VISUALISATION, 3D MODELLING, AND SPATIAL ANALYSIS OF THE RUSTENBURG LAYERED SUITE, BUSHVELD IGNEOUS COMPLEX, SOUTH AFRICA.

BY

OLUSEYI ADUNOLA BAMISAIYE

A thesis submitted in partial fulfilment of the requirements for the degree of

DOCTOR OF PHILOSOPHY

In the Faculty of Natural & Agricultural Sciences

Geology Department

University of Pretoria

JULY 2015

Thesis title: Visualisation, 3D Modelling and Spatial Analysis of the Rustenburg Layered Suite, Bushveld Igneous Complex, South Africa.

Author: Oluseyi Adunola Bamisaiye

Supervisors: Professor J. L.van Rooy

Dr. Hermanus Brynard

Department: Geology

University: University of Pretoria

Degree: Ph.D (Geology**)**

DECLARARTION OF ORIGINALITY

I, Bamisaiye Oluseyi Adunola declare that this thesis is my own original work and has not been submitted before for the award of any degree in any other institution.

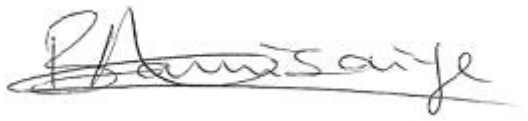

Signature:

21/07/2015

Date:

THESIS SUMMARY

The aim of the research is to describe the geometry of the Rustenburg Layered Suite (RLS) across the limbs of the Bushveld Complex through detail analysis of available borehole logs. Various spatial analytical methods ranging from interpolation methods, 3D modelling, strip logging, plotting of cross-sections and profiles and other statistical and visualization techniques were employed in interpreting the geometry and sequential structural development of each major stratigraphic unit and the units of economic importance. Interpretation was also based on published and unpublished field and geophysical data and reports on the study area.

Chapter one accentuates the importance of the study for a better understanding of the emplacement, layering, depth relationship between the various limbs and provision of information that will be useful in addressing some geological problems. The chapter also emphasizes the focus of the research, which is to determine from available borehole data, the geometry, and depth relations to modern topography of the RLS. It emphasizes the scope and limitation of the research with a detail literature review of previous research on the same area.

Chapter two describes the borehole log data format at the Council for Geoscience, Pretoria and computation detail, the software used and other data available for the study. Detailed description of lithology, position, and orientation of boreholes and other information about selected logs are given in a separate CD. The chapter gives details of the different interpolation methods employed in analyzing the borehole log data, and the basis for their choice as well as the relevance of each output in understanding the geometry of the RLSacross the limbs.

Chapter three introduces the lithologic and stratigraphic variation observed from the results of the analyses based on stratigraphic thickness and geographic contact pattern. It also describes the geometry of major stratigraphic units and the units within the Critical Zone based on lithologic correlation across the farms and limbs using strip log, models, fence diagrams, cross-sections, etc.

Chapter four gives a detail explanation of the geometry based on structural contours and isopach maps generated from downhole stratigraphic data on a local scale. Close-up views of major sub-sections of the Bushveld Complex are elaborated on to gain knowledge of the geometric patterns and general stratigraphic distribution in terms of thickness of each stratigraphic unit and the contact pattern at the top and base of the structural contours.

Chapter five addresses the variation across the Bushveld Complex limbs based on stratigraphic and structural attributes constrained from structural and isopach maps. It provides information about variation in trend and relative level of emplacement of each stratigraphic unit at different locations. The chapter also addresses some salient features within each of the limbs.

Chapter six explains trend surface analysis results of the RLS in order to gain insight of detail timing or sequence of development of structures in the study area. The relationship between structural features and thickness of each stratigraphic units were examined. This was based on the assumption that if similar relationships exist between structure contour elevation and stratigraphic unit thickness, the structure probably developed with emplaced material or it was modified during emplacement. The inverse relationship between structure contour pattern and thickness of some stratigraphic units indicate that the structure most likely pre-dates emplacement. This follows that high relief (structural high or positive structure) area that existed before magma influx received less deposit while low relief (structural low or negative structure) areas received more magma influx except where the structure has been tectonically disturbed. Stratigraphic thickness is also related to closeness to the magma source. Trend surface analysis was also used to differentiate and separate major structural and thickness trends (regional trends) from local or residual structural and isopach features.

Chapter seven illustrates some of the faults and other structural features that can be inferred from the structure and isopach maps, profiles and models generated in previous chapters. The inferred faults are described in terms of trend of the upthrow and downthrow. Strip log and sections were utilized in affirming the presence of the inferred faults and their location, while profiles were employed to show the geometry of some of the faults at the subsurface. The study provides very useful information about the geometry of some of the faults at subsurface.

Chapter eight focuses on the subsurface geometry of the RLS based on 3-dimensional model interpretation. It emphasizes the significance of the geometry in mineral exploration and magma emplacement studies.

Chapter nine summarizes and discusses the results of the findings from previous chapters.

ABSTRACT

Adequate knowledge of the regional subsurface geometry depth relationship between the limbs and distribution of mineral zones within the Rustenburg Layered Suite (RLS) is required for better understanding of the emplacement geometry, distribution of economic mineral zones and structural evolutionary issues. This will lead to improved exploration prospects that could assist in less degradation mining activities and environmental hazard control and management. Incompleteness of surface outcrops and limited availability of seismic data has been a hindrance to this. This research focused on the determination from available borehole data, the geometry and depth relations to modern topography of the RLS. Extensive Geostatistical analysis of hundreds of borehole log data was carried out to better constrain the complex geologic structural framework and architecture of the RLS. This has helped to identify and visualize the subsurface stratigraphic units, their geometric forms and improved the understanding of the geology and structure of the RLS.

ACKNOWLEDGMENTS

The contributions, assistance and guidance of the following people are highly appreciated:

- Prof. P.G. Eriksson for extensive academic and administrative guidance, and for constructive ideas and suggestions.
- Prof. J.L. Van Rooy for his support and valuable contribution to the research and
- Prof. A. Bumby for his support, valuable suggestions and constructive criticism.
- Dr. Hermanus Brynard for supervision, valuable guidance and for taking time to edit the thesis
- The University of Pretoria and home university, The Federal University of Technology Akure are acknowledged for financial support. The Management of the Council for Geoscience, Pretoria is appreciated for allowing this research collaboration and granting access to all essential data. I will also like to appreciate the following staff members of the Council for Geoscience for their contribution to the success of this research.
- Dr. Stewart Foya for administrative guidance,
- Ms. Marietjie Schalekamp for making the core logs available at all times,
- Ms Estelle van Tonder for providing access to reports and other informative documents,
- Abera Tessema, Janine Coleand Abdul Kenan for provision of geophysical data and other valuable information.
- Valerie Nxumalo for making time available to introduce me to available research facilities and for her kindness and support throughout the period.

I am also very grateful to my friends Dr. Peter Olubambi, Prof. Femi Akindele, Dr. Asiwaju-Bello, Rasidi Sule, Tunde Obadele, Biodun Adeola, Tola, Dr. Oladayo Olaniran, Mrs. Oluwaseyi Akpor, and Mrs. Helen Adekanbi, all my church members at Redeemed Christian Church of God, Mount Zion parish in Pretoria for their love, support and encouragement.

My sincere gratitude goes to my husband and friend Mr. Michael Bamisaiye for his love, perseverance, support, encouragement and prayers and to our wonderful children for being there for me.

Finally to my parents - Pastor and Mrs J.F. Olanipekun, my siblings for their support and prayers.

TABLE OF CONTENTS

LIST OF TABLES

LIST OF FIGURES

CHAPTER 1 INTRODUCTION

1.0 GENERAL INTRODUCTION

The Bushveld Complex of South Africa with an area extent of 65,000km^2 (Cawthorn and Webb, 2001) holds the world's largest deposit of Platinum group elements (Vermaak, 1995; Barnes et al., 2004; Naldrett, 2009). It intruded into the Transvaal basin about ca. 2.05 Ga (Harmer and Armstrong, 2000; Walraven et al., 1990; Barton et al., 1994) as a sill intrusive (Cawthorn, 2012) before undergoing subsidence (Letts et al., 2009). The Transvaal basin is situated in the northern parts of the Kaapvaal craton which is the best preserved and oldest continental crust (Cahen et al., 1984; Thomas et al., 1993; Youssof et al., 2013).

The Bushveld Igneous Complex (BIC) is made up of upper felsic rocks which include; the Lebowa Granite Suite, Rashoop Granophyre Suite and Rooiberg Group directly overlaying basal mafic to ultra-mafic rocks known as the Rustenburg Layered Suite (RLS). The RLS hosts layers that are economically exploited for Platinum group elements, chromium and vanadium. The RLS outcrops within the major compartments or limbs of the Bushveld Complex as indicated in Figure 1.1 below.

Research on the geology of the Bushveld Complex has been ongoing for more than one century and over this period, knowledge about the parental magma source, origin of layering, emplacement geometry, structure and evolutionary issues has continuously improved (Hunter, 1976), not only for academic reasons but also to better exploration prospects.

Despite the increase in knowledge, researchers have not been able to reach a conclusion on many of these issues. However, a key challenge is how to unravel the subsurface geometry of the entire area since field based studies could not adequately describe the

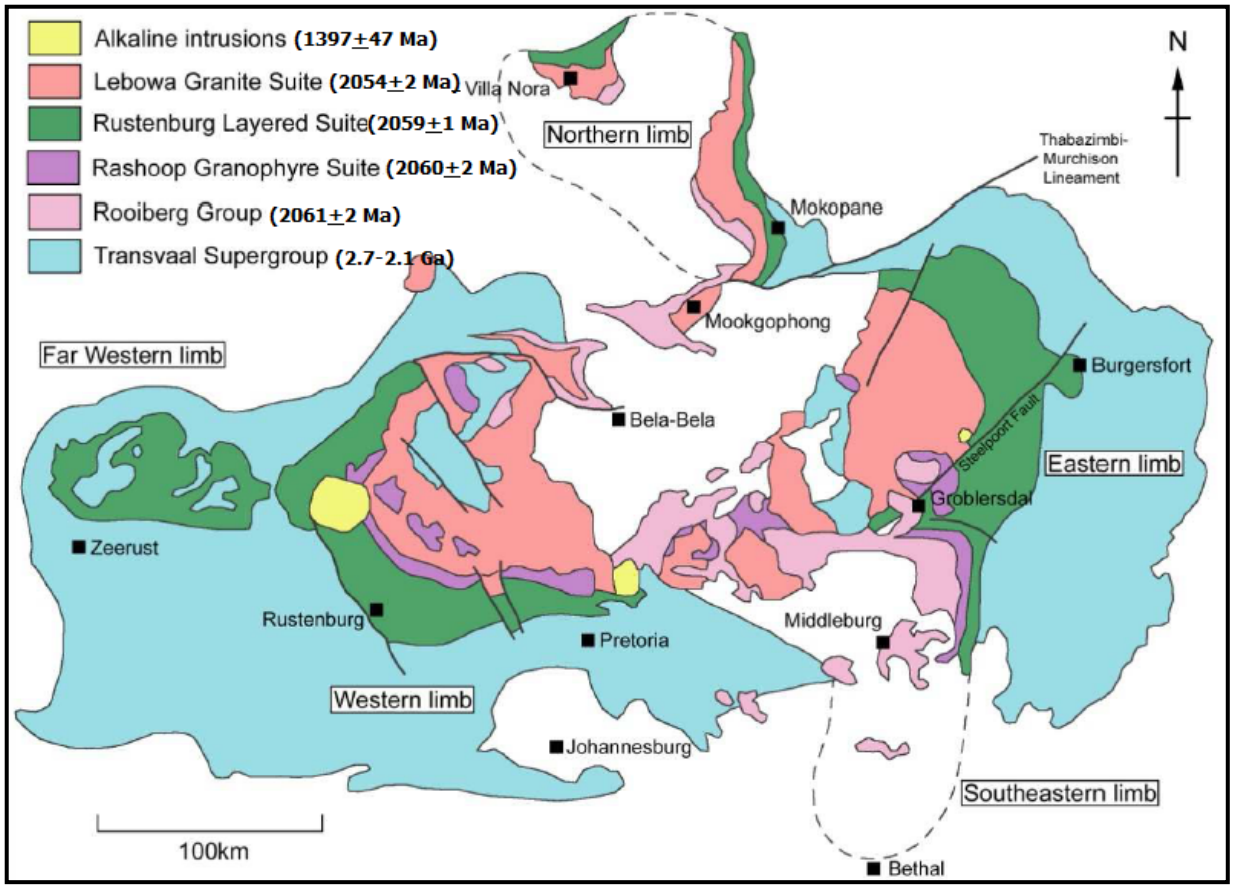

Figure 1.1: Simplified geologic map of the Bushveld Complex showing all the limbs (modified after Kinnaid, 2005) the best is to give also the range of ages related to colours

geometry due to incompleteness of outcrop exposures and limited availability of seismic data. This is important for a better understanding of the emplacement, layering, depth relationship between the various limbs. It will add to the knowledge about the distribution of the mineral bearing zones. This research focuses on the determination from available borehole data, the geometry and depth relations to present topography of the RLS.

1.1 LOCATION OF STUDY AREA

The study area is situated in the northern parts of South Africa as shown in Figure 1.1. It extends from Villa Nora in the north to Bethal in the south and from Zeerust to Burgersfort in the east (Cawthorn et al., 2006). It has total area coverage of about 65,000 km^2 which covers parts of four Provinces: Limpopo, North West, Gauteng and Mpumalanga. The

outcrops are bounded between latitude 23° and 26° S and longitude 25° and 31°E. Villa Nora section outcrop covers an approximated distance of about 39 km with a width of approximately 36 km. Potgietersrus section has a total distance of 100 km and maximum width of 12 km at the centre. Western limb spans through a distance of 239 km and the eastern limb covers a distance of about 250 km. The southeastern/ Bethal section was omitted due to lack of data.

1.2 RESEARCH AIM AND OBJECTIVES

The main aim is to determine the geometry, spatial relationship and emplacement behaviour of the RLS from available borehole log data. This aim will be achieved by following the procedures listed below;

- Determine from borehole log data the upper and lower contact of each zone and use the information to determine the geometry and thickness of each zone within the RLS.
- Analyse the RLS geometry and thickness across limbs
- Determine depth-to-horizon for each stratigraphic unit.
- Carry out limb comparisons in terms of total thickness of RLS for each limb
- Constrain nature of the floor rock spatial relationship
- Determine the paleogeography and paleo-structures of the RLS
- Identify major structural elements within the area and their surface and subsurface geometry at different horizons
- Constrain the kinematic history from the present geometry

1.3 PROBLEM STATEMENT, SCOPE, AND LIMITATION OF STUDY

Mapping the subsurface of the world's largest layered intrusion will not only enhance the understanding of underlying geology and structure, but will also assist in making better interpretations of the surface features that could not be adequately examined due to insufficient outcrops at the surface. However, subsurface data cannot be directly assessed

except through boreholes, tunnels and geophysical survey. Geophysical data has been extensively utilized for studying the emplacement and geometry of mafic rocks within the BIC. For instance, Campbell (2011) gave a summary of the advances in geophysical mapping of the RLS facilitated by technological advancement and exploration demand. Cole et al. (2013) used high-resolution gravity and aeromagnetic data to delineate the mafic rocks based primarily on physical contrast. While the study recorded high success with delineating the Upper Zone, it was unable to map with the same level of detail the other zones of the RLS due to the absence of good quality signatures.

Different geophysical data have been employed for regional study of the Bushveld Complex (Odgers et al., 1993; Odgers and Du Plessis, 1993). However, seismic reflection data seems to be more useful for local structural mapping and for mine-planning purposes (Campbell, 1994, 2006, 2009, 2011; Du Plessis and Levitt, 1987; Web et al., 2004; Cawthorn and Webb, 2001), but needs to be complemented with other datasets for better interpretation (Chunnett and Rompel, 2004).

High-resolution imaging capabilities of 2D and 3D seismic reflection surveys have been utilized for mapping underground structures in some parts of the Bushveld Complex, most of these studies are extremely localized. Another drawback in utilizing high-resolution seismic data for a regional study such as this is its availability, high cost and proprietary restriction. High-resolution seismic data are very expensive to acquire with stringent proprietary restriction on the few that are available. It might be practically impossible to acquire such data over the whole of the study area. While it is easy to constrain local (between 1 km and 5 km) subsurface geometry at the local scale with the use of seismic surveys, regional study will require a large volume of continuous seismic data which is almost impossible to access due to proprietary issues even when available.

Use of borehole log data is rather less expensive and more readily available for both local and regional studies. Regional models (>5 km) may act as a constraining medium to mineralized zones and to establish a coherent broad scale relationship between adjacent limbs across the Bushveld Complex. This will help in understanding geological processes that lead to the present day geometry (deKemp, 2000). Borehole log data are very valuable

and provide direct observation of structural and lithologic information to centimetre detail; they also provide clear descriptions of how rocks are spatially laid down. Advances in geological data processing techniques and software development coupled with 3D visualization techniques have improved the understanding of subsurface phenomenon that allows easy correlation, accurate feature detection and better morphological investigation. Each of the stratigraphic units is accurately mapped with a high level of accuracy.

These data are available at the Council for Geoscience, Pretoria and were extensively utilized for this research. The data were directly logged from borehole cores and are considered more accurate than inferred data. The data used has a good spatial distribution over the entire study area. However, most of the available borehole log data were drilled for exploration purpose and as such only terminate within the economic layers or a little below, thus making it difficult to accurately represent the geometry beyond the available depth. Therefore, the focus of this study is limited to geometry of the RLS from the surface to about 3000 m depth. Notwithstanding, the results accurately present conceptual 3D models of the study area that better define the geometric pattern of each stratigraphic interval, provide better understanding of subsurface geology, aid interpretation that serves as a basis for future exploration targets. This study also explored the potential offered by 3D interactive graphics for spatial visualization of borehole log data.

1.4 ASSUMPTIONS

- The research focuses on the Rustenburg Layered Suite (RLS) because of its lateral continuity across the limbs with the assumption that layers are laterally continues at all sample points except for minor downward transgressions into underlying layers.
- Accumulation process of layers (though igneous in nature) can be likened to sedimentary processes, either clastic or chemical (Naslund and McBirney, 1996).

1.5 GEOLOGICAL SETTING OF THE BIC

The Kaapvaal Craton and Zimbabwe Craton in South Africa are typified by extensive mafic to ultramafic complexes among which are Molopo, Trompsburg and the Bushveld Complexes. Other mafic intrusions within the Kaapvaal craton are the Vogelstruisfontein, Kaffirskraal, Losberg, Modipe, Koringkoppies and Uitloop (Viljoen and Schürmann, 1998). The most economically important of these complexes is the Bushveld Complex. The Bushveld Complex intruded into the Transvaal Basin, which is one of the basins formed at the northern part of the Kaapvaal craton about 2060 million years ago (Walraven et al., 1990;Walraven and Hattingh, 1993;Olsson et al., 2010). Other basins within the Kaapvaal Craton are the Pongola, Witwatersrand, Ventersdorp, Dominion and Waterberg Basin. The mafic rocks of the Bushveld Complex lie unconformably between clastic rocks of the Pretoria Group and overlying Rooiberg felsites (Cawthorn et al., 2006).

The floor rock to the RLS is dominated by the presence of domes, diapirs, chilled zones and minor transgression of the mafic intrusion into the underlying host rock (Uken, 1998). Holzer et al. (1999) proposed a NW-SE compressional tectonic regime for the Kaapvaal Craton as a response to collision with the Zimbabwe Craton. The Bushveld magma were emplaced due to localized transgression extension along reactivated major lineaments such as the Thabazimbi-Murchison lineament with ENE-WSW orientation (McCourt, 1995), the Crocodile River fault (Hartzer, 1989) and Steelpoort Fault (Cawthorn et al., 2002). According to Bumby et al. (1998), the first (D_1) and second (D_2) deformation events in this region pre-date Bushveld intrusion, produced folding and faulting along a NW-SE compression direction, through which the Bushveld Complex intrusion occurred along the same trend with the second deformational episode. The third deformational episode (D_3) is post-Bushveld.

The RLS of the Bushveld Complex in South Africa is the world's most enormous layered mafic intrusion (Walraven, 1982). The RLS has a thickness of about 8100 m (Eales and Cawthorn, 1996). It is divided into five major zones (Kruger, 1990, 1994; Mitchell and Scoon, 1991): the Marginal Zone, Upper Zone, Main Zone, Critical Zone and Lower Zone. Each zone is characterized by cyclic units or layering which is believed to be due to the

repeated magma addition and crystallization (Sharpe, 1981; Kruger et al., 1987; Cawthorn et al., 1991; Eales and Cawthorn, 1996; Mitchell et al., 1998: Cawthorn and Walraven, 1998; Naldrett et al., 2008; Hodge et al., 2012). New influx of magma might interrupt complete crystallization of residual magma, thus leading to incomplete or partial development of units (Maier and Eales, 1997).

The Upper Zone is made up of magnetite layers occurring mostly within gabbro which is the dominant lithology and occasionally with norite, anorthosite or pyroxenite (Ashwal et al., 2005; Tegner et al., 2006; VanTongeren et al. 2010). Total thickness of the Upper Zone varies from 1000 m to 2000 m (von Gruenewaldt, 1973; Molyneux, 1974; Kinnaird et al. 2005; Maier et al., 2012). Maier et al. (2012) recorded 26 magnetite layers in the eastern and western limbs and 16 layers for the northern limb. This zone is found at shallow depths in the Eastern limb and extends laterally along strike for about 120 km and 200 km along the western limb (Reynold, 1985b). In the western limb, the Upper Zone extends from the northern end of the western limb of Amandelbult section (<10 m) through the Union section (<30 m). It reappears again around the Boshoek section (<200 m thick) and the Brits section (with a thickness of over 400 m) and gradually thins out laterally towards the southern end of the western limb (close to Pretoria) (Coertze, 1970). The magnetite layer contains vanadium, for which it has been mined (Cawthorn and Molyneux, 1986; Wilson and Anhaeusser, 1998). The base of the Upper Zone is marked by the first appearance of cumulate magnetite and a major magma influx above the Pyroxenite Marker. This represents a major polarity reversal in the Eastern Bushveld (Lett et al., 2009) and the base of the Upper Zone in the Western and Eastern limb (SACS, 1980; Kruger et al., 1987; Harney et al., 1990; Hoyle, 1993).

The Main Zone represents the thickest zone within the RLS with a total thickness of 3000 m (von Gruenewaldt, 1973; Molyneux, 1974; Mitchell, 1990; Nex et al., 1998). It contains norite that grades downwards to gabbro-norites with minor anorthosite (Kruger, 2005a; Cawthorn and Walraven, 1998) and a distinct layer close to the top in the western limb but that is absent in some places in the Eastern limb.

The top of the Main Zone is marked by a Pyroxenite Marker interval, the base is located at the top of the Bastard cyclic unit, which is characterized by an upper contact of mottled anorthosite (de Klerk, 1992; Cawthorn and Walraven, 1998). Lateral continuity of layers

in the Main Zone is not as pronounced as in the Critical Zone (Molyneux, 1974; Mitchell, 1990; Nex et al., 1998).

Support for connectivity at depth between the Western and Eastern limbs of the Bushveld Complex was given by Cawthorn and Walraven (1998), Webb et al.(2004) (using gravity modelling). Youssof et al. (2013) gave a contrary opinion from seismic geophysical investigation and classified the thickness of the crust (45-50 km) and composition of the central Bushveld Complex as being mainly felsic.

The Critical Zone holds the largest chromite and PGM in the world (Naldrett et al., 2008, Naldrett, 2009). The zone is sub-divided into Lower, Middle and Upper Group chromitite. The Lower Critical Zone (LG) is made up of ultramafic cumulus (chromitite, harzburgite, and pyroxenite) with up to seven chromitite layers generally numbered from LG7 at the top down to LG1 at the base (Cameron, 1980, 1982). LG6 is important for its high content of chromite, which is the largest in the world (Crowson, 2001). The Middle Group consists of four major chromitite layers (MG1-4). Each of these major divisions has two to three sub-divisions. Eight cycles exist in the Upper Critical Zone while nine cycles were identified in the Lower Group. Each cycle is made up of a partial or a complete sequence of ulramafics though norite to anorthosite (Kinnaird, 2005). Detail of the thickness and distribution of the Critical Zone is provided by Wilson and Anhaeusser (1998).

The Merensky Reef and Bastard Merensky Reef are thin units occurring above the Critical Zone. The Bastard Merensky is marked by giant mottled anorthosite which also marks the top of the Critical Zone. The Merensky Reef is noted for its platinum group elements content and lateral consistency (von Gruenewaldt, 1979). This unit is also marked by influx of plagioclase bearing rocks (Cawthorn and Walraven, 1998) in magmatic composition. The typical lithology is pegmatoidalfeldspathic pyroxenite but could consist of pegmatoidalfeldspathic harzburgite, or norite with sulphide blebs bounded by narrow chromitite (Viljoen, 1994, 1999). The Reef has a remarkable planar to sub-planar nature which extends along strike for 138 km in the Eastern limb and 145 km in the western limb, the thickness varies from 2 cm to 14 m (Viljoen and Schürmann, 1998).

The dominant lithologies in the Lower Zone consist of alternating pyroxenite, harzburgite and dunite. The zone was sub-divided by Cameron (1978) into basal, lower and upper subzones which double as the lowermost unit of the Critical Zone. The zone has variable thicknesses due to floor rock topography and structure (Cawthorn et al., 2006). It is more than a 1400 m thick around the Pilanesberg, and attains up to 37 cycles according to Hulbert and von Gruenewaldt (1985). The appearance of well-defined thin layers of chromite within the upper pyroxenite marks the start of the Critical Zone.

The Marginal Zone has norite as the dominant lithology with minor pyroxenite and variable amounts of other rocks that have been assimilated from the surroundings (Cawthorn et al., 2006). It is noticeable around the Pilanesberg area in the western limb where it is in contact with the Lower Zone, has a wide distribution within the northern limb and the Eastern limb where it forms the floor rock. The thickness of the Marginal Zone of literature varies from 0 to 800 m (Naldrett et al., 2008) with evidences of crustal assimilation (Viljoen and Schürmann, 1998; Cawthorn and Walraven, 1998).

1.5.1 RUSTENBURG LAYERED SUITE OCCURRENCE

The Bushveld Complex is made up of four compartments of mafic to ultramafic layered sequence (Eales and Cawthorn, 1996) which outcrops as the Potgietersrus limb with a smaller outcrop to its western side known as the Villa Nora outcrop, the western limb with the Far Western or Nietverdiend outcrop, the Eastern Limb and the Southeastern or Bethal Limb. The Western Limb forms an arc that extends for about 241 km from the Crocodile River through Rustenburg to north of Pretoria. The Eastern Limb extends from the northern part of Belfast to Burgersfort while the northern Limb runs from Potgietersrus to Villa Nora. The four compartments of the Bushveld Complex include the Lebowa Granite Suite, the Rashoop Granophyres Suite, the Rustenburg Layered Suite (RLS) and Rooiberg Group (Cawthorn et al., 2006).

The Bushveld Complex probably developed from accretion of multiple magma injection (Cawthorn and Walraven, 1998). The magma was initially ultramafic in composition followed by later tholeiitic magma (von Gruenewaldt, 1979; Vantongeren and Mathez, 2013). Detail about parental magma composition is given by Godel et al. (2011) and

references therein. Van der Merwe (1976) gave the total thickness of RLS in the Western, Eastern and Northern Bushveld as 7750 m, 9000 m and 7 000 m, respectively.

The RLS is important not only as the world's largest deposit of mafic layered intrusion, but also as the largest source of Platinum group elements (PGEs). The RLS outcrops prominently as Western, Eastern and Northern, Far Northern, Far Western and lastly the Southwestern limb which is covered by recent deposits (Kinnaird et al., 2005). Repeated magma injection coupled with mineral precipitation and interaction with new magma addition is believed to be responsible for the repetition of mineral layers or cyclic units in the RLS (Cawthorn, 1998; Cawthorn, 2007; Naldrett et al., 2012). The Western Limb and the Eastern limbs are similar in lithology and stratigraphy and this can be attributed to simultaneous injection into both the limbs from a centrally located magma chamber (Sharpe et al., 1980) or the two limbs being connected at depth (Cawthorn et al., 1998; Cole et al., 2013).

1.5.2 THE NORTHERN LIMB

The stratigraphy in the Northern Bushveld has been grouped into four units, i.e. the Lower Zone, the Critical, Zone, the Main Zone and the Upper Zone in order to maintain the same stratigraphic order with the Eastern and Western Bushveld (Kinnaird and McDonald, 2005). The Lower Zone is dominated by harzburgite and pyroxenite. The Critical Zone is made up of norite, pyroxenite and anorthosite and contains layered orthopyroxene-chromite-clinopyroxene-plagioclase cumulates. The Main Zone is dominated by gabbros and gabbronorites, and the Upper Zone is composed of ferrogabbros with variable amounts of magnetite.

The Platreef of the northern limb is made up of mainly pyroxenite with deposits of PGEs and associated Ni and Cu. It is one of the world's most noteworthy deposits of PGEs. The distribution of PGEs in some parts of northern Bushveld is controlled by the presence of Base Metal Sulphides (BMS) (Holwell and McDonald, 2006). The base metal sulphides in the Platreef hold very high PGE (comparable with the Merensky Reef) indicating that the PGE must have been concentrated from a large volume of magma, but the source of that magma, as well as the concentration mechanism of the PGEs has not been established. However, a study of coeval diamonds provides evidence that the main source of magma

for the Bushveld Complex PGEs is the mantle rather than the crust (Armitage, 2011). Holwell and McDonald (2007) have suggested that the magma that formed the (pre-Platreef) Lower Zone may have been the source of PGE. Although, the Platreef outcrops with a N-S orientation, it is laterally irregular. The PGEs of the Northern Bushveld is more dispersed with no well-defined mineralization boundaries compared to the PGM in UG2 and the Merensky Reef (Cawthorn, 1999).

The Northern Bushveld limb differs from the Eastern and western limbs in terms of floor rock lithology, and igneous layering that shows a trangressive contact relationship different from the progressive higher stratigraphic layering displayed in the Northern Bushveld (Harris and Chaumba, 2000). The origin of the Platreef is controversial, while many researchers agree that the Platreef is a northern equivalent of the Critical Zone; others believe that the Platreef of the Northern Bushveld has a different mineralization origin, i.e. the magma composition that formed the two have different composition and source (Lee, 1996; McDonald, 2005).

The footwall lithology to the Platreef varies from Archaean basement granites/gneiss in the Northern parts to dolomitic rocks in the central section to shale, dolomite and quartzite in the southern sector (Cawthorn et al., 1985; Kinnaird et al., 2005), while the Main Zone granodiorites form the roof to the Platreef. The Thabazimbi-Murchison Lineament (TML) separates the northern limb from the rest of the complex and must have played a major role during the intrusion of the Bushveld Complex as argued by Kinnaird (2005).

1.5.3 THE WESTERN BUSHVELD COMPLEX

The Western Bushveld is sub-divided into two, the Far Western compartment and the main Western Bushveld which dips at low angles toward the centre. The Far Western outcrop shows thick harzburgite and pyroxenite layers with the occurrence of chromitite of the lower Critical Zone (Coertze, 1970). The main Western Bushveld limb consists of all the major stratigraphic units occupying the whole stretch of the Western Bushveld as layered rocks. The Pilanesberg Complex is made up of alkaline rocks, forms a perfectly circular shape with a diameter of about 28 km, and occupies the central part of the Western Bushveld. Rocks of the Main Zone are wide-spread in the area with minor transgression

by the Upper Zone rocks. The Critical Zone is also well developed and laterally continuous except for the gap areas in the Northwestern Bushveld area.

The dominant structural trends in the Western Bushveld are NNW comprising major faults such as the Rustenburg (Bumby et al., 1998), Brits and Welgevonden faults. The relationship between rocks of the RLS with the underlying Pretoria Group sediments was described by Coertze (1970) who, from field evidence, observed that the RLS concordantly overlies the Magaliesberg quartzite in the Western Bushveld with much of the quartzites forming xenoliths. Interaction between the RLS and Pretoria group sediments caused a widespread distribution of quartzite xenoliths north of the Rustenburg and southwest of the Pilanesberg, while isolated occurrences were reported towards the northern part of the Pilanesberg (Coertze, 1970, 1974). Eriksson et al. (1995) described the cross-cutting of RLS rocks into the Pretoria Group sediments and the contact metamorphism of the same rock leading to formation of xenoliths of quartzite and hornfels. Xenoliths of quartzite and dolomite were reported by Maier et al. (2000) as evidence of interaction with the floor rocks. Xenoliths of anorthosite were observed by Bristow et al. (1993), as field evidence of interaction with rocks of the Critical Zone, and thus suggesting the crystallization from residual melt (Sharpe, 1981; Eales and Cawthorn, 1996), while another model supports later injection of the Marginal Zone. Widespread folding in the floor rocks has been attributed to prevalent ductile deformation during the emplacement of the Bushveld Complex (Hatton and von Gruenewaldt, 1987).

1.5.4 THE EASTERN BUSHVELD

The RLS in the Eastern Bushveld intruded along a major regional unconformity between the Pretoria Group sediments and overlying residual zone rocks (Cawthorn, 2012) and Rooiberg felsites (Cheney and Twist, 1991). The outcrop exhibit a complete stratigraphic section from harzburgite to fayalite and apatite-bearing diorite (Cameron, 1978, 1980, 1982). They dip steeply at 60° at the contact zone, and flatten out towards the centre. Outcrops of the Eastern Bushveld are well exposed due to the rugged topography (Von Gruenewaldt, 1973; Sharp 1981). Mining is carried out at lower dips (SACS, 1980). Lithologic units that constitute the Main Zone in the Eastern Bushveld include the gabbro,

norites, anorthosites and pyroxenites with the absence of olivine and chromite (Kinnaird, 2005), while the thickness varies from 0 to 3000 m.

The Upper Zone is characterized by gabbro with bands of magnetite. Twenty-five magnetitite layers have been identified in the Eastern Bushveld Complex limb (Molyneux, 1974). Magnetitite layers occur on Mphatlele farm, Kennedy's Vale farm, Krusirivier farm, Mapochsgronde farm, Welgevonden farm, Uitvlugt farm, Doornpoort farm and Zwartkop farm. This layer is important for its vanadium content. The Lower Zone of the Eastern Bushveld Complex has been divided into lower pyroxenite, Harzburgite subzone, and Upper Pyroxenite. The Lower Zone is directly overlain by the Critical Zone (Cameron, 1963;1978). The Lower Zone thickness varies with the structure of the floor rock, attaining 1584m in thickness at the Olifants River Trough. The Marginal Zone consists of mainly norites with minor pyroxenite (Cawthorn et al., 2006), and occurs in contact with meta-sedimentary rocks of the Transvaal Supergroup. The occurrence is influenced by modification in the sedimentary floor by folds, faults and attenuation of overlying rocks (Uken and Watkeys, 1997b).The RLS in the Eastern Bushveld is penetrated by floor rock domes believed to have been formed by diapiric processes (Uken, 1998).

1.6 TECTONIC SETTING OF THE BUSHVELD COMPLEX AS IT AFFECTS THE RLS

The Bushveld Complex intruded into the Transvaal Basin which consists of a suite of both clastic and chemical sedimentary rocks with volcanic rocks, attaining a thickness of up to 12 km. Layered intrusions are important both as a tectonic feature as well as for economic reasons. Emplacement of the Bushveld rocks was controlled by reactivation along major pre-Bushveld lineaments such as the Thabazimbi- Murchison and Barberton lineaments, and the Melinda, Rustenburg and Steelpoort Faults which represent zones of weakness within the Kaapvaal craton (Du Plessis and Walraven, 1990).

The RLS was emplaced under a compression condition as proposed by Hunter (1975), Sharpe and Snyman (1980), Hatton and Sharpe (1988) and Hatton and Von Gruenewaldt (1987). Transvaal Supergroup inliers such as the Marble Hall and Dennliton and Crocodile

River domes indicate a major pre-Bushveld regional deformation pattern disrupted by Bushveld Complex emplacement (Hartzer, 1995). While one school of thought proposed a single intrusion centre for Bushveld rocks others are in agreement with multiple passageways along suture zones (Naldrett, 2009; Maier et al., 2012).

In attempting to relate the occurrence of PGE deposits to layered intrusions, Maier et al. (2013) gave the following explanations:

- Stable and light cationic crust favours the formation of large intrusions (Groves et al., 1987; Maier and Groves, 2011) and preservation of mantle derived magma (a view shared by Lee (1996)).
- Sulphides were concentrated by fractionation, periodic magma replenishment and slumping of cumulate slurries due to subsidence resulting from crustal loading.

1.6.1 CONTRIBUTION FROM GEOPHYSICAL MAPPING OF THE BUSHVELD COMPLEX

3D seismic surveys (used in conjunction with other geophysical survey methods) have proved useful in delineating underground structures in the Bushveld (Chunnet and Rompel, 2004). However, delineation of structures, reefs, potholes, iron rich ultramafic pegmatites (IRUP) slump structures, mineralization, lithologies and other features are dependent upon the presence of some physical contrasts. Although 3D seismic interpretation has become widely accepted as a routine interactive technical tool in subsurface exploration and has enhanced the understanding of the geometric relationships among interpreted surfaces, it is very expensive. Geophysical methods have been applied extensively in both lithologic and structural mapping of the Bushveld Complex with special emphasis on the RLS. Campbell (2011), in explaining the advances in the use of geophysical methods in mapping the Bushveld Complex, reported the usefulness of 2D seismic reflection and high-resolution aeromagnetic surveys in delineating faults, dykes, loss of ground and pothole structures. These geophysical surveys are also useful for blind exploration of economic zones in the RLS on a broad scale and strictly in areas or Zones with good contrast and signature. Direct delineation of the economic zones is limited due to the absence of strong

physical contrast and interpretations are based on indirect evidence (Campbell, 2011; Cole et al., 2013).

Widespread graben structures, floor domes and syn-Bushveld diapirs and graben collapse structures within the RLS were mapped by both 2D and 3D seismic surveys with high-resolution seismic interpretation, but have to be complimented with other geophysical data and field verification to avoid misinterpretation (Campbell, 2006, 2009). Gravity interpretation of RLS reveals the presence of diapirs. However, intervals between gravity stations must be carefully taken into consideration during interpretation to avoid interpretation bias. Seismic and gravity surveys reveal a thickness of between 5.0 km and 3.5 km for the RLS and about 600 m thickness over the Malope dome (Odgers and Du Plessis, 1993). Odgers et al. (1993) from the interpretation of seismic reflection of the Southern Bushveld gave credence to the regional continuity of the Transvaal sequence rocks and the RLS and pinching out of the Marginal Zone over areas with floor rock dome.

Recent aeromagnetic investigation of the RLS by Cole et al. (2012) explained the use of high-resolution aeromagnetic data for detail stratigraphic delineation on a regional scale. The study was able to map the Upper Zone with a high level of accuracy based on its consistent magnetic character, but could not delineate other zones within the RLS with the same level of detail and accuracy. Ferguson and Botha (1963) have identified structures such as IRUPs and potholes as syn-magmatic footwall extension structures.

Analyses of borehole log data provide comprehensive stratigraphic and structural information about the subsurface. Recent advances in software technology allow rapid interactive, efficient interpretation and visualization of large volumes of borehole data. 3D models created from borehole data allow a better understanding of the geometry of the RLS Zones. It also allows conceptualization of geologic features and structures in three dimensions. Geometric patterns of each Zone of the RLS were qualitatively evaluated with interval structure contour and thickness maps generated from borehole log data. These important economic layers were also directly mapped to local scale. Most of the shortcomings of geophysical data can be overcome with the use of borehole log data. Any

features of interest can be directly mapped and correlated across the limbs if the record is available.

Other prominent features common in the RLS are the gaps and pothole structures. Gap areas are areas where the Merensky Reef is either absent or have transgressed deep down. The gap areas north of Pilanesberg are generally referred to as the Northern and Southern gap areas and are associated with features such as floor rock high, thinning of stratigraphy and thickening of the Upper Zone (Viljoen, 1994).

Potholes represent areas where the planar Merensky Reef extends beyond its footwall thus disrupting the stratigraphy (Ballhaus and Stumpfl, 1985; Roberts, 1985, Roberts et al., 2007; Viljoen and Schürmann, 1998) and different types of it were identified (Viljoen and Schürmann, 1998; Robert et al., 2006). Potholes are characterized by their thickness, dip direction and the bottom contact of the Merensky Reef. Smith and Basson (2006) classified potholes based on the footwall lithology, and the shape of the pothole. Viljoen (2004) demonstrated correlation between the Merensky Reef thickness and grade, Merensky Reef facies and gravity highs. Pothole structures in the Northwestern Bushveld have been classified as Swartklip facies with subdivision into normal, pothole reef and regional subfacies, the distribution and density of the potholes, although regional in some cases are irregular (Viljoen 1994; Viljoen and Scoon, 1985; Viring and Cowell, 1999; Reid and Basson, 2002).

Due to the economic importance of the Merensky Reef as platinum-bearing zone and hindrances caused by these features to mining, it has attracted much investigation among researchers such as Ballhaus (1988), Viljoen and Heber (1986),Viljoen and Schurmann (1998), Viljoen (1999) and Smith and Basson (2006). The origins of these features are inscrutable in nature according to Carr et al. (1999) and Viljoen (1999) who, from field observations, identified the collapse of vertical dykes of the Merensky pyroxenite into vents. This resulted in the creation of pull-apart sites in response to the overloading effect of new magma addition. Isotopic studies proposed a tensional model for the formation of potholes just before the crystallization of the Merensky Reef magma. Pothole formation has also been described as a thermo-chemical erosion process by Viljoen (2004).

1.7 FLOOR AND ROOF ROCK RELATION AND STRUCTURE

Coertze (1970) described the relationship between rocks of the RLS with the underlying Pretoria Group sediments from field evidence. He observed that the RLS concordantly overlies the Magaliesberg quartzite in the Western Bushveld with much of the quartzites forming xenoliths. Interaction between the RLS and Pretoria Group sediments caused a widespread distribution of quartzite xenoliths north of the Rustenburg and southwest of the Pilanesberg, while isolated occurrences were reported towards the northern part of the Pilanesberg (Coertze, 1970, 1974). Eriksson et al. (1995) described the cross-cutting of RLS rocks into the Pretoria Group sediments and the contact metamorphism of the same rock leading to formation of xenoliths of quartzite and hornfels. Xenoliths of quartzite and dolomite were reported by Maier et al. (2012) as evidence of interaction with the floor rocks. Xenoliths of anorthosite were observed by Bristow et al. (1993), as field evidence of interaction with rocks of the Critical Zone and thus suggest the crystallization from residual melt (Sharpe, 1981; Eales and Cawthorn, 1996), while another model supports later injection of the Marginal Zone.

Some models show widespread folding in the floor rock and this has been attributed to prevalent ductile deformation during the emplacement of the Bushveld Complex (Hatton and von Gruenewaldt, 1985). Evidence from investigation of the parental magma source of the Bushveld Complex suggested an intercratonic rift setting (Von Gruenewaldt and Harmer, 1993) and a subduction zone (Harmer and Von Gruenewaldt, 1992) with some evidence of crustal contamination.

Cawthorn (2013) studied the rock succession in parts of the Southeastern Bushveld where the rugged topography permits close observation. He described a 700 m monzonitic rock occurring at the contact between the mafic rocks and the Rooiberg felsites, which was formerly believed to be the overlying rock to the mafic rocks. This rock was earlier described as ‘‘leptite’’ by von Gruenewaldt (1968, 1977). Hall (1932) mentioned the same contact zone with an appreciation of its lateral extent, though the zone may be absent in some places within the complex. The major and trace element data presented by Mathez et al. (2013) support the hypothesis that the Rooiberg and Rashoop ferroan rocks formed by fractional crystallization of Bushveld mafic liquids and described the 700 m contact zone

between the Rooiberg felsites and the RLS rocks as Stavoren Granophyre. Presence of diapiric structures (Uken and Watkeys, 1997a), up-warp at the roof contact, folds and flexure structures all contribute to the present geometry of the RLS. Hunter (1975) and Hartzer (1995) suggested that the domes formed from the interaction of NW-trending and ENE-trending folding while Uken (1998) argued that the domes and basins do not follow any regional trend, but are indications of the major crustal orientations developed during the intrusion of the Bushveld magma into the Kaapvaal craton. Some of these domes penetrate the RLS to different stratigraphic levels (Clarke et al., 2005).

Table 1.1 Summary of Major Topics on the Bushveld Complex

Age of the Bushveld Complex		
REFERENCES	METHOD OF INVESTIGATION	CONCLUSION
Hamilton (1977); Von Gruenewaldt et al. (1985).	Rb-Sr and trace element analysis Mineralogical and textural investigation	2050 Ma of RLS
Walraven and Hattingh (1993)	Zircon age determination with Pb evaporation technique	2054.4± 1.8 Ma
Scoates and Friedman (2008);	U-Pb zircon chemical abrasion technique.	2056.1±0.7 Ma emplacement age of RLS
Scoates et al. (2011)	Single-grainchemical abrasion ID-TIMS, or CA-TIMS, U-Pb zircon method	2055.3 ±0.6 Ma
Olsson et. al.(2011)	U–Pb dating of baddeleyite crystals	Proposed 2,70 and 2,66 billion age for the Transvaal basin

	Orientations of Archaean dykes	
Scoates et al. (2012)	U–Pb on zircons	UG2 footwall pyroxenite is 2059.8±1.2 Ma ca. 5 my older than the Merensky Reef with 2060.5±1.4Ma
Yudovskaya et al.(2013) and references therein	A review of the Bushveld Complex age	
PARENT MAGMA SOURCE AND CRYSTALLIZATION RATE		
Cole et al. (2013*)*	Aeromagnetic interpretation	Same parental magma source for both Western and Eastern limbs
Godel et al. (2011)	Trace element analysis	Same magma source for limbs
Vantongerren and Mathez (2011). Cawthorn (1996)	major and trace element analysis	Slow crystallization Between successive magma injections.
Naldrett et al (2012)	Cation ratio trend using Bushveld chromatites	Recognized five relative crystallization stages. Support for slow ascent of magma and slow crystallization rate
Schouwstra, Kinloch and Lee (2000)		Slow cooling and crystallization,
Wager (1963); Campbell (1978)		Due to crystal setting of magma
EVIDENCE FOR MAGMA LAYERING		
Cawthorn et al. (1991); Eales and Cawthorn (1996); Cawthorn and Walraven (1998); Irvine et al. (1987); Cawthorn (2012);	Chemical analysis using mass spectrometry	Due to multiple magma influx. Each major magma influx is identified by a reversal in mineral composition. With the last magma addition identified at the Pyroxenite Maker horizon.

Emeleus (1986); Eales (2002)		Due to crystal slurries
Eales et. al.(1986)		Due to crystallization
von Gruenewaldt (1971, 1973) and Molyneux (1970, 1974). Reynolds (1985, 1986), Klemm et al. (1985) and Cawthorn and Molyneux (1986). Cameron (1978, 1980, 1982) Teigler and Eales (1996); Cawthorn and Walraven (1998); Ashwal et al. (2005);Tegner et al. (2006)	Chemostratigraphic studies, mineral compositional studies. Field correlation	Multiple magma replenishment, multiple parental magma source, cyclicity
Yang et al.(2013)	Sr isotope analytical method	Slumping of early crystals leading to the interval layering
Brown 1956; Irvine (1970); Irvine et al. (2005); Maier et. al. (2012)	Lithologic comparison, chemical analysis	Layering
Reisberg et al. (2011)	Isotopic and chemical analysis	Evidence for genetic link between the Platreef and the Merensky Reef as a result of extensive crustal contamination at depth, possibly due to black shale assimilation
McDonald et al. (2005)	Lithologic correlation, geochemical and mineralogical analysis	Differences between Northern Bushveld Critical Zone and other Critical Zones within the complex
STRUCTURAL CONTROL		

Hall (1932); Cousins (1959); Vermaak (1976a); and Lee (1978)	Structural observation and stratigraphical studies	The NNE and ENE structural orientation within the Kaapvaal craton played a major role in the emplacement of the Bushveld Complex. Present geometry of BIC is strongly controlled by dome and basin-like structures that characterized the Kaapvaal craton
von Gruenewaldt(1979)	Review of structural and emplacement mechanism	Postulated centres of intrusions are aligned along deep-seated north-north-west and north-south-easttension fractures
Holzer et al. (1999)	Structural observation	Bushveld Complex was emplaced during a NW–SE compressional tectonic regime in the Kaapvaal craton.
Du Plessis and Walraven (1990); Von Gruenewaldt et. al. (1987); Silver et. al. (2004); Maier et. al. (2012b); Frieze (2004); Armitage et. al.(2011; 2012b)	Structural studies and seismic interpretation	Emplacement of Bushveld magma along major crustal lineaments driven by localized transpressional extension
Barnes et. al. (2004); Maier et. al. (2012, 2013);	Mineralogical and Compositional investigation	Upper Zone is 1-2 km thick.
Maier et., al. (2013)		Lower Zone with >1km thickness. Lower Critical Zone is between 700-800m thick. UG2 is approximately 500m thick

Naldrett et. al (2008)		Marginal Zone is 0-800m thick. Lower Zone is 800–1300 m thick. Critical Zone is 1300–1800 m thick. Main Zone is 3000–3400 m thick
Du Plessis and Kleywegt (1987); Meyer and De Beer (1987)		No connectivity
EVIDENCE FOR CONNECTIVITY AT DEPTH		
Cawthorn et. al.(1998); Cawthorn and Webb(2001); Webb et. al. (2004); Cole et. al. (2013). Campbell (1990); in Viljoen (1999).	Gravity, aeromagnetic and seismic interpretation.	Showed evidence for connectivity at depth.
Webb et. al. (2011)	Textural and compositional analysis of Kimberlite xenoliths	Showed evidence for connectivity at depth.
Youssof et al.(2013)	Seismic geophysical method of investigation.	Central BIC marked a paleo-collision zone with deep central root that deflected rising magma sideways to form the Eastern and Western Bushveld Complex limbs
Campbell (1990); in Viljoen (1999)		Down-dip extension of the Merensky Reef package for >50 km to the east of the Pilanesberg Complex
Iljina and Lee (2005)		Critical Zone rock found in Mineral Range some kilometres west of Eastern Bushveld.

Cousins and Fringe (1964); Cawthorn and Molyneux (1986)	Field evidence	The Merensky Reef, the UG2 andLG6 chromitites and the Main Magnetite Layer can be correlated for >100 km of strike in both the Eastern and Western Limbs
Maier and Eales (1997)	Field relations	Pseudo Reef occurrence laterally over>30kmin the Western limb
Maier, Barnes and Groves (2013).	Petro graphic evidence and field relations	Multiple magma source and injection, Shallow depth of emplacement < 2-7km
ROOF AND FLOOR ROCK RELATION		
Cameron (1963); Lee (1981); Viljoen et. al. (1986a); Maier et. al.(2013)	Field observation	Presence of small folds and schlieren in mafic and ultramafic rocks of RLS
Viring and Cowell (1999); Maier et. al. (2001); Nex (2004)	Density contract	Anorthosite diapirs
Maier et. al. (2001); Viljoen et. al. (1986a); Nex (2004)		Feldspar stringlets and dykelets in chromitite seam
Lee (1981)	Field observation and petrographic studies	Post depositional structures in the RLS
Cawthorn (2013) and references therein.	Field relations and petrographic studies	Lateral variation of RLS roof contact. Presence of Roof or monzonitic zone. Presence of diapiric structures (Uken&Watkeys, 1997) and up-warp at the roof contact area.

Eales et. al.(1993)	Filed relations,	Floor rock folding exercised significant control on the thickness, distribution and lithology of the RLS
Sharpe (1981)	Field and petrographic studies	Eastern Bushveld floor rock contact and magma succession
Scoon (2002)		Large up-warps impinge on roof rocks
Mathez (2013)	Compositional analysis of Rooiberg felsites	The relationship between the RLS and overlying felsic rocks in the immediate roof to the RLS in the Eastern Bushveld is never Rooiberg lava, Rashoop Granophyre, or Nebo, but a locally occurring rock known as ‘‘leptite’’ e.g., von Gruenewaldt (1968, 1972), same rock is described as Monzonite by Cawthorn (2013).

CHAPTER 2 METHODOLOGY AND DATA SOURCES

2.0 INTRODUCTION

The first aspect of the study involved a literature review to gain knowledge about the general geology of the area, taking cognizance of the suitability and availability of data for the study and deciding on the appropriate methodology. In order to have a thorough understanding of surface geomorphology, structural and geologic patterns existing geological maps, Landsat 7ETM images (obtained from http://glovis.usgs.gov), Google Earth images, aeromagnetic data provided by the Council for Geoscience and 30m resolution ASTER and SRTM digital elevation data were acquired and studied. This aspect was followed by data selection, collection and subsequent analyses.

2.1 DATA COLLECTION

2.1.1 Borehole data

Borehole log data were obtained from the files of the Council for Geoscience (CGS) in Pretoria. Most of these borehole log records were obtained from private companies and are classified as proprietary data because the boreholes were drilled for exploration purposes and access to the data is restricted to the public. CGS has the permission to use the data internally for preparation of maps and reports and for research purposes. Prior to this study, very little work had been undertaken regarding digital capturing of borehole records, especially with regard to lithology and structure observed in the boreholes.

The goal of this research is to compile sufficient data to study the subsurface geometry of the RLS and its distribution within the Bushveld Complex and to create a geospatial database of all the borehole log data extracted for this study, which will help provide quick and easy access to such data on request to researchers. Several hundreds of borehole log data were captured; it was, however, beyond the scope of this research to capture all the available log data.

2.1.2 Software

Quite a number of sophisticated geological modelling packages are available for borehole data management and modelling, some requiring special training and expertise, while some are mainly GIS software with a 3D analyst extension. RockWorks® 15 software, a geo-modelling software package capable of analyzing geological data for easy management and visualization (available at CGS), was decided upon not only because of availability at CGS, but also because it is user-friendly, flexible and can incorporate many analytical tools that are rare to get in most single geo-modelling software and honours basic geological principles. It also has better graphic display capability and the ability to analyze and incorporate geophysical, geochemical, and geotechnical data with statistical and survey tools thus enabling better insight into the subsurface geometry. The software also offers import and export to a variety of formats for easy dissemination of output.

2.2 DATA SELECTION

Borehole log data at the Council for Geoscience in Pretoria exist in two forms. The first set is in analogue form, stored away in files and folders in cabinets while there is a Microsoft Excel record containing the location information of all the boreholes that are stored in cabinets. Search for borehole data was initiated by digitizing the available record on the digital map of the area in the Arc Map 10.1 environment for easy geographic search of boreholes, and in order to get a visual understanding of the spatial distribution and identify boreholes that intercept the Rustenburg Suite layers. This is due to varying positional accuracy of some of the boreholes from existing records: some boreholes were wrongly located and did not actually fall within the area of interest. Information on existing record includes: the map number, farm name, borehole ID, location and orientation information. This information was subsequently used to locate the borehole logs in the cabinet. The entire borehole log for each farm was carefully examined and compared with adjacent borehole information in order to determine and capture any slight variation or change in lithology to ensure that no detail is left out. Although the available borehole log data is enormous, not many are deeper than 500 m.

Data collection was done by assessing the log files stored in cabinets at the Council for Geoscience though not all the logs were available. The level of detail on the lithologic description and structural information on dykes, faults, etc. varied in most of the borehole records. However, known marker horizons were clearly indicated on most of the logs. This information was used in distinguishing the boundary of the RLS Zones. Some of the borehole cores are available at the CGS Core Library at Donkerhoek and a few of them were visually inspected and validated against the borehole record in order to become familiar with the different log descriptions. Since the boreholes were logged by different people and varying descriptions were used in describing different units, synchronization of lithologic descriptions of different borehole records was done in order to build a consistent dataset.

2.3 DATA CAPTURING

Prior to capturing pre-selected borehole records into a Microsoft Excel database, files containing the records were carefully examined and preference was given to borehole that penetrated more than one stratigraphic unit of RLS with a detail lithologic description.

All these data were later linked to the RockWorks® 15 software. The borehole database captured so far consists of five individual Excel files containing about 1200 individual borehole data well distributed over the entire the western, eastern, and Far-western limbs of the Bushveld Complex. Information included for each borehole is as follows:

- Borehole locations in longitude and latitude latter converted to Universal Transverse Mercator(UTM) meters
- Borehole name (unique identity for the borehole)
- Farm name where the borehole is located
- A district where the borehole is located
- Borehole ID (unique numbering code)
- Ground elevation of borehole (in meters)
- Total depth of hole (in meters)

- Borehole orientation (Inclination and direction of hole)
- Lithologic peak (measured depth to top of the first lithologic interval)
- Lithologic ending (measured depth to the base of the first lithologic interval)
- Down hole geology logs
- Lithological description

The data were categorized as follows:

- Location information: Consists of latitude and longitude of borehole location, borehole name and code, farm name, map reference of the borehole location, collar elevation, and ground elevation.
- Borehole orientation information: Consists of azimuth, inclination and down-hole direction of each borehole.
- Log information: Consists of top and base of each lithology intercepted and lithologic description.

2.4 DATA ANALYSIS

This involved importing data into the RockWorks 15®environment, conversion of Latitude/longitude to UTM meters and plotting of borehole location maps. This was followed by picking of the stratigraphic top and base. Only boreholes that sufficiently penetrate the top and base of each stratigraphic unit were included in this process. Major marker horizons that were clearly identified in the logs were utilized in grouping the lithologies into stratigraphic units (these include- the Pyroxenite Marker, Giant Mottled Anorthosite layer, Bastard Merensky Reef, the Merensky Reef, UG2 and UG1 layers, etc.). The stratigraphic classification was based on SACS (1980) classification scheme and on work of Coertze (1974), Molyneux(1974), Cameron(1978), Eales et al.(1993) Teigler and Eales (1992), Barnes and Maier(1999) and several unpublished mine reports on RLS and the BIC. Based on these previous studies, the base of the Upper Zone in this study was placed above the Pyroxenite Marker horizon while the base of Giant Mottled Anorthosite marks the base of the Main Zone and directly overlay the Bastard Merensky layer or the Merensky Pyroxenite. The Upper Critical Zone is identified by the appearance of the

Merensky Reef and chromitite layers. The Middle chromitite unit is marked by the presence of alternating norite/pyroxenite/anorthosite layers with chromitite layers and transforms to another cycle of pyroxenite and chromitite layers which define the Lower Critical Zone. Later intrusions occurring as dykes, pipes, boulders, etc. and other lithologies that could not be correlated or grouped with the major stratigraphic units occurring between the marker horizons were grouped as footwall to the overlying stratigraphic unit. A stratigraphic and lithology type table derived from lithological grouping is presented below:

Table 2.2: Borehole Downhole Lithostratigraphic Description

Serial no	Name	Description	Column stratigraphic
1	Overburden	Mostly soil, sand, clay or percussion drilled section	1
2	Post Bushveld (RLS)	Mostly Pilanesberg Complex rocks, Bushveld Granites and Granophyres	2
3	Upper Zone	Magnetite layers occurring mostly with gabbro/ anorthosite	3
4	Main Zone	Gabbro, norites, anorthosite, pyroxenite	4
5	Bastard Merensky Reef		5
6	Bastard Merensky Footwall (BMR)	Lithologies occurring between the BMR and the MR	6
7	Merensky Reef (MR)		7
8	Merensky Footwall unit (MR FW)	Lithologies occurring between the MR and the UG2 (when the Pseudo Reef is absent)	8
9	Platreef		9
10	Platreef footwall	Metasediments, granites (unclassified), Archaean granites and gneisses.	10
11	Pseudo Reef		11
12	Pseudo Reef Footwall	Lithologies occurring between the Pseudo reef and the UG2	12
13	UG2	chromitite layers	13

14	UG2 Footwall	Lithologies occurring between theUG2 and UG1	14
15	UG1	Chromitite layers	15
16	UG1 Footwall Unit	Lithologies occurring between theUG2 and UG1	16
17	Middle Group Chromitite (MG)	chromitite layers with pyroxenites (MG4-MG0)	17
18	Middle Group Chromitite FW	Lithologies occurring between the MG and LG	18
19	Lower Group Chromitite (LG)	chromitite, harzburgite, pyroxenite (LG7-LG1)	19
20	Lower Group Chromitite FW	Lithologies occurring between the LG1 and Lower zone	20
21	Lower Zone	Pyroxenite, harzburgite and dunite.	21
22	Marginal Zone	Mostly norite	22
23	Pre-Bushveld/Transvaal Supergroup	Metasediments belonging to the Pretoria Group/ Transvaal Supergroup	23
24	Archaean Granite	Archaean granites and gneisses	24

2.5 METHODS AVAILABLE FOR PROCESSING BOREHOLE DATA

RockWorks 15® software used for this study operates on a set of embedded algorithms that make use of borehole coordinates, depth at the top of each well, total depth (which is the true vertical depth of vertical wells), measured depth (for inclined or deviated well) and borehole orientation detail to calculate the true XYZ location. These data were adjusted to UTM meters with Zone 35 as central meridian and WGS-84 as datum specified. Different methods for processing the acquired data were implemented and the purpose for each is discussed below.

2.5.1 Structure contours for representing subsurface geometry

The use of the correct mapping method is essential for accurate and reasonable subsurface interpretation. The concept of utilizing structure contours to illustrate the geometry of the subsurface initiated from the work of Benjamin Smith Lyman (1870) as reported by Zieglar

(2005) (http://www.aapg.org/explorer/2005/03mar/lyman.cfm). This method of studying topographical relief with the use of topographic contours was adopted to examine the disposition of subsurface rock units with the use of structure contours. Structure contours connect points with the same elevation on a geological surface; they are also oriented parallel to the strike direction of the rock contact and are assumed to be straight (without undulation especially for a horizontal or sub-horizontal horizon) before tectonic movement (Groshong, 2006). Once the structure contours of a particular horizon is accurately determined, altitudes of other horizons above or below it are determined by adding or subtracting the distances above or below it respectively. Each stratigraphic horizon was mapped separately to create 3D stack which is essential for 3D modelling.

In essence, the ability to adequately verify the fitness of interpretation at multiple stratigraphic horizons will improve the level of confidence in the interpretation of the subsurface geology and confirm the geological suitability of the applied technique (Tearpock and Bischke, 2002). Horizontal or sub-horizontal horizons are expected to show straight contour lines. However, when the contour lines are disrupted it is assumed that tectonic movement caused the dislocation and components of dislocation can be measured directly from structure contours. This is very useful in detecting structures at the subsurface (Evenick, 2008; Mossop and Shetsen, 1994). Structure contour maps are generated by gridding with interpolation methods that help transform spatially distributed borehole log data into continuous data that can easily be modelled in 3D.

2.5.1.1 Gridding of top and base of stratigraphic units

Grid interpolators available in RockWorks® (a detailed discussion on this is given below) were used to generate contours for the top and base of each stratigraphic unit. These contour lines are termed structure contours, connecting points with the same elevation on a lithologic/stratigraphic contact or surface. They are equivalent to strike lines because they trend parallel to the strike of the surface and illustrate the shape of structures and patterns of outcrop at the subsurface. The program estimates strike and dip direction by computing changes in elevation between grid nodes to determine uphill and downhill direction. Structure contour maps of the selected stratigraphic units were generated with the

Automatic Kriging interpolation method, which allows the program to select the best variogram for gridding the input data. However, variogram tests were carried out to ascertain if the automatic Kriging method was actually the best choice.

The Triangulated Irregular Network (TIN) method available in the RockWorks Utility platform was utilized for data verification and to check for selected interpolation methods. This is because the result of the TIN method is usually close to hand-drawn contours and data integrity is preserved (because the computation honours all data values) and high accuracy is maintained. However, RockWorks does not allow 3D computation and isopach map production with this method.

Isopach maps show 3D variation in thickness of a stratigraphic unit. Stratigraphic thickness is generally influenced by subsurface structure, geology and post-emplacement erosion. Interval isopach maps were generated by first determining the top and basal contact of each stratigraphic unit, gridding the surface elevation of each and subtracting the lower contact elevation from the upper or top elevation taking the orientation of each well and collar elevation into consideration.

Interpolation techniques such as Kriging, trend surface residual, inverse distance and trend polynomial were used to generate structure contour and isopach maps. The Kriging technique was useful because it calculates unknown variables from measured points and gives account of accuracy or suitability; it is also useful in identifying directional trend patterns across data points.

Trend surface residual method is equally useful in differentiating between regional and local (residual) trend, by computing different polynomial trends, and fitting measured data to the computed data to determine the best fit. The trend surface polynomial method has special relevance in determining the regional trends in the input data. Different orders of trend surface polynomial were used to generate structure contour and thickness maps. Interval isopach and structural maps were stacked separately to show their approximate structural position relative to each other, and to illustrate time sequence patterns representing the structural or the tectonic history of each stratigraphic unit and thickness variation between each stratigraphic unit.

Interpretation of structure contours is based on the following assumptions adopted from Groshong (2006) and references therein.

- Same or similar patterns on successive intervals can be used to confirm the presence or otherwise of a geologic feature such as faults, folds, basin, etc.
- Surface fluctuations on structure contour maps are caused by displacement since undisturbed surfaces are supposed to be smooth.
- The stress condition that modified the present-day geometry is regional.
- Similar geometries are formed by similar processes and can be classified as such.
- Prevalent outcrop orientation on structure contours might be related to the stress or pressure condition at the time of rock emplacement.

Problems associated with fault movement are easily overcome by determining piercing points and slip motion using structure contours (Huerta and Rodgers, 1996; Xu et al., 2004; Barclay et al., 1990). At the initial stage of structure contouring, the contours are usually without fault trace. Presence of faults on structure contour maps could be detected from contour geometry during interpretation, which is usually smoothly curved or may show gentle undulation when a fault is present. The exact location of faults is confirmed by mapping and interpreting closely spaced contours on successive stratigraphic unit intervals and correlating across the two sides of the suspected faults. Surface undulations are usually aligned in the fault slip direction as reported by Groshong (2006).

2.5.2 Isopach generated from structure contour map

Structure contour maps for the top and base of each stratigraphic unit were constructed using Inverse Distance, Kriging, and Trend Surface Residual interpolation methods. Necessary precautions were taken to avoid data clustering and redundancy, which could affect the interpolation result. The Decluster point option was used to decluster points with multiple entries. The High Fidelity option was also pre-selected to ensure that the contours generated honour the control points. The thickness of each stratigraphic interval was then computed by subtracting the structure contours grid at the base of each stratigraphic unit from structure contour grids at the top using the grid-grid math option under arithmetic operations. Isopach maps were generated for each stratigraphic unit represented by

perpendicular measurement taken from the top and base of structure contours in the dip direction using grid calculation mathematics within the RockWorks environment, thus giving the true stratigraphic thickness (TST). Consequently, the resultant grid maps were imported to the Global Mapper12 software.

True stratigraphic thickness is the distance between the top and bottom of a stratigraphic unit measured perpendicular to the unit. Measured thickness in a vertical well is the true vertical thickness otherwise known as TVT and is different from the thickness measured in an inclined or deviated well. Thickness variation on isopach maps were used for fault detection since thickness will normally change along a fault trace (Hintze, 1971). Assuming the two surfaces were originally subhorizontal, an isopach map would reveal the total structural movement of the top surface when the lower surface was undisturbed (Lee and Merriam, 1954).

2.5.3 Structural feature identification

Fault displacement on structure contours were detected using the bow-and-arrow rule given by Elliott (1976). This method is used to separate a marker horizon into footwall and hanging wall. However, offset of structure contours were used to detect fault motion on structure contour maps and fault slips were subsequently calculated since subsurface fault slip cannot be directly observed on a structure contour map (Xu et al., 2004).

Profiles were drawn across the stratigraphic interval structure contour map to show the shape of the stratigraphic unit along the profile line. These maps are also scale dependent and choice of map scales and contour interval (used to generate maps in this study) were critically considered during this investigation. Choice of contour interval was carefully moderated such that the selected interval is small enough to show structures of interest. Small contour intervals were selected for areas with low dips (areas with low relief).

Profiles were drawn across the interval structure and isopach maps in the Global Mapper ™ software environment. These profiles form the framework for the interpretation of the subsurface geometry and structure because it adequately defines the subsurface geometry, thus making it easy to detect subtle changes along structure contours and measure fault slip

displacement (Gibson et al., 1989). Profiles drawn on each structure contours makes visualization and measurement of fault and fold components easy. Areas with subtle relief or geometries with small dips were emphasized using vertical exaggeration. This has helped to:

- Emphasise subtle changes in relief,
- Make subsurface geometry more obvious and show small features.

The layered mafic rocks of the Bushveld Complex were deposited as sills with low relief (Cawthorn, 2012). In order to draw conclusions on the dynamics and possible mechanism of emplacement of each stratigraphic unit, the interval structure contour pattern as well as the thickness pattern was investigated. Any deviation from the normal horizontal layering is assumed to be caused by deformation, which could be classified as either syn- or post-magmatic depending on the stratigraphical units affected. Subsequent chapters will focus on a discussion of the structure contour map of each stratigraphic interval in the RLS. The emphasis is to take a close look at local geologic features represented on the structure contour and to study the geometry of features by drawing profiles across structure contour intervals and isopach maps.

2.5.4 Trend Surface Analysis

Structure and thickness residual maps were derived by subtracting trend surface grid orders from structure contour grid data. Positive residual values indicate that the vertical location of a pick is higher in elevation than the calculated trend surface while negative values show that the calculated surface is lower than the lowest surface trend.

This method is useful in separating regional trends from the residual trend; it also helps to identify small or local displacements and other small-scale structures that were previously masked by the regional trend. In order to measure the error in the interpolation method, the residuals from the first order to the sixth order were mapped out and examined where the trend surface was predicted at a higher or lower value than the actual measured data. Residual maps are essential because they represent the best data set that could be obtained in the field (Evenick, 2008).

Interval structure and thickness maps are presented in order to identify the correlation between structure and thickness as well as structural time sequence developmental patterns. This in essence will provide evidence for the progressive change in emplacement controls during accumulation and provide useful information on the deformation that pre- or post-dates the emplacement and those that are synchronous with the multistage emplacement.

Diagrams showing depth-to-top of each stratigraphic unit were created by subtracting the stratigraphic top grid of each unit from an ASTER DEM of the study area. Isopachs of specific stratigraphic units were hanged from the surface elevationto get the present day geometry of the unit. 3D path profiles were drawn across the structure and isopach maps to visualize the subsurface geometry.

2.5.6 3D modelling and visualization

Visualization is essential in interpretation and characterization of geologic features. 3D visualization diagrams in the form of 3D grid models, stratigraphic solid models, isosurfaces, fence diagrams, structure and isopach stacks, strip log, and surface maps were generated to enhance the understanding of the subsurface and for interpretation purposes. Visualization of subsurface lithostratigraphic relations and structural features within the first few hundreds of meters will be of tremendous economic benefit in mineral exploration and in making inferences about Paleo-geometry and present day geometry of the subsurface.

Modelling horizons at shallow depths is more accurate than modelling horizons at deeper depths since more boreholes will penetrate horizons at shallower depth than deeper depths (Lemon and Jones, 2003). 3D solid modelling was done by defining the project boundary and creating multiple-layered interval structure contour and isopach grid models defining the top and base of each stratigraphic unit along with the thickness. The contact between the units is defined based on input stratigraphic order designed on a stratigraphic-type datasheet in RockWorks Borehole Manager. The program automatically selects boreholes that fully penetrate the stratigraphic units to define the top and base of the unit (note that a minimum number of boreholes are required to define the top and base of the unit). This may limit the number of boreholes to only those that fully penetrate each of the

stratigraphic units while the gaps between the selected boreholes are interpolated with a pre-defined interpolation method. However, it is also possible to modify the top and base to be used in defining the contact if additional information such as geophysical logs is available. Lower units are given priority when the Onlap option is checked, this instructs the program to build models from the base upward and modify the model when a unit is missing (this option is used for fixing units that extend below the base of a lower unit).

2.5.7 Borehole database creation

Prior to data analysis with RockWorks all the borehole log data were imported from Excel spreadsheets into the Borehole Manager platform in RockWorks where they are stored in Microsoft Access-compatible database or MDB file. Each project has anMDB file assigned as the project folder and contains all the information about each borehole, including the location, lithology, stratigraphy, borehole orientation, grid files, 3D models and all information pertaining to the project. This ensures data validation (same unit and format for borehole location data) and helps maintain rational integrity by linking information on related tables and for building queries. The database allows for incorporation of geochemical, geophysical and geotechnical measurements and observations.

A geo-database was also created with the ArcCatalogue for the borehole logs for easy access to the database since ArcGIS is widely available. Point feature classes were created since they are the main component of our borehole data. Different columns were used to store the attribute data, borehole coordinates, farm names, top and base of each lithology unit, lithological description, etc. The existing digitized geological map of South Africa at a scale of1: 1 000 000 (Keyser et al., 1997) was incorporated into the database.

2.6 OVERVIEW OF INTERPOLATION METHODS

Interpolation is a process of estimating values for unmeasured points that fall between measured points (deKemp, 2000; Li and Heap, 2011). Spatial interpolation is a process of calculating values for unknown data points from a set of known data points that are distributed across an area (Lunardi, 2009). The principle of spatial interpolation is based

on the first law of geography formulated by Tobler, (1970) which states that everything is related to everything, but near things are more related than distant things.

Each interpolation method is based on different assumptions. The choice of interpolation method depends on many factors, but the appropriate technique must simulate minute changes in measured parameter, an idea of the real world knowledge about variation patterns of the measured parameter will assist in making an appropriate choice. A good number of interpolation methods offered by RockWorks® 15 include; Closest point, Cumulative, Directional Weighting, Distance to Point, Inverse-Distance, Kriging, Multiple Linear Regression, Sample Density, Trend Surface Polynomial, Trend Surface Residual and Hybrid. Ultimately, different interpolation methods were tried for this study and the results compared before choosing three of the methods for detail computational analysis and final interpretation. This choice was based on close geological plausible trends that correlate well with known geology.

All interpolation methods are estimation methods that operate on a set of algorithms; each with its merits and demerits. A short review of each spatial interpolation method is given by Li and Heap (2008) and in the summary below. Interpolation algorithms give average values of what is being estimated leading to underestimation of high values and overestimation of low values in the result (Bohling, 2005).

2.6.1 CLASSIFICATION OF SPATIAL INTERPOLATION METHODS

- **Global and Local**

The spatial interpolation methods can be categorized into global or local methods. These are two basic techniques of approximating a regular grid of points from scattered observations.

Global methods use all input data of the region of interest to calculate or estimate values at unknown points in order to capture the general trend. Local methods use only the

information that is within the vicinity of the point being estimated and capture the local or short-range variation (Burrough and McDonnell, 1998).

- **Exact and inexact**

Exact interpolation methods honour all data points on which the interpolation is based, i.e. the estimated value is the same as the measured value. In-exact methods do not necessarily make use of the exact value of measured points or do not pass through all the sample points, so the predicted value of such points is not the same as with observed values (Burrough and McDonnell, 1998). The exact technique is suitable for high quality datasets.

- **Stochastic and Deterministic**

Stochastic methods calculate or estimate unknown points without previous assumption of pattern variation and provide information about possible errors. Deterministic methods give estimates for unknown points based on assumptions of pattern variation, but do not provide information about associated errors (Li and Heap, 2008).

- **Gradual and Abrupt method**

Methods that produce a smooth and continuous gradual surface are termed Gradual methods. Methods that produce a small, discreet and abrupt surface are called abrupt methods.

- **Geostatistical and non-Geostatistical method**

Geostatistical methods usually employ both mathematical and statistical functions to predict and estimate values at un-sampled points and also provide probabilistic estimates of the quality of interpolation based on spatial autocorrelation of data input (Li and Heap, 2008).

2.6.2 KRIGING INTERPOLATION METHOD

The Kriging method is a local, exact, stochastic and Geostatistical method of interpolation that makes use of a least-square regression algorithm developed by Krige (1951).

Geostatistical interpolators such as Kriging can be used to describe spatial patterns and the calculation of variables at unmeasured points and to estimate surfaces. Advantages of Kriging include: ability to compensate for data clustering by treating clustered data as a single point, versatile in identifying geometry, patterns and trends in irregularly spaced data makes available error estimates which helps improve confidence in the estimated result (Goovaerts, 1997; Bohling, 2005). In this study, different variogram models were tested and compared with the Automatic mode, which gave the best variogram model. Consequently, all subsequent models are based on Automatic Kriging.

There are different types of Kriging and each has its unique features which make it useful for geological analysis, the underlining difference is the way the mean values are determined and utilized during the interpolation process (Wackernagel, 1995; Chambers et al., 2000). Clark and Harper (2001) give assumptions and essential Kriging equations. Kriging interpolation methods include: Simple Kriging (not adaptable for local trend modelling), Ordinary Kriging (use local mean for re-estimation), co-Kriging, Ordinary Kriging (a standard method without a pre-assumed trend of input data), Universal Kriging (assume an overriding trend in the input data) Block Kriging, Factorial Kriging and Dual Kriging. Details on each Kriging method and the equations can be found at http://www.nuim.ie/staff/dpringle/gis/gis09.pdf and in Appendix 1. For multivariable modelling different types of co-Kriging can be applied.

2.6.3 TREND SURFACE ANALYSIS METHOD

This is a global, inexact, stochastic and deterministic method of interpolation, originally used for modelling depths of stratigraphic horizon. It makes use of geographic coordinates in predicting values for un-sampled points by using least squares regression to fit a polynomial surface on control points. It is useful in separating local trends from regional trend. Local or residual trends give information about local variations (Collins and Bolstad, 1996). Residual patterns are the product of multiple linear regressions. Model validation depends on the distribution of data. Clustering of data often introduces distortion in Trend

Surface Analysis, but this is overcome if there are control points outside of the cluster, which might provide useful regional information for geologic interpretation (Davis, 1973).

The Trend Surface Analysis method is essential in computing closer to field scale data and regional trends by the polynomial development of geographic coordinates of control points using a least square method in determining the coefficient of polynomial expansion (Evenick et al., 2008; Unwin, 2009) especially in area with low relief such as the study area. It can also be used as a tool in separating a regional map component from local fluctuations. Larger scale structures are expressed in the trend component, while the small scale structures are expressed in the local fluctuation component, i.e. residual (Davis, 1973; Wren, 1973; Wharton, 1993; Davis, 2002). This method is widely used in studying the geometry and structural pattern in areas where a change in relief pattern between successive stratigraphic units can be related to structural movements (Davis, 1986; Salvador and Riccomini, 1995).

Agterberg (1984) warned against heavy reliance on statistical test and confidence belts which can be exerted only if the residuals are stochastically independent. Moreover, geologic correlation based on the interpreter's background knowledge is a better test of fitness and validity.

The Trend Surface Analysis method shows the best results in both regional and local analysis of structural features (Davis, 1973; Davis, 1986, 2002). Mei (2009) introduced an improved method of Trend Surface Analysis that allows for more geological control on a local-fit procedure with the option of choosing the number of neighbouring points. With recent improvements in computer programming other options exist, such as the high fidelity option (which utilizes a recursive algorithm to grid the residual repeatedly in order to ensure that the cumulative error drops below the threshold), the declustering, logarithmic and power options that help in exercising geological control on data interpretation. The resultant residual thickness and structural maps are void of secondary factors such as compaction during deposition and paleo-bathymetry of involving strata and can be related directly to illustrate similarities between the original deformation and later deformation structures by accentuating important local anomalies. Some of the results show variation

in trend with increasing polynomial order. The Trend Surface Residual technique has been applied to demonstrate its use in identification of blind structures and trends in areas with adequate, well data and limited seismic information (Evenick et al., 2008).

2.6.4 INVERSE DISTANT METHOD

This is an interpolation method that makes use of a distance-based weighting technique to assign relevance to data points; the closer a point is, the more relevant it is in determining the value of the nearest data point. It is an exact and deterministic method of interpolation. Major drawbacks include the generation of bull's eye contours around observing positions within a grid. Spatial distribution of data is considered when applying the distance weighting parameter to data points (Lu and Wong, 2008). The power setting was adjusted to increase or decrease the influence of distant sample points over the interpolated points. Lowering the power setting will reduce the influence of sample points that are far away and thus enhance the regional trend to produce a smooth surface while an increase in the power setting results in the more localized output.

CHAPTER 3 DOWNHOLE LITHO-STRATIGRAPHIC VARIATION ACROSS FARMS

3.1 INTRODUCTION

This chapter will focus on the lithostratigraphic distribution and correlation of the major sub-divisions of each unit from borehole log data. The chapter highlights the different lithologies that make up different stratigraphic units at different locations and correlates stratigraphy across farms. Strip log and hole-to-hole sections were employed in describing stratigraphic variation along profiles while 3D models were used to illustrate the features and geometry formed as a result of lateral stratigraphic correlation. Figure 3.1 shows the aerial view of borehole distribution across the Bushveld Complex.

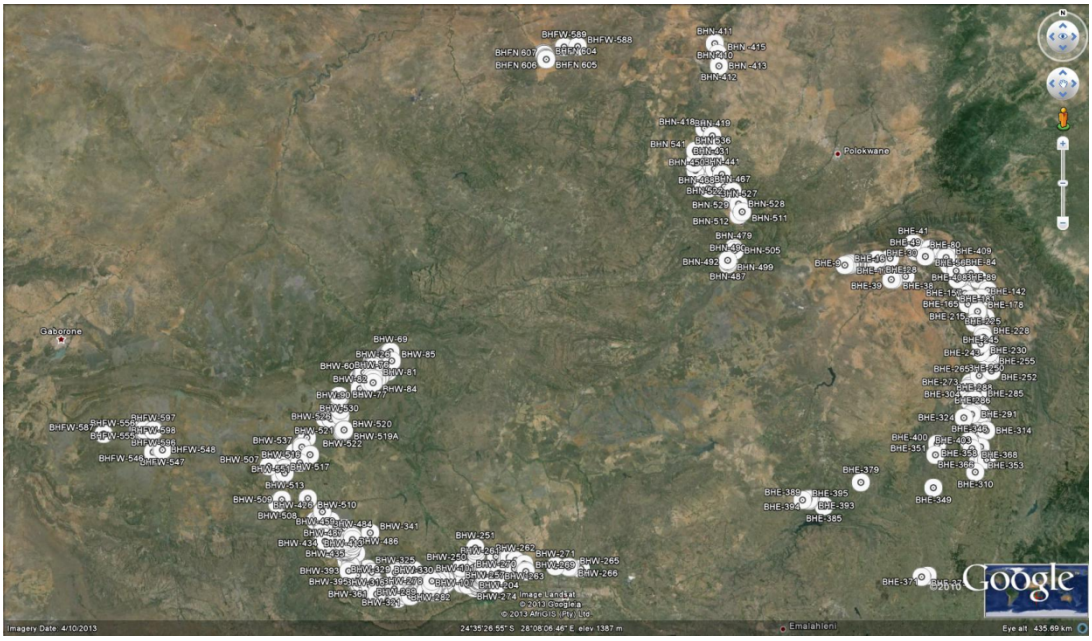

Figure 3.1: Borehole locations overlain on a Google image.

3.2 THE WESTERN BUSHVELD

The Western Bushveld with its conspicuous layering spans from the northeastern edge of the Crocodile River fault (south of Thabazimbi through the Pilanesberg Complex) to east

of Brits as shown in Figure 3.2. The RLS outcrop occurrence has been grouped into sections. The Northam and the Union section are situated in the northern parts of the Pilanesberg Complex. The Impala, Rustenburg and Wolhuterskop section occur south of Pilanesberg and west of the Brits area, while the Schietfontein section occurs at the Eastern side of the Brits. The Pilanesberg Complex occurs almost midway through the Western Bushveld. For the purpose of this discussion, the Western Bushveld is sub-divided into the Northwestern Bushveld, central parts of the Western Bushveld and Southwestern Bushveld. The Far Western Bushveld is also included in the discussion.

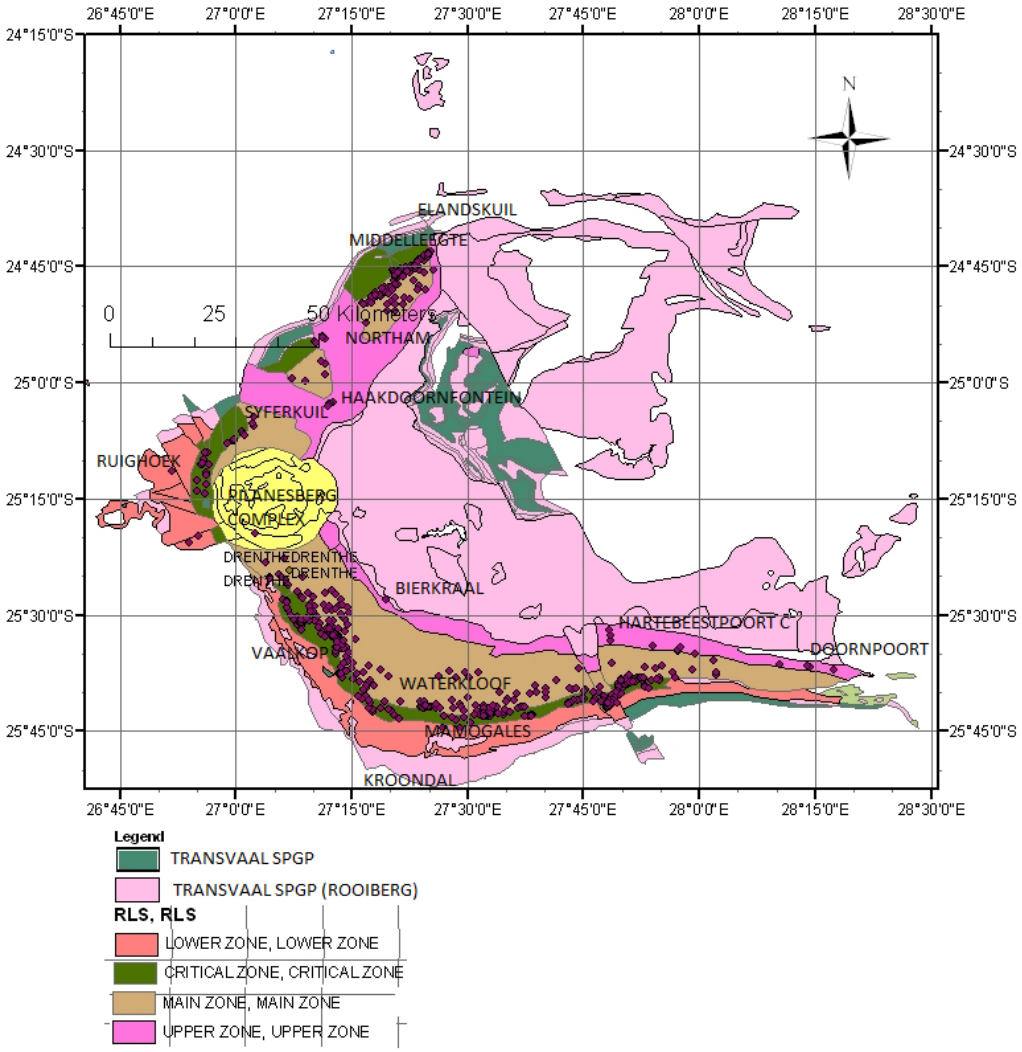

Figure 3.2: Geologic map of the Western Bushveld with farm names and borehole locations.

3.2.1 NORTHWESTERN BUSHVELD

This is the area north of the Pilanesberg Complex to the northeastern end of the Crocodile River fault representing an area of about 70 km.[2] The area is divided into the Amandelbult section and the Union section (see Figure 3.3).

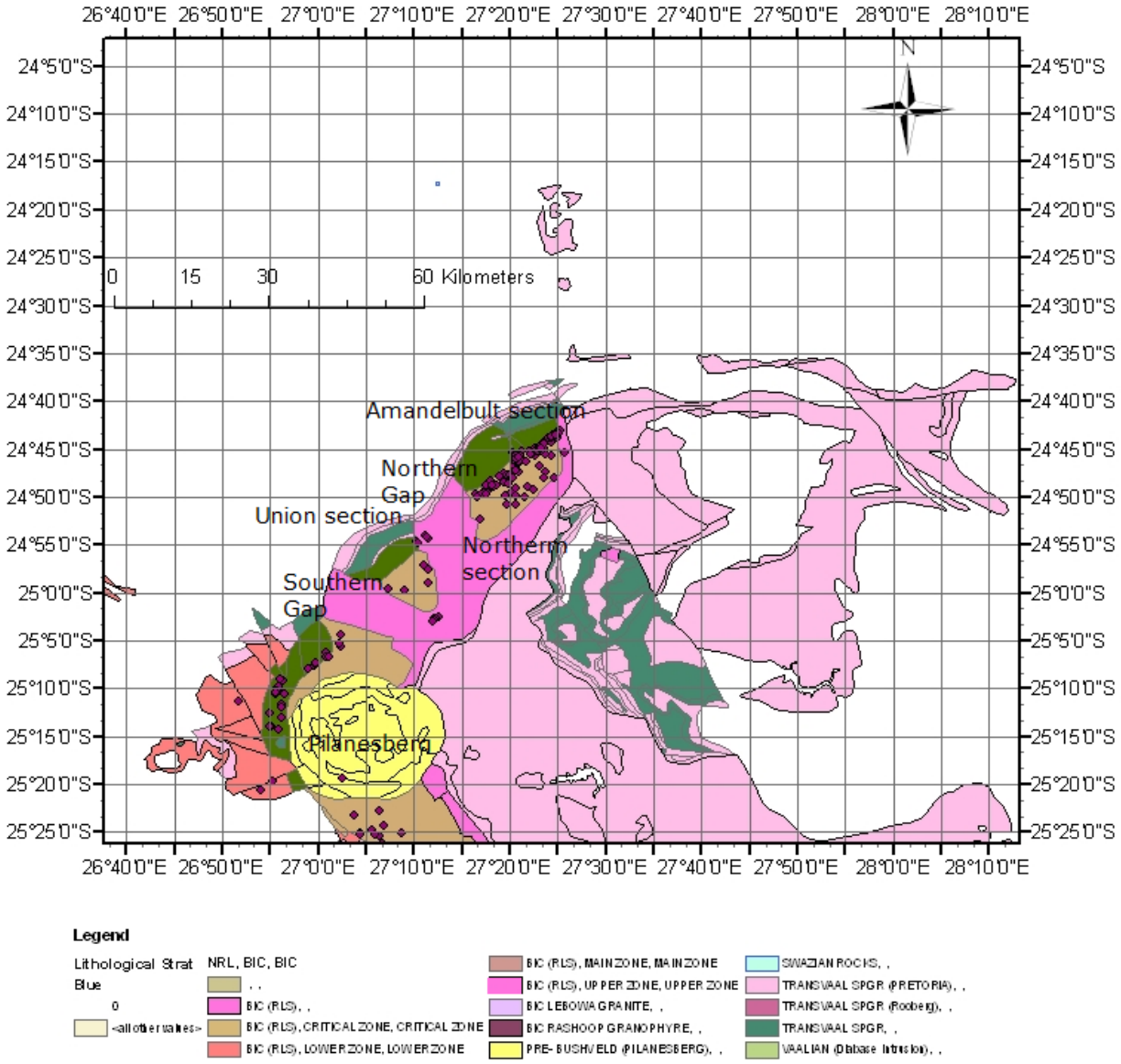

Figure 3.3: Geologic map of Northwestern Bushveld Complex showing the main sections mentioned in the text with the Amandelbult section at the northeastern edge and part of the Pilanesberg Complex in the south.

3.2.1.1 Amandelbult Section

This section strikes southeast and cover distances of about 20 km, prominent farms in the area from the north are: Haakdoorndrift, Elandskuil, Middellaagte, Amandelbult, Schildpadnest, and Elandsfontein. From the southwest: Kaalvlakte, Zondereinde, Kopje Alleen, Middeldrift, Elandskuil, and Grootkuil as shown in Figure 3.3. From borehole lithologic records the area is occupied by rocks of the RLS and is tabular at the surface. The Upper Zone and Main Zone form the topmost units in the area and are madeup of a thick succession of homogeneous rocks which directly overlies the critical zone while the UG2 units are overlain by Pseudo reef.

The Main Zone is characterized by a thick succession of gabbro/norite with minor occurrences of anorthosite and pyroxenite. The ratio of norite and gabbro varies laterally across the area while chromitite and magnetite are absent from this stratigraphic unit. The Main Zone usually directly overlies the Bastard Merensky unit or the Merensky Pyroxenite. The Main Zone thickness increases southward in the middle of this section with a thickness of over 2000 m. The mottled anorthosite marker horizon is prominent from borehole lithologic records on farm Zondereinde, Kopje Alleen, Grootkuil, Middeldrift and Kaalvlavkte, all occurring south of the Amandelbult section. The Bastard Merensky seems to be replaced by pyroxenite to the north of these farms. Mottled anorthosite directly overlays the Bastard Merensky unit and the Merensky unit at these farms and minor intrusives are also very common. The pyroxenite marker horizon is only well defined in a few of the boreholes in this section. Each separate layer in the 3D model is a stratigraphic unit characterized by the unique cumulate composition. The 3D model of the area reveals a featureless surface. The thickness of the feldspathic rocks (norites, anorthosite and pyroxenites) in the UG2-Merensky interval increases gradually from 36 m in the southwestern to 45 m in the northwestern part of this section.

The entire 20 km stretch of this section is marked by downward-dipping transgression of all the stratigraphic units as indicated in Figures 3.4, 3.5and 3.6. The Merensky Reef unit exposure is shallow in the north and deepens at a depth of 50 m around Middellaagte in the north, to about 2400m at Zondereinde farm in a step-like fashion. Mining operations occur

over the entire section in a down-dip direction, with different mining companies exploring the reefs at different depths.

Figure 3.4: Diagram showing borehole interception of different stratigraphic units in a down-dip direction with corresponding location indicated on Main Zone interval structural map draped with geologic contacts of the Amandelbult section of Western Bushveld.

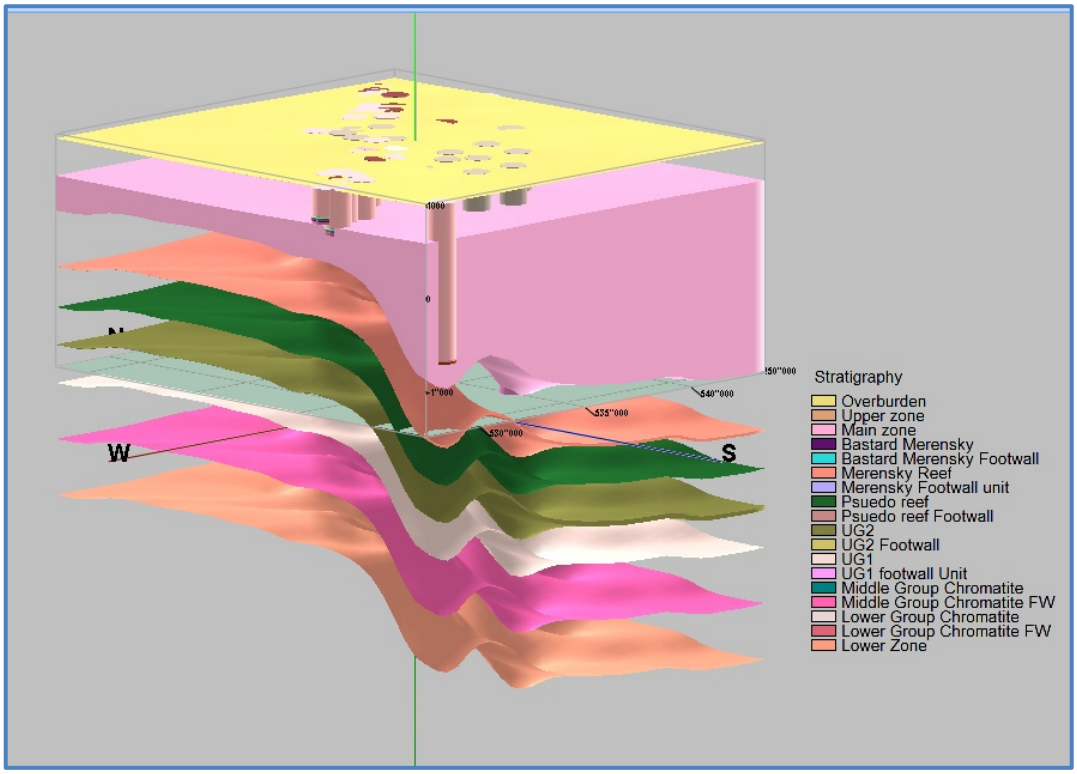

Figure 3.5: Exploded 3D Model of the Amandelbult section (some of the stratigraphic units were exempted for clarity)

The structure is about 3 km wide in the northern part and the width increases downwards to the south. The structure is confined between the base of the Main Zone and the Lower Zone but does not extend to the surface. The western limb of the structure shows a throw of about 700m, while the Eastern limb is about 500m down. Figures 3.6 and 3.7 shows a graben shape at the central part of the Amandelbult section.

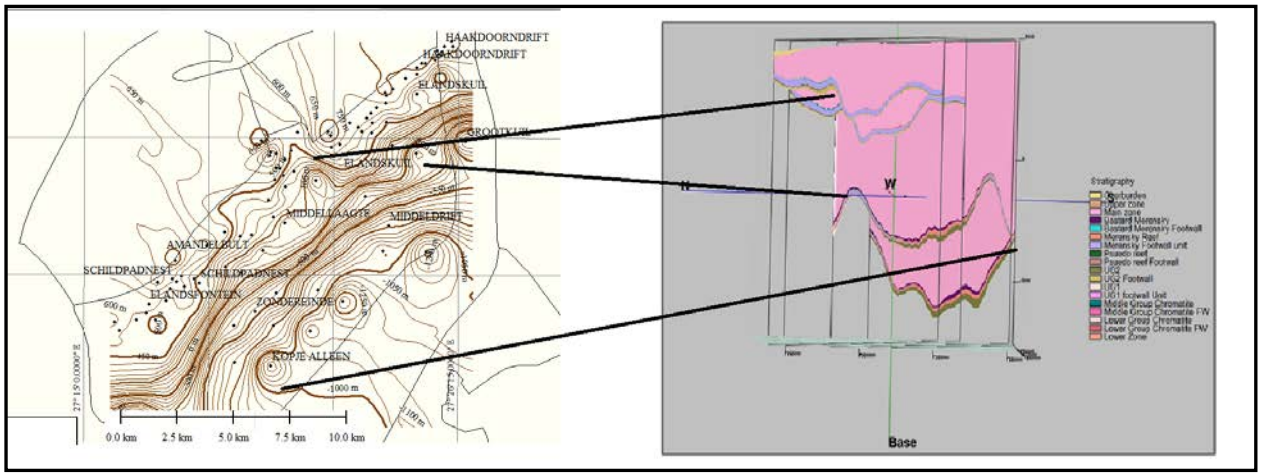

Figure 3.6: Diagram of Amandelbult section showing the different levels of the stratigraphic horizon on the structure contour map and stratigraphic fence.

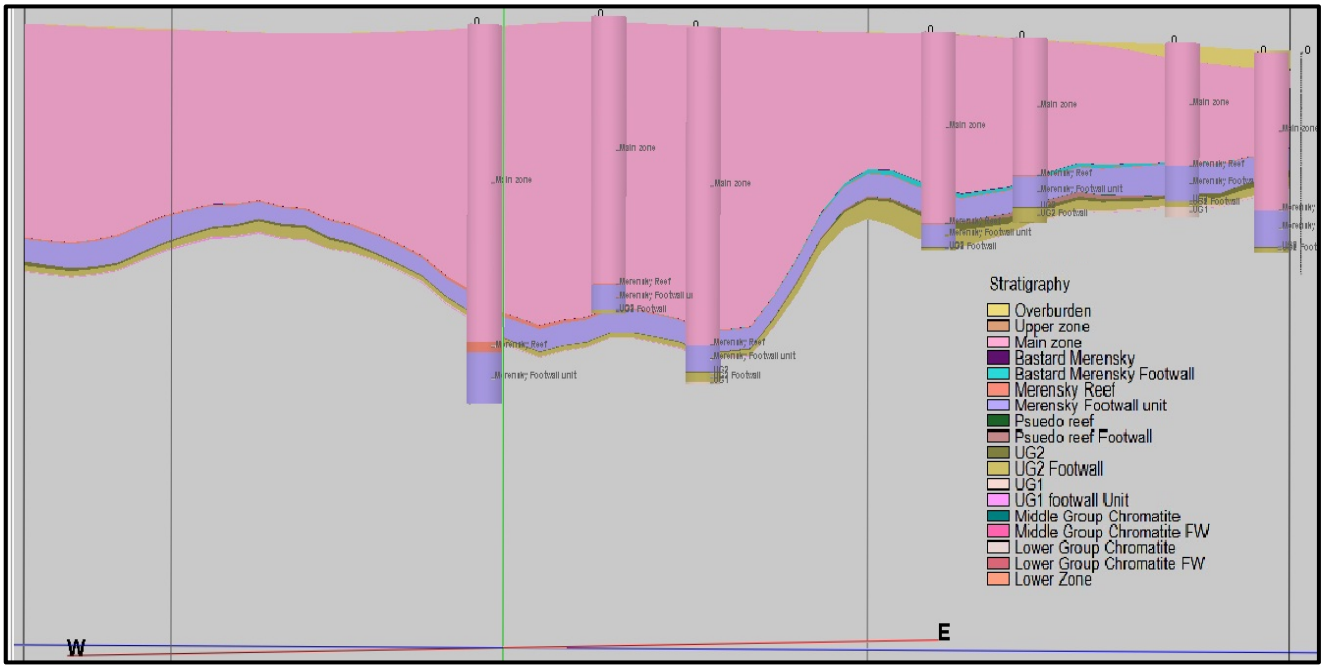

Figure 3.7: Section with few borehole strip log in Amandabult section of northwestern Bushveld

3.2.1.2 UNION SECTION

The Union section is located at the western side of the Amandelbult section and the Northern gap separates these two sections with an average distance of about 11km. The Union section is an extension of the RLS layers at the Amandelbult section with a thick succession of the Main Zone gabbronorites. Farms represented in the area include Haakdoorn, Spitskop, Syferkuil, Haakdoornfontein and Zwartklip as shown in Figure 3.3. For example, the thickness of the feldspathic rocks in the UG2- Merensky Reef interval in this section is about 30m, while it is about 20m at Amandelbult section. A thick succession of mottled anorthosite is present at Spitskop and Haakdoorn farms. The Upper Zone occurs in the central part of the section and at the boundary. Pseudo Merensky Reef is not reported in this section.

3.2.1.3 GAP AREAS BETWEEN AMANDELBULT AND UNION SECTION

Two gap areas have been identified in Northwestern Bushveld Complex by Wilson et al. (1994), Reid and Basson(2002),and Smith and Basson (2006). The first is known as the Northern gap that separates the Amandelbult section from the Union section with a distance of about 11km. Slopes that dip towards the Amandelbult section mark this area. The other gap area is the Southern gap area and exists between the Union section and southeastern fringes of the Pilanesberg Complex. The Northern and Southern gap areas are characterized by the presence of the Upper Zone rocks. Although there is limited borehole information in the Southern gap area, the model reveals a gradual increase in elevation from the southwest to northeast, interrupted by the presence of domes and a small basin structure (see Figures 3.8 and 3.9).

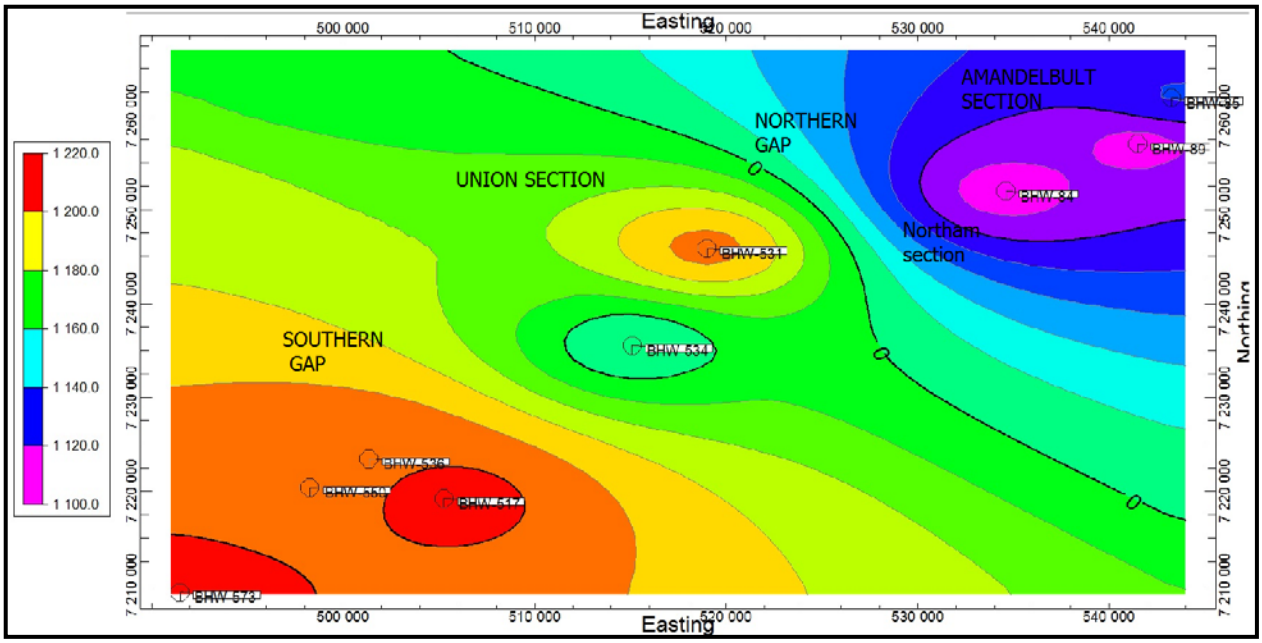

Figure 3.8: Presence of isolated local dome structure on grid model of Northwestern Bushveld.

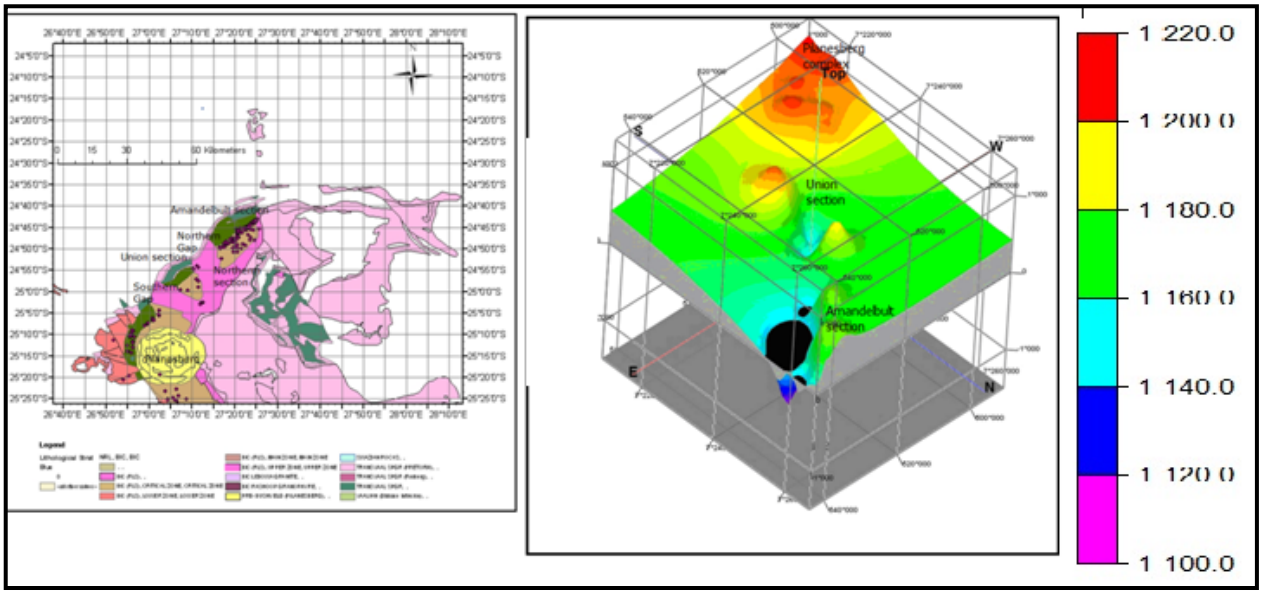

Figure 3.9: 3D grid model of the Northwestern Bushveld Complex, with the gradual slope to the NE.

3.2.2 OTHER FEATURES

Path profiles were drawn across the top of the Amandelbult section for each stratigraphic interval to gain knowledge of the geometry of the area. From the base of the Main Zone, the result shows a wide basin-like structure with a depression at the centre. The shape of

the structure on the lower Critical Zone and the Lower Zone interval changes to a basin-like structure with minor intersections. This structure is missing in the Upper Zone and Marginal Zone intervals.

3.2.3 DESCRIPTION OF EACH ZONE IN THE NORTHWESTERN BUSHVELD

A. UPPER ZONE

The Upper Zone overlies the Main Zone with mostly gabbro intersections. It is more prominent in the Northern gap area and southwestern part of the Northwestern Bushveld, but is not underlain by the Main Zone rocks in some boreholes. From borehole records, the Upper Zone is present as magnetite pipes and minor intersections at the eastern section of the Northwestern Bushveld.

B. MAIN ZONE

The Main Zone has a general southward dip. Hence, the zone thickens southwards. The Pyroxenite Marker Zone is not present in all the boreholes. The mottled anorthosite is prominent in the southern part of the section, while the upper parts (or pyramid gabbro) are dominated by the presence of gabbro/norite, anorthosite and pyroxenite layers.

C. CRITICAL ZONE

The Critical Zone is rather missing in the gap areas. However, the zone thickens toward the east of the Union section. The Lower Group Chromitite layer is exposed close to the surface in the west. The level of the Merensky zone varies sporadically from one borehole to another.

3.2.4 Regional 3D model of the Northwestern Bushveld

The regional trend in the Northwestern Bushveld is NE-SW. The region dips towards the southeast, interrupted by the presence of an isolated domes and basin-like structures around the Union section. Hence, the rocks thicken southeastwards, and the deepest depth

occurs at the Eastern end. Consequently, gap areas developed over floor rock high or occupy the structural high areas. On the contour map, Northern and Southern gap areas are represented by NE-SW trending contours that gradually slope toward the east (Amandelbult section). The thickness of the Critical Zone interval also increases eastwards.

3.3 THE CENTRAL PARTS OF WESTERN BUSHVELD

This section describes the area in the central parts of the Western Bushveld, starting from the northern fringes of the Pilanesberg Complex to the southwestern parts of the Brits section covering about 100 km in the distance. The area host the Ruighoek section, the Boshoek section and the Rustenburg section. The regional stratigraphic strike is NNW-SSE.

Prominent farms in the area include:Waterval, Waterkloof, Paardekraal, August Mokgatles, Wildebeestfontein, Town and Townlands, Vaalkop, Kookfontein, Styldrift, Frischewaagd, Bon Accord stock, Goedgedacht, Vlakfontein, Turffontein, Boschhoek, etc. The Main Zone thickness varies sporadically in this area. The Middle and Lower Critical Zones are well developed in the western and southwestern parts of the Pilanesberg Complex. However, there are several intrusions and faulting but the Upper Zone rocks are not common in this area. Very few borehole records are available in the Pilanesberg Complex. The Main Zone is virtually missing in this area, but it is well developed at the northern parts (towards the southern gap area) and southwards. The area is also very much intruded by dykes of various compositions while the Marginal Zone is extensively developed especially at Vlakfontein farm. The Middle Critical Zone is well-developed on most farms while the Upper and Lower Critical Zones are well-developed at Waterval, Kroondal, August Mokgatles and Styldrift farms while Pre-Bushveld rocks occurring as quartzite are common in this area as reported in the borehole logs.

The abrupt termination of some of the stratigraphic units on the southeastern part of the Pilanesberg Complex was noticed on the model and strip log. The Main Zone is also well

developed to the immediate south of the Pilanesberg while the Critical Zone started with Bastard Merensky and consists of mostly anorthosite.

3.4 SOUTHWESTERN BUSHVELD

This area extends from the western fringes of Brits to NNE of Pretoria and covers a distance of about 90km. The area hosts the Marikana section and the Brits section. Farms in the area include: Brakspruit, Buffelsfontein, Bokfontein, Roodekopjes, Mamogales, Schaapkraal, Hartebeestpoort, Uitvalgrond, Zandfontein, Hoekfontein, Klipfontein, Sjambokzijn, Oudekraal, De Onderstepoort, De Kroon and Krokodildrift.

The regional outcrop trend is east-west. The Main Zone and Middle Critical Zone are well developed in the west while the Upper Zone rocks are well developed around the Brits graben. The thickness of the Upper Zone varies from 2m towards the end of the Rustenburg section to about 14 m around the Brits section. The Upper Zone rocks dominate the Eastern end of the Brits section.

3.5 THE FAR WESTERN BUSHVELD

The Far Western Bushveld section (also known as the Nietverdiend sector) is located about 45 km away from the Pilanesberg Complex, and covers a horizontal distance of approximately 50km. The lithologies in the area are basically pyroxenite and chromitite (these lithologies were grouped as the Lower Critical Zone) surrounded completely by a thick layer of Marginal unit (aureole). A profile from this sector to Pilanesberg Complex shows that the two areas are separated by a depression. Outcrop trend is NNW-SSE. Figure 3.10 shows a grid model of the Nietverdiend sector and the main Western Bushveld Complex. Farms located in the area include: Draalaaigte, Strydfontein, and Rooderand farms. Few borehole records are available for this area.

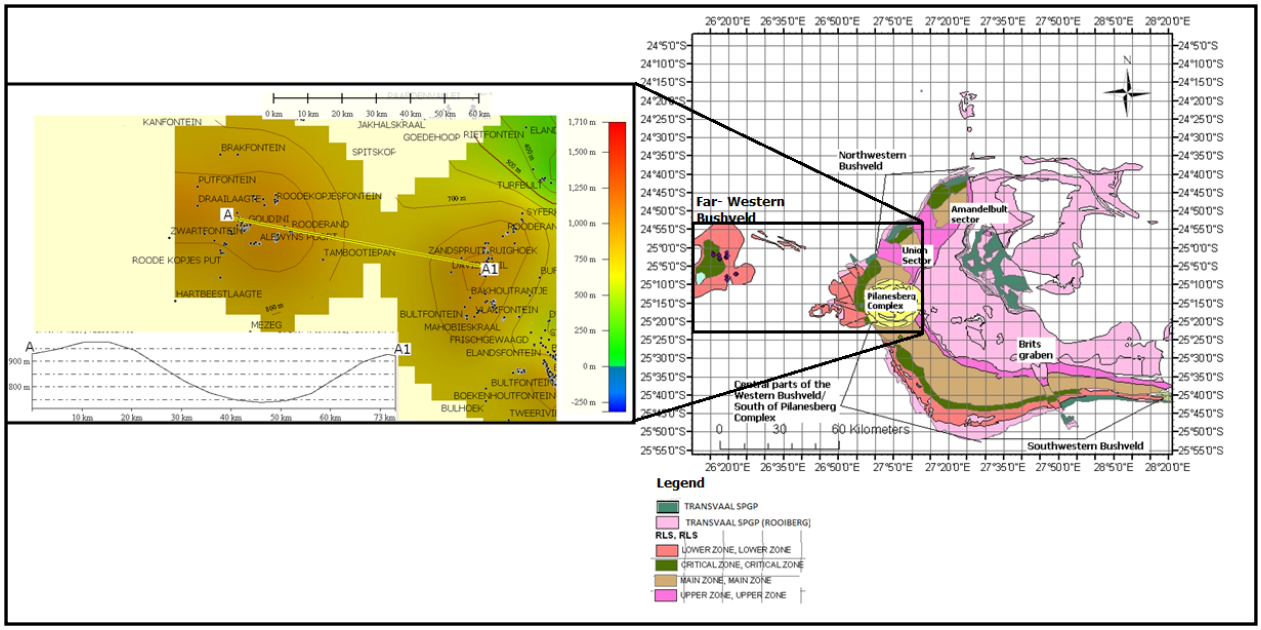

Figure 3.10: Far Western Bushveld and Pilanesberg Complex grid model showing the link between the two areas on the Main zone structural interval.

3.6 THE EASTERN BUSHVELD

The Eastern Bushveld Complex spans from Lebowakgomo area in the Northeastern Bushveld through Penge, Burgersfort, Lydenburg to Middelburg in the south. The Main Zone in the Eastern Bushveld reaches a thickness of approximately 1600m at Belvedere in Lydenburg. Figure 3.11 shows the geologic map of the Eastern Bushveld with the farm names. At Voorspoed farm in the northeastern Bushveld, the Main Zone is made up of mainly gabbronorite, pyroxenites and anorthosites. On Doornvlei farm the composition changes to an intercalation of norite and anorthosites while at Middelpunt farm the succession changes to gabbro, anorthosite and norite and continues up to Umkoanesstad farm where some pyroxenite layers were reported.

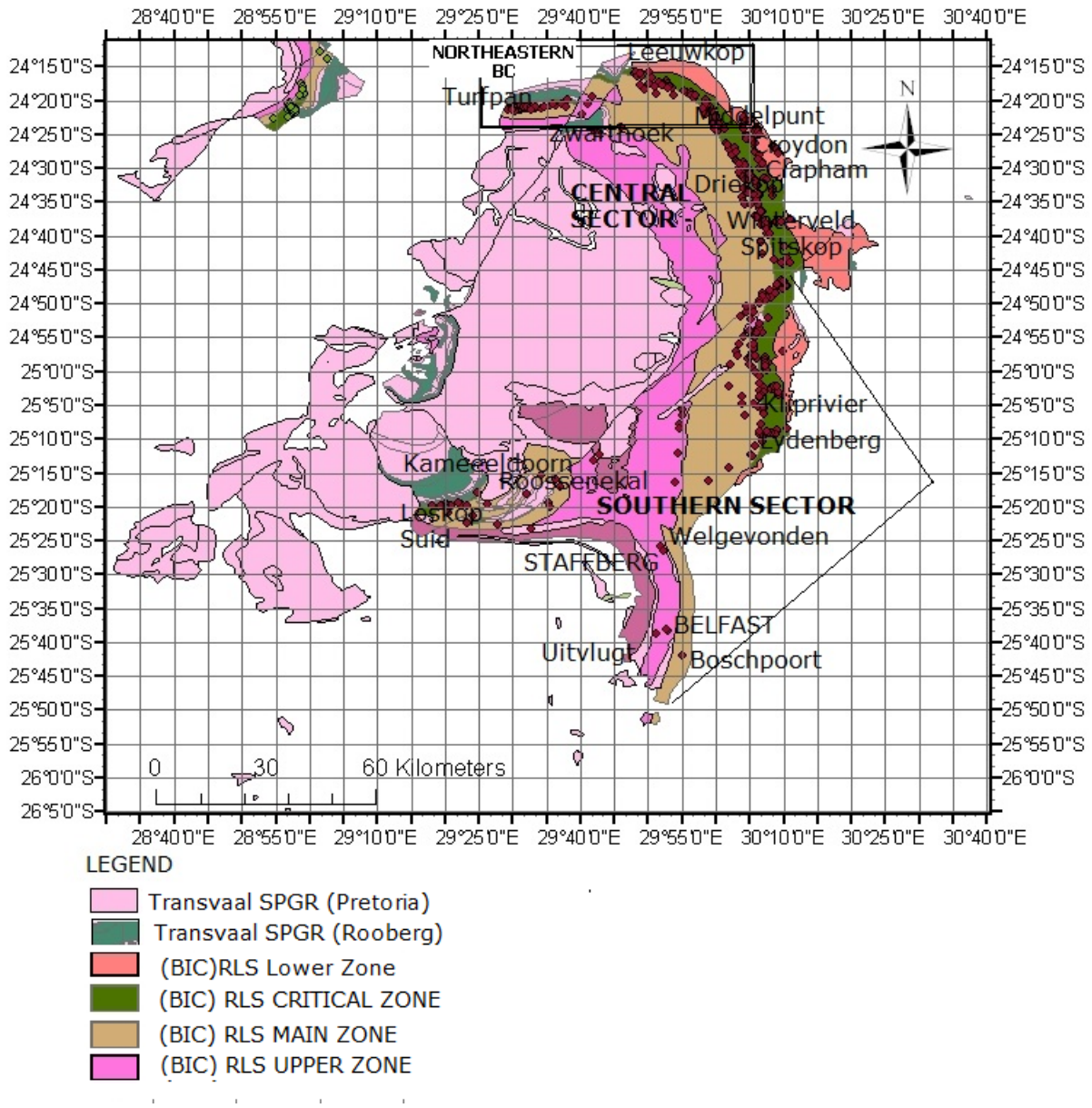

Figure 3.11: Geologic map of the Eastern Bushveld Complex showing some of the major lithostratigraphic units and farm names mentioned in the text (modified after the Geological map of South Africa (1: 1,000,000 scale) from the Council for Geosciences (1997).

3.7 THE NORTHEASTERN BUSHVELD

The Northeastern Bushveld extends for 18km west of the Wonderkop fault (Doornvlei section) in the Lebowakgomo area, and covers an additional length of approximately 45km east of the Wonderkop fault (Jagdlust-Winterveld section), all occurring at the southeastern

part of TML in the Eastern Bushveld Complex. Some of the farms in the area are:Voorspoed, Turfpan, Doornvlei, Mphatlele location, Zwarthoek, Eerste Regtees, Diamond, Middelpunt, Brakfontein and Umkoanesstad.

The Main Zone in this area consists of gabbronorite, anorthosite and pyroxenite while the pyroxenite marker and mottled anorthosite marker horizon can be correlated from one borehole to another. The Merensky Reef unit is very close to the surface in this area with a depth of less than 15m from the surface at Voorspoed.

3.8 CENTRAL PART OF THE EASTERN BUSHVELD

This area marks the northern and southern parts of the Steelpoort fault. Along the central part of this fault the level of Merensky Reef is deep, reaching a depth of approximately 1700m at Belvedere farm. To the south and north of this sector the Merensky Reef occurs at very shallow depth of less than 100m while at Booysendal farm it occurs at less than 4m from the surface. The Critical Zone is exposed at the surface in some places with chromitite layers covered with just a thin layer of norite or pyroxenite for instance at Zeekoegat, southeast of the Wonderkop fault. The deepest depth recorded for the Merensky Reef is about 1254m around Middelpunt farm in Lydenburg. The immediate west of the Wonderkop fault is characterized mainly by rocks of the Upper Zone however, about 8000m from here the Critical Zone reaches a depth of about 2500m. The Upper Zone rocks occur on the western side of this area. The UG2- Merensky Reef interval varies from 2m to well over 200m. The Marginal Zone is well developed at Kameeldoorn, southeast of the Dennilton Dome and around Groblersdal area. Elevation increased from Blaauwbank to Mapochsgronde.

3.9 SOUTHEASTERN BUSHVELD

This area is marked by a gradual increase in ground elevation from the Mapochsgronde farm to the central part of the southeastern sector with a depression in-between. Figure 3.11 shows the profile across the Far western and western parts of the Southeastern Bushveld, the centre of the depression marks the location of the Laersdrift fault that separates the two

sections and represents two NNE-SSW trending isolated hills. Widespread occurrence of Upper Zone rocks dominates this sector.

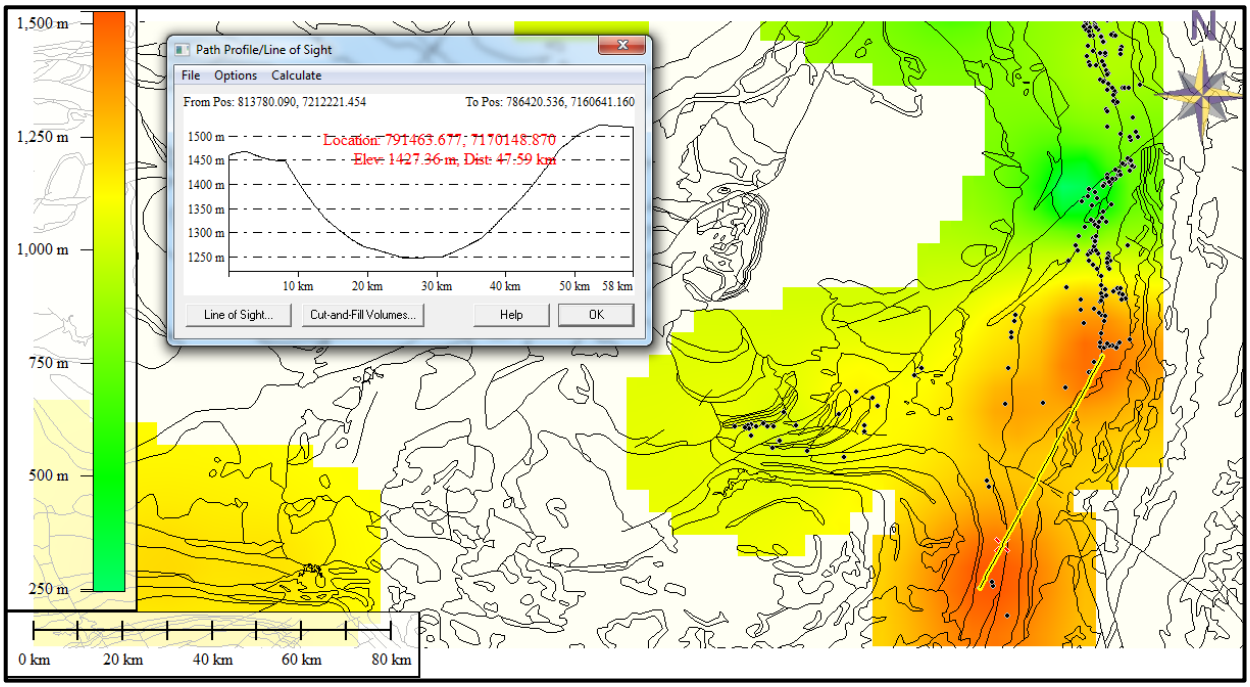

Figure 3.12: Superimposed grid model on geological contact to show the Laersdrift Fault at the southern part of the Eastern Bushveld. Small dots indicate the borehole locations used for the model.

3.10 THE NORTHERN BUSHVELD

The Northern Bushveld Complex consists of the Potgietersrus limb (see Figure 3.13) and the Villa Nora sector or Northwestern sector (Van der Merwe, 1978), a subdivision based on outcrop distribution. The Potgietersrus Limb is divided into a northern sector; central sector and southern sector. The sequence in the Potgietersrus region shows a conspicuous north-south trend with an outcrop length of about 120km. It is truncated in the south by the Zebediela Fault and in the north by the Melinda fault. Prominent RLS rocks in this area are:the Lower Zone, the Critical Zone, the Main Zone and the Upper Zone. The Lower Zone is well developed in the southern sector on Jaagbaan, Grasvally and Volspruit farm south of the Potgietersrus limb with a thickness of over 1400m. The Upper Zone is best represented in the northern sector where it rests on Archaean granites. The Upper Zone is also present on Harriets Wish, Aurora, Elandsfontein, Gezond and Witrivier. The Platreef is overlain by Main and Upper Zones. The Platreef is more concentrated in the central

sector of the limb. The Main Zone consists of norites, anorthosites and pyroxenites. The Merensky Reef and The Upper Critical Zone are well developed in the southern parts of the Potgietersrus limb while the Marginal Zone is not so conspicuous, but is present in the Grasvally area.

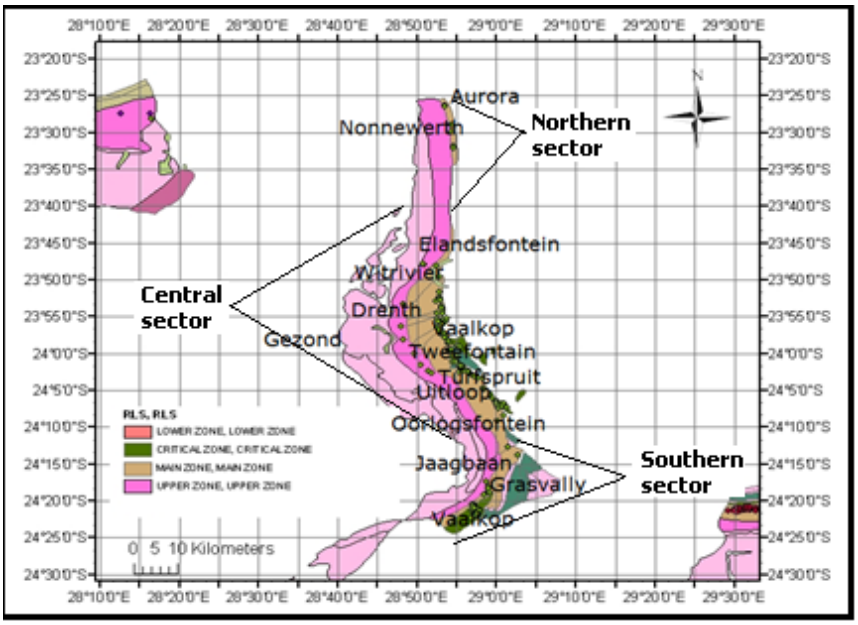

Figure 3.13: Geological map of the Northern Bushveld Complex with farm names.

A. The Northern Sector of Potgietersrus limb

The Platreef is absent for over a distance of 10 km south of Nonnenwerth, where the Upper zone is well developed and lies directly on the floor rock. It consists of gabbro, norite and magnetite. In farm Harriets Wish the Upper Zone lies directly on the Archaean granite floor rock and extends to Elandsfontein farm. On Aurora, a sequence of pegmatitic gabbro and magnetite lies on basal hornfels, however at the Drenthe area sequence of pyroxenite, norites and melanorites together lies on granitic floor rock. The Marginal Zone in the area consists of norites, hornfels and metasediments. The Platreef lies between the Main Zone and Archaean granite floor rocks. The floor rock in this sector varies from granite, gneisses to Archaean granite.

The Platreef rests mostly on the Archaean rocks in this sector as shown on Figure 3.14.

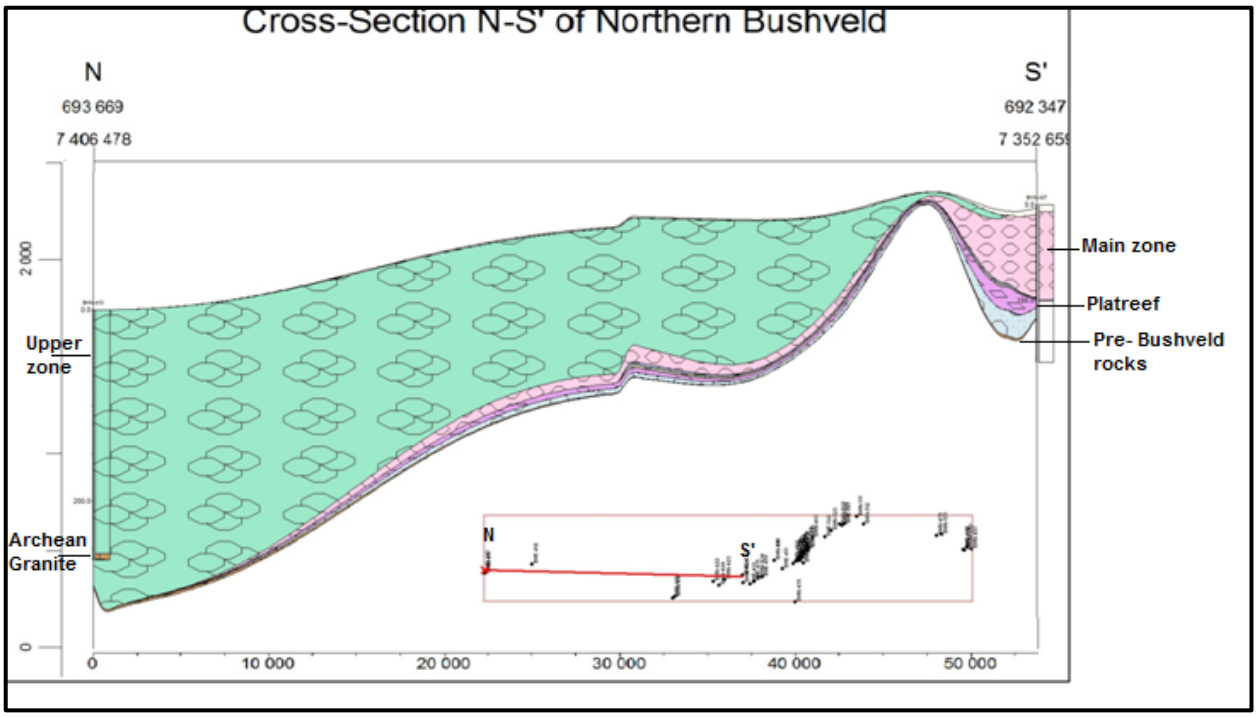

Figure 3.14: Cross-section of northern sector of the Northern Bushveld Complex.Give the legend of nature of rocks

B. The Central sector

The Platreef is overlain by the Main Zone and the Upper Zone. The Main Zone is dominated by gabbronorites, anorthosites, norites and pyroxenites. The Main Zone rests directly on metadolomite on Dorstland farm. The meta-carbonate floor rock continues to Sandsloot and Zwartfontein farms. At Overysel farm the Platreef is well developed with Platreef and its footwall reaching a thickness of over 200 m. Interaction between the lower Platreef and the Marginal Zone hornfels is very pronounced on Overysel, Tweefontein and Turfspruit farms. Metasediments occur sporadically towards the base of the Main Zone and Platreef sequence in the area. Floor rock of granite is also common. The Upper Zone is characterized by gabbro/norite and magnetitite, this unit is present on Elandsfontein, Witrivier and Gezond farm. The Platreef rests mostly on Transvaal Supergroup rocks at the central sector. At the central sector the Platreef is characterized by pyroxenite whiles serpentinite forms part of the Main Zone at Uitloop, Merensky Reef was reported at Vaalkop. The Marginal Zone occurring as hornfels is very extensive in this sector reaching a thickness of more than 100m on some farms.

C. The Southern sector

The Ysterberg-Planknek fault cuts across the southern sector. The sector is characterized by the presence of well-developed Lower Zone especially on Grasvally 293KR and Zoetveld 294KR. The Lower Zone is overlain by the Platreef, and consists of pyroxenite, serpentinites, harzburgite and chromites, the Main Zone and the Critical Zone overly the Lower Zone of over 600 m thick. The Lower Zone is common on Volspruit, Grasvally and Turfspruit farms. The Main Zone consists of gabbro, anorthosites and norites while the Platreef is made up of pyroxenite with variable proportions of norites, gabbros, serpentinite and meta-sediments. The Critical Zone consists of chromitites of the Upper and Lower Groups. The Marginal Zone is made up of hornfels with norites. Quartzite interference that is common on Uitloop farms is missing in this area. The top of this sequence is made up of xenoliths. The floor rock in this sector is mostly quartzite. On Grasvally farm a sequence of norite-pyroxenite-anorthosite with chromitite characterizes the Platreef reef while at Turfspruit and Rietfontein the Platreef is made up of pyroxenites, melanorites, pegmatitic pyroxenites with interference of metadolomites and hornfels. The Merensky Reef and the Upper Critical Zone (similar to the Western and Eastern Bushveld sequence) occur only in this sector, along with the Platreef that is common to the limb. Figure 3.15 and 3.16 illustrate the geometry of the Northern Bushveld Complex across the different sectors with fence diagrams and model of the Northern Bushveld Complex.

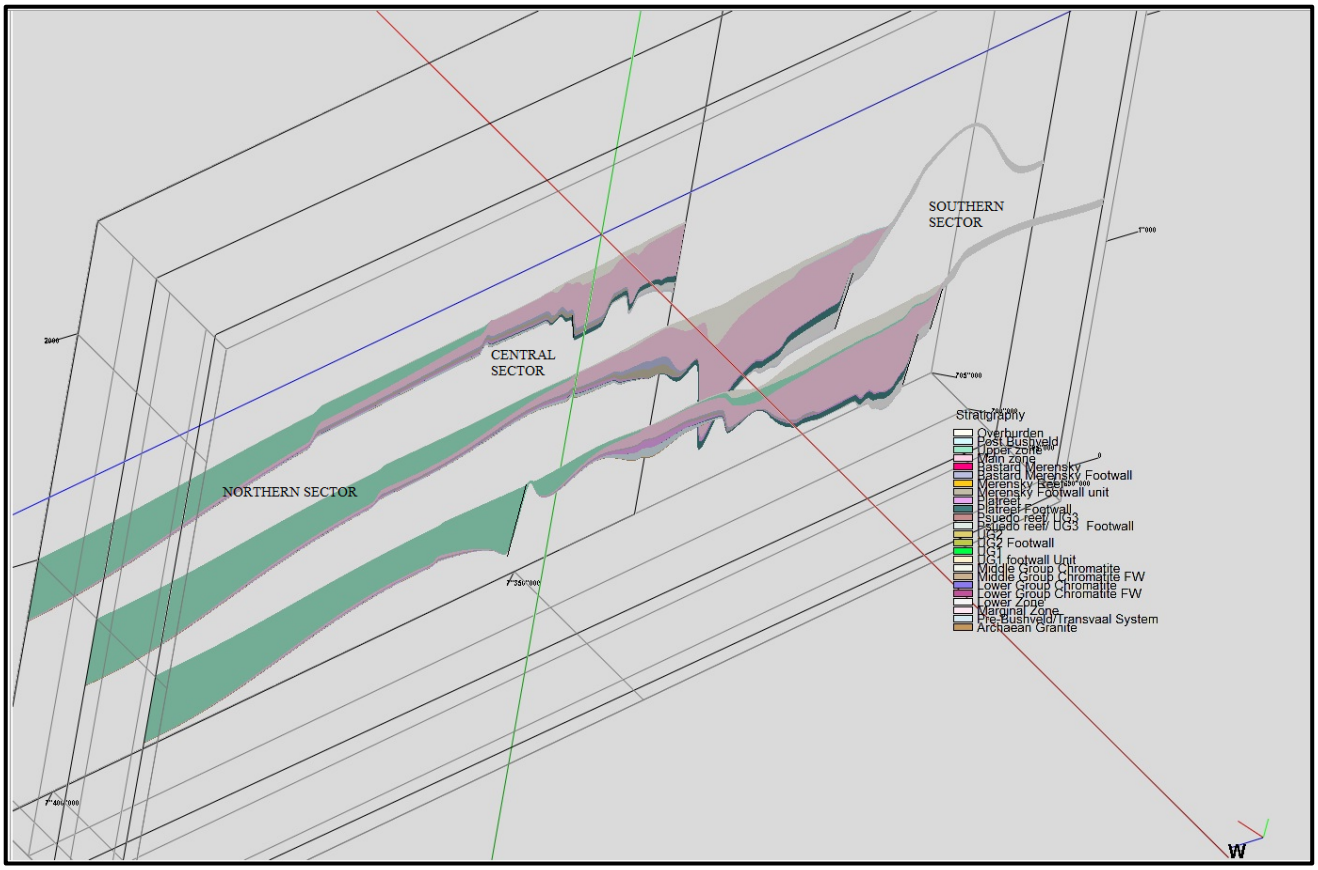

Figure 3.15: Fence diagram of the Northern Bushveld Complex.

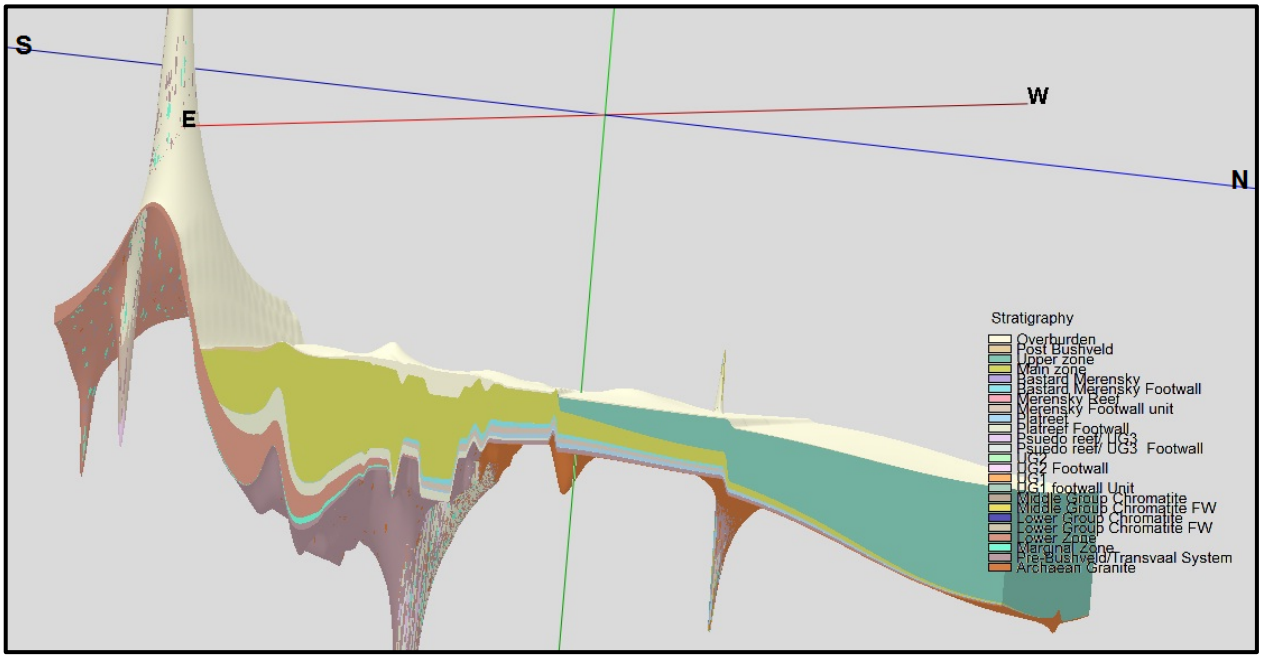

Figure 3.16: 3D model of the Northern Bushveld Complex showing the geometry of the area (Vertical exaggeration is 40).

3.11 VILLA-NORA SECTOR OR NORTHWESTERN SECTOR

This fragment is located about 56km west of the Potgietersrus limb and covers a distance of 35 km (see Fig.3.17). The regional strike is east-west and the main lithologies are gabbro, norites and anorthosite of the Main Zone.

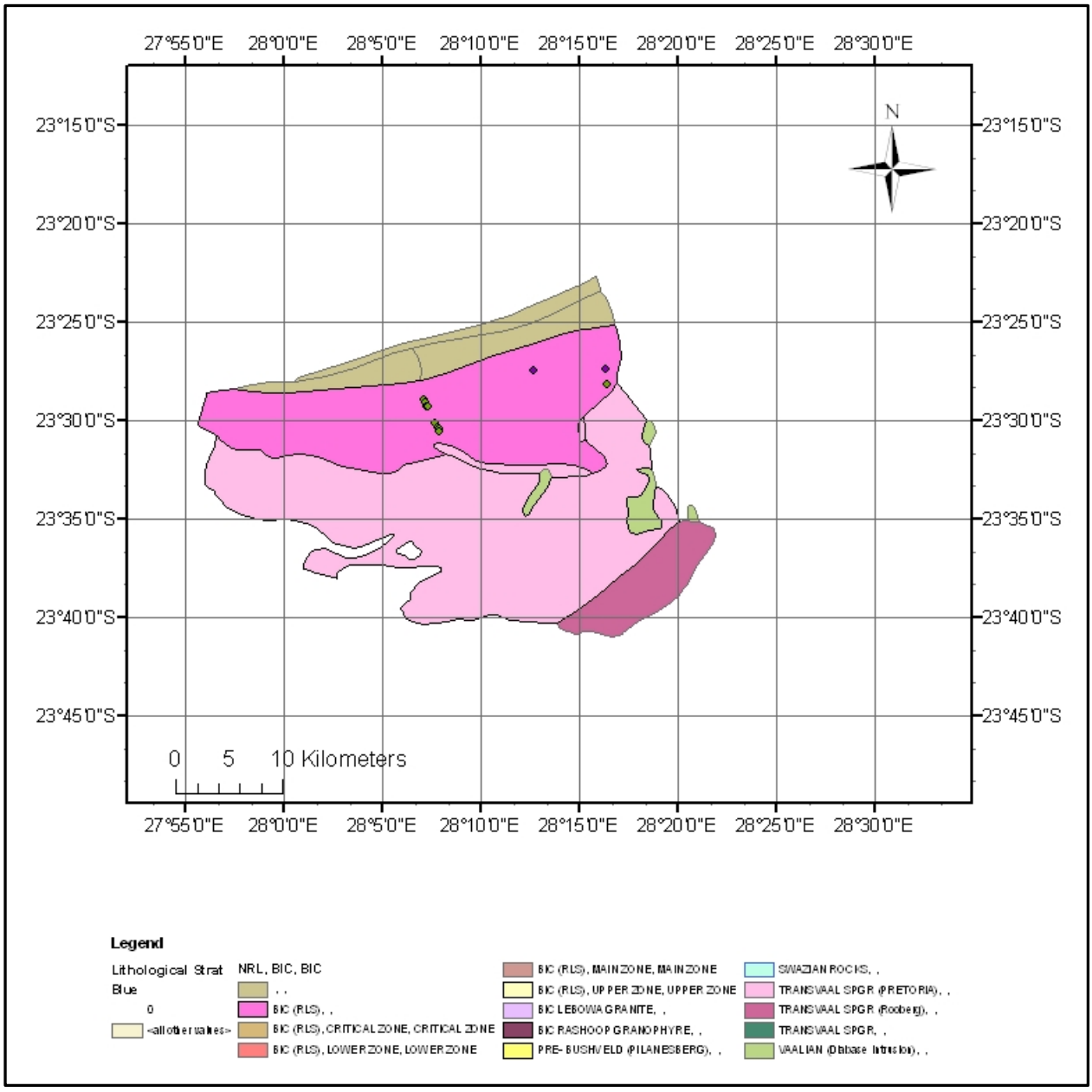

Figure 3.17: Geological map of the Villa Nora sector of the Northern Bushveld Complex.

CHAPTER 4 STRUCTURE AND ISOPACH MAPS OF PARTS OF THE RLS

4.1 INTRODUCTION

This chapter reports the result of the analysis of borehole log data of the Rustenburg Layered Suite (RLS) stratigraphic unit within the Bushveld Complex. The RLS is currently the major source of PGEs and other metals. The purpose of this chapter is to highlight the geometry as well as the structural features present in the study area with the use of structural contours, isopach maps and profiles. The result of this study provides both local and regional perspective of the geometry of the RLS and has implications for constraining the relative timing and sequence of deformation events. This report will provide information about the geology of the subsurface and serve as baseline data for subsequent research in the area.

4.2 STRUCTURE CONTOUR MAPS

Structural contour maps were generated for each stratigraphic unit represented in the study area in the following stratigraphical order:

- Overburden (Sand, coreless, turf, percussion drilled areas without core)
- Post-Bushveld (RLS), (Bushveld granites and granophyres, Pilanesberg lava)
- Upper Zone (gabbro, magnetitite)
- Main Zone (Gabbro, norites, anorthosites, Pyroxenites)
- Bastard Merensky Reef and its footwall,
- Merensky Reef and its footwall,
- Pseudo Reef unit,

- UG2 and UG1 units
- Middle Critical Zone,
- Lower Critical Zone,
- Lower Zone
- Marginal Zone
- Pre-Bushveld /Transvaal Supergroup, and
- Archaean granite unit.

The contour pattern from the top of the Post-Bushveld unit through the Upper Zone to the top of the Main Zone interval is similar to each other. This might suggest a similar emplacement mechanism explain more.

4.2.1 AMANDELBULT SECTION OF NORTHWESTERN BUSHVELD

This area is divided into two sectors for the purpose of this discussion. The first area is the extreme southeastern part or the Amandelbult area (Figure 4.1A). The structure contour intervals of the stratigraphical units reveal similar patterns from the Overburden unit to the top of the Main Zone. Structure contours in this area trends mostly NW-SE except at the southwest, that shows some contours trending SW-NE as shown in Figure 4.1B. This conforms to the general outcrop trend in the area. Structure contours in the NNE part of the map show a gradual slope with a fairly uniform rise in elevation in the southwest and slight bend to the NE.

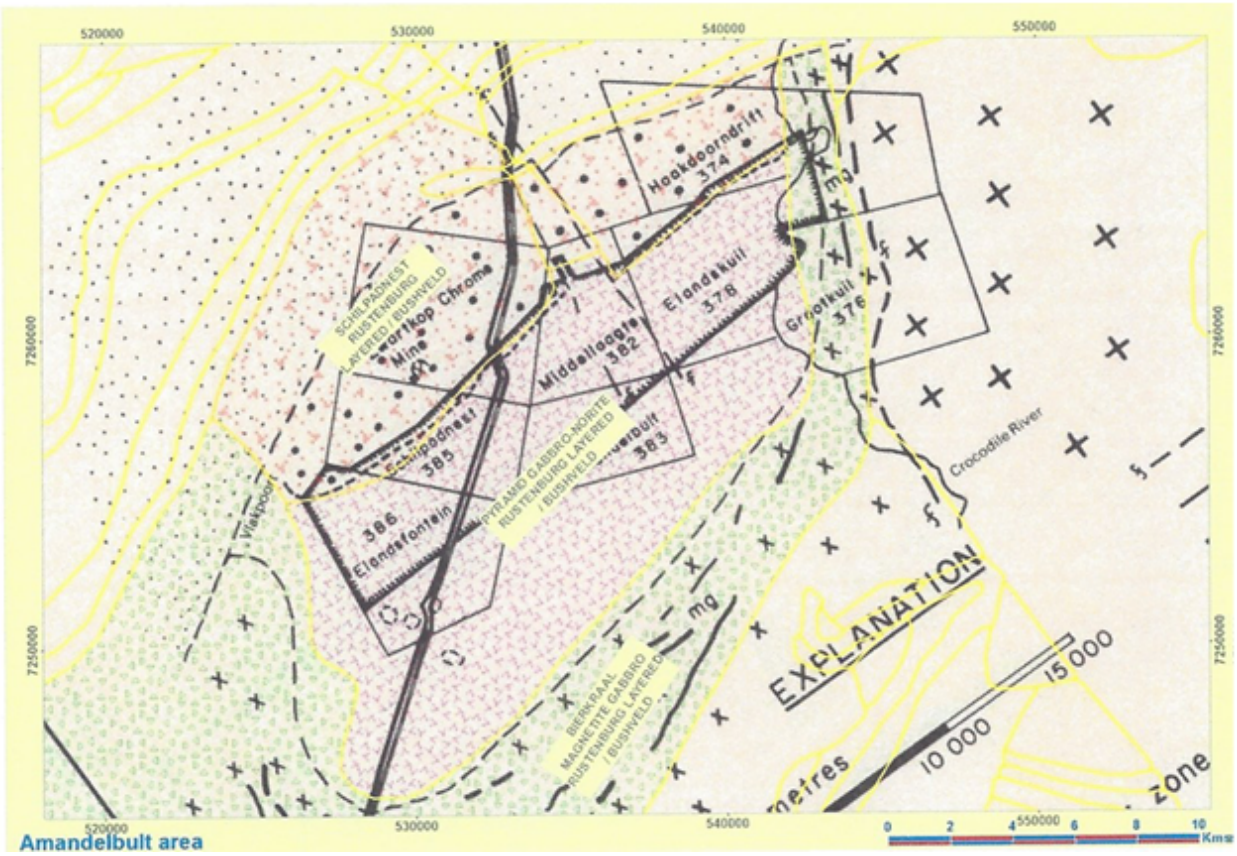

Figure 4.1A: Diagram showing the Amandelbult area of Western Bushveld (after Viljoen et al.1998).

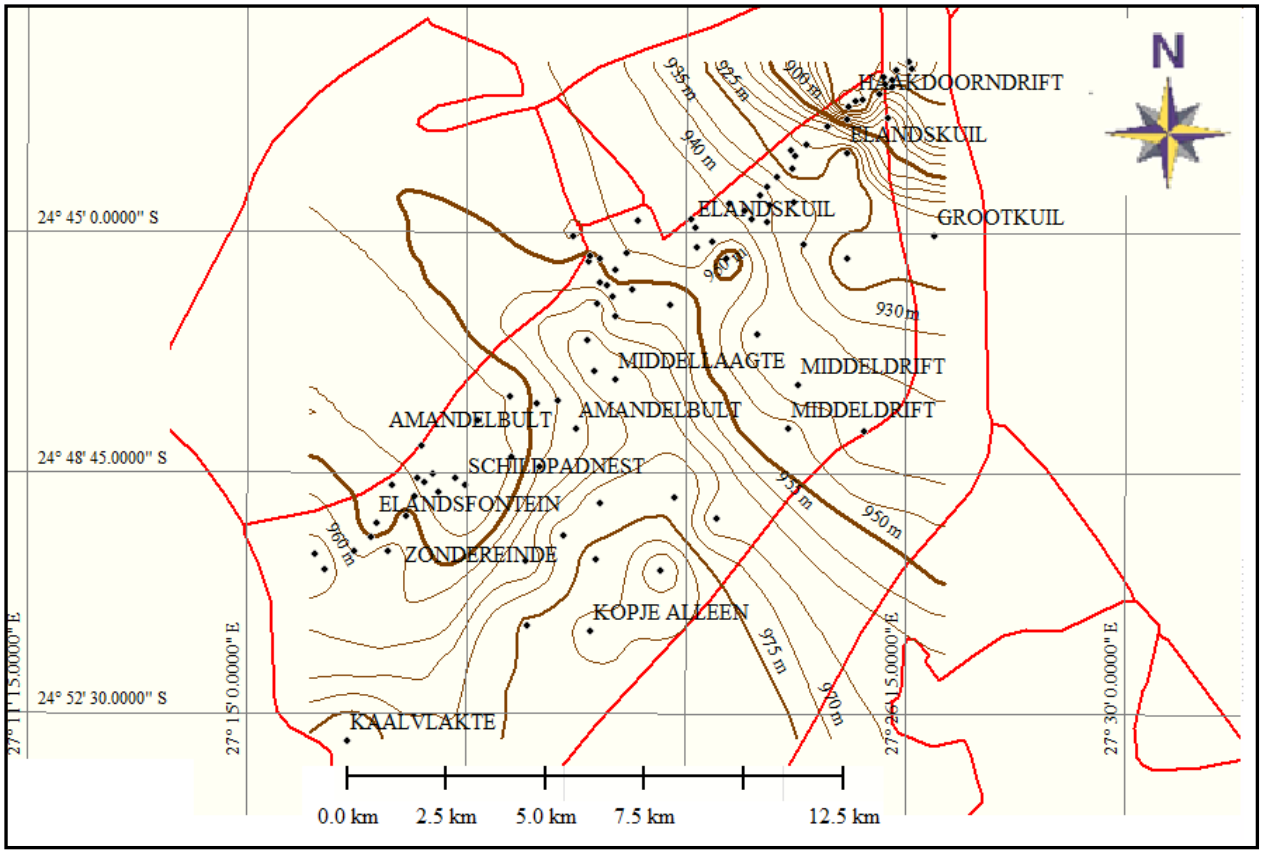

Figure 4. 1B: Top of the Upper Zone structural contour interval of the Amandelbult section of the Northwestern Bushveld.

Structural lines at the base of the Main Zone to Lower Zone (as shown in Figure 4.2) reveal a different pattern entirely. The base of the Main Zone interval, with central SW-NE trending and closely spaced contours (Figure 4.2) cut across the area, separating the NW-SE trending contour into two parts i.e., northwest and southeastparts (implying that the NW-SE structural trend is older than the SW-NE structural trend).The elevation of the Main Zone rocks in the northwestern part decreases gently from more than 750 m, to almost -1300 m in the southeast, representing a steeply subsiding section.

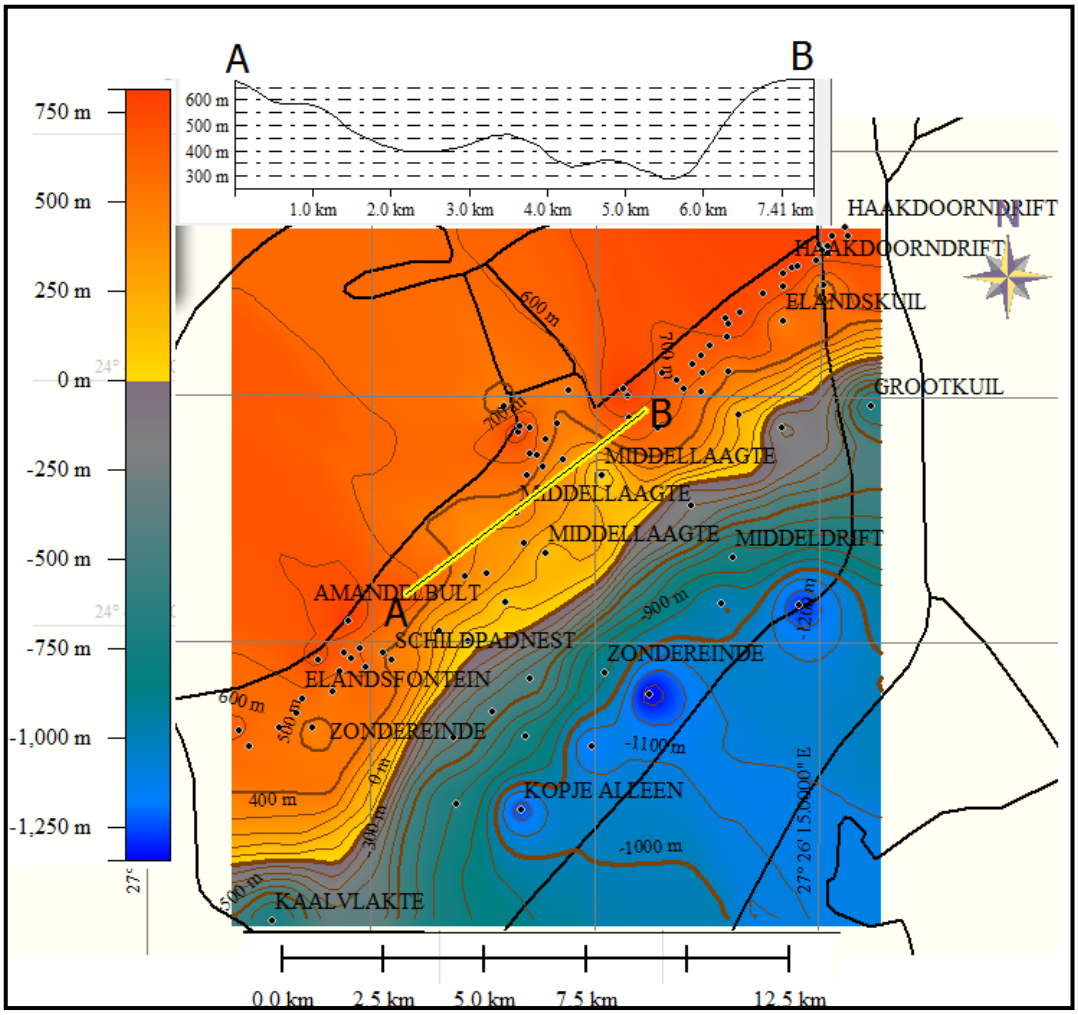

Figure 4. 2: Structural contours at the base of the Main Zone interval in the Amandelbult area of the Northwestern Bushveld.

The NW-SE trending structure widens southwards from about 4 km at the northwestern part to over 11 km at the southeastern part.

The two extreme ends of the SW-NE trending contour lines show a slight bend to the south (from the profiles in Figures 4.2 and 4.3 these represents the position of the bounding faults).

Profile A-B drawn on the Main Zone base interval shows a gradual vertical slope. Elevation dropped from 610 m to 448 m on the western part of the structure and a sharp drop in elevation from 700 m to 409 m in the eastern part and a trough-like structure at the centre (Figure 4.3). The second profile on the lower end shows a similar structure with the two sides becoming more pronounced (Figure 4.3). A profile drawn on the Main Zone structure

contours and isopach map for part of the Amandelbult section shows a similar pattern to pothole structures as indicated in Figure 4.4.

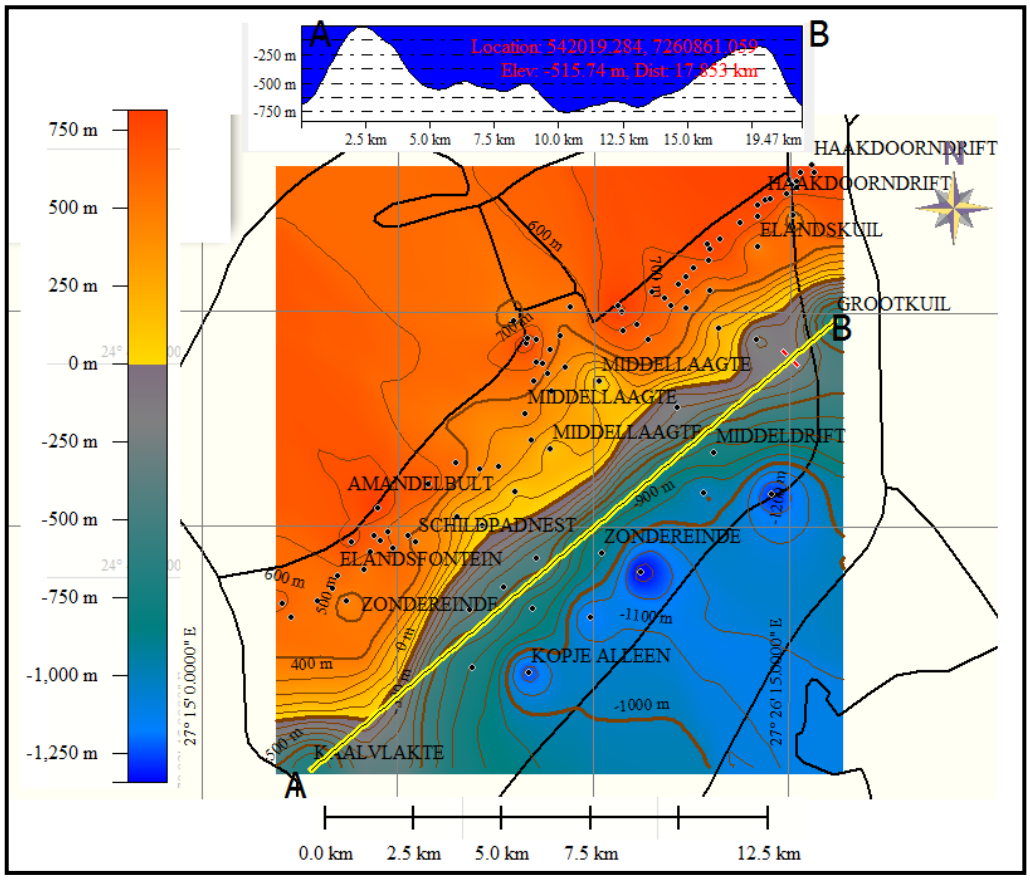

Figure 4.3: Profile A-B across the Northwestern part of the trough at Amandelbult and northern section.

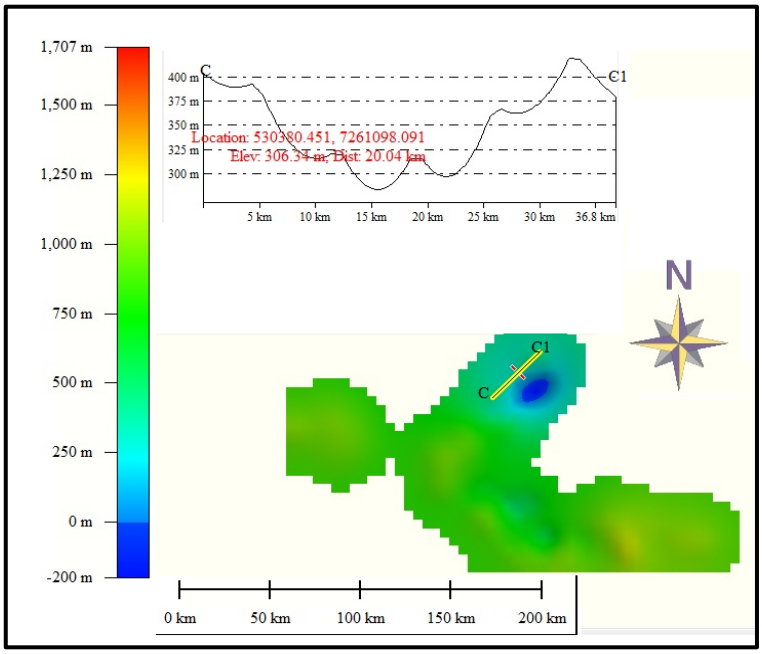

Figure 4.4: Isopach grid model of the Western and far Western Bushveld Complex with Profile C-C1 drawn across the northern part of the Amandelbult area showing a basin-like structure (pothole).

The Main Zone isopach map of Amandelbult section (see Figure 4.5) shows the thickness variation in the area. Thickness varies from less than 100 m at the northern part to over 2000 m in the south. There is a close resemblance between the structural map and theisopach map in this area. Thickness atthe central part varies steeply from 500 m to 2250 m and it is about 20km distance across. The thickness varies steeply from the centre of the map southeastwards. A similar pattern of thickness variation was observed on the isopach map of the Main Zone to the Lower Zone interval. The whole of this area dips steeply to the south, and the complete sequence of RLS rocks (from the Main Zone to Lower Zone) occurs at different depths of less than 100 m in the north to over 2200 m south. This continuous southward dipping structure and thickness, pattern might suggest that the structure in this area is pre-Bushveld and was probably reactivated during the intrusion of the RLS. The complete magma sequence at different depths and southwards thickening of the RLS rocks in this area (as illustrated with 3D models and fence diagrams in chapter two) indicate that the structure in this area is pre-Bushveld.

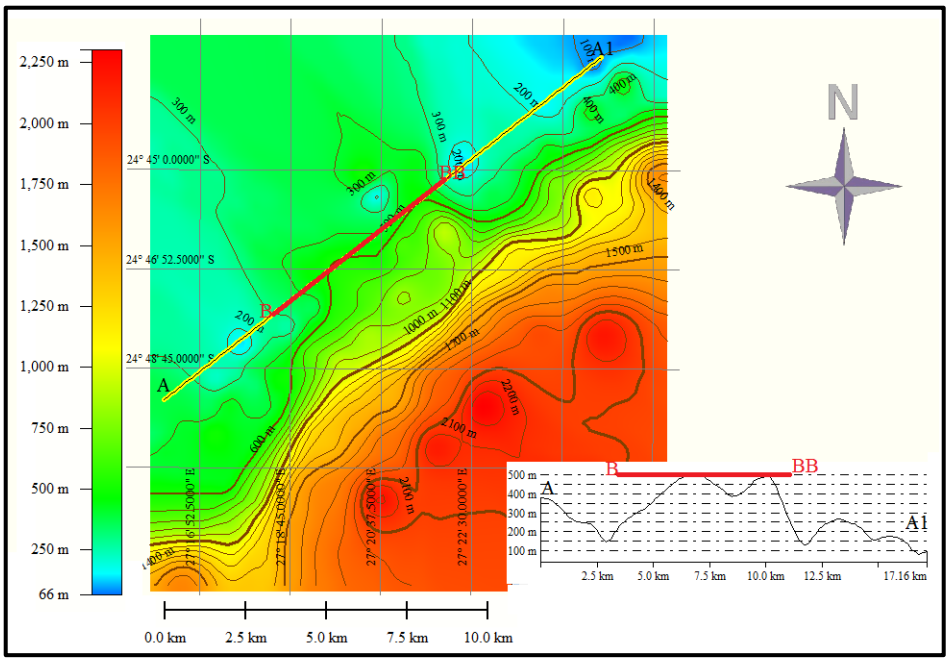

Figure 4.5: The Main Zone isopach map of the Amandelbult section, Northwestern Bushveld showing the thickness distribution.

OVERVIEW OF AMANDELBULT SECTION

1. The Upper Zone interval at the Amandelbult section indicates a central NW trending anticlinal structure, with the western limb deflected horizontally (NE)
2. The structure at the base of the Main Zone interval of the Amandelbult section indicates the presence of a graben that dips steeply to the south in the centre of the anticlinal structure, thus dividing the anticlinal feature into two (one part of the northwest and the other in the southeast).
3. As shown in Figures 4.2 and 4.3, the structural pattern for the horizon in the Northwestern Bushveld persists up to the top of the Main Zone, however the pattern changed abruptly at the base of the Main Zone and continues with only slight changes down to the Lower Zone stratigraphic unit. The abruptness of the change in the structural pattern might suggest a change in deformation pattern.
4. The Upper Zone structure contours define a NW-SE structural trend pattern
5. The structural contour pattern from the base of the Main Zone for the Lower Zone interval is marked by a SW-NE trend.
6. The northern part of the Amandelbult section reveals a basin like feature on the structural map.

4.2.2 OTHER PARTS OF NORTHWESTERN BUSHVELD

4.2.2.1 Structure Contour Maps of The Northwestern BushveldComplex

The structural contour map from the Main Zone base interval to the Lower Zone interval shows close resemblance. The Main Zone rocks occur between elevations -651 m to 1700 m. The southwestern part is an uplifted area and the height decreases gradually from this area towards the centre. The central portion consists of a small depression between two uplifted areas; one to the north (over 750 m high) and the other to the south (over 900m high). The northern uplifted area is part of the Union section, adjacent to the Amandelbult section, and the elevation decreases gradually from 400m to -125m within this area. The area marked by this slight elevation decrease coincides with the Northern gap area (Figure 4.6). The Southern gap area between the Union section and the northern part of the Pilanesberg Complex is also marked by a gradual decrease in elevation from about 750 m to less than 350 m around the Union section. The slope on the eastern side is more pronounced than the one on the western side. The contour lines at the centre trend SE and tend to bend slightly westwards at the centre. L-shaped structural contours around the Southern gap area indicate the presence of strike slip movement (Figure 4.6). Structural contours at the Amandelbult section regionally, has a lobate shape appearance with slightly flattened top and broad sides that dip southward in a step like manner as shown in Figure 4.7.

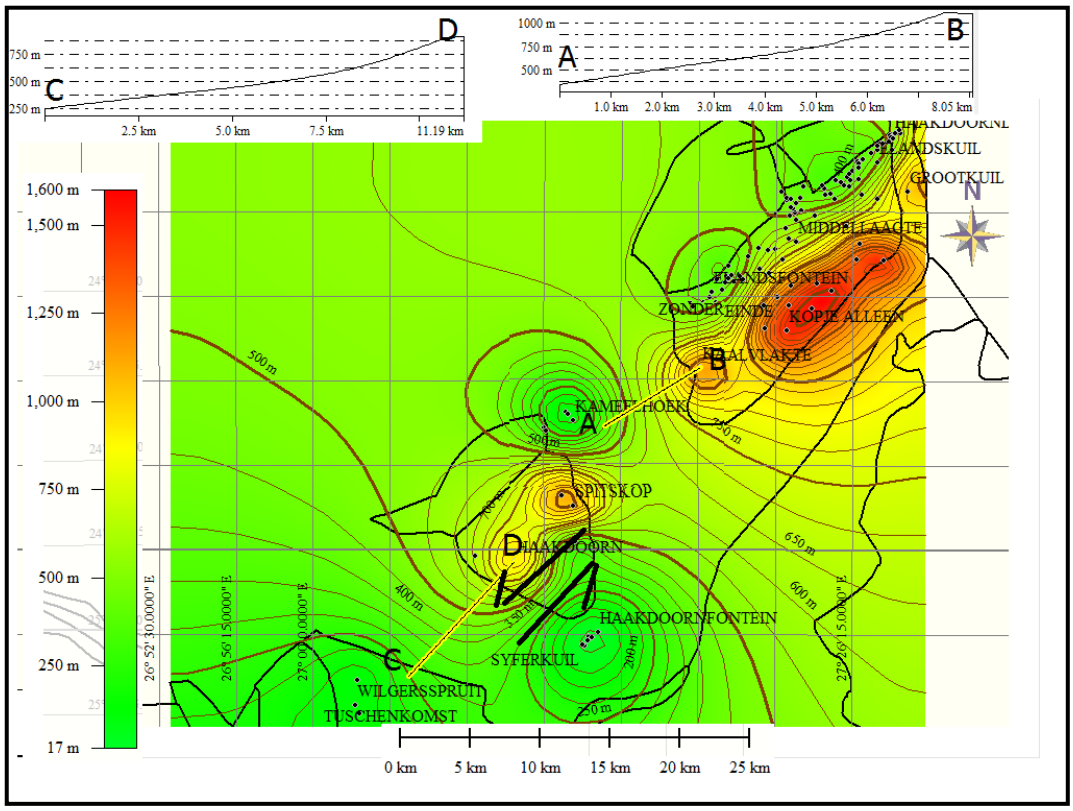

Figure 4.6: Base of the Main Zone structure interval with profile across the Northern gap area.

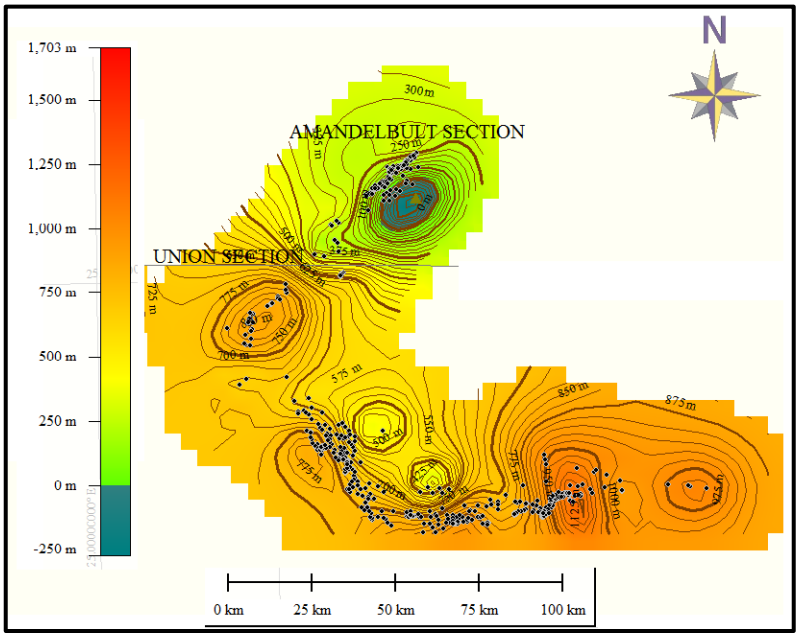

Figure 4.7: Structural contours on the Lower Zone base interval showing the geometry of the Amandelbult section

.

4.2.2.2 Isopach Maps of Northwestern Bushveld Complex

The Upper Zone isopach map of the northwestern parts of the Western Bushveld Complex shows pronounced central thickening as indicated in Figure 4.8. The thickness on the Main Zone isopach map varies from 17 m at the southwest to about 750 m at the centre and to over 1600 m at the southeastern part (Figure 4.9). The thickness at the central part shows a central thickening zone submerged between two thin zones at the Union section. Figure 4.10 and 4.11 shows the Main Zone and Merensky Reef isopach respectively.

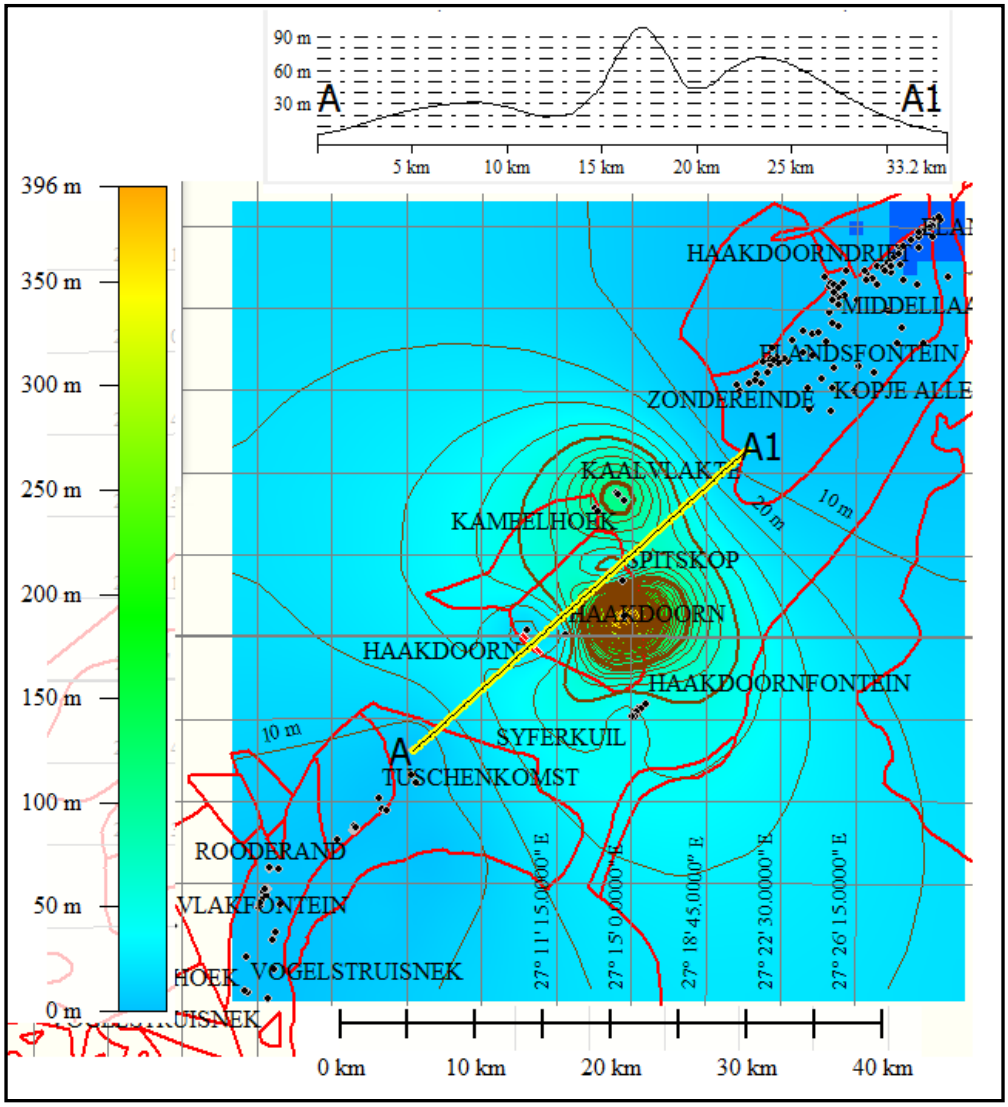

Figure 4.8: The Upper Zone interval isopach map with profile A-A1 showing the thickness variation around the Northern and Southern gap areas.

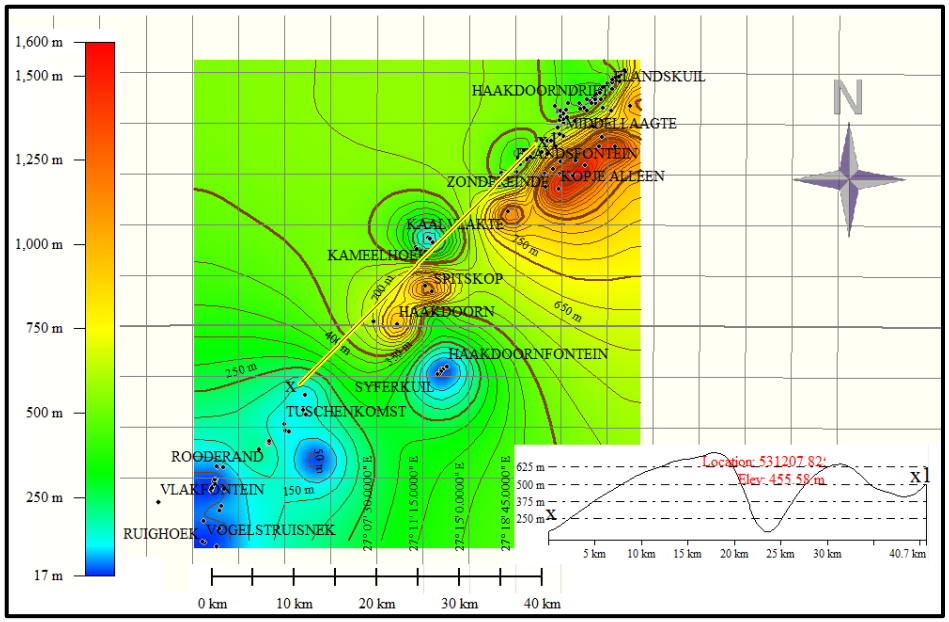

Figure 4.9: The Main Zone interval isopach map with profile X-X1 showing the depression (drop in thickness of the Main Zone rocks) between the Union section and the Amandelbult section, which represents the Northern gap area and the gradual increase in the Main Zone thickness

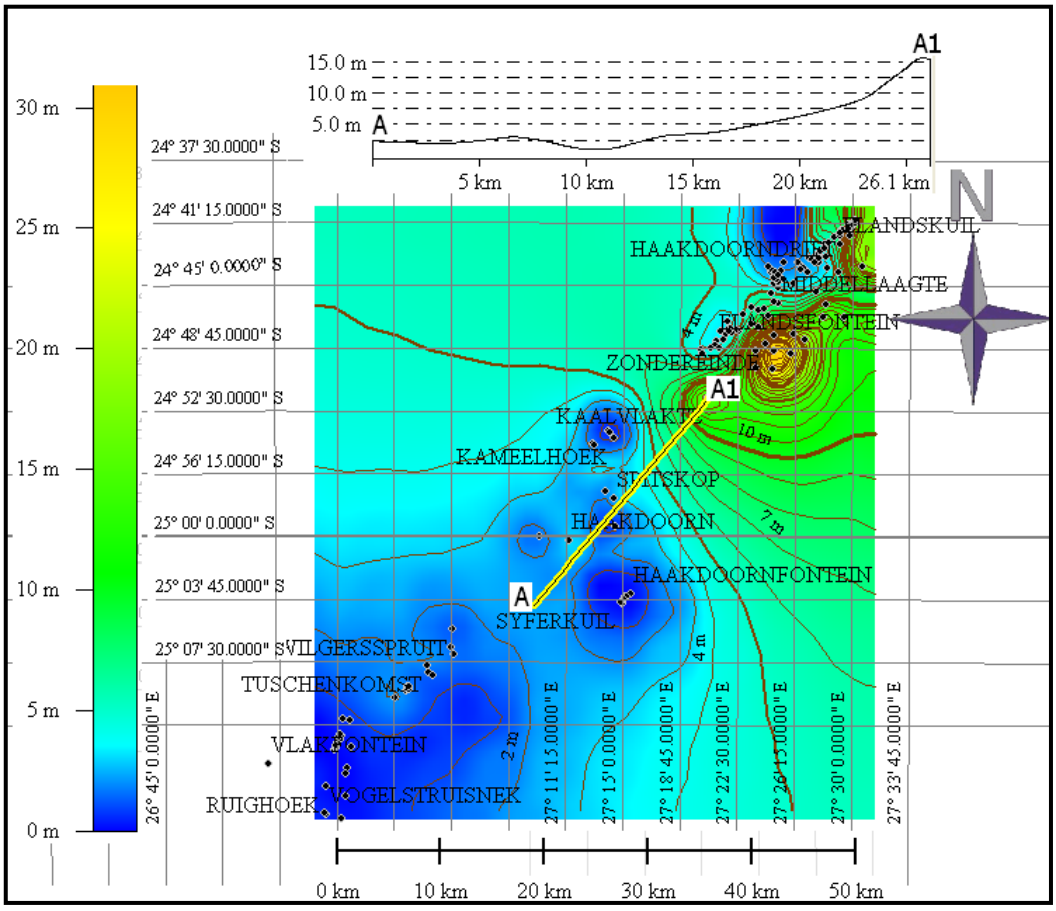

Figure 4.10: Merensky Reef isopach mapwith profile A-A1 in the Northwestern Bushveld.

Change in thickness is related more to variation in the elevation of the Main Zone surface. The more pronounced eastern thickness is due to complete filling of the synclinal structure at the Amandelbult section with RLS rocks. The Critical Zone thickness increased progressively from SW to NE.

SUMMARY OF FEATURES OBSERVED AT THE NORTHWESTERN PART OF THE WESTERN BUSHVELD COMPLEX

1. Pronounced thickness of the Upper Zone unit is present around Union section
2. L-shaped isopach lines at Union section are indication of lateral or strike-slip movement.
3. The Southern gap and Northern gap areas are marked by gentle and steep slopes respectively
4. Depth of occurrence of the Main Zone range from 1100 m on the southwestern edge (northern fringe of Pilanesberg Complex) to less than -1000 m in the Amandelbult area.
5. Thickness of all the stratigraphic units increases from SW to NE except for the Upper Zone of which the thickness is concentrated at the centre (Union section) and reduced sideways i.e., to the east and west.

4.3 CENTRAL PARTS OF THE WESTERN BUSHVELD

4.3.1 STRUCTURAL CONTOURS OF AREA AROUND PILANESBERG COMPLEX

Structural contours at the top of the Post Bushveld interval are widely spaced, with the immediate south of the Pilanesberg Complex showing east-west trending contours, interrupted by two isolated structures. These east-west trending contours represent a gentle slope. The immediate north of the Pilanesberg Complex is marked by NW-SE trending contours. Structural contours at the base of the Main Zone show that the Pilanesberg Complex forms a major positive structure with radially distributed gentle slope around a circular shaped complex. However, the available borehole information is not sufficient to

describe the Complex adequately. The contours surrounding the Complex to the immediate south are closely spaced with a west plunging nose that turns southwards (trending parallel to the Rustenburg Fault) and continues with this trend down to the southern edge before turning east (with more closely spaced contours) on Kroondal farm around the Spruitfontein upfold. Structural contour pattern from the Main Zone interval to the Pre-Bushveld interval issimilar and differs slightly from structural contours on Overburden to the Upper Zone interval, which are similar to each other with low relief of evenly spaced contours over the entire area. The profile through the area shows a slope from over 900 m from the periphery of the Pilanesberg Complex southwards to below 600 m (see Figure 4.11).

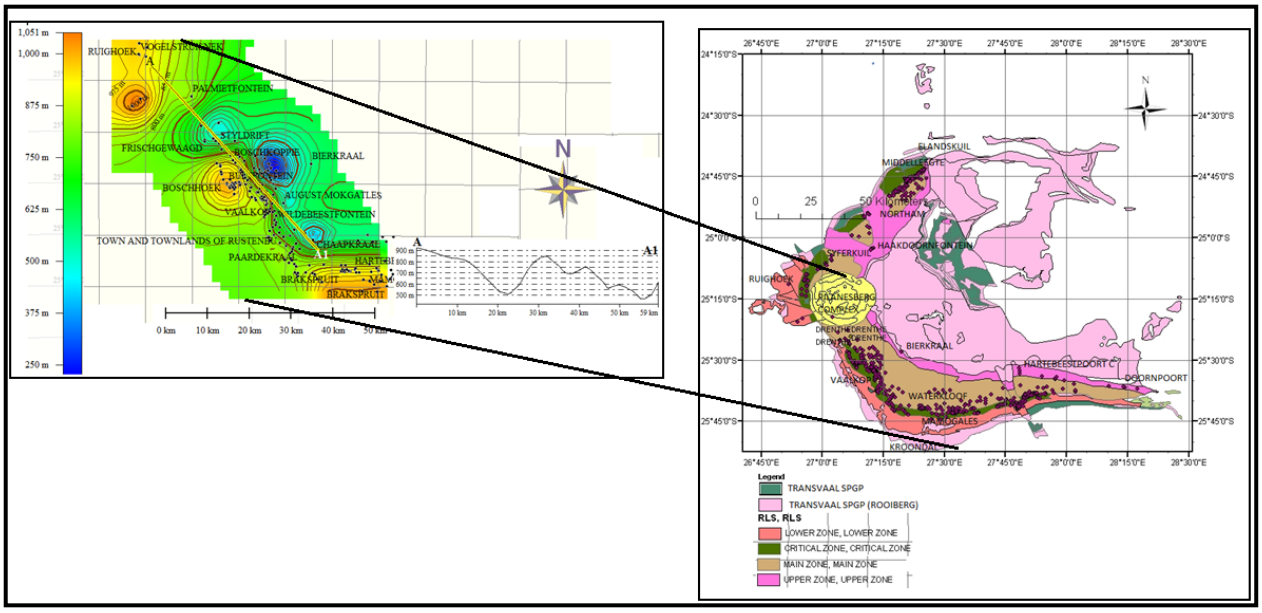

Figure 4.11: Central parts of Western Bushveld the Main Zone structural contour interval with profile.

4.3.2 ISOPACH MAP OF AREA AROUND PILANESBERG COMPLEX

The Main Zone isopach map and the structural contour maps have a similar pattern but show an inverse relationship (Figure 4.11 and 4.12). The Main Zone thickness increases eastwards from the western edge. The Main Zone thins out around Vaalkop farm in the west and at the southern edge. From the Pilanesberg Complex the thickness increases sharply from less than 200 m to over 350 m. The structural feature to the southwest

probably represents part of the Brits graben. The Styldrift farm area exhibits a positive structure. Contours in this area trend mostly NNW-SSE.

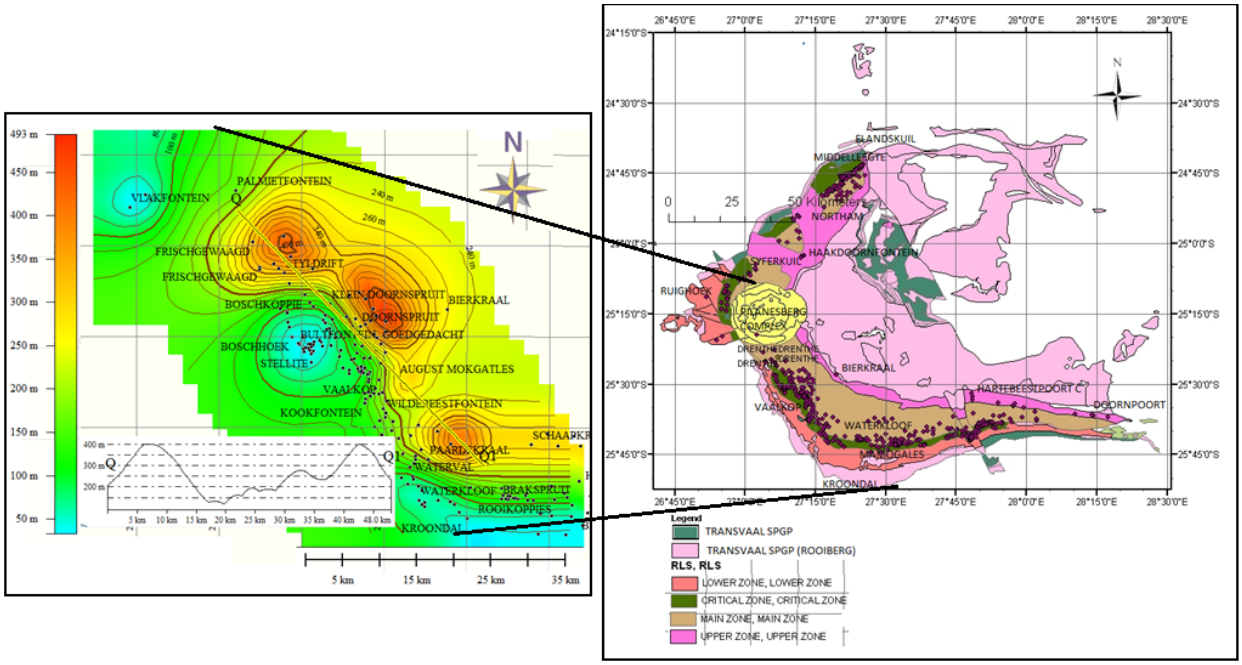

Figure 4.12: The Main Zone isopach with profile Q-Q1 across the southern parts of the Pilanesberg Complex in the Western Bushveld

OVERVIEW OF SOUTHERN PARTS OF PILANESBERG COMPLEX, WESTERN BUSHVELD

1. Structural contours and isopach interval maps are inverse to each other
2. Archaean rocks are not indicated on borehole log records for this area.
3. The Pilanesberg Complex forms a positive circular structure occurring midway in the Western Bushveld Complex.
4. The rock units dip to the east.
5. A NW-SE trend (parallel to the Rustenburg Fault trend) is prevalent in the central part

4.4 SOUTHWESTERN BUSHVELD

4.4.1 STRUCTURAL CONTOURS OF THE SOUTHWESTERN BUSHVELD COMPLEX

The Upper Zone structure contours show two shallow areas, one around Hartebeestpoort B (east of Middelkraal farms) and the other around Roodekopje farm both areas located on the western side of the Brits. The contours at Roodekopjes farm are mostly NNW trending, while those at Hartebeestpoort B are circular in shape and terminate against NNW trending contours to the west i.e. around the Kroondal structure. The eastern side of the Brits is marked by a uniform rise in elevation. Structural contours on the Main Zone base interval show a complex pattern, on the western side, NNW-SSE closely spaced trending contours with a central depression as shown in Figure 4.13. The depression is bounded on both sides by the closely spaced contours, which indicate steeply sloping sides. The southern end of the depression is slightly curved northwards (might be due to floor rock topography or presence of Spruitfontein inliers), while the eastern edge exhibits a southeast plunging structure partly surrounded by a steep slope.

The Lower Zone base interval shows a similar pattern to that of the Main Zone base, except for the eastern limb of the graben, which has a wide, plunging nose that developed southeastwards. Figures 4.15 shows the central part consists of an isolated hill and depression, with the eastern sides of the central isolated hill consisting of east verging and closely spaced L-shaped contours with the superimposed geological contact from the geological map on the Main Zone grid model of the Brits graben area. The grid model of the Lower Zone base structural contour interval is shown in Figure 4.15.

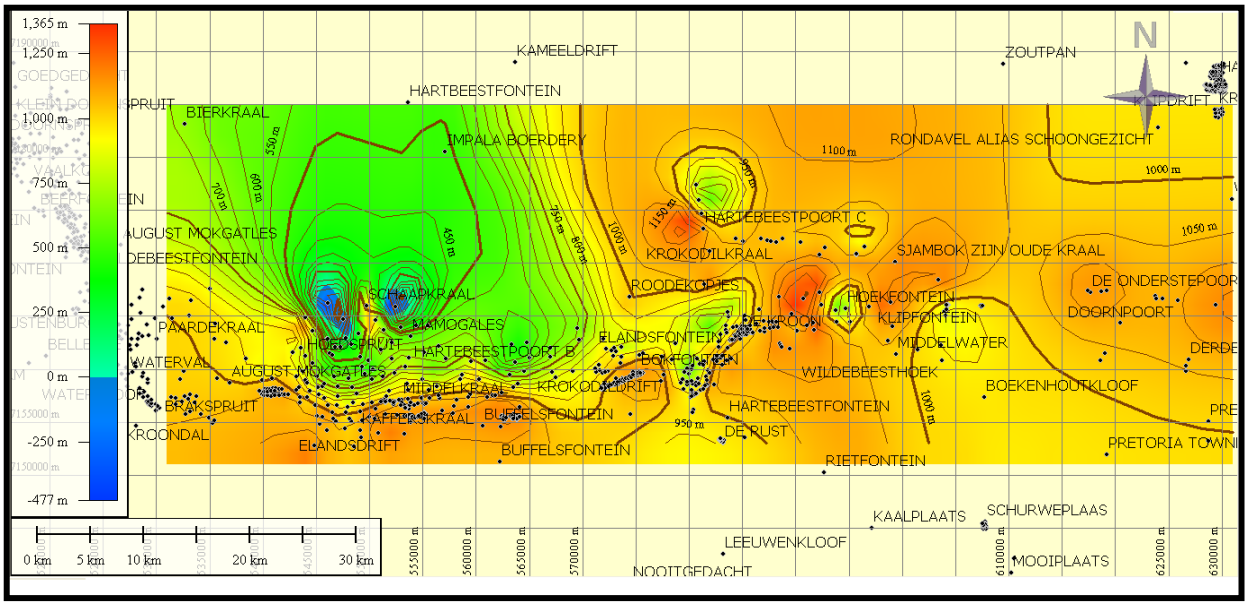

Figure 4.14: Profile A-A1 on the structural contour model at the base of the Main Zone interval of the Southwestern Bushveld Complex. Shape of the profile reveals the presence of more than a single graben.

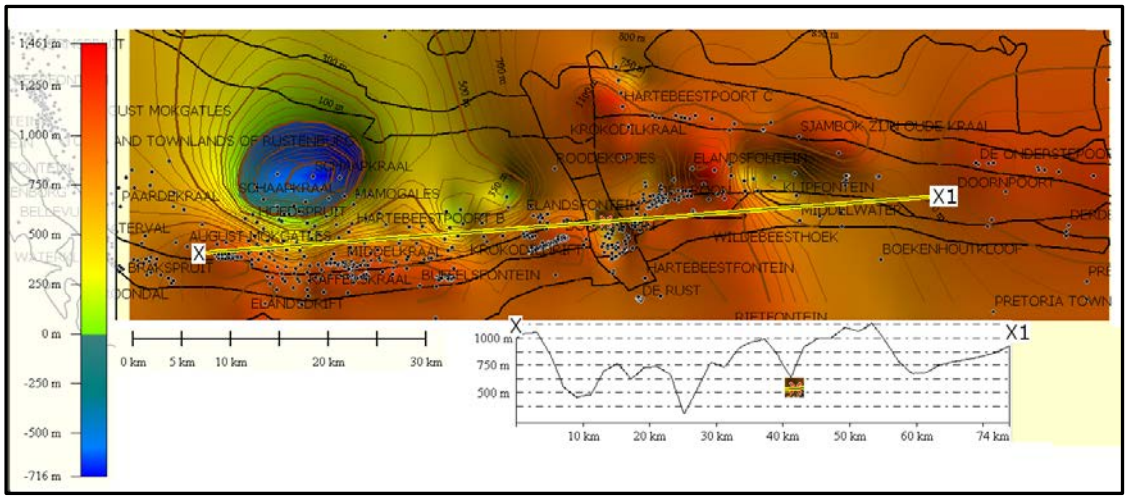

Figure 4.15: Structural contour model for the base of the Lower Zone interval of Southwestern Bushveld Complex showing profile x-x1 and the location of Brits graben and other graben-like structures in the area.

4.4.2 ISOPACH MAP OF THE SOUTHWESTERN BUSHVELD COMPLEX

The Upper Zone isopach map reveals an eastward increase in thickness especially around the Brits area (see Figure 4.16). It also shows a NNW-SSE displacement around the Brits graben, with contours adjacent to the displacement showing an uphill pointing V-shape. On the Main Zone isopach map (Figure 4.17), the western part has a negative structure and positive thickness. The Main Zone thickness varies from over 1100 m on the western side to less than 50 m in the eastern part. Centrally located NNW-SSE trending contours with

derivatives (horizontal) may show discontinuities which could be possible faults in the area (Figure 4.18).

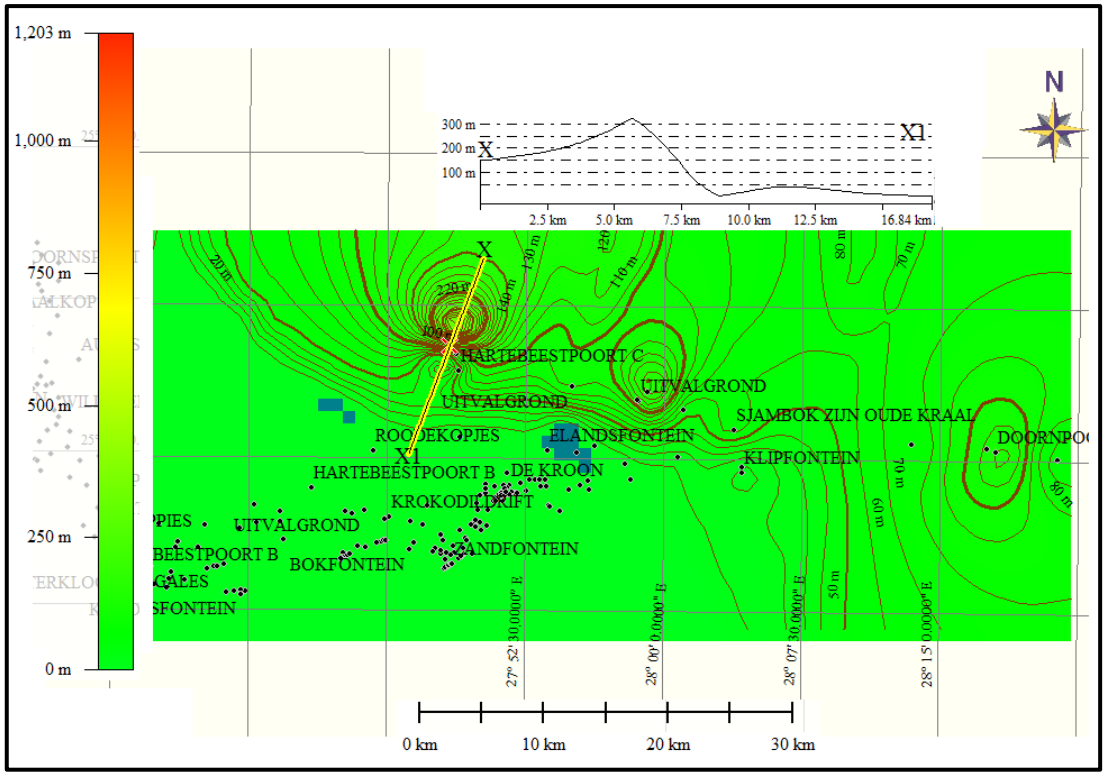

Figure 4.16: The Upper Zone isopach map of Southwestern Bushveld with profile X-X1.

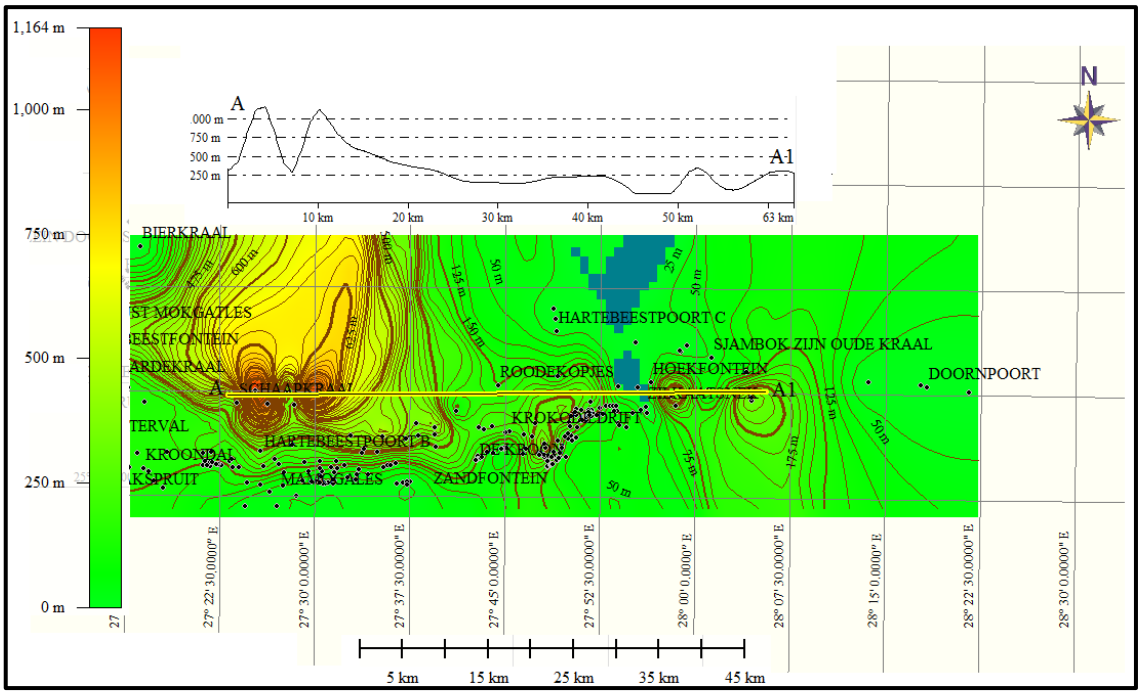

Figure 4.17: The Main Zone isopach map of Southwestern Bushveld Complex with profile A-A1.

4.4.3 SUMMARY OF FEATURES IN THE SOUTHWESTERN BUSHVELD

1. The Upper Zone thickness increases eastwards from the west
2. Main Zone thickness decreases from west to east.
3. More graben-like features apart from the Brits graben can be inferred from the structure contour and isopach maps.
4. An L-shaped thickness, pattern at the central part of Southwestern Bushveld might indicate lateral movement
5. Most of the structures trend NNW.
6. Areas with negative structure have positive thickness
7. Tight isopach lines on successive interval maps might probably represent faults

4.5 THE EASTERN BUSHVELD

4.5.1 NORTHEASTERN BUSHVELD

4.5.1.1 Structural Contour of the Northeastern Bushveld Complex

The Eastern Bushveld geological map (Figure 4.18) showing the Northeastern part, the central sector and the southern sector of the Eastern Bushveld. The structural contour pattern on the Upper Zone interval of the Northeastern Bushveld reveals the presence of side-by-side structural high and depression (likely due to faulting), relatively flat and uniform surfaces. The Upper Zone rocks occur between depths1280 m to -1383 m at the central part of the Eastern Bushveld Complex. The prominent faults such as the Wonderkop Fault caused a downthrow along the western side of Northeastern Bushveld Complex. The centre slopes towards the north. This central depression represents the location of the Sekhukhune Fault. The western part of the Sekhukhune Fault is marked by a steep slope, while the eastern side is marked by widely spaced southwest trending contours representing a uniform rise in elevation.

The structure contour map indicates a downthrow of over 5.3 km on the western side of Sekhukhune Fault and over 11 km downthrow on the eastern side. Two other faults occur to the west, each with a downthrow of less than 250 m and a central deep of about 46 km between the two. A structural high (Fortdraai Anticline) exists adjacent to the Sekhukhune

Fault. Profile A-A' and B-B' drawn across the Northeastern Bushveld reveals the geometry of the faults and other features (Figure 4.19 and 4.20). The 3D model of the area is shown in Figure 4.21.

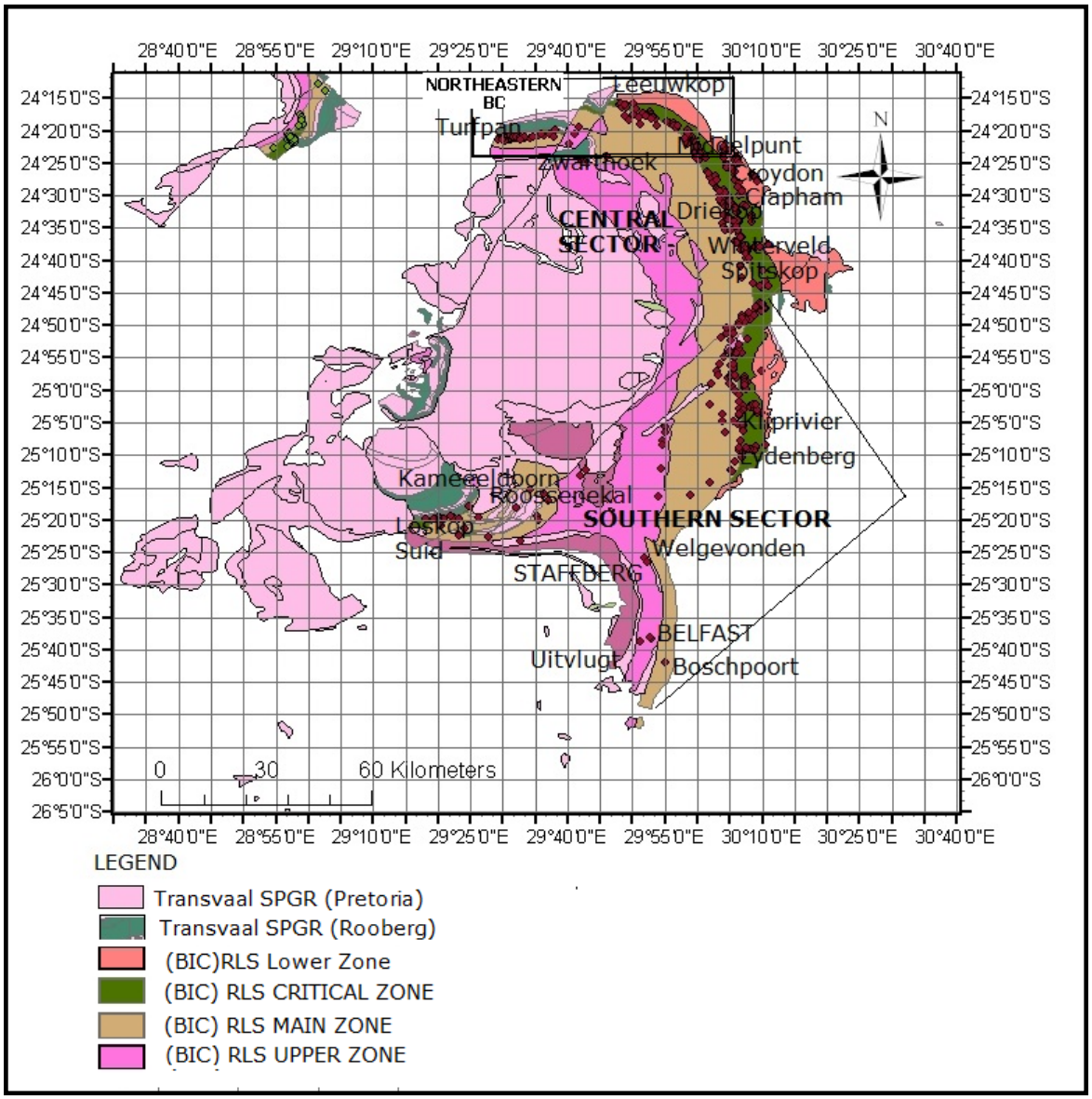

Figure 4.18: The Eastern Bushveld geological map showing the Northeastern BIC at the northern part of the map (around Leeuwkop), the central sector and the southern sector occupying the southern parts of the Steelpoort fault down to Boshchpoort.

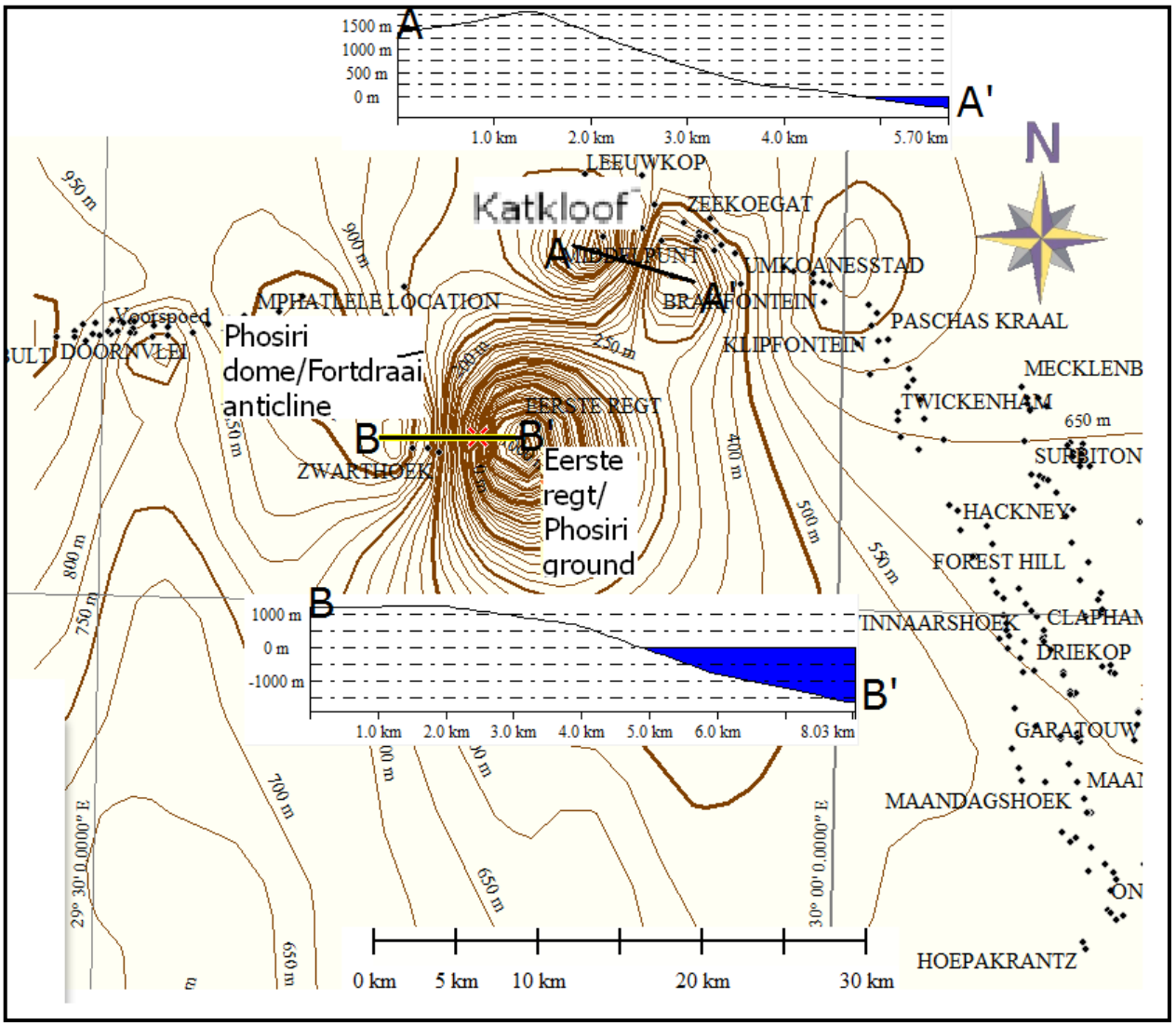

Figure 4.19: The Main Zone structure contour map of the Northeastern Bushveld Complex showing profile B-B' across Fortdraai anticline and adjacent depression at Eerste Regt and profile A-A' across north-eastern part of Fortdraai anticline (along Katkloof dome and adjacent structure low area). Note the eastward dipping of faults in this section of the Eastern Bushveld.

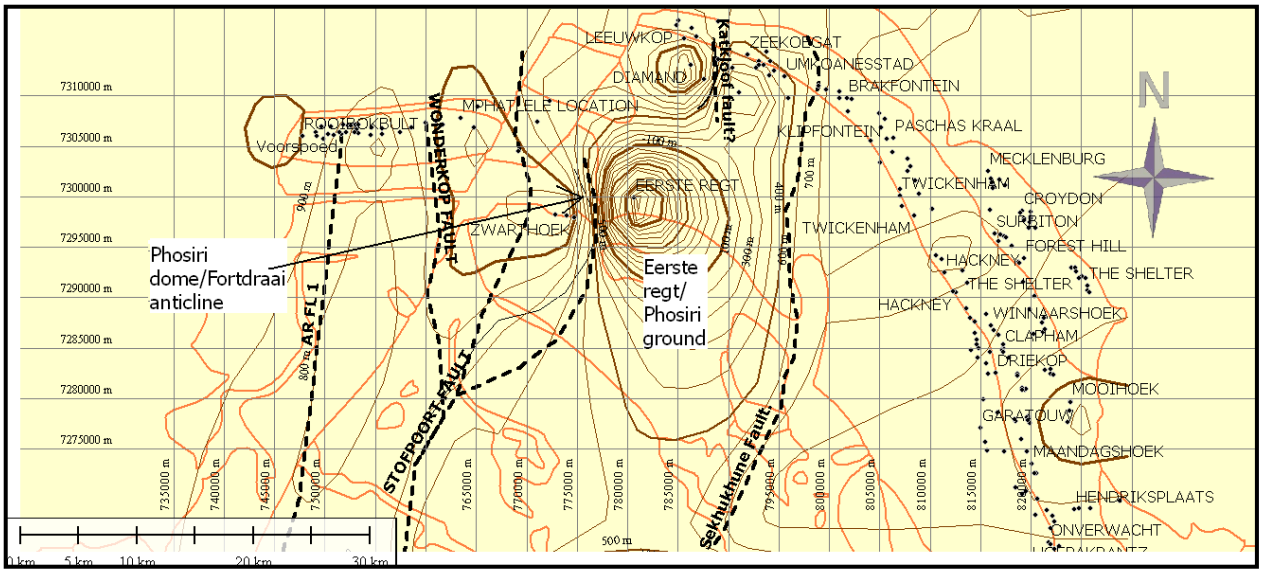

Figure 4.20: Profile C-C1 showing the geometry of a fault adjacent to part of the Sekhukhune Fault in the north causing a downthrow of about 120 m to the southwest.

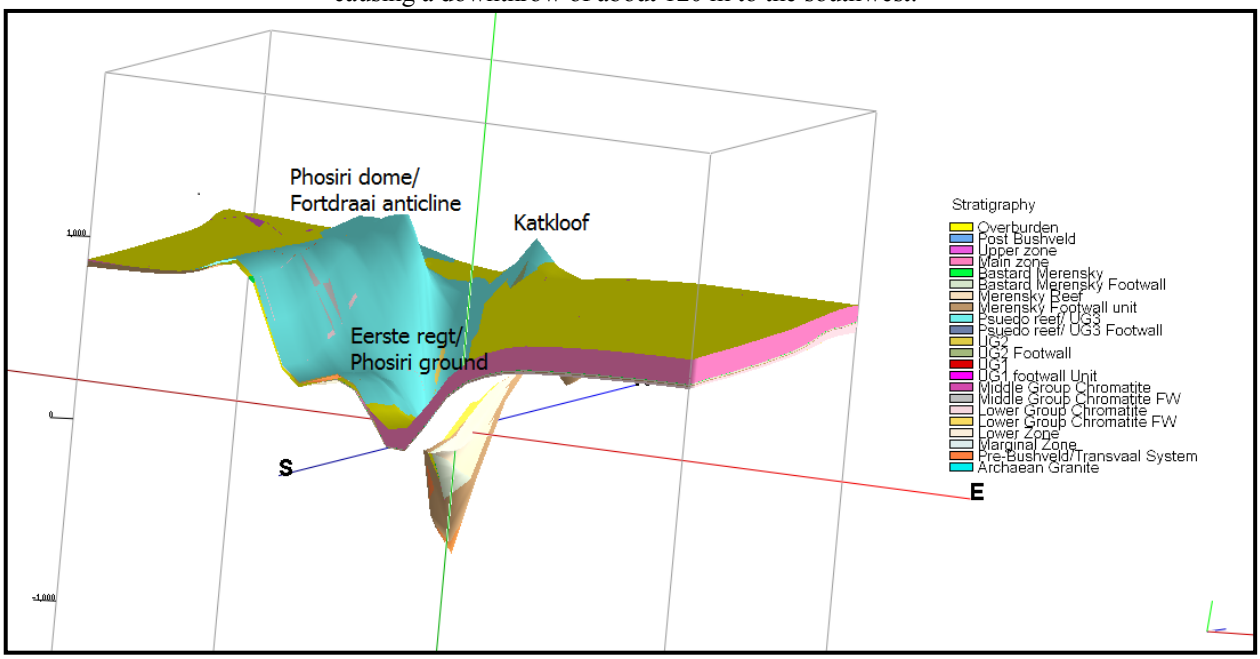

Figure 4.21: 3D model of the Northeastern Bushveld (VE 10x)

4.6 CENTRAL SECTOR OF THE EASTERN BUSHVELD COMPLEX

4.6.1 STRUCTURE CONTOURS ON UPPER ZONE TOP INTERVAL OF THE CENTRAL EASTERN BUSHVELD COMPLEX

The centre sector extends from the southern end of the Wonderkop Fault to the northern parts of the Steelpoort Fault as indicated in Figure 4.22, 4.23 and 4.24. The structural contours on top of the Upper Zone interval show three sets of contours that merged southwards and converged on the centre of the Eastern Bushveld Complex (Figure 4.24). The structural contours to the extreme west of the Wonderkop Fault are represented with N-S trending contours, with the downthrown side to the west of the Wonderkop Fault. Structural contours between the Wonderkop Fault and the small arch adjacent to it are slightly curved to the west and later converge along a southwest trending fault. The contours on the western side of the Sekhukhune Fault (part of Sekukhune Fault) are also curved westwards and form a depression southeastwards. Centrally located east-west trending contours from the west (almost opposite the gentle sloping structural high in the southeast (maximum elevation 1000 m)) with a downthrow to the north joined the Wonderkop Fault southwards.

The southern sector consists of N-S trending structures that bend to the west, with a plunging nose to the Northwest. The southeastern parts consist of east-west trending contours; also, there are few isolated hills and structural highs at the southeastern part of the map. The structural high, attained a height of approximately 1800 m at the southeastern part of the sector, and slope gently to the south and steeply to the west. The southern sector, ‘thus forms the structural high part of the Eastern Bushveld Complex and dips to the northern part (Figure 4.23). The structural pattern on the Archaean floor rock and successive upper layers (up to the Main Zone) are similar. This probably indicates that most of the structures are basement controlled. Figure 4.24 shows the profile across the southern part of the Wonderkop Fault. The northwest trending contours around the Laersdrift Fault probably represent the northern extension of the Laersdrift Fault, which separates the southeastern Bushveld Complex from the rest of the Eastern Bushveld Complex. The geometry of the Laersdrift Fault on the Upper Zone top intervals is indicated

in Figure 4.25, while Figure 4.26 shows the profile across the Southeastern Bushveld Complex.

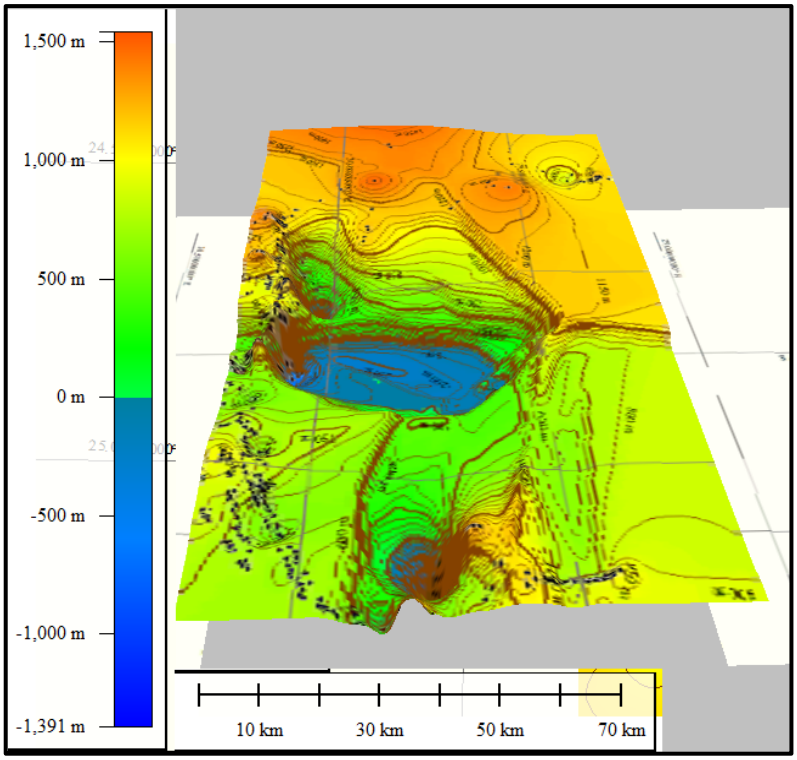

Figure 4.22: Eastern Bushveld structural model with the Lower Zone base.

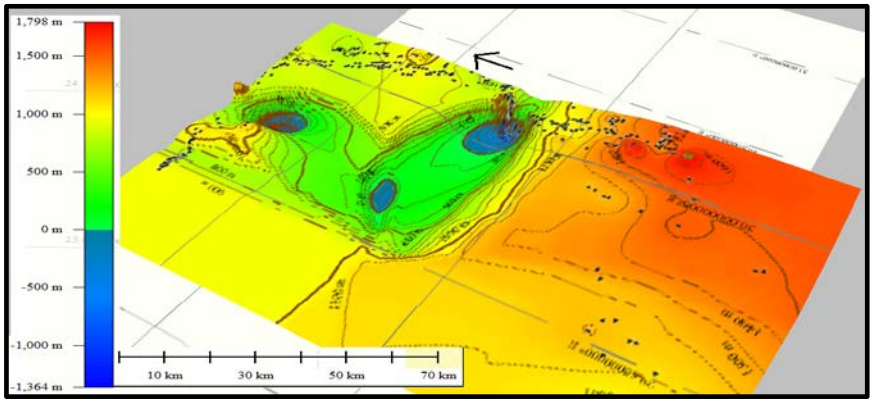

Figure 4.23: Eastern Bushveld structural contour model on the Upper Zone unit top.

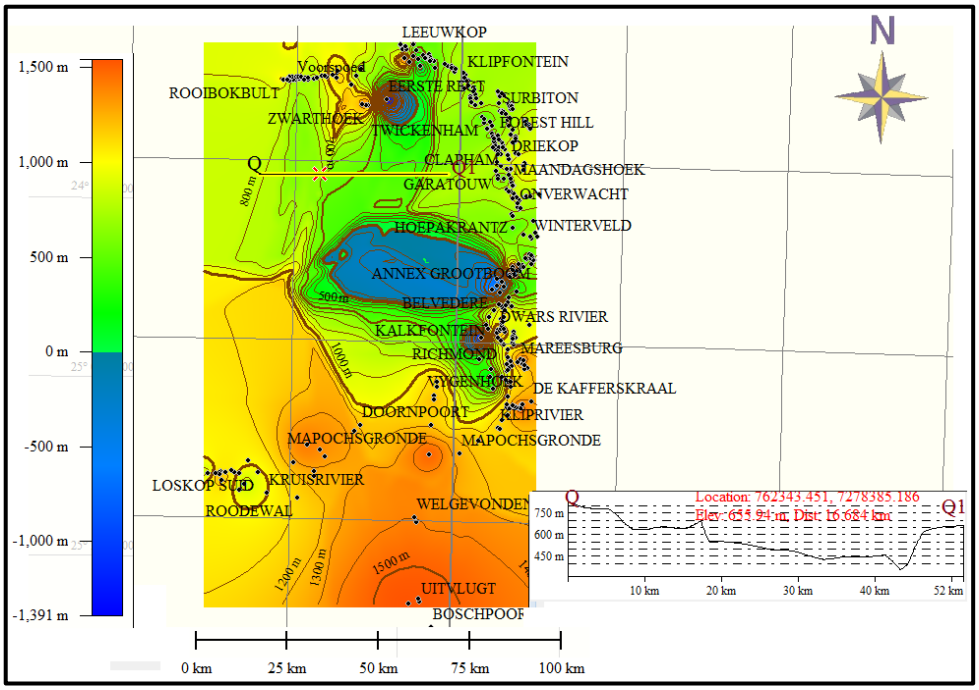

Figure 4.24: Structural contours at the base of Archaean rocks with a profile across line Q-Q1, south of the Wonderkop Fault.

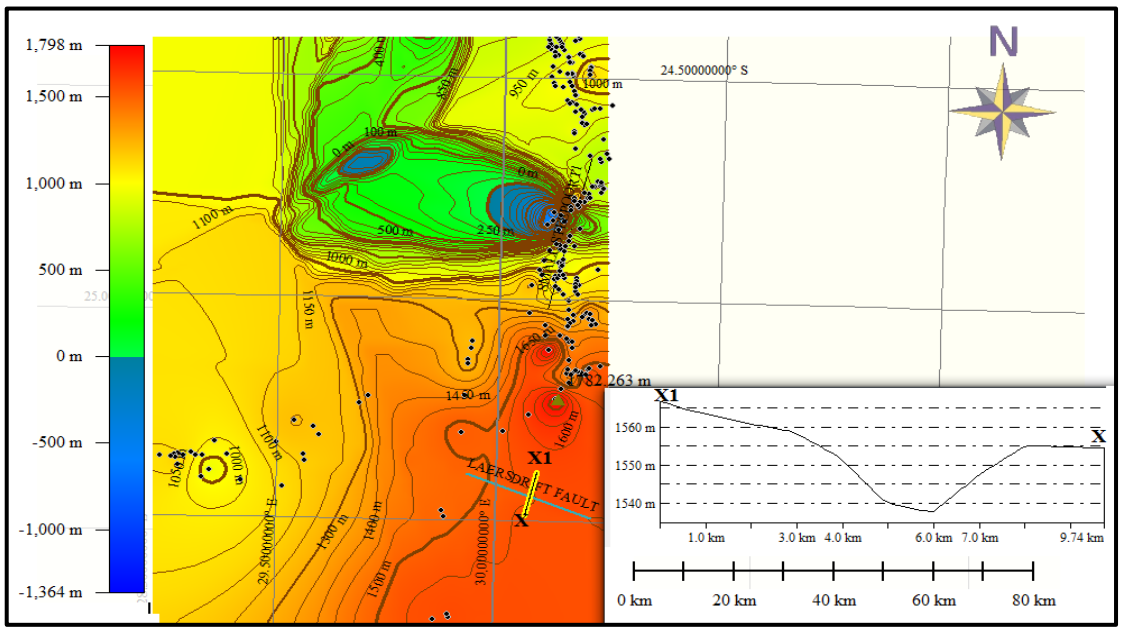

Figure 4.25: Geometry of the Laersdrift Fault at the top of the Upper Zone interval in the eastern limb of the Bushveld Complex.

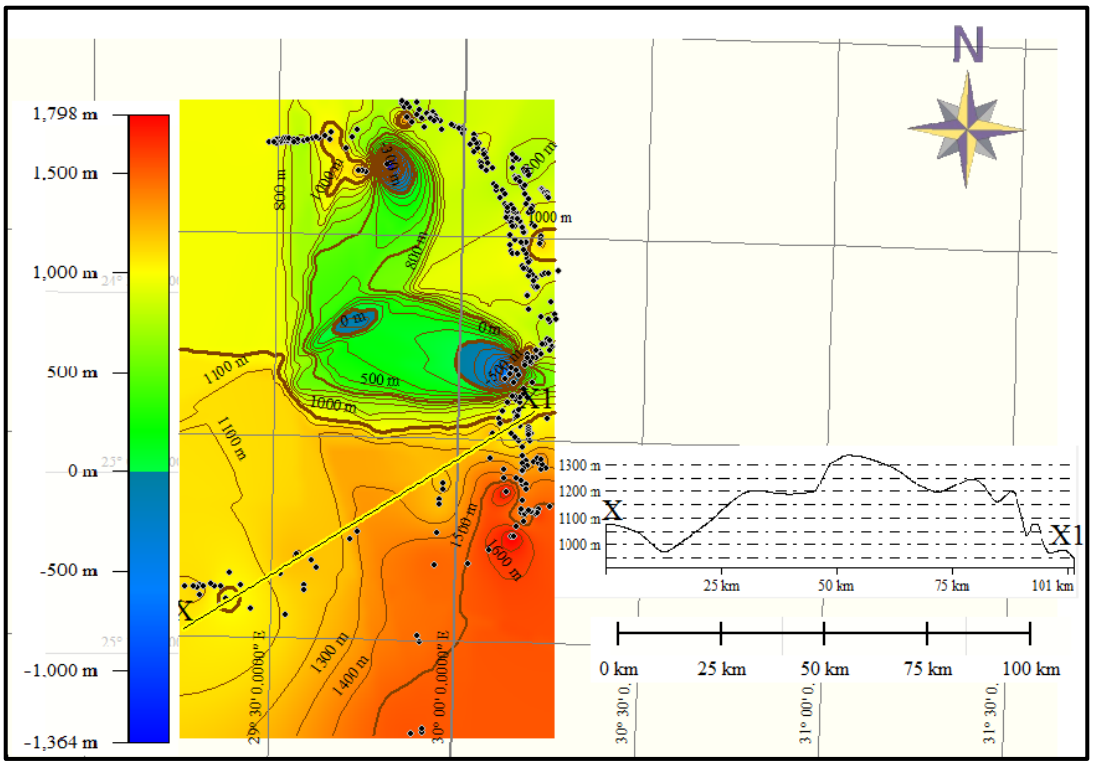

Figure 4.26: Profile X-X1 at the top of the Upper Zone structural contour interval in the eastern limb of the Bushveld Complex

4.6.2 ISOPACH MAPS OF THE EASTERN BUSHVELD COMPLEX

The thickness of the Upper Zone unit in the Eastern Bushveld Complex varies from about 2 m in the northern parts to over 40 m in the south (see Figure 4.27). The isolated (thickness) peaks are arranged in a N-S trending pattern starting from the central part of the Eastern Bushveld to the southern edges.

The Main Zone thickness attained its peaks in the southeastern part of the Eastern Bushveld Complex (Figure 4.28 and 4.29). The central peak has a maximum thickness of over 1000 m and the peaks are arranged in an NNW- SSE trending pattern, with a decrease in thickness towards the west and the northeastern part. Figures 4.30 and 4.31 show the Merensky Reef and Lower Zone isopach maps respectively, with profiles indicating the thickness.

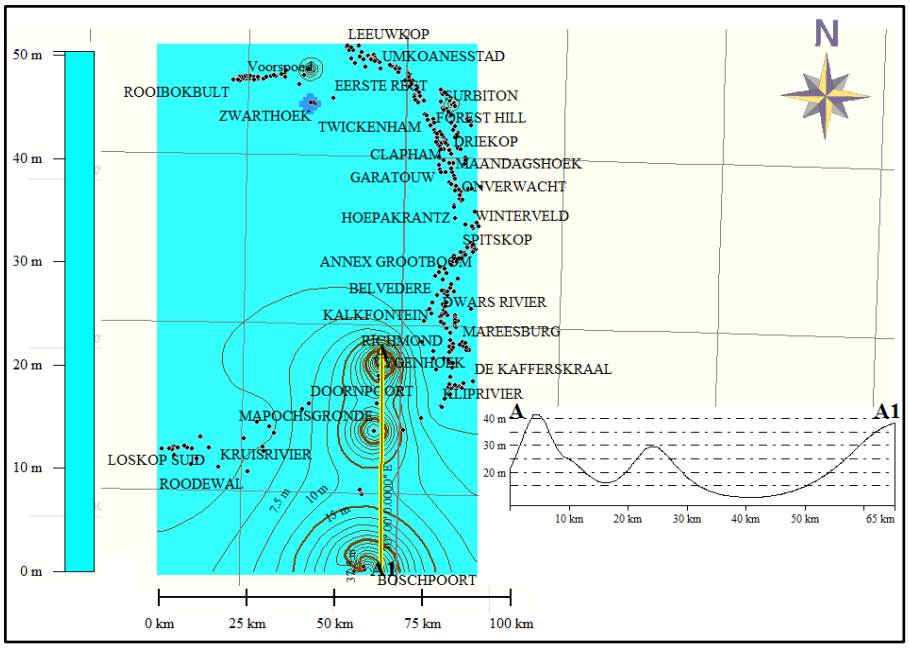

Figure 4.27: The Upper Zone isopach map of the Eastern Bushveld Complex showing an hourglass shape

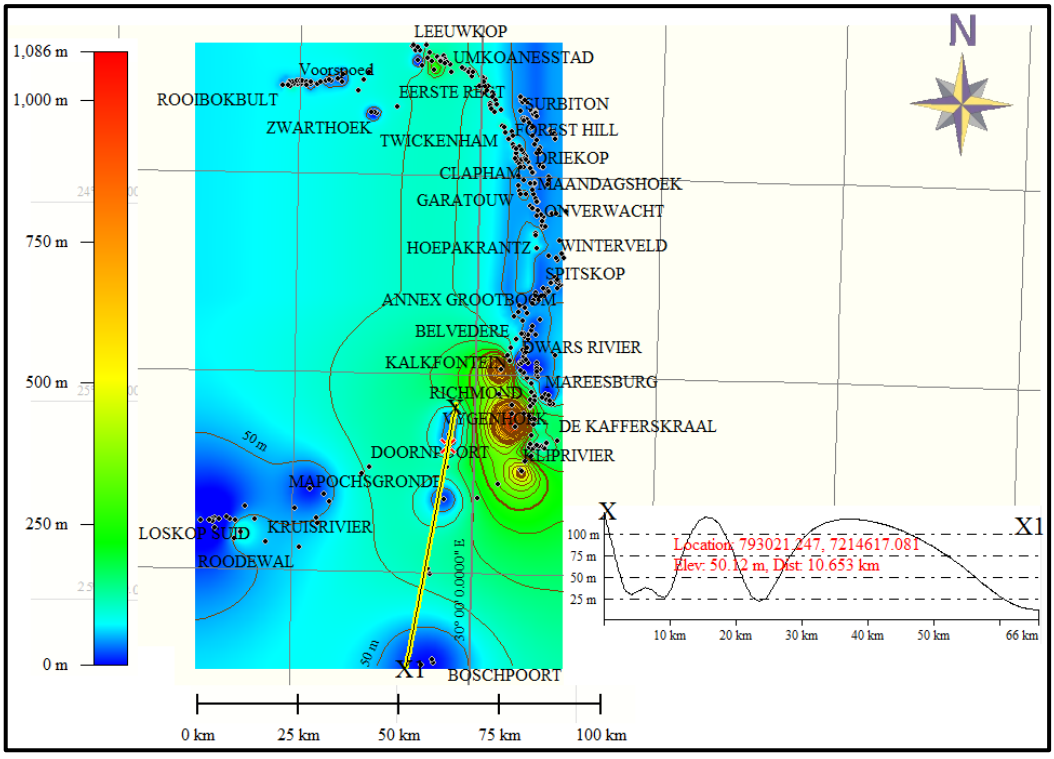

Figure 4.28: The Main Zone isopach map of the Eastern Bushveld limb

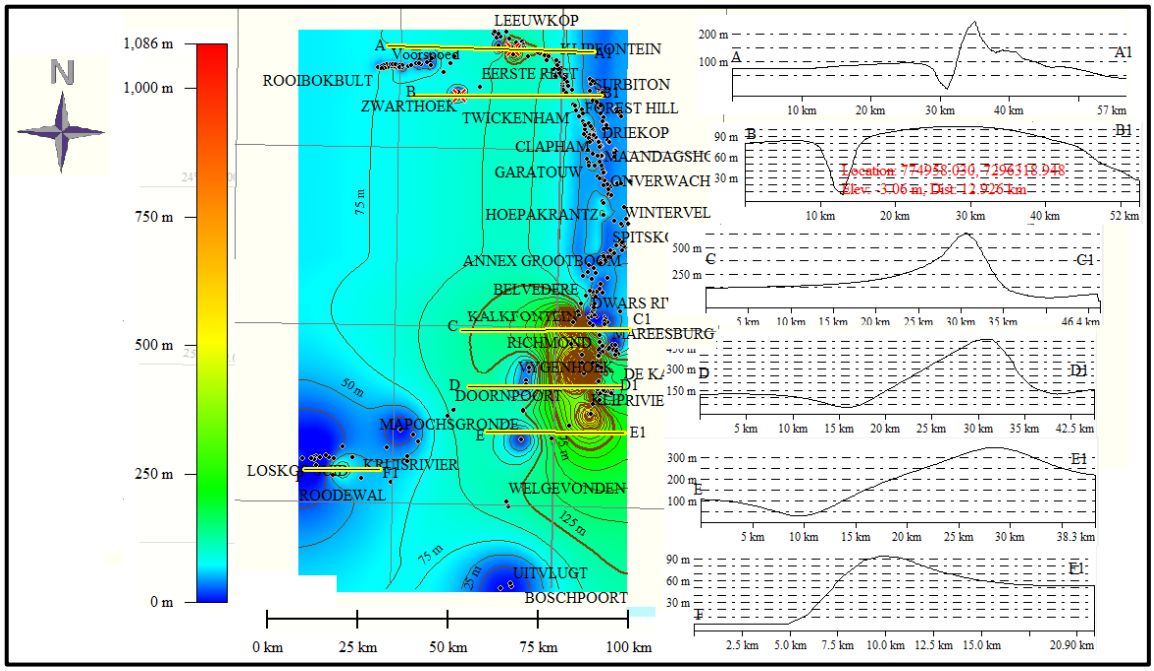

Figure 4.29: Profile on the Main Zone isopach map. Profiles A-A1, D-D1, E-E1 and F-F1 showing downthrow to the west.

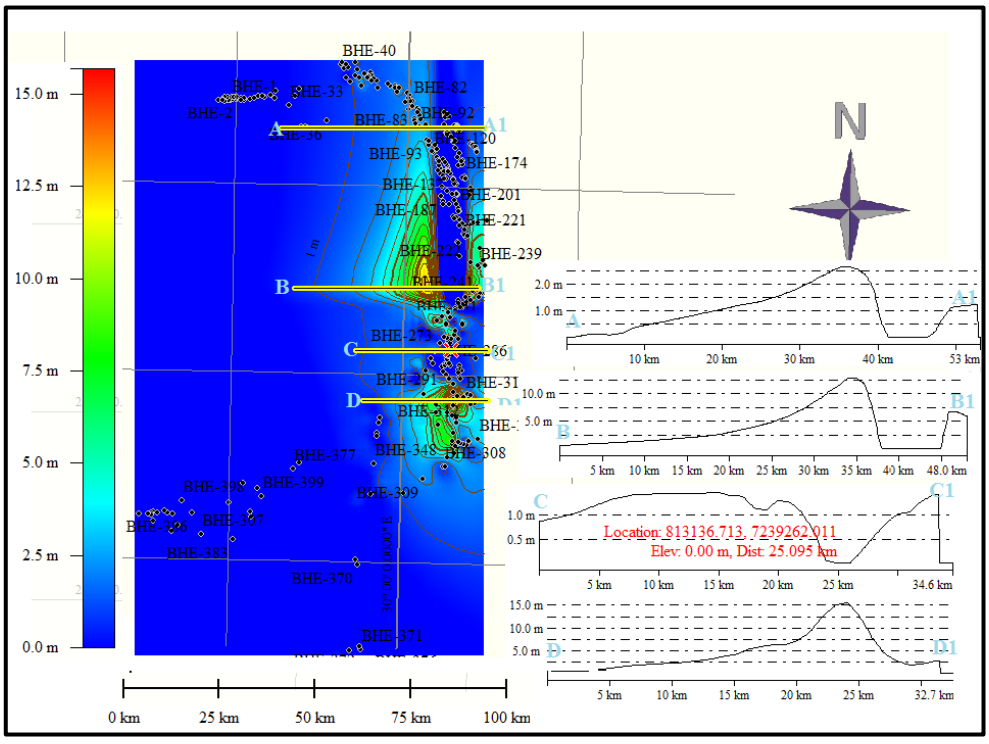

Figure 4.30: Merensky Reef isopach map of the Eastern Bushveld limb showing profiles. Profiles A-A1, B-B1 and D-D1 show downthrow to the east.

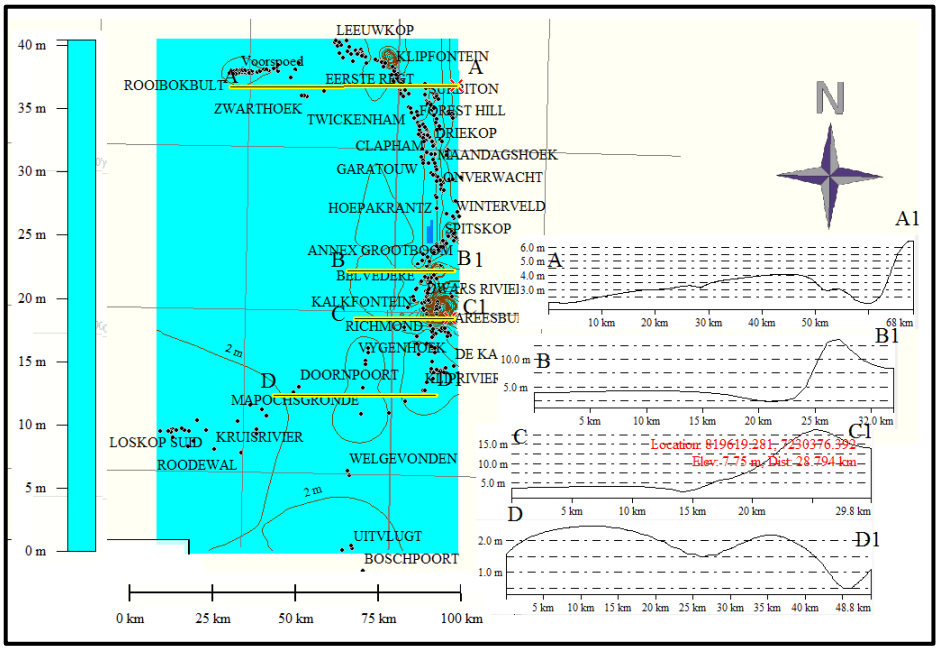

Figure 4.31: Lower Zone isopach map of the Eastern Bushveld Complex with profiles.

4.6.3 SUMMARY OF FEATURES ON EASTERN BUSHVELD COMPLEX.

1. The southern sector is higher than the northern sector (Figure 4.26)
2. The southern sector shows a downthrow to the north at the centre, and to the west (Figure 4.27)
3. The northwestern part dips to the east in a step-like manner
4. A heart-shaped depression (i.e.Kennedy's Vale) dominates the central part of the area.
5. The Laersdrift Fault extends to the NW and terminates at the centre
6. The Lower Zone is more developed in the Groblersdal sector
7. Normal dip and strike slip movements dominate

4.7 NORTHERN BUSHVELD

4.7.1 NORTHERN SECTOR STRUCTURAL CONTOUR MAPS

The pattern on the Upper Zone structural interval (Figure 4.32) is similar to that on top of the Archaean rocks; however, the downthrow to the north is about 150 m. The Main Zone is not well represented in this sector. Structural contours at the top of Archaean granite (Figure 4.33), in the north parts of the Northern Bushveld Complex are mostly curved or

circular in shape and slopes down to the extreme northern edge. The elevation increases gradually to the south, but is interrupted by east-west trending contours close to the northern edge. A profile across the area shows a downthrow of about 60 m to the north (Figure 4.33).

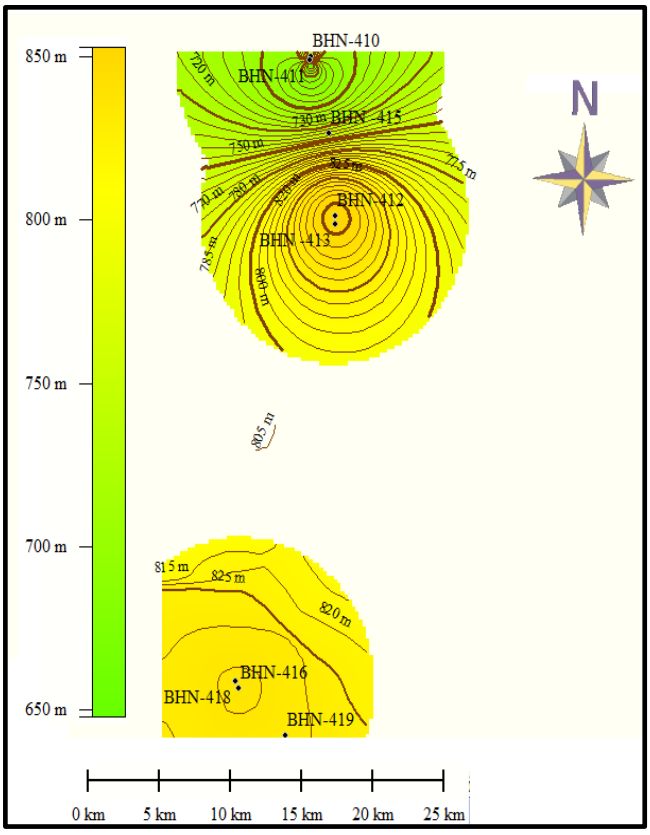

Figure 4.32: Structures on the Upper Zone interval of the Northern Bushveld Complex. The best is to show it on a ~NS section as for Fig. 4.36

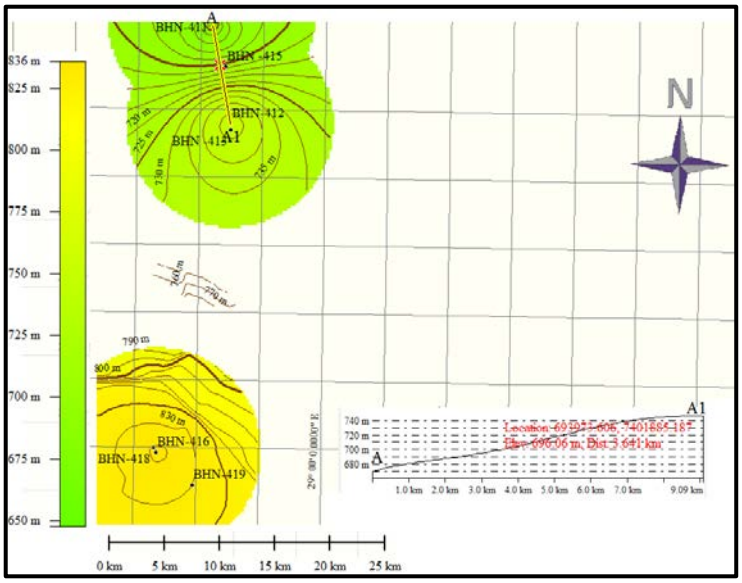

Figure 4.33: Structure at the top of Archaean rocks, north of the Northern Bushveld Complex.

4.7.2 NORTHERN SECTOR ISOPACH MAPS

The Upper Zone isopach map (Figure 4.34) shows that thickness increases northward and thins out southwards. The middle area consist of closely spaced contours oriented almost east-west.

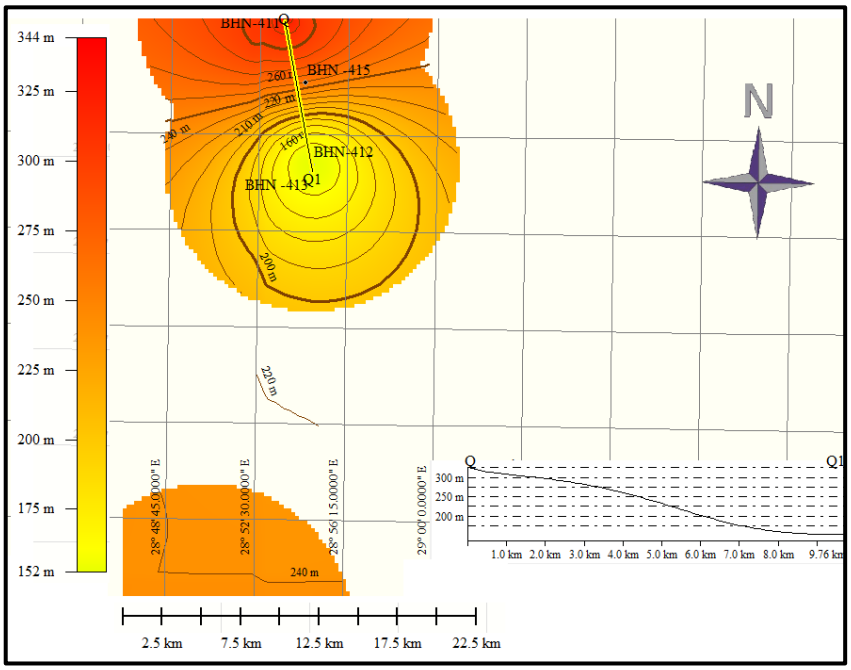

Figure 4.34: The Upper Zone isopach of northern parts of the Northern Bushveld Complex.

4.7.3 OVERVIEW OF NORTHERN SECTOR OF THE NORTHERN BUSHVELD COMPLEX

1. Archaean floor rocks dip to the north.
2. The Upper Zone rocks thicken northwards from the centre; shallow floor enhanced thick accumulation of magma, while high floor permitted thin deposits.
3. This indicates that the Archaean floor rocks must have influenced magma accumulation and also reflect ancient floor rock topographic pattern of this area, with the deep areas receiving more magma influx than the structural high areas.

4.8 SOUTHCENTRAL SECTOR OF NORTHERN SECTOR OF THE NORTHERN BUSHVELD COMPLEX

4.8.1 STRUCTURAL CONTOURS OF THE NORTHERN BUSHVELD SOUTH-CENTRAL SECTOR

Structural contours of Archaean floor rocks of the central-south sector exhibit a very complex pattern. The northwestern part is marked by the presence of a structural low area with steep contours on the southeastern side of the deepening structure and gentle spaced contours on the northwestern side.

The centre of this sector (between Witrivier and Overysel farm) consists of two isolated structure highs, each occurring side by side with a depression (forming an anticline-syncline shaped structure). The sides of each of the structural highs slope steeply towards the depression. The downthrow from the structural high (i.e high relief area) to the depression at the northern end is about 250 m while the southern feature exhibits a downthrow of about 300 m (Figures 4.35 and Figure 4.36). Contours trend along these features (i.e., the structure high and depression) is approximately east-west. The centre of this sector dips sideways. The western side of the sector consists of semi-circular contours representing an undulating surface.

The southern parts of the sector also contain the structural high and adjacent depression structural feature; the structural high is the Tweefontein hill (from a geological map and borehole location correlation) and the adjacent deep structure represents a synformal structure that dips to the southwest. The structure contours between the hill and the depression trend NW-SE and turn southeastwards before finally veering southwards. Contours at the turning plunges southwest and tend to separate the southeastern structure high from the Tweefontein hill.

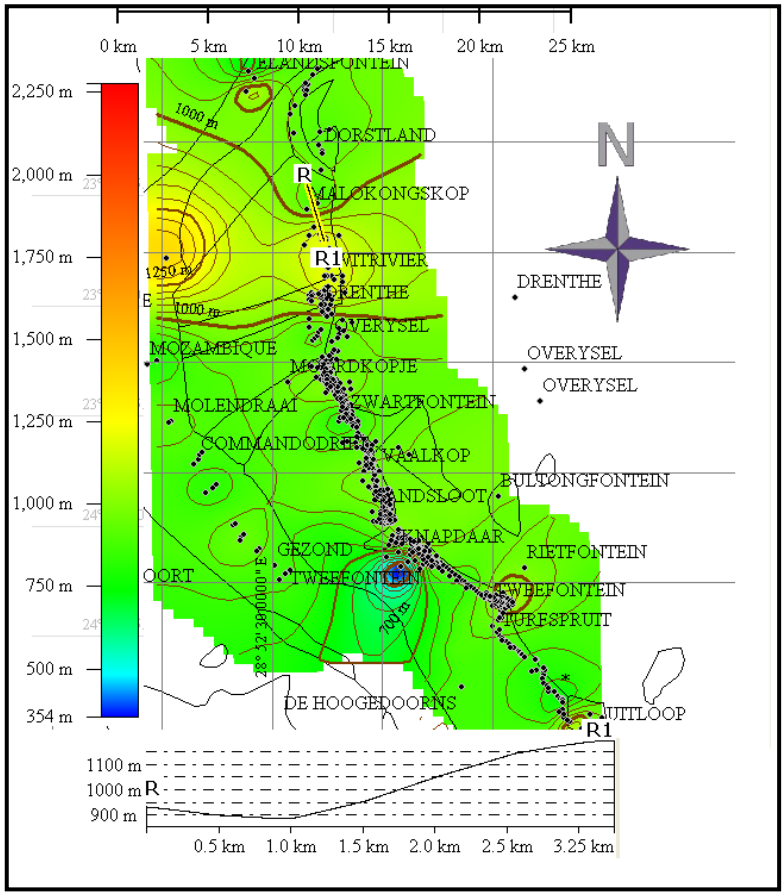

Figure 4.35: Structural contours at the top of Archaean floor rocks of the Northern Bushveld south-central sector.

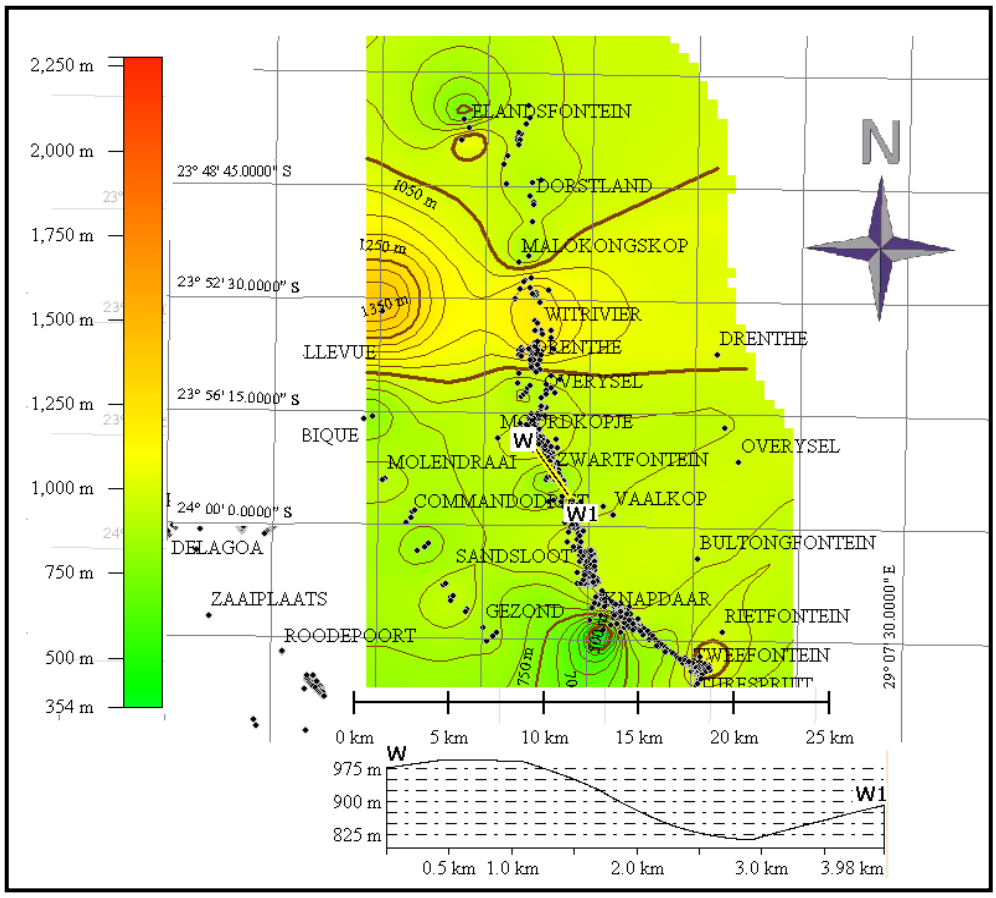

Figure 4.36: Structural contour map on top of Archaean rocks of the Northern Bushveld southern sector with profile W-W1.

While the boundary of the southeastern structure high is marked by closely spaced contours, the northern border has east-west trending close contours and the western side is marked by south verging contours.

Structure contours on the Marginal Zone interval exhibit similar patterns to that of the Archaean rocks interval, however, the structural contours at the base of the Platreef interval is different especially in the northern parts of this area. The contours trend north-south and plunges southwards, later deviates to the southeast. While the central part consists mostly of east-west trending contours interrupted by the presence of an isolated structural high. The structural contour pattern at the southern part of this sector is similar to that on the Archaean rocks and Marginal Zone interval, thus indicating that the southern parts of this section were not affected by significant tectonic activities during the emplacement of the RLS.

The structural contours on top of the Main Zone interval is similar in pattern to that on the Archaean rocks interval in the northern parts, differing slightly in the centre due to the presence of southwest dipping structure in the centre. The contours trend southeastwards at the centre, and bend eastwards around the synformal structure (less than 1000 m deep).The contours maintain a north-south trend in the south adjacent to the southern structural high (about 1180 m high). The structural high at the centre is truncated by east-west trending contours that slope steeply NNW.

The structural contours at the base of the Upper Zone interval closely resemble the pattern on the Main Zone interval. However, the structure contours at the top of the Upper Zone interval differs slightly. At the northern parts a central depression with steep slopes on the western side and gradual slope on the eastern side exists. The southern parts consist of a structural high with downthrow of about 60 m to the north and 40 m to the south. The central part is marked by multiple curved structural contours likely due to compressional movement.

4.8.2 ISOPACH MAPS OF SOUTHCENTRAL SECTOR OF THE NORTHERN BUSHVELD COMPLEX

Archaean rocks are more concentrated at the northern part of this sector based on available data. The thickness varies from about 2 m in the south to over 55 m in the north. Due to paucity of data a detail isopach map for the Archaean rocks cannot be constructed.

Transvaal rocks have a maximum thickness and concentration at the centre and at the southeastern corner of this sector. Marginal Zone rocks are more concentrated at the southern part of the sector with the maximum thickness occurring with a NW-SE trend as indicated in Figure 4. 37.

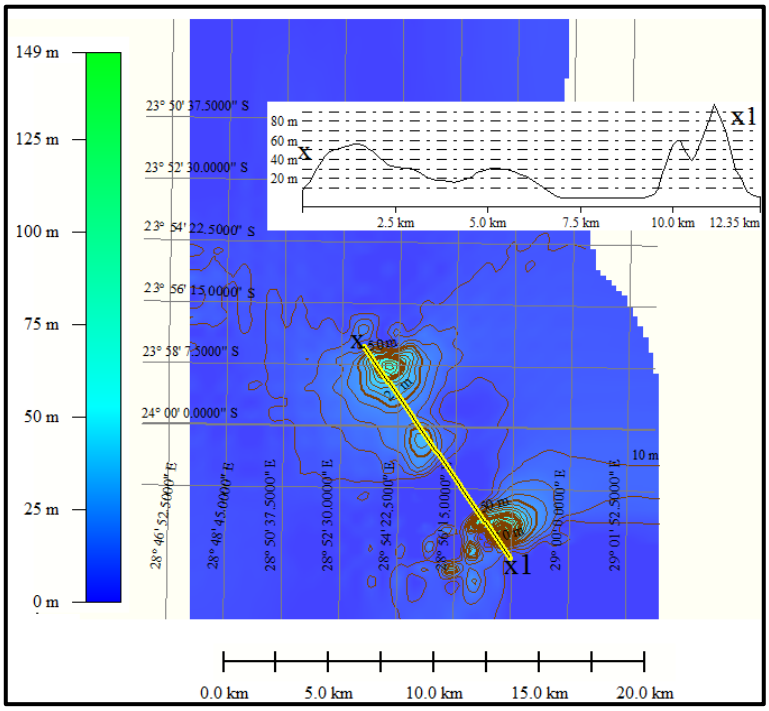

Figure 4.37: Marginal Zone isopach of the Northern Bushveld south-central section of Northern Bushveld with profile X-X1.

The Main Zone isopach map of the central part shows the three zones of thickening: the first is in the northwestern part of the sector with nearly N-S thickening trend represented by wedge shaped contours (Figure 4.38). From this area, the Main Zone thins out eastwards. In the north central part (Witrivier farm) the Main Zone thickness increases gradually towards the south with a thin zone in-between. The second thick zone is located southwards between Overysel and Zwartfontein farms, a steep slope that trends SE marks the boundary between the thin zone to the north and the thick zone to the southeast as shown by profile B-B in Figure 4.38. Tweefontein hill trends NW-SE and defines a narrow zone of thinning with two closures, while the adjacent synformal area marks the maximum thickness zone (Figure 4.39).

Pronounced thickness of the Upper Zone dominates the northern and the western part of this section. The unit thins gradually from the west to east in the south and thins out sharply from the north.

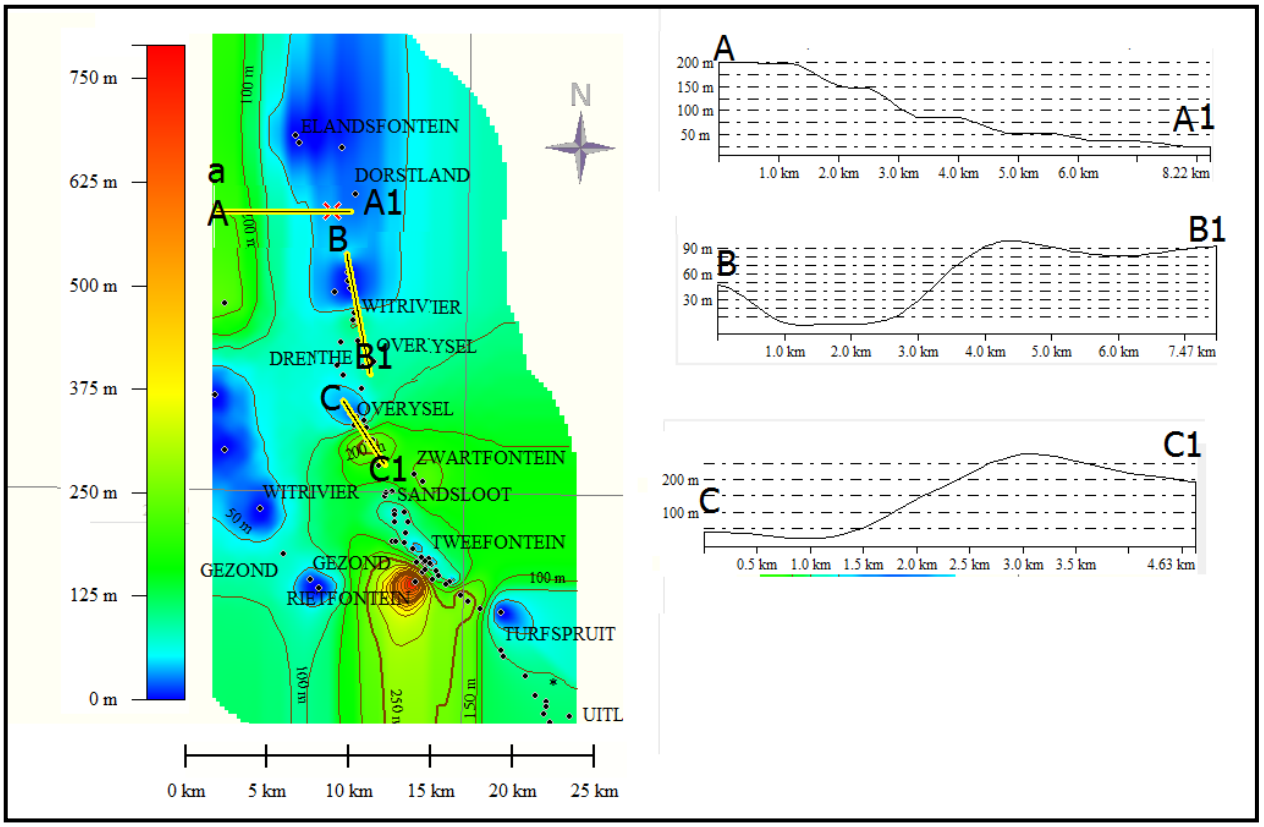

Figure 4.38: The Main Zone isopach of the south central part of the Northern Bushveld Complex showing profile A-A1 with step-like structures Profile B-B1 shows strong thining of the Main Zone around Witrivier area. Profile C-C1 shows graben structure around Zwartfontein farm. The structural high area is about 4 km wide and a height of 1050 m, the shallow area is about 4.4km wide and 250 m deep.

4.8.3 SUMMARY FOR SOUTHCENTRAL SECTOR OF NORTHERN BUSHVELD

1. The Main Zone contours and isopach lines indicate that the northern and southern parts are dominated by N-S trending outcrop.
2. Archaean rocks dominate the northern parts
3. Side by side depression and structural high features (similar to anticline-syncline feature) characterize this sector.
4. The contract between the structural high and depression structures define an east-west trend.
5. Most of the structure contours are not perfectly straight but step-like features were also identified.
6. Tweefontein hill and adjacent depression define a downthrow of over 700 m to the southwest.

7. Archaean floor rocks are more preserved in the northern part than in the southern part of this sector
8. The Marginal Zone seems conformable to the Archaean floor rocks.

4.9 SOUTHERN SECTOR OF THE NORTHERN BUSHVELD COMPLEX.

4.9.1 STRUCTURAL CONTOURS OF THE NORTHERN BUSHVELD SOUTHERN SECTOR

Structural contours of the Archaean rocks in this sector indicate a structural high in the northern part, while the central part is marked by a gentle decrease in elevation, and the southern part is marked by a structural low. Adjacent structural low and structural high features occur on Uitloop (with about 300 m downthrow to the northwest) and Grasvally farm (with over 900 m downthrow to the north).The contour pattern at the base of the Marginal Zone indicates a N-S deepening trend. The northern part reflects a structural high area with circular contours that open to the north and trend NE-SW towards the south. The centre defines a uniformly rising area, compared to the northern part. This area is marked by the presence of a depression and an adjacent hill with steep slopes and a downthrow of about 200 m to the southeast on Uitloop farm (see Figure 4.39). The southern extreme (Grasvally farm) is marked by pronounced deepening (Grasvally structure) with circular contours at its centre and east-west trending contours towards the north. Adjacent to this dipping surface is a structure high that slopes steeply into the deep structure with a down throw of over1000 m to the north as shown in Figure 4.40. Similar structural features also occur at the southwest of the Grasvally structure with a downthrow of over 100 m to the south as indicated in Figure 4.41. The pattern on the Marginal Zone interval is similar to the Lower Zone and the Main Zone interval where the structural high at the north peaks at about 1125 m.

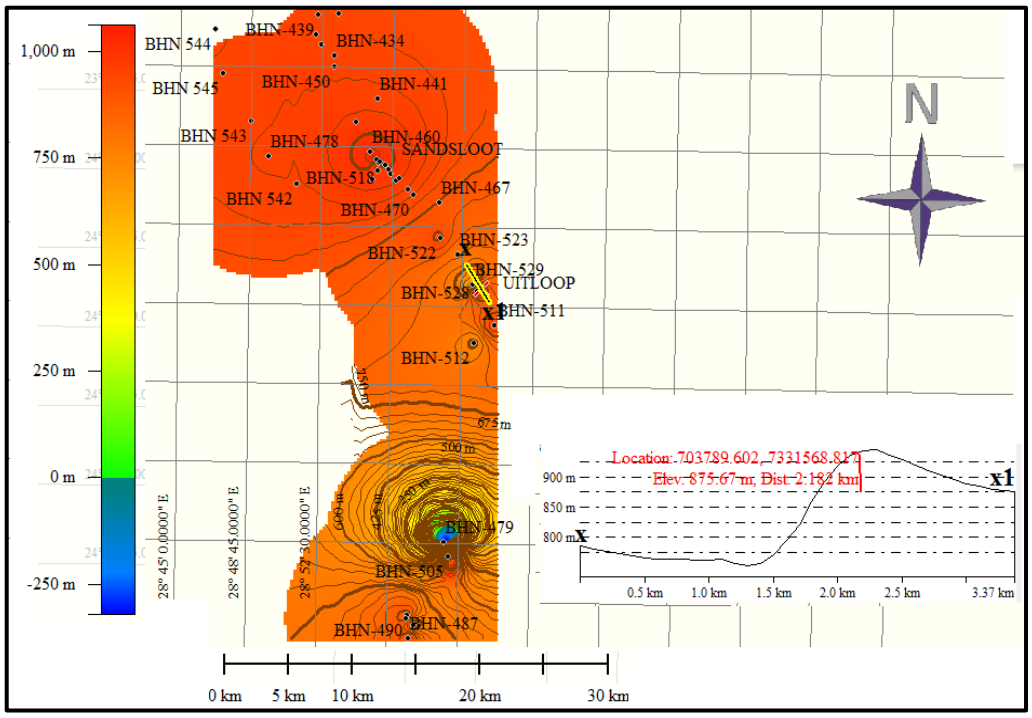

Figure 4.39: Structural contours at the base of the Marginal Zone on the southern sector of the Northern Bushveld Complex with profile showing downthrow to the west.

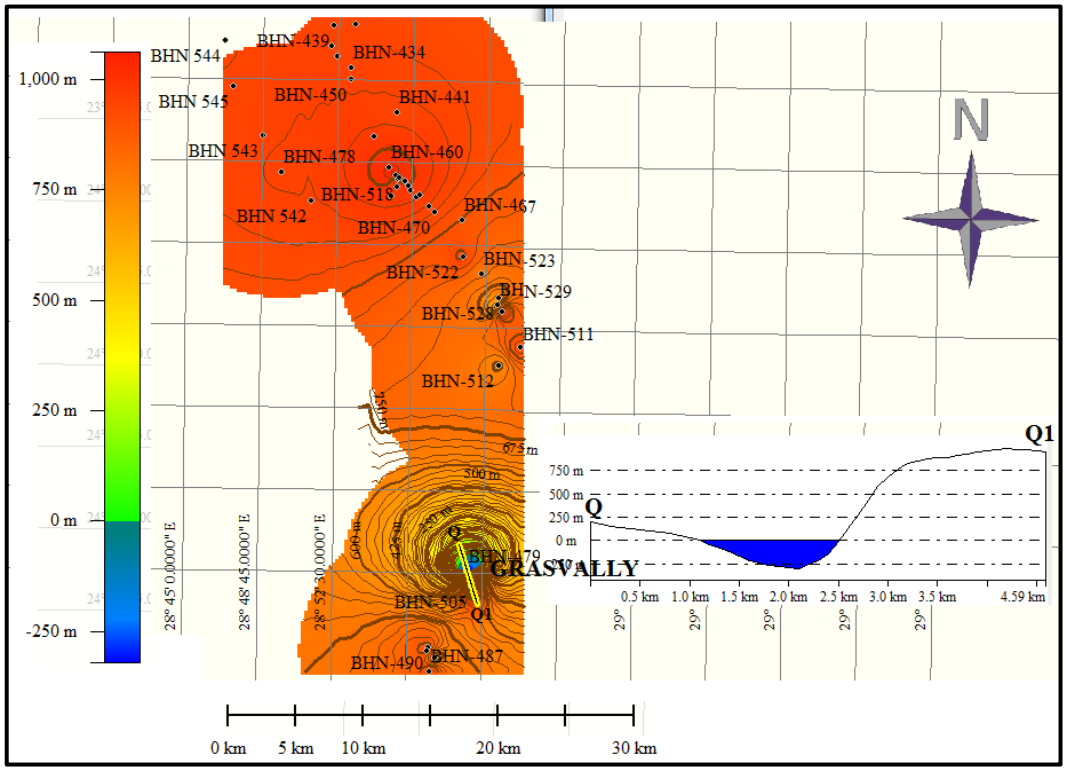

Figure 4.40: Structural contours at the base of the Marginal Zone of the Northern Bushveld southern sector with profile on the Grasvally structure.

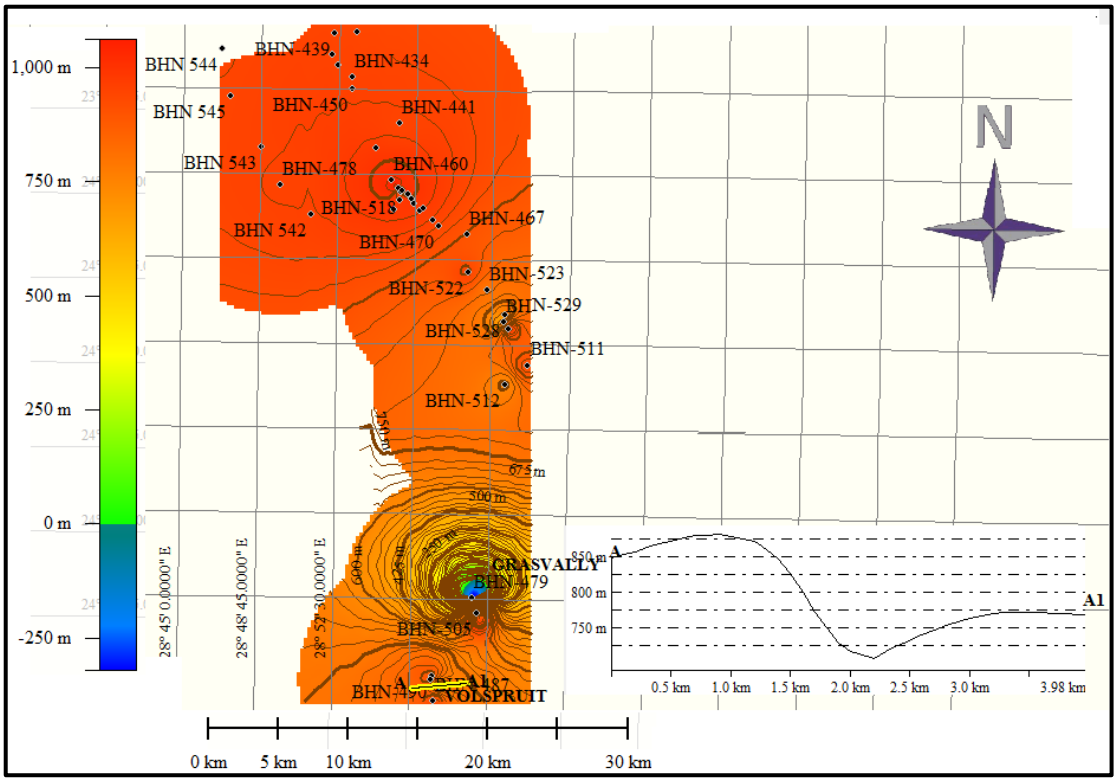

Figure 4.41: Structural contours at the base of the Marginal Zone with profile showing downthrow to the east on Volspruit farm, southern sector of the Northern Bushveld Complex.

4.9.2 ISOPACH MAPS OF NORTHERN BUSHVELD SOUTHERN SECTOR

The Lower Zone isopach map shows southwest thickening in the southern part of this sector, while in the northern parts a SE-thickening trend dominates. Around Uitloop farm in the north a structural feature with adjacent depression and structural high is present as indicated on Profile A-A1 in Figure 4.42. This type of structure is also present at Volspruit farm in the south (profile Z-Z1 in Figure 4.43). Southwest trending contours dominate the steep slope from the maximum thickness area at Volspruit farm into the Grasvally structure.The Marginal Zone isopach indicates a NW-SE thickening trend with a central thin zone between the two thick areas (Figure 4.44).

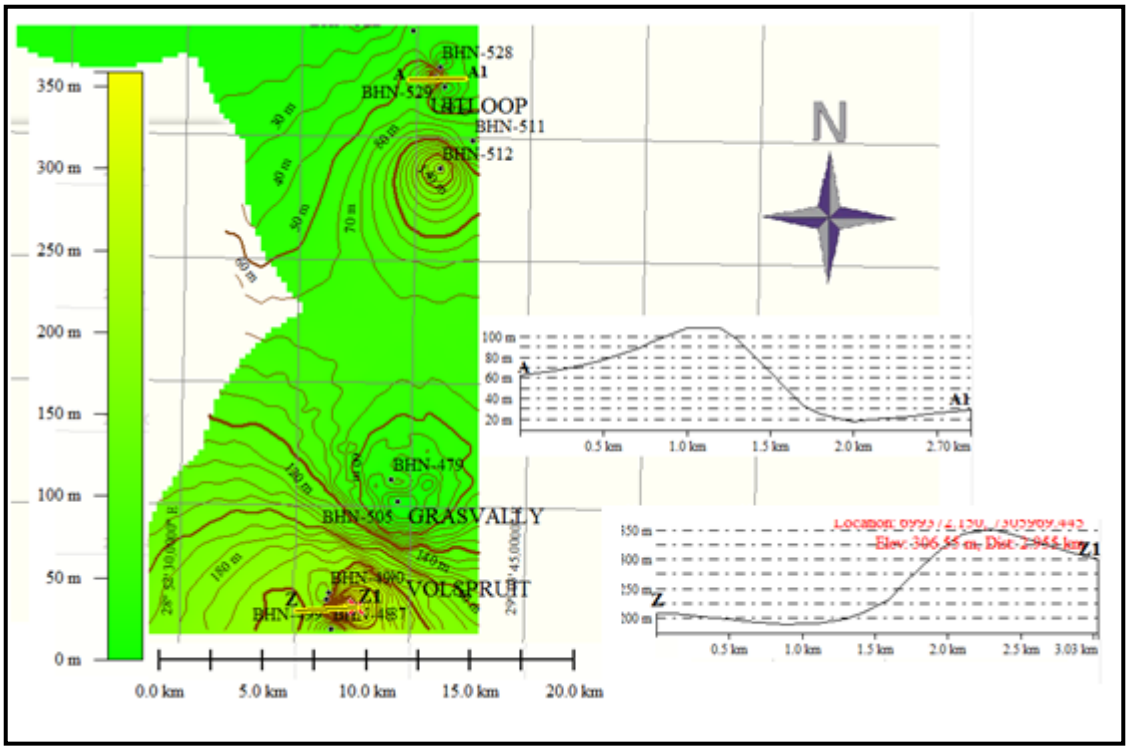

Figure 4.43: Lower Zone isopach of southern sector of the Northern Bushveld Complex profile A-A1 shows the geometry of a fault on Uitloop farm with Profile Z-Z1 across a fault on Volspruit farm

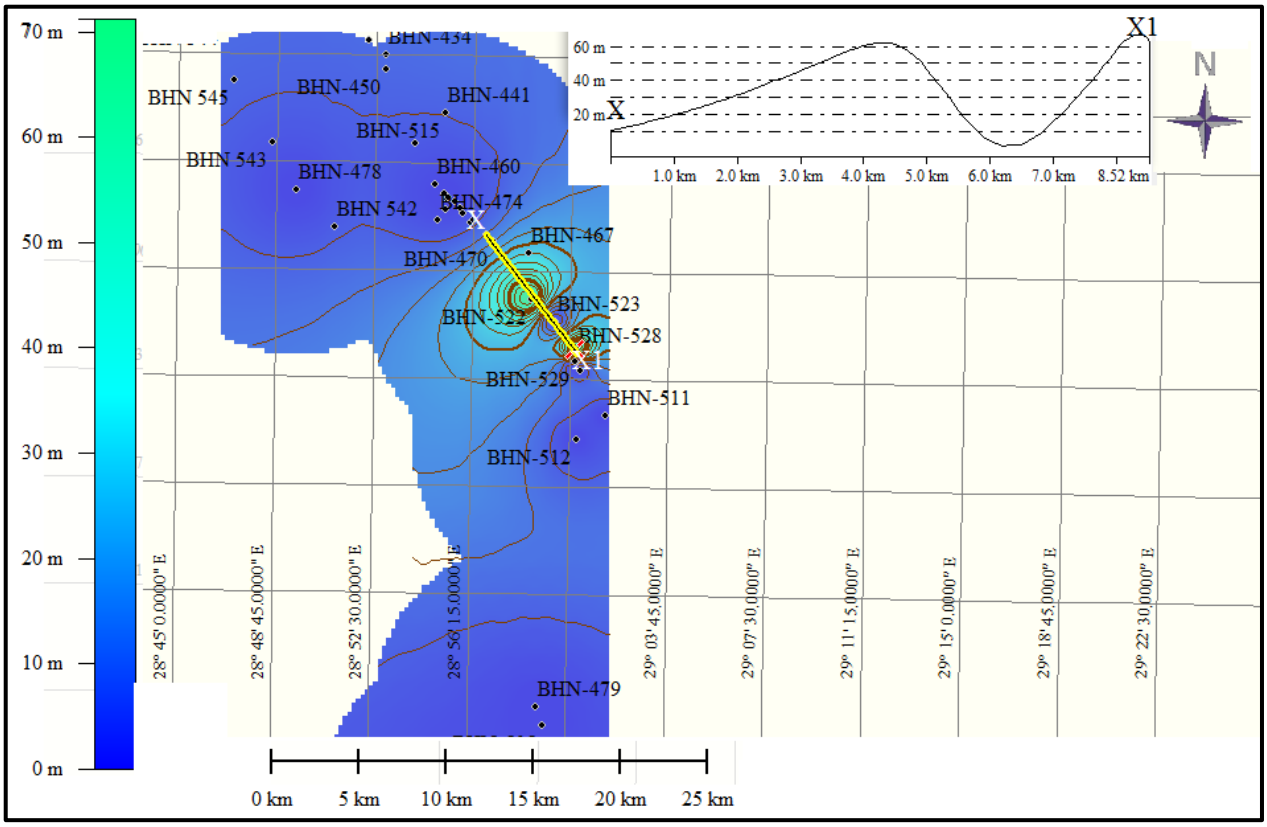

Figure 4.44: Marginal Zone isopach map of the Northern Bushveld southern sector with profile showing the thickness trend around Uitloop farm.

The Main Zone isopach map shows two isolated thin zones in the northern part (Figure 4.45). The northern thin zone, however, thickens to the southeast with the contours trending NE-SW.

The structure contours between the two isolated thin zones trends SW with curves pointing to the NW (Figure 4.45 shows the profile across the NW bend around Uitloop farm, profile X-X1). The southern thin area is adjacent to Grasvally structure and shows a SW thinning. The Grasvally area indicates southeast thickening on the synformal structure, and this is truncated by a structure adjacent to the Grasvally synformal structure. From the northern part of Grasvally, the Main Zone thins out northwards, before being truncated by another thick zone around Uitloop farm where another adjacent depression and structural high is present (Figures 4.45, profile A-A1 around the Grasvally structure).

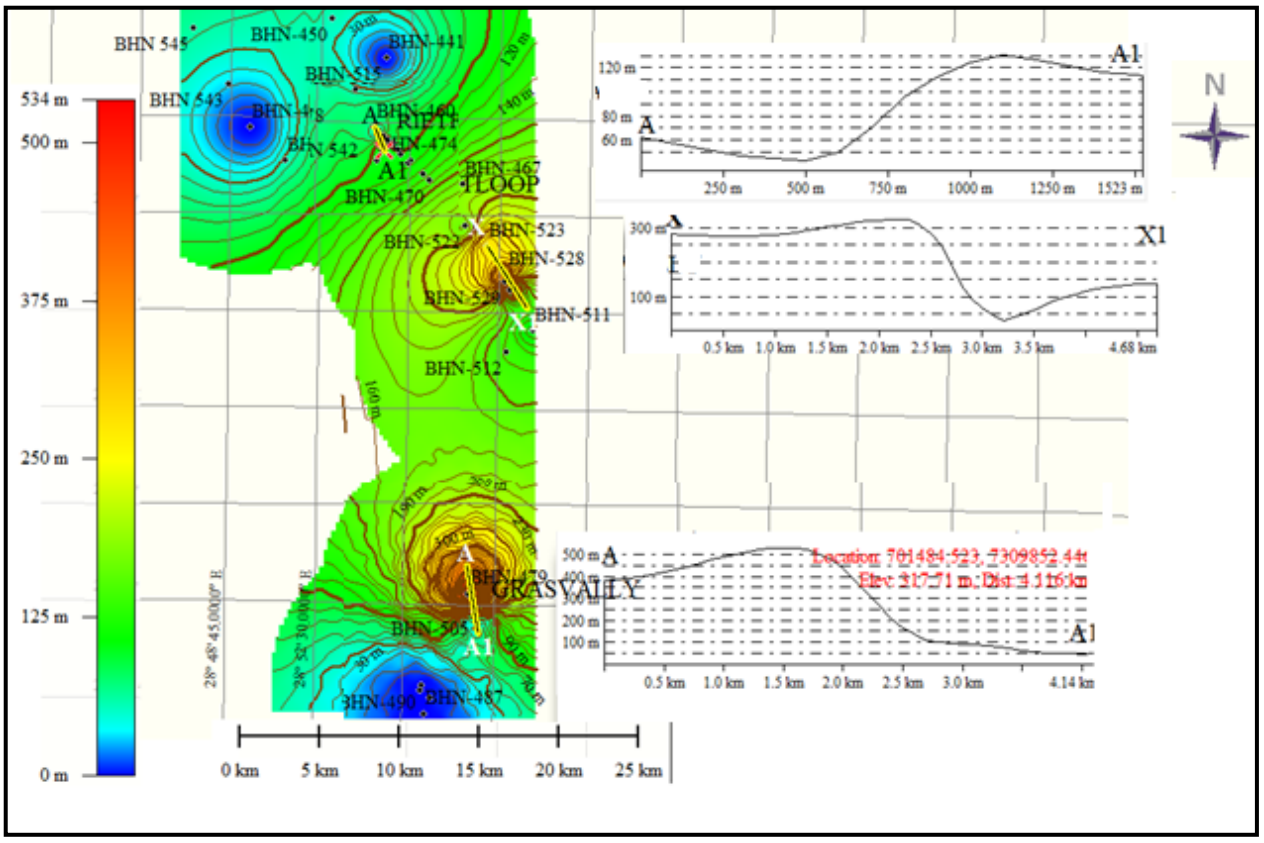

Figure 4.45: The Main Zone isopach map of the Northern Bushveld southern sector with profile A-A1 around the northern part. Profile X-X1 showing structure on Uitloop. The low relief area is about 10 km wide and 200 m deep on the Main Zone structural contour interval, the adjacent structural high is about 1 km wide and 175 m high. Profile A-A1 across Grasvally structure. This structure is about 7 km wide and 500 m deep at the base of the Main Zone interval. It is truncated by a structure that is over 1000 m high.

4.9.3 OVERVIEW OF SOUTHERN SECTOR OF NORTHERN BUSHVELD

1. Structural contour pattern indicates a general N-S deepening trend
2. Depression and adjacent structural high features at Uitloop farm, Volspruit and Grasvally structure show downthrows to the south.
3. Thickness is thin over structurally positive areas, while structural low areas have maximum thickness.
4. Lower Zone rocks thickness increases southwards

4.10 FAR WESTERN BUSHVELD SECTION

Structural contours of the Archaean floor rock are only represented at the centre of the Nietverdiend section appearing circular and open to the west. Structural contours on the Upper Zone down to the Marginal Zone are all open to the west or continue westward Figure 4.46 and 4.47 shows the structure contour map for the Main Zone and the Lower Critical unit respectively.

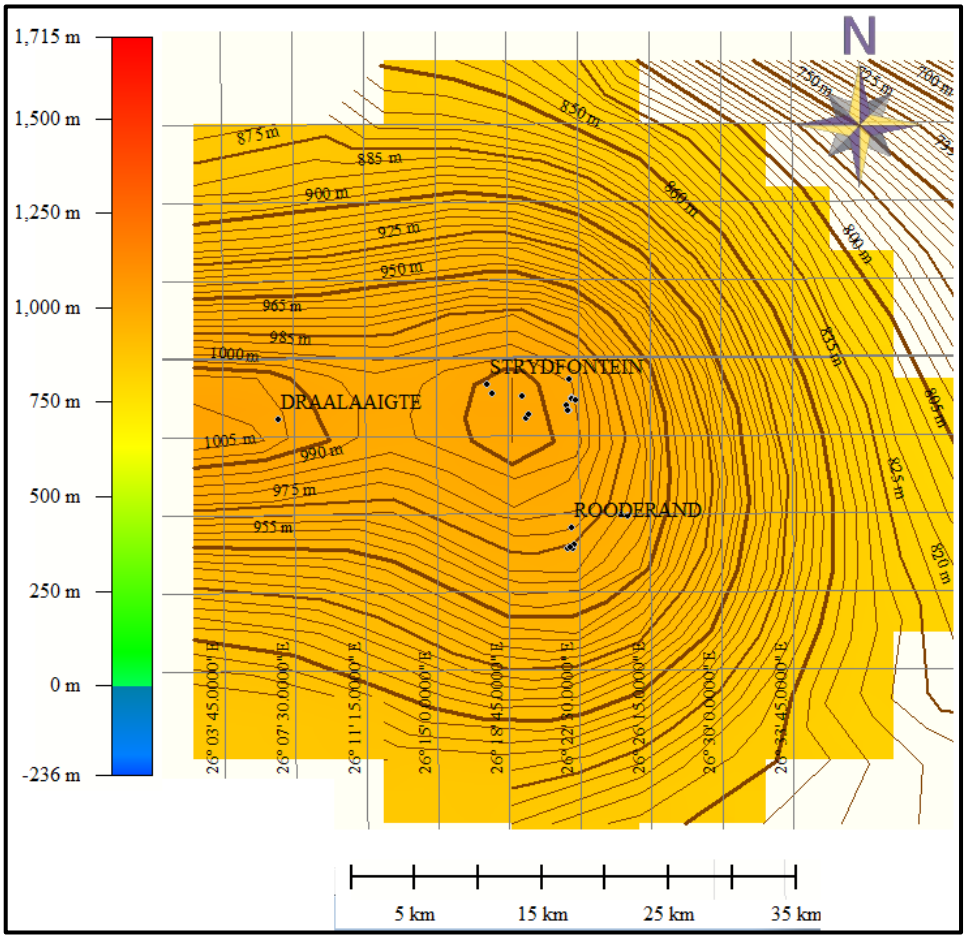

Figure 4.46: Structural contours on the Main Zone interval of the Far Western Bushveld.

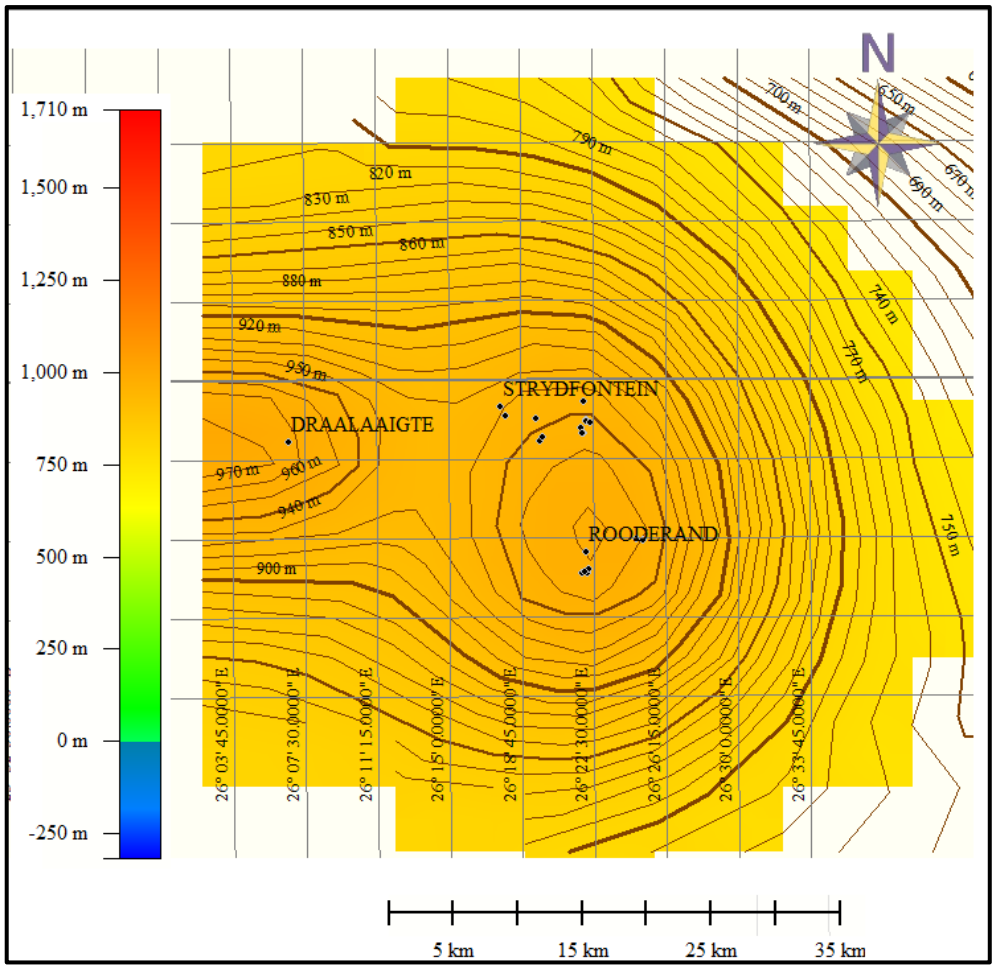

Figure 4.47: Structural contours on the Lower Critical Zone interval of the Far Western Bushveld Complex.

The isopach map for the Lower Critical Zone shows increased thickening from the SE to the NW with a steep thinning between the NW and the SE ends. Figure 4.48 shows the isopach for the Lower Critical Zone and the profile across the section while Figure 4.48 indicates the Main Zone isopach with thickening from the margins to the centre. Figure 4.49 shows the strip log of some boreholes within the area.

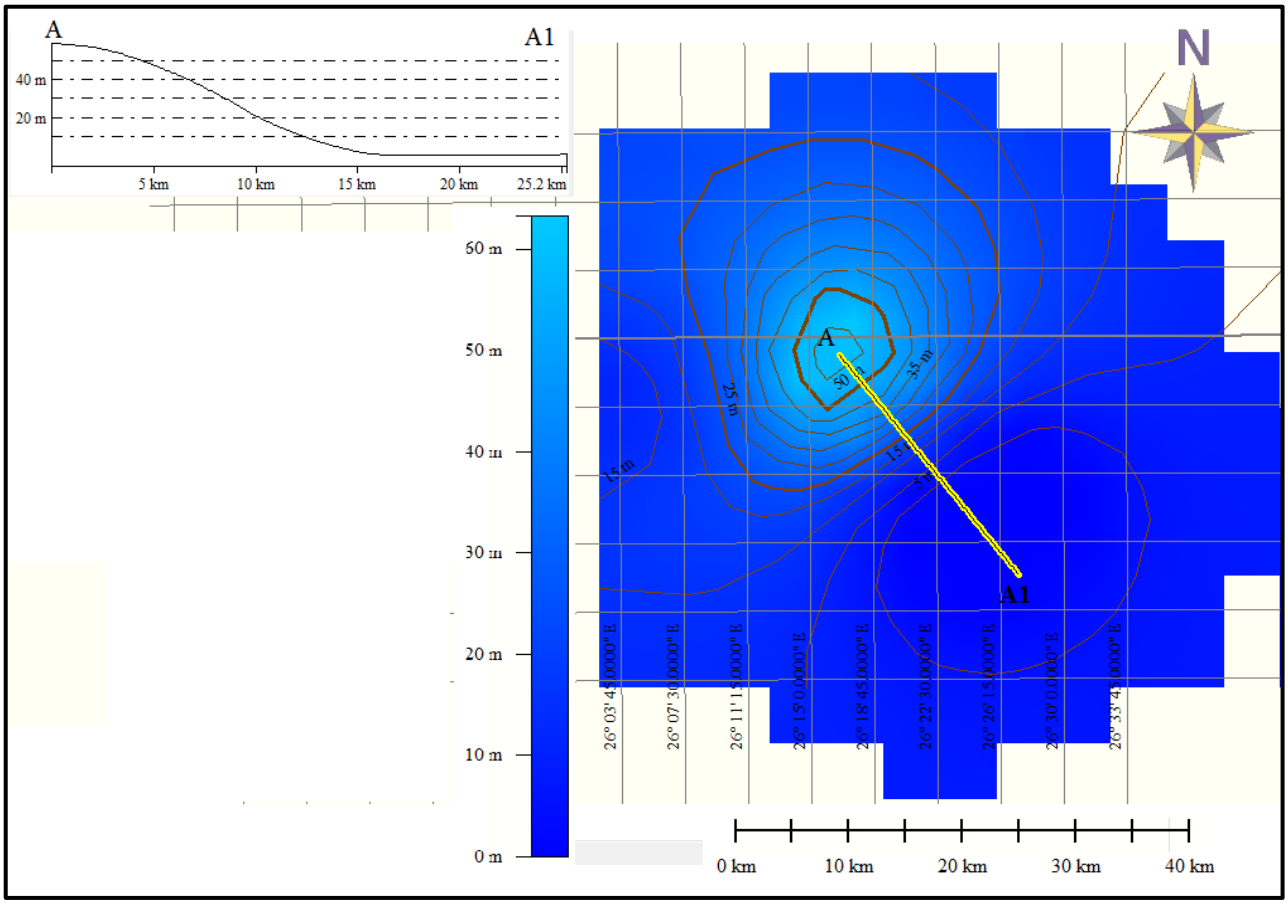

Figure 4.48: Lower Critical unit isopach of the Far Western Bushveld Complex.

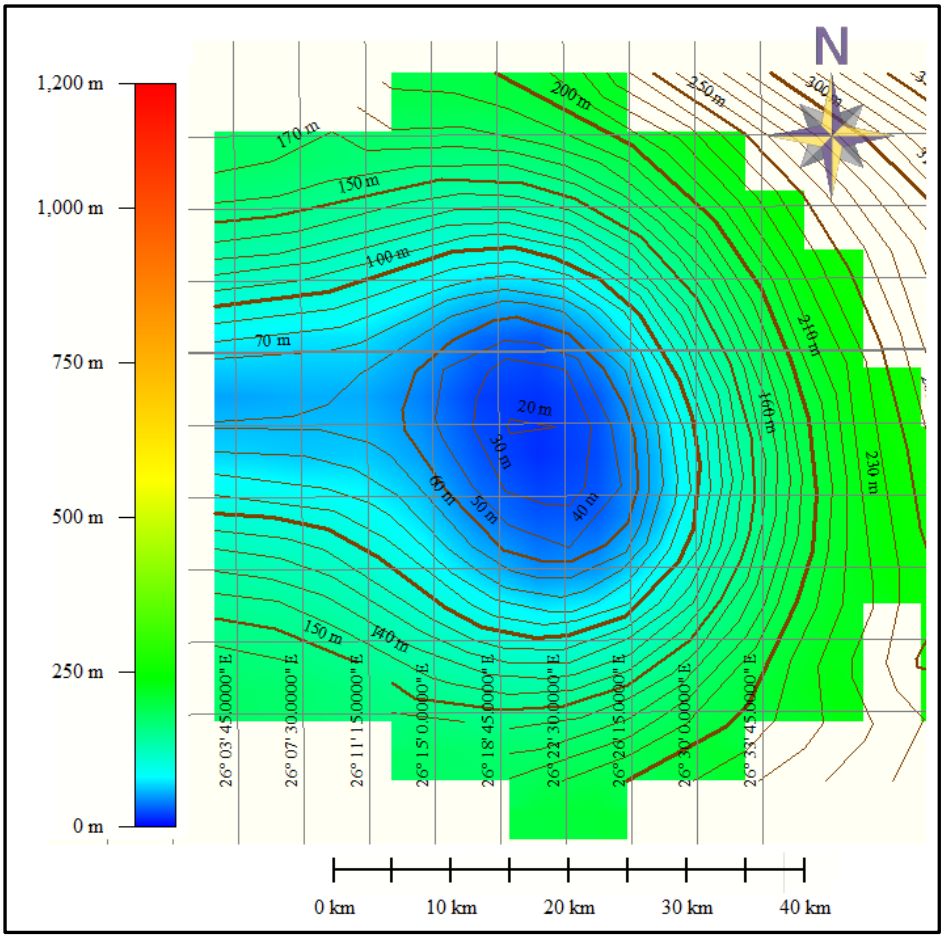

Figure 4.49: The Main Zone isopach map of the Far Western Bushveld.

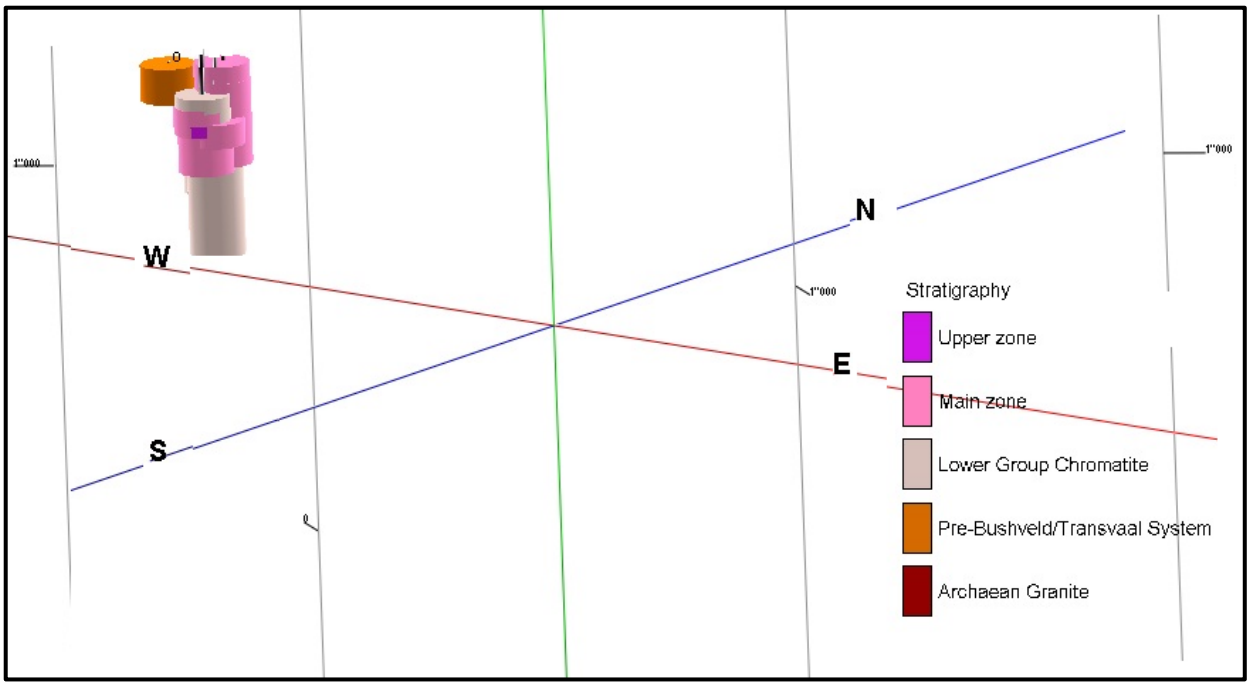

Figure 4.50: 3D borehole strip log in the Far Western Bushveld area.

4.10.1 OVERVIEW OF FAR WESTERN BUSHVELD COMPLEX

1. The opening to the west of most of the structural contours and isopach lines show that this section might extend to the west.
2. No structural feature that could have disturbed the normal deposition model was identified.

4.11 FAR NORTHERN BUSHVELD COMPLEX

This area is dominated by rocks that belong to the Main Zone stratigraphic unit. The structural contours at the base of the Upper Zone interval increase from NW to SE (see Figure 4.51), while the structural lines at the base of the Main Zone interval increase from SE to NW (see Figure 4.52). Isopach lines on the Main Zone interval trend NE (see Figure 4.53); however, the thickness increases from NW to SE.

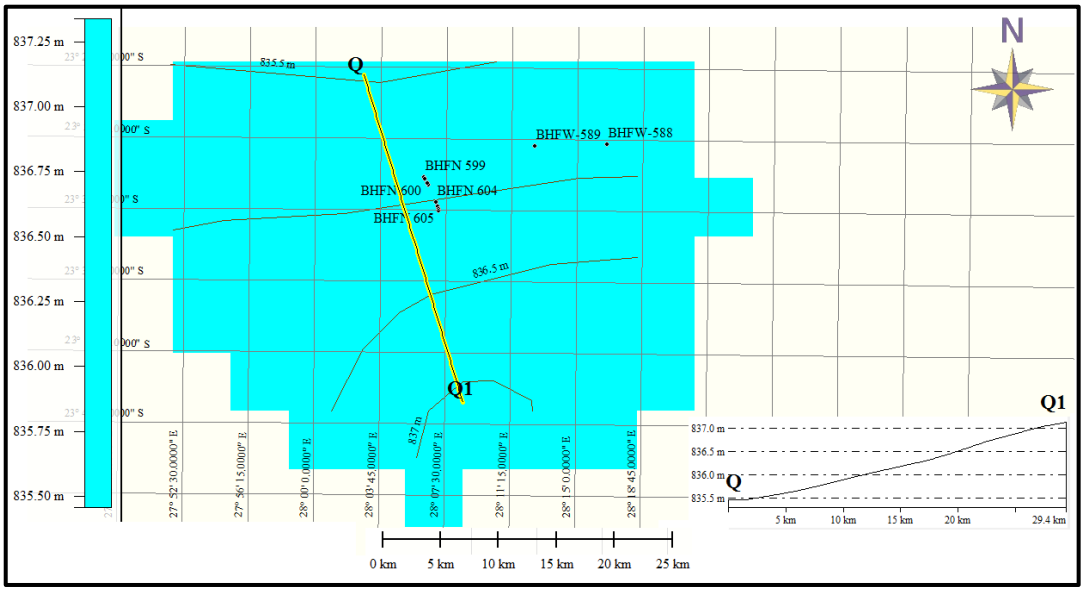

Figure 4.51: Structural contours at the base of the Upper Zone in the Far Northern Bushveld Complex.

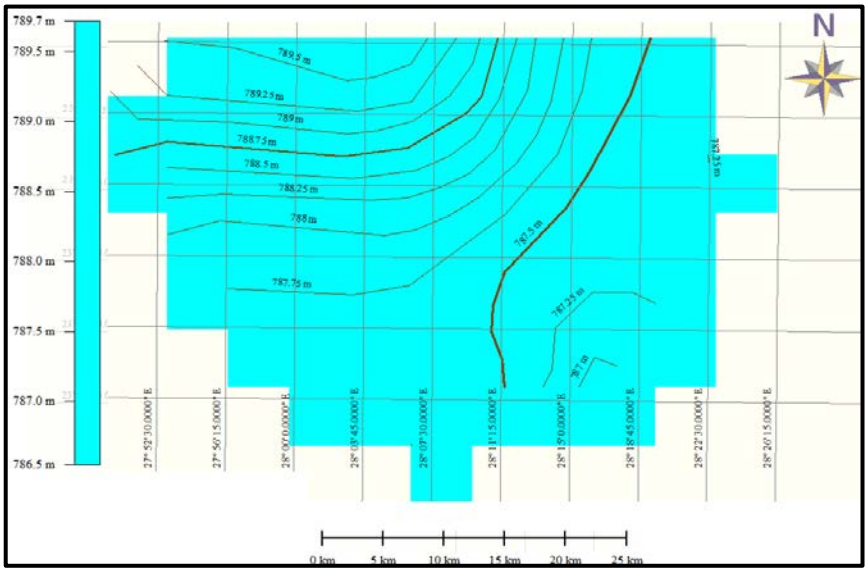

Figure 4.57: Structural contour pattern at the base of the Main Zone interval of Villa- Nora area (Far Northern Bushveld Complex)

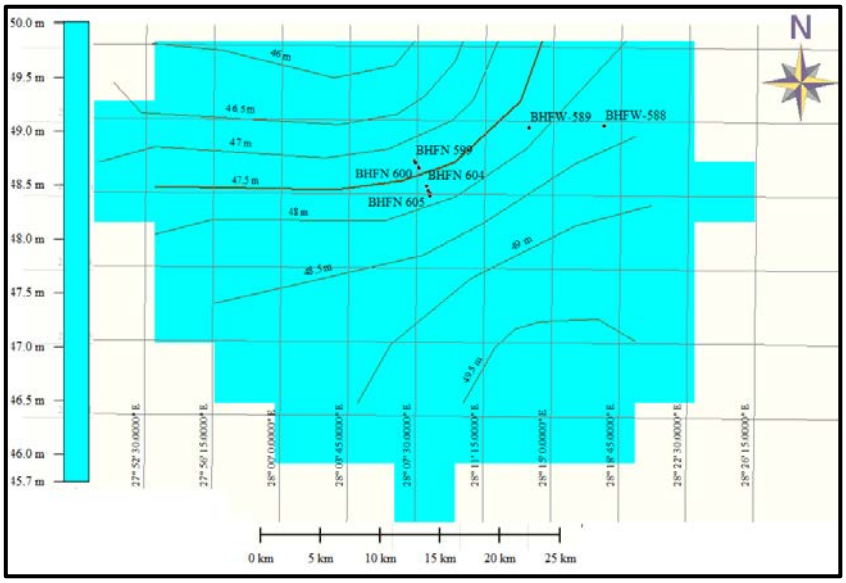

Figure 4.52: The Main Zone isopach map of the Far Northern Bushveld or Villa-Nora.

GENERAL OVERVIEW

Abrupt termination of thickness may be due to the presence of faults and these are further probed by drawing a profile across such features to reveal their geometry.

Deposits thicken towards their source: It might be common knowledge that the magma source is closer where the Main Zone is thickest. However, the concentrations of economic zones are also controlled by structure.

CHAPTER 5 GEOMETRY OF RLS ROCKS ACROSS THE BUSHVELD COMPLEX

5.1 CHAPTER INTRODUCTION

This chapter presents the results of the borehole data analysis on a regional scale by examining the geometry of each stratigraphic unit using interval structure contour and isopach maps. Major structural features were also identified from the study of interval isopach maps, which also aided in classifying the feature into pre-, syn- and post-Bushveld ages. The study allows the structural and geometric investigation of large areas and stratigraphic intervals with relative rapidity and accuracy. Better appreciation of the Bushveld Complex, especially the Rustenburg Layered Suite (RLS) rocks were gained. This understanding will assist with a better appreciation of the subsurface geology and could aid in investigation of special geologic problems in this area.

This discussion will be based on unit-by-unit investigation of the major stratigraphic units starting with the youngest to the oldest as reported in the borehole log record.

5.2 THE OVERBURDEN

Karoo sediments, sand, clays and overburden rocks were classified together as Overburden rocks. These rocks are not present in most places where the topmost stratigraphic unit is exposed. However, percussion drilled sites were not considered. The layer is also very thin in most places and not geologically important except for the benefit of Mine planning or exploration. Figure 5.1 reveals the elevation at the top of the overburden which ranges from 1600 m to 200 m. Highest and lowest elevations were recorded in the Eastern Bushveld. The highest ground elevation occurs in the southern and southeastern part of the Eastern Bushveld while the lowest ground elevation was recorded in the central part of this complex. The overburden is very thin or absent in most parts of the Eastern Bushveld. The ground elevation in the Northern Bushveld ranges between 1000 m and 1100 m. Around Villa-Nora, the elevation varies from 1000 m at the eastern edge to 850 m at the centre.

Overburden thickness is less than 10 m in most parts of the Northern Bushveld except around Tweefontein farm where the thickness increased to over 35 m with a NE-SW trend. Ground elevation in the Western Bushveld varies from 900 m in the northwestern part to 1200 m in the southwest. However, overburden thickness in the Western Bushveld is usually less than 1 m except for the northwestern edge where it increased sharply to about 10 m.

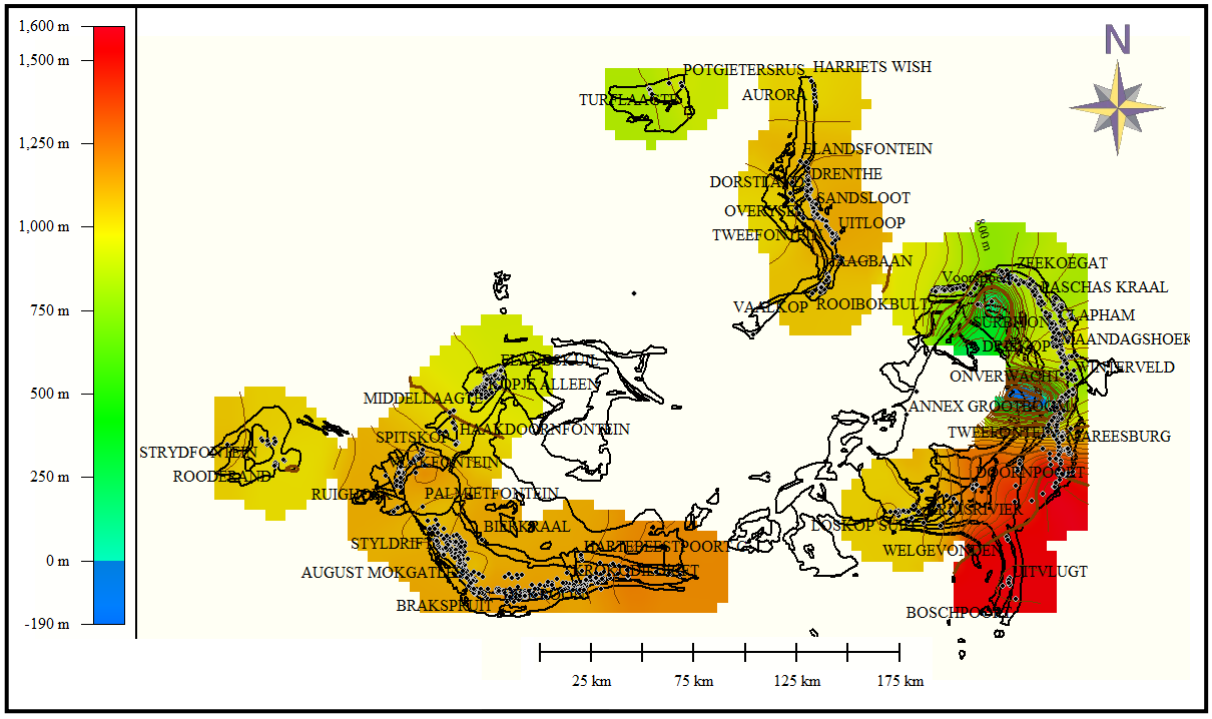

Figure 5.1: BIC Overburden top structure contour interval using the Kriging interpolation method

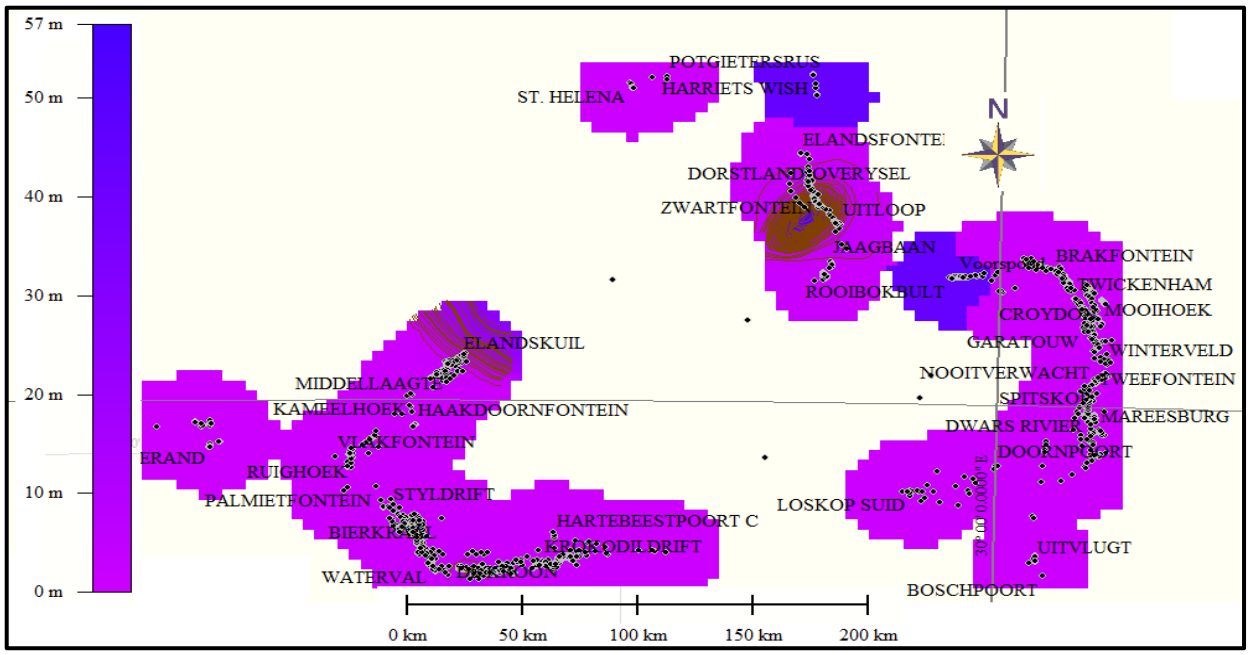

Figure 5.2: BIC Overburden isopach map with farm names.

5.3 THE POST-RLS STRATIGRAPHIC UNIT

This unit consists mostly of Pilanesberg Complex rocks which are located at the central part of the Western Bushveld (Figure 5.3 and 5.4) as a circular shaped outcrop and consist of tuffs, foyalites and 'Lava'. At the Bierkraal farm (southeastof the Pilanesberg Complex) the litho-stratigraphy consist of chromitite, pyroxenites and norites at the top and further down the lithology changed to granites and granophyres underlain by quartzites, while towards the end the lithology changed again to ferrogabbro and magnetite-rich gabbro and extends to the east. On the isopach map in Figure 5.4 the rocks have a NNW orientation.

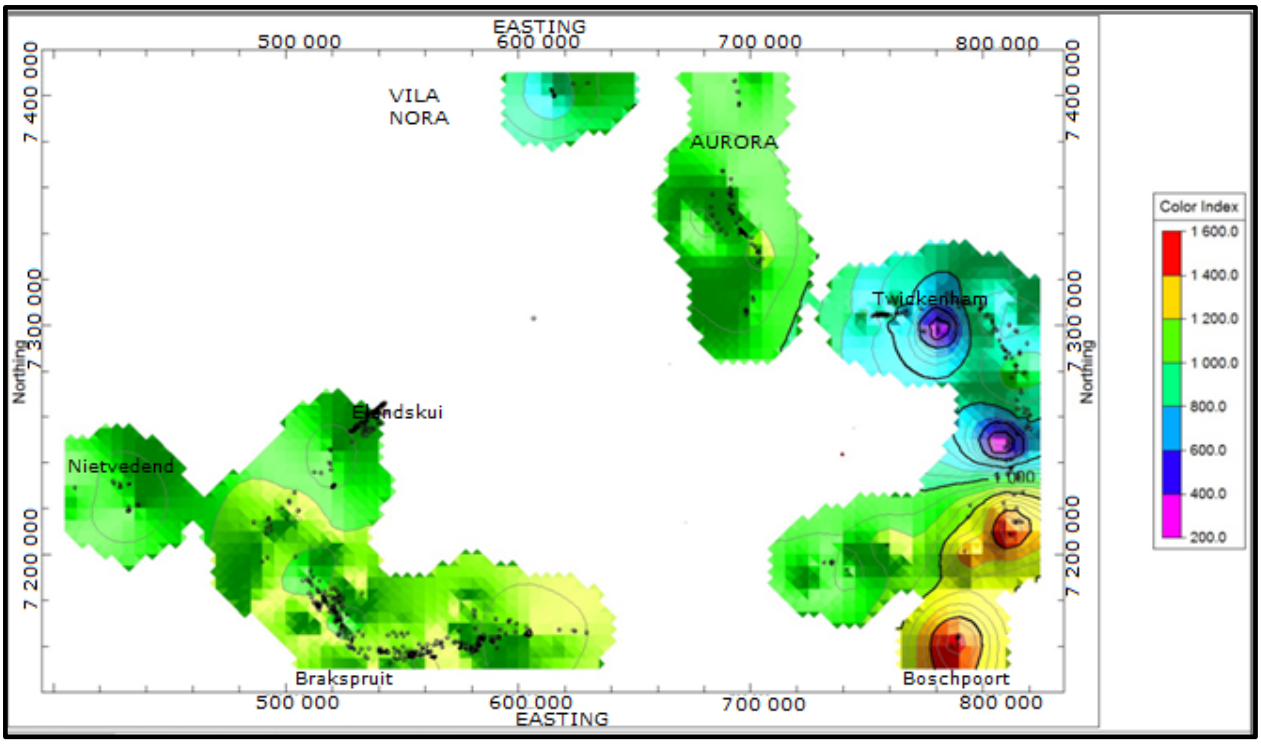

Figure 5.3: 2D Grid model map of Post RLS top using the Kriging method

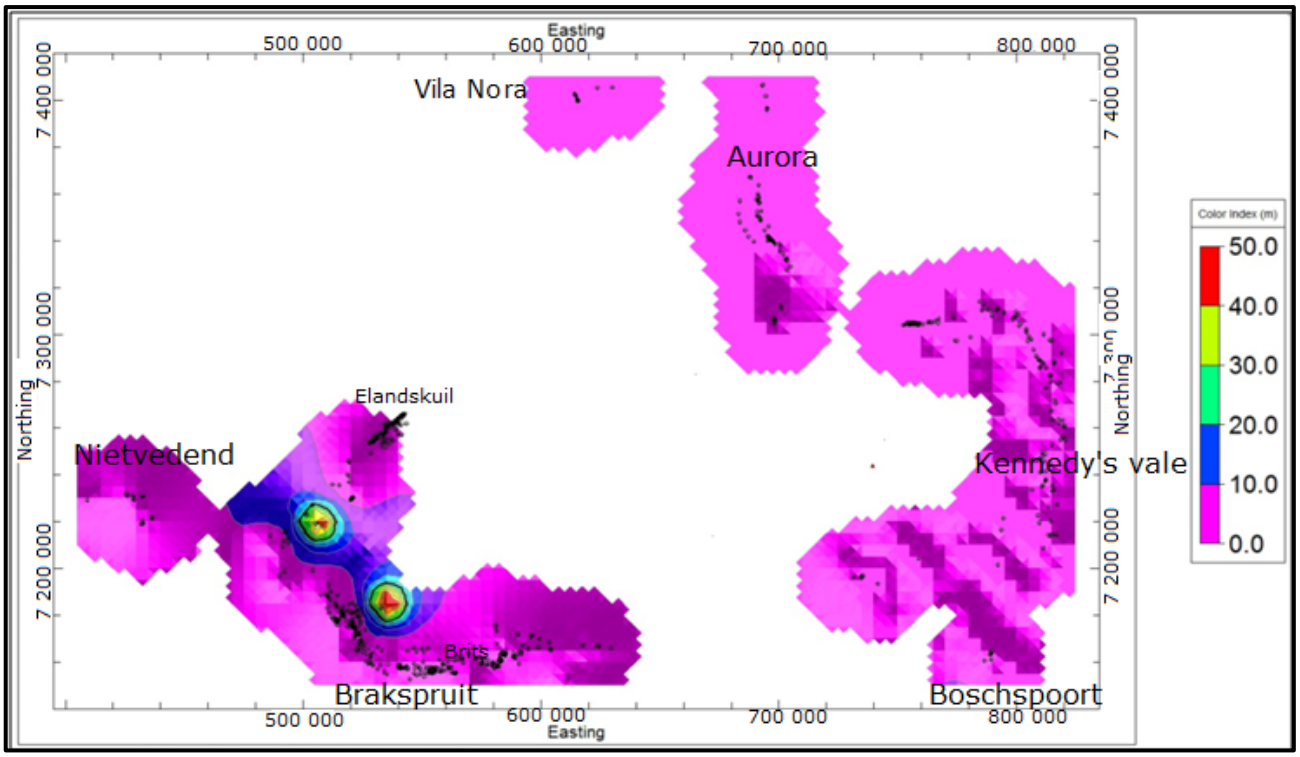

Figure 5.4: 2D isopach map of the Post RLS unit of Bushveld Complex using the Kriging method.

5.4 THE UPPER ZONE STRATIGRAPHIC UNIT

The Upper Zone structural pattern in the Northwestern Bushveld trends mostly SE and dips to the NE. The depth of occurrence of the Upper Zone unit ranges from about 900 m at the Haakdoornfontein farm at the southeastern edge to over 1000 m around the Pilanesberg Complex and about 1200 around the Brits section as indicated in Figures 5.5-5.6.

The thickness of the Upper Zone in Figure 5.6 increased from between 1 m and 20 m at Amandelbult section to over 30 m around the northern parts of the Union section, but decreased gradually towards the northern fringe of the Pilanesberg Complex. The unit is thick between the Amandelbult section and the Union section (i.e. over the Northern Gap area) forming a closure that extends to the NW and SE. Towards the southeastern part of Pilanesberg Complex where the area is tilted to the southeast the unit extends southeastward and thickens towards the centre. It forms a small dome close to the Kroondal structure and further eastwards the unit thins out completely leaving a gap that extends eastwards. Further east around the Hartebeestpoort C farm, it slopes steeply over a gap fault with a NW-SE trend. Adjacent to the fault are two valleys, one on Uitvalgrond farm and the other at Doornpoort farm, north of Pretoria. The two isolated depressions (probably a horst and graben structure) are separated by a structural high.

One of the major structural features of the Eastern Bushveld the Upper Zone structural contour interval is the north plunging arch or anticline that extends from north to south across the southeastern part of the Complex. Its thickness increases from the northern part of the structure southwards on the isopach map while on the structural map the same structure forms two concentric structural highs; one in the southeastern part and the other to the extreme southern part. They are separated by a shallow area, which coincides with the position of the Laersdrift Fault. From the southeastern part the structural contours (i.e. towards the central part of the Complex) decreased in elevation steeply (across a fault zone) into the central valley (Kennedy's Vale) where the Upper Zone rocks virtually thins out.

The central part of the southeastern Bushveld hosts a depression that extends eastwards and a SW trending anticlinal structure that opens to the NE. separates it from the depression at Kennedy's Vale area. The Upper Zone rocks occur between 20 m (in the valley) and 1600 m on the structural high area of the southeastern Bushveld. The thickness of the Upper Zone unit in the southeastern and central parts of the Eastern Bushveld ranges between 10 m and 200 m.

The Northern Bushveld is marked by prominent thickening of the Upper Zone rocks at the northern edge of the northern sector and in the western part of the central sector. These two areas are shallow areas in the structural interval of the Upper Zone. Upper Zone was reported only on Potgietersrus farm of the Vila-Nora section. However, the pattern and trend could not be verified due to insufficient information.

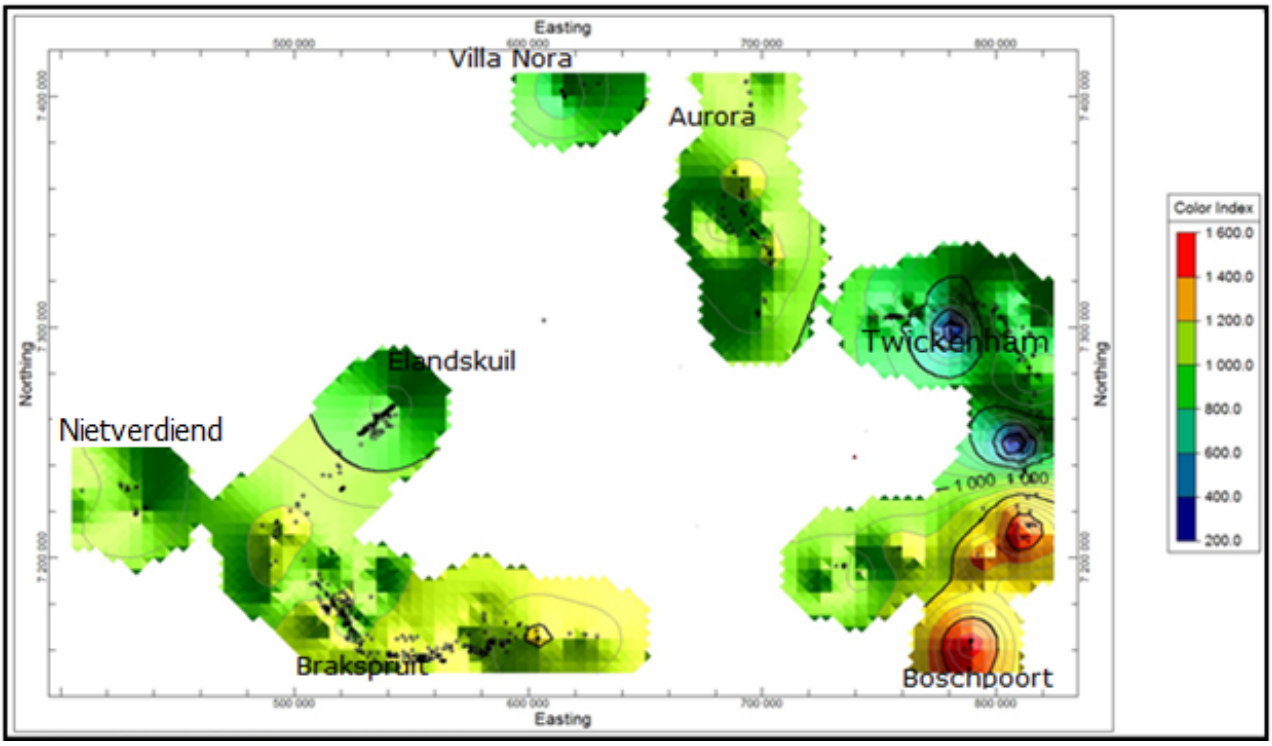

Figure 5.5: The Upper Zone top interval grid model of the Bushveld Complex by using the Kriging interpolation method.

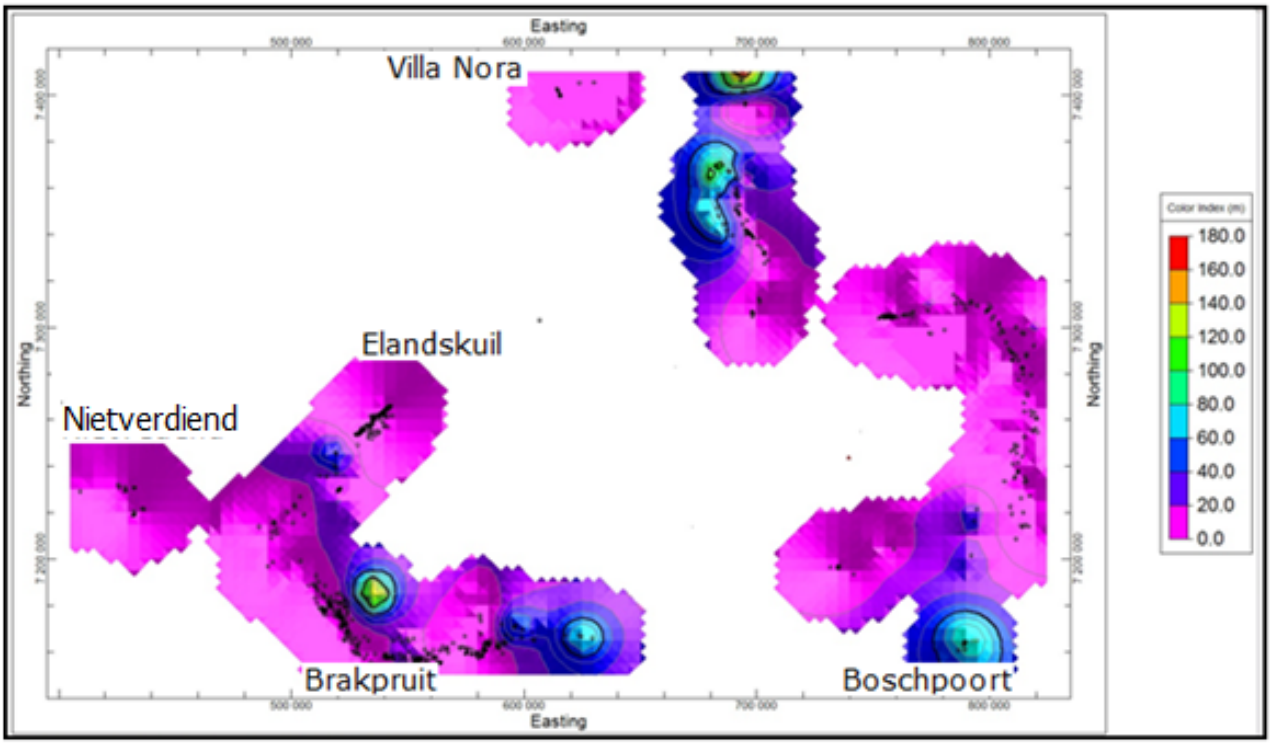

Figure 5.6: The Upper Zone 2D isopach map of the Bushveld Igneous Complex using the Kriging interpolation method.

5.5 MAIN ZONE

The structural pattern at the top of the Main Zone interval is different from the one at the base for some part of the Complex (see Figure 5.7 and 5.8). These areas include the Northwestern Bushveld and Far Northern Bushveld, while the former changed to a synclinal structure with a lobate shape around Amandelbult section, the other area experienced uplift with an anticlinal structure, which opens to the north and is surrounded by steep slopes especially on the western side. The Main Zone dips to the southeast from northern parts of Pilanesberg Complex, while at Amandelbult section the unit dips southeastwards.

The Far Western Bushveld the Main Zone dips to the east towards the Pilanesberg Complex, the southeastern side of the Pilanesberg Complex is marked by an east dipping (fault zone) and southeast trending contours that are parallel to the Rustenburg fault. Sharp bending of the contours occur around the Kroondal structure to form a southeast plunging U-shaped structure which is significant and might be related to the presence of the

Kroondal structure in the area. Adjacent to the U-shaped structure are series of closely spaced NNW trending contours that coincide with the location of the Brits fault. Further east are two structural highs with a small depression between them. The isopach map for the Amandelbult area thickens towards the centre and thins out at the sides defining an anticline surrounded by steep limbs.

The isopach map and the structural contour map for the Western Bushveld show inverse correlation. The slope becomes gradual around the Union section and continues southwestward towards the Pilanesberg Complex. The Main Zone thickens eastwards at the southern part of the Pilanesberg Complex as revealed on Figures 5.9.

The Main Zone in the southeastern Bushveld indicates a steeply dipping zone between the northwestern side and the Fortdraai arch with NS trending structure contours in Figure 5.8. The centre of the Eastern Bushveld is marked by the presence of Kennedy's Vale while the southeastern part is incised midway by a NE trending depression. The southeastern part formed an hourglass shaped structure that extends from the central part to the extreme southern part. Midway between these structures is a depression which coincides with the position of the Laersdrift fault. The Groblersdal sector is marked by two NE trending isolated structural highs (indicated as valleys on the isopach map) incised by a structural low area (indicated as hills on the isopach map). This sector is separated from the southeastern sector by a synclinal structure. The southeastern side is made up of another set of two east trending structural highs with a depression in between. However, around Lydenburg on the isopach map (Figure 5.9) the synclinal structure (in-between the southeastern structural highs) area is marked by a NW-SE trending valley with steep slopes on the sides (probably representing a fault-bounded basin or graben).

The Main Zone is more prominent in the central and southern sector of the Northern Bushveld. In the central sector where the zone is more prominent it reaches a thickness of over 450 m on a synformal structure at Rietfontein farm, adjacent to Tweefontein hill in Figure 5.9. The isopach lines opened to the east on this sector and it is truncated by faults. On Overysel farm (a SW trending fault with downthrow to the south, i.e. on Zwartfontein farm); another one is a N-S trending fault with downthrow towards the synclinal structure

on the Rietfontein farm while the third is on Tweefontein farm and looks like a southeastern extension of Tweefontein hill. This fault is at a corner around Uitloop farm and trends partly N-S and E-W.

In the Far Northern Bushveld the Main Zone thickness increases to the southwest, thus reflecting the presence of a positive structural feature in the southeast.

The Main Zone base interval (Figures 5.7 and 5.8) in the Western Bushveld occurs between depths of 970 m (in the northwestern Bushveld) to 1170 m (in the southwestern Bushveld), while the depth of occurrence in the Eastern Bushveld ranges from less than 100 m around the valleys to 1400 m in the southeastern part. In the Northern Bushveld the Main Zone is prominent in the central sector and occurs at depths of about 1000 m to 1070 m while in the far northern Bushveld the Zone occurs between 840 m to 1005 m. However, at Nietverdiend section the same zone showed up at about1070 m at the western edge, shallowing down to 1000 m at the centre and 1050 m towards the main Western Bushveld.

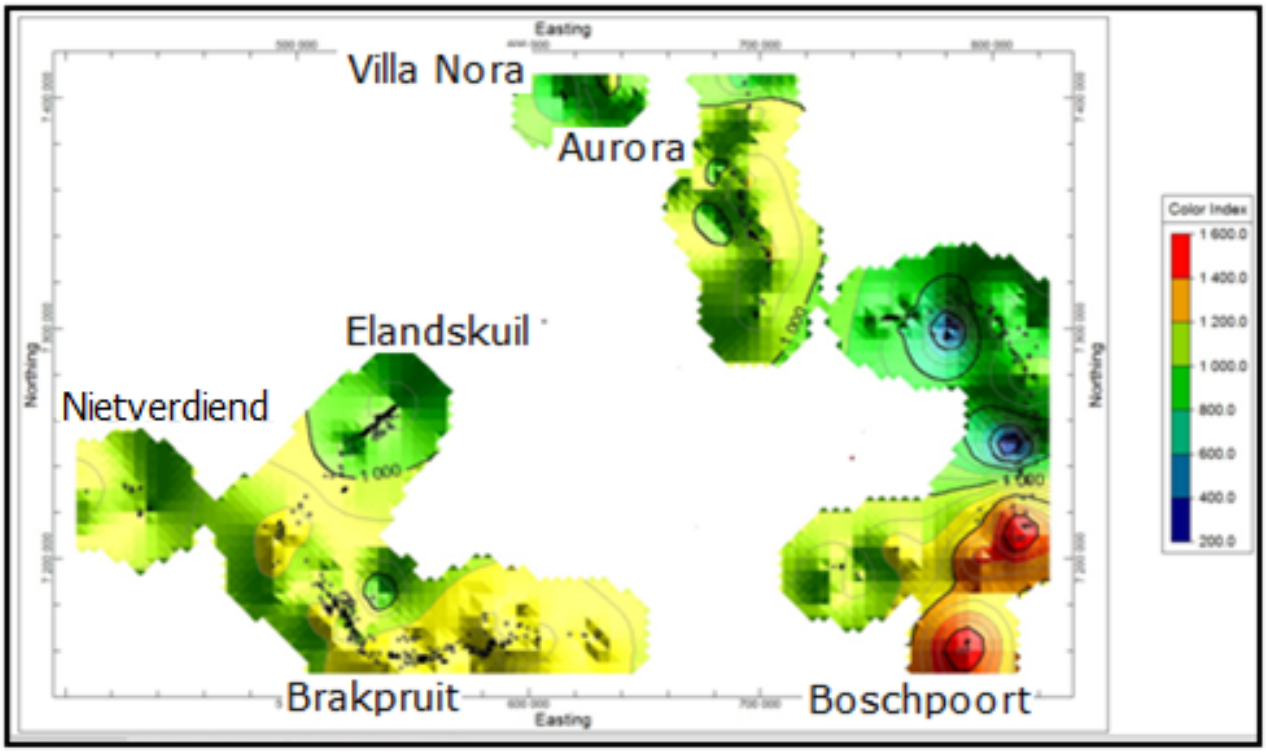

Figure 5.7: The Main Zone top 2D grid model using the Kriging interpolation method.

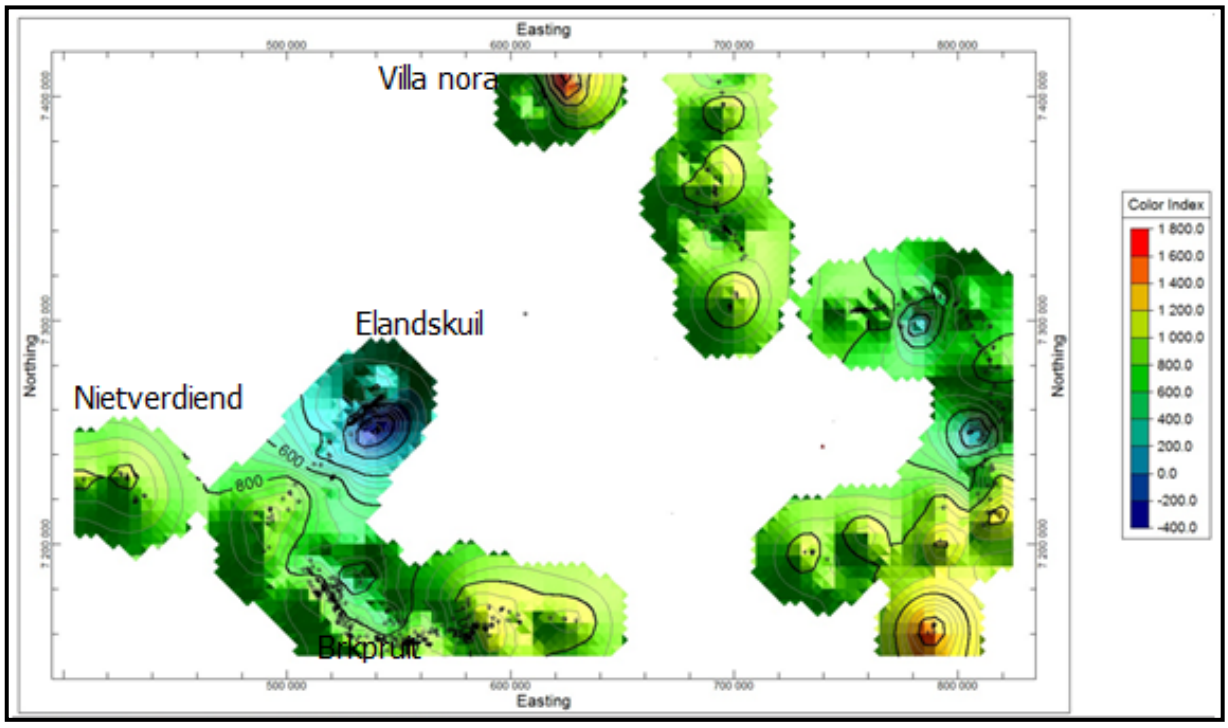

Figure 5.8: 2D Grid model of the Main Zone base using the Kriging method.

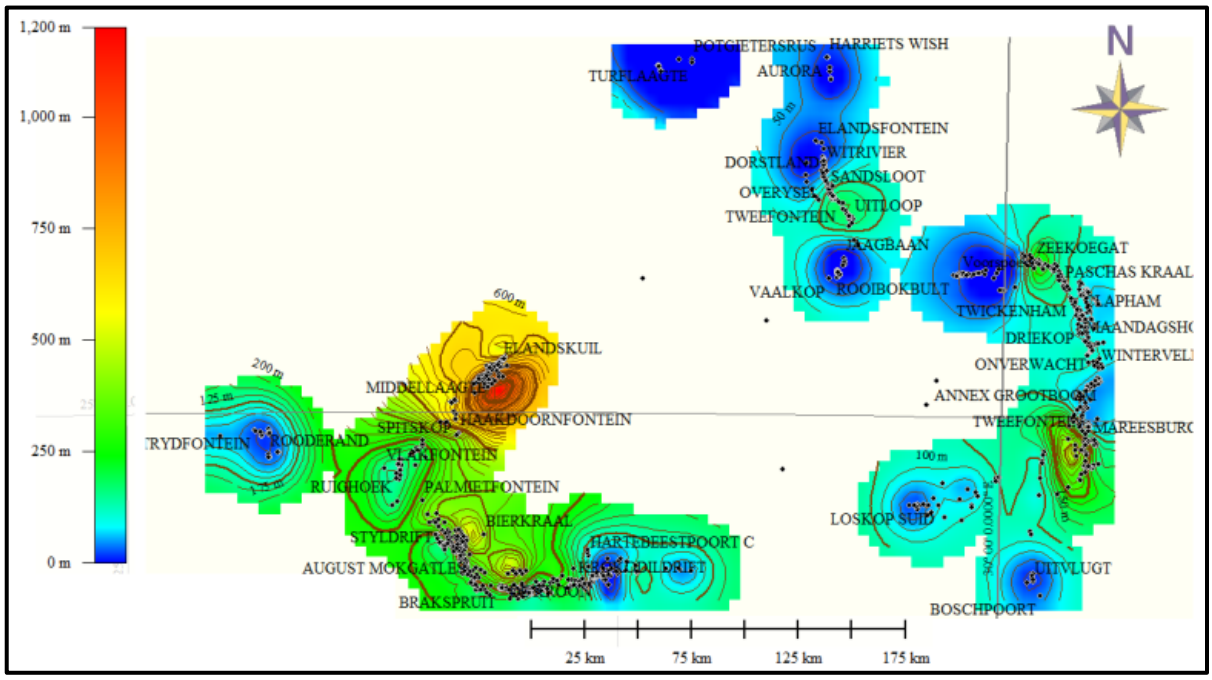

Figure 5.9: 2D Isopach map of the Main Zone using the Kriging interpolation method

5.6 BASTARD MERENSKY UNIT

This unit has a pronounced thickness around the Union section and the Northern gap, but thins towards the Amandelbult section of the Northwestern Bushveld Complex. The unit formed an L-shaped thickness trend (i.e. N-S and E-W) around this area and has it maximum thickness around the Northern gap (Figure 5.11).Structural contours on this unit have a similar pattern to the one at the base of the Main Zone interval. The deepest depth of occurrence is around the Amandelbult section, while the highest elevation occurs around the Union section as shown in Figure 5.10 and 5.11.

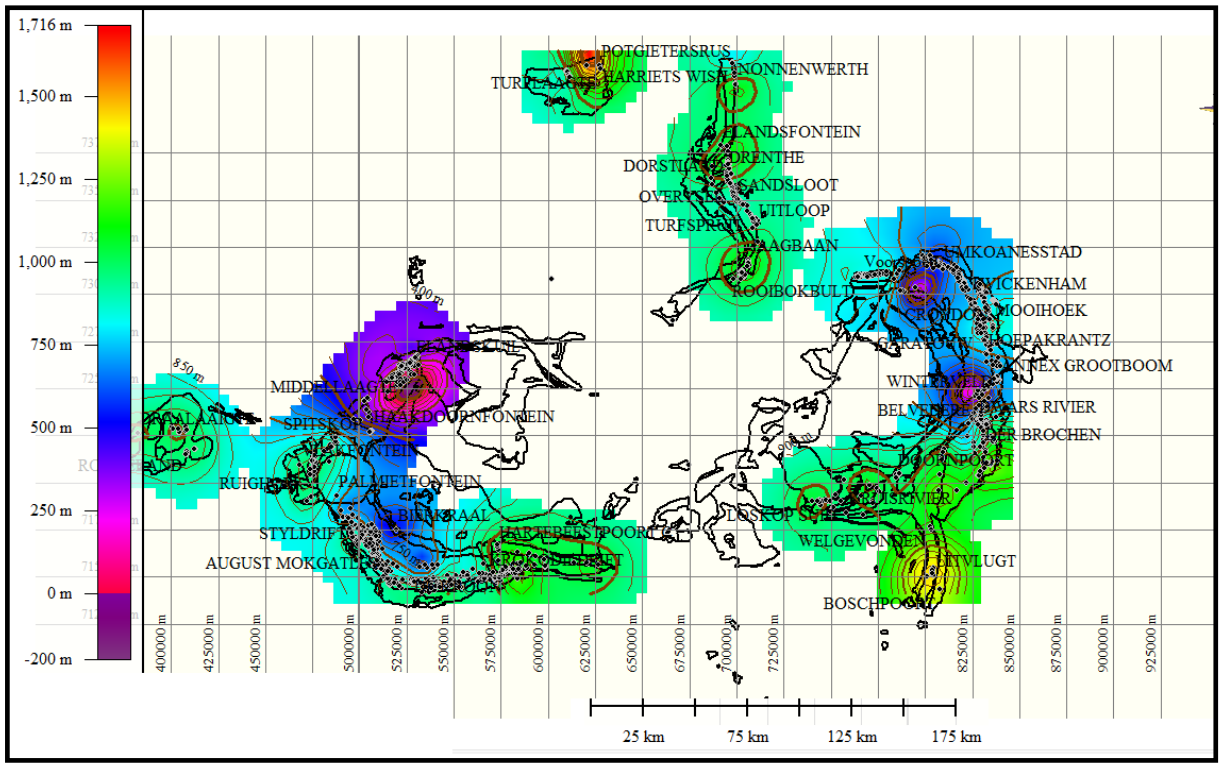

Figure 5.10: Bastard Merensky Reef structure contour top using the Kriging interpolation method

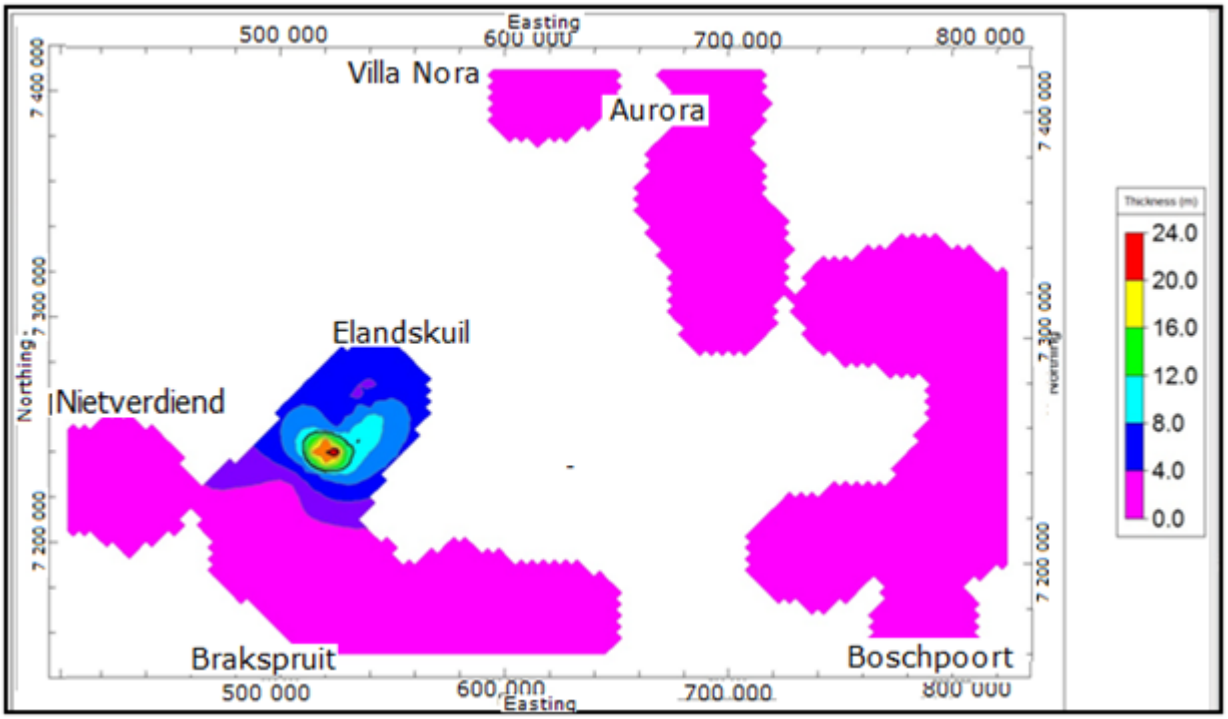

Figure 5.11:2D grid model of Bastard Merensky Reef isopach of Bushveld Complex using the Kriging interpolation method and showing prominent concentration around the Northwestern Bushveld.

5.7 THE MERENSKY REEF

The Merensky reef is present in most part of the Western Bushveld as indicated in Figure 5.12 to 5.13 but the thickness is almost uniform over the area except for the Northwestern part (where it formed a NW–SE trend) and around the Brits section (forming an east–west trend). However, around the Northern gap area, the isopach lines form closely spaced NW-trending (faults), while on the western part, the unit thins over the Union section and Southern gap area with a southeast plunging nose at the centre. Around the Brits section, the thickness increases steeply into a graben to the immediate west of the Kroondal structure (parallel to the Kroondal fault) and thins out abruptly around Hartebeestpoort farm. The graben is bounded on the western side by faults that are probably related to the Kroondal fault and the eastern side by the Brits faults. Further eastwards the unit thins across the Brits faults; however, the thickness increases abruptly again eastwards across another synclinal structure or graben (Figure 5.12 and 5.13).

The thickness is also uniform over the Eastern Bushveld. However, there is pronounced thickness around the southeast, where the contours open to the east (probably indicating a

continuation in this direction).The Far Northern Bushveld and Northern Bushveld have minor occurrences of the Merensky unit.

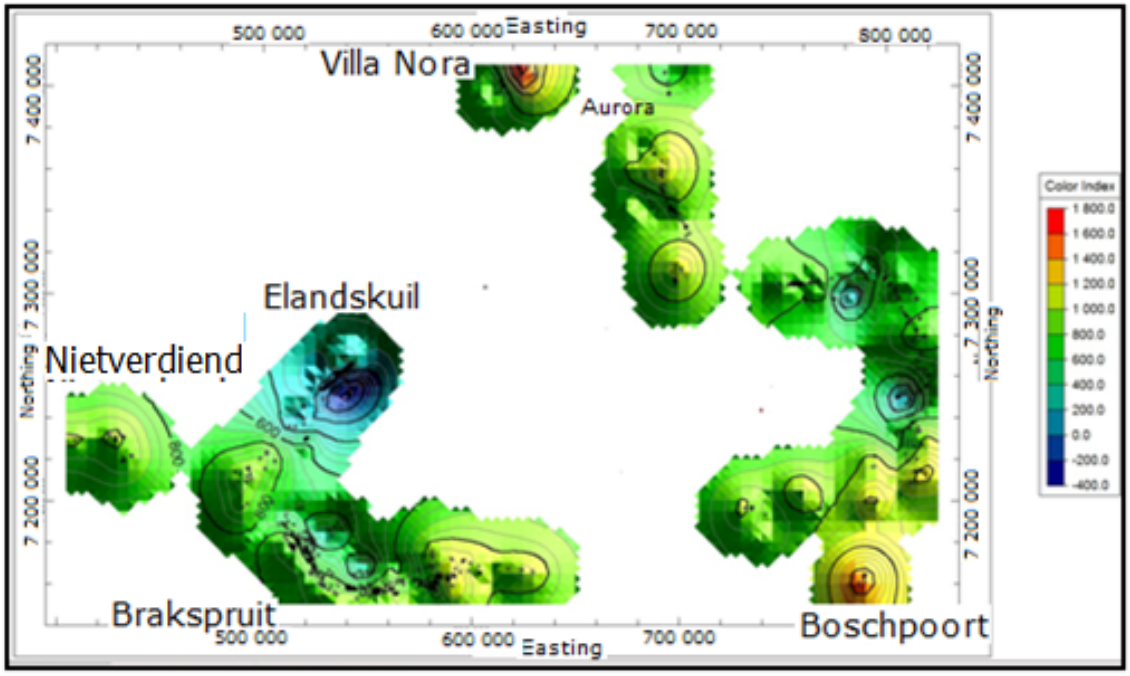

Figure 5.13: 2D Grid model of The Merensky reef top of Bushveld Complex using the Kriging interpolation method.

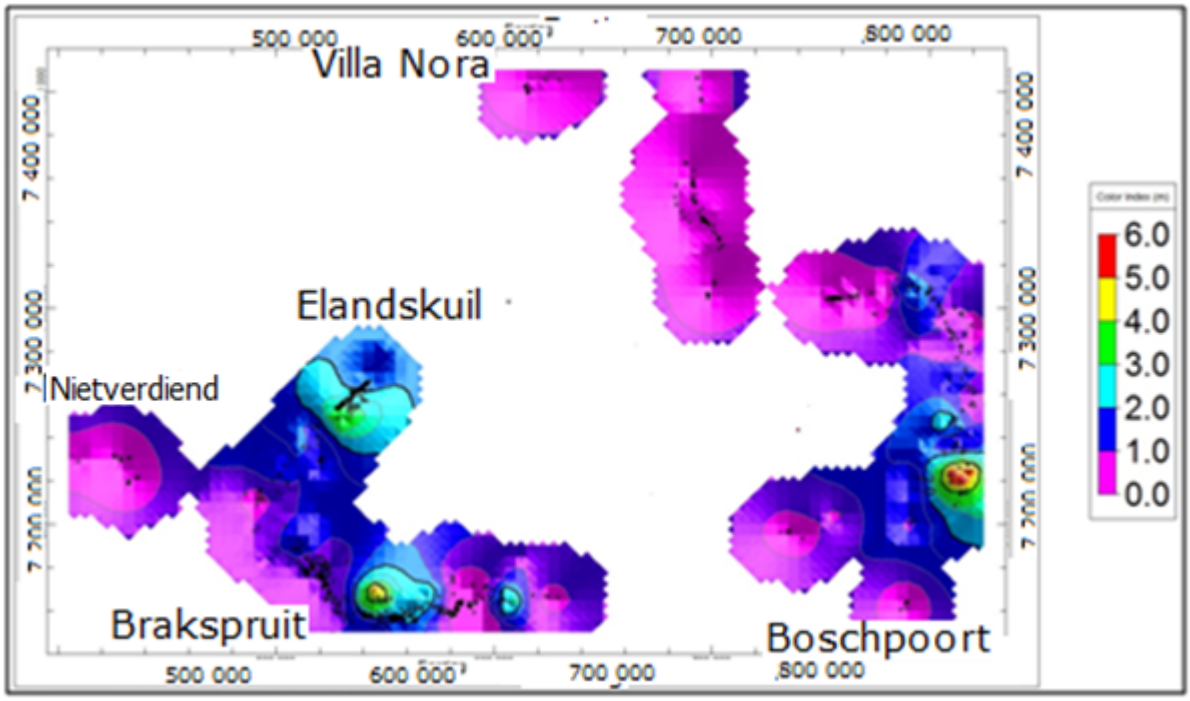

Figure 5.14: 2D Isopach map of the Merensky reef unit of the Bushveld Complex using the Kriging method. Nietverdiend

5.8 PLATREEF

The Platreef 2D grid model reveals a structural high at the extreme northern part while the southern parts indicate widespread structural lows (as indicated in Figure 5.15). The unit occurs between 800 m and 1280 m. However, the thickness as revealed in Figure 5.16 shows that the central part is irregular probably due to the underlying structures. The Platreef in the Northern Bushveld limb has a NNW-SSE regional trend (see Figures 5.17 and 5.18) and the thickness steadily reduce northwards; it is highest around the central part of the Northern Bushveld.

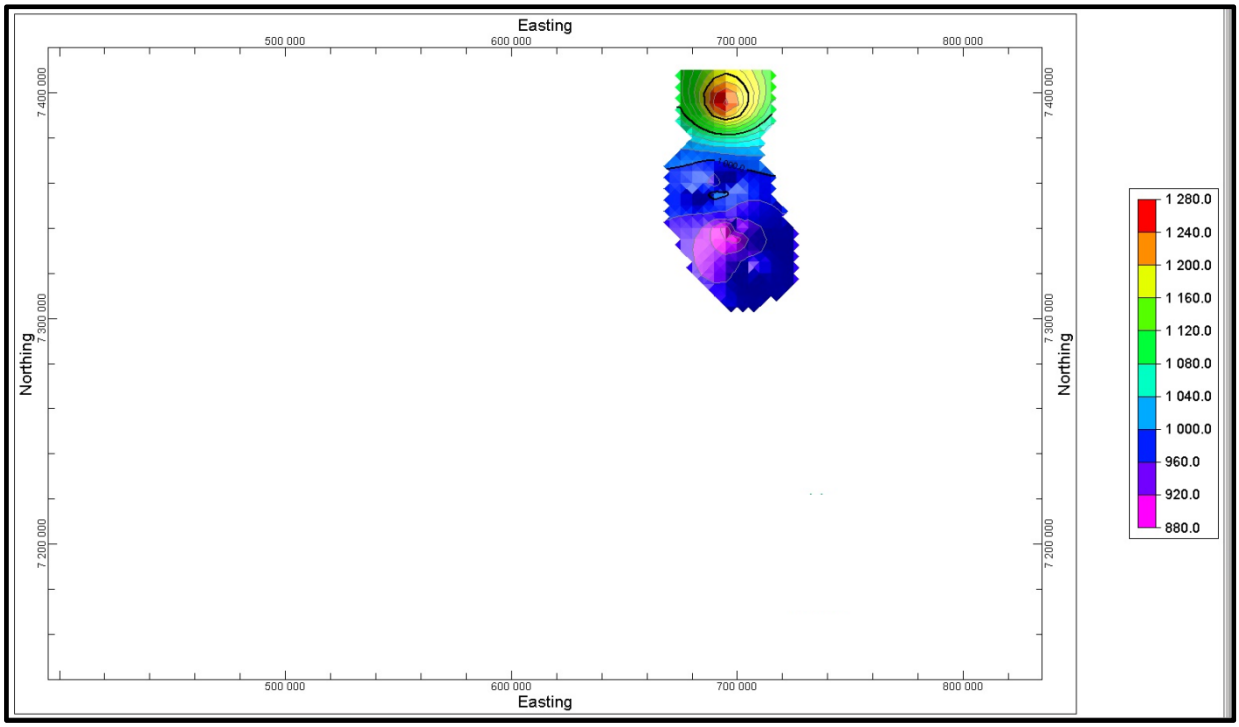

Figure 5.15: Platreef structure top interval of the Bushveld Complex using the Kriging interpolation method.

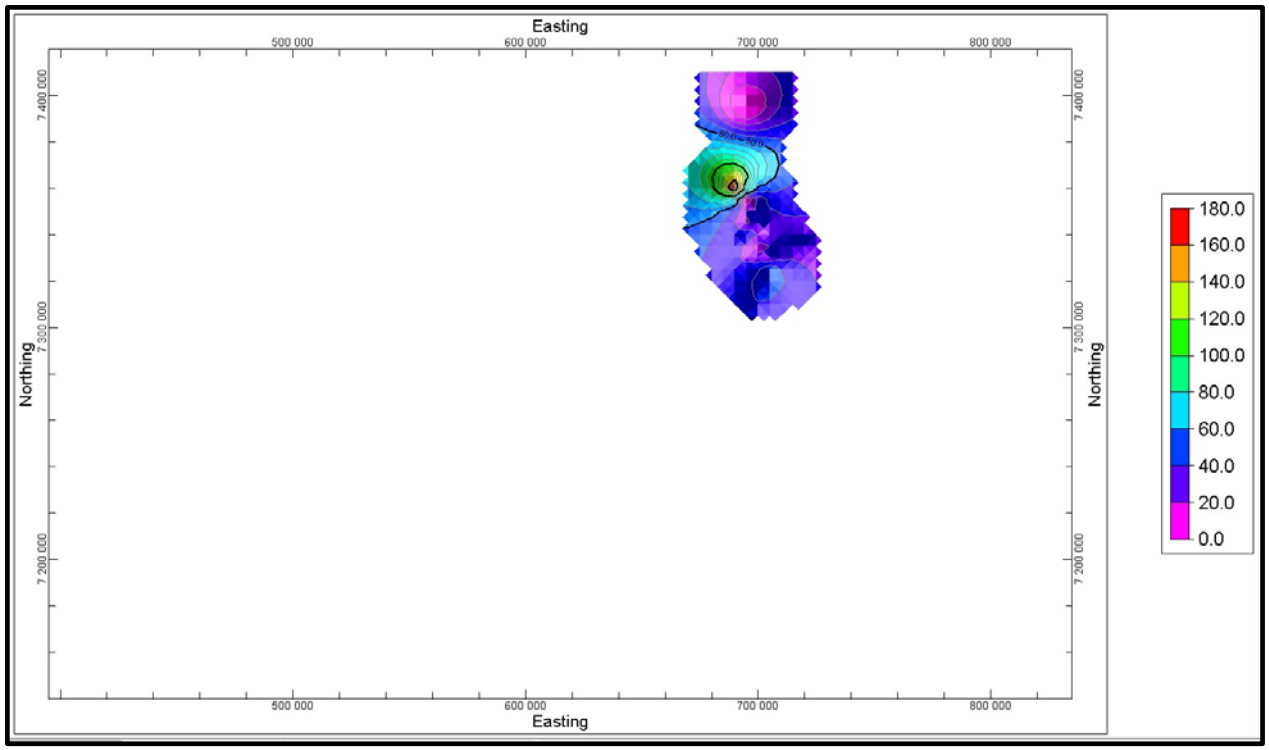

Figure 5.16: Platreef isopach of the Bushveld Complex using the Kriging interpolation method.

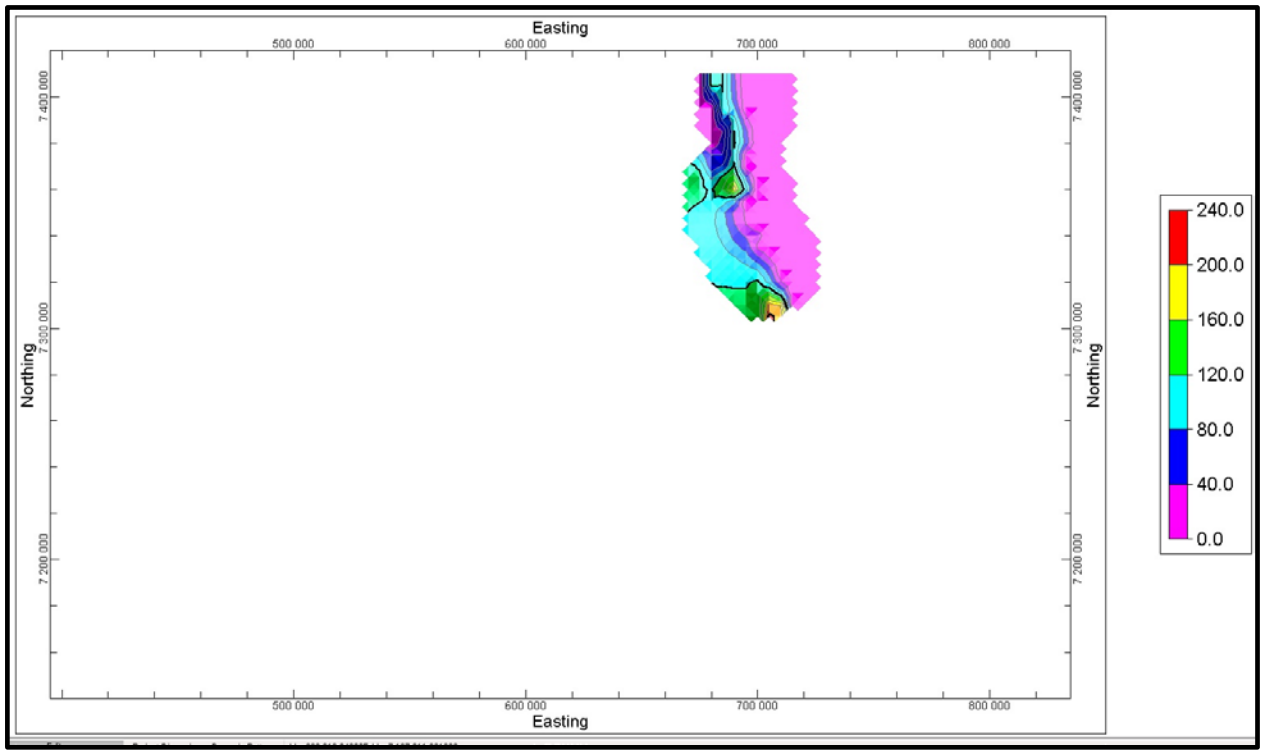

Figure 5.17: 2D model of Platreef isopach showing the regional trend of the Platreef in the Northern Bushveld Complex using the Trend Polynomial interpolation method.

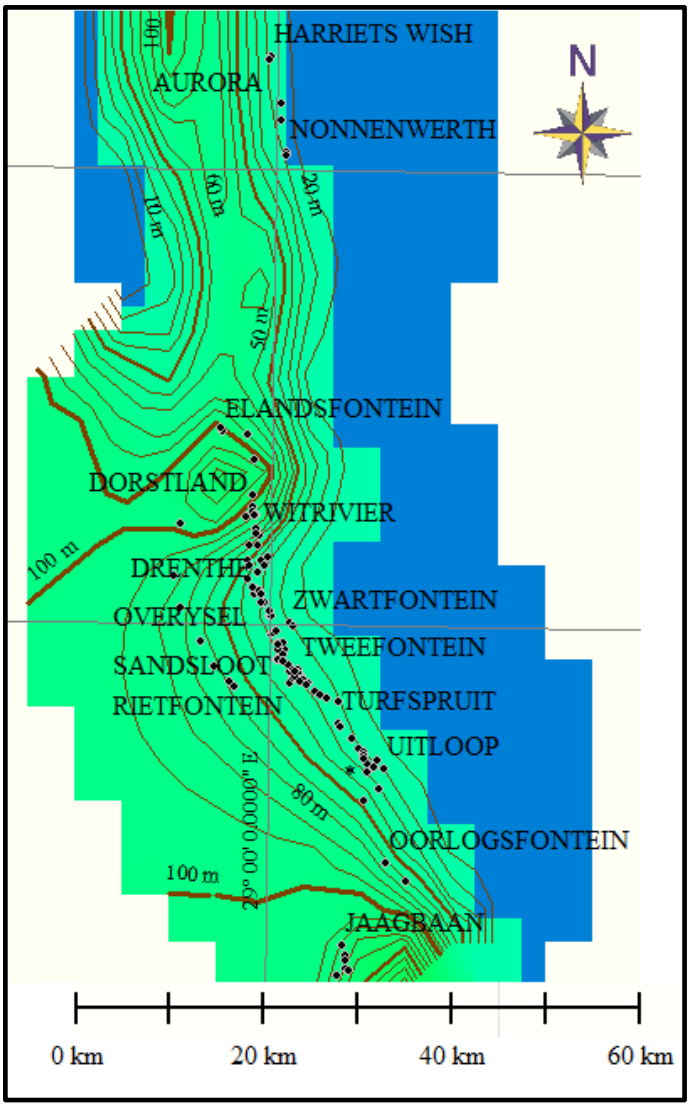

Figure 5.18: Platreef isopach map showing the regional Platreef thickness trend and farm locations using the Polynomial Trend interpolation method

5.9 PSEUDO REEF

The 2D grid models in Figures 5.19 and 5.20 shows the range of occurrence of the Pseudo reef around the Northwestern Bushveld. This unit occurs at the Northwestern Bushveld especially around the Northern gap and Amandelbult section. Most part of the structure c

contour is similar to the overlying stratigraphic unit. The thickness varies from 0.25 m to about 0.8 m as shown in Figure 5.31.

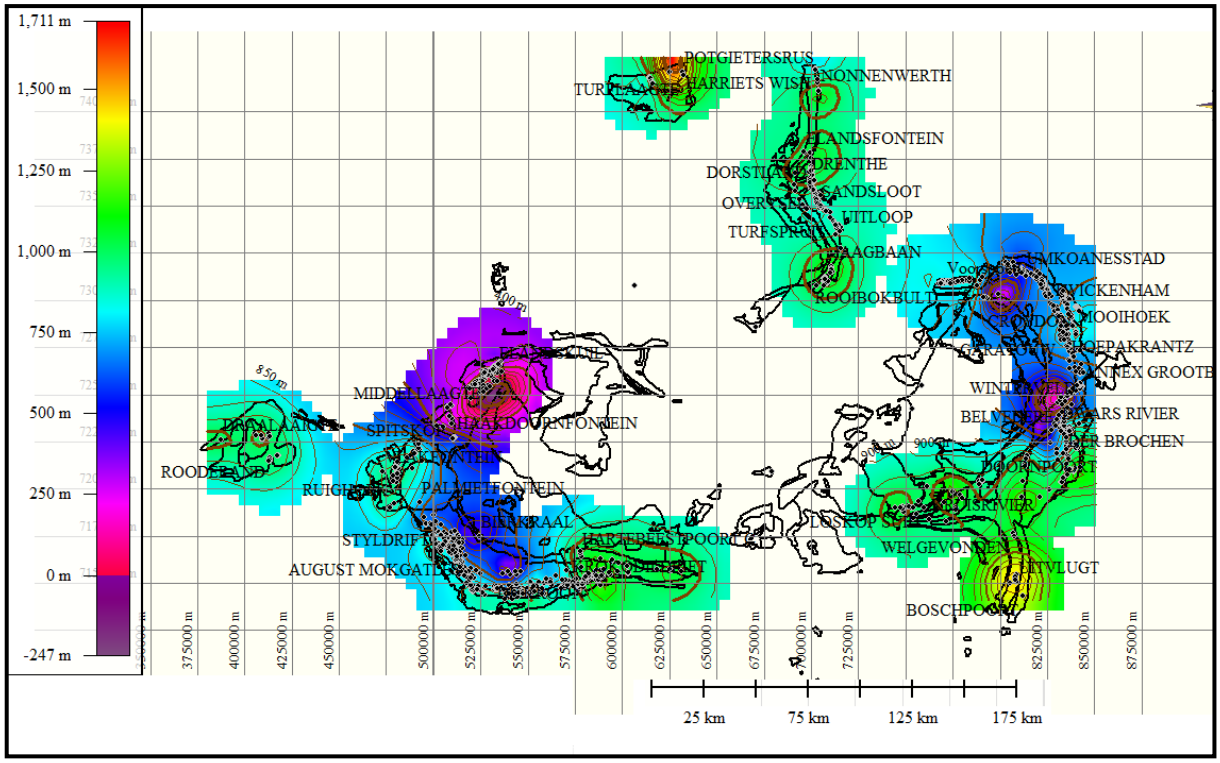

Figure 5.19:2D Grid model of Pseudo Reef interval of the Bushveld Complex generated with the Kriging interpolation method.

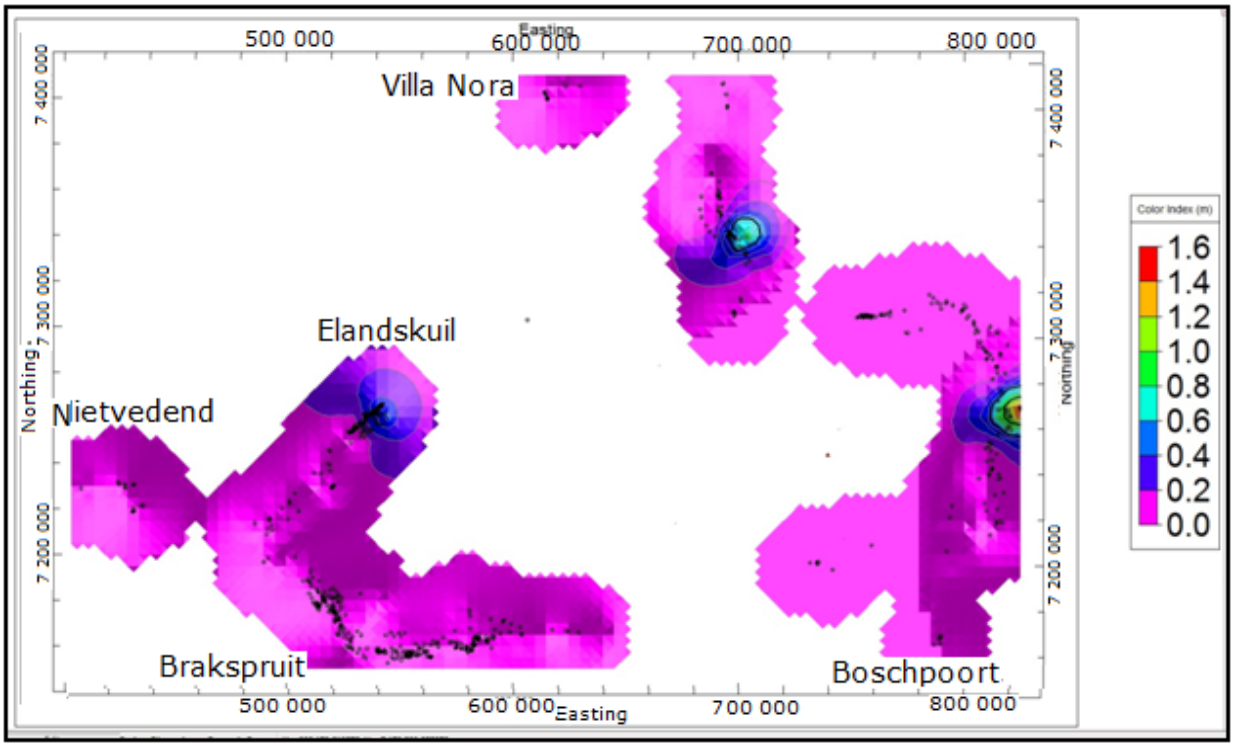

Figure 5.20: Grid model of the Pseudo Reef unit isopach in the Western Bushveld, the UG3 isopach in the Eastern Bushveld and chromitite in the Northern Bushveld isopach using the Kriging method

5.10 UG3 UNIT

The UG3 unit occurs mostly in the central part of the Eastern Bushveld (Figure 5.19 and 5.20 above). On the isopach map, it thickens towards the east on Winterveld farm, occupying a structure that dips eastwards. However, the structure contour map shows a similar pattern to the overlying horizons.

5.11 UG2 UNIT

This unit has a widespread occurrence in the Western Bushveld section with more pronounced thickness around the northwestern Bushveld and around the Brits section of the Western Bushveld as indicated in Figure 5.21. The unit occupies two shallow areas with a small uplift in the middle of the northwestern section. The first shallow area occurs in the Amandelbult section and forms a NW- SE trend, the second shallow area occurs around the Union section and forms a NW-SE trend, while the small uplifted area occupies

the Northern gap area. The structural pattern around the Brits section is unaffected, and remains similar to the pattern on the upper horizons.

The UG2 unit has a prominent thickness in the southeastern part of the Eastern Bushveld and occupies a structural high at about 1000 m depth around Kliprivier farm. The isopach lines open to the east, thus indicating that the unit might probably extend to the east. In the Northern Bushveld this unit occurs in the southern section on Jaagbaan and Grasvally farm.

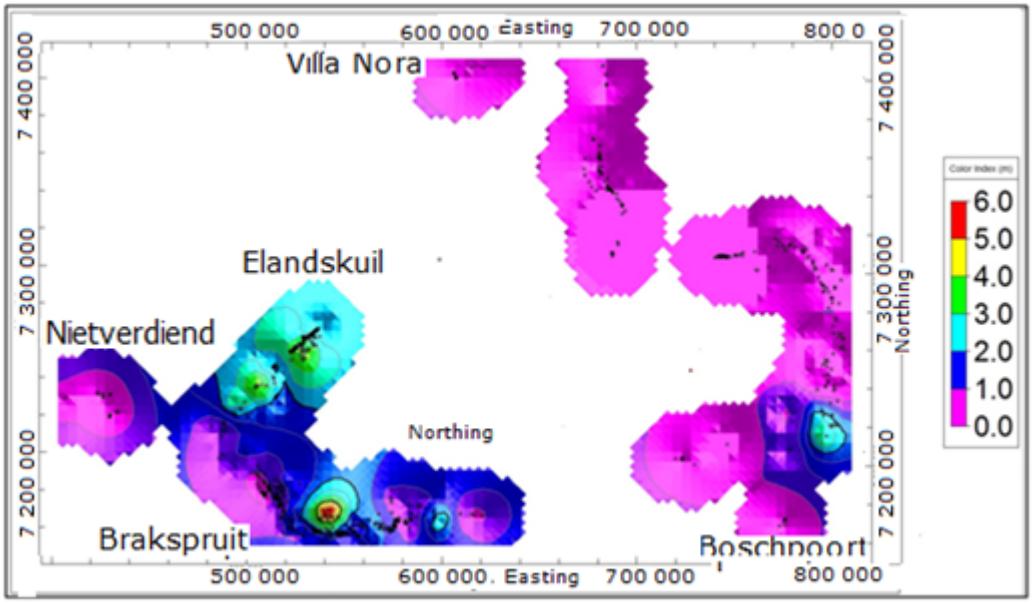

Figure 5.21: 2D Isopach map of the UG2 unit of the Bushveld Complex using the Kriging method of interpolation.

5.12 UG1 UNIT

The UG1 unit is present in the Northwestern Bushveld and forms a lobate shape on the structural contour map (see Figure 5.22). The shape widens to the SW towards the Southern gap area, but further southwest the structure descends steeply towards the Union section with a slight bend to the southwest at the centre. The unit occurs between depths of 670 m and 248 m with a SW-NE trend and slopes steeply over the Northern gap area in the northwestern Bushveld. The unit thickens towards the NE and dips steeply from the Northern gap area towards the Amandelbult section.

The unit occurs around the southeastern Bushveld, forming a small shallow that opens to the east. The structural contour pattern is similar to patterns on overlying units. It occurs at about 1000.4 m depth in this section.

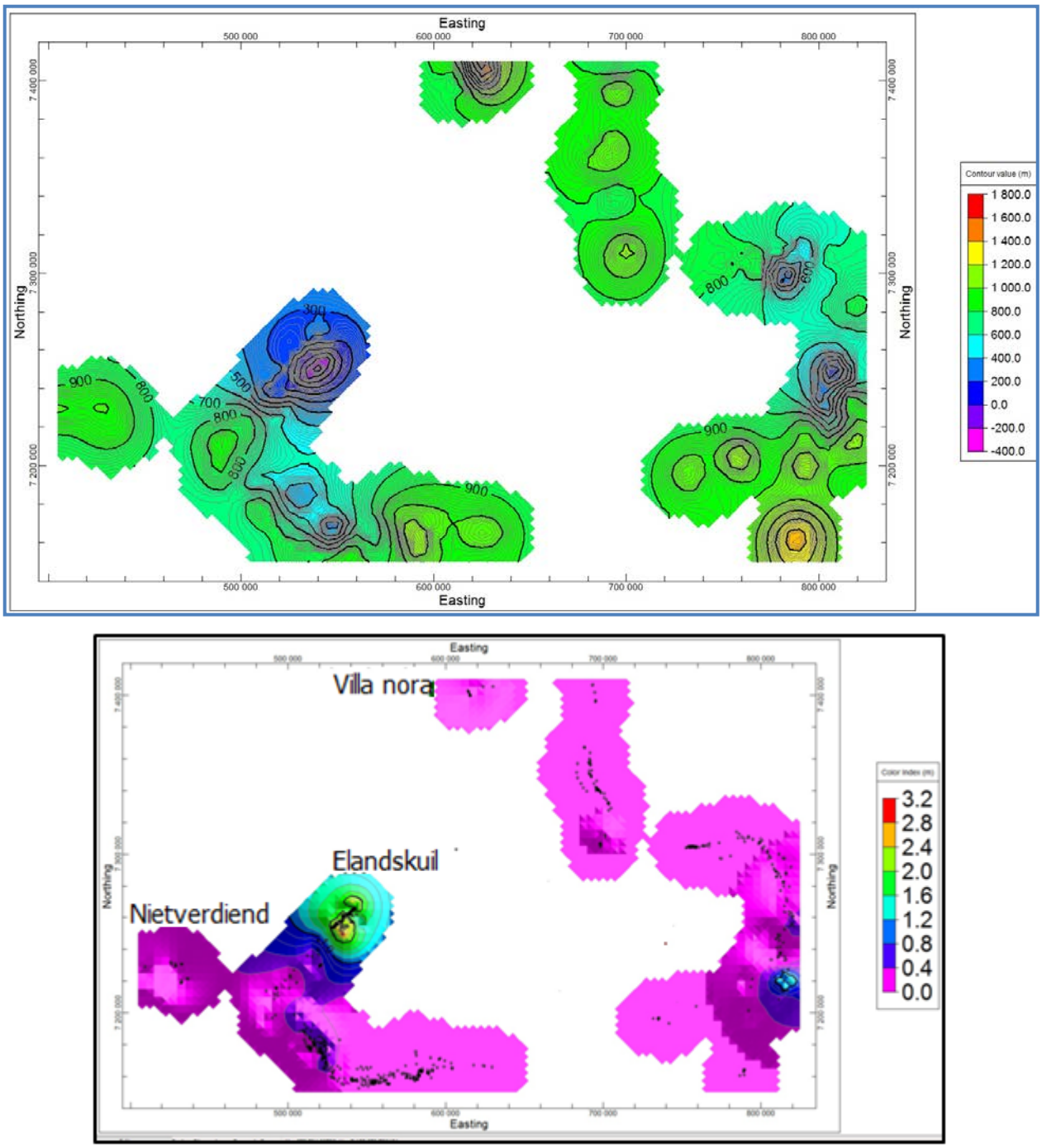

Figure 5.22: 2D isopach map of the UG1 unit of the Bushveld Complex using Kriging interpolation method.

5.13 THE MIDDLE GROUP CHROMITITE

The Middle Group Chromitite layers (MG) are widely distributed over the Western Bushveld, The Northwestern part is marked by a NE-SW trend as shown in Figures 5.23; however, the trend is incised around the Northern gap by a shallow depression. The unit thickens southwards from the Pilanesberg Complex and peaks on a steep-sided synclinal structure that opens to the south around Kroondal farm. Further southeast, the unit thins out across the southwestern Bushveld from Hartebeestpoort B farm to Doornpoort farm in the east. The unit occurs between the depth of 250 m and 800 m in this area as shown in Figure 5.23. The unit also indicates pronounced thickness in the central part of the Eastern Bushveld Complex, occupying a steep-sided synclinal structure that extends across Tweefontein, Dwarsrivier and Mareesburg farms, and opens to the east. This unit thins to the south and west. It occurs between depths of 800 m and 1100 m.

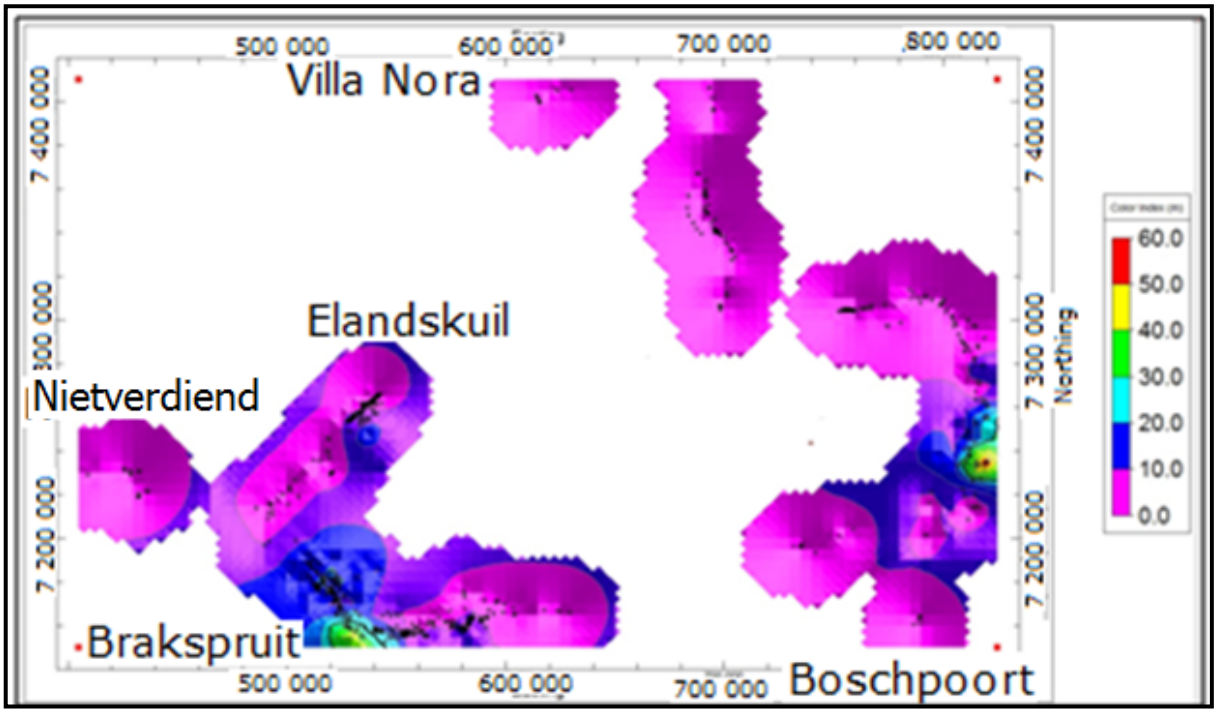

Figure 5.23: 2D isopach map of the Middle Group Chromitites of the Bushveld Complex using the Kriging interpolation method.

5.14 THE LOWER CRITICAL ZONE

This unit occurs in the Far Western Bushveld, Northwestern Bushveld, and west and southeast parts of the Pilanesberg Complex (Figure 5.24). On the isopach map, the unit thickness increases from the NW to the centre before decreasing sharply to the SE and SW. In the Western Bushveld, thickness of the unit is consistent over the entire Western Bushveld, except beyond Brakspruit farm where it virtually thins out.

The unit occurs in the southeastern part of the Eastern Bushveld where it trends SW with southward thickening, while the one in the southeastern part, trends eastward with increasing thickness to the east.

The Lower Critical Zone unit is also present in the southern sector of the Northern Bushveld where it was classified as having lower seams.

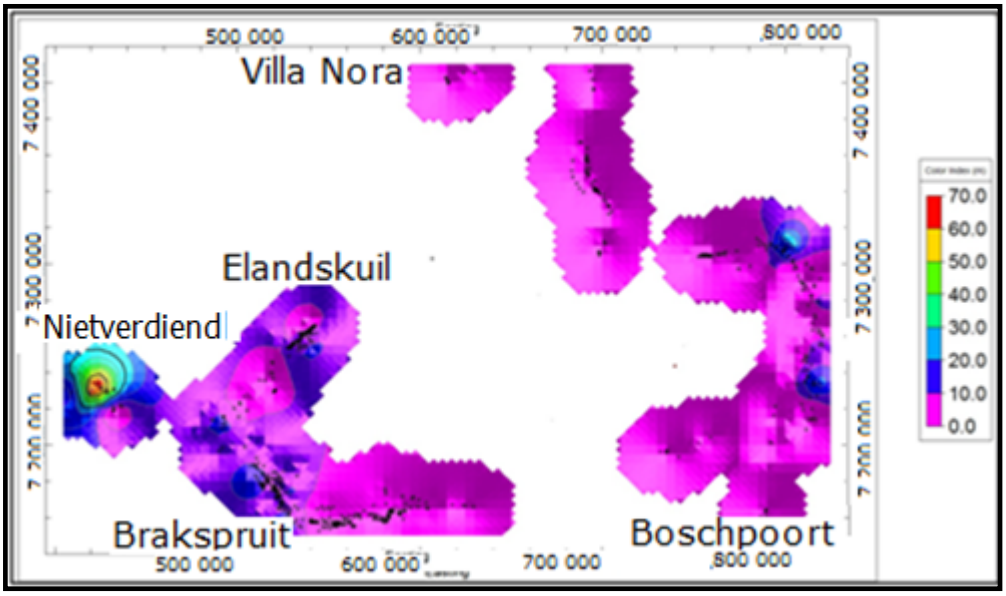

Figure 5.24: 2D isopach map of Lower Group Chromitites of Bushveld Complex using the Kriging Interpolation method.

5.15 LOWER ZONE

The Lower Zone occurs conspicuously around the Pilanesberg Complex of the Western Bushveld as indicated in Figures 5.25 and5.26. Here, there is sharp thickening of the unit to the south below the Pilanesberg Complex, thus the unit occupies a synclinal structure at

the lower parts of the Pilanesberg Complex. The synclinal structure dips steeply on all sides (this probably implies that the structure is fault bounded), extends over a 43 km stretch and opens to the SW. The unit might extend both to the west towards the Far Western Bushveld area and southwestwards. Figure 5.26 shows that the area is structurally positive or high relief and occurs between 750 m and 912 m depth in the area.

In the Eastern Bushveld, this unit occurs in the Groblersdal sector forming a small trough in an area that is structurally positive. The unit occurs between depths of 900 m and 1027 m.

Lower Zone rocks are prominent in the southern sector of the Northern Bushveld. The unit trends N-S and is delimited in the northern edge by a SW trending fault (probably the Ysterberg-Planknek fault) and occupies the positive structure on Grasvally area.

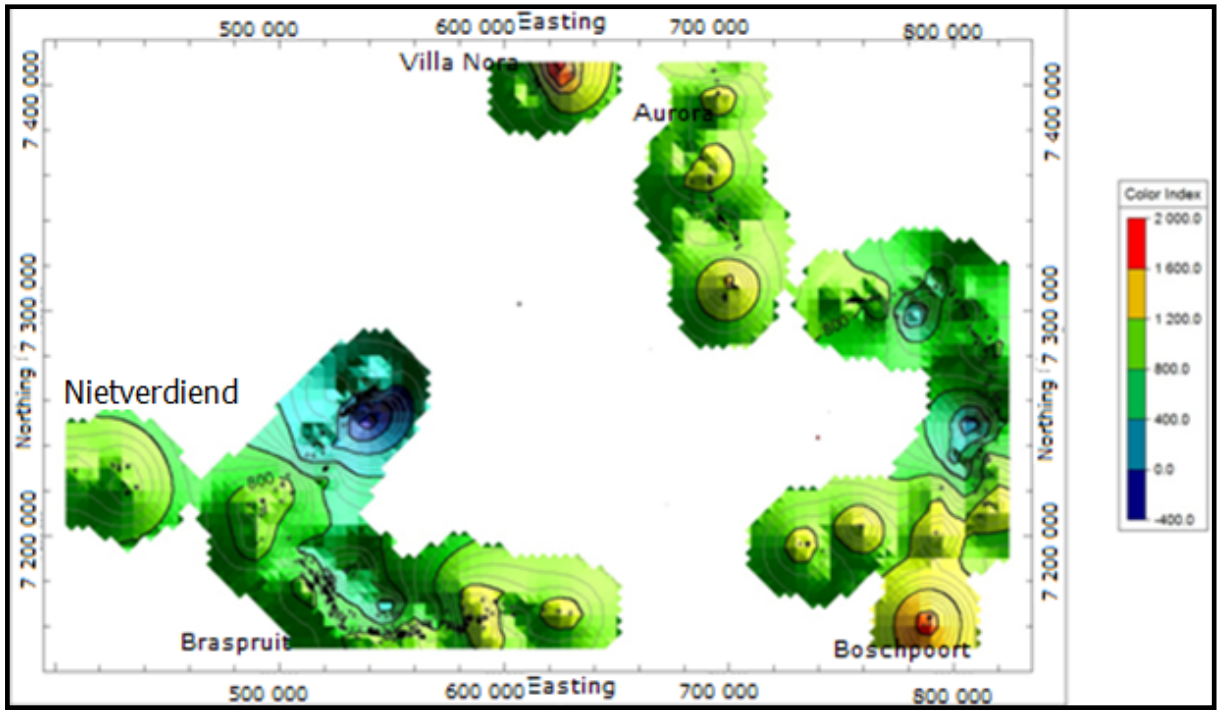

Figure 5.25: 2D grid model of the Lower Zone interval of the Bushveld Complex using the Kriging method.

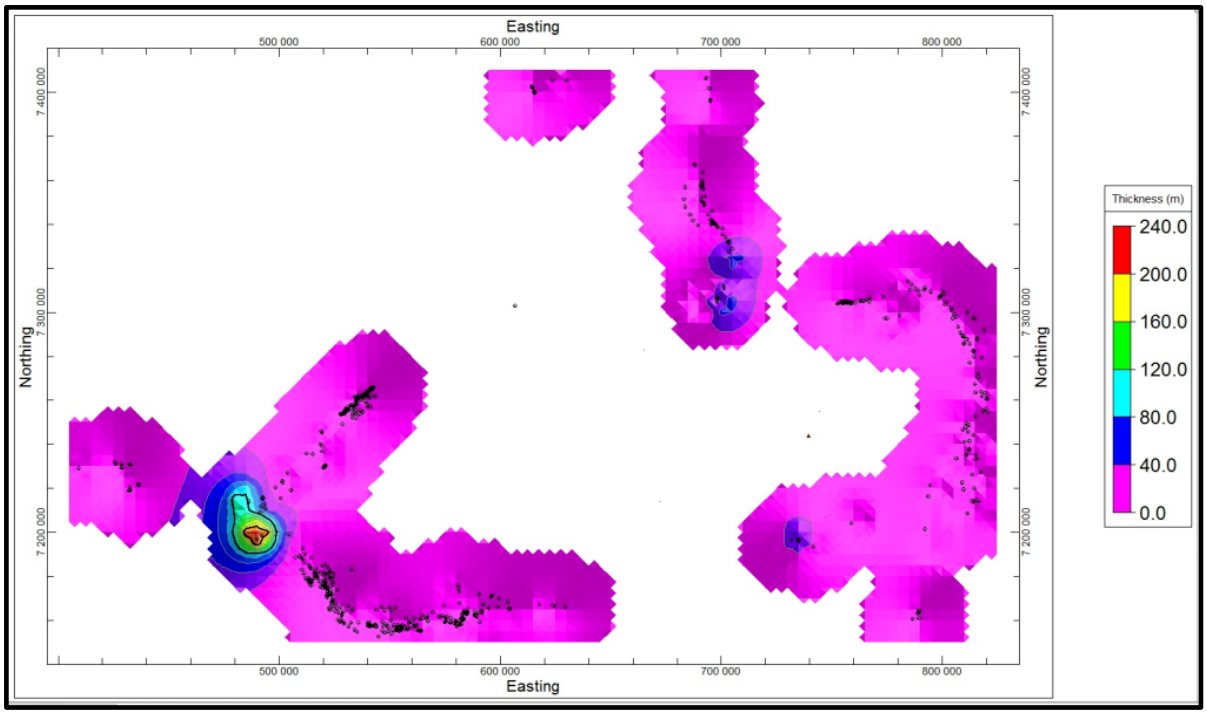

Figure 5.26: 2D isopach map of the Lower Zone of the Bushveld Complex using the Kriging method.

5.16 THE MARGINAL ZONE

The Marginal Zone occurs below the Pilanesberg Complex in the Western Bushveld Complex where it forms a circular closure that thickens eastwards as indicated in Figures 5.27 and Figure 5.28.The unit extends to the Far Western Bushveld and immediate south of the Pilanesberg Complex and occupies the steep-sided trough below the Complex. The unit occurs between depths of 677.4 m and 877.4 m around the Pilanesberg Complex.

Within the Eastern Bushveld Complex, the Marginal Zone is prominent towards the southeastern edge and around the Groblersdal sector. In the southeastern edge, the unit thins westwards. While in the Groblersdal sector the unit thins to the southeast (Figure 5.28). The unit occurs between depths of 927 m and 1002 m.

The Marginal Zone extends across the northern and central sector of the Northern Bushveld. The unit thickens to the north over a shallow trough (at depths between 827.4 m and 927.4 m) that opens to the north on Harriet Wish farm at the northern edge. Towards the south, the unit trends southeastward and forms two isolated shallow areas, separated by

a small uplifted area, and the unit terminates against an E-W trending fault around the southern part as it thins out. The structure contour pattern shows two structural high areas in the north-central part and another structural high in the Grasvally area while a small shallow area occurs between these two on Sandsloot and Uitloop farms (see Figures 5.27).

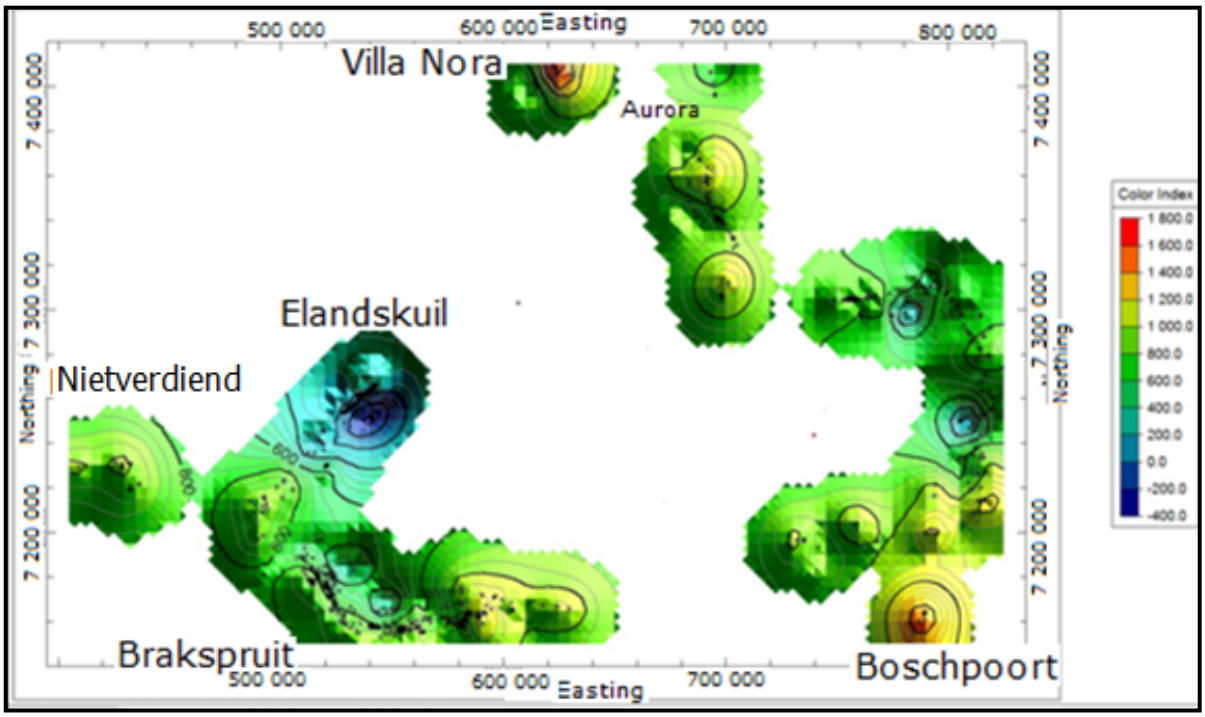

Figure 5.27: Grid model of the Marginal Zone top of the Bushveld Complex using Kriging interpolation method.

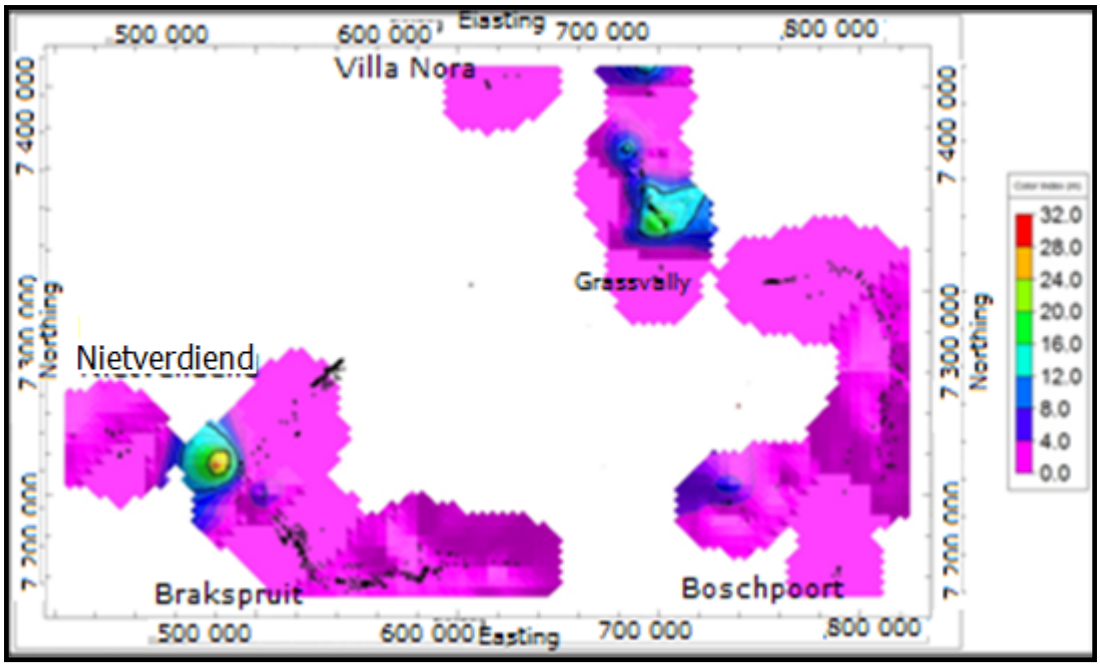

Figure 5.28: Isopach map of the Marginal Zone of the Bushveld Complex using Kriging interpolation method.

5.17 THE PRE-BUSHVELD OR TRANSVAAL GROUP ROCKS

Pre-Bushveld rocks occur below the Pilanesberg Complex and extend to the immediate southwestern part of the Complex. Below the Pilanesberg Complex, the occurs as metasediments and extend between depths of 777.4 m and 877.4 m, while in the Far Western Bushveld, they occur between 777.4 m and 977.4 m as indicated in Figure 5.29.

The rocks thicken westward at the Groblersdal sector of the Eastern Bushveld, but gradually thin out eastwards from Blaauwbank farm to Welgevonden farm (the thinning probably defines a fault zone as shown on the isopach map in Figure 5.30). The depth of occurrence in this sector varies from 1002.4 m to 902.4 m.

Pre-Bushveld or Transvaal Supergroup rocks also occur extensively in the Northern Bushveld Complex with varying lithologies, which includes dolomite, shale and quartzite. The thickness is more pronounced in the central sector of the Northern Bushveld.

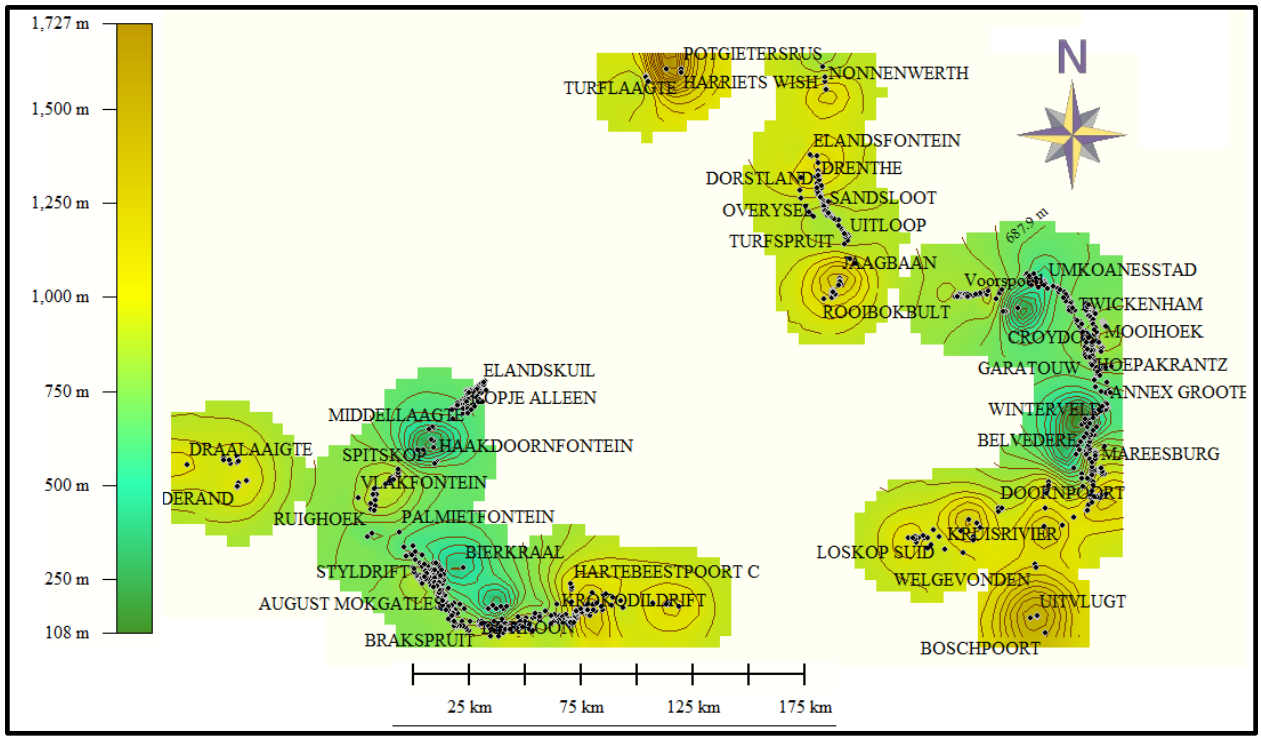

Figure5.29: Pre-Bushveld or Transvaal Supergroup rocks top interval structure contour map using the Kriging method

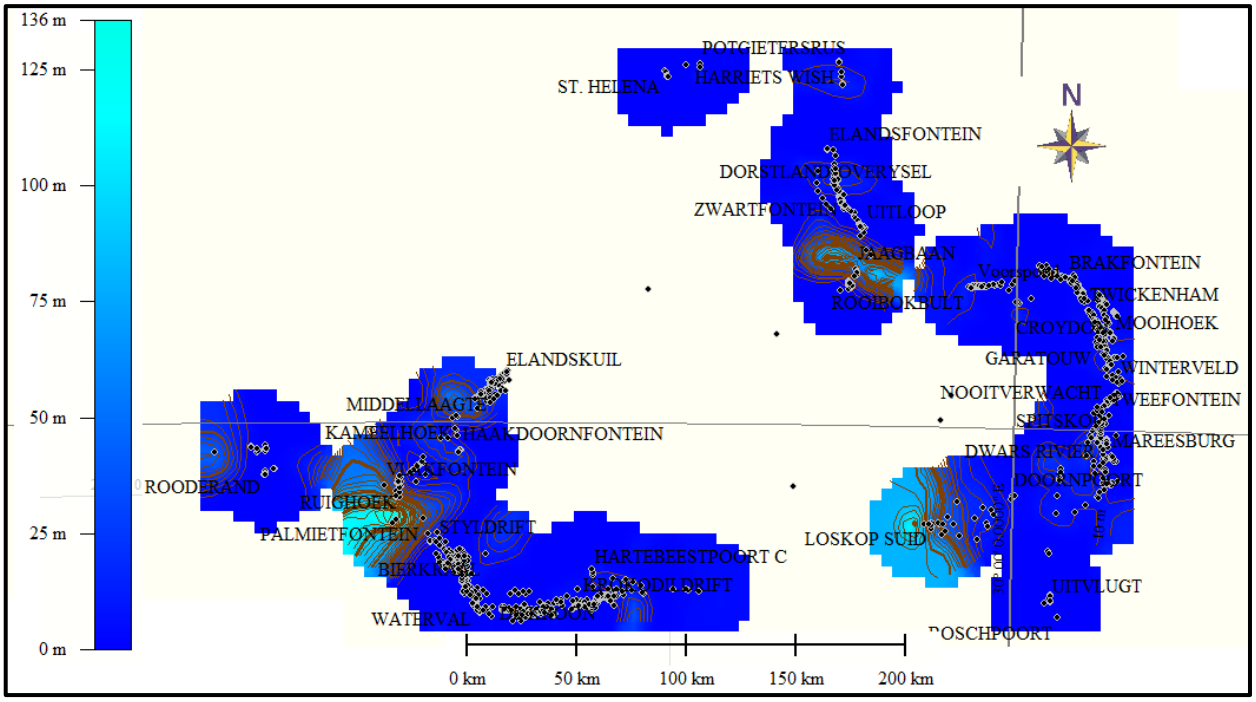

Figure 5.30: Pre-Bushveld or Transvaal Supergroup rocks isopach map using the Kriging method

5.18 THE ARCHAEAN FLOOR

The Archaean floor rocks occur in the Far Western Bushveld at depths of about 352.4 m at the centre, and -147 m at the fringes. It forms a positive structure at the centre and extends to the west. These rocks are not reported in the Western Bushveld Complex log either, because they are not present or might occur at deeper depths in this area.

The Archaean floor rocks of the Northern Bushveld occur between 127 m and 464 m approximately at the northern edge and form a synformal structure that plunge to the north. The rocks extend from depths of 352.4 m at the edges to 752.4 m at the centre, trend southeastwards from the central to the southern sector, dip to the west, and east, except around the area of Turfspruit farm where there is another synclinal structure, which extends from west to east and plunges to the west.

Archaean floor rocks structure contours pattern in the Eastern Bushveld Complex show the presence of a steep-sided valley that extends from the north to the centre. The valley is surrounded by structural high areas. Their depth of occurrence ranges from 748 m (in the valley) to 252.4 m at the edge. The valley has a N-S extension of about 77 km. The southeastern Bushveld is marked by a structural high that extends westwards to the Groblersdal sector and Bethal area. The depth of Archaean floor rocks in the southeastern Bushveld Complex range from 1000 m at Uitvlugt farm in the southern section to 760 m at the southeastern edge and 500 m in the Groblersdal sector. Figure 5.31 and 5.32 shows the 2D grid models of the Archaean floor rock occurrence around the BIC.

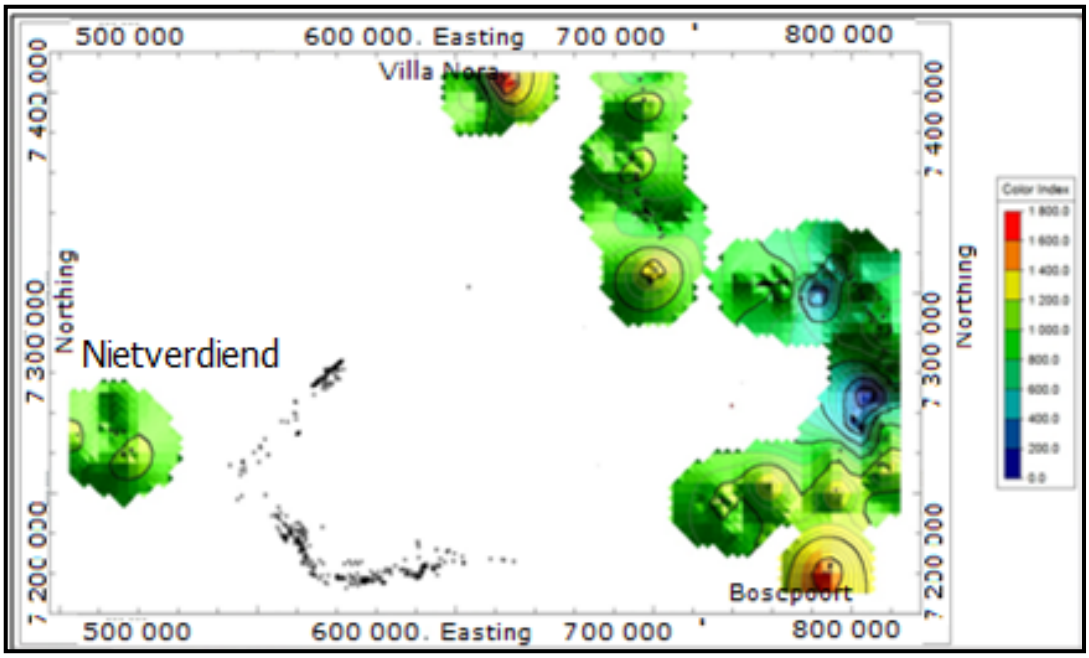

Figure 5.31: 2D grid model of Archaean granite top of the Bushveld Complex using Kriging interpolation method.

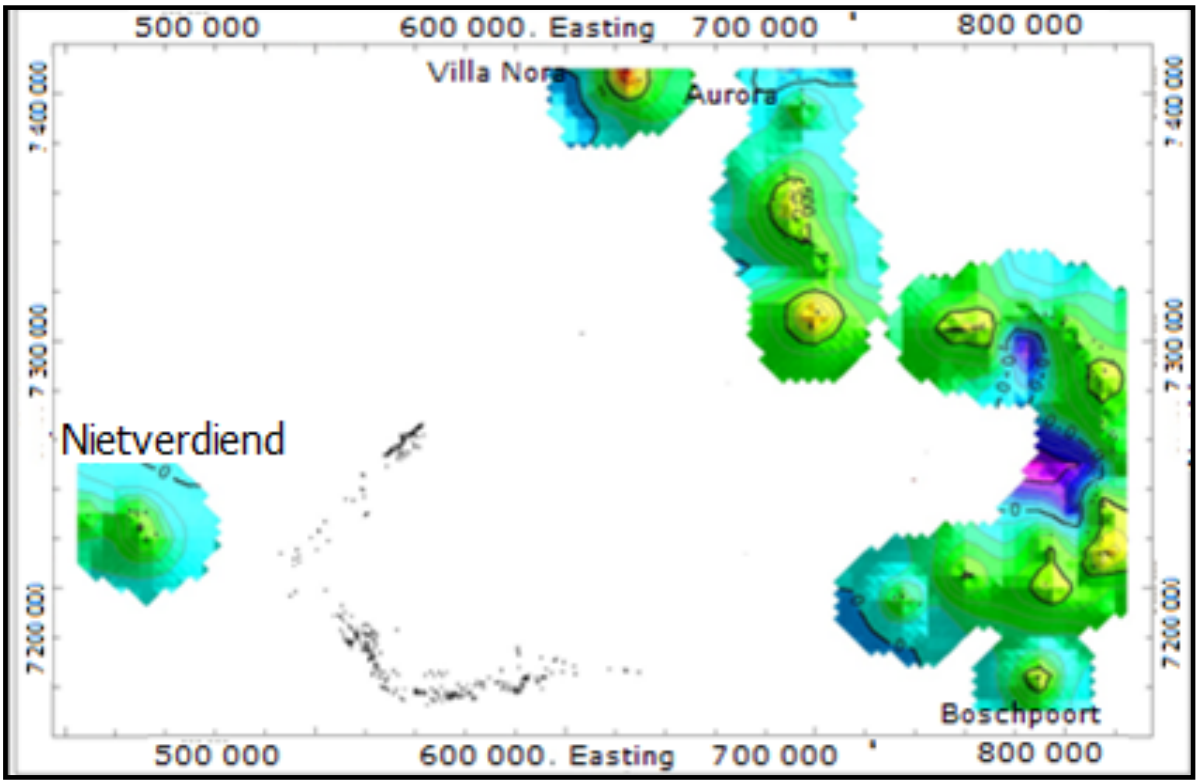

Figure 5.32: 2D grid model of Archaean granite top in the Bushveld Complex using the Auto Trend Surface Residual method.

The Archaean rock thickness is not well defined in most places because most of the boreholes did not fully penetrate this unit. Hence, in describing the floor rocks the interval structure contour map of Archaean rocks will be utilized.

At Far Northern the Bushveld area, the floor rocks slope southwest due to the presence of an anticlinal structure in the southeast. The anticlinal structure plunges southwards and opens to the north. It slopes gently to the southeast while the slope in the southwest is rather steep. A profile drawn across this structure in Figure 5.33 shows a downthrow of more than 500 m in the southwest and less than 100 m in the southeast.

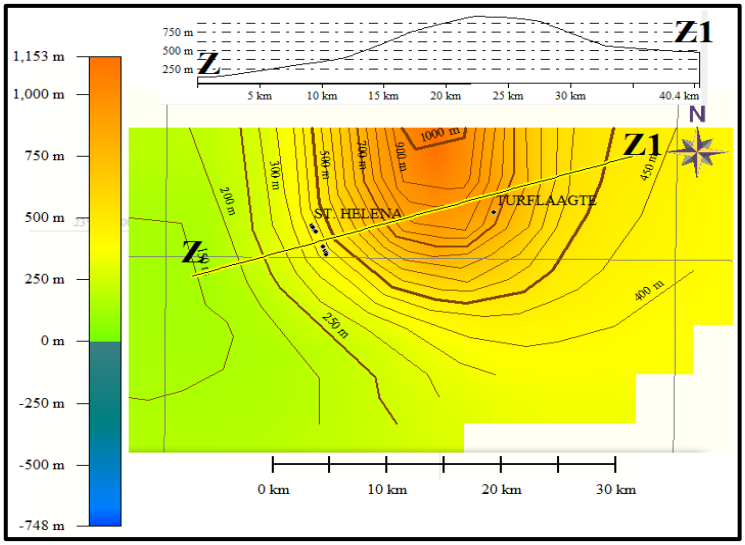

Figure 5.33: Profile across the Far Northern Bushveld Complex area structural contour intervals. Archaean rocks top interval respectively shows the structural trend in the Far-Northern Bushveld.

CHAPTER 6 TREND SURFACE ANALYSIS OF RLS

6.1 CHAPTER INTRODUCTION

In order to enhance the understanding and ability to make better and easier geological interpretations of the subsurface, especially in economically important regions such as the BIC, the Trend Surface analysis was utilized. This technique analysed and described the interaction between trend and residual structure to the thickness of stratigraphic units with the aim of distinguishing between pre-, syn- and post-emplacement structures. This will also help to unravel the development and timing of the growth of these structures. The study also attempts to find out the mechanisms responsible for the location and geometry of structures as well as to reconstruct the developmental history of the Rustenburg Layered Suite (RLS).

The relationship between the structure in which magma accumulates and thickness of the deposit is usually inverse. The reason for this is that previously structurally negative areas i.e., low land areas such as synclines and basins formed before the deposition will receive more influx than positive or structural high except if the area has been structurally disturbed by later tectonic activities. The RLS although igneous in origin exhibits stratigraphic layering that is very similar to sedimentary layering and is analyzed as such.

An attempt was made to relate stratigraphic unit thickness of the RLS units to positive and negative structural features by comparing the isopach and structural contour maps computed with the trend surface analysis technique. This technique has a long history of application in delineating structural trends and related features which might be difficult to detect using other interpolation methods due to masking by dominant regional trends. The effectiveness of this technique in studying subsurface structures was first demonstrated by Krumbein (1959) but has since been employed in different aspects of geology for stratigraphic and structural controlled resource exploration (Cook, 1969; Baird et al., 1971; Davis, 2002; Evenick, 2008; Evenick et al., 2008; Mei, 2009).

The overall geometry reveals the deposition of the major stratigraphic horizons as well as the inverse relationship between structure and thickness of pre- and syn-Bushveld structures, with some few exceptions, which could be classified as post-Bushveld structures. The general landscape is dominated by low undulating bedrock surface with little relief.

While most parts of the RLS show some correlation in terms of residual structure and thickness at the subsurface, the Amandelbult section of the Northwestern Bushveld shows a relatively flat Upper Zone unit masking a terrain of buried graben.

6.2 VARIATION IN STRUCTURE AND THICKNESS

The Rustenburg Layered Suite (RLS) ranges in thickness from a few cm to more than 8000m (Cawthorn and Web, 2001; Manyeruke 2003; Kinnaird, 2005). However, there is little relief on the upper surface of the RLS; changes in thickness are related not only to variations in the depth of the RLS surface, but to some other factors. The thickness is influenced mainly by (1) subsurface geology, (2) pre, syn- and post-Bushveld structures that influenced the geometry and distribution of the RLS. The Northwestern sector of the Bushveld Complex will be discussed in detail with all the relevant diagrams. However, most of the figures showing identical trends will not be repeated in subsequent sections.

6.3 TREND SURFACE ANALYSIS OF PARTS OF THE RUSTENBURG LAYERED SUITE

6.3.1 NORTHWESTERN BUSHVELD UPPER ZONE RESIDUAL STRUCTURE

First order Upper Zone structural residual map shows a general decrease in gradient from the SW to the NE. The structure contours are more regular in the SW (west of the Union section) than in the northeast. The NE part of the Union section shows gradual decrease in gradient compared to the southwestern side. A similar pattern is exhibited by higher residual orders. Figures 6.1-6.4 show the Upper Zone residual structural maps and structural trends for the northwestern Bushveld Complex

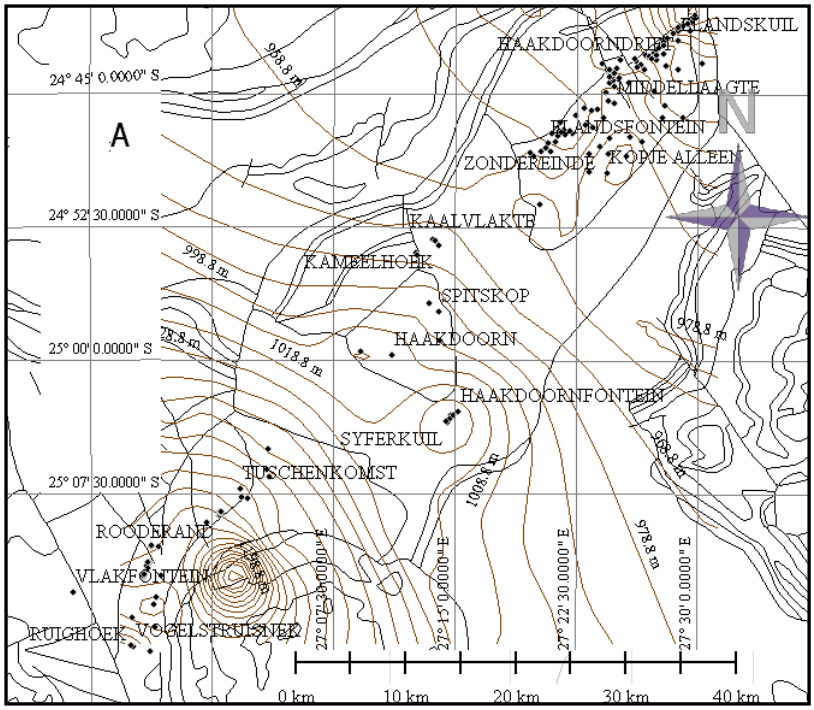

Figure 6.1: First-order residual structure map of the Upper Zone top in the RLS of the Northwestern Bushveld Complex with surface geological contacts (contour interval 10).

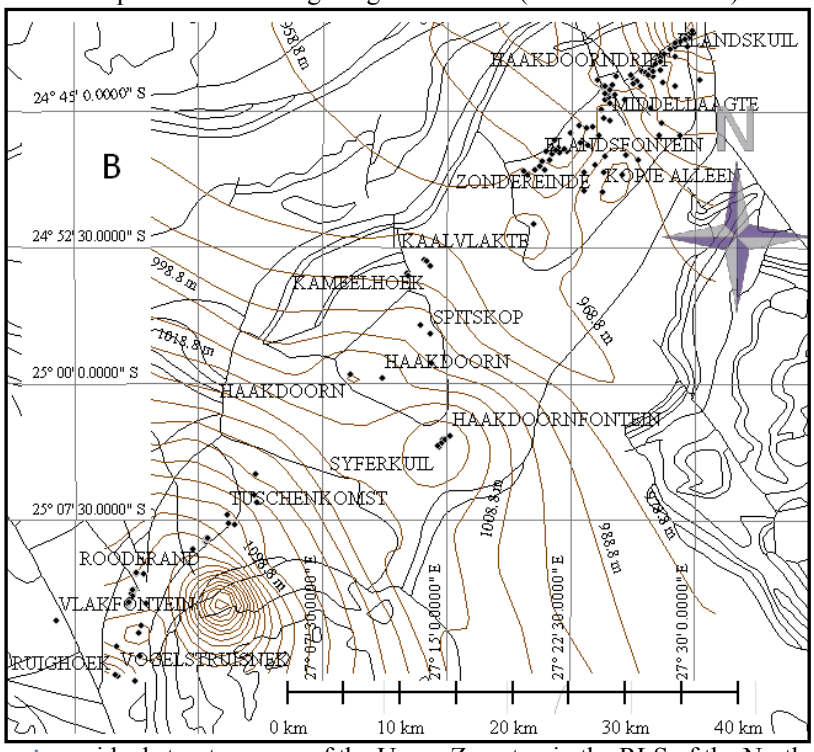

Figure 6.2: Second-order residual structure map of the Upper Zone top in the RLS of the Northwestern Bushveld Complex (contour interval 10).

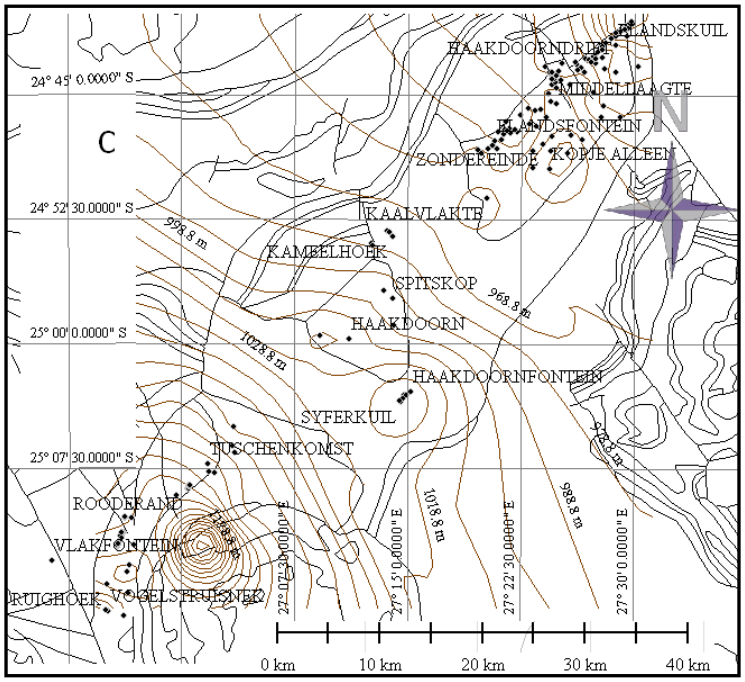

Figure 6.3:Third-order residual structure map of the Upper Zone top in the RLS of the Northwestern Bushveld Complex (contour interval 10).

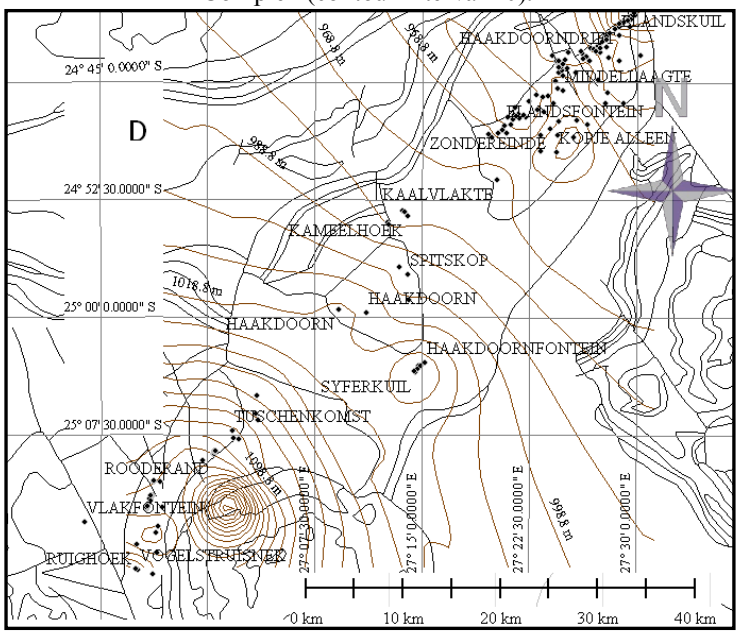

Figure 6.4: Fouth-order residual structure map of the Upper Zone top in the RLS of the Northwestern Bushveld Complex with draped geological contacts (contour interval 10).

6.3.2 NORTHWESTERN BUSHVELD MAIN ZONE RESIDUAL STRUCTURE

Patterns and trends on the Upper Zone top is the same with the Main Zone top interval. However, the first order Main Zone base residual structure shows a major NE decrease in gradient. The NE extreme exhibits a sharp slope to the southeast from the NW and SW. The central portion of the map exhibits a contracting structure in the northern and southern part. The southern part is marked by a wide structural high while the northern part has a depression that extends to the NW in Figure 6.5-6.8. An isolated structural high exists around the Kameelhoek farm at the centre. The structure in the Amandelbult section shows a structural low in the south and structural high in the northern parts as indicated in Figure 6.3. This central section is also marked by an irregular or rapidly undulating structural surface compared to its southwestern side.

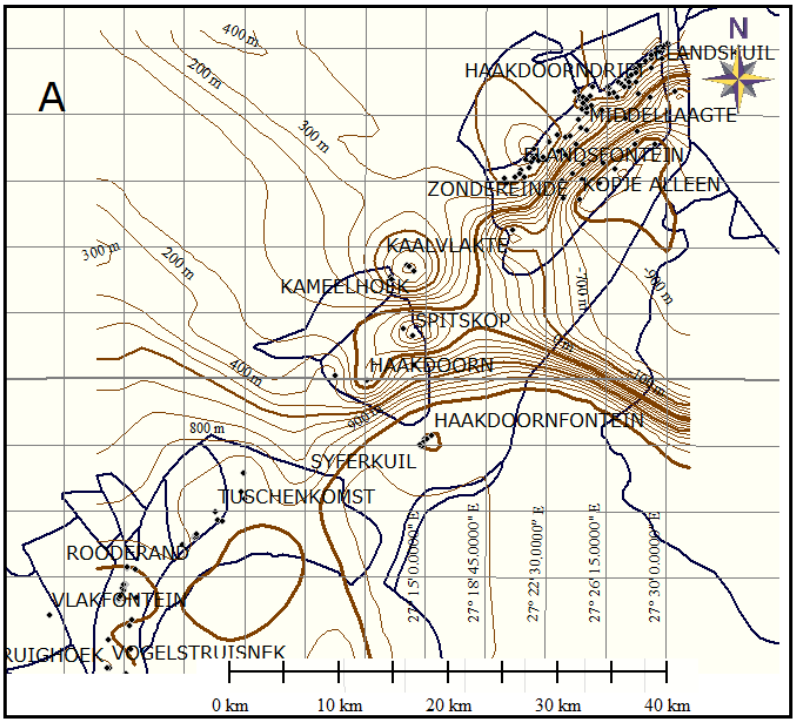

Figure 6.5: First-order (A) the Main Zone residual structure maps of Northwestern Bushveld Complex.

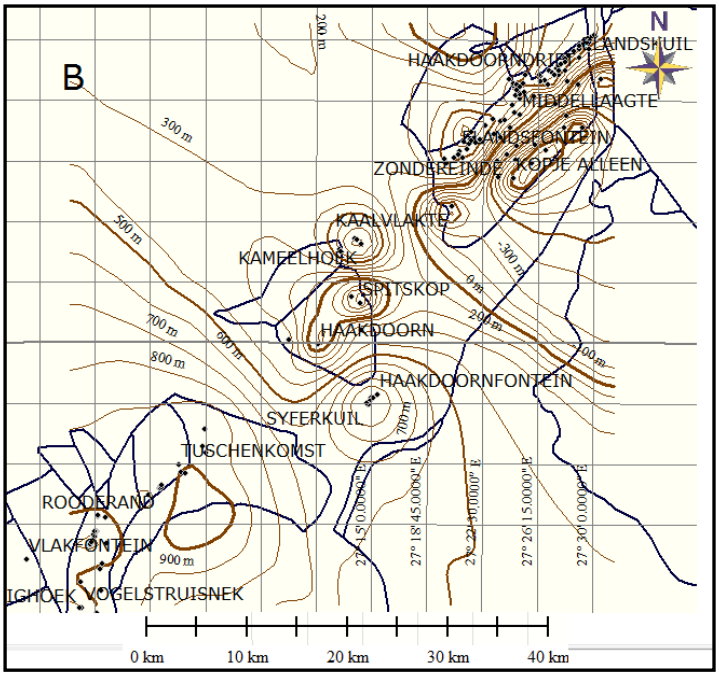

Figure 6.6: Second- order (B) of the Main Zone residual structure maps of Northwestern Bushveld Complex.

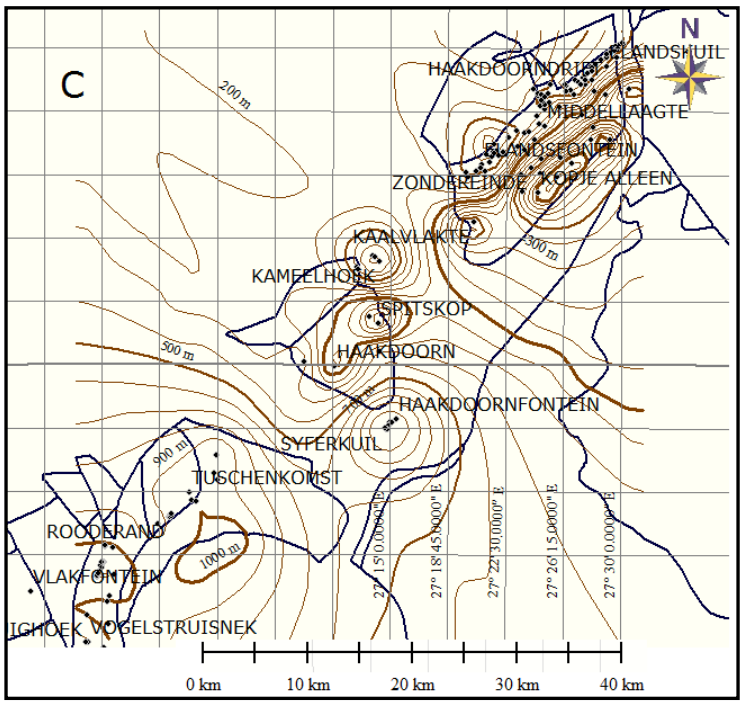

Figure 6.7: Third- order (C) of the Main Zone residual structure maps of Northwestern Bushveld Complex.

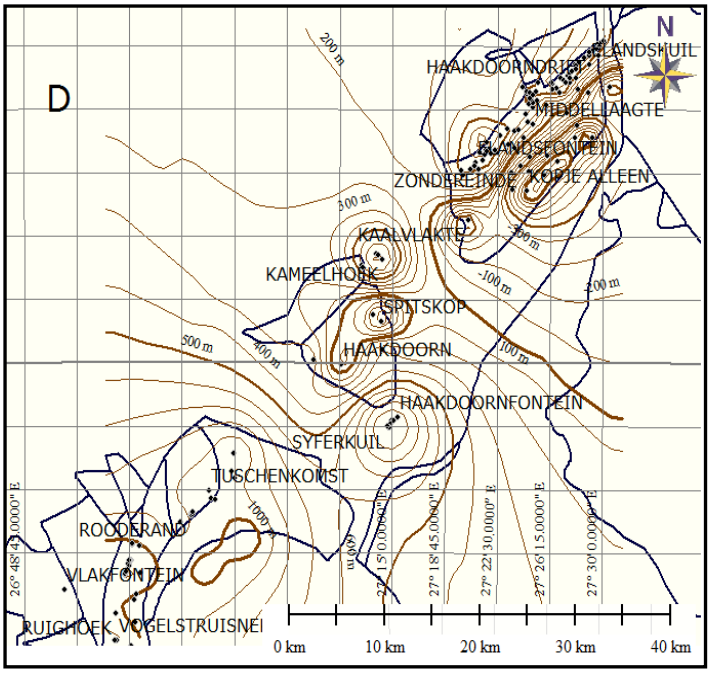

Figure 6. 8: Fourth order (D) of the Main Zone residual structure maps of Northwestern Bushveld Complex.

6.3.3 NORTHWESTERN BUSHVELD CRITICAL ZONE STRUCTURE RESIDUAL

The structure and isopach maps of the Merensky Reef indicate close similarity with the Main Zone base interval structure and isopach maps. Figures 6.9 to 6.12 reveal the prominent NE trending structure, negative domain and concomitant SE thickening pattern from the west. The central thinning domain coincides with the fault zone around the Brits section. Figures 6.13-6.16 represent the Merensky reef isopach maps with strong thickening around northeast.

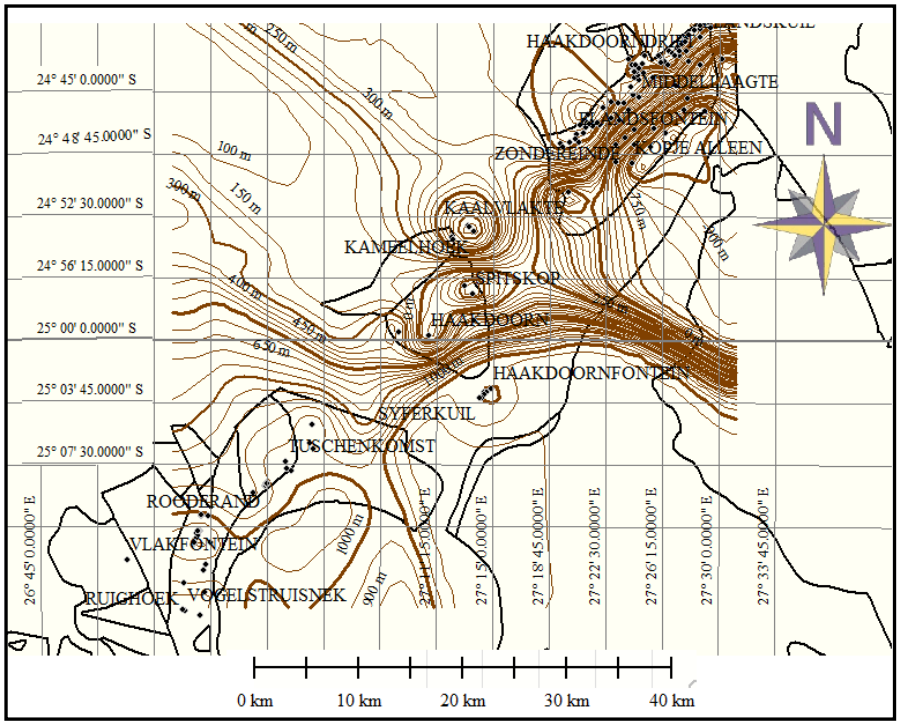

Figure 6.9: First - order (A) the Main Zone residual isopach map of Northwestern Bushveld Complex.

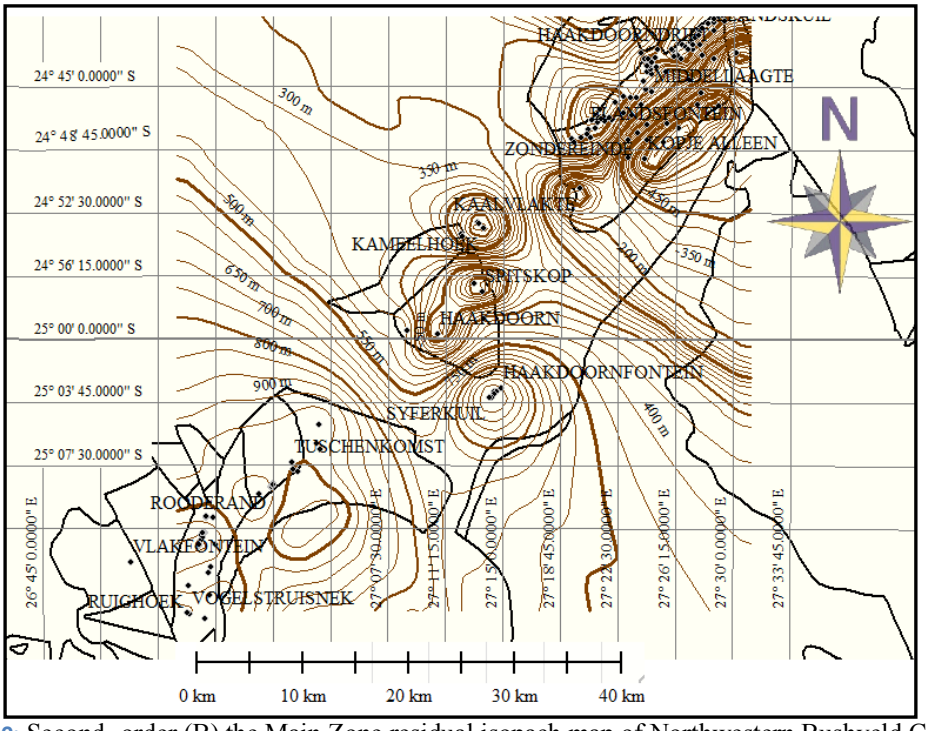

Figure 6.10: Second- order (B) the Main Zone residual isopach map of Northwestern Bushveld Complex.

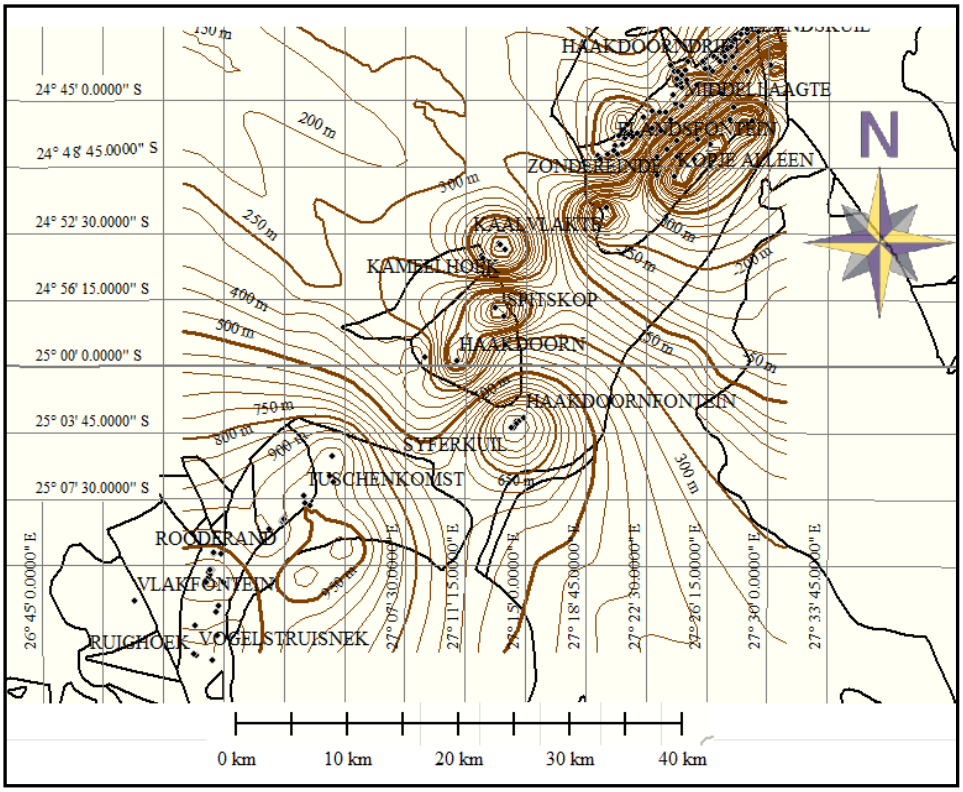

Figure 6.11: Third - order (C) the Main Zone residual isopach map of Northwestern Bushveld Complex.

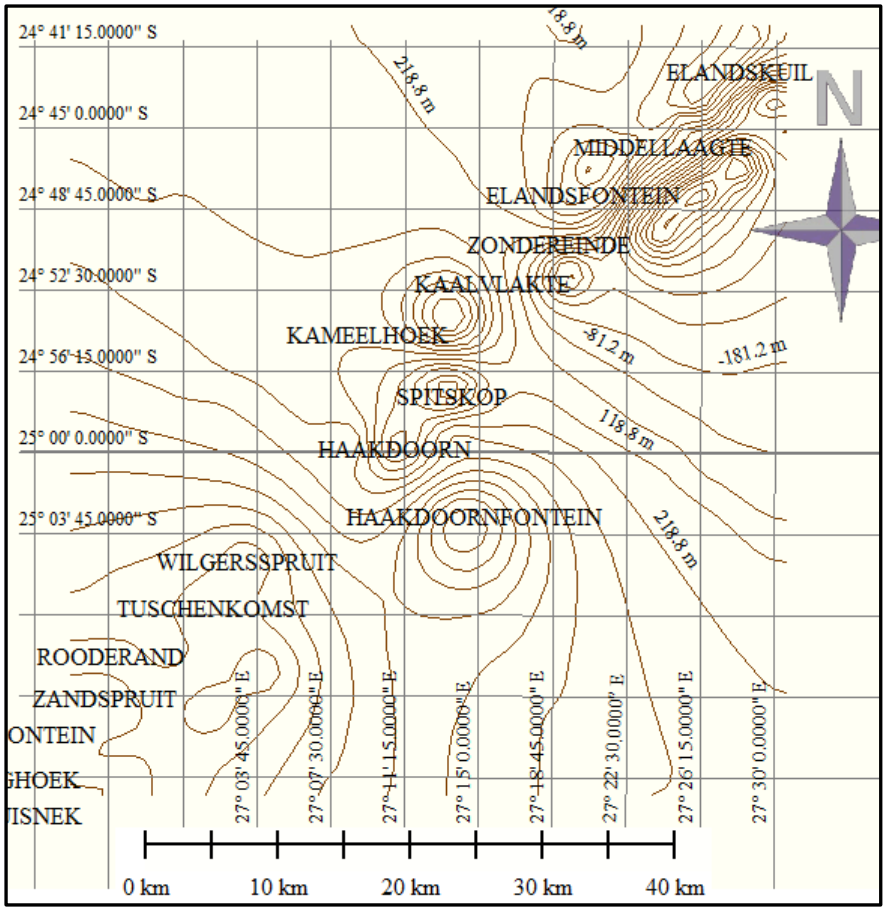

Figure 6.12: Fourth - order (D) the Main Zone residual isopach map of Northwestern Bushveld Complex.

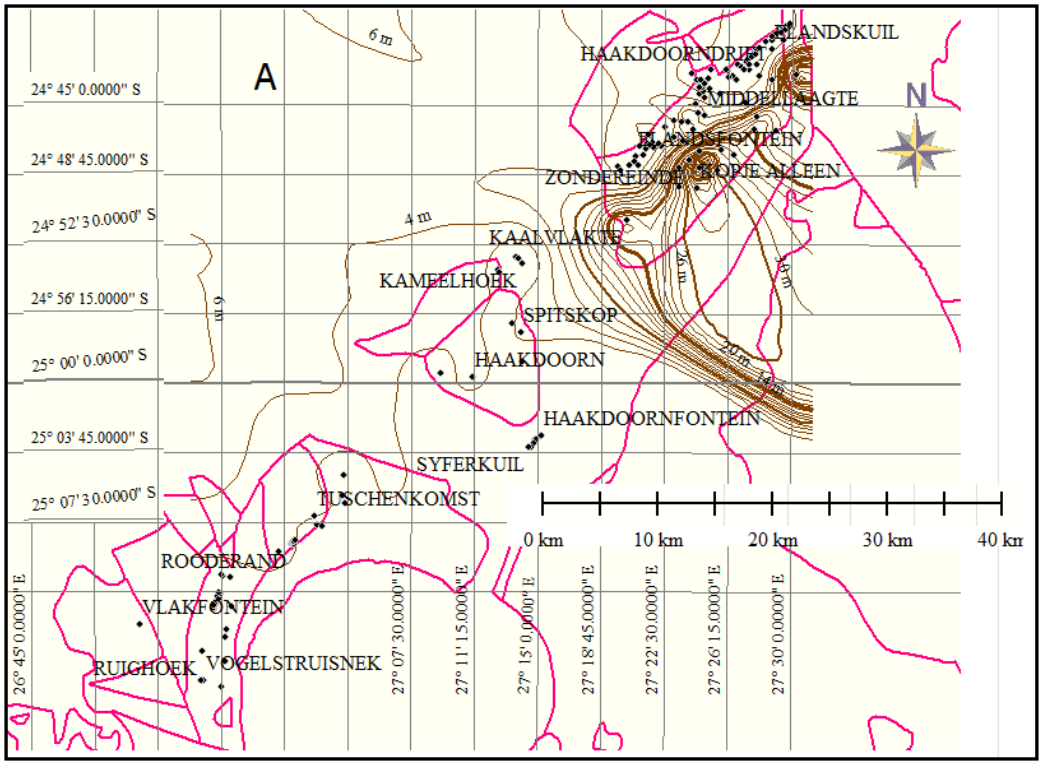

Figure 6.13: First order (A) Merensky Reef residual isopach map of the Northwestern Bushveld Complex

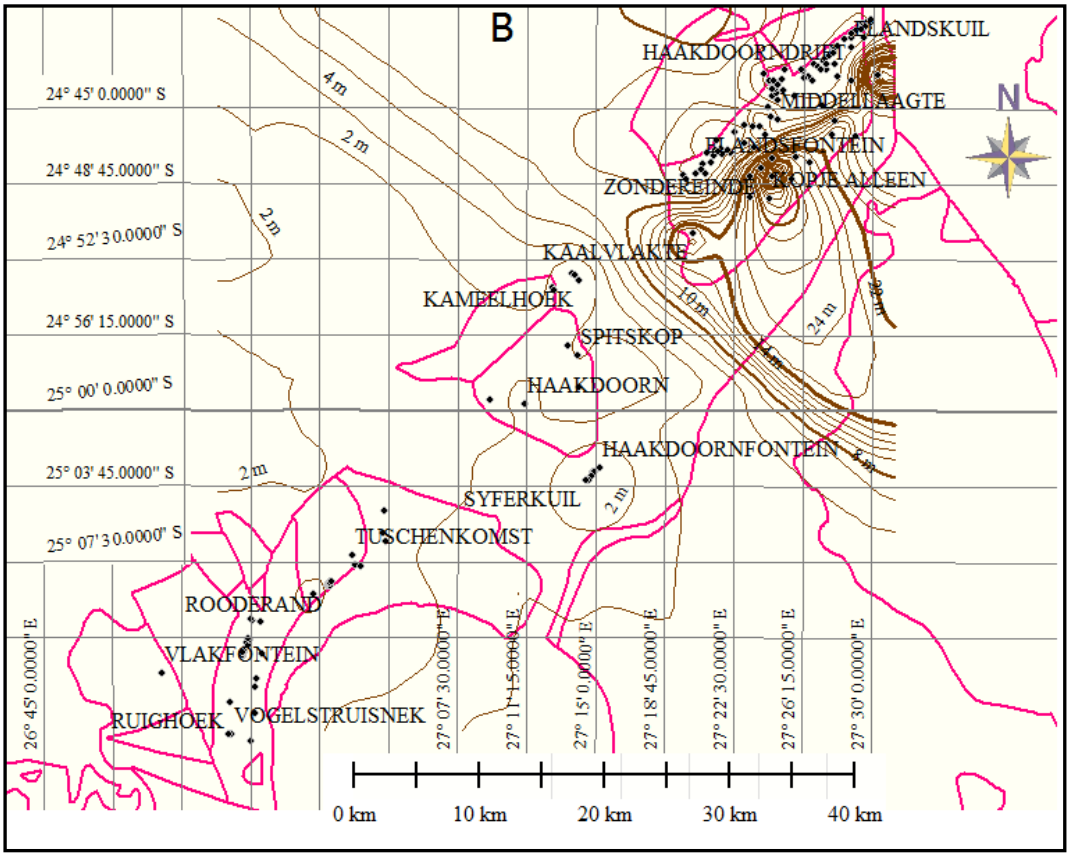

Figure 6.14: Second order (B) Merensky Reef residual isopach map of the Northwestern Bushveld Complex

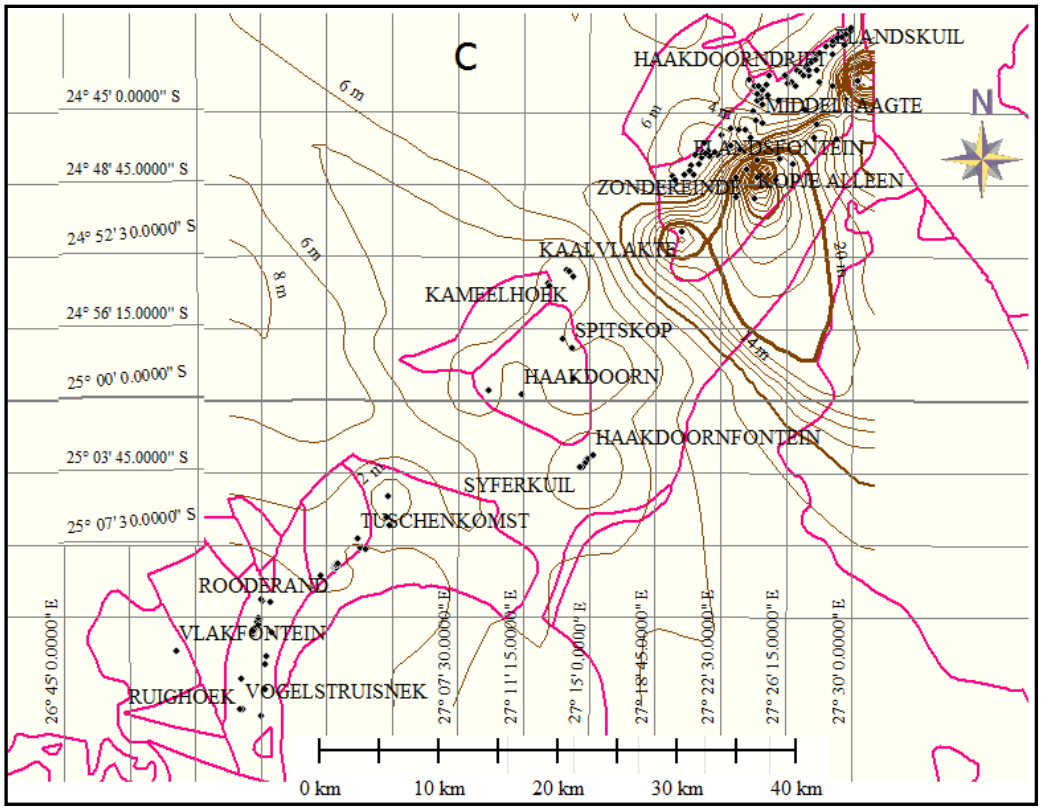

Figure 6.15: Third- order (C) Merensky Reef residual isopach map of the Northwestern Bushveld Complex

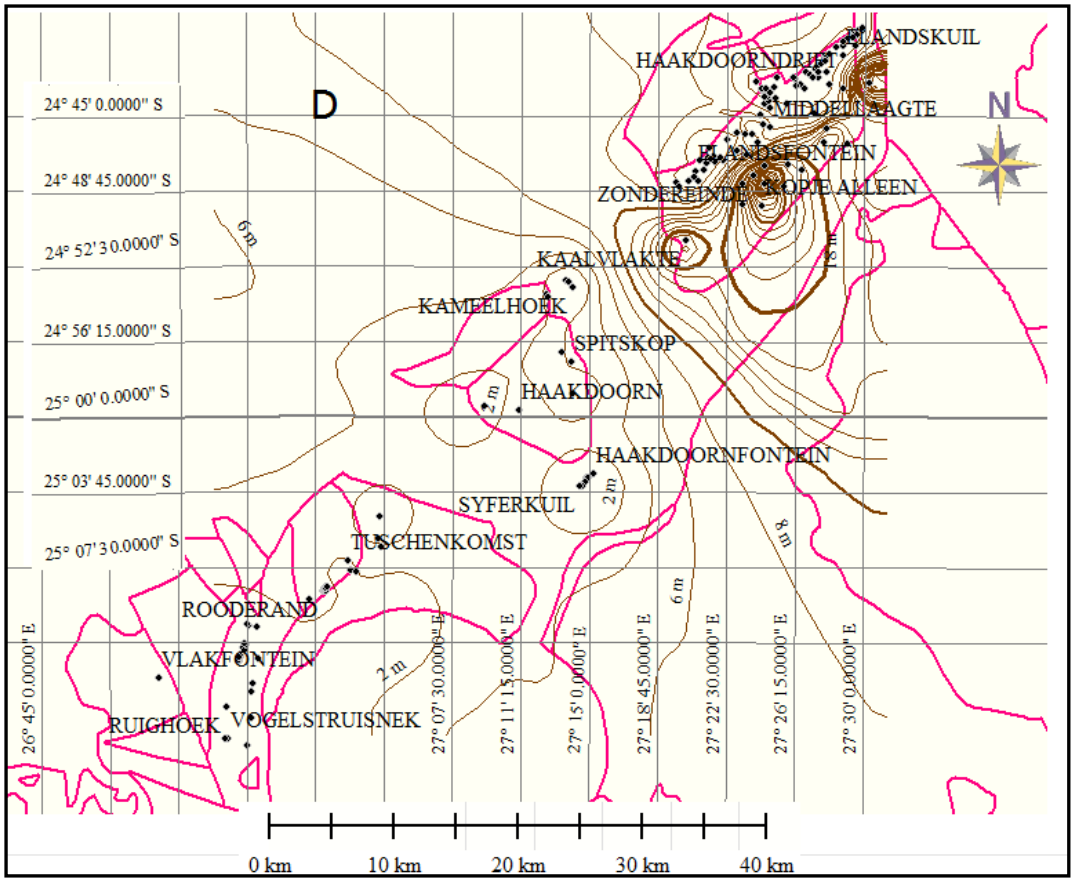

Figure 6.16: Fourth order (D) Merensky Reef residual isopach map of the Northwestern Bushveld Complex

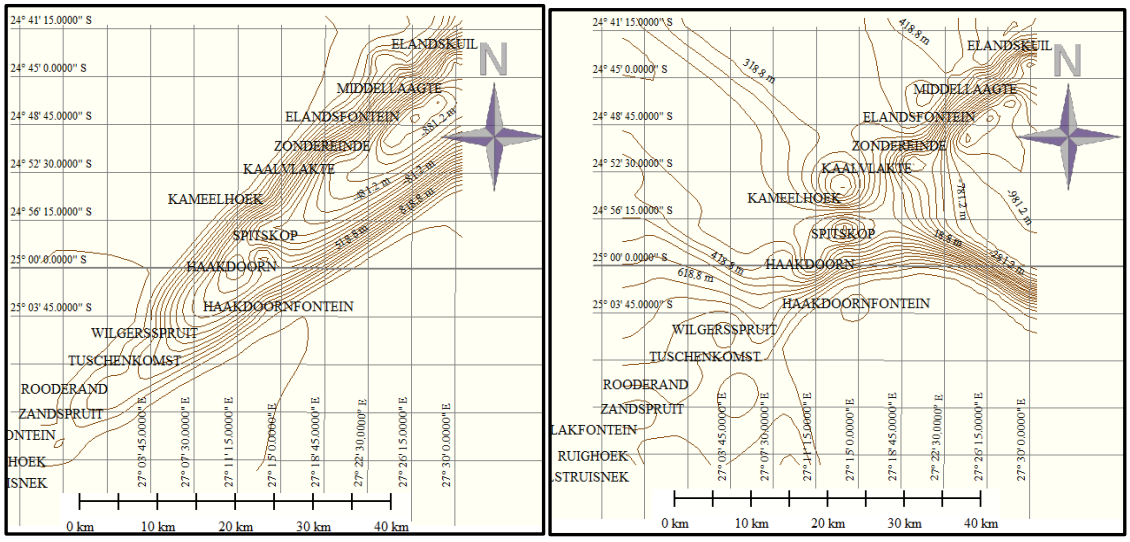

Figure 6.17: Second order Merensky Reef structural trend (left) and second order Lower Zone residual isopach map (right) of Northwestern Bushveld Complex

6.3.4 NORTHWESTERN BUSHVELD UPPER ZONE TREND RESIDUAL

ISOPACH MAP

The first order residual isopach map of the Upper Zone in the southwestern Bushveld Complex shows a prominent NW-SE thickening trend as indicated in Figures 6.18- 6.21. However, at the centre i.e. around Union section there is an isolated thickening that thins out, first gradually and later abruptly to the NE and SW. This abrupt decrease in thickening in the NE coincides with the Northern gap area while the other corresponds to the Southern gap area. A profile drawn across these three farms show a downthrow to the north. The same pattern is indicated on the residual structure map in Figure 6.22. Higher order Upper Zone isopach maps show a similar pattern. Figure 6.23 shows the profile across the northern part of the Amandelbult section with residual amplitude and a synclinal shape around the Middellaagte farm (see profile in Figure 6.23). The corresponding anticlinal shape is present on the Upper Zone structure map of the same area, thus indicating an inverse relation between structure and thickness.

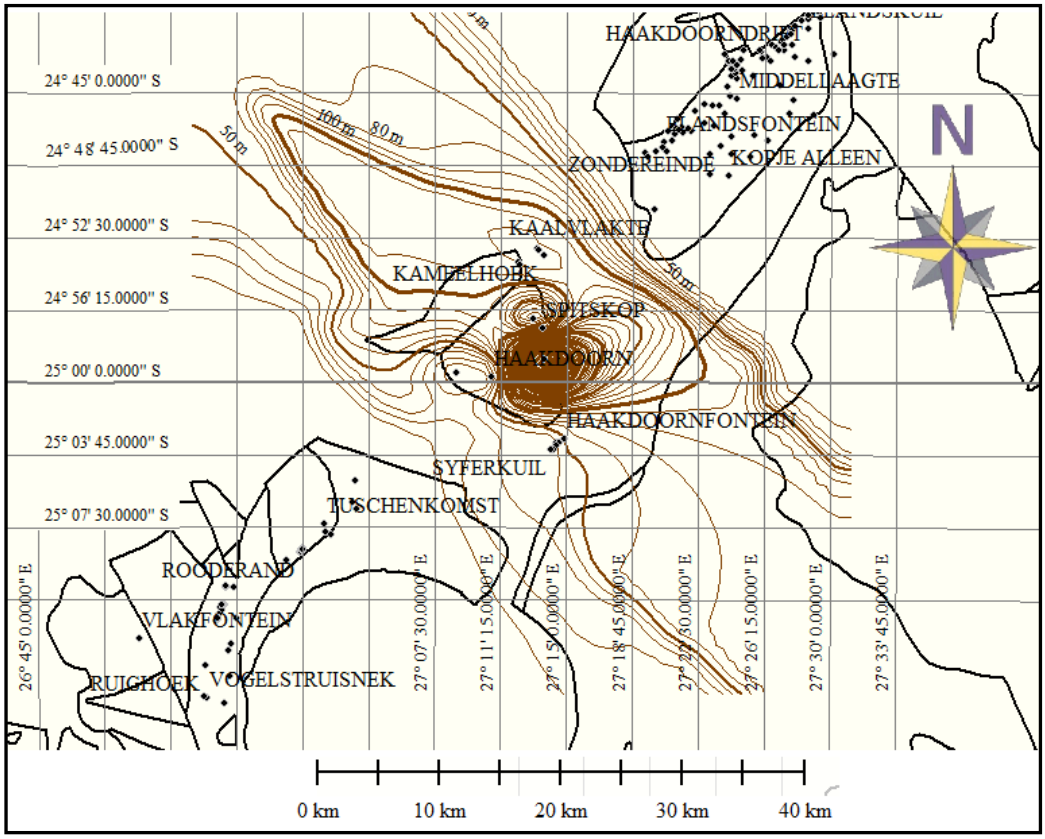

Figure 6.18: First-order (A) residual isopach for the Upper Zone of the Northwestern Bushveld Complex (contour interval is 10)

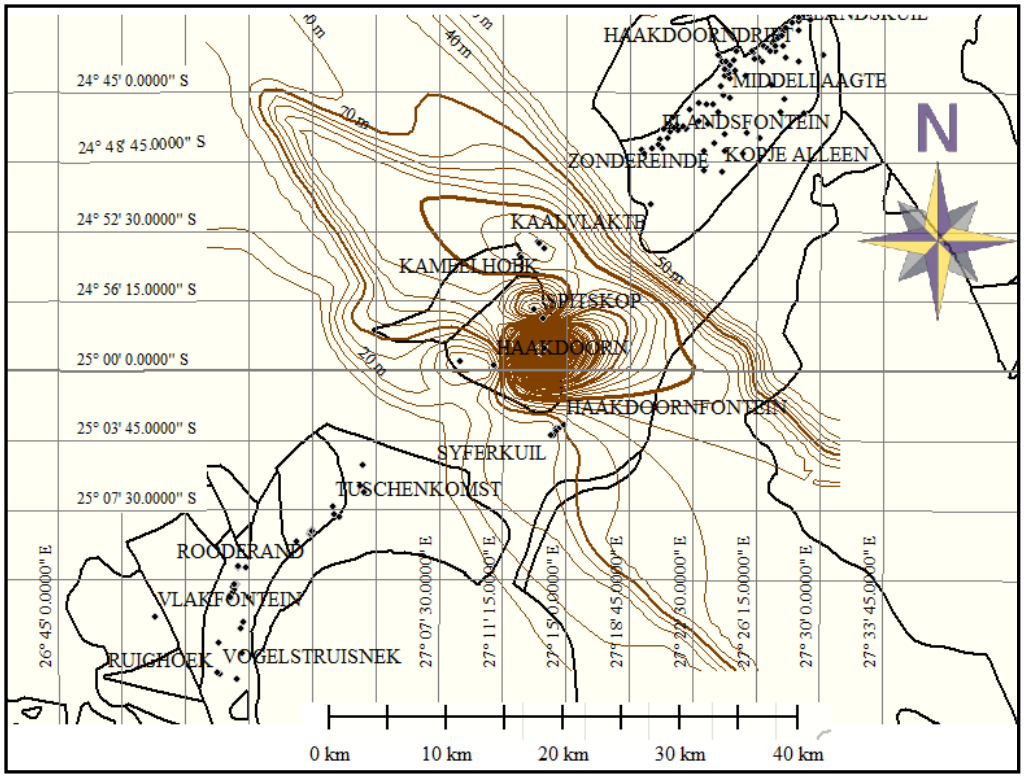

Figure 6.19: Second-order (B) residual isopach for the Upper Zone of the Northwestern Bushveld Complex (contour interval is 10)

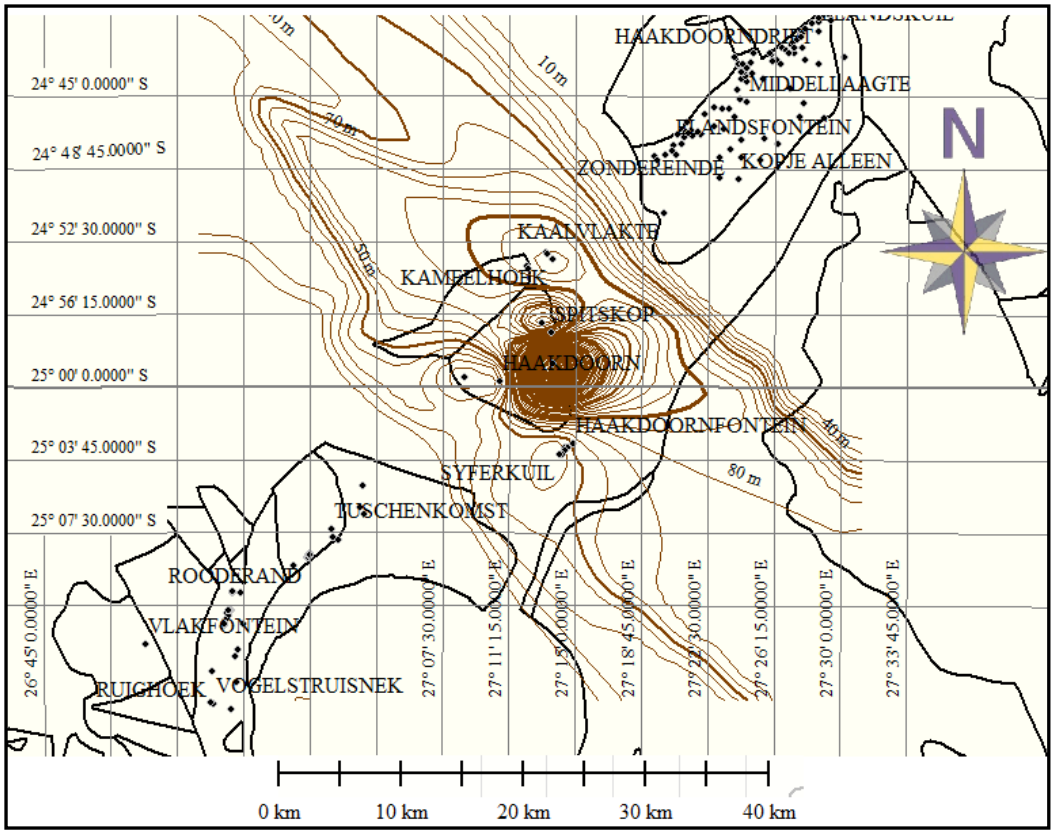

Figure 6.20: Third-order (C) residual isopach for the Upper Zone of the Northwestern Bushveld Complex (contour interval is 10)

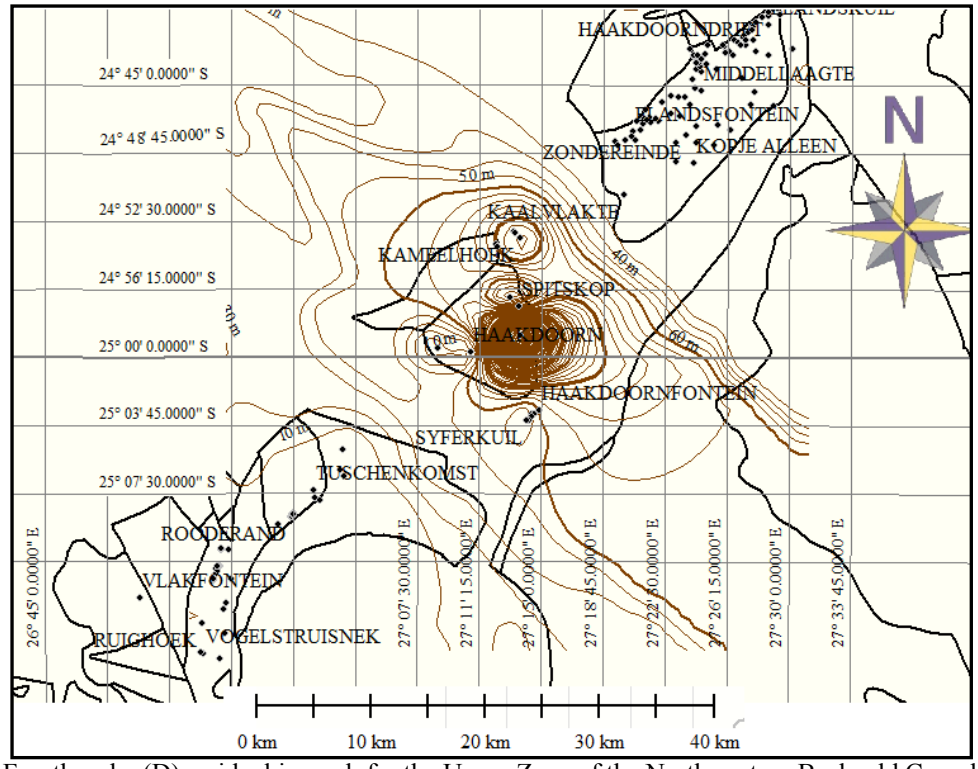

Figure 6.21: Fourth order (D) residual isopach for the Upper Zone of the Northwestern Bushveld Complex (contour interval is 10)

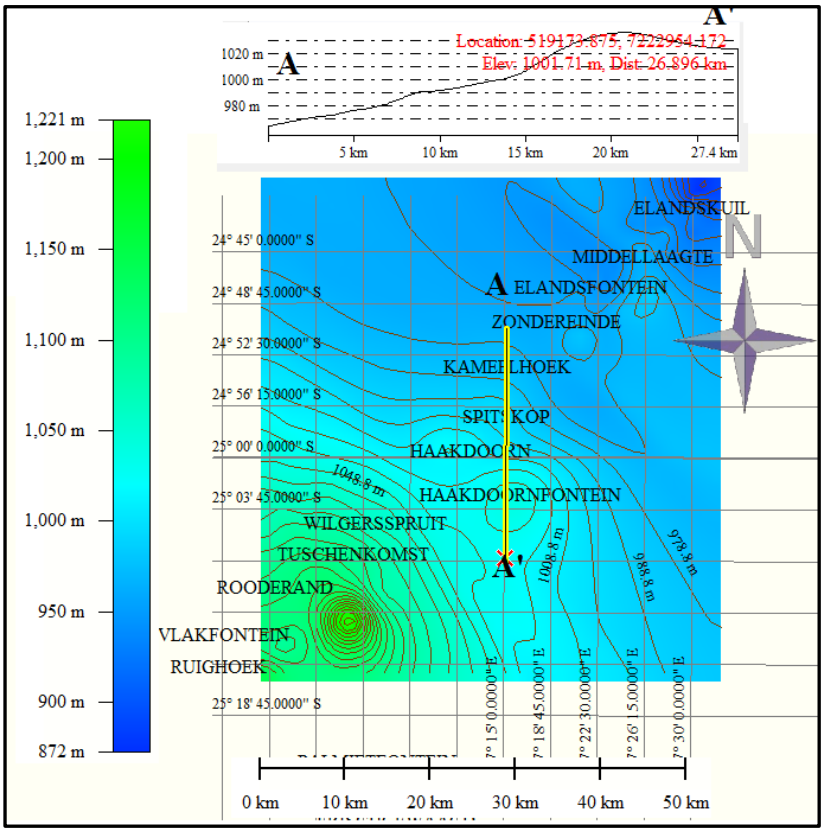

Figure 6.22: Profile across the Upper Zone top structure interval in the central part of the Northwestern Bushveld.

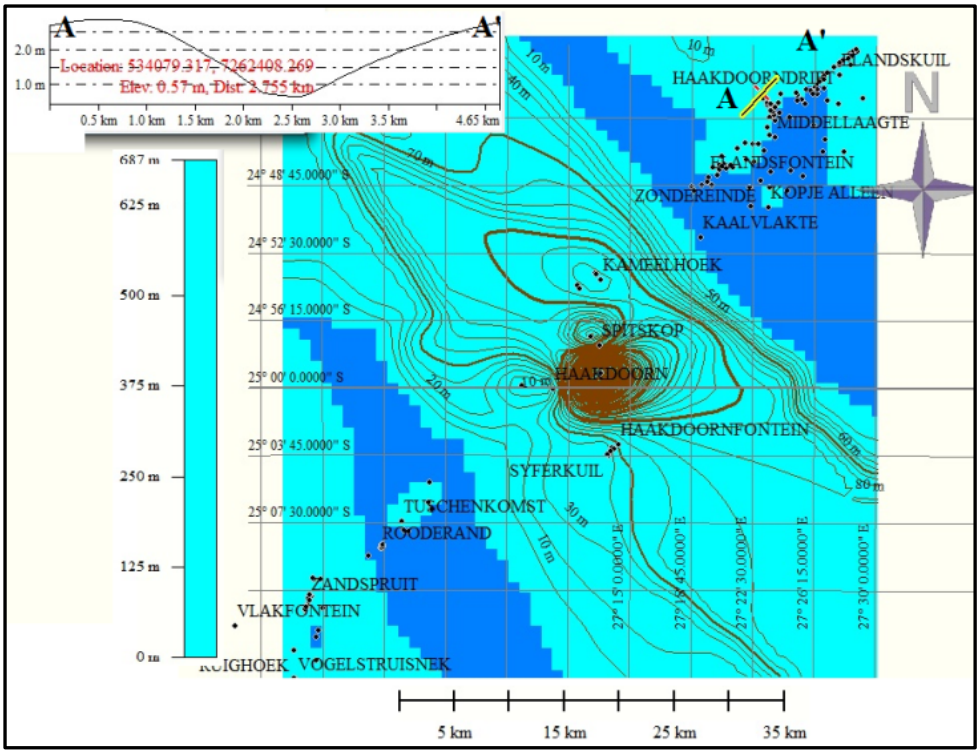

Figure 6. 23: Profile across Middellaagte showing the graben in the Northwestern Bushveld Complex.

6.3.5 RESIDUAL STRUCTURE MAPS OF NORTHWESTERN BUSHVELD

The contour pattern at the base of the Main Zone, especially around the Northwestern Bushveld indicates a SW-NE trending 'basin'/graben (Figure 6.24 shows a close-up of the NW of the Western Bushveld). The Northwest trending contours correspond to the Southern gap between the Northwestern section of the Western Bushveld and the Pilanesberg Complex. The Northern gap between the Amandelbult section and the Union section is represented by sharply decreasing contours to the east i.e. Amandelbult section and gradually increasing contours to the west, around the Union section.

The contour pattern also reveals the circular nature of the Pilanesberg Complex with a gentle plunge to the west. Contour lines are more broadly spaced south of the Pilanesberg Complex and closely spaced to the north.

The Main Zone is thickest in the Northwestern Bushveld Complex around the Amandelbult section.

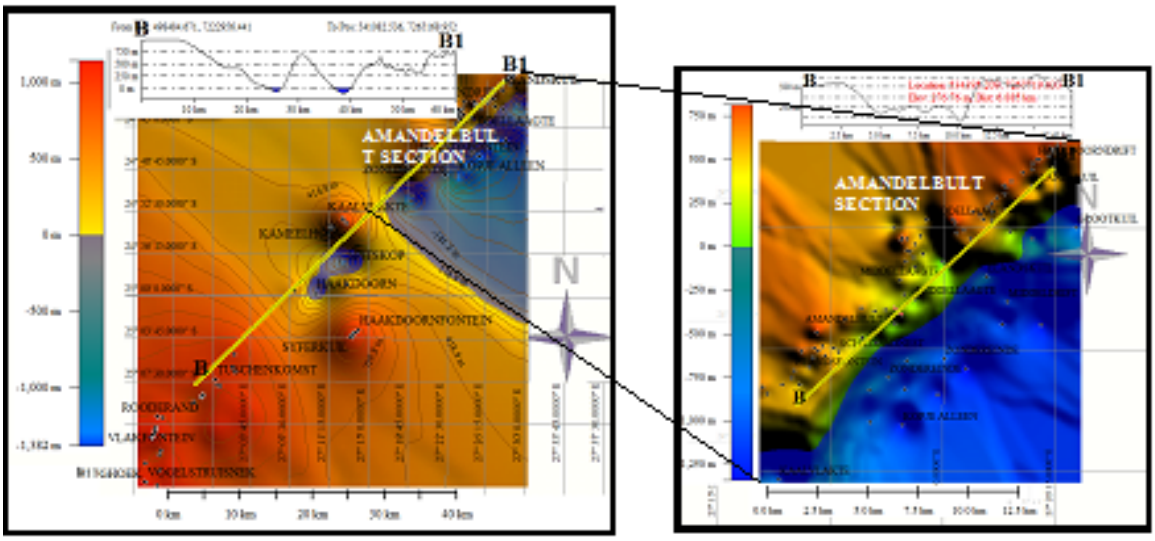

Figure 6.24: Close-up view of the Amandelbult section of the Northwestern Bushveld.

6.3.6 NORTHWESTERN BUSHVELD MAIN ZONE TREND RESIDUAL ISOPACH MAP

On the first order the Main Zone isopach residual map in Figures 6.25-6.28, the structural high areas correspond to areas with thinning while the structural low areas correlate with areas with thick deposition. Both the trend and residual structures match up with the structural grain. The southeastern parts of the maps are marked by abrupt thickening to the east, around the Amandelbult section.

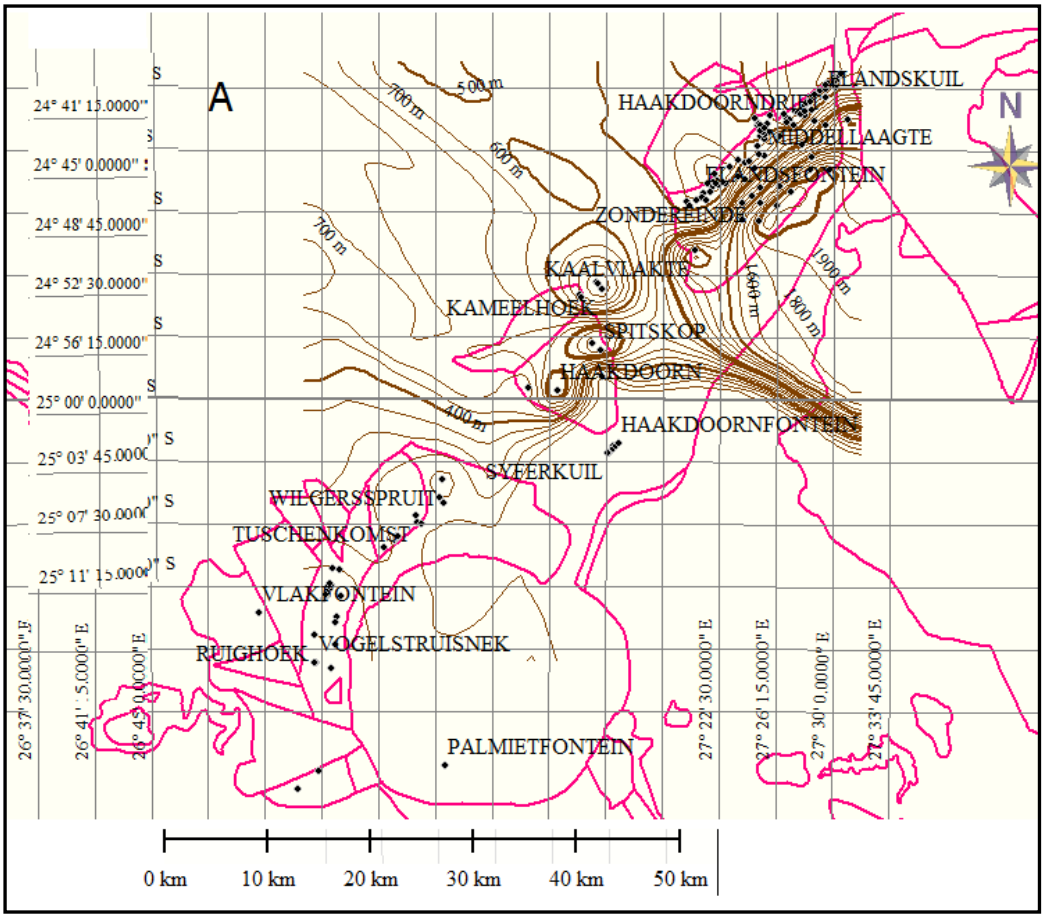

Figure 6.25: First - order (A) the Main Zone residual isopach maps of the Northwestern Bushveld Complex.

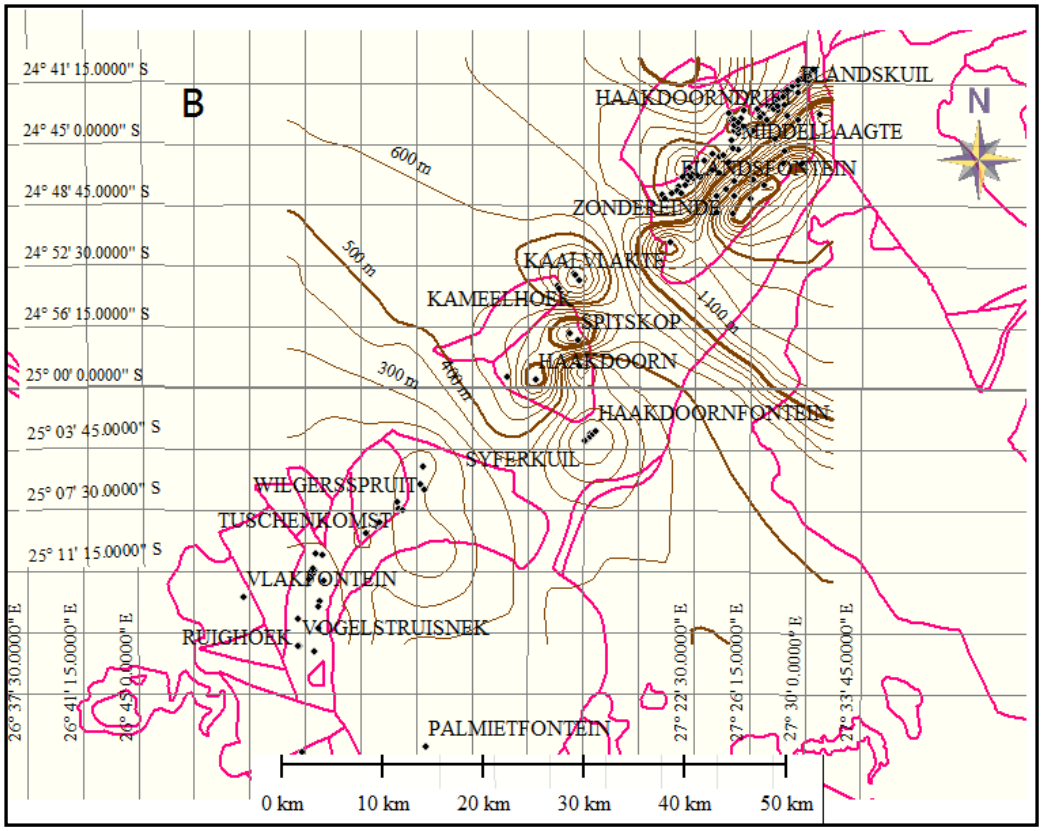

Figure 6.26: Second- order (B) the Main Zone residual isopach maps of the Northwestern Bushveld Complex.

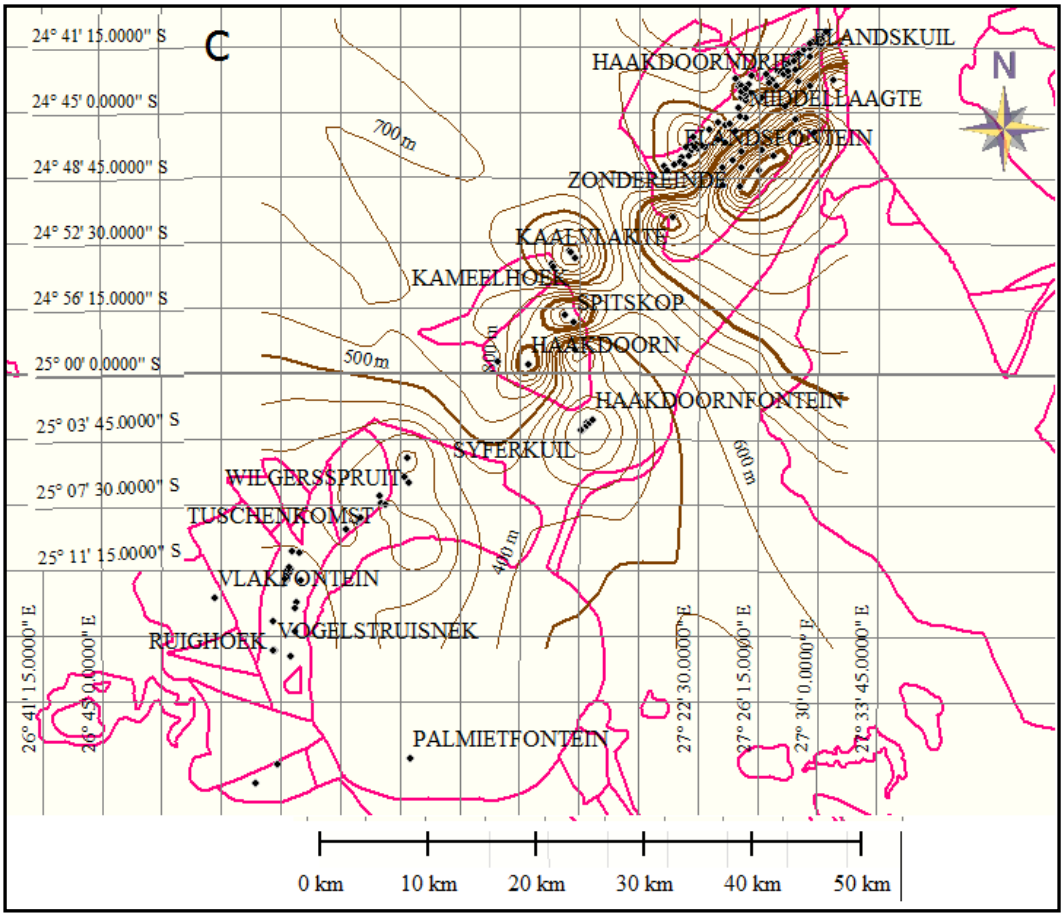

Figure 6.27: Third-order (C) the Main Zone residual isopach maps of the Northwestern Bushveld Complex.

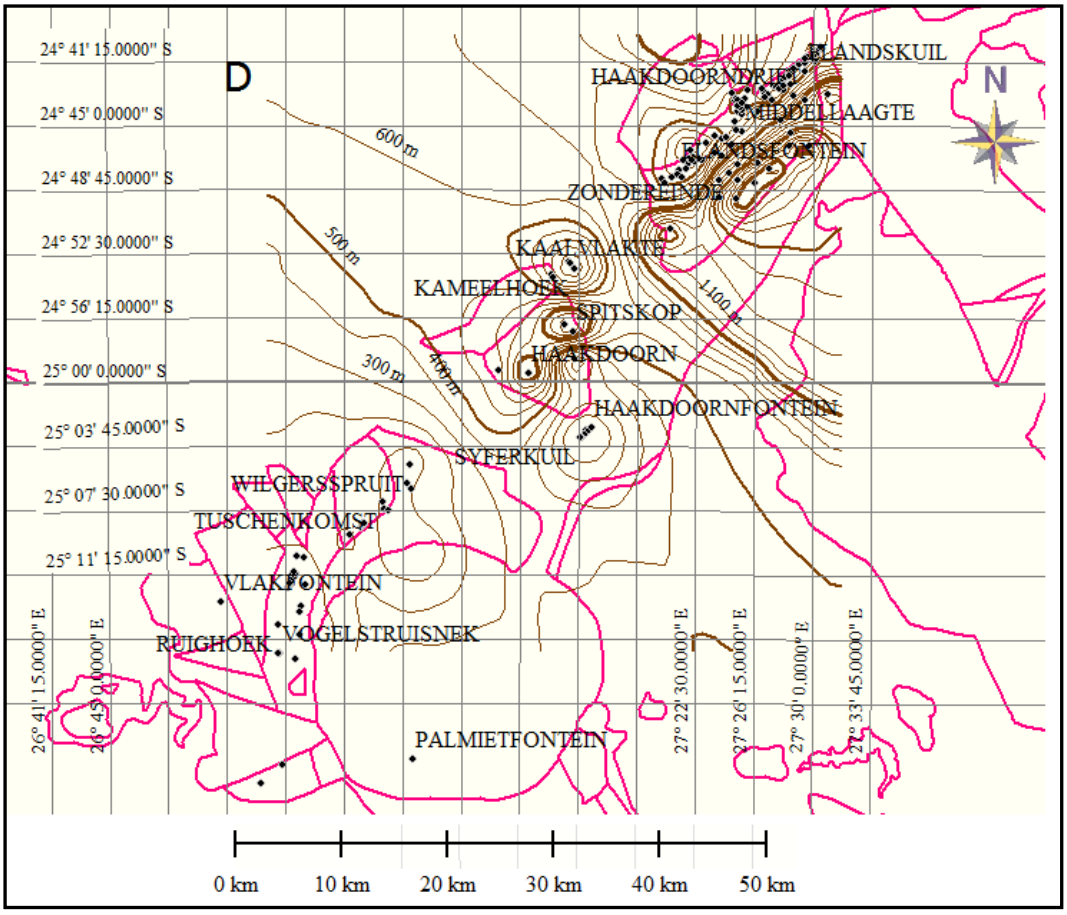

Figure 6.28: Fourth order D) the Main Zone residual isopach maps of the Northwestern Bushveld Complex.

6.3.7 NORTHWESTERN BUSHVELD STRUCTURE AND THICKNESS RELATIONSHIP

Strong abrupt thinning on both sides of the central section of the Upper Zone isopach residual map coincides with the gap areas. A profile across the area in Figure 6.29 reveals that the gap areas coincide with the downthrown sides of a centrally located positive thickness domain. Using the first order residual isopach for illustration, the central part of the Northwestern Bushveld on the Upper Zone residual isopach maps show a centrally located NW thickening trend with abrupt thinning to the east and west. However, on the Main Zone residual isopach map the same central portion is marked by a NW thickening trend in the north and Southeast thickening trend in the south. Figures 6.30) indicates the

independent relation between the Upper Zone residual isopach and structure while Figure 6.31) reveals a strong inverse correlation between theMain Zone residual isopach and structure. Strong southeast thickening coincides with a structural negative or a structural low area of the Amandelbult section; thickness is maximal in the axial part of this structure. This area is marked by structure controlled down-dip accumulation of sequence of RLS rocks.

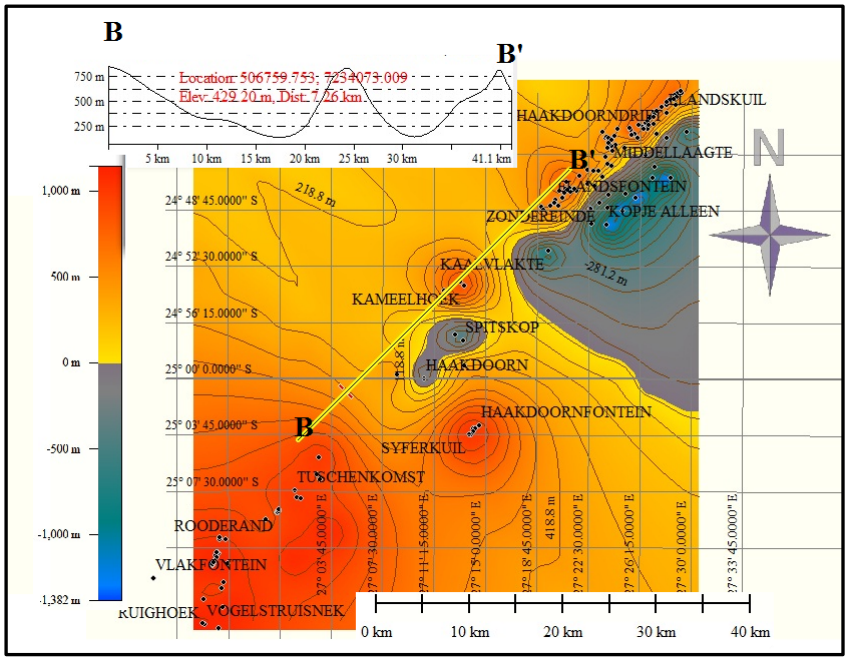

Figure 6.29: : Profile across the gap area on the Main Zone structure contour interval of the Northwestern Bushveld

Formation of most of these structures such as normal faulting and layer parallel slip movement has been attributed to structural readjustment of the underlying Transvaal Supergroup rocks (Carr and Groves, 1994; Eriksson and Reczko, 1995;Smith and Basson, 2006). Others are said to be syn-magmatic due to density contract, intrusion of syn-veins and pegmatites, slumping (Viljoen and Scoon 1985; Lee 1981; Ballhaus 1988; Scoon and Mitchell, 1994; Wilson et al., 1994; Viljoen, 1999; Reid and Basson 2002). This irregular structure might account for the formation of potholes in the area.

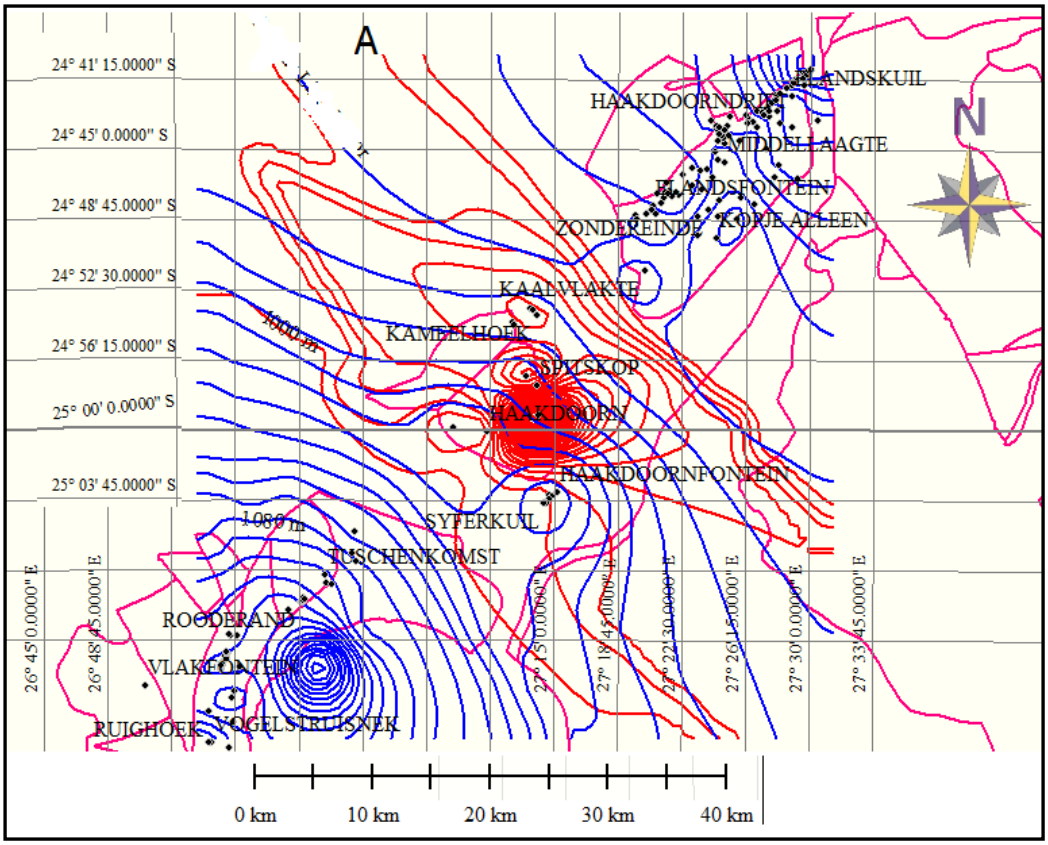

Figure 6.30:The Upper Zone structure (blue contours) and isopach (red contours)

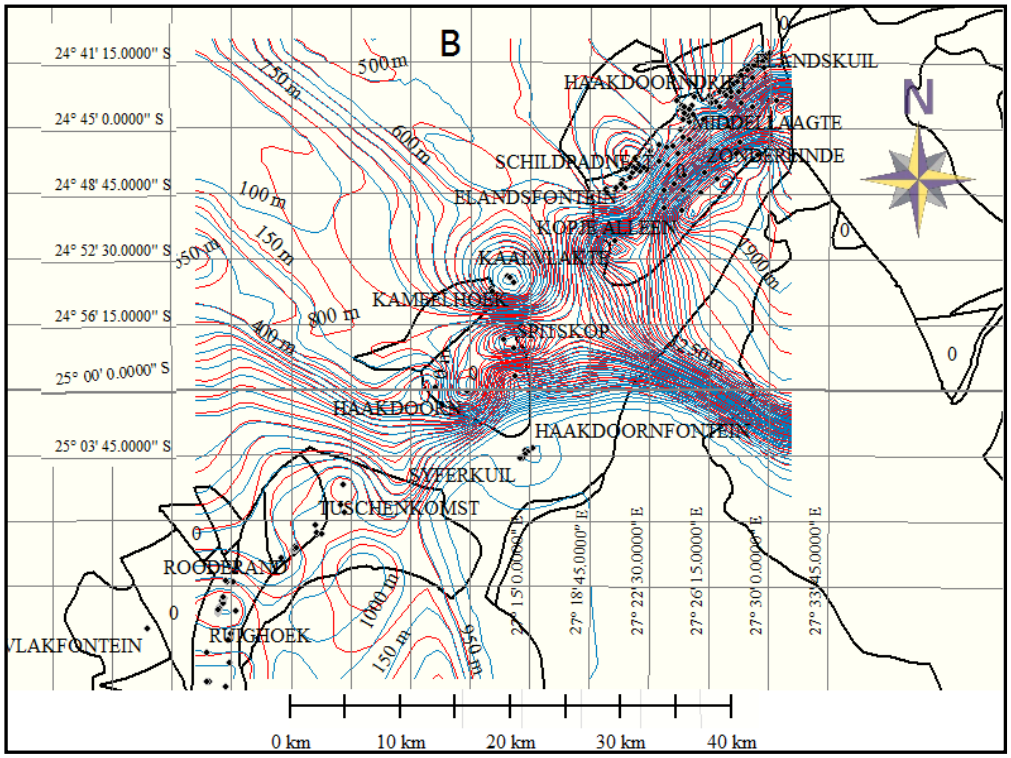

Figure 6.31: Main Zone structure (blue lines) and isopach maps (red lines).

6.4 TREND SURFACE ANALYSIS OF CENTRAL PARTS OF WESTERN BUSHVELD

6.4.1 RESIDUAL STRUCTURE OF CENTRAL PARTS OF WESTERN BUSHVELD COMPLEX

The western parts of the Pilanesberg Complex (Figure 6.32) also exhibits abrupt changes in the structural pattern with an abrupt increase in structure around Ruighoek farm. A structural negative domain probably controlled by the presence of faults dominate the area occupied by the Upper Zone around the Pilanesberg Complex. In spite of difference in orders the residual maps still show strong similarities to each other. Figure 6.32 shows the pattern onthe Upper Zone residual structure in the central part of the Western Bushveld Complex and reveals a strong NNW-SSE positive structure to the immediate south of the Pilanesberg Complex. Another positive domain that opens to the west exists to the immediate north of Pilanesberg Complex.

The Main Zone residual isopach surfaces are marked by a wide positive structural domain with a NE trend around the northern parts of the Pilanesberg Complex. The southern part shows a dominant eastward thinning at the centre with a steep slope to the west and a general SE trend. The extreme southern part shows thinning to the north. Two isolated structural negative domains (depressions/valleys) that are separated by a structural positive domain (hill) occur between around the Schaapkraal farm at the northern part of a Rooikoppies farm in the southwestern Bushveld Complex.

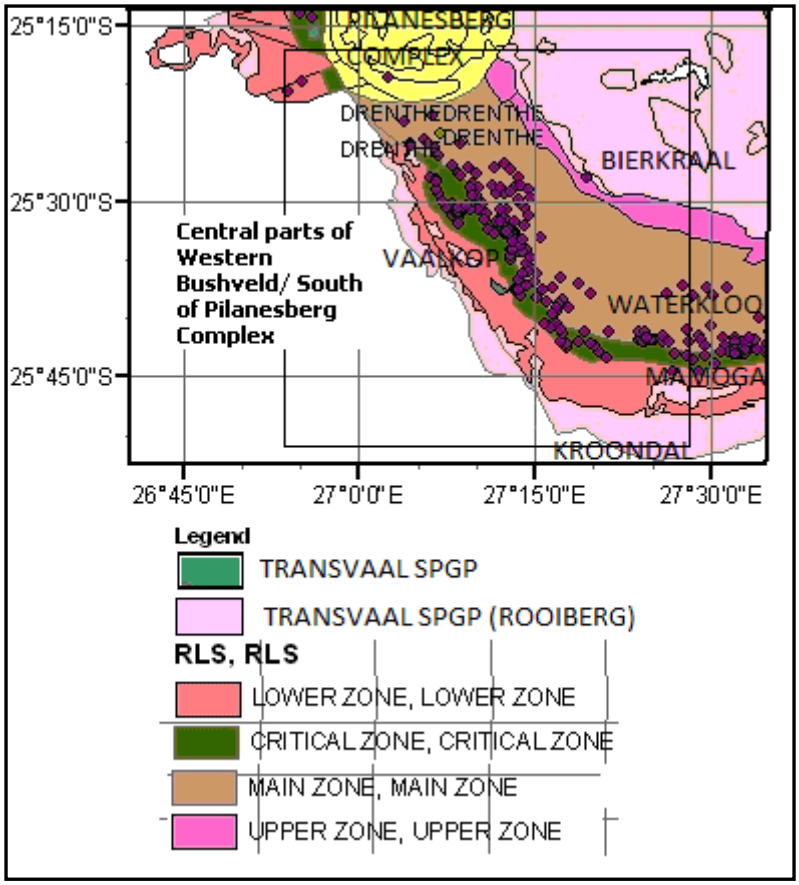

Figure 6.32: Geological map of Pilanesberg Complex area.

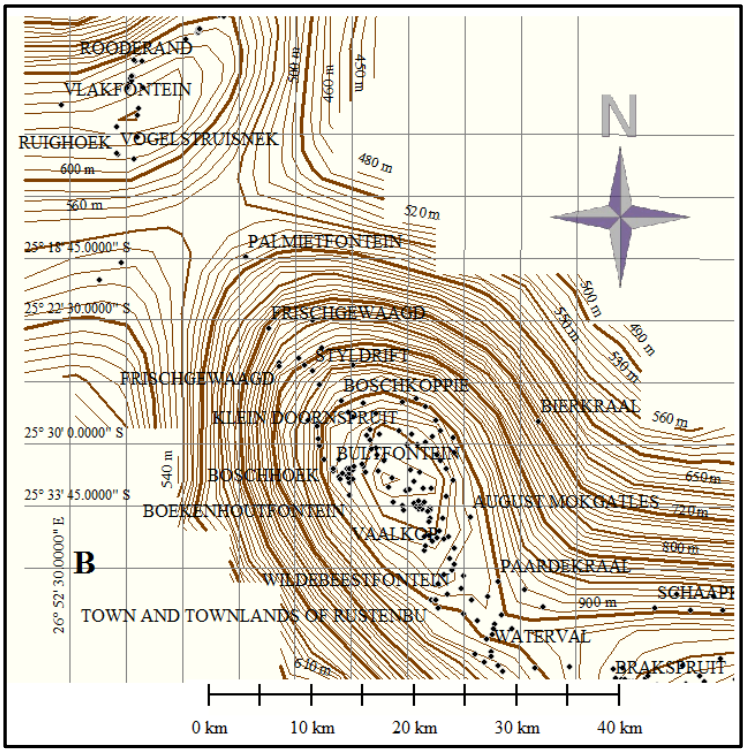

Figure 6.33: Second order (B) Upper Zone residual structure of central parts of the Western Bushveld Complex

6.4.2 RESIDUAL ISOPACH OF CENTRAL PARTS OF THE WESTERN BUSHVELD COMPLEX

The Upper Zone residual isopach map in Figure 6.34 indicates positive thickening towards the centre of the map and especially at the Bierkraal farm. It also reveals a sudden increase in thickness between Kroondal and Mamogales in the southern parts. This area coincides with a negative structural domain (a depression) on the residual structure map.

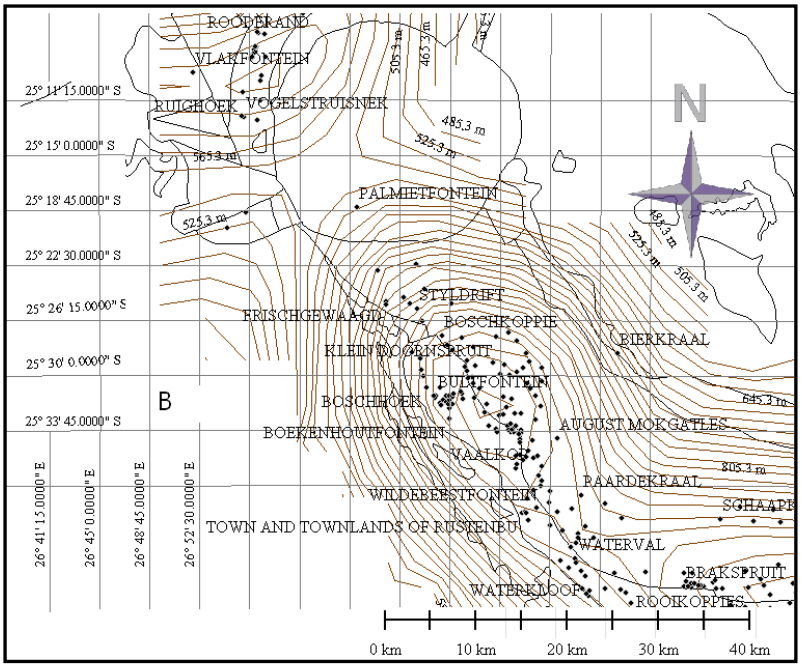

Figure 6.34: The Upper Zone residual isopach of central parts of the Western Bushveld Complex (contour interval 20 m).

The Main Zone isopach maps in Figure 6.35 show a progressively eastward thickening trend (with abrupt thinning in the west and south) at the southern parts of the Pilanesberg Complex. The northern parts indicate a strong NE thickening trend.

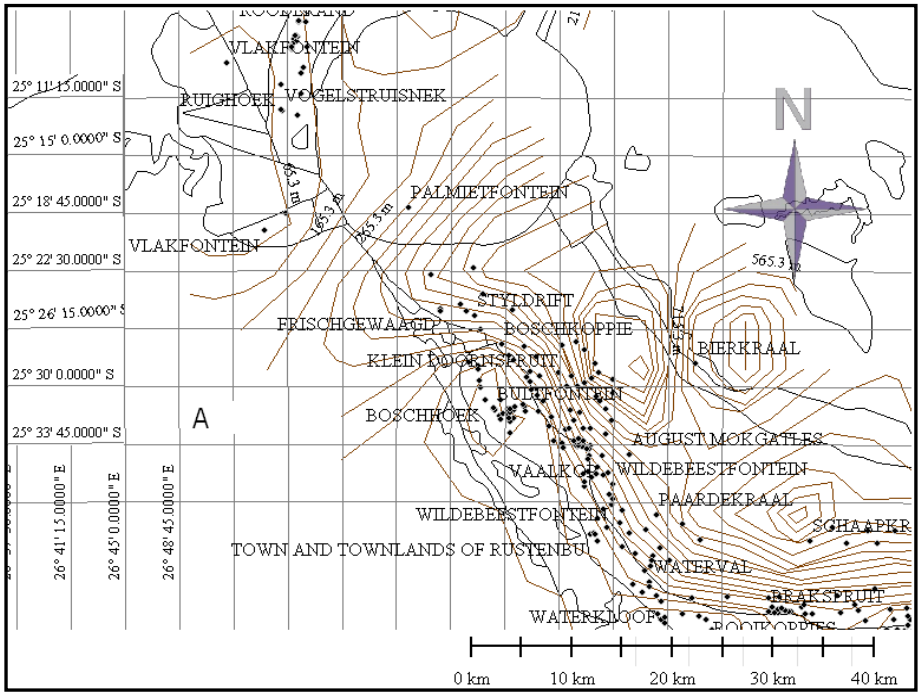

Figure 35: The Main Zone residual isopach of central parts of the Western Bushveld Complex showing the major structural trends in the area (contour interval 50 m)

6.4.3 STRUCTURE TREND SURFACE OF CENTRAL PARTS OF THE WESTERN BUSHVELD COMPLEX

The first order Upper Zone trend surface in the Upper Zone in Figure 6.36 is marked by NE trending contour lines around the Pilanesberg Complex while the immediate southern parts are dominated by NNW- SSE trending contours. The extreme southernpart of the Complex is marked by slightly curved (folded) east-west trending contours around the Kroondal structure. The whole area is dominated by a progressively negative structure towards the east. This trend is, however, more prominent around Bierkraal farm. Random change in structure is prevalent in this section. Second to fourth order trend surfaces show strong similarities.

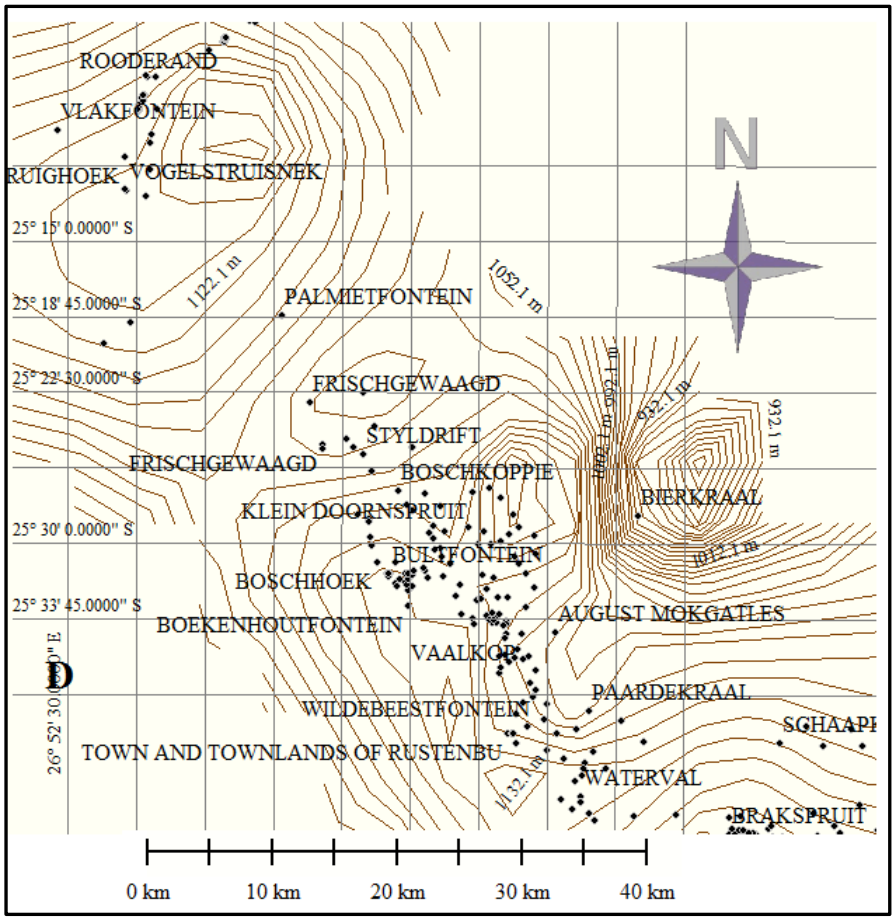

Figure 6.36: The Upper Zone structural trendsin the central parts of the Western Bushveld Complex

The Main Zone structural trend of the northern Pilanesberg Complex is mostly NE while the trend in the southern parts of the Complex is NNW-SSE (parallel to the trend of Rustenburg Fault) as indicated in Figure 6.37. A positive structural domain dominates the western part of the fault and a negative domain is prominent in the eastern part i.e. towards the centre.

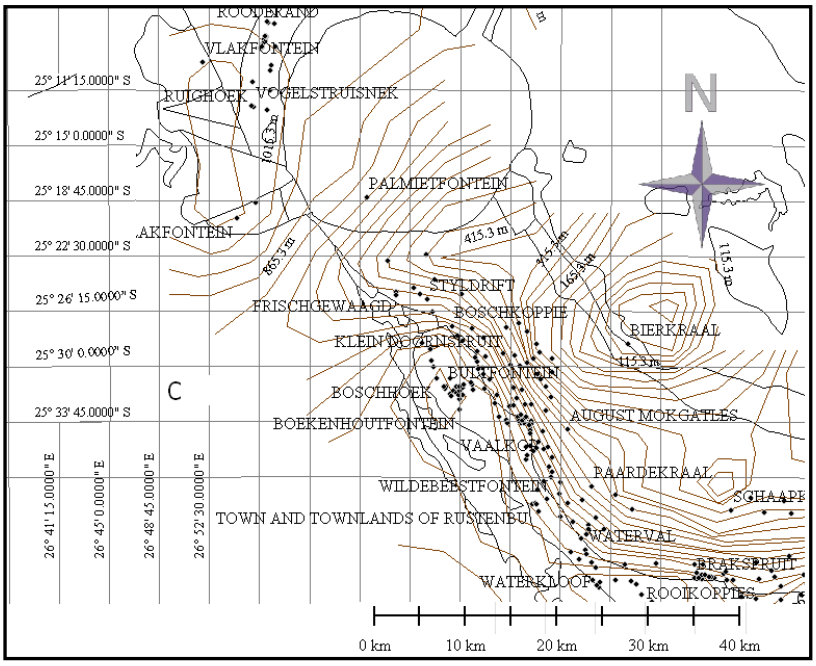

Figure 6.37: The Main Zone residual structure of central parts of Western Bushveld Complex showing prominent NE structural trend around Pilanesberg Complex; NNW-SSE trend (in the centre) parallel to Rustenburg Fault and E-W trend around the Brakspruit farm west of Brits (contour interval 50 m)

6.4.4 ISOPACH TREND SURFACE OF CENTRAL PARTS OF THE WESTERN BUSHVELD COMPLEX

The northern part of the Pilanesberg Complex is dominated by a NE thickening trend while the southern part of the Complex is dominated by a SE trend with an anomalously high thickening trend around the Bierkraal farm. Figures 6.38 shows the isopach trend surface of the Upper Zone.

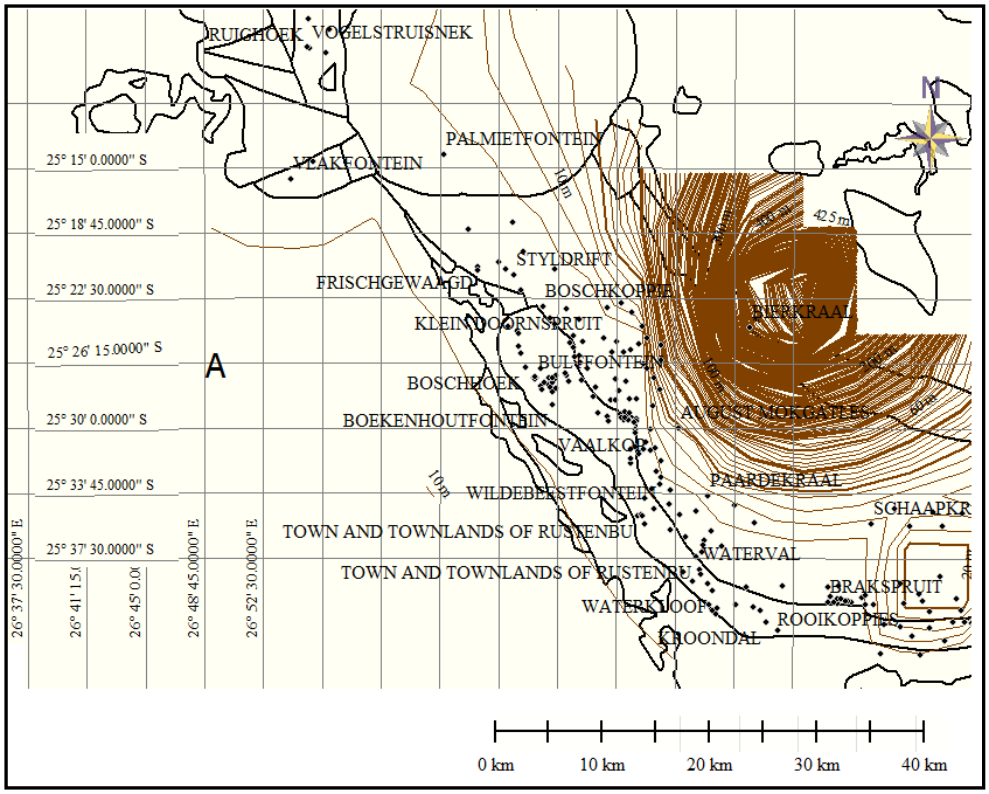

Figure 38:The Upper Zone isopach trend of central parts of the Western Bushveld Complex (contour interval 20 m).

The Main Zone isopach maps in Figure 6.39 represent isopach trend surface for the Main Zone and show a strong inverse relation to the structural trend surface both in pattern and trend except for the area around Bierkraal farm and Schaapkraal farm. These two areas show a negative structural domain on the structural trend surface and coincides with negative isolated thickening at Bierkraal farm and positive thickening on Schaapkraal farm.

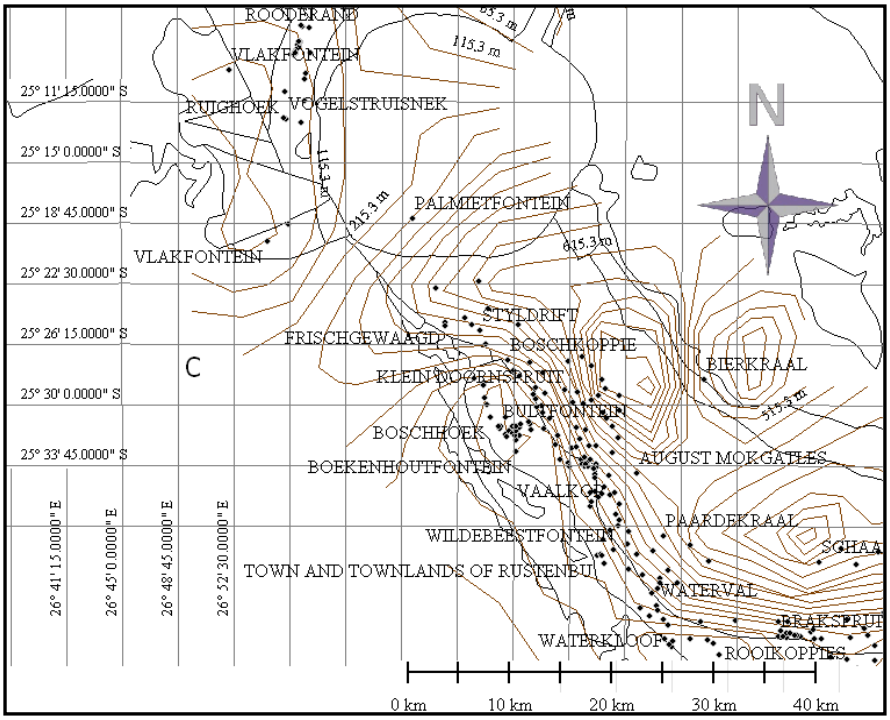

Figure 39: Third -order (C) the Main Zone isopach trend of central parts of the Western Bushveld Complex (contour interval 50 m).

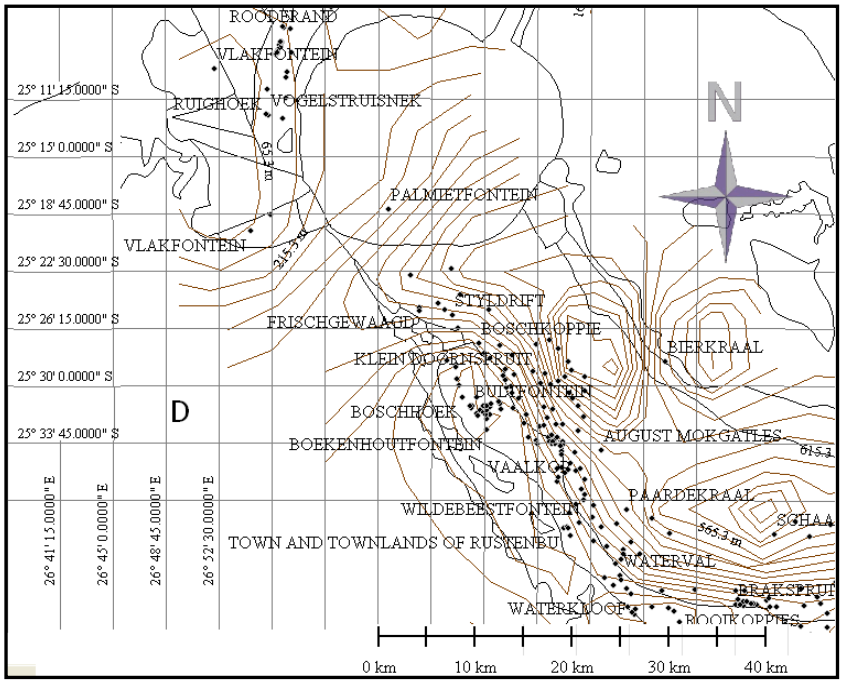

Figure 6.40: Fourth order D) the Main Zone isopach trend of central parts of the Western Bushveld Complex (contour interval 50 m).

6.4.5 RELATIONSHIP BETWEEN STRUCTURE AND ISOPACH OF CENTRAL PARTS OF THE WESTERN BUSHVELD COMPLEX.

The Upper Zone of this section in Figure 6.41 did not show an inverse relation between structure and isopach as indicated in the Main Zone (see Figure 6.42) of the same area. The Main Zone to Lower Zone units show strong correlation in structure, especially around the Rustenburg Fault where the trend is predominantlyNNE-SSW.

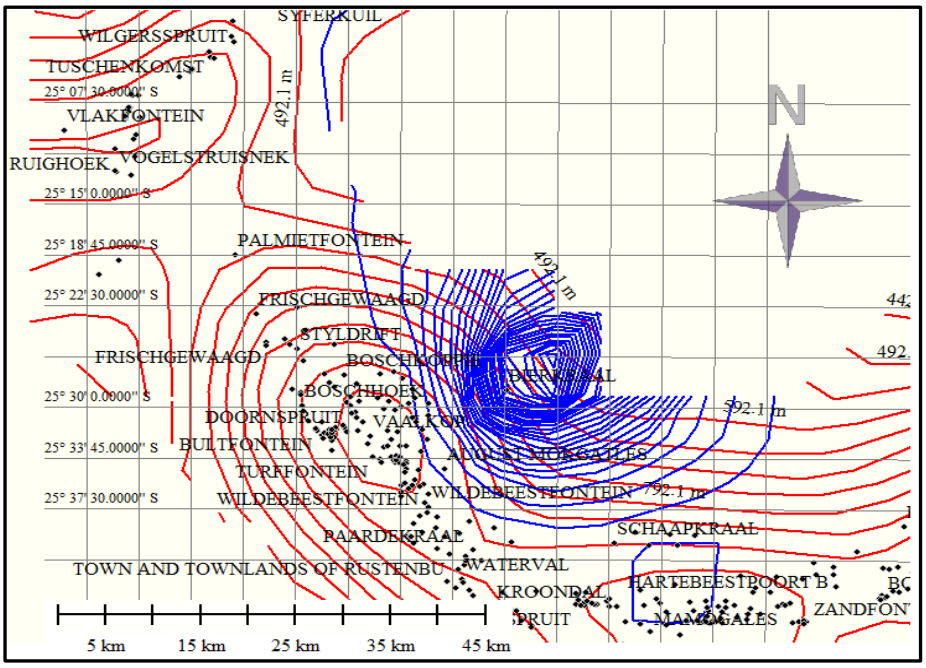

Figure 6.41: The Upper Zone residual structure (red) of central parts of the Western Bushveld Complex overlain with the Upper Zone residual isopach (blue) of the same area.

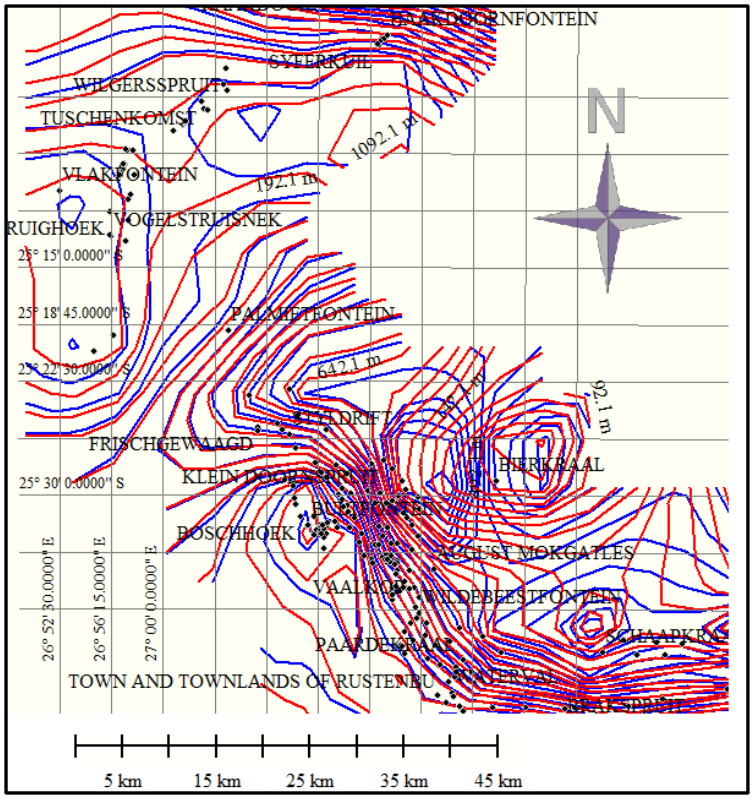

Figure 6.42:The Main Zone residual structure (red) of central parts of the Western Bushveld Complex overlain with the Main Zone residual isopach (blue) of the same area.

6.5 TREND SURFACE ANALYSIS OF THE SOUTHWESTERN BUSHVELD COMPLEX

6.5.1 SOUTHWESTERN BUSHVELD UPPER ZONE STRUCTURE RESIDUAL MAP

The geological map of southern parts of Western Bushveld Complex (6.43) showing the Brits graben and some farm names mentioned in text. The Upper Zone residual structure maps indicated in Figure 6.44 are marked by a NNW structural trend from the western side. While the eastern end shows east-west trend with a westward dip. The eastern side has a positive structure while the western side indicates a negative structure. Small-scale structural features correspond to the synclines or grabens which plunge to the south. The

residual structure maps show close resemblance with increasing orders of trend surface thus implying stability with increasing order of trend surface.

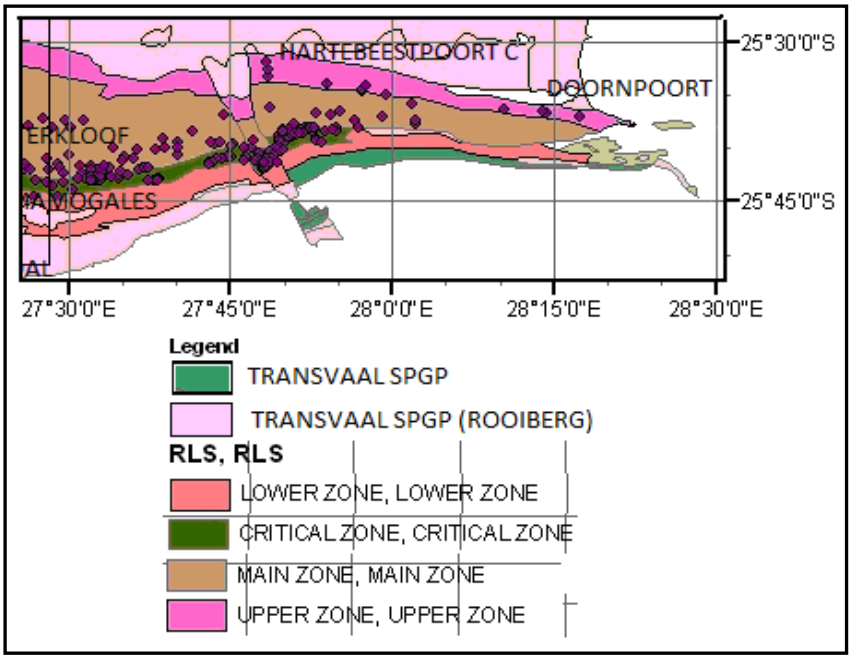

Figure 43: Geological map of the southwestern Bushveld Complex.

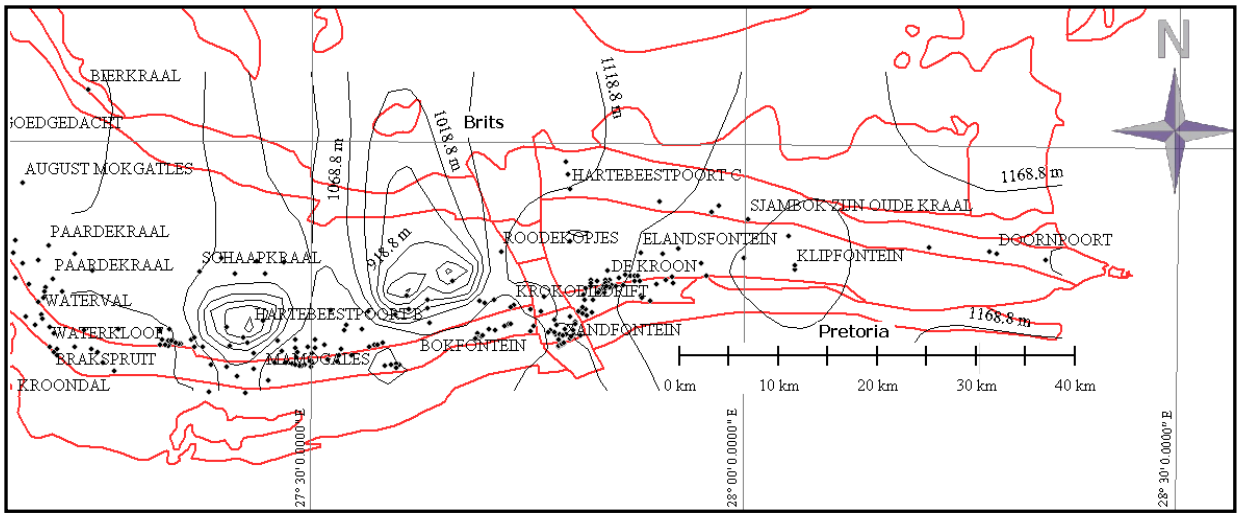

Figure 6.44: The Upper Zone top interval residual structure of the Southwestern Bushveld

6.5.2 SOUTHWESTERN BUSHVELD MAIN ZONE STRUCTURE RESIDUAL

Small scale structures characterize the Main Zone residual maps in Figure 6.45. The area around the Brits section is marked by a dominant NNW trend while east-west trends

dominate the eastern side of the Brits section. A small structure with a downthrow to the north occurs in the north-central part of map i.e. around the Hartebeestpoort C farm. Another structure occurs in the southeast, with a downthrow to the east. The residual structure map shows close similarities with the structural grain (style) of the area.

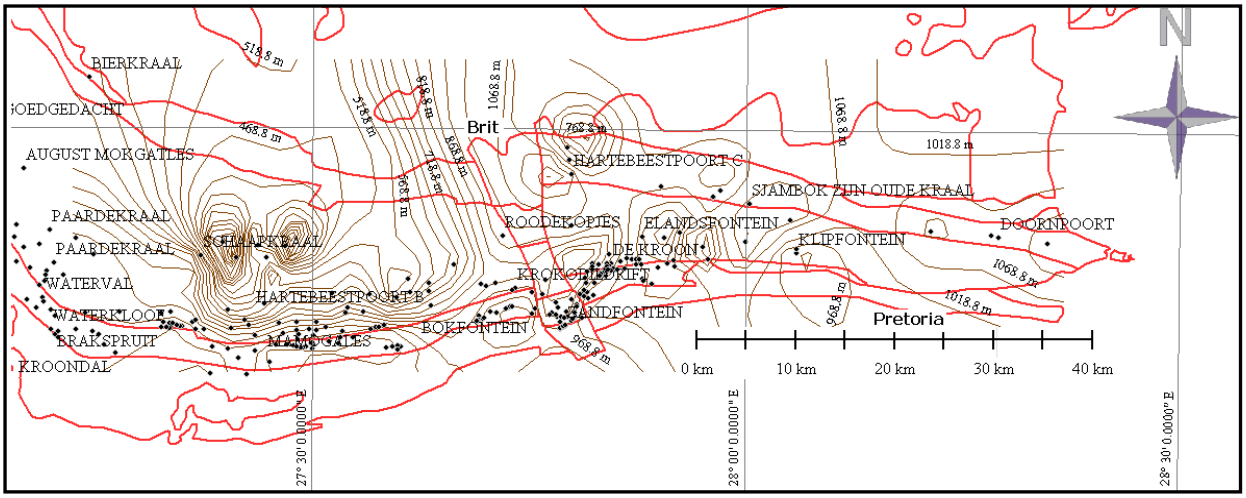

Figure 6.45: The Main Zone residual isopach maps of the Southwestern Bushveld

6.5.3 SOUTHWESTERN BUSHVELD CRITICAL ZONE RESIDUAL STRUCTURE AND ISOPACH

The structural trend in the Critical Zone is similar to the Main Zone base structure interval. All the residual isopach maps for the Merensky Reef of the southwestern Bushveld exhibit positive thickening in the western part and thins out eastwards except for an isolated thickening southeast of the Brits section (detail in Figure 6.46 and 6.47). There are also gaps and repeated contours around the Brits section. The UG2 unit in Figure 6.48 and 6.48 thickens southwestwards in the west, while in the eastern part it thickens to northeastwards with the isopach lines trending NNW.

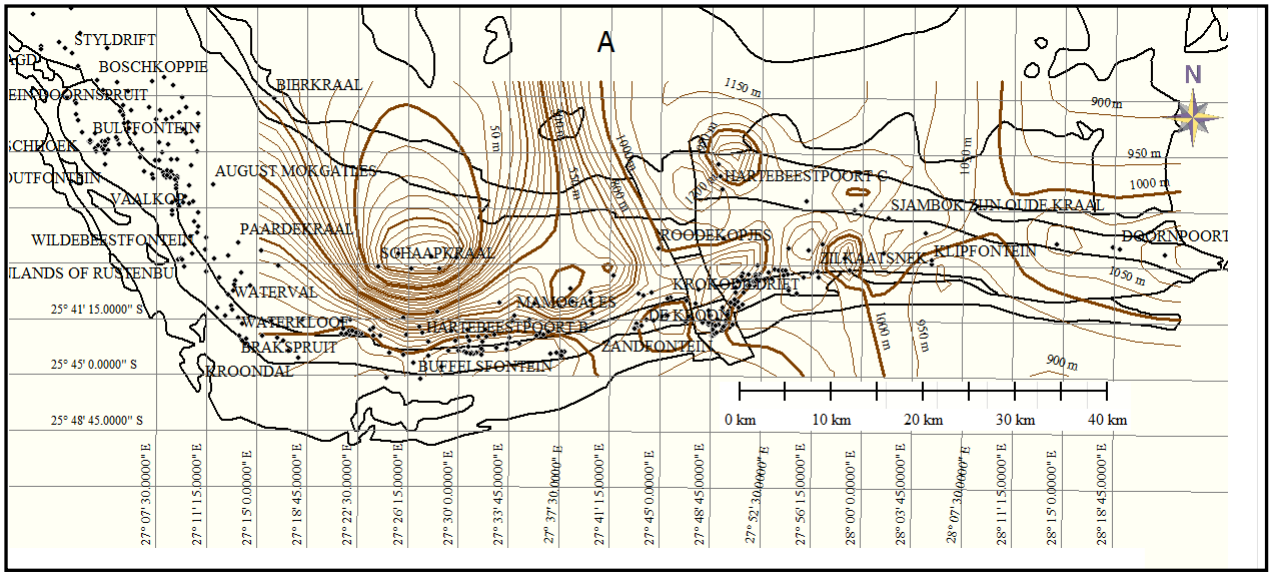

Figure 6.46: The Merensky Reef residual structure of the Southwestern Bushveld (A)

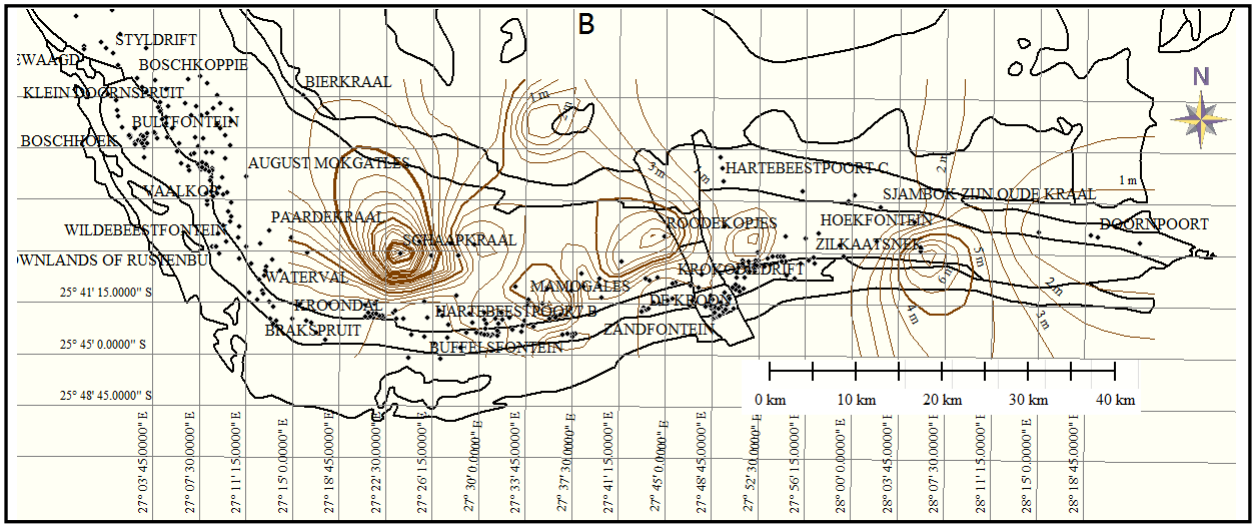

Figure 6.47: The Merensky Reef isopach map of the Southwestern Bushveld (B)

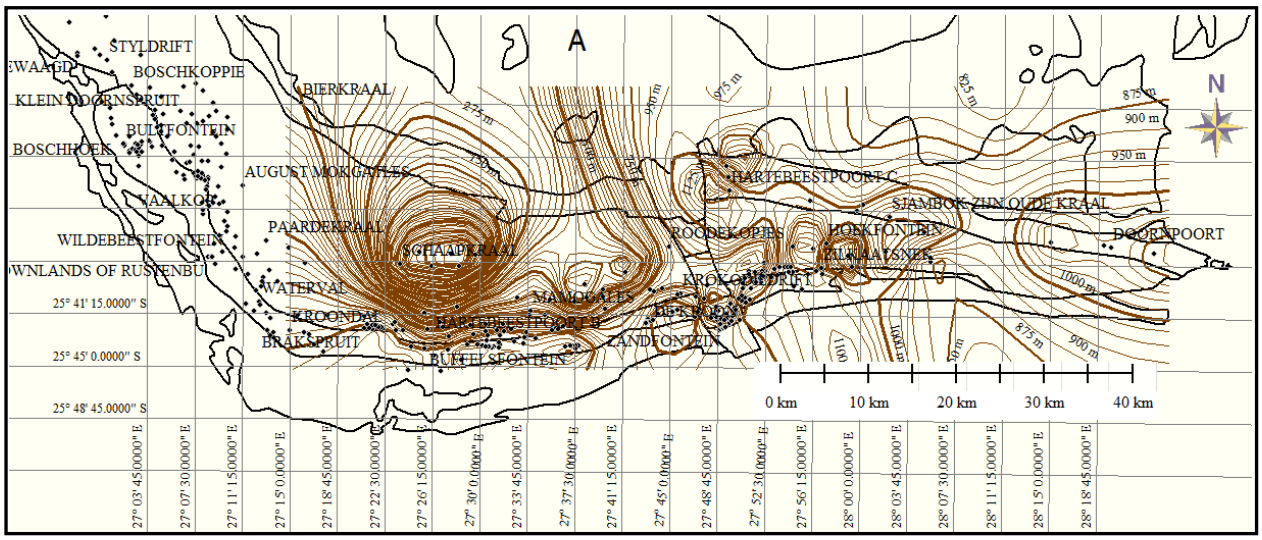

Figure 6.48: UG2 unit residual structure (A) of the Southwestern Bushveld Complex

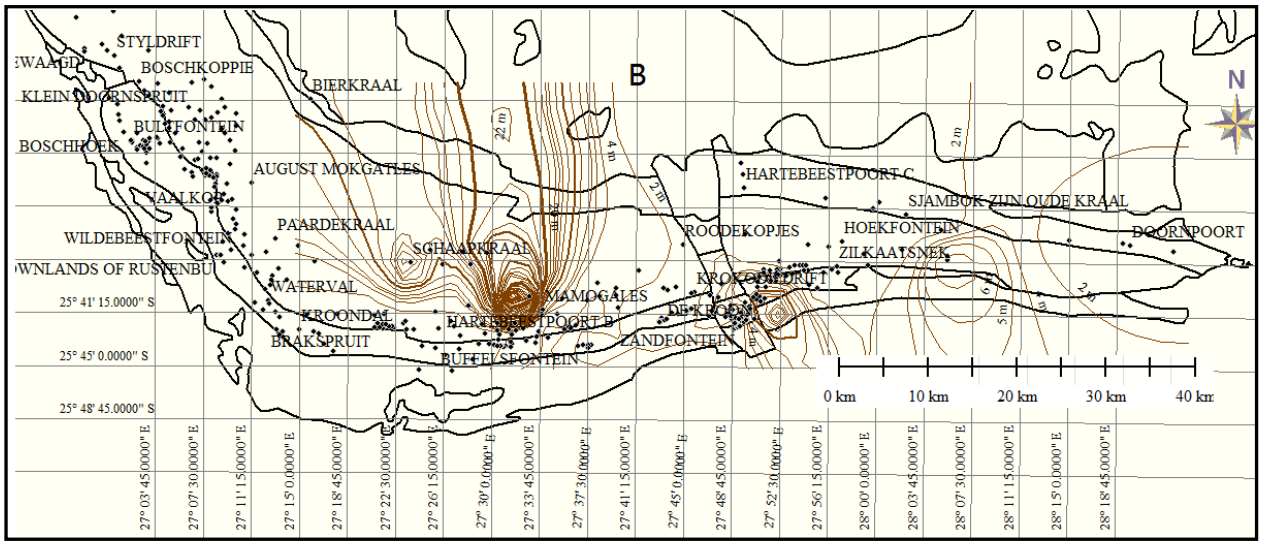

Figure 6.49: UG2 isopach map (B) of the Southwestern Bushveld Complex

6.5.4 SOUTHWESTERN BUSHVELD MAIN ZONE STRUCTURE TREND SURFACE

The western side of the Main Zone base interval maps shows a prominent NNW-SSE trend, however, this NNW-SSE trend was disrupted midway upward by a southeast trend. Repeated structural contours and gaps are present around the Brits section; a profile across the area indicates the presence of NNW trending faults and sags (Figures 6.50 and 6.51).

The same pattern is exhibited on the Merensky Reef unit, UG2 unit to the Lower Zone unit of the RLS.

6.5.5 SOUTHESTERN BUSHVELD UPPER ZONE STRUCTURE TREND SURFACE

The structural trend surfaces for the top of the Upper Zone are shown in Figure 6.52 and 6.51. First to second degree trend surfaces indicate a dominant NNW trend with a SW trend becoming more prominent from the east with increasing order. The fourth to sixth order shows a dominant east-west trend. Repeated contour lines and gaps dominate the western and central part of the map, i.e. around the Brits section. A profile across the gap shows two sets of upthrown blocks dipping towards each other with a central drop (gap) in-between (see Figures 6.52). These two sets of horst and graben structures possess a NE trend and are very conspicuous on all the trend surfaces. A profile drawn through this section shows downthrows of an order of over 300 m on the Upper Zone unit and deeper downthrows on underlying units.

6.5.5.1 The Southwestern Bushveld Upper Zone Residual Isopach Map

The Upper Zone trend surface isopach maps are dominated by a northward thickening trend. However, this trend was interrupted at the centre by two isolated structures with a southward thickening trend. These structures were truncated by an abrupt thinning trend from the west and south. Figures 6.53 shows gap and repeated isopach lines around the Brits area; this confirms the presence of faults and sags.

The Upper Zone residual isopach maps are marked by a NNW thinning in the west, northeast thinning in the centre and westward thinning in the southeast with two isolated structures at the centre (also present on the trend surface isopach maps). Generally the unit thickens to the north.

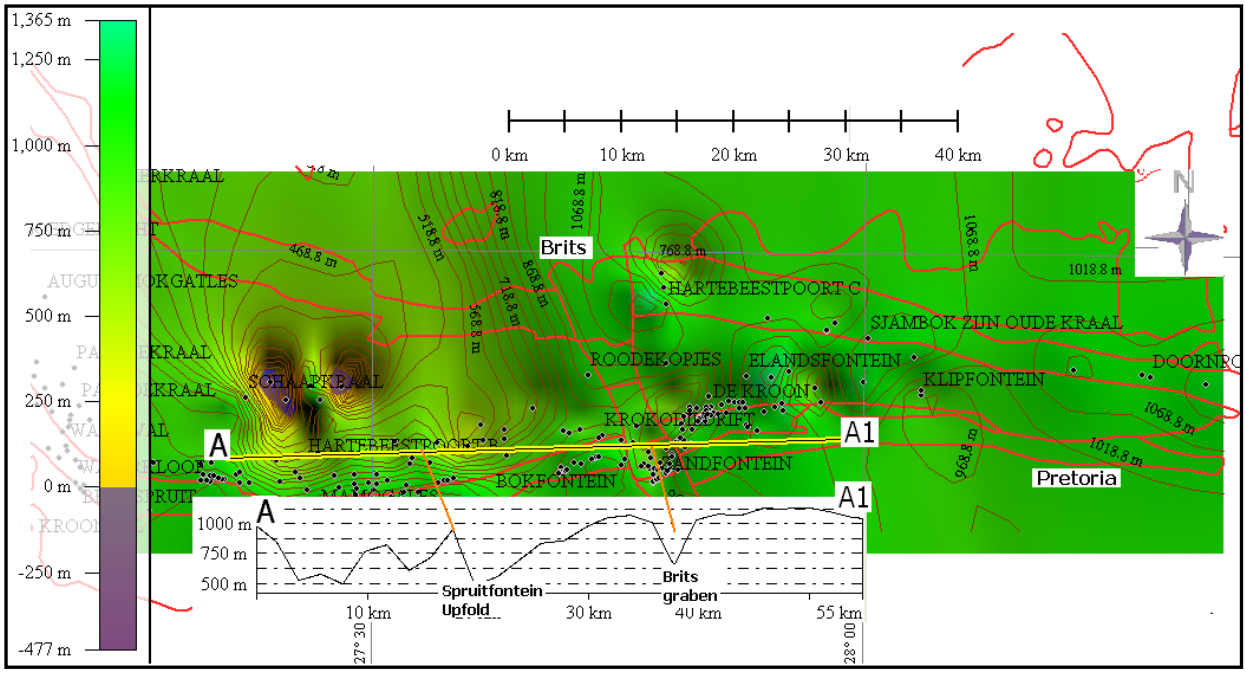

Figure 6.50: Profile A-A1 across the Brits grabens on the Main Zone structure interval in the Southwestern Bushveld

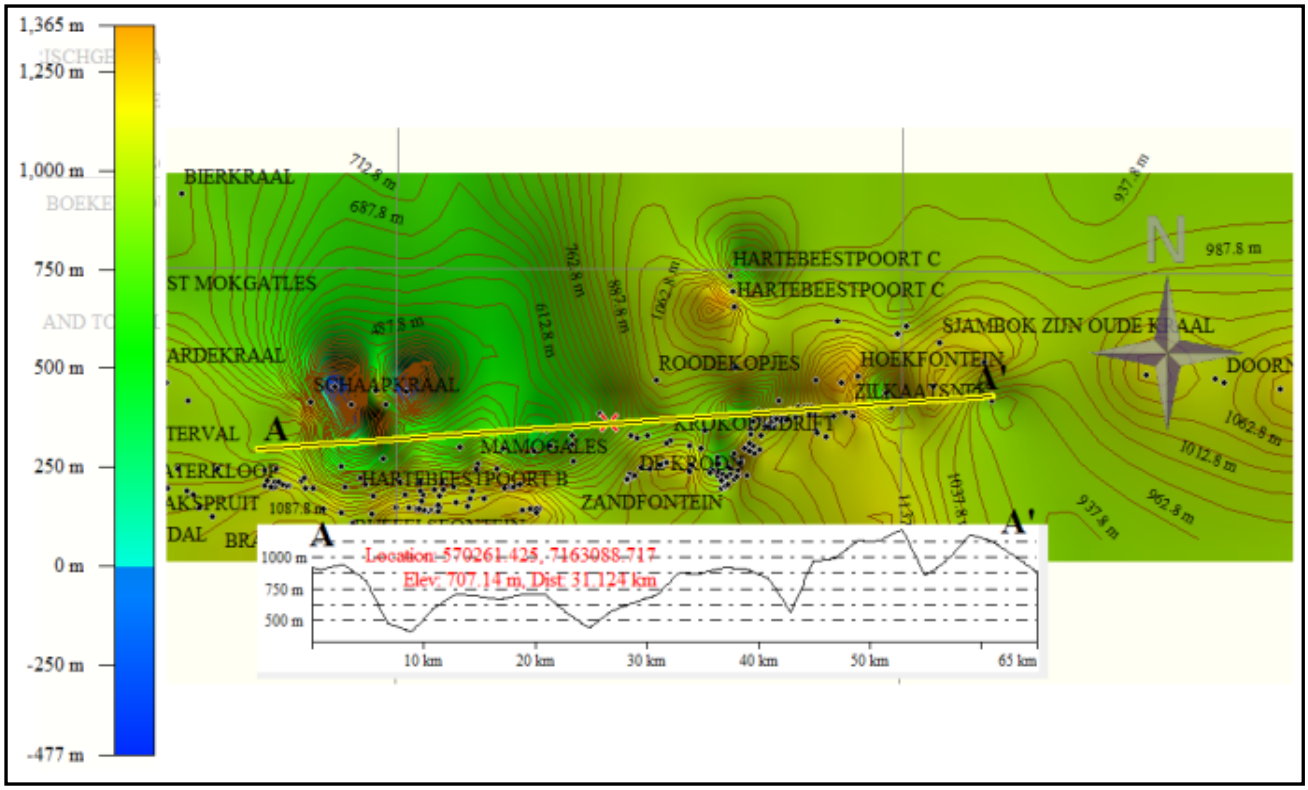

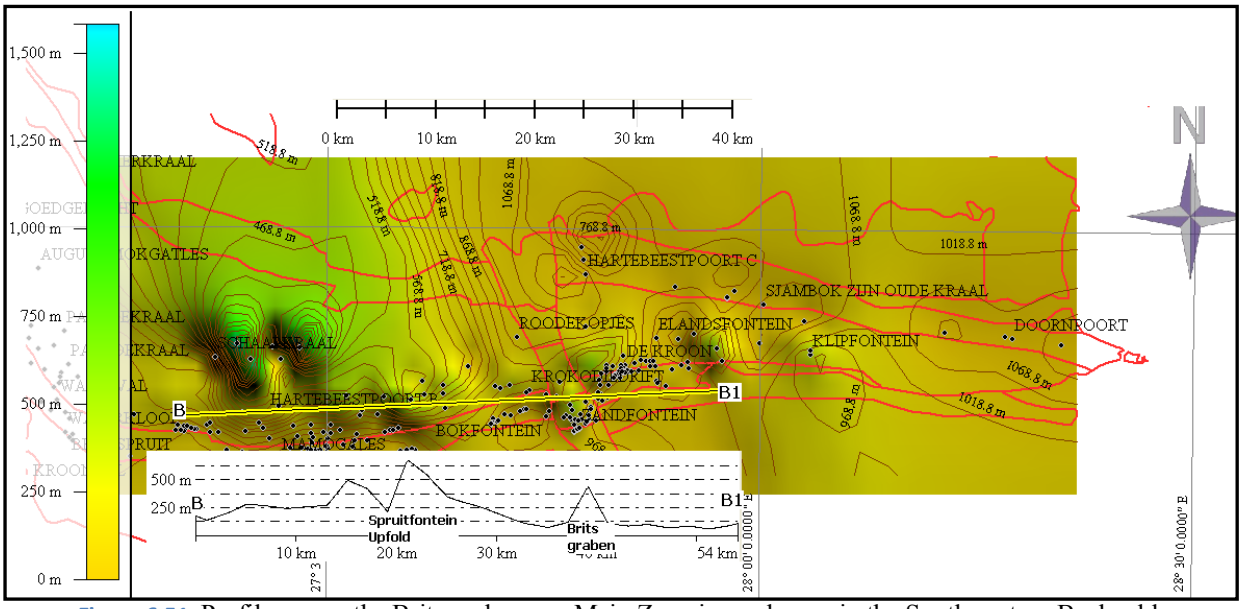

Figure 6.51: Profile across the Brits grabens on Main Zone isopach map in the Southwestern Bushveld

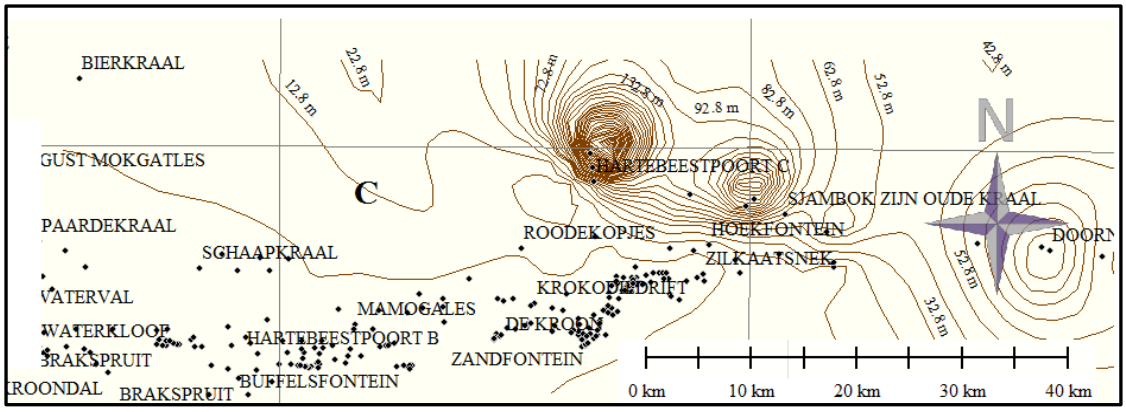

Figure 6.52: The Upper Zone top interval residual structure of the Southwestern Bushveld Complex.

6.5.5.2 Southwestern Bushveld Main Zone Residual Isopach Map

The Main Zone in Figure 6.53 is well developed in the west, but thins towards the northeastern part and around the Brits graben probably due to faulting. The unit is, however absent in the southern parts of the Brits graben.

The Main Zone trend surface isopach maps in Figure 6.53 show a prominent NNW thickening trend except for minor isolated thickening at the centre (around Brits section).

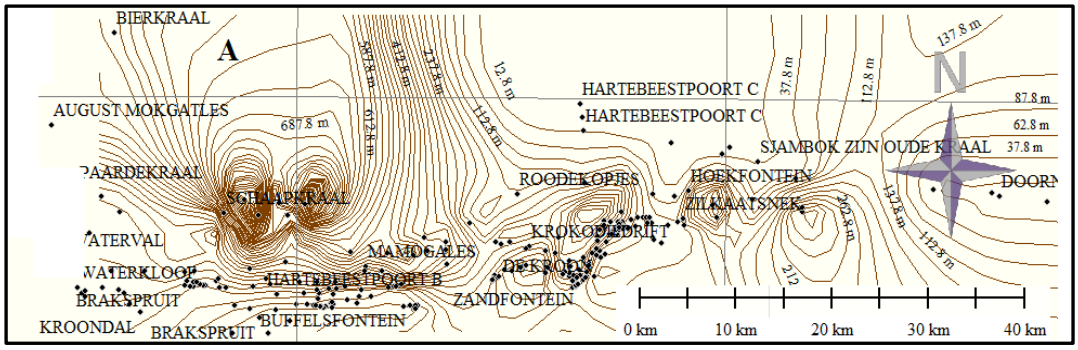

Figure 6.53: The Main Zone residual isopach maps of the Southwestern Bushveld Complex

6.5.5.3 Trend Surface Analysis of Formation Thickness of the Southwestern Bushveld

The effect of subsidence due to compaction is minimal on these stratigraphic units because the lithologies involved are igneous and not sedimentary, original thickness at the time of emplacement was preserved except for alteration due to syn- or post-emplacement movement. Due to close similarities between the Upper Zone top interval and the Main

Zone top interval and lack of significant variation in structure between the Main Zone base and all the lower stratigraphic units only the Upper Zone and the Main Zone will form the core of this discussion.

There is little correlation between the structure and thickness trends and residuals for the Upper Zone in the Southwestern Bushveld Complex; this might be due to poor structural control. Conversely, the Main Zone structure and thickness exhibit inverse correlation both in trend and with the small scale structures. The western part of the Brits section is structurally low and received more influx than the eastern part. However, most of the units thin out around the structurally high areas while the structurally low areas (graben or sag) show isolated thickening. This is responsible for the alternating or random thickening and thinning around the central part of the map. The northeastern part seems to be more structurally stable in comparison with the southwestern section. This same pattern was observed on the Merensky Reef and UG2 trend and residual structure and thickness.

6.5.5.4 Relationship between Residual Structure Contour Maps of the Southwestern Bushveld

At the northern part of the residual structure contour map of the Southwestern Bushveld Complex, there are isolated structural negative areas, the western isolated negative structure forms an anticlinal shape and opens to the north. The eastern isolated negative structures occur on the northeastern side and open to the north. Most of the structural negative areas correspond directly to thickness positive areas.

The Brits Graben faults are NNW trending faults in the Southwestern Bushveld (Bumby et al., 1998). Prominent faults around the Brits Graben include the Bokfontein Fault, Kommandonek Fault, Hartebeestpoort Fault and De Kroon Fault (Judeel and Hartmann, 2008). The faults strike in the same direction, but dip in opposite directions and are located about 200 m away from each other. There is an inverse correlation between the structural elevation and thickness in this area (Figures 6.52 to 6.53). A positive structural trend is associated with a negative thickness trend. A strongly negative structural domain coincides with graben areas, while a strongly positive structural domain coincides with horst areas. The central part of the Western Bushveld i.e. south of the Pilanesberg Complex also shows inverse correlation between structure and thickness. The trend of the Brits Graben

coincides with the regional structural trend within the Kaapvaal Craton and thus signifies that the structures were probably formed in early Transvaal times and reactivated during the intrusion of the Bushveld Complex according to Hartzer (1989).

6.5.2.5 The Southwestern Bushveld Upper Zone and Main Zone Structure Trend Surface

The Main Zone trend surface pattern in Figure 6.54 shows that the prominent trend is NE with northeast regional strike and northwest dip. This coincides with the outcrop trend in the area. Figure 6.54 and 6.55 shows the Main Zone second and third isopach trend maps.

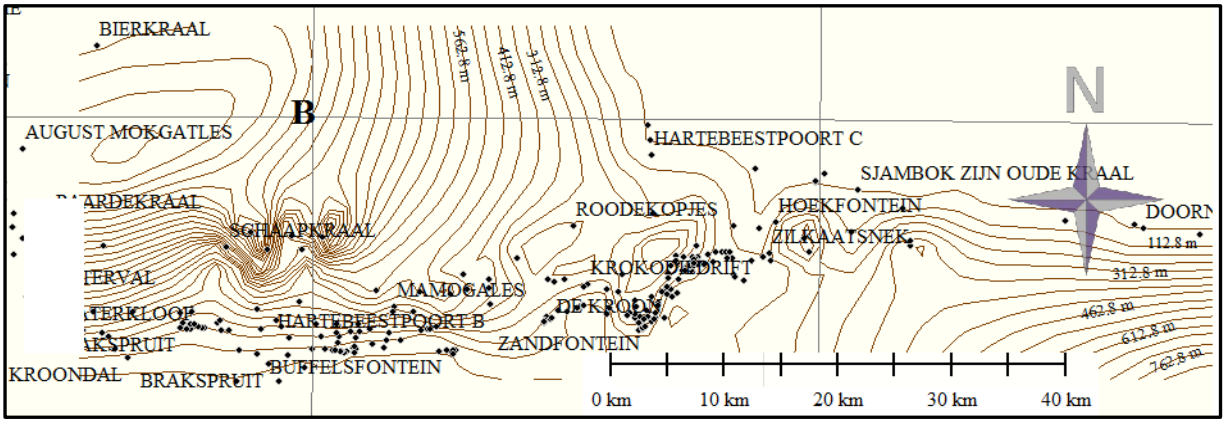

Figure 6.54: The second-order Main Zone structural trend of the Southwestern Bushveld Complex

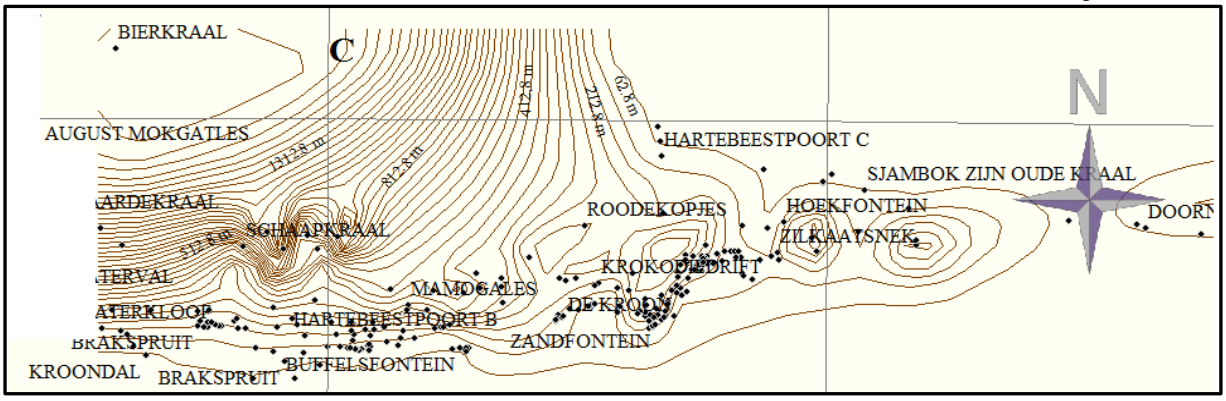

Figure 6.55: The third-order Main Zone structural trend of the Southwestern Bushveld Complex

:

6.5.4 TREND SURFACE ANALYSIS OF THE NORTHEASTERN BUSHVELD

6.5.4.1 Northeastern Bushveld Residual Structure

The geological map of northeastern part of the Eastern Bushveld (Figure 6.56) showing the farm names mentioned in test. The residual structural map in Figures 6.31 and 6.32 shows several positive and negative structural domains. Around the Voorspoed farm in the northwest, there is a small negative structural domain. Further eastwards i.e. east of Wonderkop Fault are two positive domains trending southwest and parallel to the WonderkopFault. The positive domain in the northeastern part of the Wonderkop Fault is an anticline plunging NNW (the structure is probably part of the Katkloof structure) and adjacent to a small negative structure while the other one coincides with the Fortdraai Anticline when overlain with the geological map. There is, however, an anomalously strong structural negative domain (this particular data was re-verified before inclusion) adjacent to the Fortdraai Anticline; this might be due to the level at which the RLS occurs in the area, thus the structure revealed occurs only in the subsurface since there is no corresponding surface signature on the surface. The Upper Zone residual structures in Figures 6.58 trend NE, with positive structures in the north and negative structures in the south. The central portion, however, shows plunges to the south. In the northern part the trend extends from west to east and separates the negative structure in the extreme northeastern part from the extensive southeast negative structure.

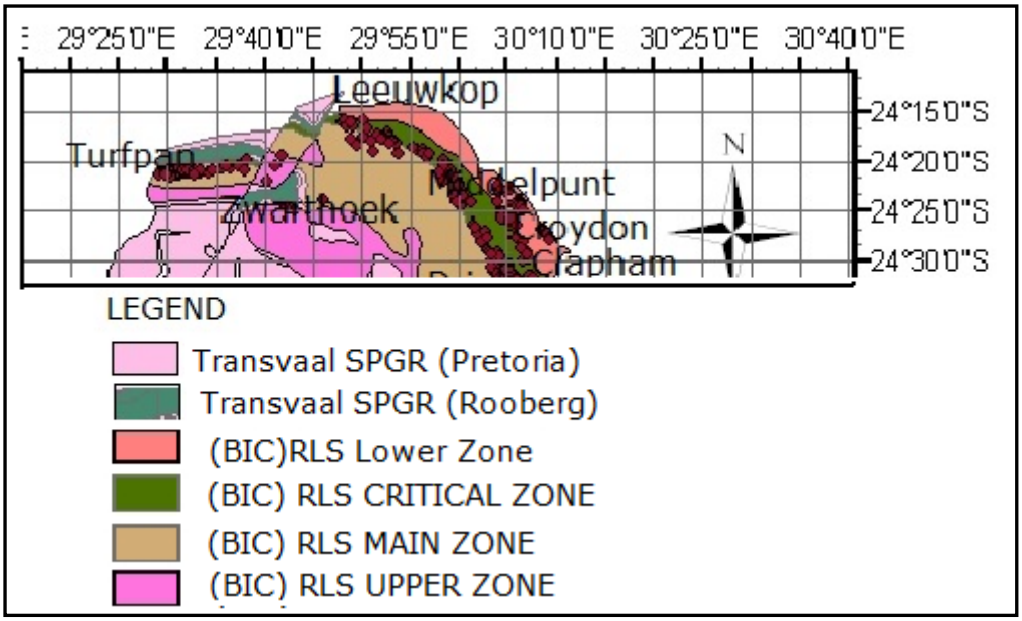

Figure 6.56: The geological map of northestern part of Eastern Bushveld Complex.

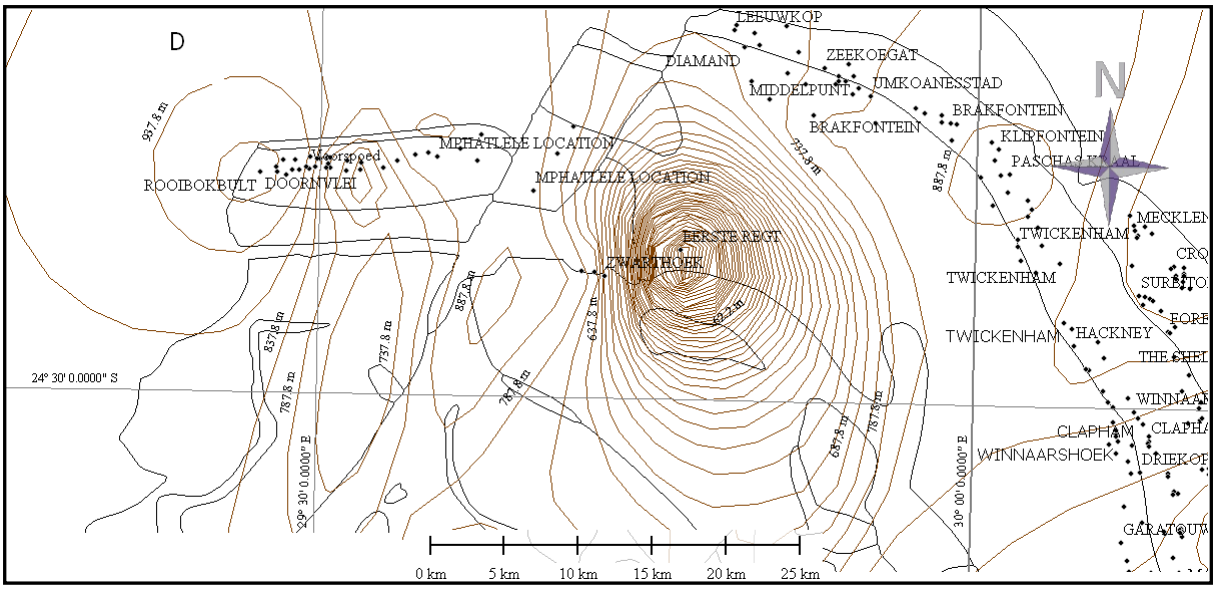

Figure 6.57: The Northeastern Bushveld Upper Zone residual structure contour map

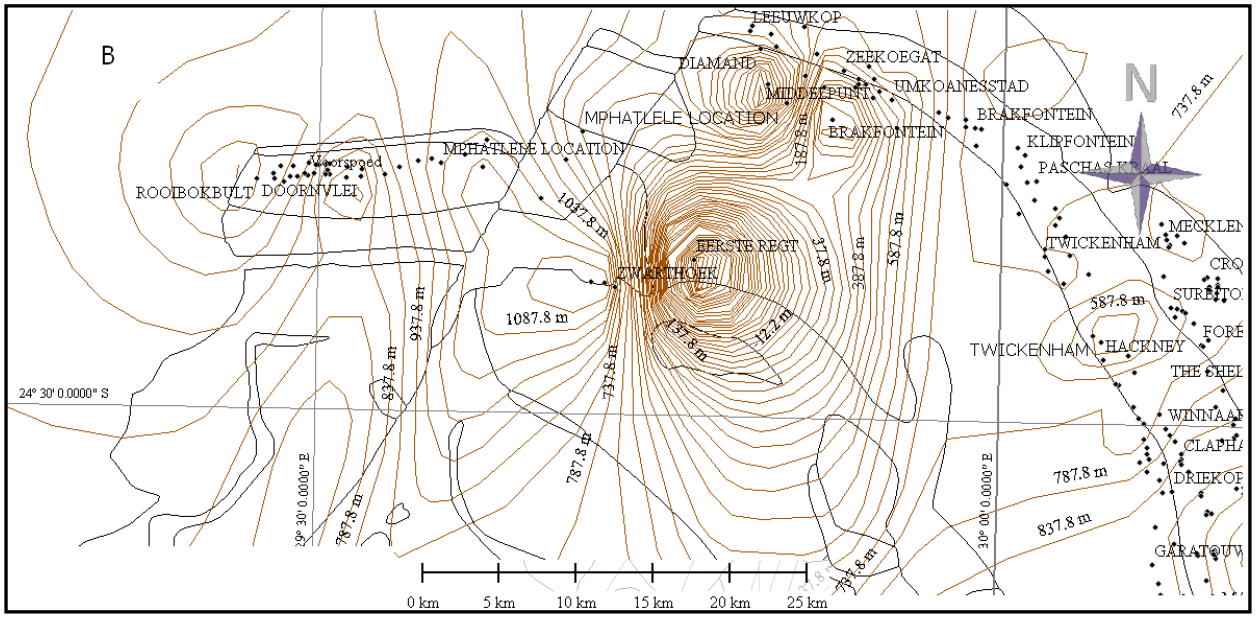

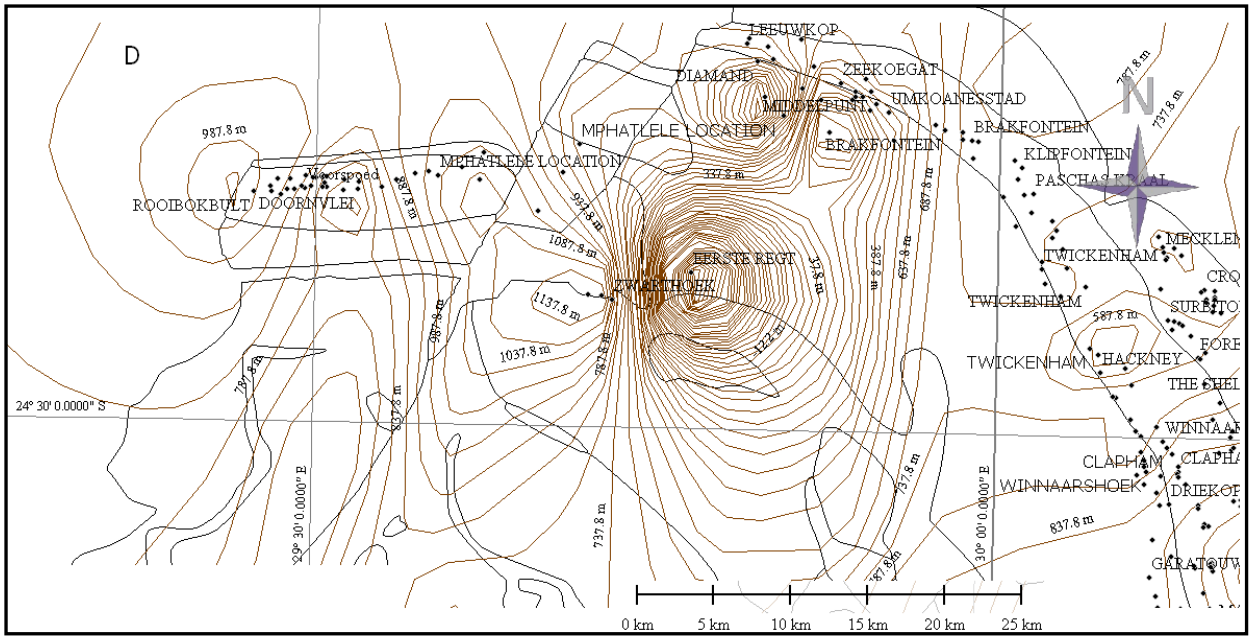

Figure 6.58: The Main Zone second-order (B) and fourth-order (D) residual structure with contour interval of 50 m

The Main Zone residual structures in Figure 6.58 is marked by a steep sided synclinal structure of about 2 km in the north, around Middelpunt farm. Adjacent to this structure on the western side is a small structural high. Another steep sided synclinal structure occurs in the southwest, around Fortdraai Anticline.

6.5.4.2 Northeastern Bushveld Residual Isopach

The Upper Zone residual isopachs for the Northeastern Bushveld Complex indicate isolated positive thickness around Mphatlele location in the north and negative thickness towards the southeast (Figure 6.59).

The Main Zone residual isopach maps in Figure 6.60 show a similar residual domain with a central NNW oriented positive thickening. The northern part is dominated by an anticline structure that slopes eastwards into an adjacent structural low domain.

The Merensky residual isopachs are marked by negative thickness residuals in the west and positive residual isopachs in the east. The negative residual potion is also bounded on both sides by fault zones with centrally located thinning. In the northern part, the presence of positive thickness domain between two isolated positive thickenings residual structures oriented southeast

was observed. There are steep isopach lines on the western side while the eastern part is marked by more gentle slope. These two residual structures coincide with two small adjacent positive and negative structures in the northern parts. Areas around the Fortdraai Anticline show up as a syncline on the residual structural map and as an anticline on the residual isopach map. A small residual negative structure also exists on Voorspoed farm; this structure shows up as small positive thickness on the thickness residual map thus supporting inverse structure and thickness correlation of both trend and residual structures.

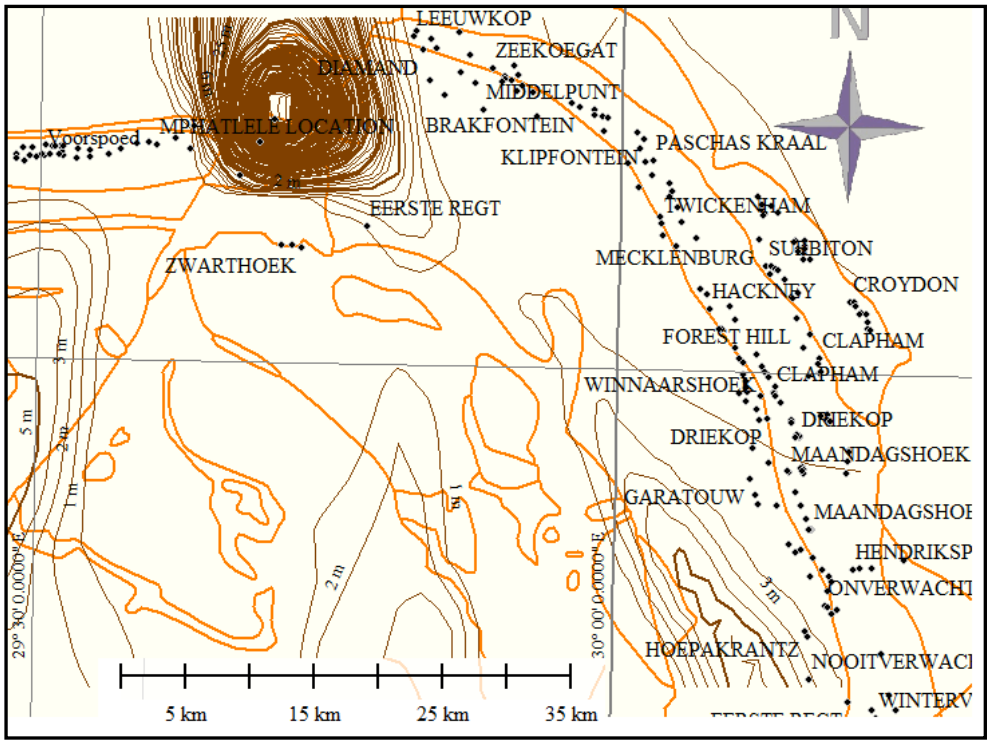

Figure 6.59: Upper Zone residual isopach map showing NNW-SSE trend.

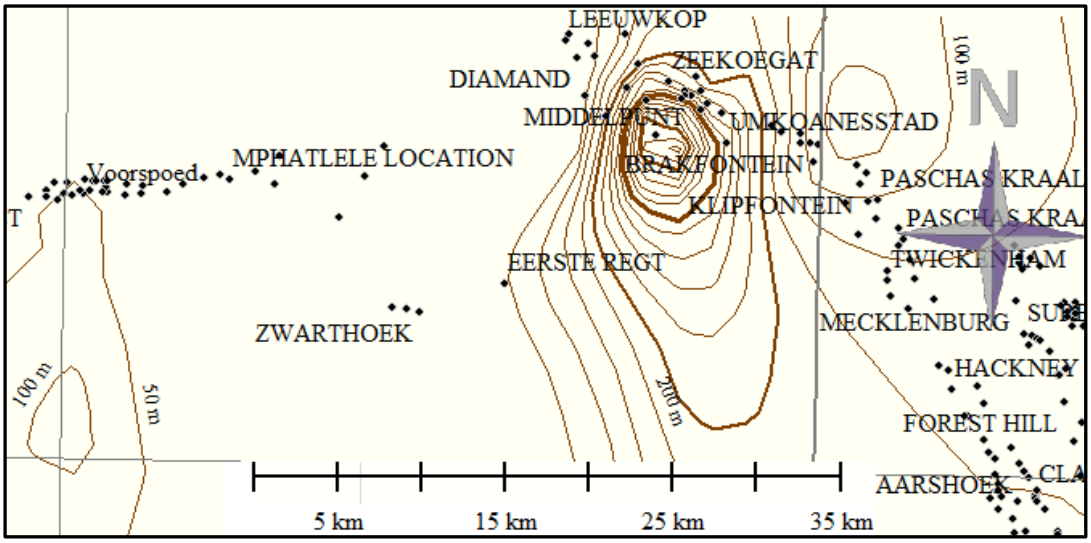

Figure 6.60: The Main Zone isopach residual with a contour interval of 50 m

6.5.4.3 Southeastern Bushveld structural trend

The Upper Zone structural map in Figure 6.61 trend NE with a centrally located structural low area that dips towards the centre. The residual map shows a NNW trending structural low area at the centre.

Figure 6.62 indicates that the Main Zone structural trend maps reveal a NE trend with a centrally located steep sided synclinal closure trending northwestward and plunging southwards.

The Merensky Reef in the Southeastern Bushveld trends NE on structure trend map and plunges southwards at the centre of the map. A positive structure on the northern side and wide negative structure in the south. The northern part also exhibits an east-west trend. The third order structure exhibits a strong structural negative with an east-west trend in the north-central part. This shows strong correlation with existing geology.

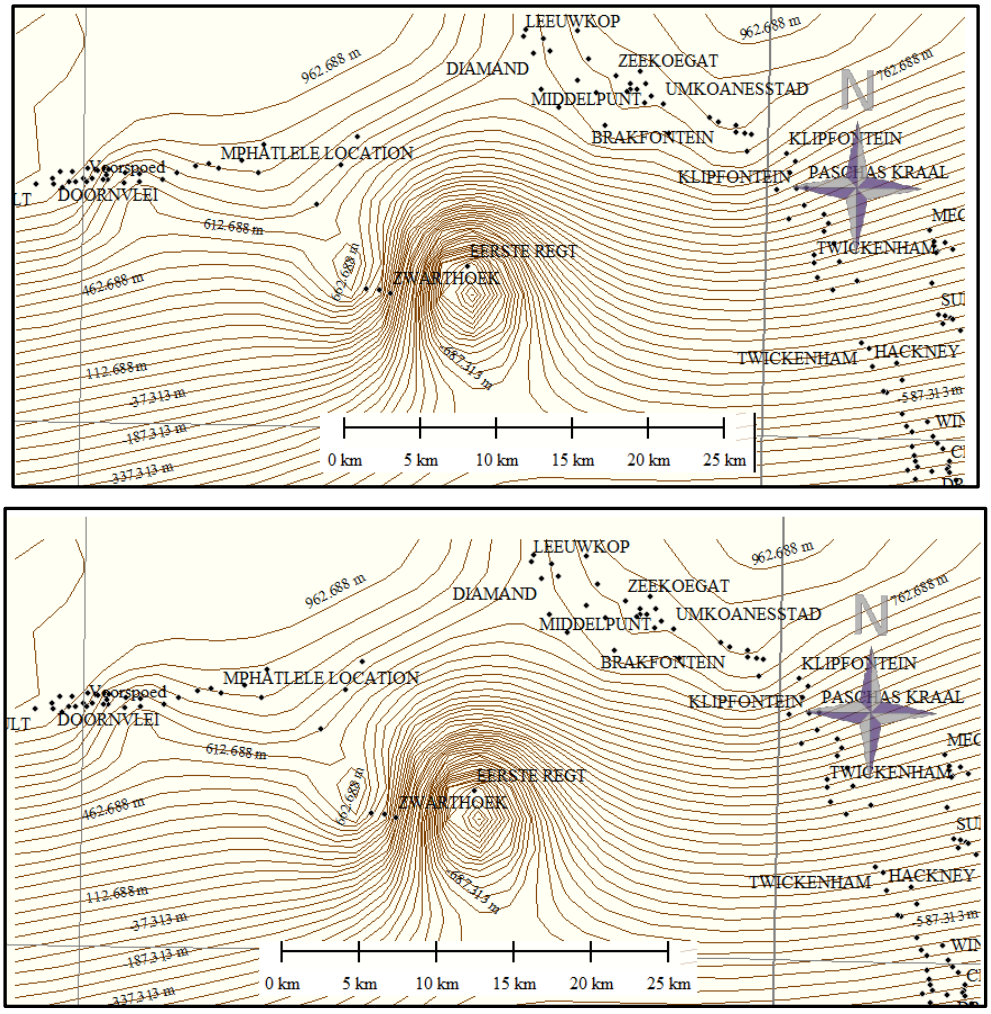

Figure 6.61: The Southeastern Bushveld Upper Zone first-order (up) and second order structural trend map

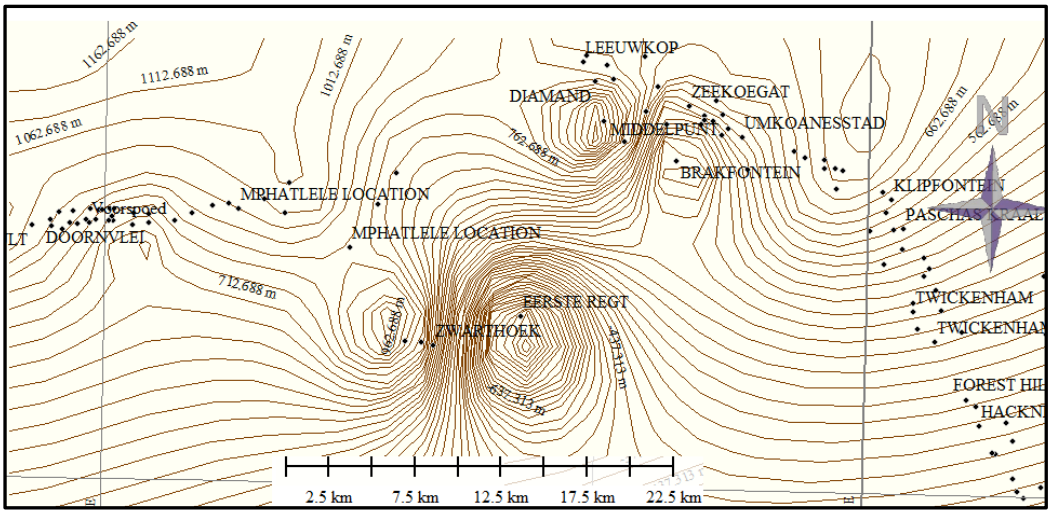

Figure 6.62: The Main Zone structural trend of the Southeastern Bushveld Complex

6.5.4.4 Southeastern Bushveld Isopach Trend

The east-west thickening trend dominates the northern part of the Southeastern Bushveld (Figure 6.63). Isopach contour trends NNW at the centre.

The Merensky Reef isopach exhibits a weak NW thinning trend. The third order isopach trend exhibits an east-west thickening trend, which geographically coincides with the east-west structural negative domain on the structural map.

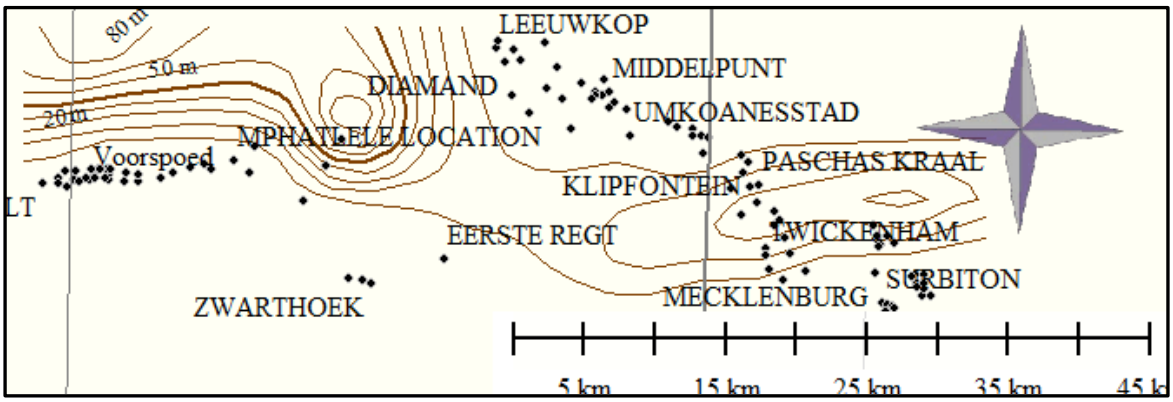

Figure 6.63: The Upper Zone isopach trend of Northeastern Bushveld.

6.5.4.5 Relationship between Structure and Isopach of the Southeastern Bushveld

There are few similarities between the structure on the Upper Zone and the Main Zone units. However, the Main Zone and the Archaean floor rock structures have more similarities as indicated in Figure 6.64. In addition, the thickening trends between the Upper Zone and the Main Zone vary strongly. While the structures indicate more of a NNW trend, the thickness shows more of an east-west trend. The thickness of each of the stratigraphic units in the Southeastern Bushveld Complex indicates that individual unit developed independently and did not show close similarities with the present day structures. Structure and thickness trends of each unit in the Southeastern Bushveld Complex did not exhibit much correlation. Despite this, Figure 6.65 to 6.66 with profiles drawn across both the thickness and structure map of some parts of the area indicate a very

strong inverse relationship. This indicate that most of the structures are probably syn-Bushveld or post-Bushveld.

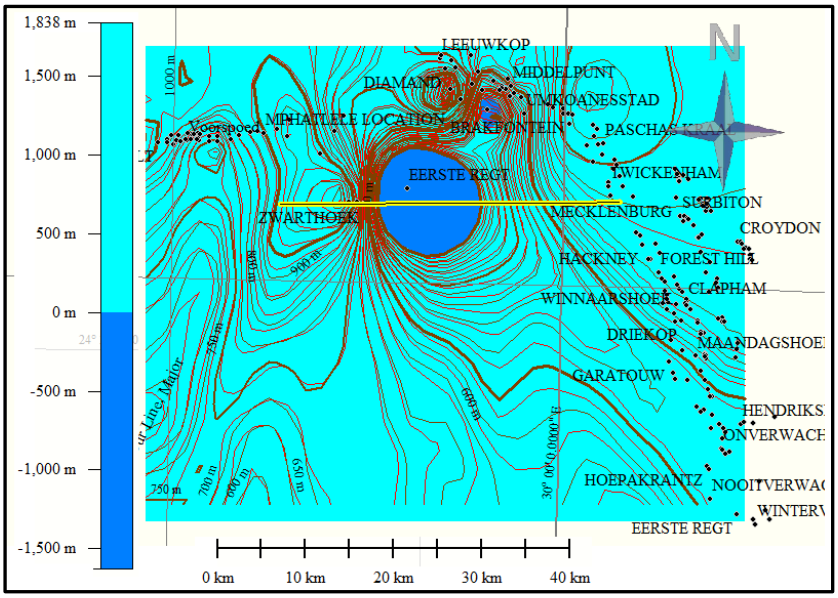

Figure 64: Draped Archaean floor structure on the Main Zone base interval structure showing close correlation between the two units (contour interval is 50 m).

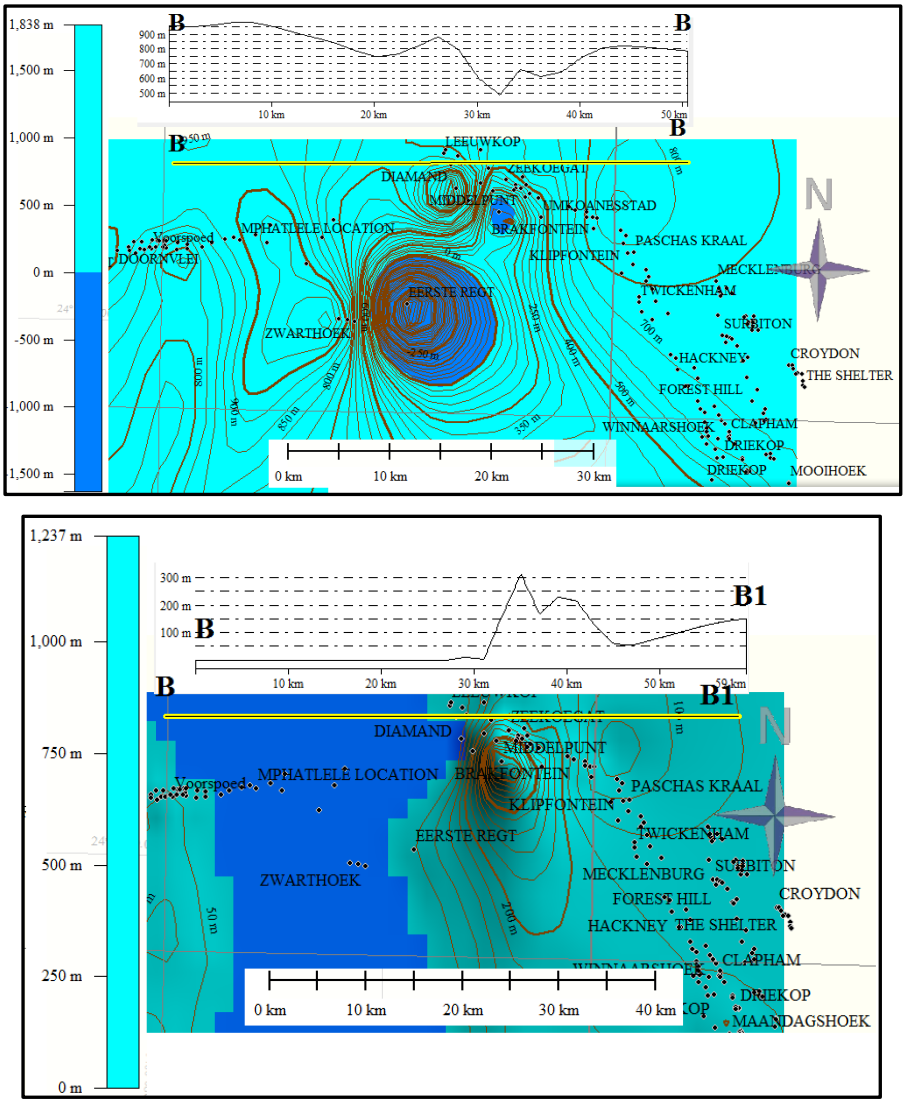

Figure 6.65: Profiles showing inverse correlation between the Main Zone residual structures (up) and isopach (down).

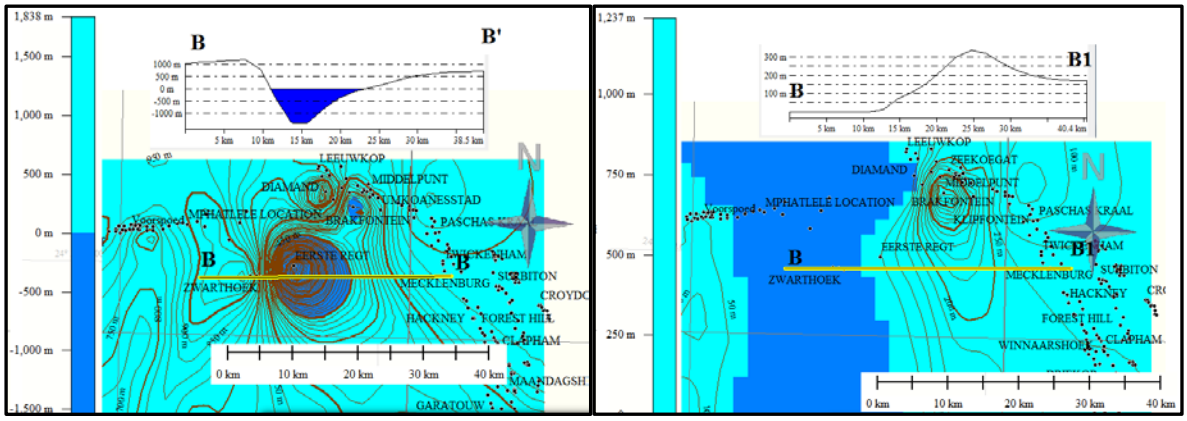

Figure 6.66: Profiles showing inverse correlation between the Main Zone residual structure (left) and isopach (right).

6.5.5 TREND SURFACE ANALYSIS OF CENTRAL PARTS OF THE EASTERN BUSHVELD COMPLEX

6.5.5.1 RESIDUAL STRUCTURE AND ISOPACH OF CENTRAL PART OF THE EASTERN BUSHVELD COMPLEX

Small-scale structures include the depression (central dipping) at Kennedy's Vale in the east and the adjacent structural high at Spitskop.

6.5.5.2 STRUCTURE TREND OF CENTRAL PART OF EASTERN BUSHVELD COMPLEX

The central part of the Eastern Bushveld as indicated in Figures 6.67 and 6.68 dips centrally from the surrounding structural positive areas forming a triangle like basin in the centre. The western side dips inward with a NS trend, while the southern part dips inward with an east-west trend. The southeastern part dips inward following the Sekhukhune Fault outline and a southeast trending structural high in the southeast. However, the Lebowa Granite Suite overlies most part of this area.

6.5.5.3 ISOPACH TREND OF CENTRAL PART OF THE EASTERN BUSHVELD COMPLEX

The Upper Zone and the Main Zone as shown in Figures 6.69, to 6.70 show a positive thickening in the centre and thin out to the northwest.

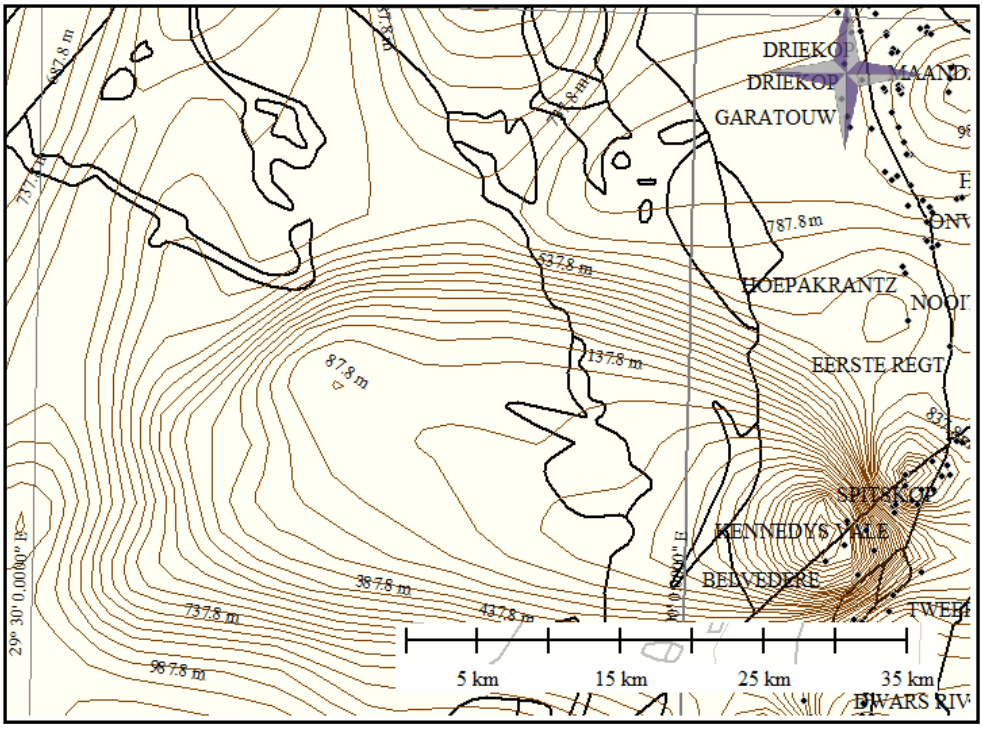

Figure 6.67: The residual isopach contour map for the Upper Zone unit of the central Eastern Bushveld Complex (contour interval 1 m).

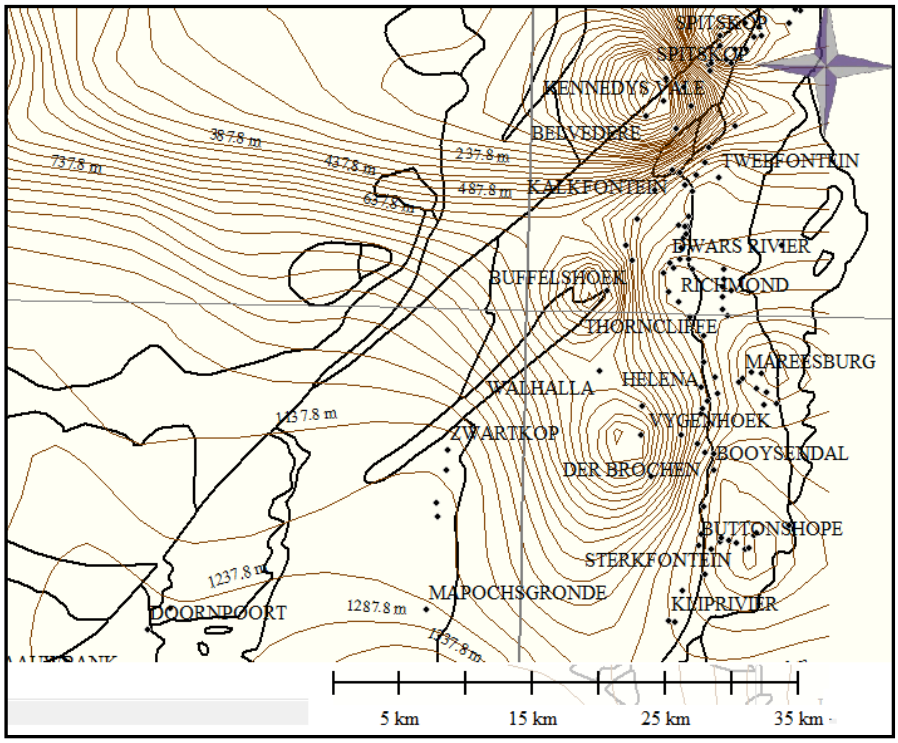

Figure 6.68: The residual isopach contour map for the Main Zone unit of the central Eastern Bushveld Complex (contour interval 50 m).

Residual structure contours for the Upper Zone and the Main Zone reveal a structural low domain in the centre of the Eastern Bushveld Complex.

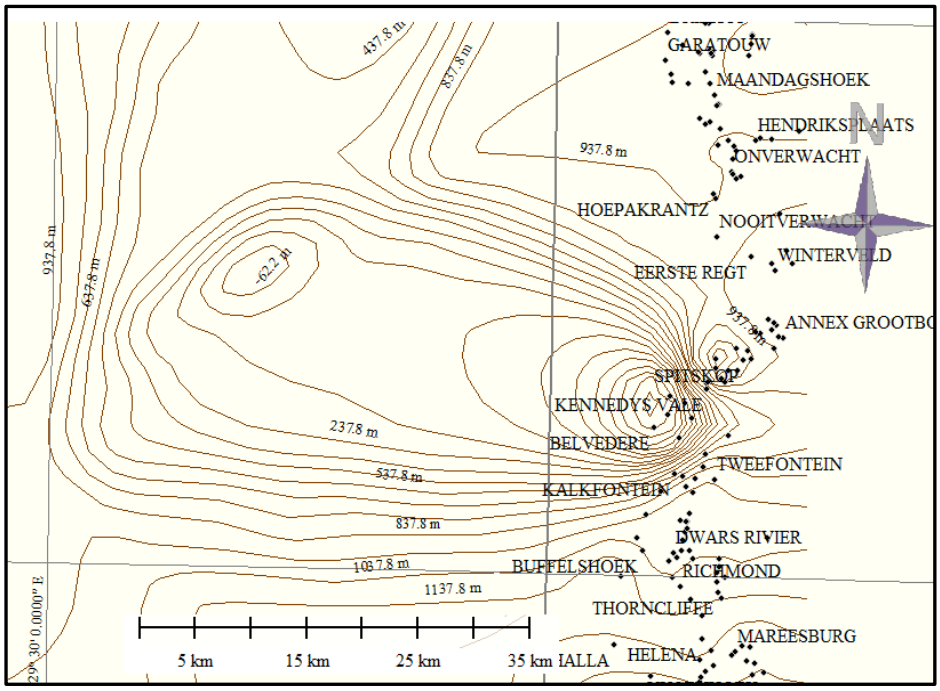

Figure 6.69: The second-order residual structure contour map for the Upper Zone unit of the central Eastern Bushveld Complex

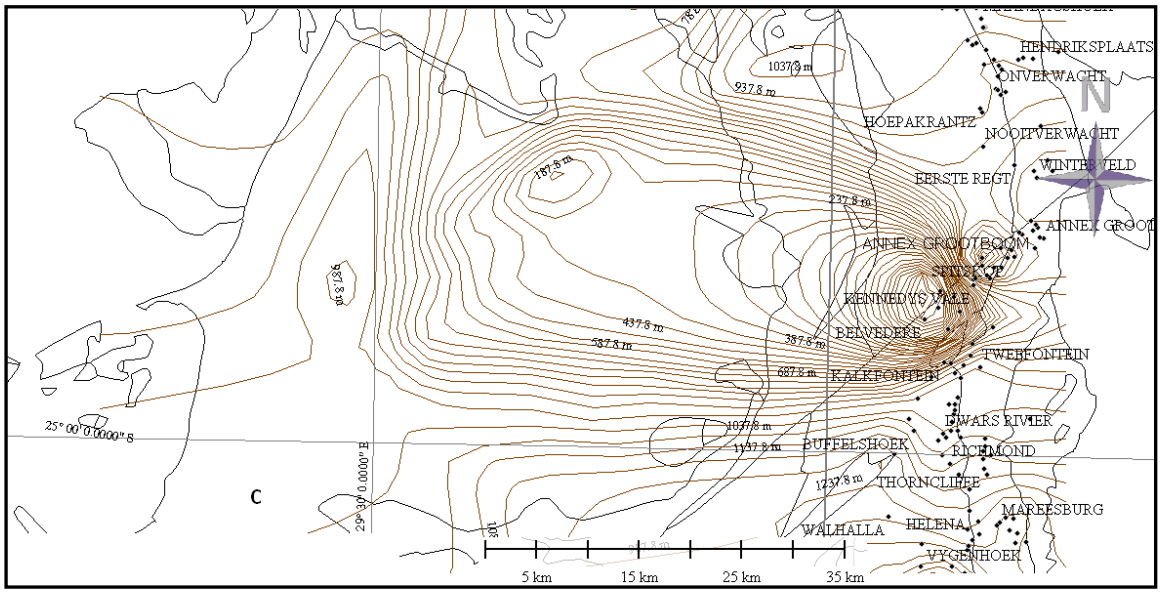

Figure 6.70: The third- order residual structure contour map for the Upper Zone unit of the Central Eastern Bushveld Complex

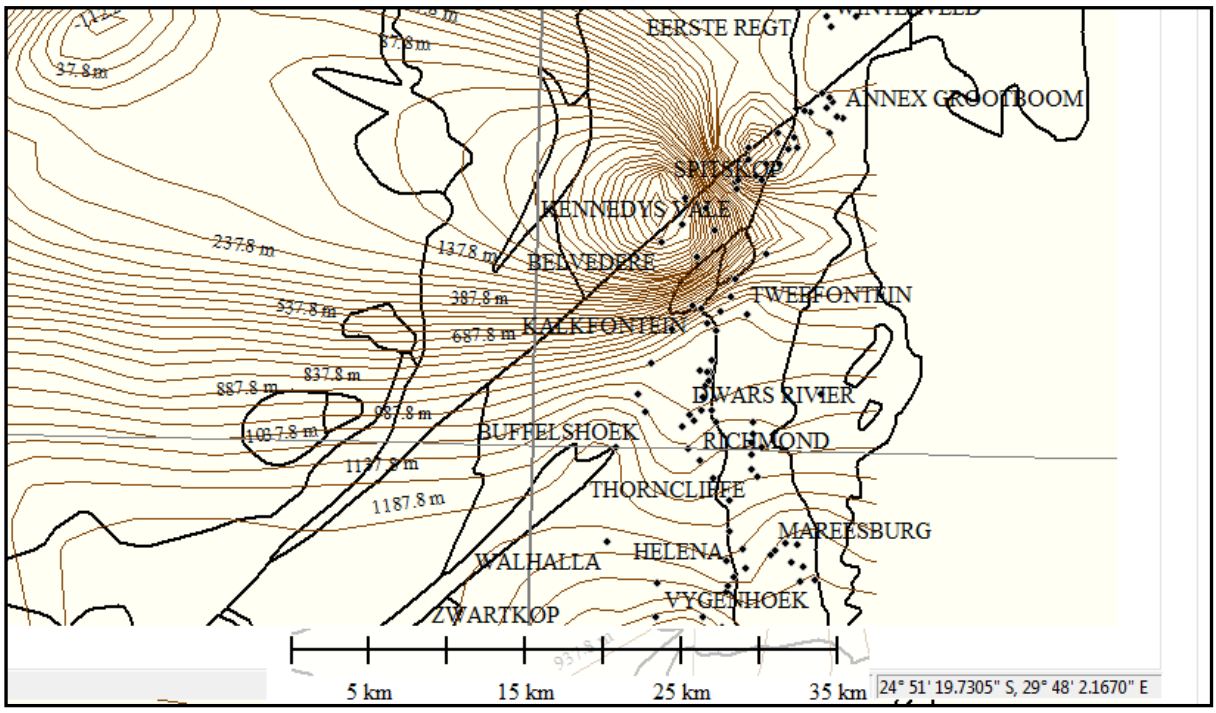

Figure 6.71: The residual structure contour maps for the Main Zone unit of the central Eastern Bushveld Complex

6.5.5.4 STRUCTURE AND ISOPACH RELATIONSHIP OF CENTRAL PARTS OF EASTERN BUSHVELD COMPLEX

The Upper Zone and the Main Zone residual isopach and structural maps shown in Figure 6.72 and re 6.73 reveals an inverse correlation at the centre although, they both trends differently. While the Upper Zone isopach trend is SE that of the Main Zone is more of N-S with widespread thinning at the centre this is clearly indicated in Figure 6.73. However, the other stratigraphic units show random correlation structure and thickness correlation.

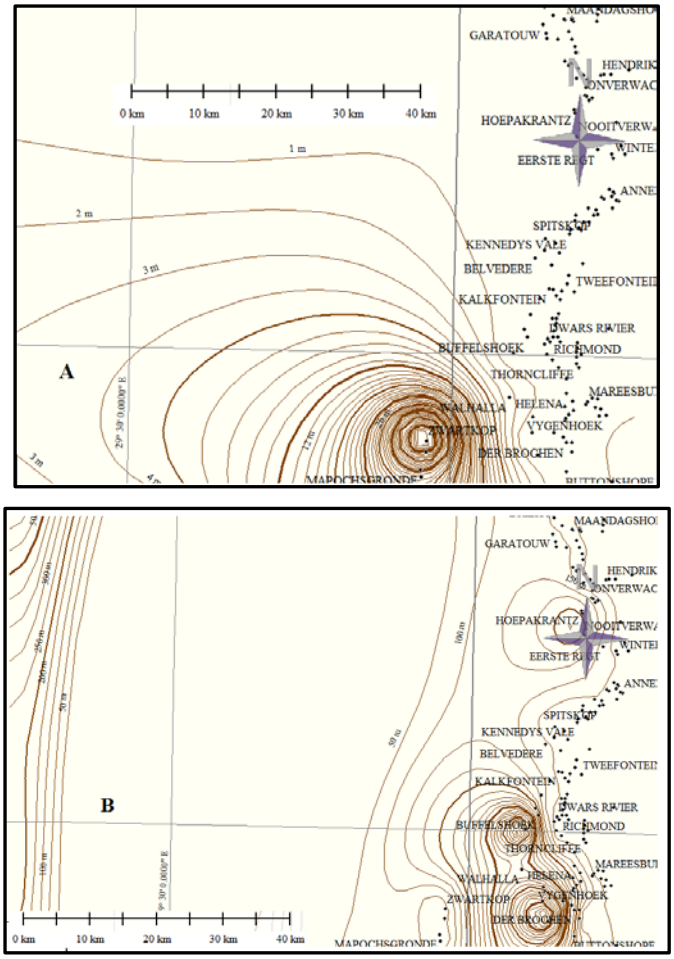

Figure 6.72: The Upper Zone isopach trend (A) and the Main Zone isopach trend (B) of central parts of the Eastern Bushveld Complex.

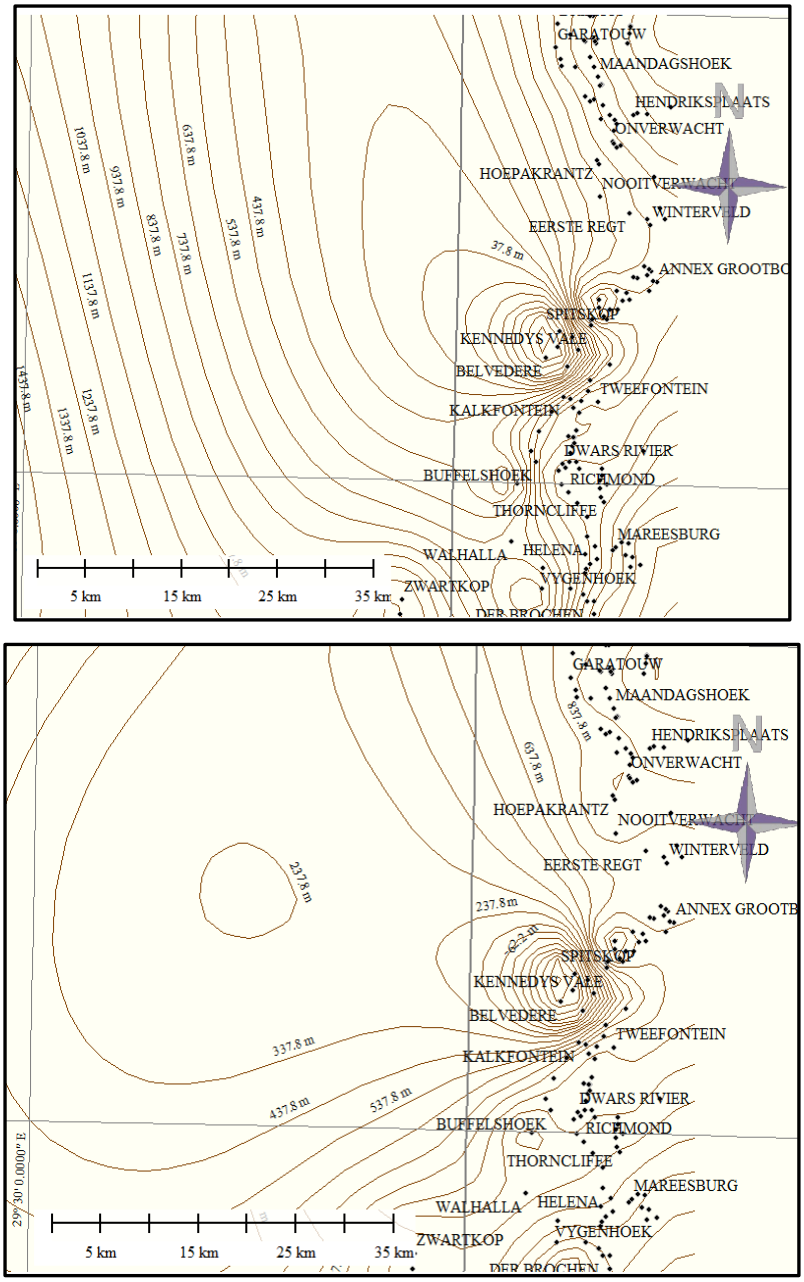

Figure 6.73: Structural trend for the Upper Zone (up) and the Main Zone (down) of the central parts of Eastern Bushveld Complex

6.5.6. TREND SURFACE ANALYSIS OF SOUTHEASTERN BUSHVELD COMPLEX

6.5.6.1 SOUTHEASTERN BUSHVELD RESIDUAL STRUCTURE

A few numbers of positive and negative structures are evident on contoured the Upper Zone stratigraphic unit of Southeastern Bushveld Complex as shown in Figures 6.74. The

Groblersdal sector consists of a syncline, which is about 100 m deep at the centre, while the immediate east of this structure consists of gradually increasing northwest elongate positive domain. Further eastwards in Figures 6.74 are extensive positive domain that opens to the east implying possible continuous positive domain to the east. Within this extensive positive domain are three isolated strong positive residuals, one occurs at the centre around Mineral range i.e., north of Welgevonden. The other two residual structures occur in the extreme eastern part. The southern parts of Stoffberg in Southeastern Bushveld are marked by strong positive domain separated from the Mineral range positive domain by a negative domain.

The Main Zone residual structure contour in Figure 6.75 exhibits a few small-scale structure negative domains that slope to the west around Buffelshoek and Der Brochen farm south of Steelpoort. Area around Groblersdal sector on Loskop suid farm also exhibits negative domain.

Pattern on residual structure map for the Main Zone up to the Archaean granite surface are the same while the residual isopach varies randomly.

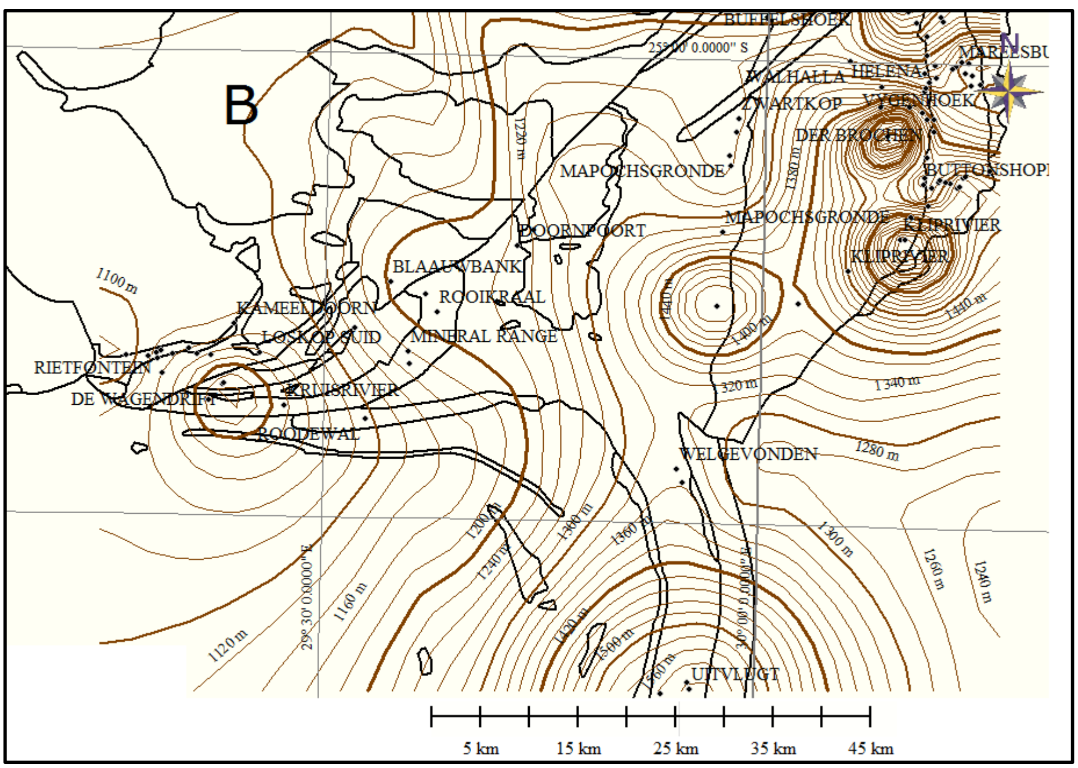

Figure 6.74: The second-order Upper Zone residual structure map and superimposed geological contact of central part of Eastern Bushveld Complex geologic map.

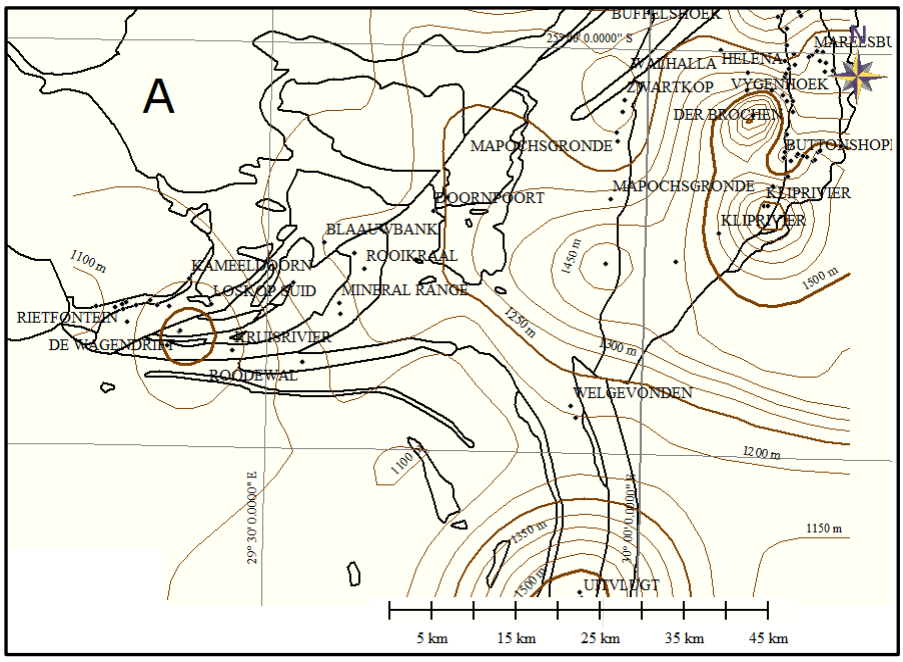

Figure 6.75: : The first-order (A) Main Zone residual structure and geologic map of central part of Eastern Bushveld Complex.

6.5.6.2 Southeastern Bushveld Residual Isopach

Small scale isolated positive thickness domains can be identified on the Upper Zone residual isopach map. As revealed in Figure 6.76, the structures are aligned NS and dominate almost the central part of the Southeastern Bushveld Complex. The structures are also surrounded by steep slopes of the east and more gradual slope in the western part. The eastern parts around Kliprivier farm is marked by negative thickness while the Groblersdal section is marked by an eastward thickening trend. Two adjacent anticlines are present in the extreme southern section of the map. The one on the western side represent the down thrown block to the uplifted section in the immediate east.

The Main Zone first order residual isopach map in Figure 6.77 reveals a prominent thickening in the eastern part of Mineral range and around Groblersdal section which geographically coincides with areas with negative domain on the residual structural maps. The Merensky Reef is prominent around the southern parts of Steelpoort especially around Richmond and Mareesburg farms (as indicated in Figure 6.78). The thicknesses however, terminate abruptly to the north (around Steelpoort fault).

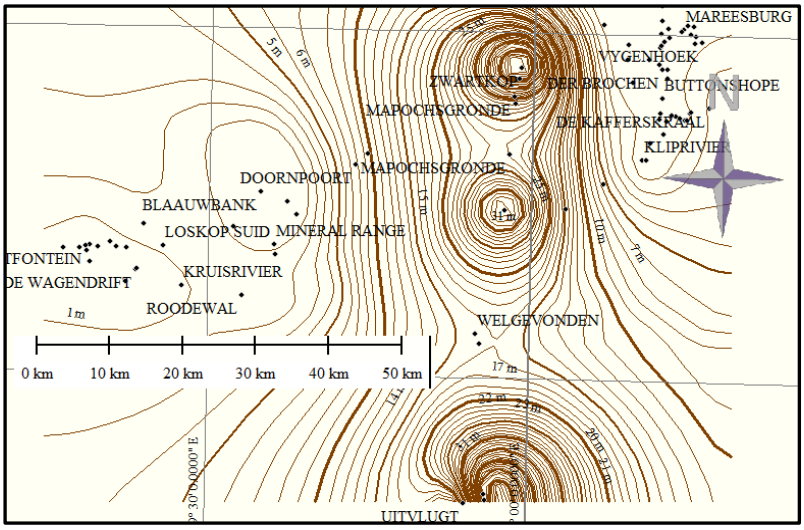

Figure 6.76: First order Upper Zone residual isopach for part of Southeastern Bushveld Complex.

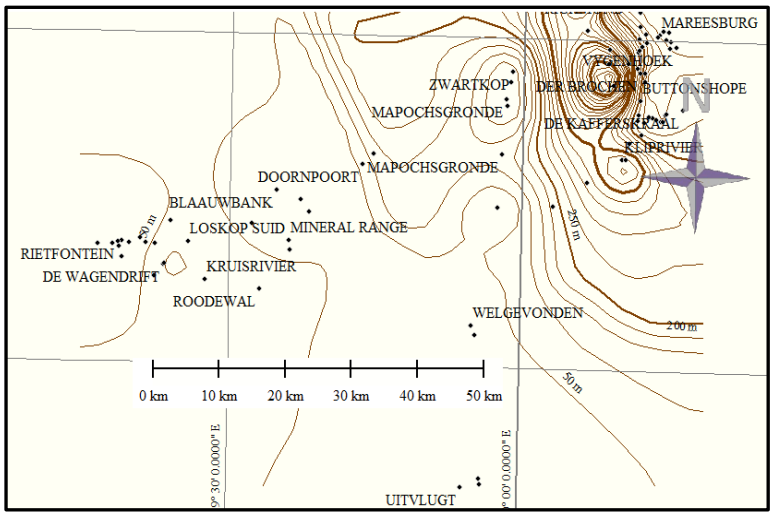

Figure 6.77: The Main Zone thickness in the central parts of the Southeastern Bushveld Complex indicating the residual isopach.

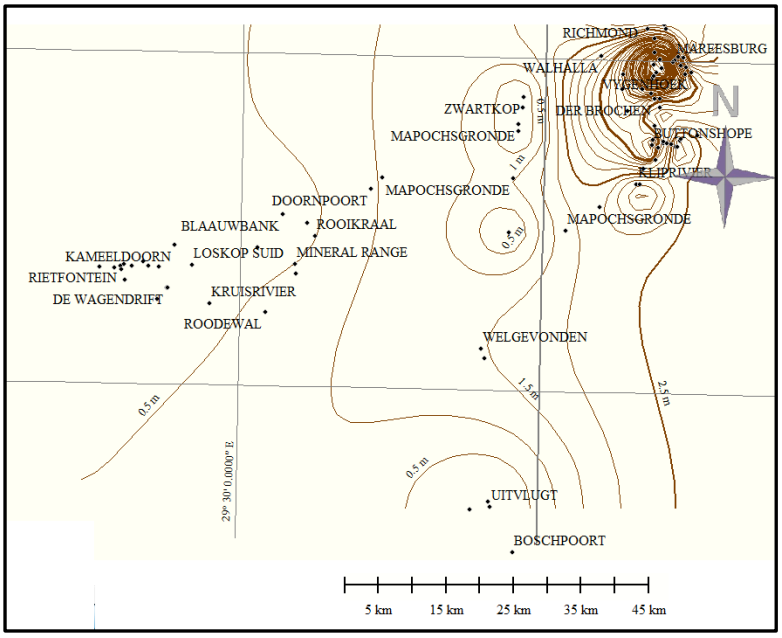

Figure 6.78: Merensky reef isopach trend map of parts of Southeastern Bushveld Complex.

:

6.5.6.3 Southeastern Bushveld Structure Trend

The Upper Zone first order structural trend of the Southeastern Bushveld area in Figure 6.79 can be separated into four broad trends: the Groblersdal synclinal area, the Stoffberg area dominated by an anticline structure, the Kliprivier area with anticlinal closures that open to the east and the central i.e. east of the Groblersdal area with an increasing structural high that trends east-west.

First order Main Zone structure trend in Figure 6.80 is marked by a NNW thickening trend around the southern parts of Steelpoort. The area also coincides with the shallow dipping part of the Eastern Bushveld Complex.

6.5.6.4 Southeastern Bushveld Isopach Trend

The Upper Zone isopach trend map in Figure 6.79 exhibit prominent N-S and NNW-SSE trend with inward bend around Welgenonden and open outward in the southern extreme. However, on the Main Zone residual isopach, the former north-south structural positive domain in the centre now coincides with the absence of the zone in the centre. First to third order Main Zone trend shows strong inverse correlation between structure and isopach while higher orders show very random correlation. The second-order Main Zone trend

surface in Figure 6.80 reveals dominant ENE thickening trend that slopes to the NW. On the other hand the isopach lines run mostly N-S and NNW-SSE, the Critical zone displayed prominent NE trend in this section of the Eastern Bushveld Complex.

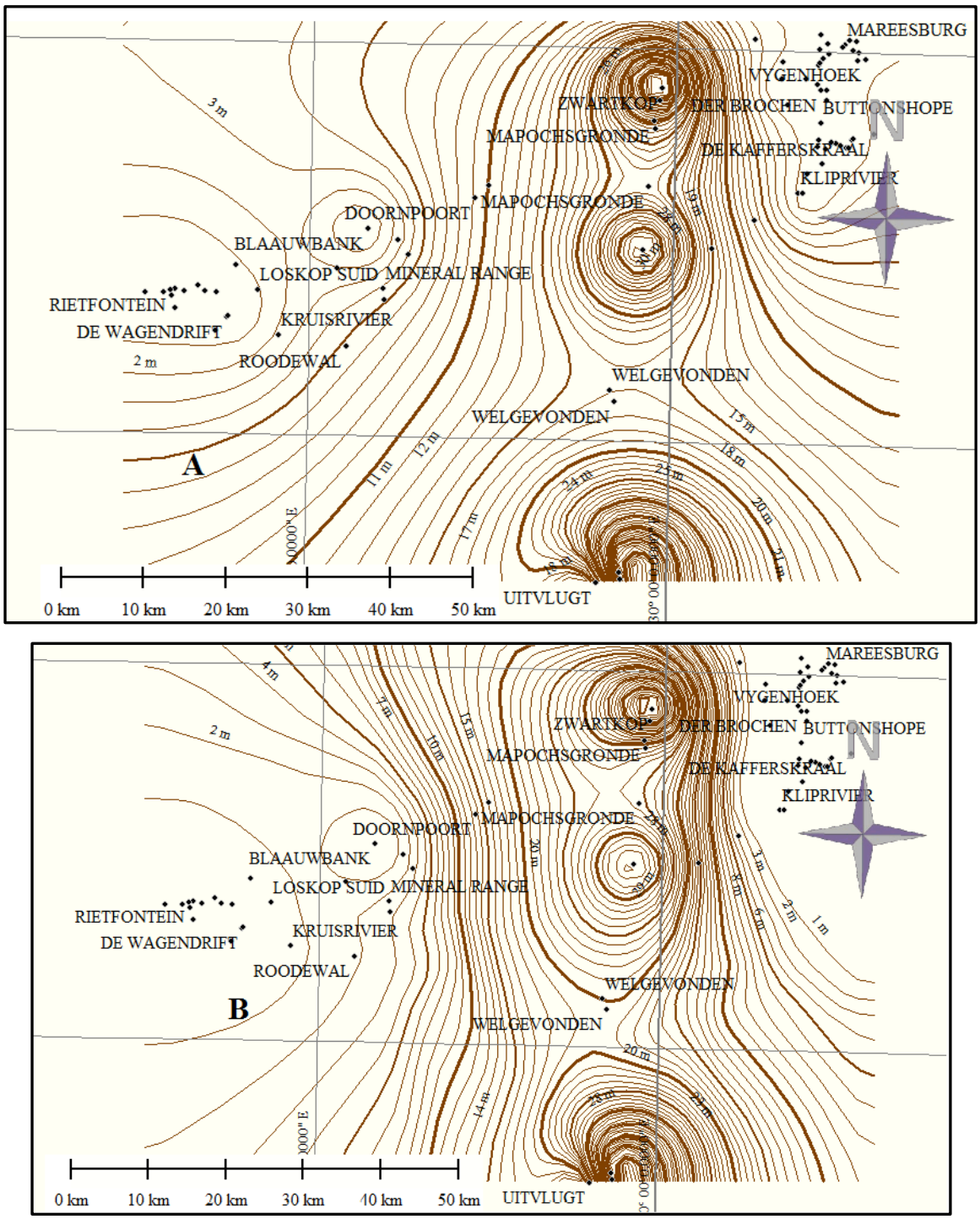

Figure 6.79: First and second order Upper Zone isopach trend of Southeastern Bushveld Complex

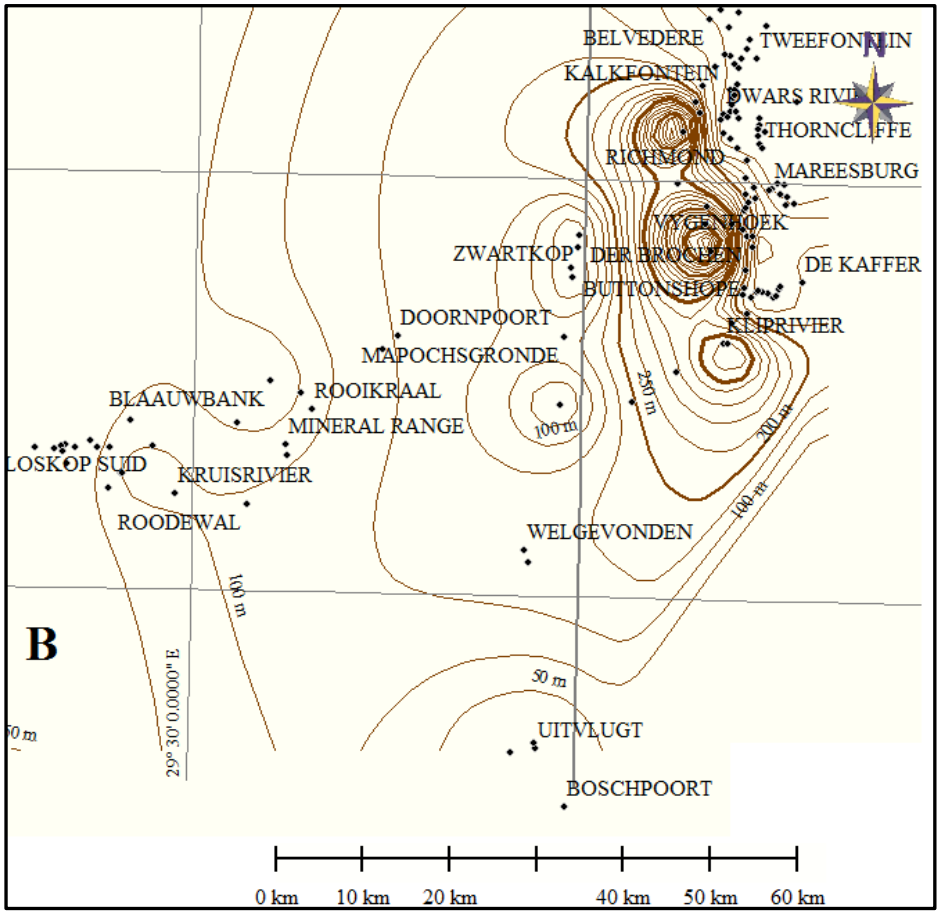

Figure 6.80: The second-order Main Zone isopach trend of Southeastern Bushveld Complex

6.5.6.5 Relationship between Trend Residual Structure and Isopach of Southeastern Bushveld Complex

First to fourth order (A-D) residual structure and isopach exhibit inverse correlation in the eastern extreme section, while the other parts show a similar relationship in terms of residual structure. However, the trend on both structure and isopach maps are similar. On the trend surface maps the general trend is increasing east verging positive structure and dips eastwards.

There is an inverse correlation between the structure and isopach residual of the Upper and the Main Zone. First and second structure and isopach trend also exhibit similar inverse correlation.

Inverse correlation between the Main Zone residual thickness and structure for the most part of southeastern Bushveld especially the shallow dipping portion of the Eastern

Bushveld Complex shows that the inward shallowing geometry is probably pre- or syn-Bushveld. Correlation of structure and isopach of higher orders is however, random.

The residual structure and thickness for the Merensky Reef in Southeastern Bushveld Complex varies randomly from first order to sixth order.

The Main Zone base and Archaean floor rock structure interval shows close similarities as indicated in Figure 6.54A, this indicates strong floor rock influence on most parts of RLS layers. However, Figure 6.54B indicates that the Upper Zone structure interval only shows close similarities with the Archaean floor in the southern and western parts.

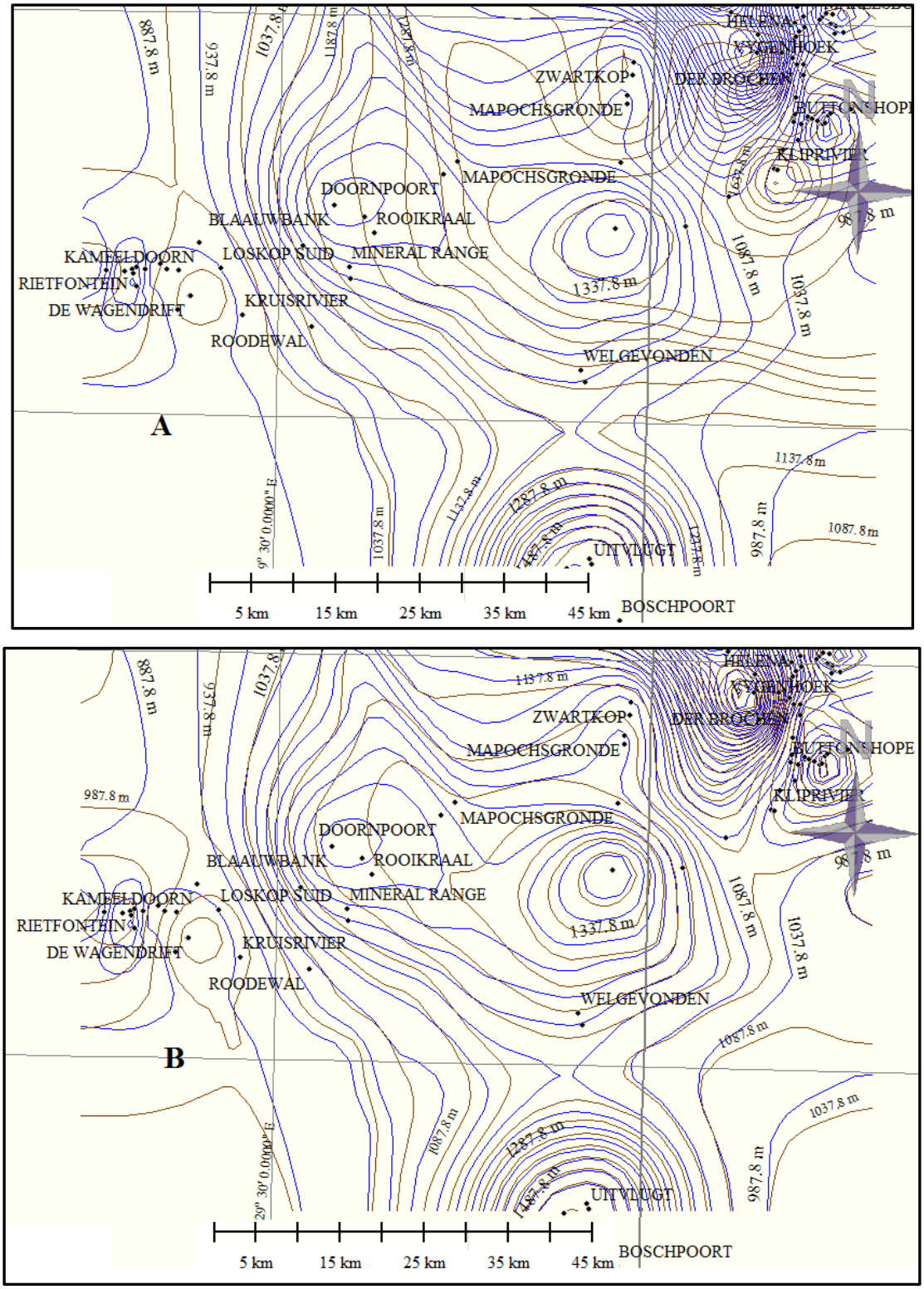

Figure 6.81: Draped structure contour map of the Upper Zone (A) on Archaean floor rock. (B) indicates close pattern correlation between the Archaean floor and the Main Zone base interval structure contour of the Southwestern Bushveld Complex define red and blue contours

.

6.5.7 TREND SURFACE ANALYSIS OF NORTHERN BUSHVELD

6.5.7.1 Northern Bushveld Residual Structure

Upper Zone residual structure map in Figures 6.82- 6.86 reveals isolated structure, high domain among a dominant low structural trend in the extreme northern parts of the Northern Bushveld Complex on farms Aurora, Harriet's wish and Nonnenwerth. The isolated structural high trends NNW-SSE to each other while the northern structural high domain extend northwards, the one on Nonnenwerth farm forms a closure. Southwards towards Elandsfontein farm (located as indicated in Figure 6.83 is a fault with downthrow of about 20 m to the north. Isolated structure negative domains occur on farm Dorstland 776 and Rietfontein in the central part of the Northern Bushveld. Another east-west trending fault with downthrow to the north occurs south of the Dorstland farm. However, the northern parts of Drenthe farm, is marked by strong isolate structural high domain especially around the Witrivier farm. This structure is elongated east-west and shortens along the N-S direction. Between Drenthe and Overysel farm there is a significant change in orientation, from the east-west trend in the western side to north-south in the centre and back to east-west trend on the eastern side (as indicated in Figure 6.84 and 6.85).

The central part of the northern Bushveld as indicated in Figure 6.86 hosts most of the small-scale isopach positive and negative domains for Upper Zone unit. These small-scale domains coincide geographically with that of Upper Zone unit isopach residual maps.

The Main Zone residual structure surfaces in Figure 6.87 shows close similarities with the Upper Zone residual structure surfaces and are marked by small-scale positive and negative domain in the central parts.

Platreef residual structures in Figure 6.88 and 6.89 indicate a structural high at the extreme north of the Northern Bushveld Complex. This structural high forms a closure that opens to the north. This section descends gradually to the south with a small gap between it and the central section. The central section shows an irregular residual structural pattern with many small-scale structures almost forming a NNW trend.

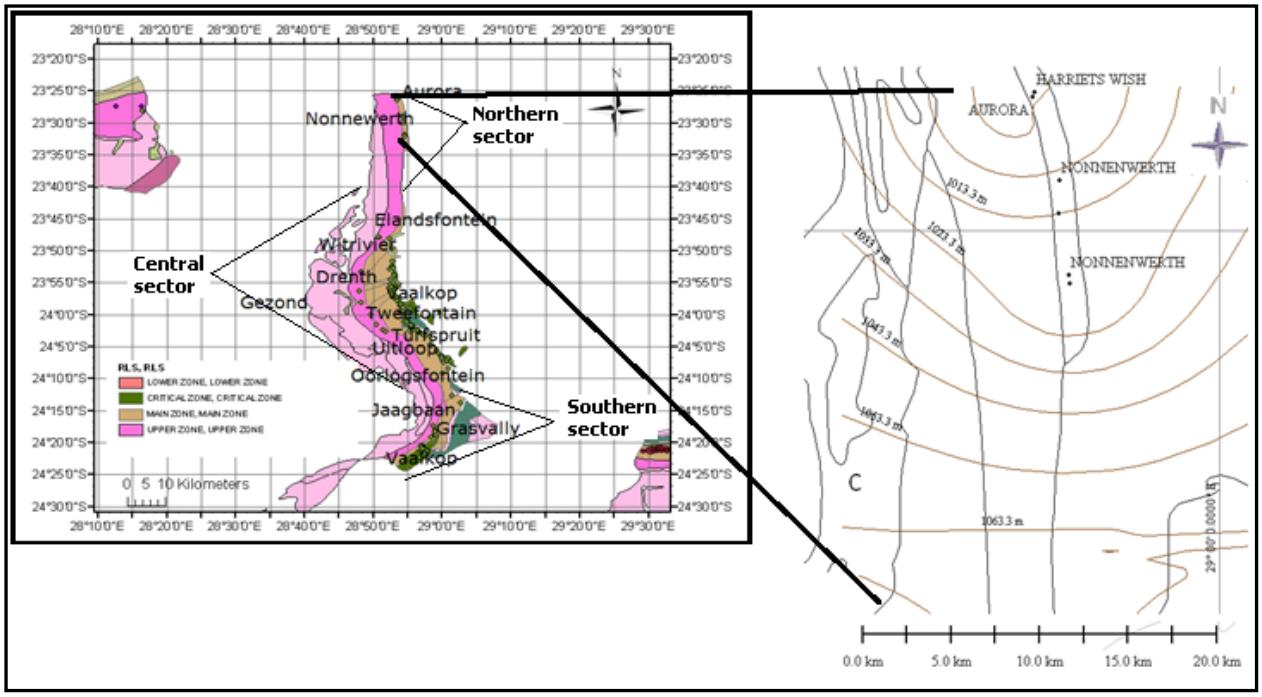

Figure 6.82: The Upper Zone top interval structure contour map for the northern part of Northern Bushveld

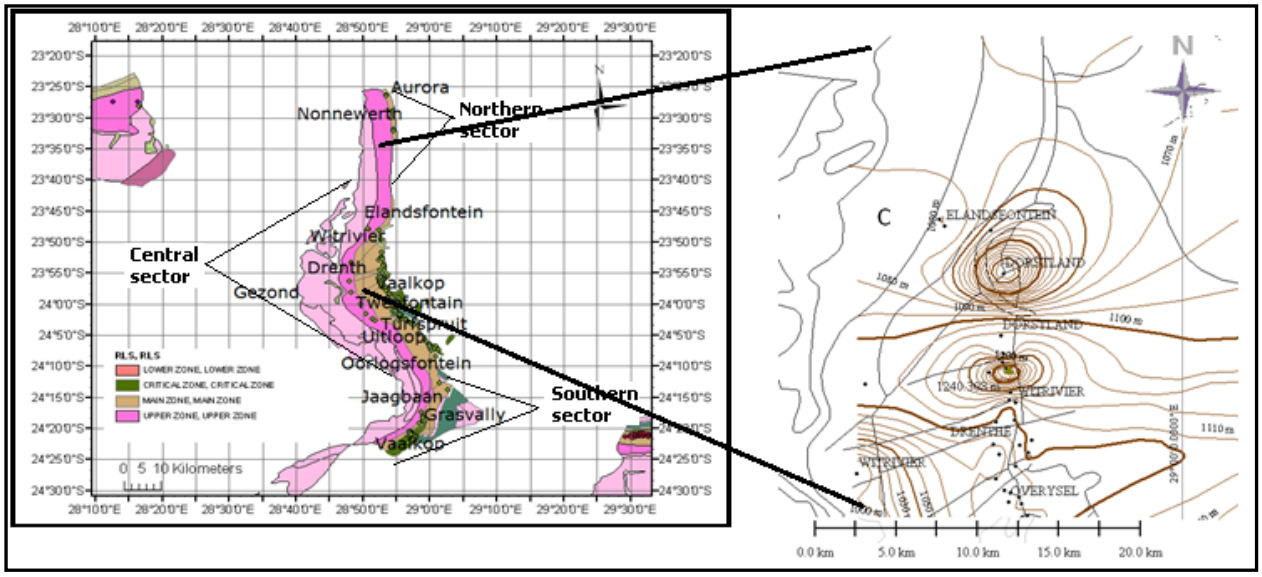

Figure 6.83: The Upper Zone top interval structure contour map for central part of Northern Bushveld.

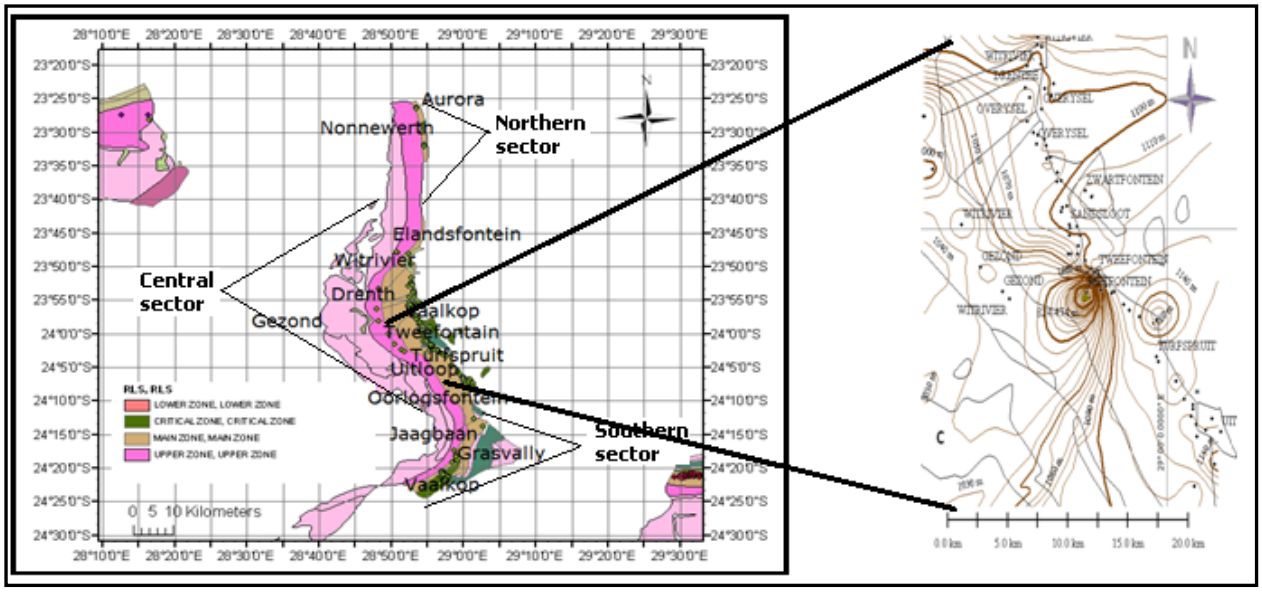

Figure 6.84: The Upper Zone top interval structure contour map for central part of Northern Bushveld.

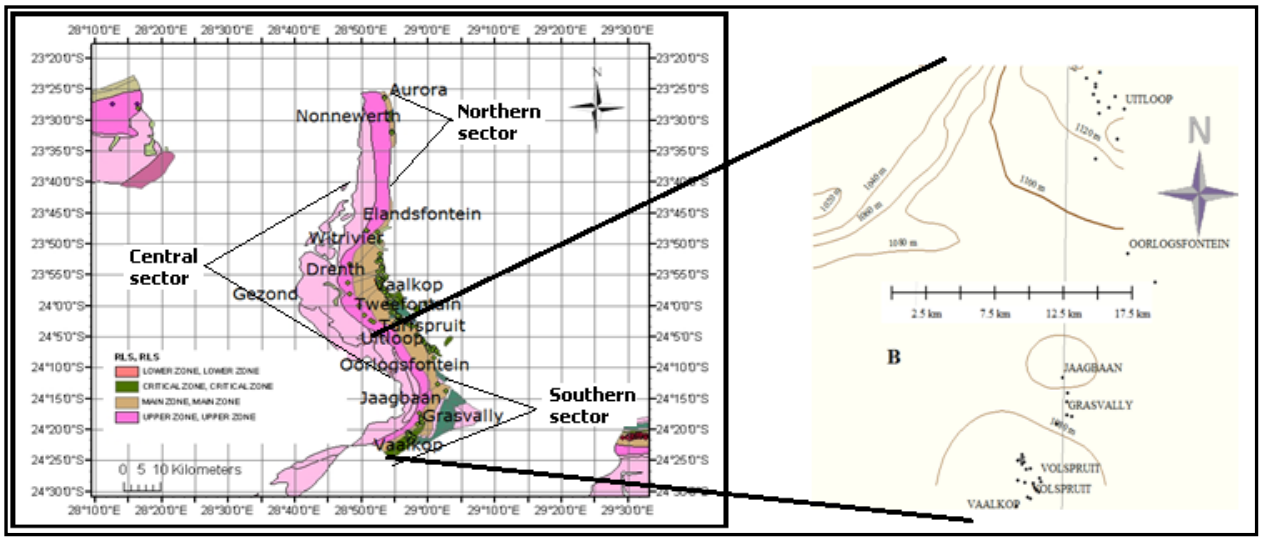

Figure 6.85: The Upper Zone top interval structure contour map for southern part of Northern Bushveld.

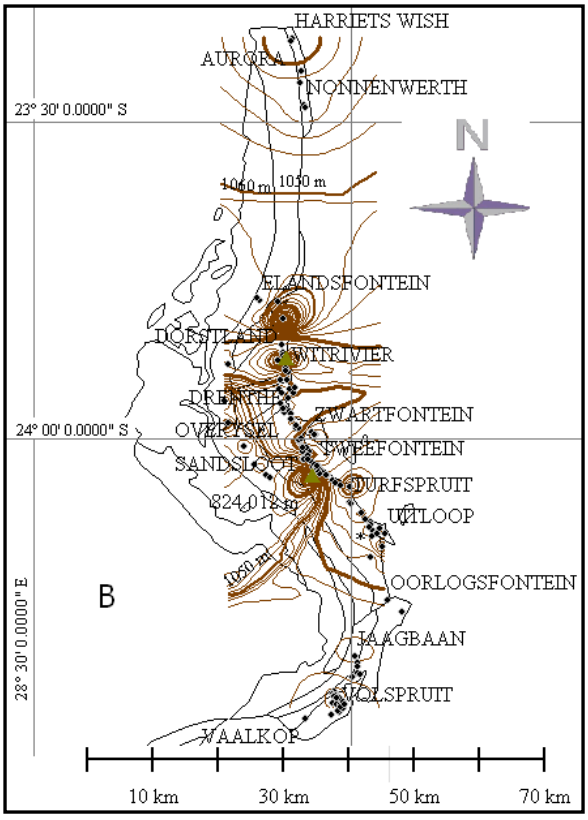

Figure 6.86: The Upper Zone interval residual structure map showing second order (B) surfaces

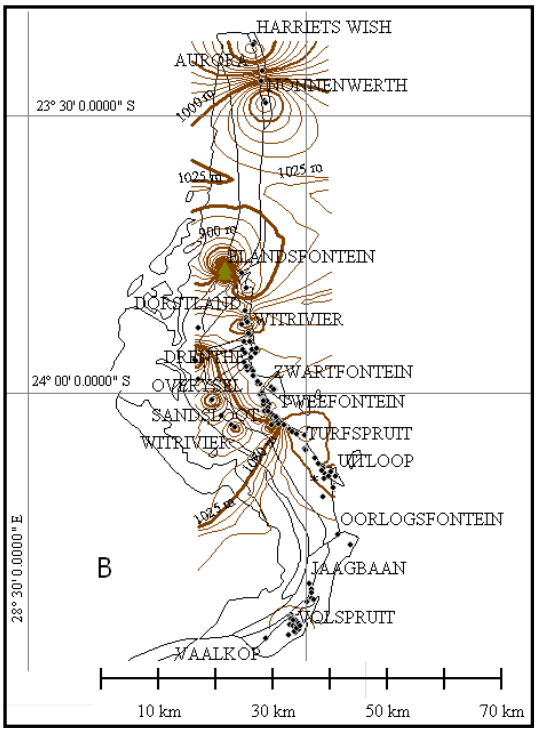

Figure 6.87: The Main Zone interval residual structure map of Northern Bushveld southern sector showing second order (B) surface (with a contour interval of 25 m).

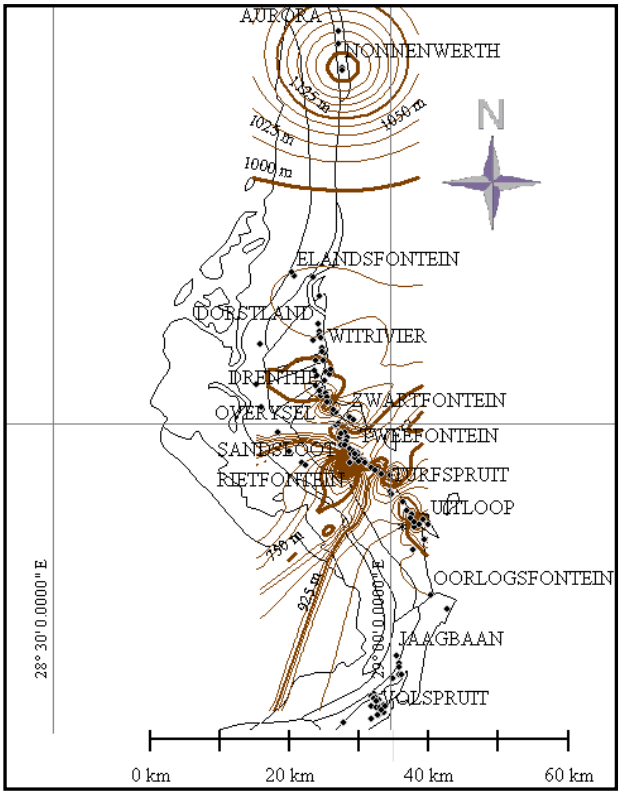

Figure 6.88: First order Platreef residual structure map of the Northern Bushveld

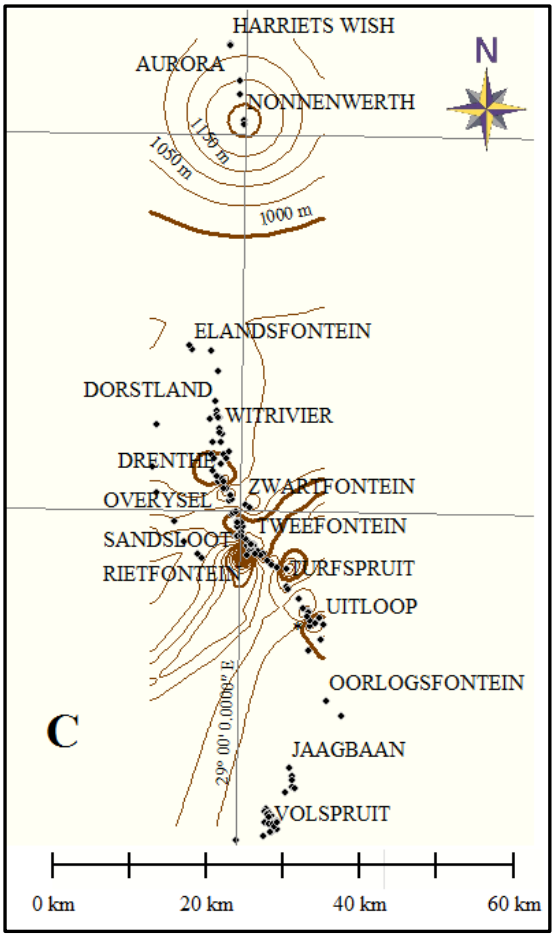

Figure 6.89: Third order Platreef residual structure maps of the Northern Bushveld.

6.5.7 2 Northern Bushveld Residual Isopach

The second- order isopach trend surface in Figure 6.90 reveals that the extreme northern part of the Northern Bushveld Complex shows northward thickening of the Upper Zone stratigraphic unit. Immediate south of this area is marked by an east-west trending fault with a down throw to the south around Nonnenwerth farm. Southwest of Nonnenwerth farm, the Upper Zone thickens southwards and terminates abruptly around Dorstland farm. This is followed by NNW-SSE oriented alternating thickening and thinning in the western part and widespread southeast thinning to the east.

The Main Zone residual isopach maps in Figure 6.91 and 6.92 indicate prominent central thickening of the Main Zone unit with thinning to the north and south. This central thickening is rather irregular. For example, on Overysel farm there is a prominent adjacent thickening and thinning with southeast plunging. Another similar structure occurs around

Tweefontein farm with thinning on the Tweefontein Hill and thickening on the adjacent southwest plunging Syncline. Also in Uitloop farm south of the Turfspruit same type of structure is replicated with thickening on the downward side that is oriented to the NNW and adjacent thinning occurring across an isolated structural high. This central thickening trend terminates southwards with east-west oriented steep sloping downthrow to the south. However, an isolated positive thickening is present on Grasvally farm.

Platreef residual isopach maps in Figure 6.93 and 6.94 show gradual thinning northward towards the extreme north. While southwards, it formed an anticlinal closure around Dorstland farm. However, the Grasvally area did not indicate any structure on the residual isopach map as indicated on the Main Zone residual isopach map probably due to the absence of sufficient borehole data on Platreef in the area.

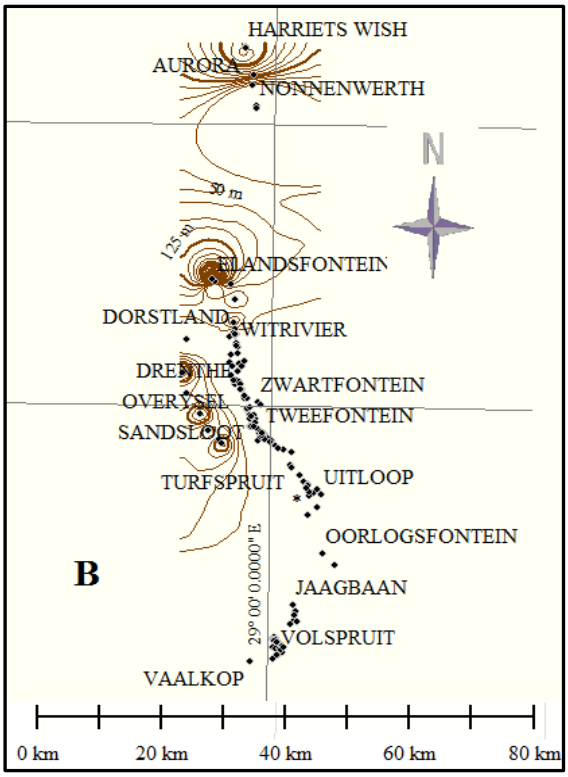

Figure 6.90: The Upper Zone interval residual isopach maps showing second order (B) surface

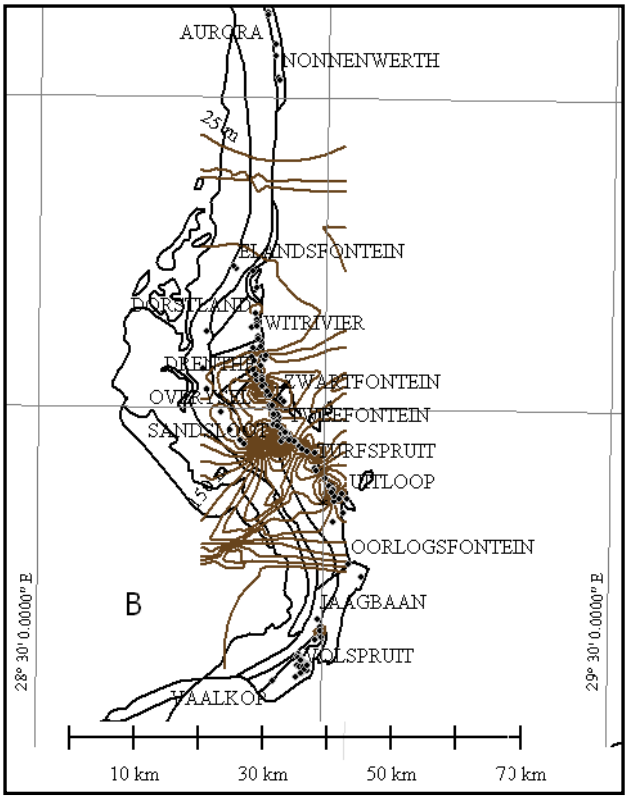

Figure 6.91: The Main Zone interval residual isopach maps of the Northern Bushveld southern sector showing second order surface (with a contour interval of 25 m)

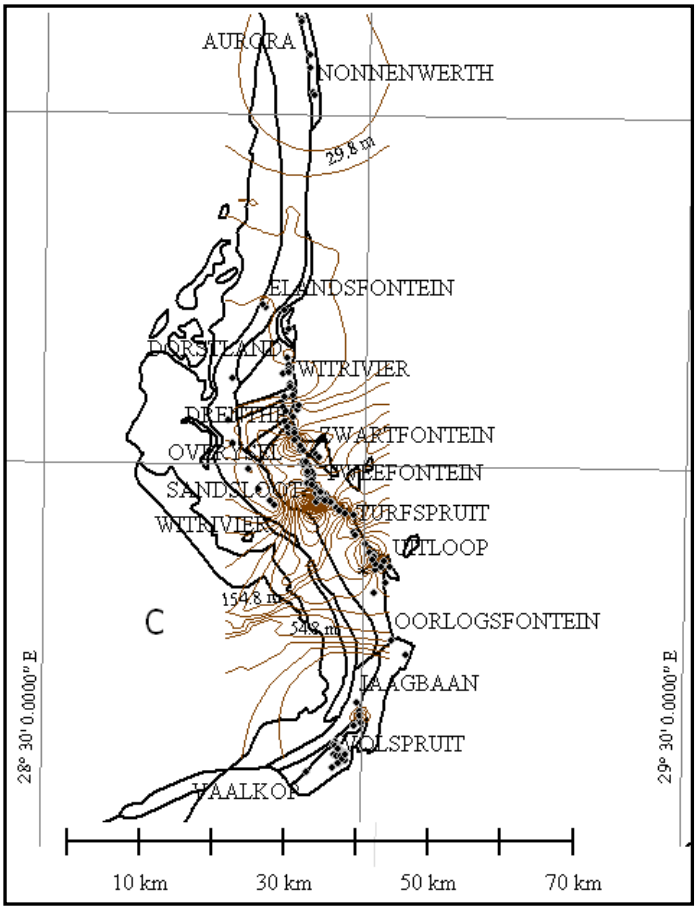

Figure 6.92: The Main Zone interval residue structure map of the southern sector in the Northern Bushveld showing third order (contour interval of 25 m)

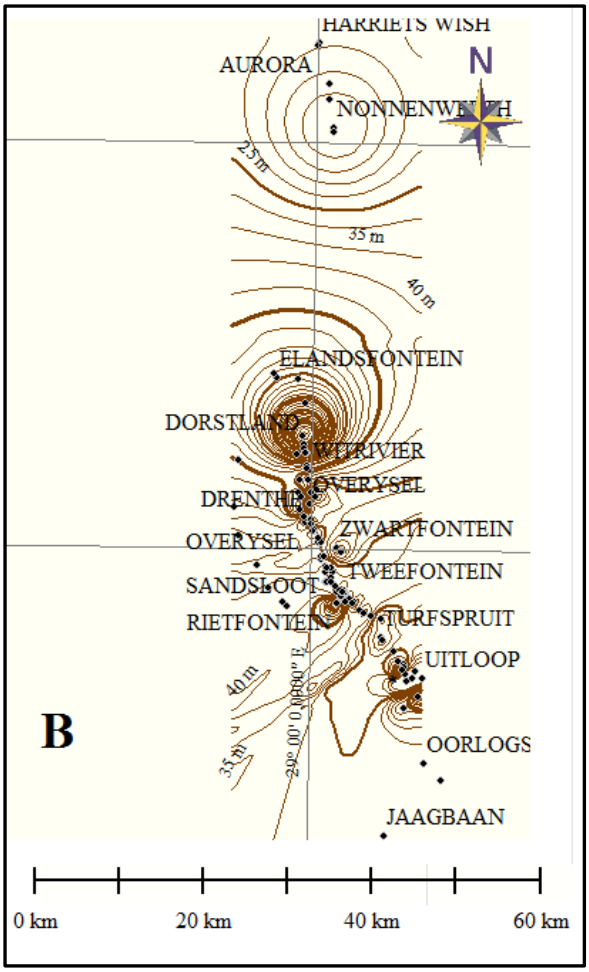

Figure 6.93: : Second order Platreef residual isopach map of Northern Bushveld Complex.

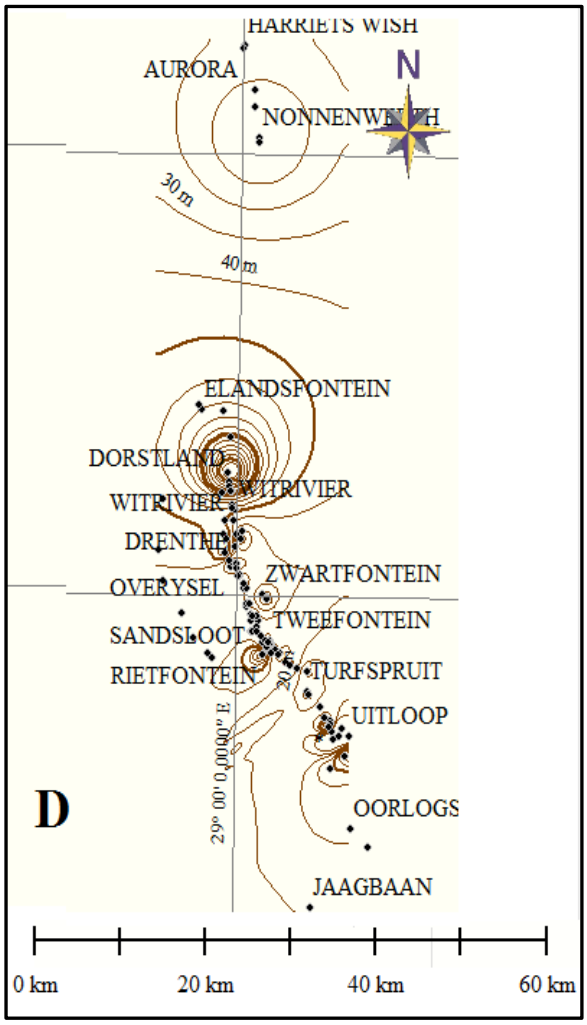

Figure 6.94: The fourth order Platreef residual isopach map of the Northern Bushveld complex.

6.5.7.3 Relationship between Residual Isopach and Structure of Northern Bushveld

The structures revealed on the Upper Zone, Main Zone, the Lower Zone down to the Archaean floor, and the thickness of each of these units for most part of the Northern Bushveld Complex show strong inverse correlation.

6.5.7.4 Northern Bushveld Structure Trend

On first order structural trend surface in the Upper Zone, the extreme northern part forms the structural negative portion with a regional dip to the north in Figure 6.95. The southern

and southwestern parts reveal depression or trough . However, the central part forms a structural positive area with NW-SE trend. Regionally, the western part of the central portion is dominated by structural high while the southwestern side is made up of sharply descending structural low area. There is another significant change in orientation. Northwest of Sandsloot farm, the unit trends NNW and dips to the southwest. However, on Sandsloot farm and south of Zwartfontein farm, the trend changed to approximately ESE and dips southwards. The western part of Tweefontein slopes steeply Southeastwards thus demarcating the structural low trend in the west from the western structural high trend. Further south between Jaagbaan and Volspruit, there is a structural high domain that separates these two farms.

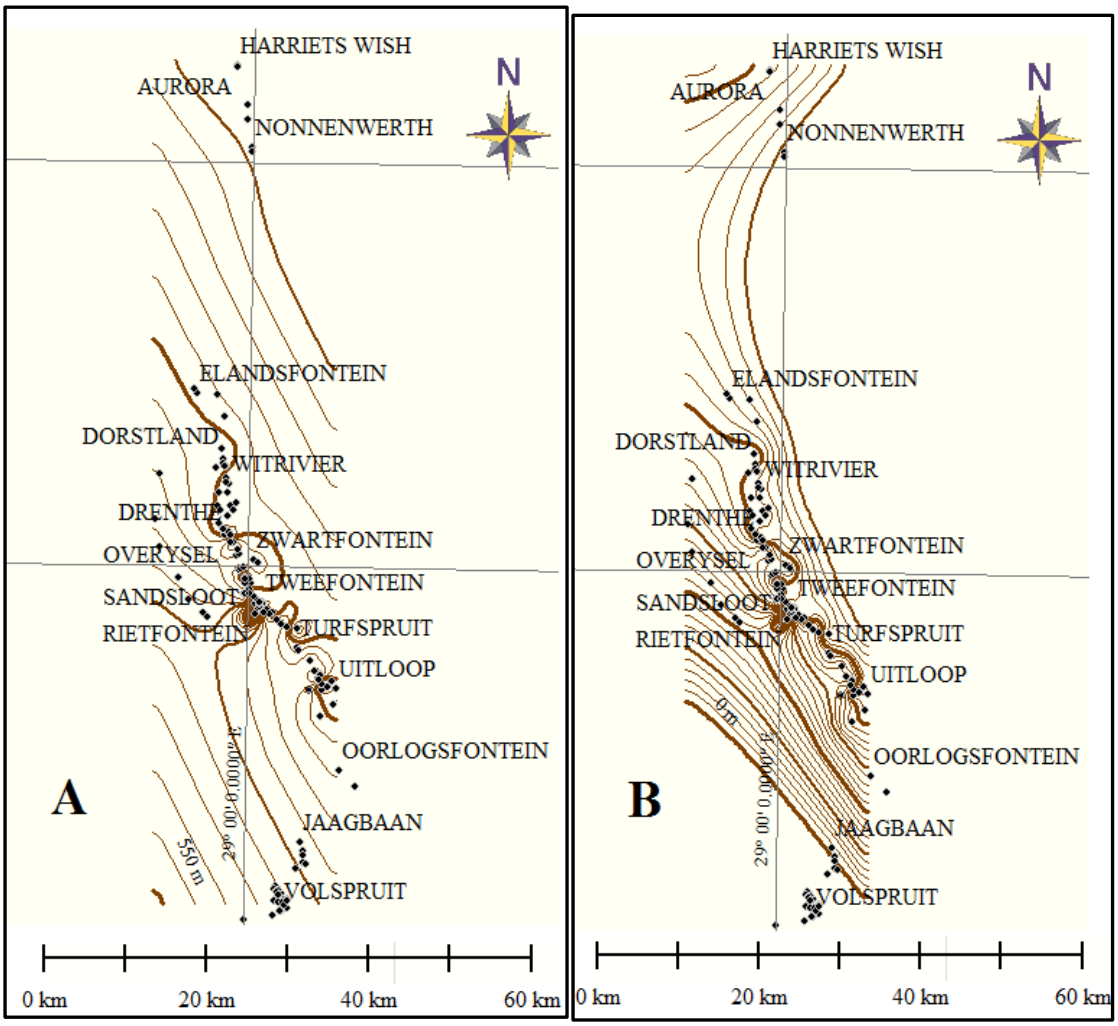

Figure 6.95: Platreef first (A) and second (B) order structural trend of Northern Bushveld Complex

6.5.7.5 Northern Bushveld Isopach Trend

First and second order isopach surface ofthe Upper Zone unit in Figure 6.96 has a prominent NE thickening trend in the north between Nonnenwerth and Elandsfontein the trend changed to NNW thickening in the west and thins out towards the east. This trend continued in the centre except for the presence of isolated thickening and thinning in the western part in the extreme southern part the trend is almost N-S with thickening to the west. Higher orders display similar trends with slight variation.

The Main Zone unit exhibit eastward thickening trend as indicated in Figure 6.97. This trend is, however, irregular and wider at the centre due to the presence of isolated thickening and thinning domains which are oriented almost NNW-SSE except for the Tweefontein area where the trend changed to NE-SW. Around Overysel farm the thickening trend extends eastwards and thins out in the west. While in the Rietfontein area (adjacent to Tweefontein) the thickening trend is southwest.

First order Platreef isopach trend in Figure 6.98 reveals strong N-S trend while the second order indicates a NW-SE trend in the northern part and NNW-SSE trend in the southern part with the central part showing some irregularities.

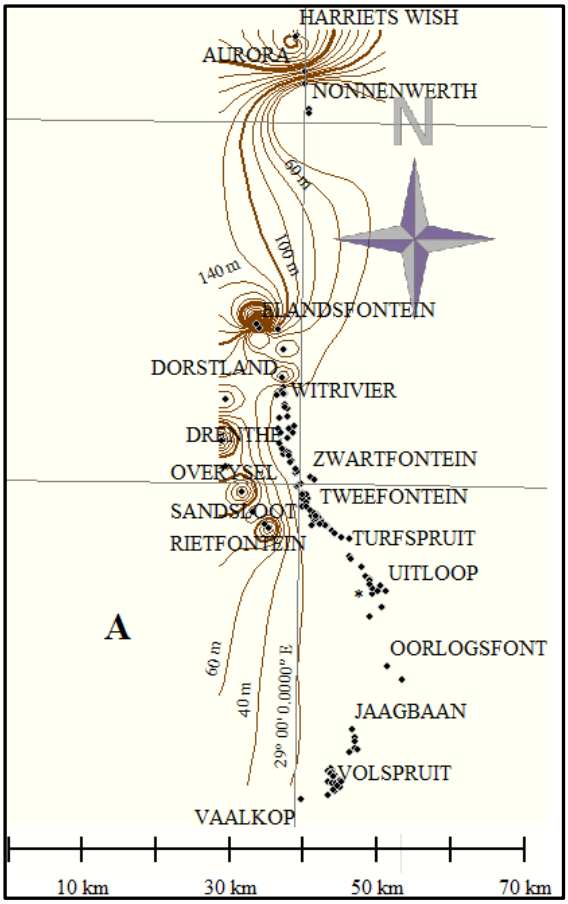

Figure 6.96: The Upper Zone isopach first order trend surface of the Northern Bushveld Complex

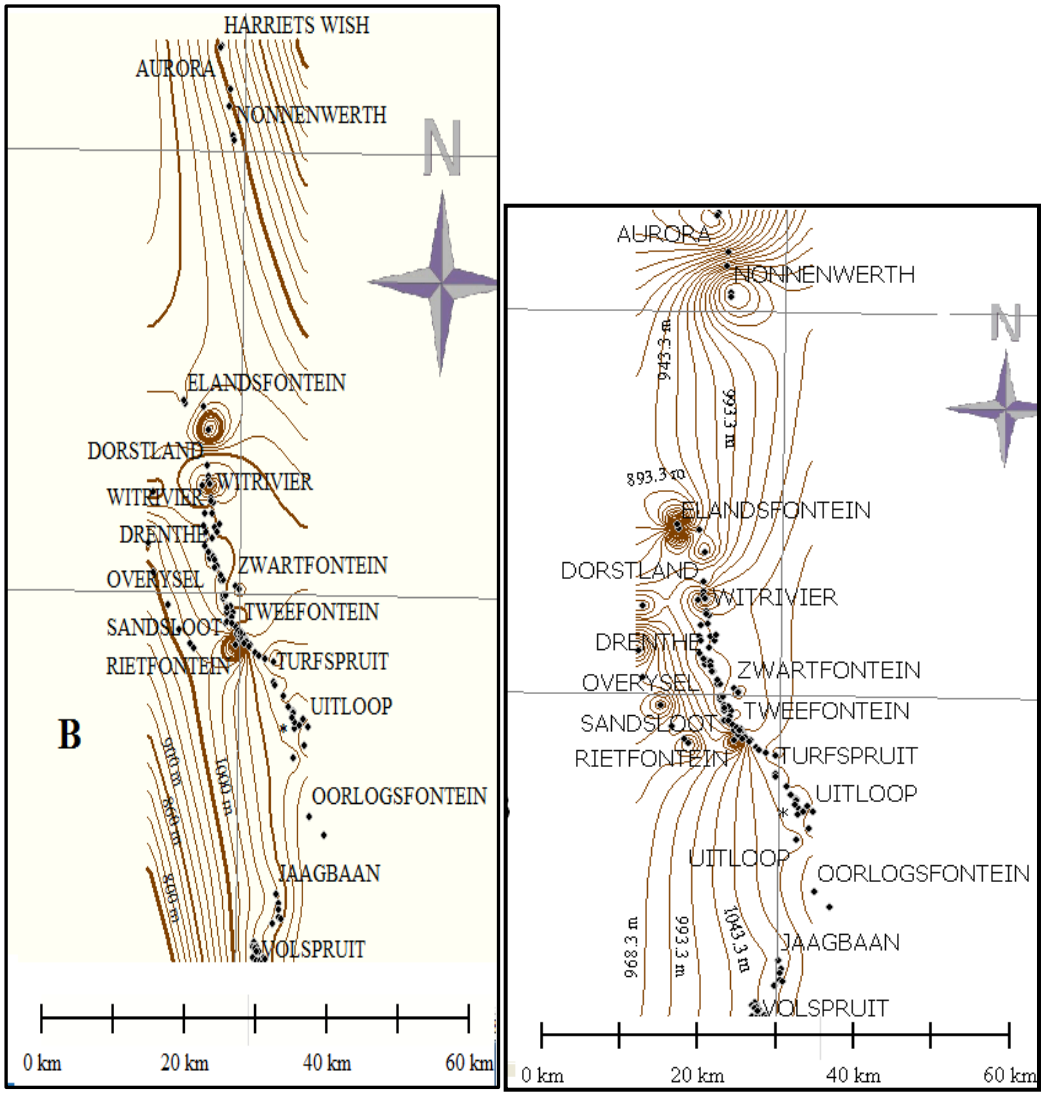

Figure 6.97 The Main Zone isopach (left) and structural (right) second order trend surface of the Northern Bushveld Complex

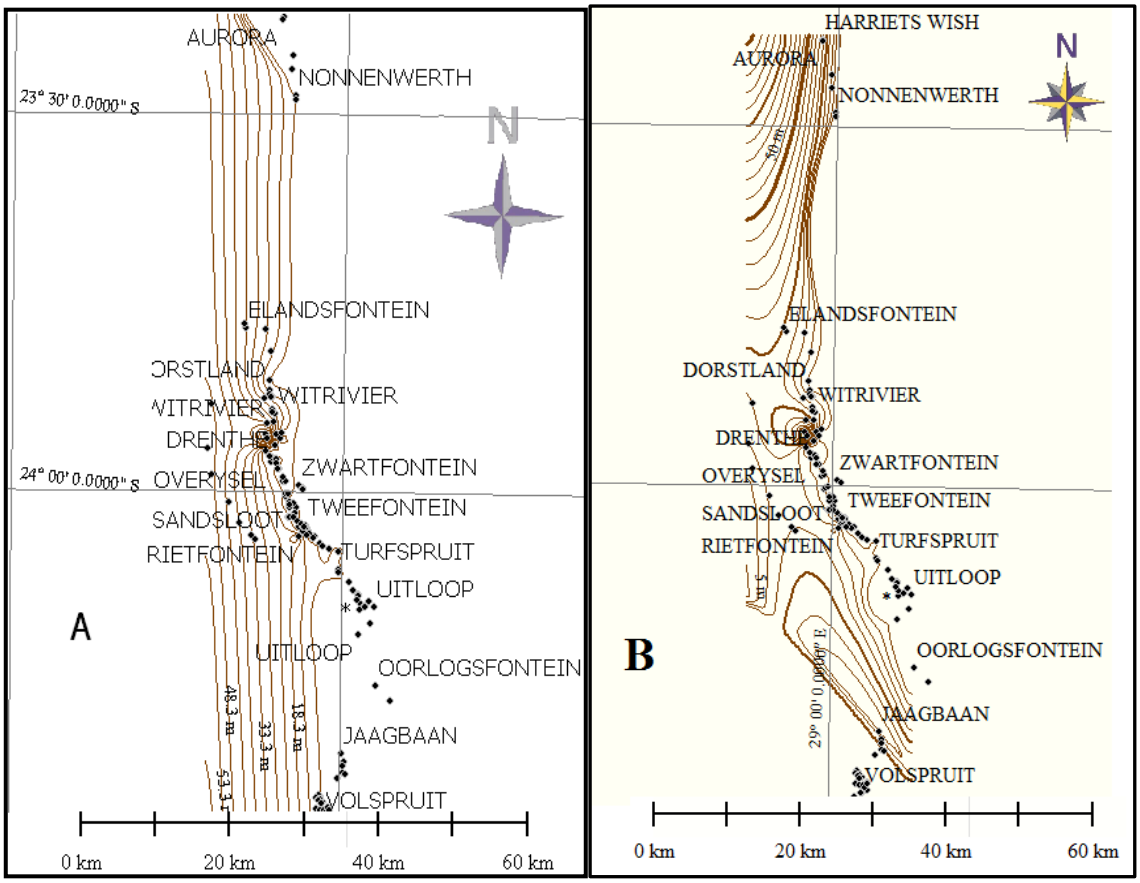

Figure 6.98: Platreef isopach first and second order trend surface of Northern Bushveld Complex

6.5.7.6 Relationship between Northern Bushveld Isopach and Structure Trend

Both the residual and trend structure, and isopach indicate inverse correlation for most parts of the Northern Bushveld Complex from the Upper Zone unit to the Archaean floor rock unit. This implies that most of the present day structures are either pre- or syn-Bushveld.

A major horst structure is indicated in the centre of the northern limb on the residual structure map for first to sixth- order. Figure 6.99 and 6.100 reveal the centrally located horst structure with the northern parts slightly higher than the southern part. This is particularly obvious on the Upper Zone and the Main Zone residual structure maps. It is however, not pronounced on Platreef residual structure map. The horst structure is very irregular and multi-peaked on the Archaean floor residual structure map (see Figure 6.100). On corresponding isopach maps in Figure 6.101 the horst structure geographically coincides with a depression or graben structure at the centre of the Northern Bushveld Complex. Since the same signature is observed on most of the intervals down to the

Archaean floor, the centrally located graben structure may probably signify a post-Bushveld structure or reactivated Archaean structure. Change in regional dip direction from eastward in the northern parts of the Elandsfontein farm to westward in the southern parts of Witrivier farm is also noteworthy. An isolated small-scale positive domain exists on Grasvally farm, the structure slopes down northwards toward Jaagbaan and southwards toward Volspruit farm forming a horst-like structure.

A similar structure exists on Archaean floor rock residual structure between Uitloop and Turfspruit farm, this structure shows a structural high that slopes steeply to northwest and gently in the southwest. Same structure seems to be modified on the Main Zone structure map to a fault with down slope to the northwest. Southward on Volspruit farm is a negative structure bounded by positive structures on both east and west. However, most of the faults in this area strike NE to ENE parallel to Ysterberg fault. More explanation about faults and other structures will be discussed in the next chapter. The structural pattern from the Upper Zone unit down to the Archaean floor rock did not indicate any major difference.

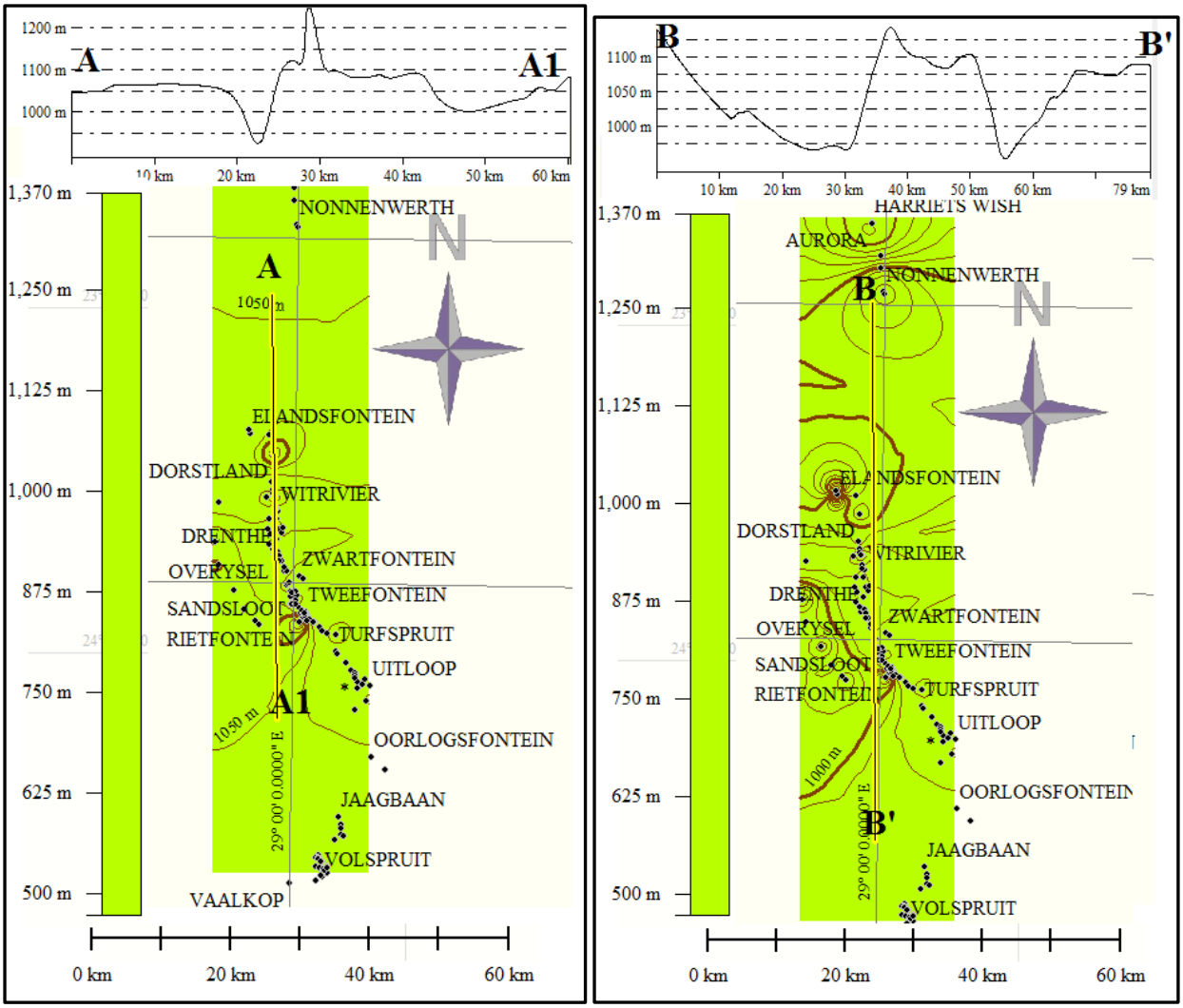

Figure 6.99: Profile A-A1 on the Upper Zone (A) and B-B1 on the Main Zone (B) residual structure of Northern Bushveld Complex showing a horst structure in the central part (Contour interval 50 m for (A) 25 m for (B).

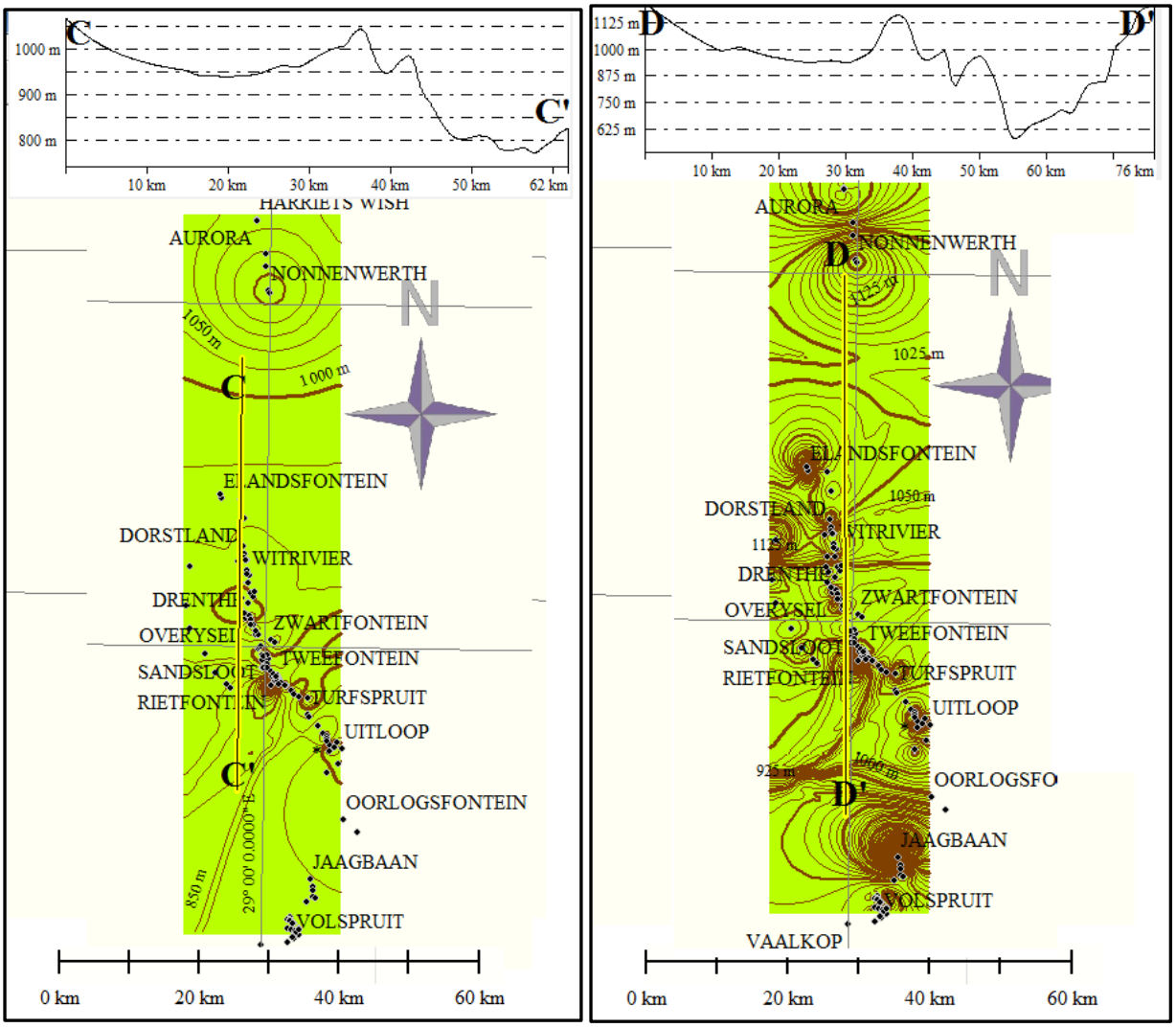

Figure 6.100: Profile C-C' on Platreef (A) and D-D' on Archaean floor rock (B) residual structure of Northern Bushveld Complex showing a horst structure in the central part (Contour interval 25 m).

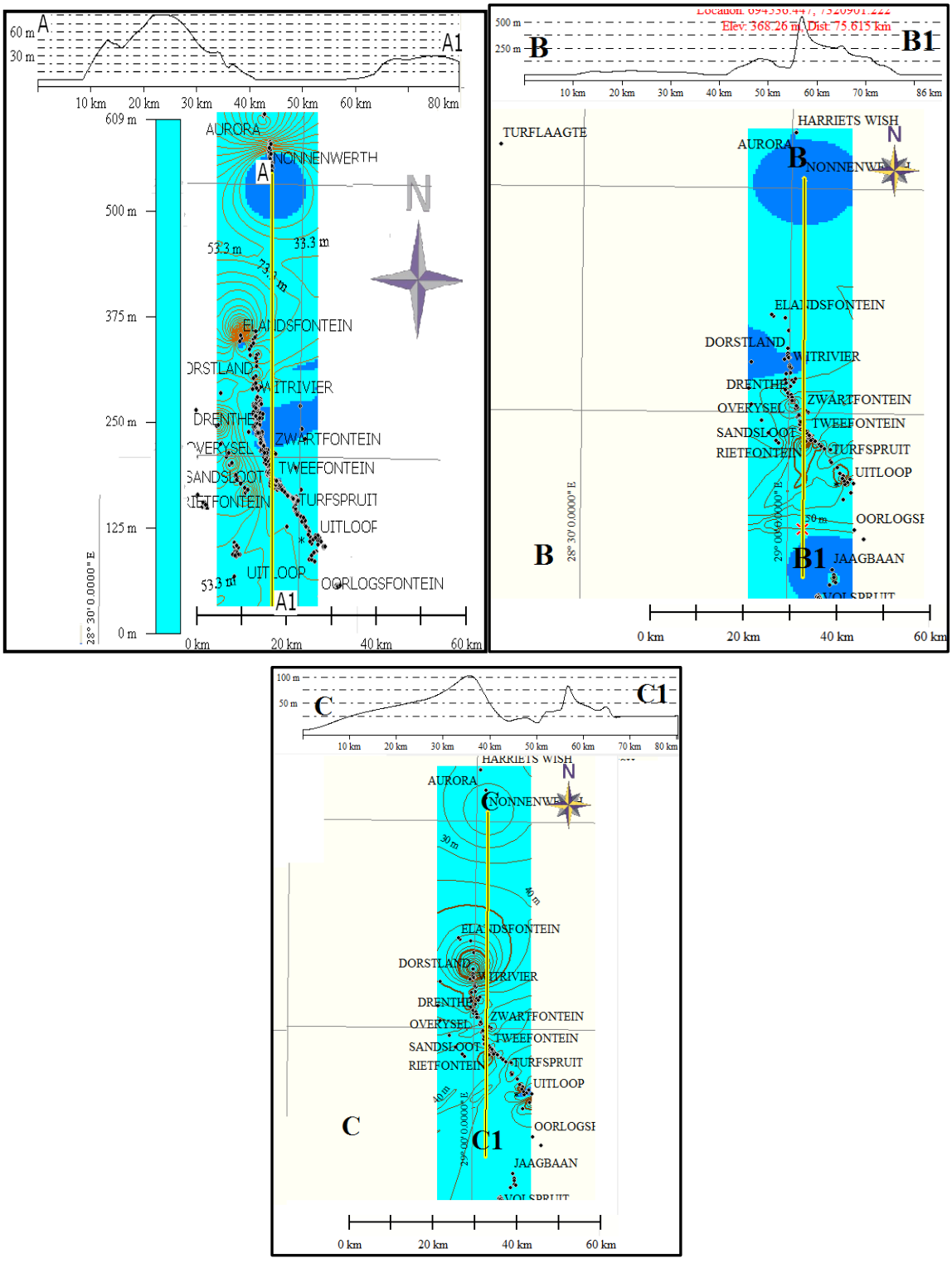

Figure 6.101: Profile A-A1 on the Upper Zone residual isopach (A), B-B1 on the Main Zone (B) and C-C1 on Platreef (C) residual isopach of the Northern Bushveld Complex showing a graben structure in the central part.

6.5.8 Discussion on Stratigraphic Top Structure Contour

The structural pattern from the top of the Upper Zone and the Main Zone top for most part of Western Bushveld Complex bear close similarities to one another. This suggests that there was no differential structural movement during deposition. However, the structure on top of the Main Zone differs from the structure at the base thus confirming some structural movements during the magmatic intrusion of the Main Zone and succeeding stratigraphic zones shows structural resemblance with the base of the Main Zone, indicating similar structural movement.

6.5.9 Summary

Patterns formed by structure contours at the base of the Archaean basement floor rock also reveal the influence of the floor rock on the morphology of the layered rocks. The geometry and thickness of RLS are also controlled by the presence of valleys and positive physiographic elements during its emplacement and can be attributed to alternating tension and compression (Uken, 1998; Holzer et al., 1999: Bumby et al., 1998 missing in the reference list). Faulting and up doming are more prominent in lower units of RLS (i.e. from the base of the Main Zone downwards) than reflected in the upper units such as the Upper Zone unit (Uken, 1998). The RLS is thick along deep-rooted valley systems that were scoured into pre-Bushveld rocks or the Transvaal sequence in which it is emplaced. The sill-like geometry of the RLS confirms the predominance of tensional stresses during early Bushveld times. Most parts of the RLS show inverse correlations between the structure in which it was emplace and thickness of the intrusion, this imply that most of the structures are pre or syn-Bushveld.

1. Most of the isopach maps in some parts of the RLS show thickening and thinning trends which coincides strongly with variation in structural grain (faulting) on the structure maps. Areas with positive thickening coincide with negative structural residual (structural lows, sags, troughs or synclines) areas. While positive structural residuals such as structural highs or anticline correspond to negative thickness residual.
2. Inverse relationship between structure elevation and thickness was used to discriminate between pre- and syn-Bushveld structures and relate the time sequence pattern of each stratigraphic unit). This signifies an inverse correlation between structure and isopach

trend surfaces. Hence indicating that most of the present day structures are intensification of structures in place before the RLS were emplaced and only slight modification has occurred since their emplacement.

3. Prominent tectonic features have been highlighted from the residual mapping of each of the stratigraphic units of RLS. Also by overlaying adjacent horizons and determining if the positive and negative areas coincide, relation between adjacent horizons was established.
4. The use of 3D path profile with trend surface interpolation methods for structural analysis has facilitated the detection of regional features and their subsurface geometry.
5. The Northern and Southern gaps of Northwestern Bushveld are associated with NW- SE trending fault along the gap area. The fault shows up as close contours on the structure contour for the Main Zone base and successive stratigraphic zone structure maps.
6. Two distinct structural domains were identified based on difference in structural features observed, the overlying stratigraphic zones down to the top of the Main Zone differs from the underlying stratigraphic zones. Structures at the surface from the Post Bushveld unit to the Upper Zone are very similar and differ from structural features at the base of the Main Zone through the critical zone to the Lower Zone. Except for the Brits graben area, that shows inverse correlation between structure and thickness on Post Bushveld unit indicating that Brits graben is probably Pre- or syn-Transvaal.

CHAPTER 7 FAULT IDENTIFICATION

7.1INTRODUCTION

Numerous faults were identified within the Rustenburg Layered Suite (RLS) of the Bushveld Complex. This is primarily due to extensive exploration for PGM and chrome within this economic suite, which has contributed immensely to knowledge about major and minor surface structures within the area. Information from mine plans has also permitted more detail mapping of some of these faults at a local scale. However, this chapter further revises some of the inferred faults that are inherent from previous interpretation of structure and isopach maps, strip log, 3D modelling and other analysis of borehole log data in the area. The purpose is for a credible interpretation of subsurface features to determine the nature and age relationship of faults and other features that might not be apparent at the surface, through the correlation of stratigraphic horizons and detail structural interpretation.

Structural investigations are restricted to the RLS units because of the paucity of borehole data that fully infiltrate beyond these units. Many of the borehole logs used provide lithostratigraphic information of horizons that can be correlated continuously across limbs of the Bushveld Complex.

7.2 FAULTS DETERMINED FROM PROFILES, STRUCTURE AND ISOPACH MAPS

Structural mapping was based on interpretation of structure contour maps, thickness variation, shaded relief, structural profiles (used to identify and measure offset in interval structure and isopach maps) and information about existing structural styles in the area. Attention was given to trends of closely spaced contours and undulations along structural contour surfaces. Integration of existing fault surfaces with interval structural contours and isopach maps at different horizons was carried out in order to better constrain the geometry of the underlying structure. Structural profiles drawn across stratigraphic interval structure contours were used to accurately depict the location of fault planes and to infer the

underlying geometry. 3D models were used to relate the displacement of stratigraphic units to its down-dipping direction along fault planes.

For the purpose of this study and to enhance detail investigation, each of the limbs will be subdivided into sections.

7.3 WESTERN BUSHVELD STRUCTURES

The structure at Amandelbult section trends NNW and shows many characteristics: The central part descends in a step-like manner with complete lithostratigraphic cycle (i.e. from the Main Zone layer to Lower Zone unit) on each of the steps as illustrated in Figure 3.6. The Upper Zone and the Main Zone structural contours show the same NNW trend in the northern part and the southern part. However, it only shows close similarity in the western side of the central region where the trend is NE, while the eastern part shows contrasting trend as illustrated in Figures 4.1 and 4.2. This indicates that the NNW structural trend might be younger than the NE trend since the latter is more prominent on the lower unit (from the Main Zone base to the Lower Zone unit). This structure coincides with the Roodedam Graben and it is located at the NE part in the northwestern Bushveld Complex. Figure 3.7 shows the section with selected borehole logs of the area.The strip log shows selected borehole sections of the area; the deep penetrating boreholes coinciding with the central depression (graben) while the short boreholes at the sides represent the horst. The bounding fault seems to be closer at the north and widens southward. This graben structure is probably pre-Bushveld since the structural contours and the isopach maps indicate an inverse relationship showing that the structure was already in place before the influx of the magma, but might have been reactivated or modified by the magma addition.

Maximum displacement (from the Main Zone interval) on the eastern side of the graben is about 500 m and is slightly more than the 400 m displacement on the western side. The structure extends horizontally over a distance of approximately 22 km. The present day uplifted section is the southern part of the Amandelbult section where the Main Zone is more preserved with a thickness of over 2200 m based on available borehole record. Undulations around this area are typically aligned NE. Figure 7.1 shows the upthrow and

downthrow side of inferred faults around the Amandelbult area using the isopach map (note that on the structural map the downthrow sides coincide with upthrows and vice versa).

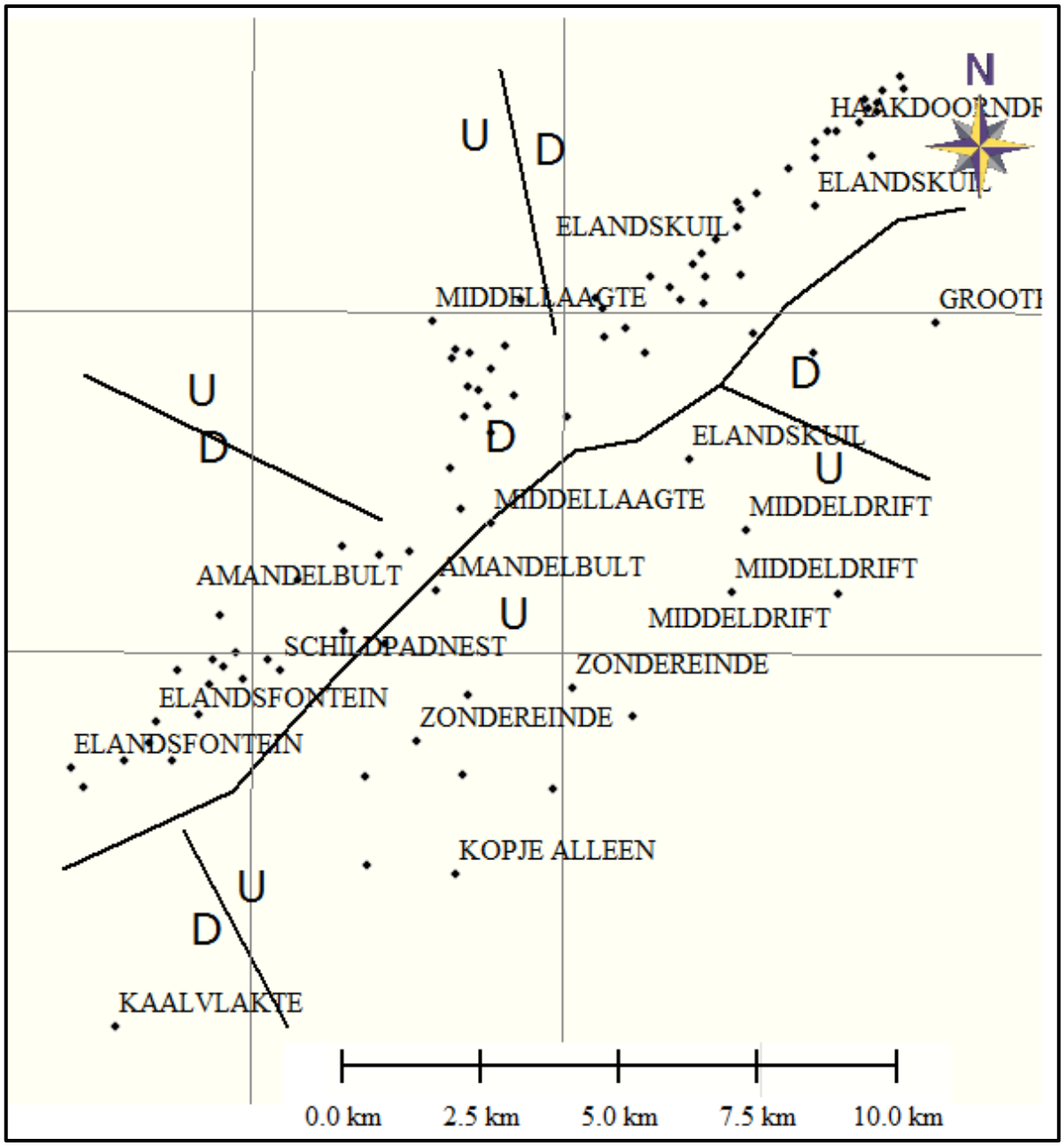

Figure 7.1: Inferred fault planes extracted from the Main Zone isopach map of the Amandelbult section of the Northwestern Bushveld Complex showing the upthrow side indicated as U, and downthrown side indicated as D along the major fault zones.

Two NNW trending faults were inferred in the central part of the Northwestern Bushveld Complex. The first one coincides with the Northern gap area while the second coincides with the Southern gap area. Centrally located L-shaped isoclines on the Main Zone isopach map may also represent strike slip faulting (Paulson and Peascatore, 1979). A profile across the Upper Zone isopach map indicates a central upthrow and a gradual downthrow to the east around the Northern gap area, while the Southern gap area shows a sharp downthrow to the west on the Main Zone isopach map (see Figure 4.12). This central part is marked by central thickening with thinning to the east and west on the Upper Zone isopach map. However, the thickening trend is eastward on the Main Zone isopach map and underlying stratigraphic units, with a possible fault plane (indicated by closely spaced parallel isoclines which represent a rapid decrease in thickening trend with steepening in structural gradient) separating the Amandelbult section from the Union section of the Northwestern Bushveld Complex. These closely spaced isoclines coincide with the Northern gap area and shows up distinctly on all the isopach maps from the Upper Zone down to the Lower Zone. The Southern gap also coincides with closely spaced parallel contours on the Upper Zone and the Main Zone isopach maps, but it is less pronounced in underlying units.

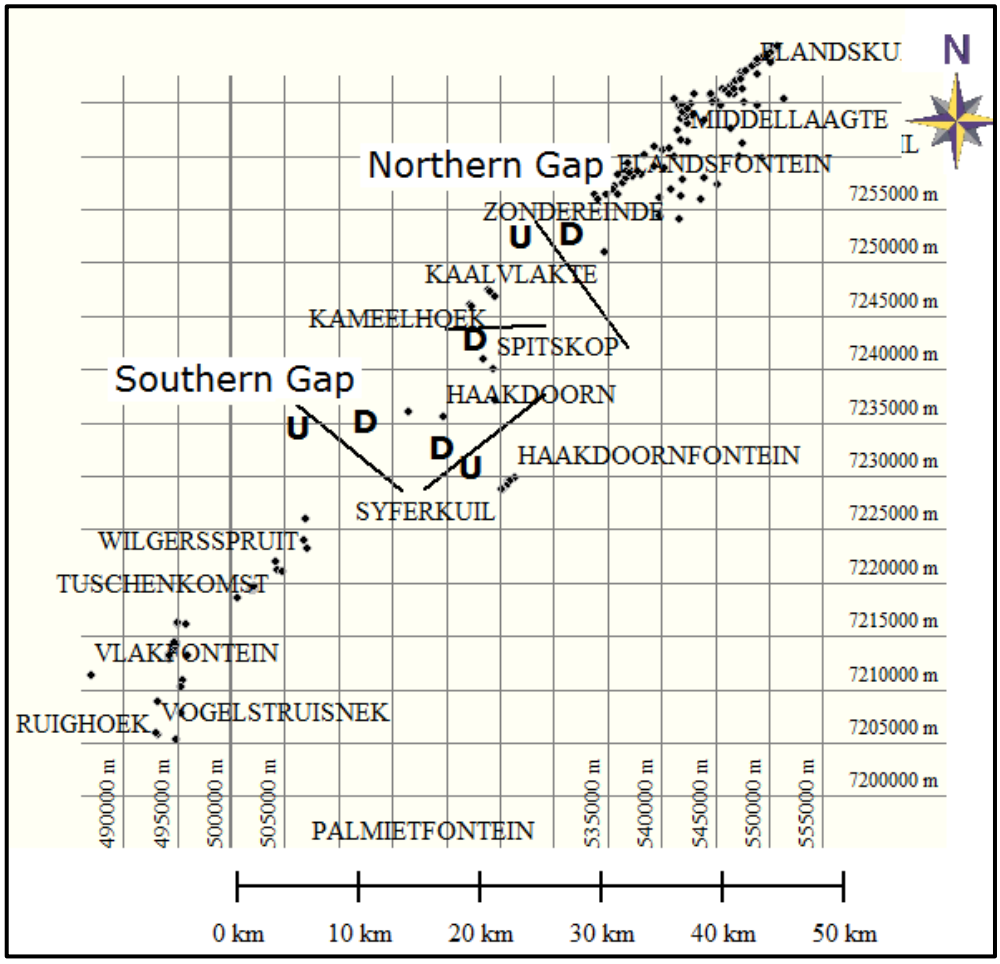

Figure 7.2: Map showing the NNW trending faults along northern and Southern gap areas of the Northwestern Bushveld Complex, the NE trending fault around the Union section and the E-W trending fault in the northern part of the Union section same remarks as previously

The Pilanesberg Complex is located almost midway between the Western Bushveld Complex where it forms a circular shape as indicated in Figure 7.3. The southern part of the Pilanesberg Complex is marked by NNW-SSE trending isopach lines which are parallel to the trend of the Rustenburg Fault. The western part of the fault is made up of a NNW trending narrow structural high that dips towards the centre. The Complex is fault bounded thus displacing the other units sideways. The NNW trending fault is located between the Profile B-B1 in Figure 7.4. On the Upper Zone isopach map the eastern part of the NNW trending forms a structural high that descends to the centre.

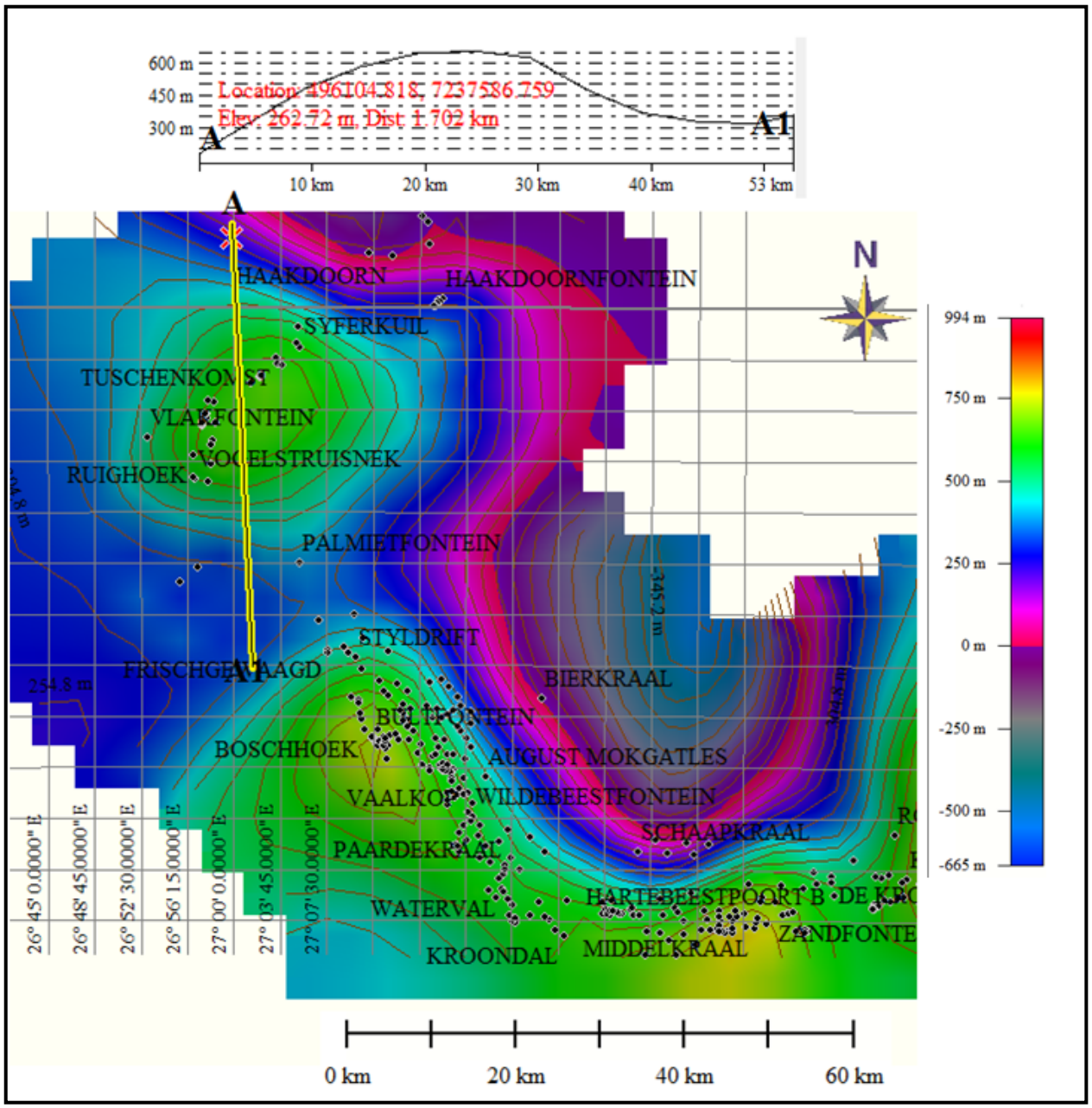

Figure 7.3: Illustrating the circular shape of the Pilanesberg Complex in relation with other parts of the Western Bushveld Complex at depth (I suppose depths are the same as in Fig. 7.4).

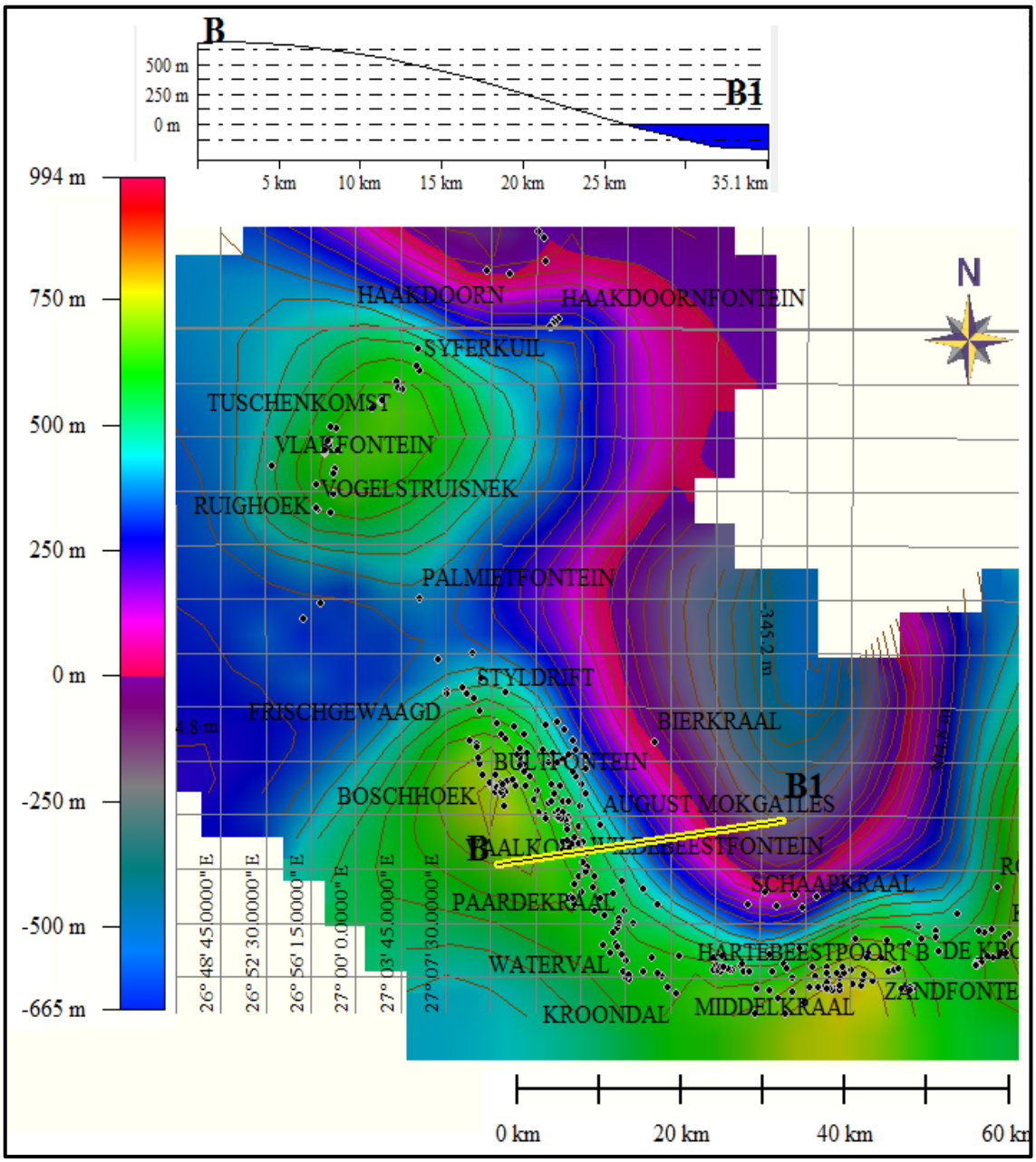

Figure 7.4: Profile B-B1 drawn across the NNW-SSE trending isoclines parallel to the trend of the Rustenburg Fault showing the central dipping from the west.

NNW trending faults around the Brits area on both the structural and isopach maps dominate the southwestern part of the Bushveld Complex. Most of these structures are aligned in a NE trend relative to each other (as indicated in Figure 6.29). The Main Zone base residual structure reveals the presence of two graben-like structures in the western part of the Southwestern Bushveld around Schaapkraal farm. These two structures are separated by an anticlinal structure or structural high of over 1000 m higher than

downthrown sides which coincides with the graben structures. Another graben-like structure occurs in the southeast around the Krokodildrift farm with a downthrow of about 400 m at the centre of the graben and flanked by two opposite dipping faults, a NNW trending fault on the western part and a NE trending fault at the eastern part. A smaller graben-like structure is located in the southeastern section of this area.

A NNW trending fault can be inferred on the Hartebeestpoort C farm. This fault shows a downthrow of more than 1200 m in the southeast. The residual isopach and structural maps indicate an inverse relationship indicating that the present day structure grew from an already existing structure. The Lower Zone structure contour shows more NNW trending structures than the Main Zone, also more graben-like structures other than the Brits graben occur in this sector. There is thickening on the downthrown side and thinning on the upthrow side. Figure 7.5 illustrates the spatial distribution of some boreholes in the Southwestern Bushveld, with boreholes on the western side much deeper than those in the eastern side. The borehole logs on the western side show stratigraphic thickening and gradual thinning eastwards. Figure 7.6 shows the upthrow and downthrow sides of inferred faults extracted from structural contour and residual maps of the Southwestern Bushveld.

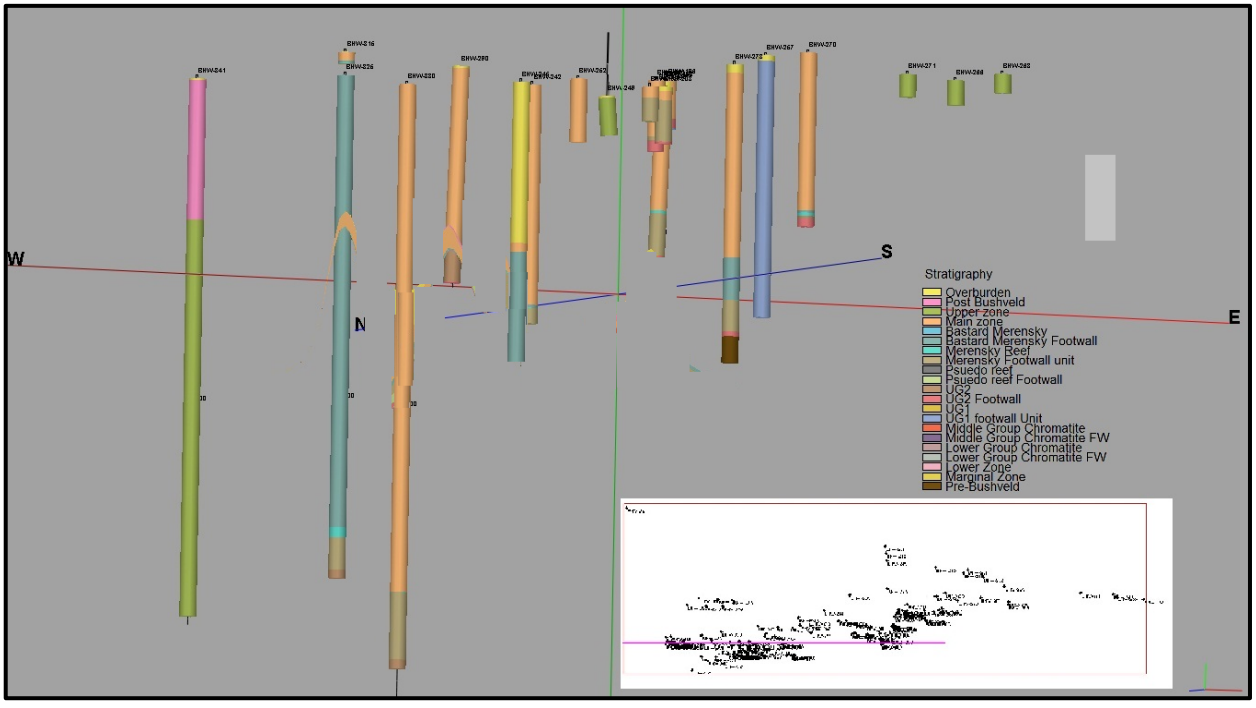

Figure 7.5: Multi-strip log from west to east of the Southwestern Bushveld.

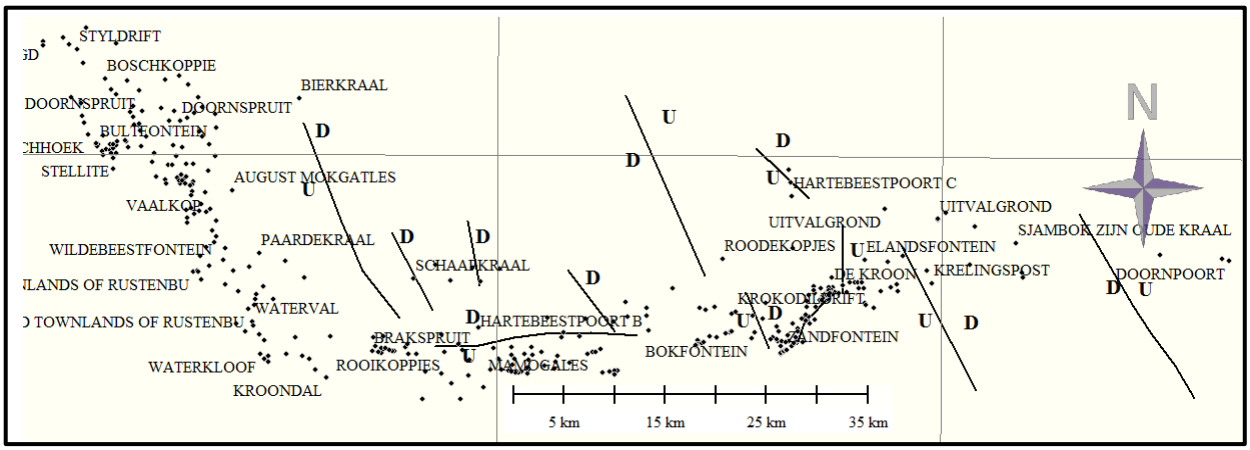

Figure 7.6: Diagram showing all the inferred faults with the upthrow and downthrow sides extracted from the structure and residual maps of the Southwestern Bushveld

7.4 THE EASTERN BUSHVELD STRUCTURES

The Eastern Bushveld Complex is marked by complex undulation caused primarily by faulting and doming in the floor rock. Major faults such as the Wonderkop Fault, Stoffpoort Fault, the Sekhukhune Fault Zone, Laersdrift Fault and the Steelpoort Fault are all indicated in varying degrees on the isopach and structural contour maps as well as the strip log.

A couple of faults were inferred from closely spaced structure contours, variation in thickness across the inferred faults at different stratigraphic horizons and sharp slope on profiles drawn across the inferred fault plane. The extreme western side of the Northeastern Bushveld Complex hosts a number of faults. The western side and south of Zebediela, a NNE-SSW striking fault parallel to the Wonderkop Fault can be inferred, another fault which coincides with the Stoffpoort Fault occurs at the eastern side of the Wonderkop Fault. An additional fault can be inferred at the eastern end of the Fortdraai Anticline; this fault separates the anticline from the eastward downthrown side. On the structure contour map, the eastern part of the Fortdraai Anticline in the northeastern Bushveld is flanked by a synclinal structure or depression of about 2000 m deep. The eastern boundary of the depression coincides with Sekhukhune Fault zone.

A profile across the eastern edge of the Fortdraai Anticline and the Eeste Regt structural low area also suggests a fault with displacement to the east as indicated in Figure 7.7. Further northeastward around Kalkloof Dome, a fault is proposed based on a combination of structure, isopach and profile interpretation (see in Figure 7.7). This fault also indicates a downthrow to the east. The extreme eastern fault coincides with the Sekhukhune Fault Zone. The location of these faults coincides with known faults in the area and most of the faults have NNE-SSW trend with downthrow to the east except for the Sekhukhune Fault with downthrow to the west. The throw on each fault varies from 150m to 2 km across the stratigraphic units. The Sekhukhune Faults trends almost N-S and has a maximum throw of about 2 km, east of the Fortdraai Anticline. The fault around Kalkloof Dome and the one at the eastern edge of Fortdraai Anticline are not indicated on the geological map.

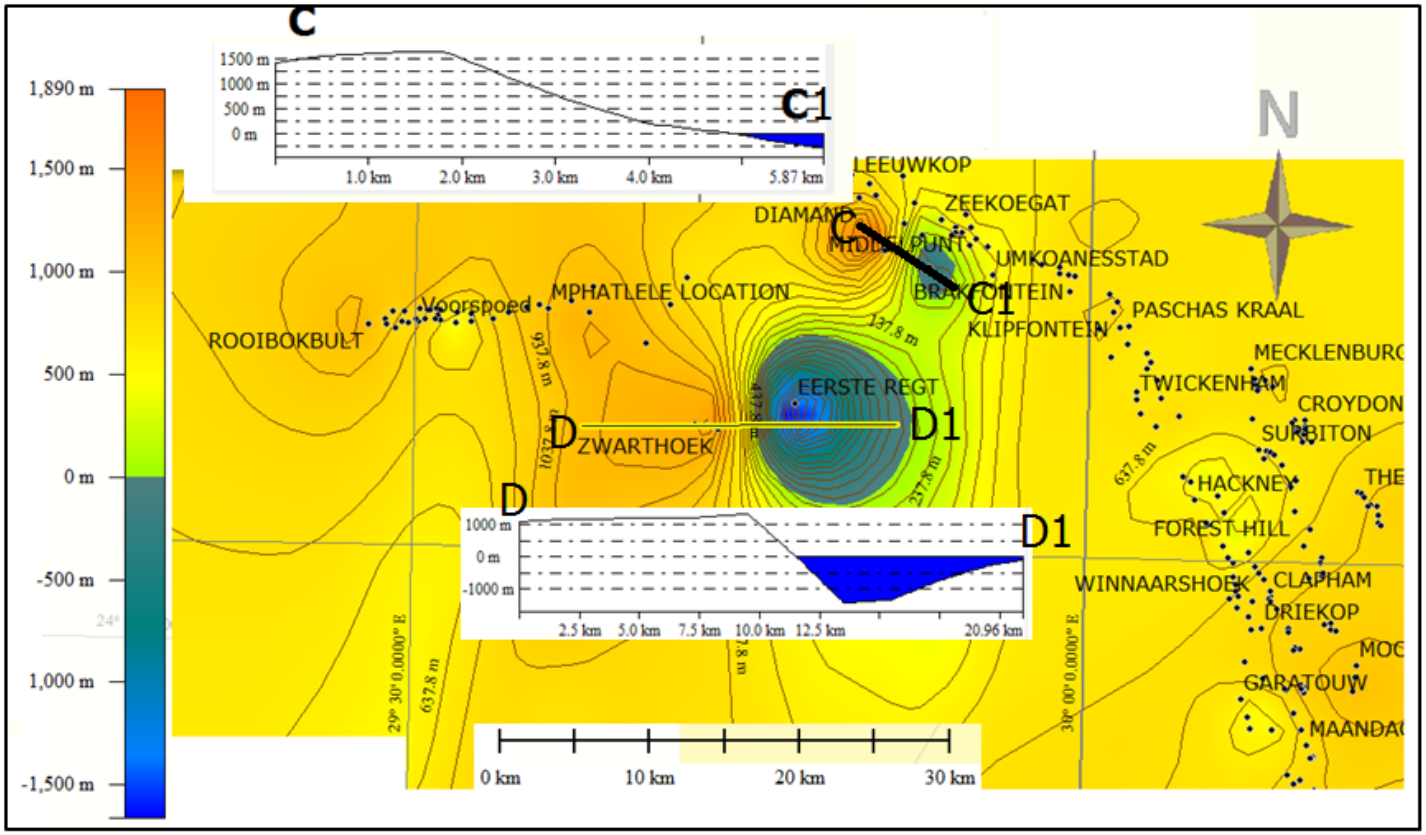

Figure 7.7: Structural contour map of the Northeastern Bushveld Complex showing Profile (C-C1) along Kalkloof Dome and adjacent structural low area and profile (D-D1) across the Fortdraai Anticline and adjacent depression at Eerste Regt.

Both Kalkloof Dome and the Fortdraai Anticline show inverse structures and thickness relationship while the Eerste Regt area exhibits similar relationships between structure and thickness on both the Main Zone and the Upper Zone.

The central part of the Eastern Bushveld Complex is marked by east-west trending faults in the centre and around the western side. The eastern side is made up of a pair of slightly curved faults with downthrow to the west (i.e. to the centre). Two sets of E-W striking parallel faults could be inferred in the central part of Eastern Bushveld section; the northern E-W parallel fault dips to the south while the one at the south dips to the north thus creating a synclinal structure or depression in the central part of the limb. Thickness of stratigraphic units across the fault changed from northward thinning to thickening towards the southwest. The Main Zone thickness variation across the northern and southern part of the Steelpoort Fault indicate (dextral) lateral movement of the southern unit to the west and the northern portion to the east thus indicating about 3.3 km right-lateral movement of the unit and a gap around the Kennedy's Vale as indicated in Figure 7.8. This provides an evidence for a syn-Bushveld Complex movement along the Steelpoort Fault and possibly a reactivation of this fault from an earlier fault, contrary to Uken (1998).

A NNW trending fault could be inferred around the southeastern portion of the Eastern Bushveld (Figure 7.9); it extends from Kalkfontein farm southwards to the Klip River valley area. The thickness of the Main Zone varies across the fault as indicated by closely spaced structural contours with a downthrow to the west. The Main Zone rocks exhibit a westward thickening trend around the valley area while the same unit thins out eastwards towards the structural high. The Upper Zone unit in the area also exhibits an inverse thickening and thinning trend thus indicating an inverse relationship between the structure and thickness, i.e. the structure was already in-place before the influx of the RLS rocks.

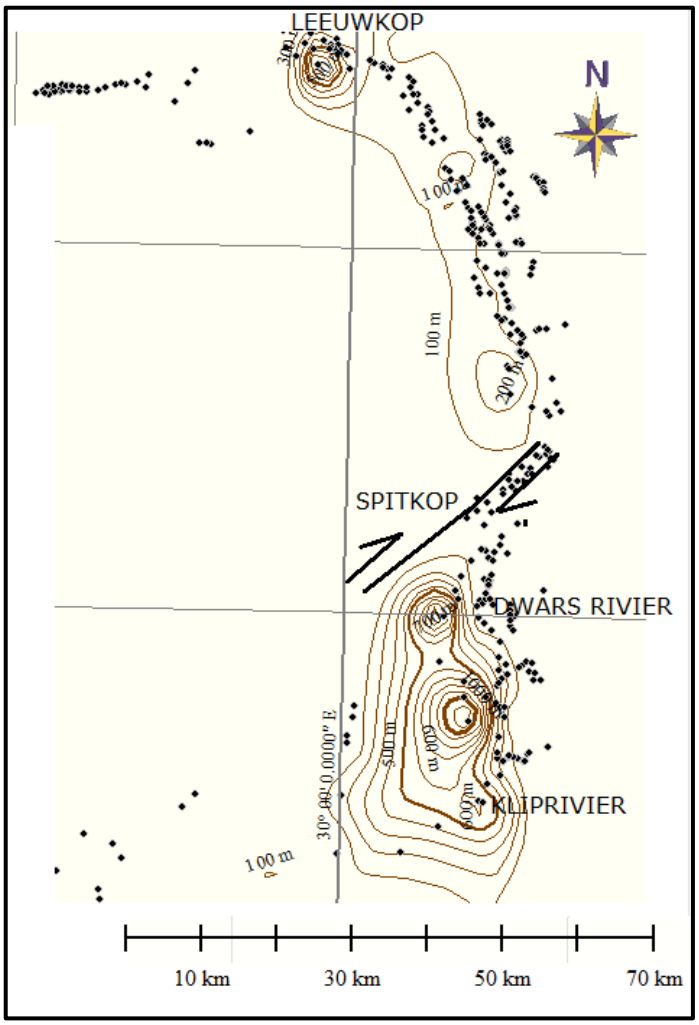

Figure 7.8: The Main Zone fourth order isopach poly trend of the Eastern Bushveld showing a gap and right lateral movement between the northern part and the southern parts and the thickness variation of the Main Zone rocks across the Steelpoort Fault.

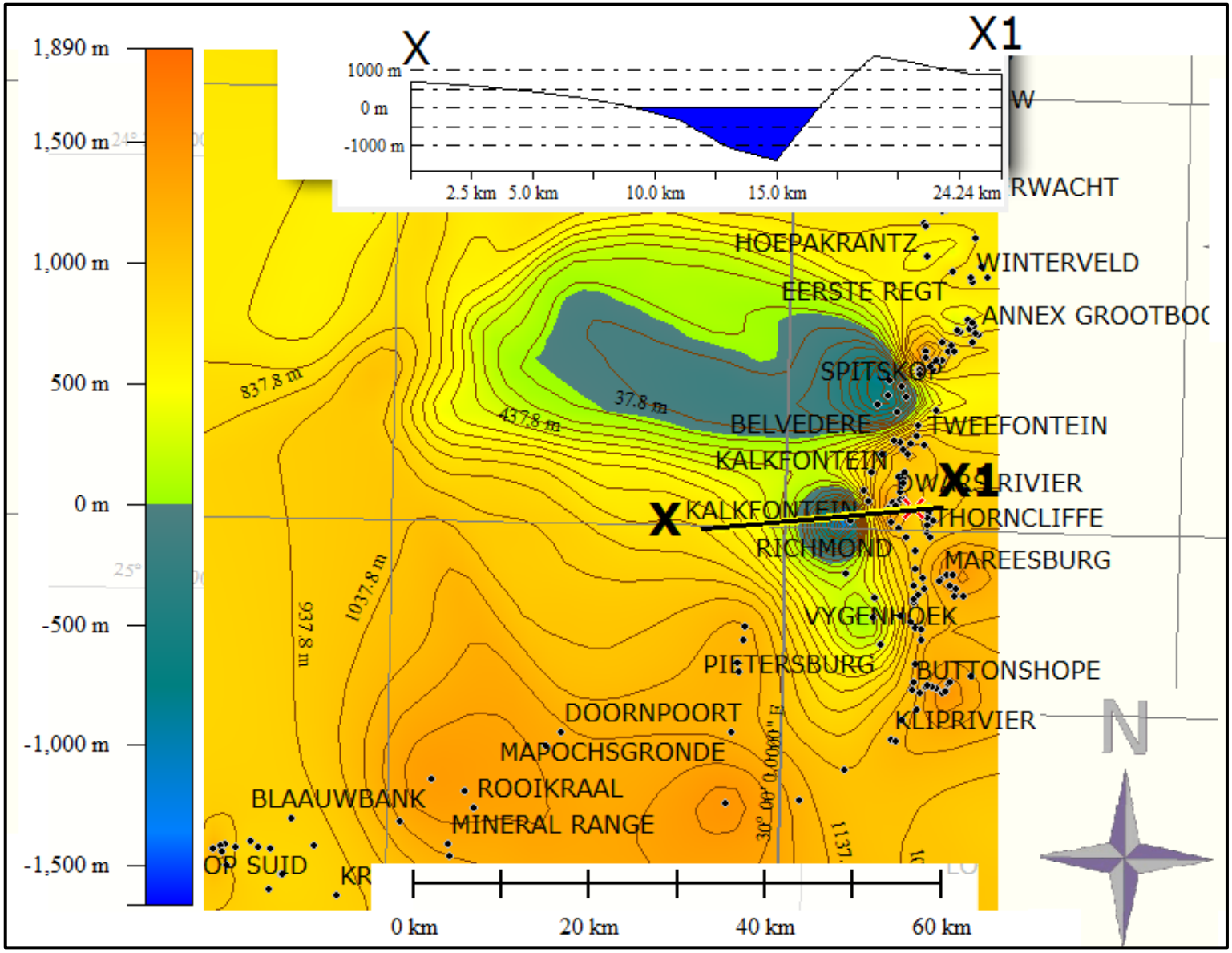

Figure 7.9: Profile across an inferred fault around Kalkfontein farm in the Southeastern Bushveld.

An additional NNW trending fault occurs around the northwestern part of Laersdrift Fault and seems to be a northwestern extension of the Laersdrift Fault. The fault extends northwards and terminates against an east-west trending fault at the centre of the limb. The map in Figure 7.10 shows the trend of the inferred faults with the upthrow and downthrow sides. Most of the faults in the Northeastern Bushveld trend NE with downthrow to the east while a few trend NNW.

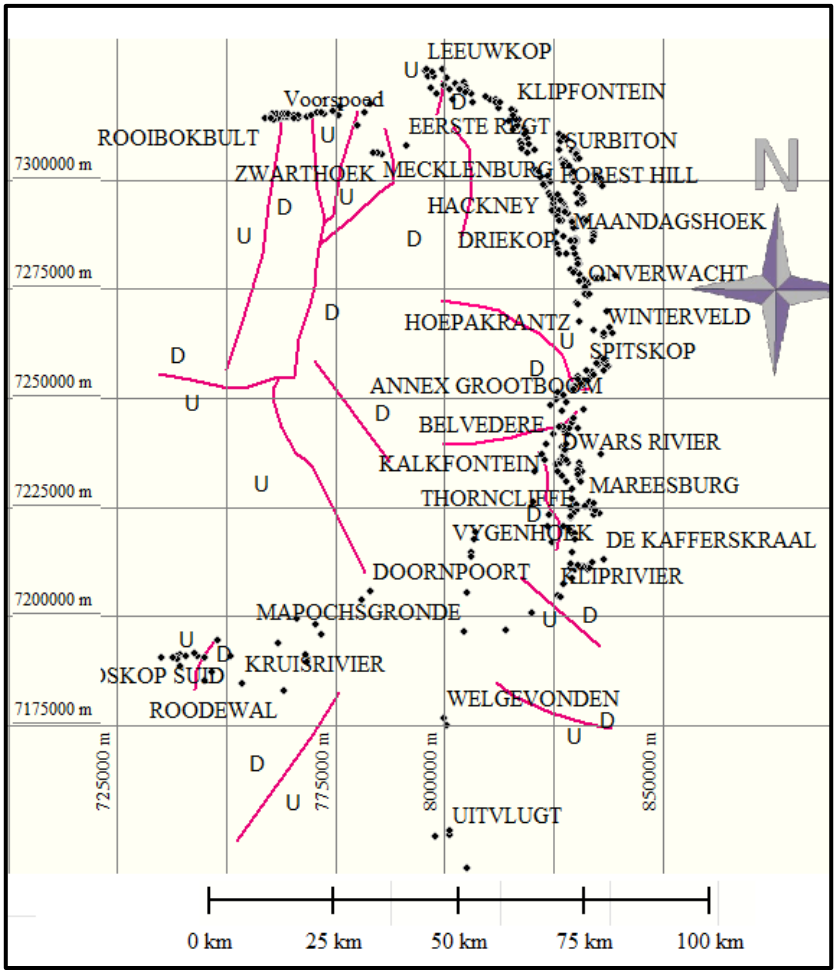

Figure 7.10: Diagram showing some of the inferred faults in the Eastern Bushveld Complex extracted from both the structure contour maps and the isopach maps.

7.5 NORTHERN BUSHVELD STRUCTURES

The far northern part of Potgietersrus limb or the Northern Bushveld slopes down sharply with a downthrow to the north, suggesting a NE trending fault between Aurora farm and

Nonnenwerth farm. Further northward toward the terminal edge of the limb, a NW striking fault can be inferred between Harriet farm and Aurora farm. This fault has a downthrow of approximately 120 m to the SW.

Around Elandsfontein farm in the north central part of the Northern Bushveld Complex a series of NE to ENE striking faults were inferred at different horizons. On the Archaean floor contour map the inferred faults trend ENE while on the Marginal Zone and the Main Zone interval it strikes NE with downthrow to the NW. Further southeast, similar faults occur between Dorstland and Witrivier farms with downthrow to the north on Drenthe farm. At the southern parts of Overysel two sets of faults can be inferred: the first set is E-W trending faults while the other exhibits NE trend with downthrow to the south. NNW striking faults with downthrow to the SW can be inferred at the separation point between the Tweefontein Hill and the adjacent valley on Rietfontein farm. This valley is present on the Archaean floor structural interval and shows thick deposits of RLS rocks, suggesting that the structure was already in place before the RLS rocks were deposited on it. Other N-S trending faults were inferred at the northwestern part of the Turfspruit farm with upthrow to the east of Tweefontein farm.

Uitloop farm in the southeastern extreme of the Northern Bushveld hosts a slightly curved NE striking fault which appears on all the stratigraphic unit interval maps with the upthrow side in the southeast. A different E-W striking fault that separates the central part of the Complex from the southern part can be inferred at the southern part of Uitloop farm. This fault is joined to another fault elongated to the NE and parallel to the Ysterberg-Planknek Fault. This NE-trending fault displays an upthrow to the east at its northern edge and west at the southern edge.

The western part of the central northern Bushveld displays a SE trending rolling surface while the central part defines an irregular horst structure. The eastern part of Grasvally structure is marked by NNW-SSE trending structures contours while the Upper Zone and the Main Zone isopach maps exhibit a northward thickening truncated southwards by an E-W striking fault with a downthrow to the north. However, the Lower Zone isopach map exhibits southwards thickening modified around Volspruit farm by a fault which trends

NW with downthrow to the NE. The trend of this fault coincides with that of the Potgietersrus and Pruizen Faults. The Archaean floor also exhibits downthrow to the SE around Grasvally structure with an ENE trending fault.

This aspect of the thesis has been able to highlight faults constrained from an interval structure and isopach maps that bear credence to the existence of some previously identified faults and their geometry at the subsurface. Figures 7.11 to 7.14 indicate the strip log and sections while Figure 7.15 shows the inferred faults around the Northern Bushveld Complex.

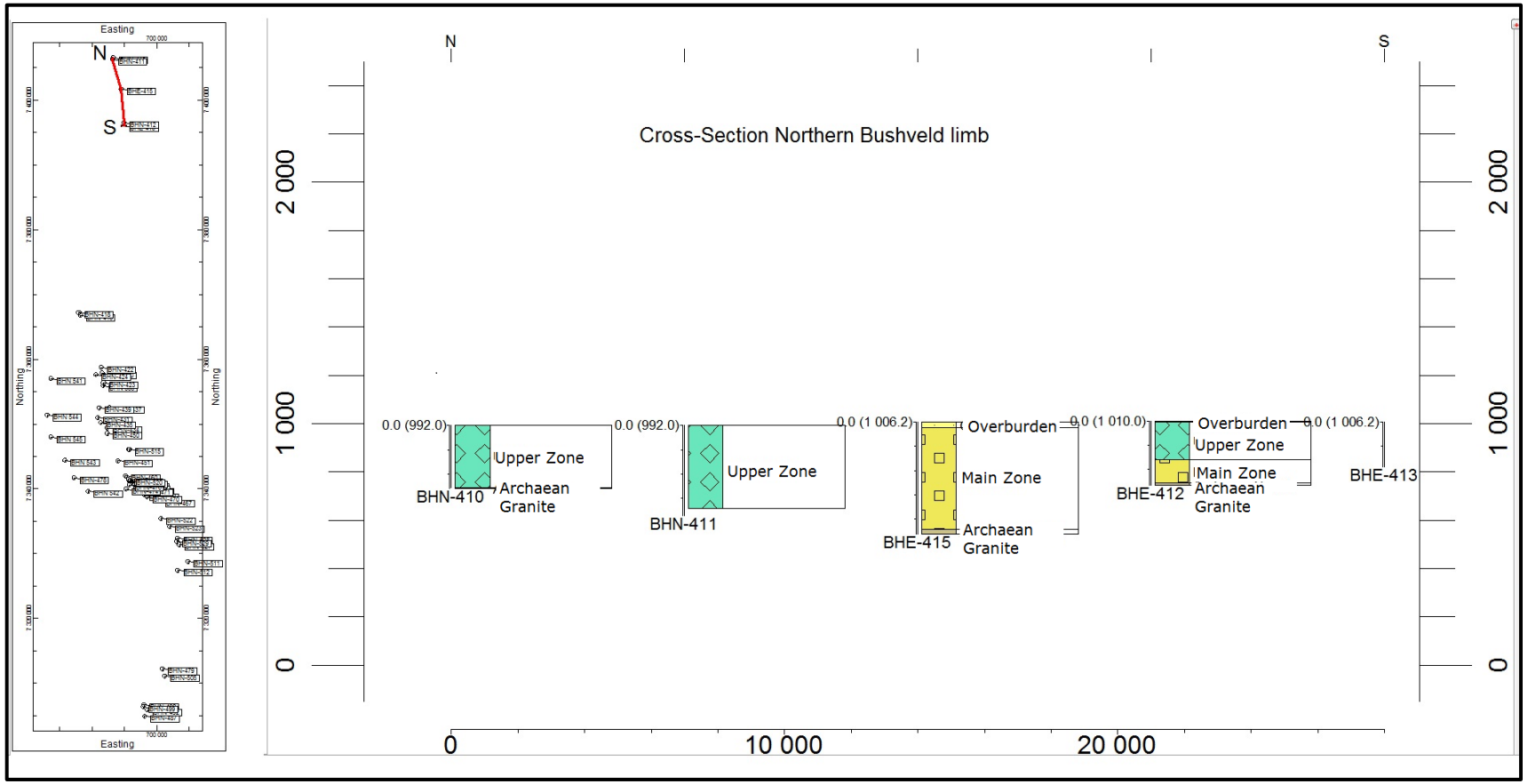

Figure 7.11: Strip log section of part of the Northern Bushveld Complex.The units are indicated beside each of the strip-logs

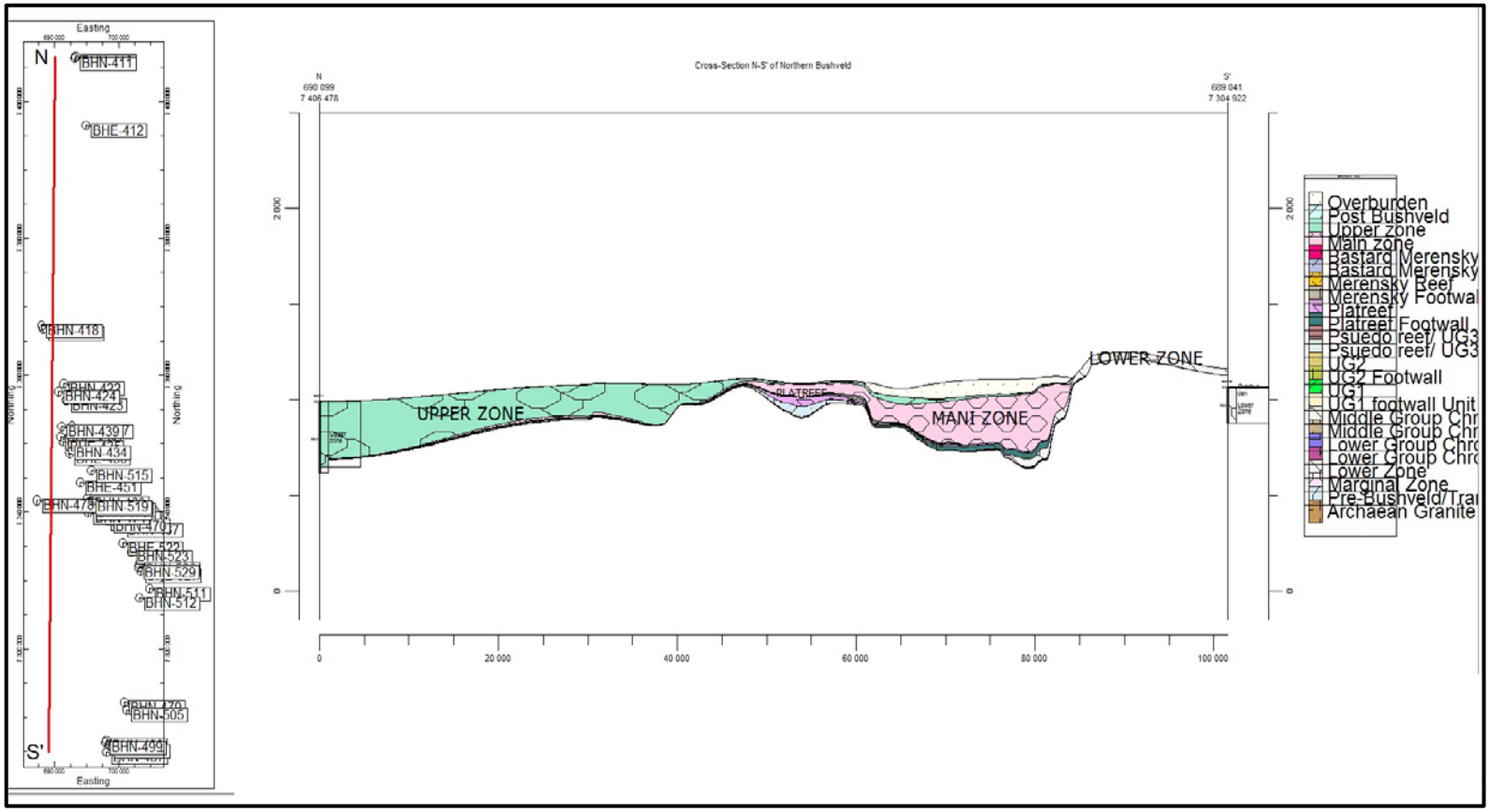

Figure 7.12: N-S cross section of western part of the Northern Bushveld Complex.

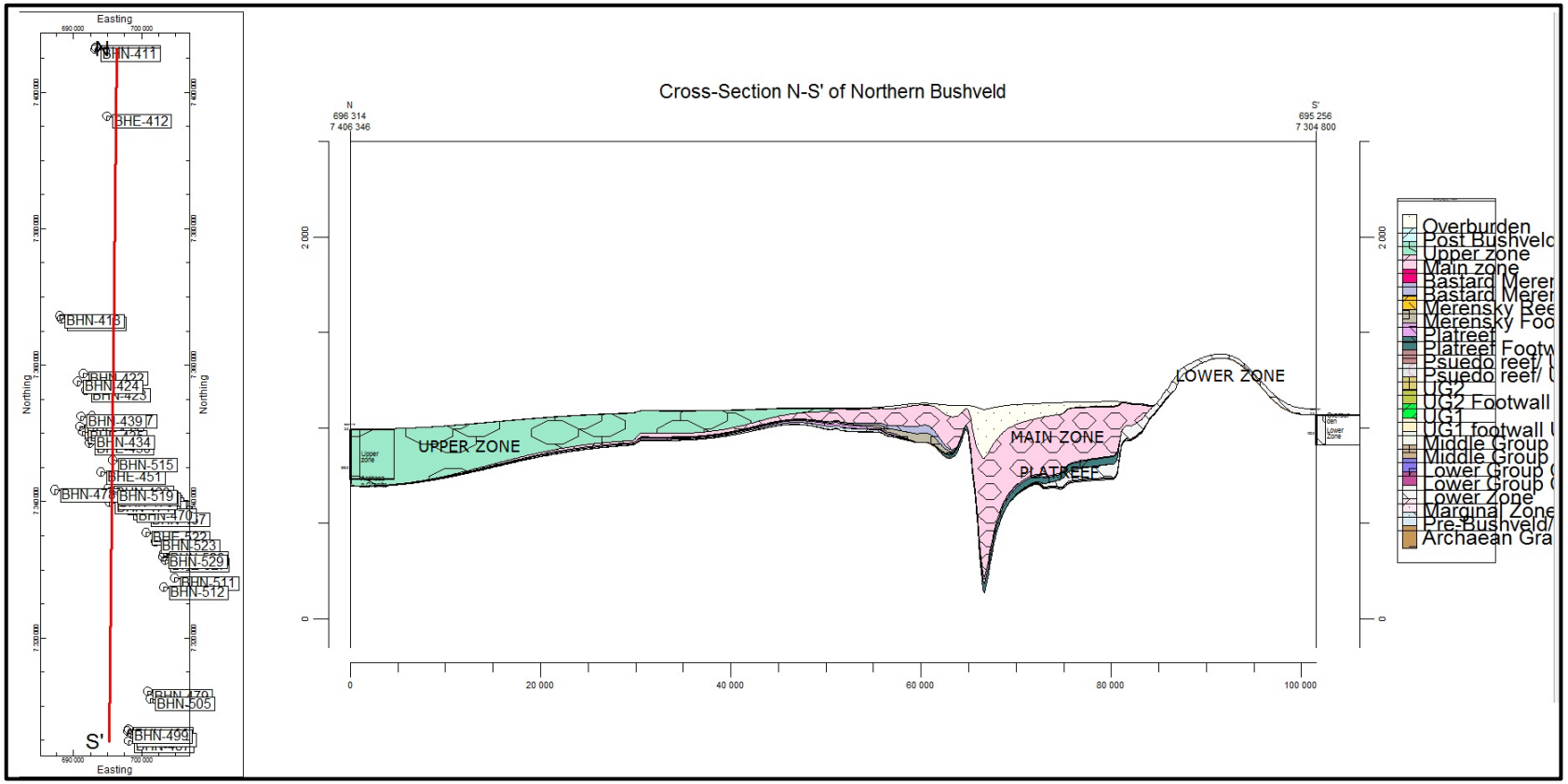

Figure 7.13: N-S central cross section of the Northern Bushveld Complex

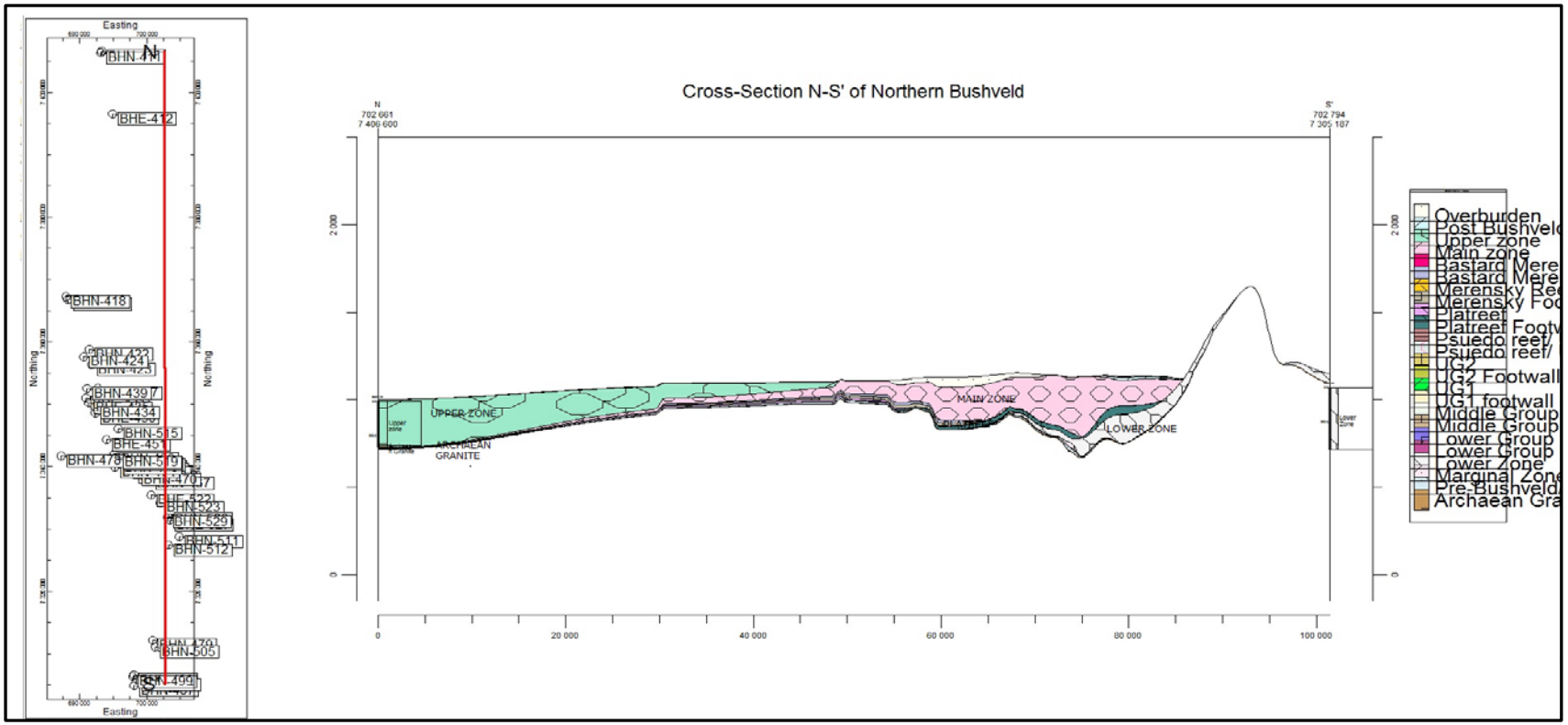

Figure 7.14: N-S cross section of eastern parts of the Northern Bushveld Complex.

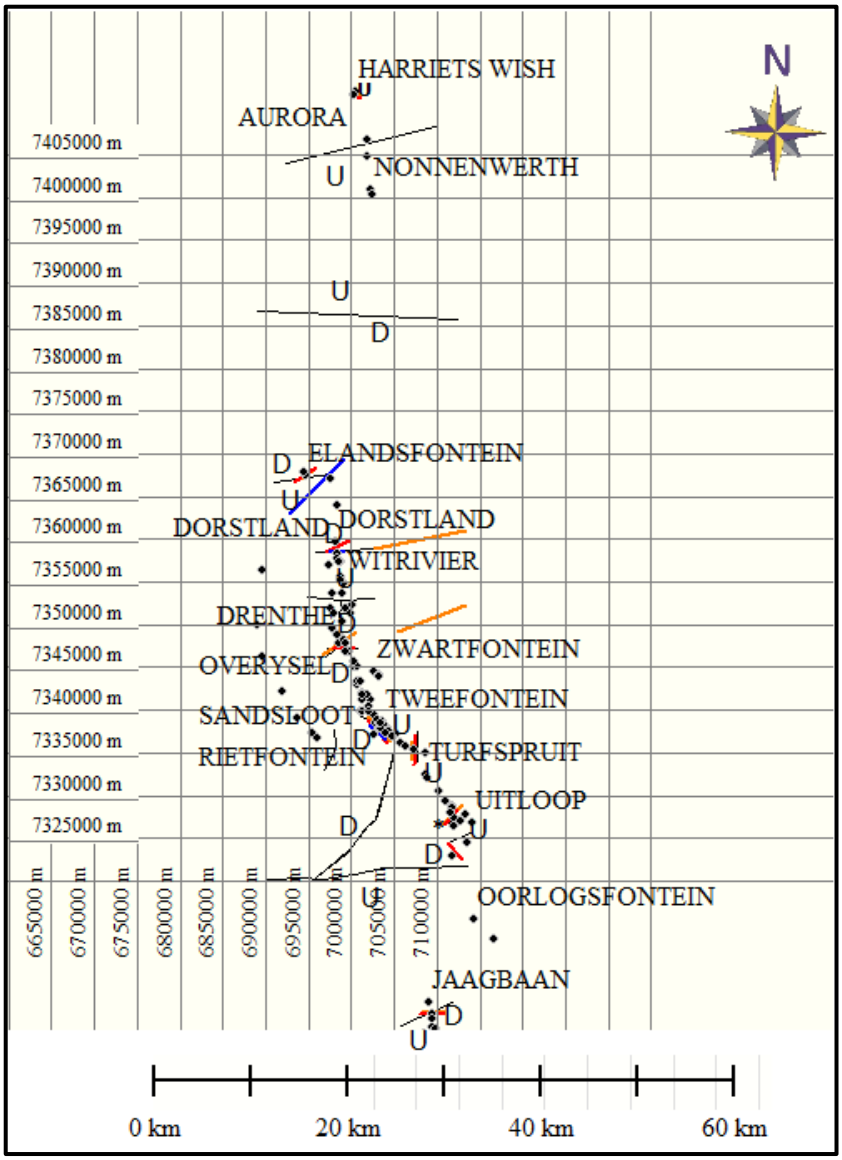

Figure 7.15: Diagram showing the upthrow and down throw part of inferred faults within the Northern Bushveld Complex. The inferred faults were extracted from both interval structure and isopach maps of the area; hence the difference in colour

CHAPTER 8 THREE-DIMENSIONAL GEOMETRY OF RUSTENBURG LAYERED SUITE

8.1 INTRODUCTION

The Rustenburg Layered Suite (RLS) occurs as a sill between the overlying volcanic mass of Rooiberg felsites and Rashoop GranophyreSuite and the underlying Transvaal Supergroup rocks at shallow depths (Kinnaird, 2005). Three-dimensional models at each stratigraphic interval is presented here to enhance the understanding of the geometry of the Rustenburg Layered Suite (RLS) and to constrain the mode of emplacement on a large-scale. It has been discovered from recent studies that the 3-dimensional geometry of rocks can be used to explain the shape and contact relationship of rocks (Bayer and Dooley, 1990; Rosenberg and Handy, 2005; Hogan et. al., 1998; Ameglio and Vigneresse, 1999). Field observation alone might not be adequate to delineate an accurate 3Dmodel (Ameglio and Vigneresse, 1999). 3D models of sheet-like intrusion have been found to be significant in the study of volcanology and hazard management (Auger et al., 2001), underground water monitoring (Zhou et al,2007; Kresic, 2006), climate change (Sheppard, 2005; Koca et al.,2006; Svensen et al., 2007), resource evaluation (Groves et al., 2000; Aarnes et al., 2011), magma emplacement and geometry (Gudmundsson et al.,2009; Galindo and Gudmundsson, 2012; Skytta et al., 2013).

The geometry of the BIC was first described as a lopolith by Hall (1932). Further probe into the geometry revealed funnel-shaped intrusions (Wilson, 1956;Willemse, 1964; Wager and Brown, 1967). Roberts et al. (2007) proposed sills of horizontal to sub-horizontal geometry that transgresses into underlying floor rocks. Both geophysical investigation and other studies were corporated to describe the actual geometry of the BIC (Kruger,2005b and references therein). Major hindrance to this has been the small piece

nature of the investigation. This chapter provides a synoptic evidence of the shape of the BIC with special reference to the RLS.

Subsurface features are most accurately illustrated with 3D models, however, strip log sections and fence diagrams are also used to illustrate the disposition of borehole cores for easy understanding of subsurface lithologic and stratigraphic layout. A 3D model is created from borehole log, orientation data and depth information of each stratigraphic top and base. Different interpolation methods such as - Kriging, Trend Surface Analysis (TSA) and Inverse Distance Weighing (IDW) were employed to create a continuous surface from space borehole data.

8.2 3D MODELS OF WESTERN BUSHVELD COMPLEX

Figure 8.1 reveals the surface geometry of the RLS in the Western Bushveld Complex. The figure shows the elevated rim and the general central dipping nature of the RLS rocks. It also indicates shallowing toward the Amandelbult section and the central dipping at this section. The surface geometry is rather smoother than the floor. The floor to the RLS probably reveals the nature of the underlying floor rock with pipe-like features, irregular undulations, step-like down dipping and doming in some parts while some parts are sill-like. Step-like and down-diping geometry is prominent at Amandelbult section and this enhanced the volume of magma deposit in the area (the step-like geometry could have acted as “trap” for the magma). Huge deposit of magma in this area might also signify closeness to the magma source. It is assumed that towards the end of magma expulsion, most of the magma would be deposited close to the magma chamber. Southward dipping of this area might have influenced the magma transport direction. Tectonic changes such as sinking and/or rotations about inclined axes might have also influenced the formation. This structure is most probably pre-Bushveld since the structure and thickness of RLS are inverse. If the down dip circular features shown in Figure 4.6 can be attributed to the presence of potholes in this area, then pothole structures can be described as structural features.The area around the Pilanesberg Complex shows subsidence and faulting of the RLS rocks especially at the subsurface while at the surface it reveals a circular geometry. Figures 8.2 and 8.3 show the geometry of the Western Bushveld compartment as

continuous layers with overburden.Figure 8.4 reveals the geometry of the same area without the thin zones.

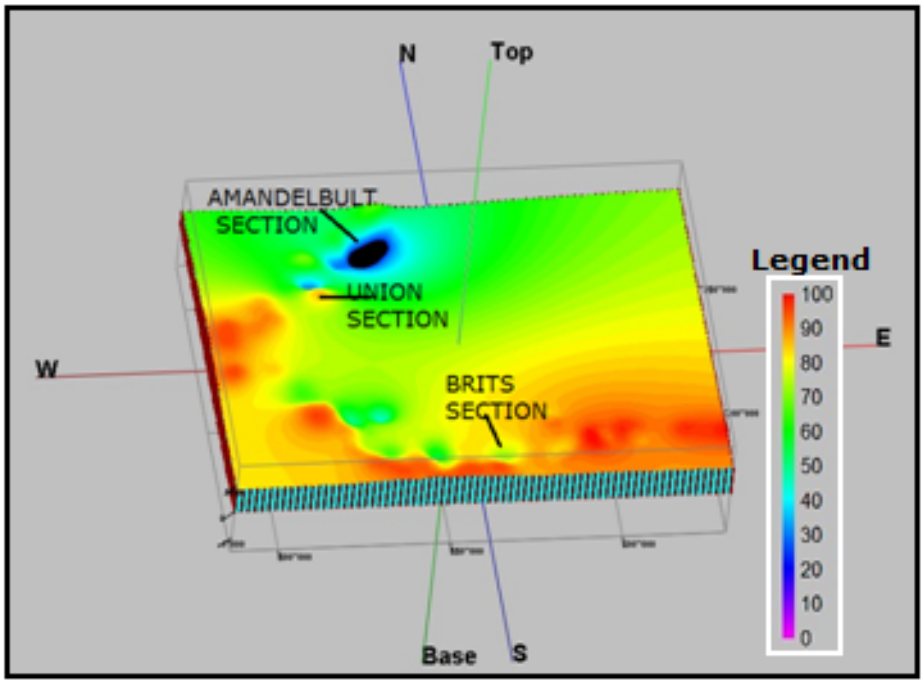

Figure 8.1: The Main Zone of Western Bushveld display uplifted rim dipping to the centre. The extreme northeastern edge is very shallow while the southwestern edge is uplifted.

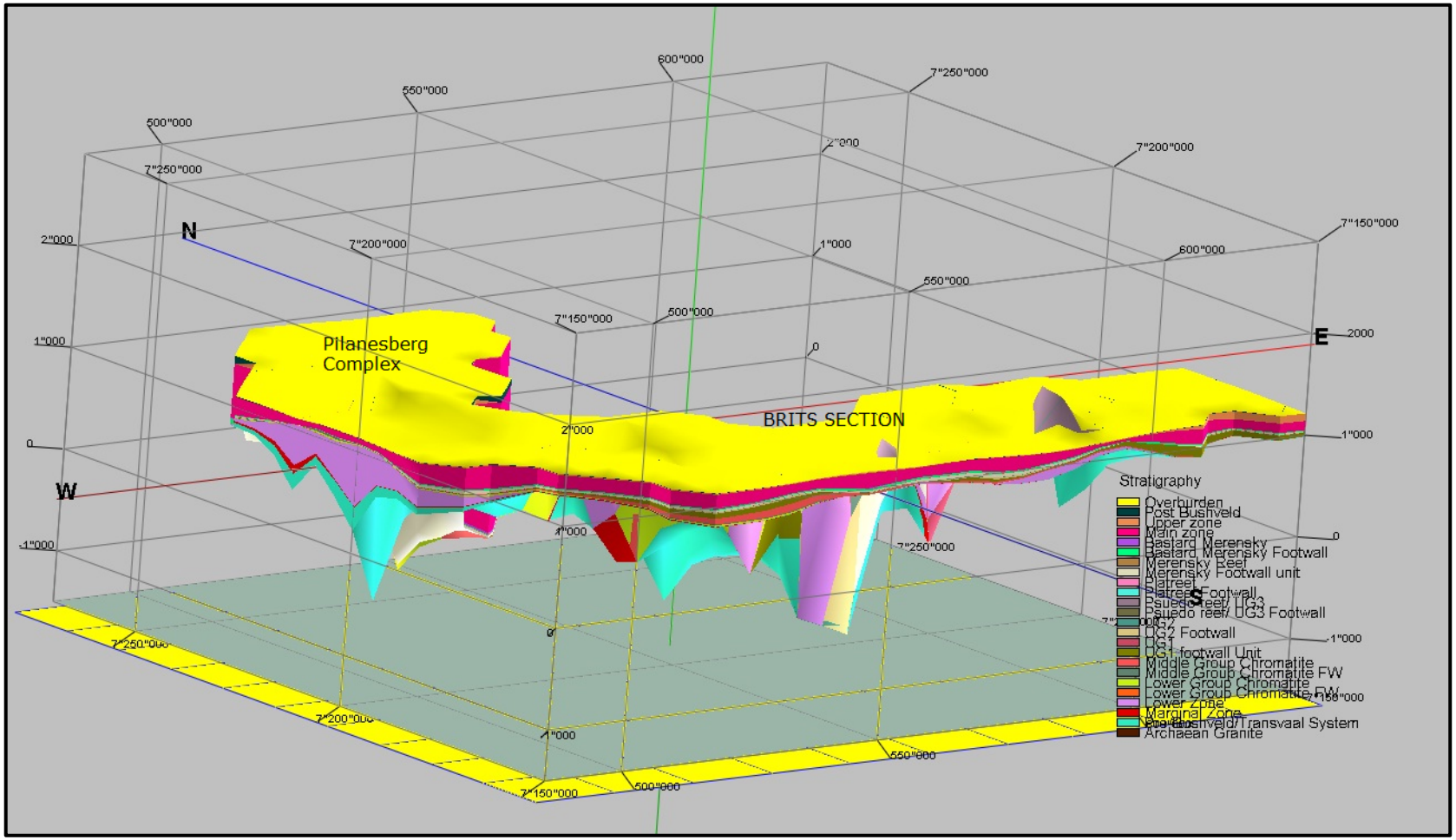

Figure 8.2: 3D model showing the sill nature of RLS rocks at the surface and the varied nature of the floor geometry of the Rustenburg Layered Suite (VE-16).

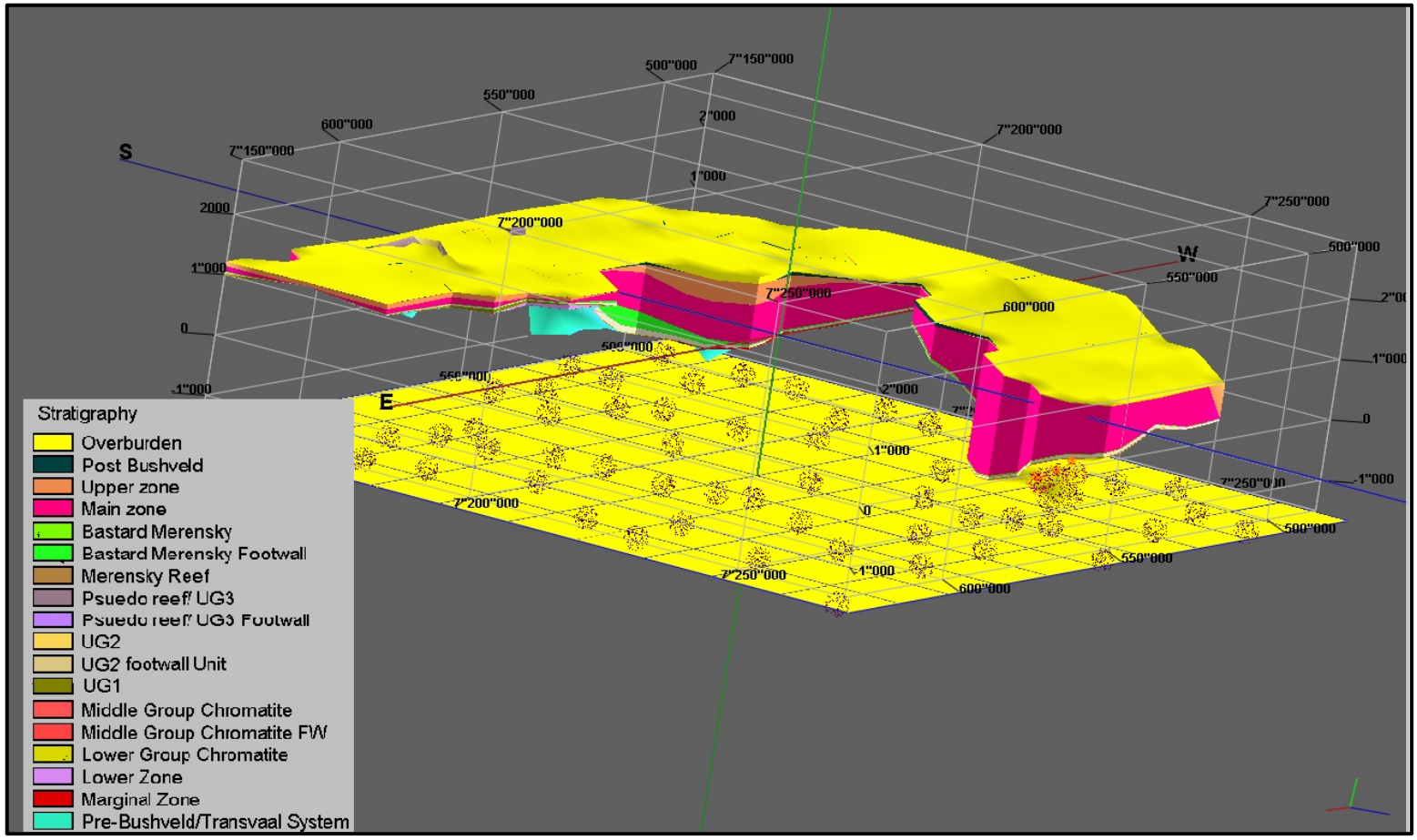

Figure 8.3: E-W view of the Western Bushveld 3D model showing the sill-like nature of the intrusion (VE-45).

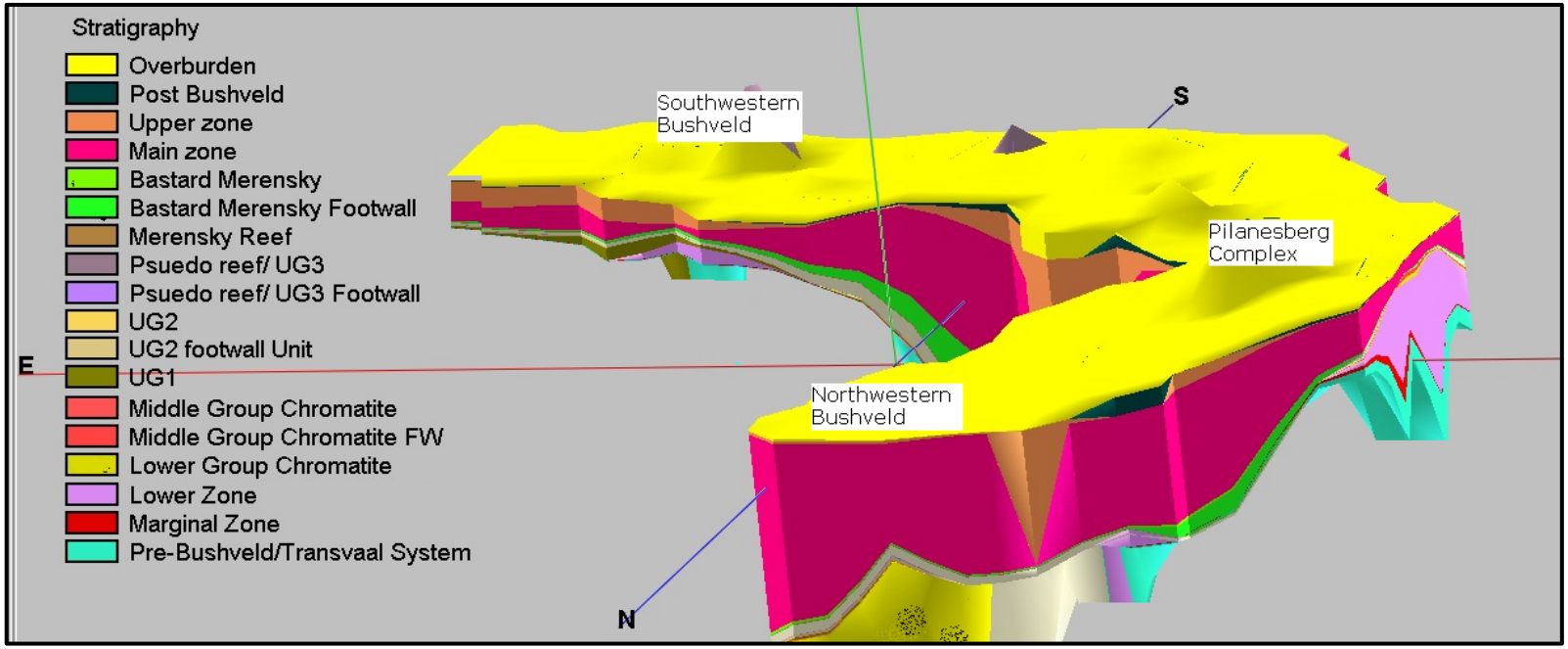

Figure 8.4: 3D model of Western Bushveld Complex showing the geometry and lateral distribution of each stratigraphic zone.

8.3 3D MODELS OF THE EASTERN BUSHVELD COMPLEX

The Eastern Bushveld geometry in Figures 8.5, 8.6 and 8.7 reveals rugged surface undulations especially along the edges. Most of the layers dip in the same way. This doming in the area might be responsible for the exposure of some of the RLS units at the surface (Uken and Watkeys, 1997a).

3D models of the RLS rocks in the area reveal that the doming influenced the entire stratigraphic units. The RLS at eastern Bushveld is dominated by floor rock domes believed to have formed by diapirc processes (Uken and Watkeys, 1997b) Most of the faults such as the Wonderkop and the Stoffspoort at Southeastern Bushveld dip to the east. The Kalkloof and Schwerin domes coincide with a structural high area and steep down eastward towards an adjacent structural low. Inverse correlation exists between the dome (structural high) area and thickness, i.e. there is thinning of the RLS over the dome and thickening over the adjacent structural low area. The southeast verging synclinal structure developed adjacent to Fortdraai Anticline in the Southeastern Bushveld. The Central part of the Eastern Bushveld is marked by the presence of valleys that separate the northern part from the southern parts. Not all parts of the Eastern Bushveld show inverse correlation in terms of structure and thickness and this might be due to syn- or post-depositional activities in the area. The southern part of the Eastern Bushveld in particular did not exhibit inverse correlation in structure and thickness and might have developed during the emplacement of the RLS or after.

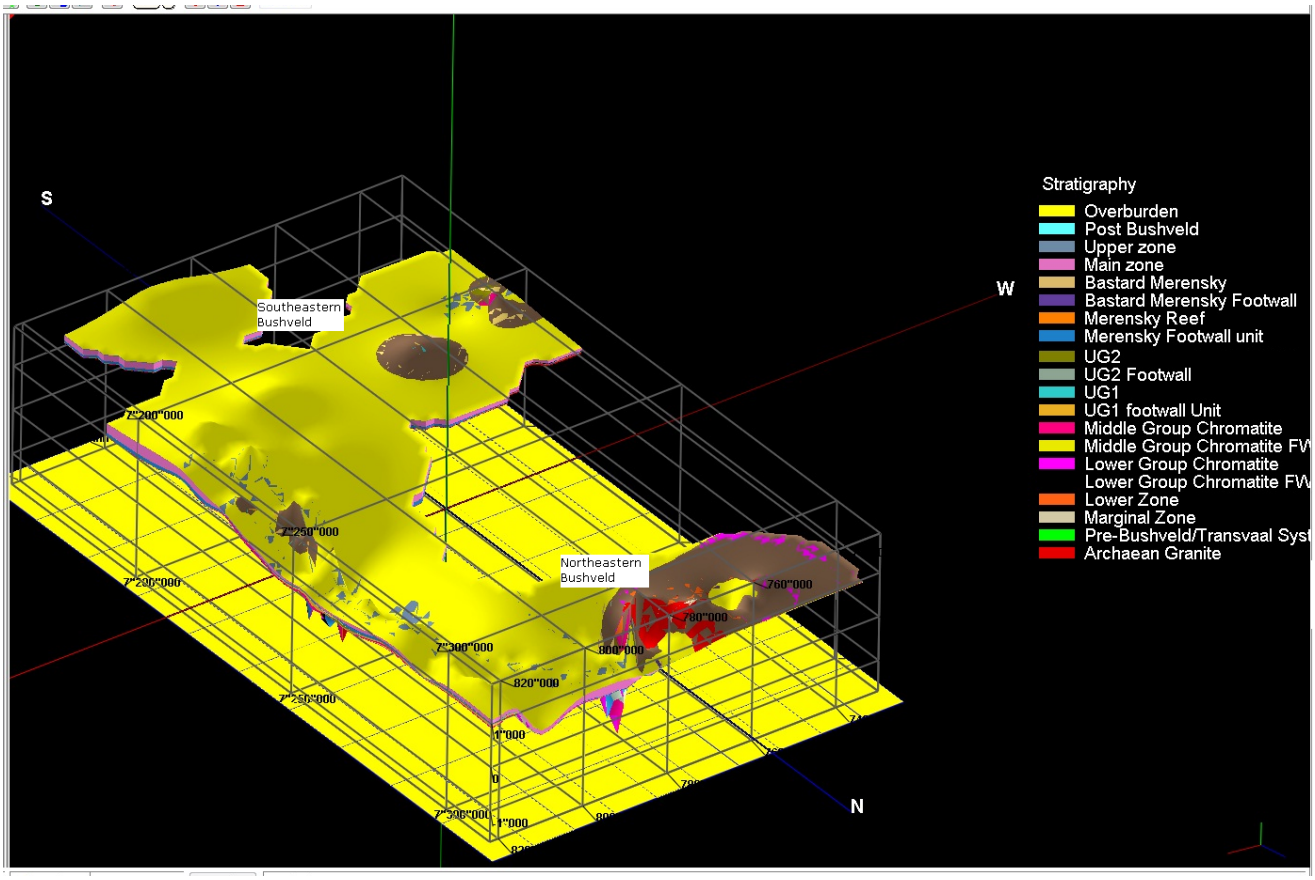

Figure 8.5: 3D model of the Eastern Bushveld.

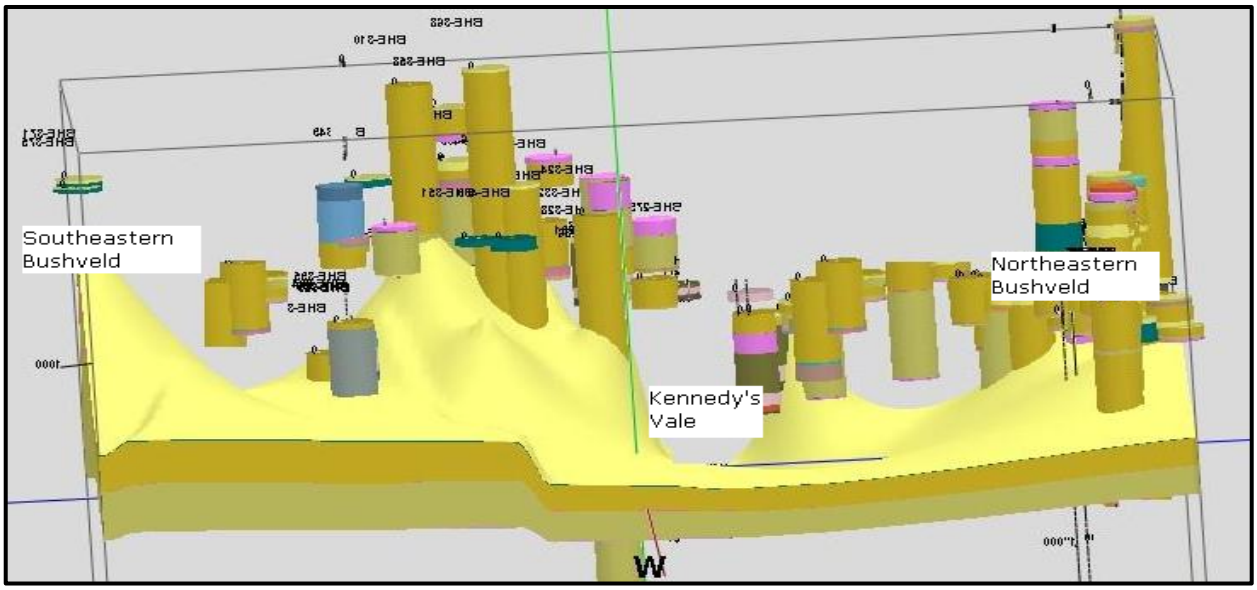

Figure 8.6: The Eastern Bushveld 3D model with strip log.

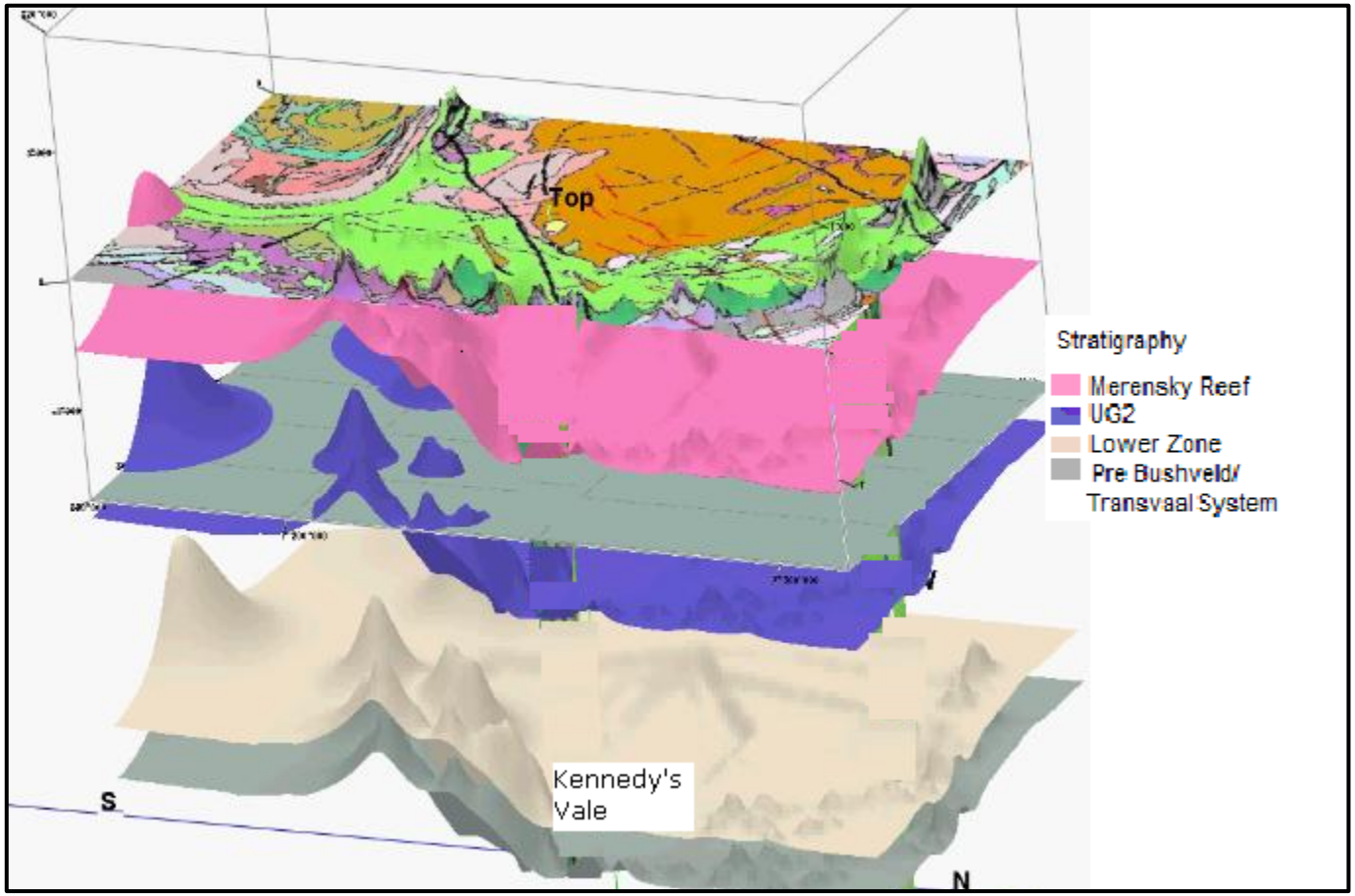

Figure 8.7: Exploded 3D model of the Eastern Bushveld Complex (not to scale) showing some layers of the Rustenburg Layered Suite with the draped geological map at the top (Stratigraphic index does not apply to draped geological map).

8.4 3D MODELS OF THE NORTHERN BUSHVELD COMPLEX

The Northern Bushveld or Potgietersrus sector is marked by northward dipping of the stratigraphic unit in the northern sector. The Upper Zone lithologies thicken northward in this sector, this was enhanced by structural dipping in the same direction. The unit also transgresses northwards down to the Archaean granite floor rock. More stratigraphic units and structural features (such as horst and graben structures, normal faults, folds as indicated in Figures 8.8 and 8.9) are exposed in the central section. The central sector exhibits a graben structure at the centre. Alternating downthrow and upthrows are also very common in this sector. Lower Zone rocks dominate the southern sector; a structural high or upwarp is prominent in this sector and this might be related to the presence of the Pretoria-Zebediela anticline.

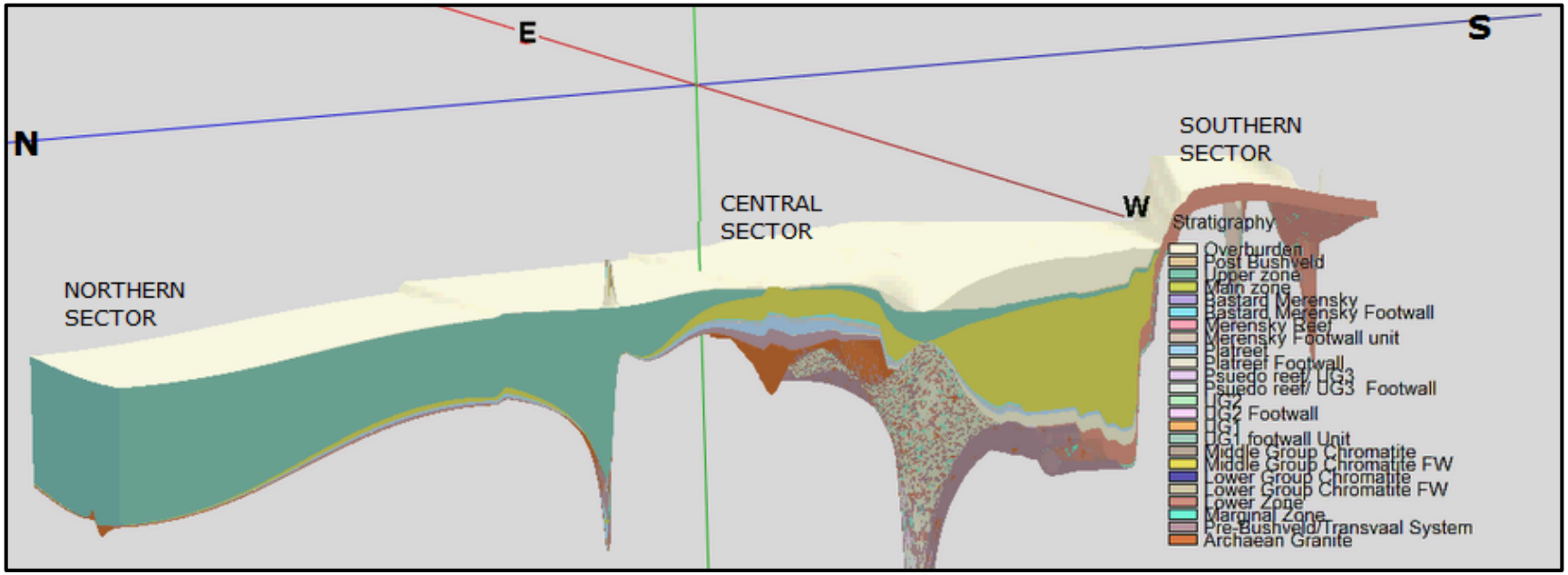

Figure 8.8: West to east view of 3D model of the Eastern Bushveld with some borehole logs.

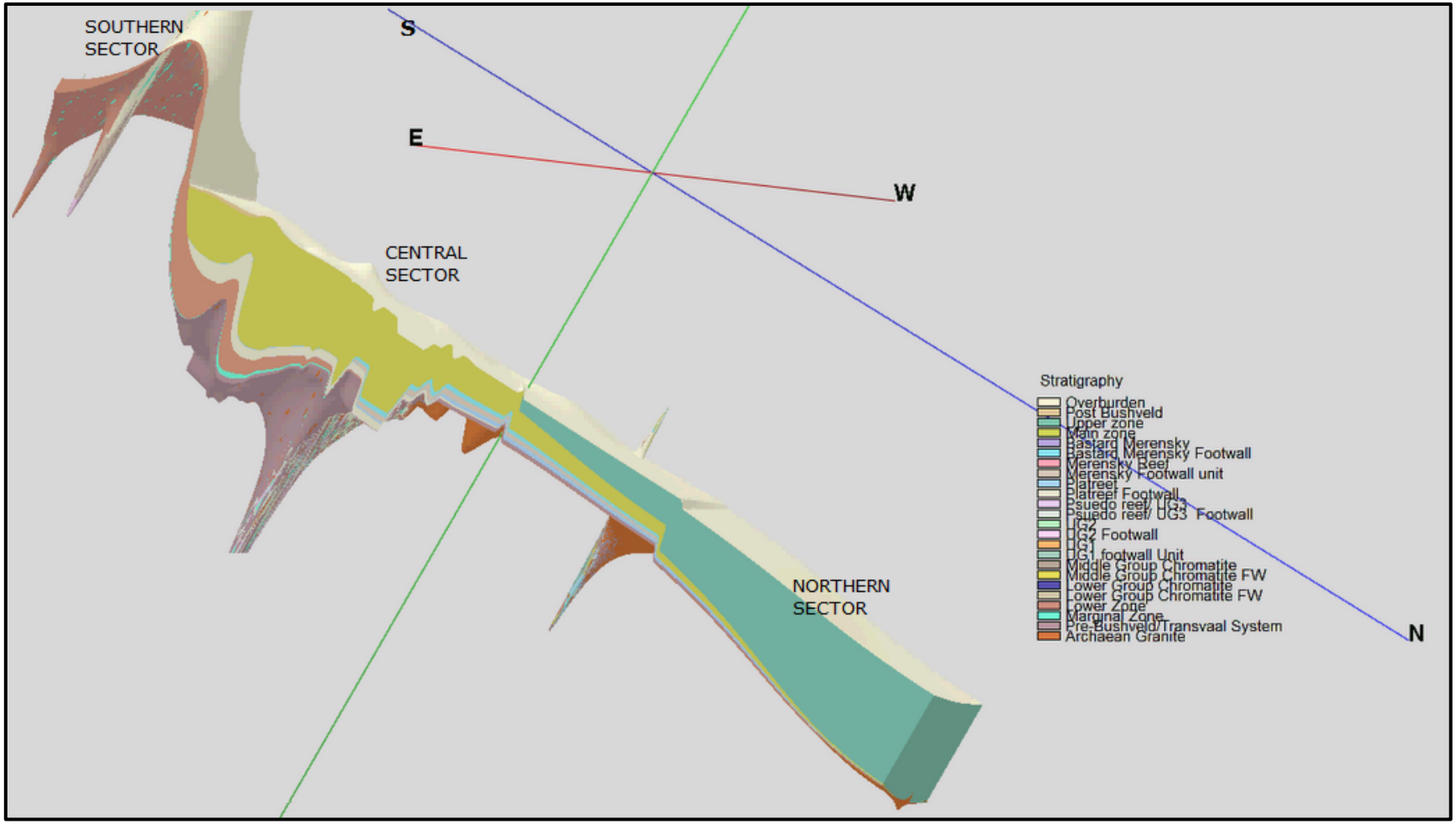

Figure 8.9: Southwest view of the Northern Bushveld 3D model with borehole logs showing the geometry and the rugged nature of the central part.

8.5 3D MODELS OF THE RUSTENBURG LAYERED SUITE ACROSS THE BUSHVELD COMPLEX

A look at the whole of the BIC shows that the southeastern part, the northern limb and the far western section were structural high areas before the emplacement of the RLS with the Southeastern Bushveld floor sloping to the northwards. Consequently, the southeastern part must have been the highest part while the extreme edge of Northwestern BIC and central part of the Eastern Bushveld occurred at the lowest points before the emplacement of the RLS rocks as indicated in Figure 8.10 below.

8.5 3D MODELS OF THE RUSTENBURG LAYERED SUITE ACROSS THE BUSHVELD COMPLEX

A look at the whole of the BIC shows that the southeastern part, the northern limb and the far western section were structural high areas before the emplacement of the RLS with the Southeastern Bushveld floor sloping to the northwards. Consequently, the southeastern part must have been the highest part while the extreme edge of Northwestern BIC and central part of the Eastern Bushveld occurred at the lowest points before the emplacement of the RLS rocks as indicated in Figure 8.10 below.

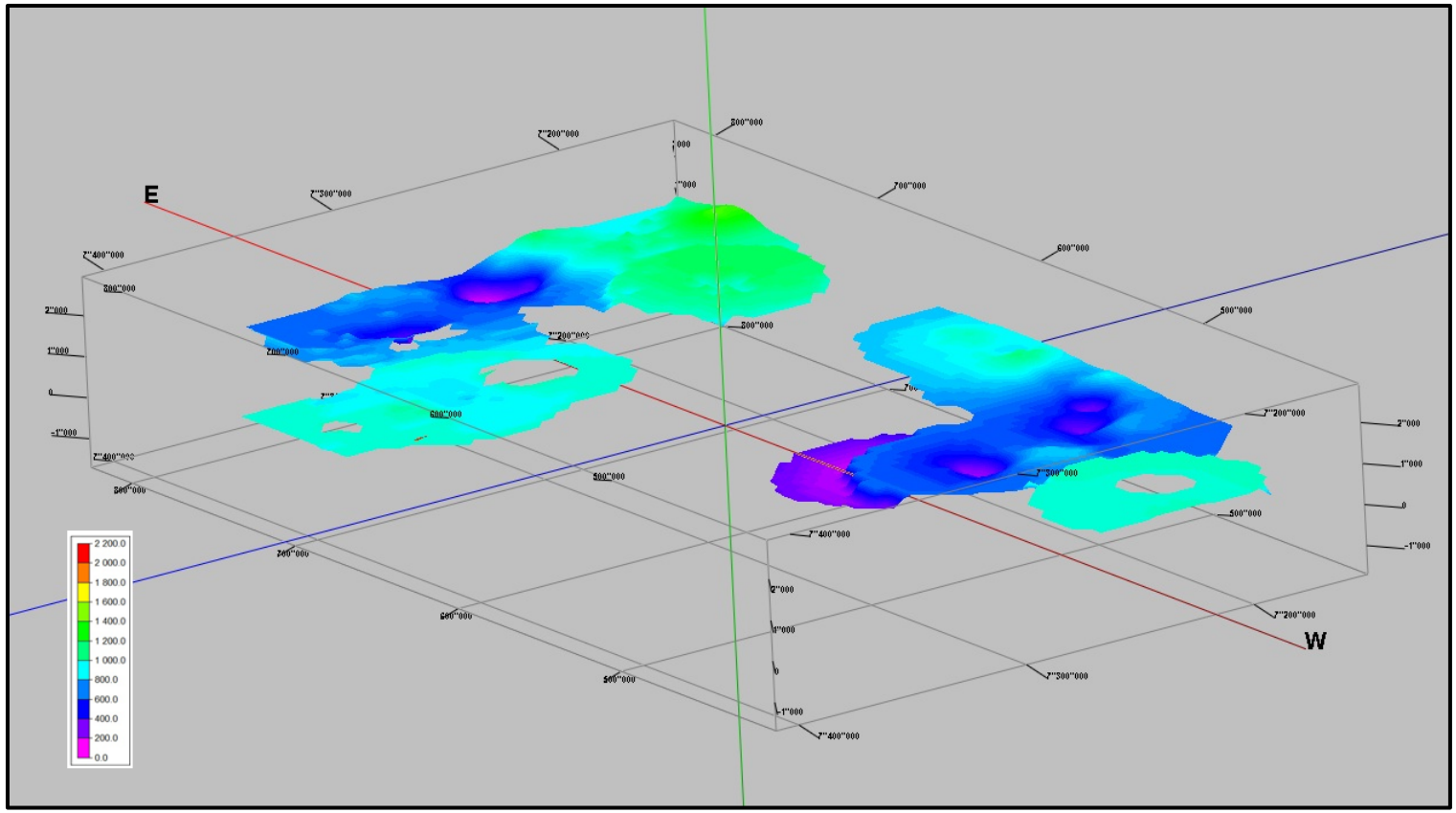

Figure 8.10: Diagram showing the base of the Main Zone interval for the whole of RLS rocks in the BIC. The main Western compartment is approximately at the same elevation with the Southeastern part while the NE edge of the Main Western compartment slope to the southeast.

Most of these models reveal strong tectonic control, resulting in elongations that are parallel to the trend of regional structures. A good example of this is the NNW-SSE outcrop elongation parallel to the Rustenburg Fault. Horizontal magma emplacement is favoured by vertical compression. Figures 8.11 and 8.12 indicate the strip log and the 3D model for the Bushveld Complex.

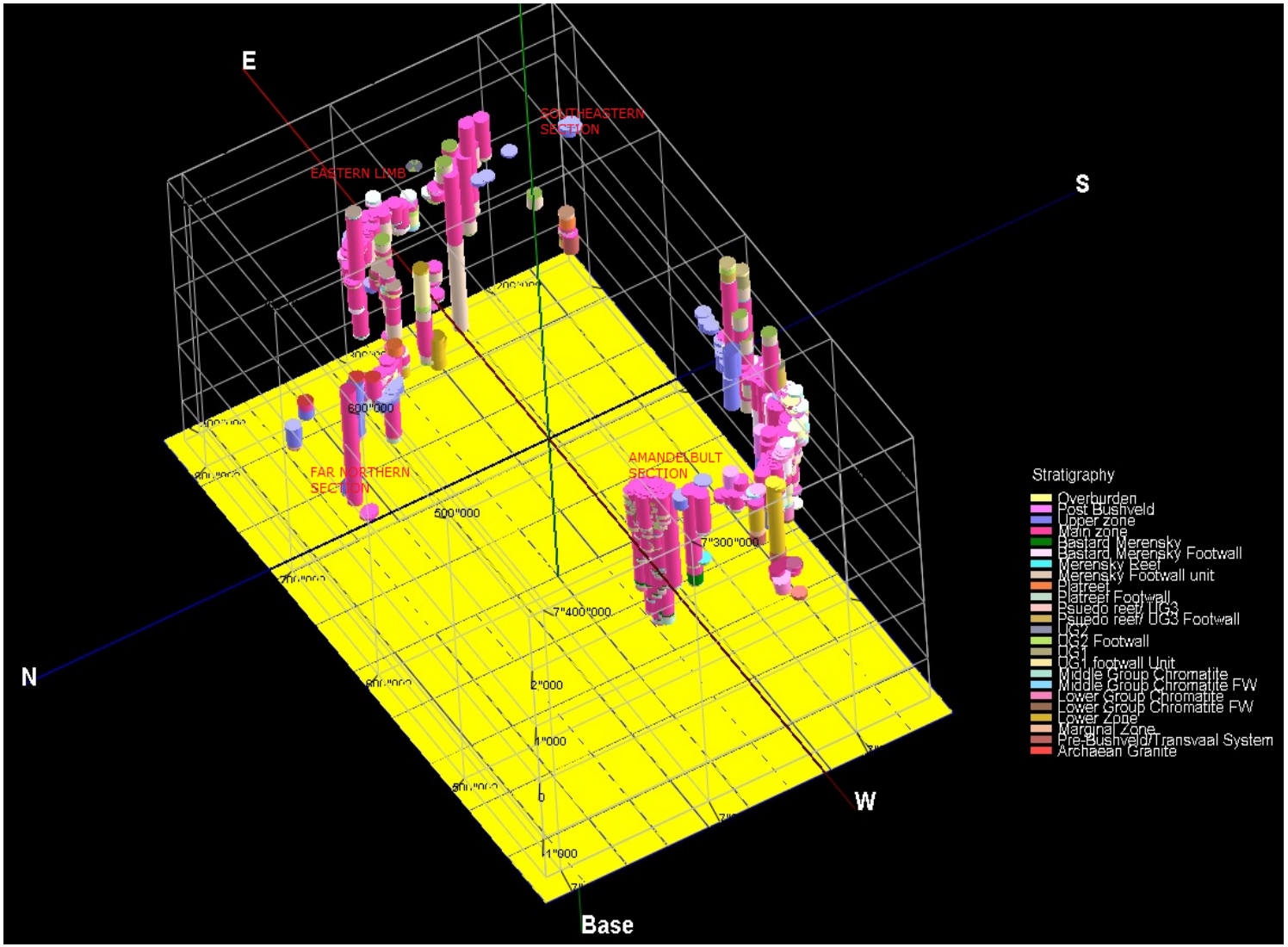

Figure 8.11: Multi-striplog image of some of the boreholes across the BIC.

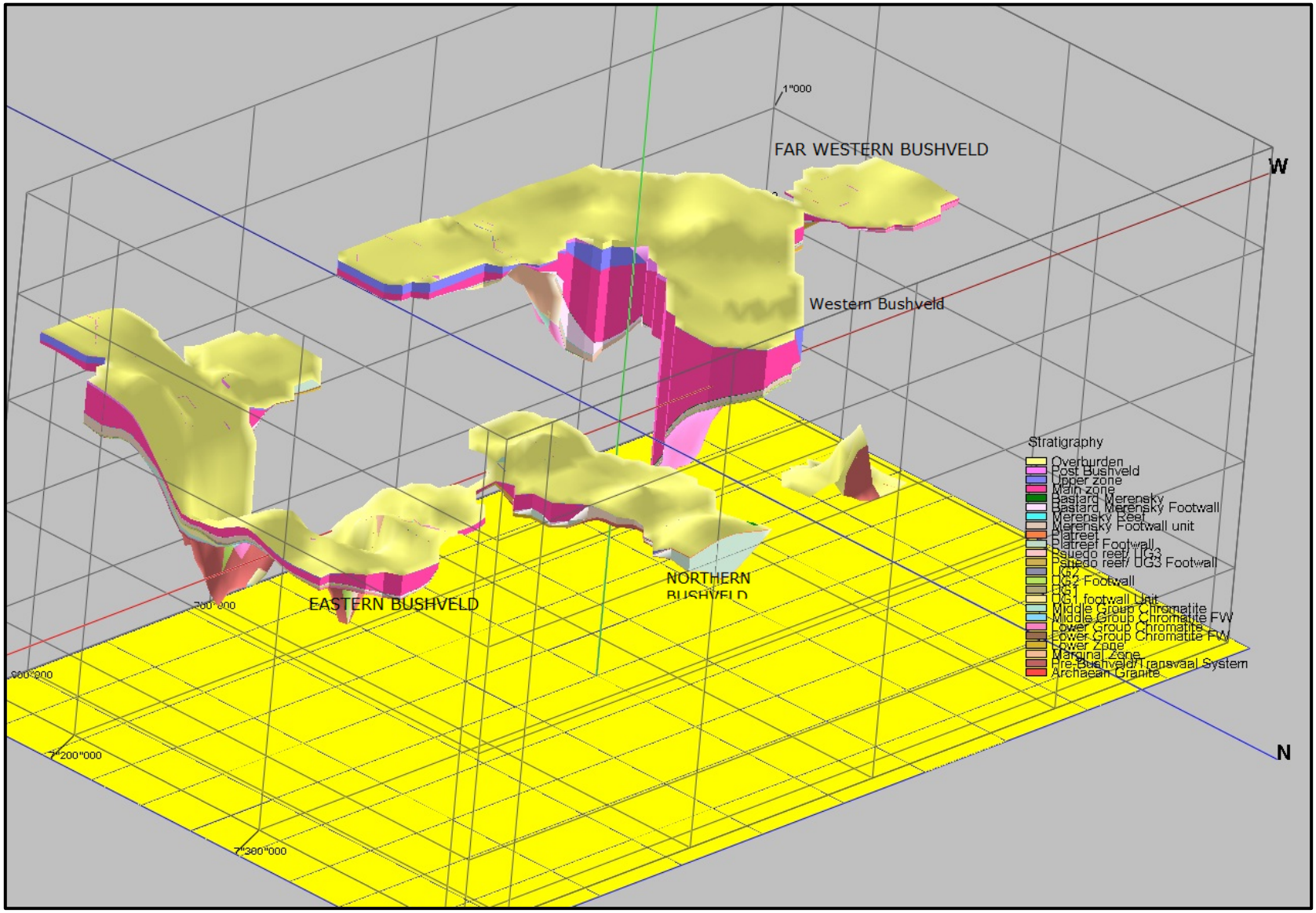

Figure 8.12: 3D model from the overburden to the floor of the Rustenburg Layered Suite (VE-46).

CHAPTER 9 CONCLUSION

9.1 INTRODUCTION

The aim of this chapter is to integrate the entire concept from previous chapters in order to adequately define the geometry of the Rustenburg Layered Suite in the Bushveld Igneous Complex based on available borehole log data. This will include; the description of the geometry of stratigraphic top and base contact through interpolation of sparse borehole data; using interval structure contour lines and isopach maps; structural interpretation from variation on thickness and attitude across infer structures; and systematic development of structures using trend surface analysis.

The interpolated subsurface geometry and faulting pattern allowed better understanding of regional stress pattern that produced the constrained models and geometry.

9.2 SUMMARY AND DISCUSSION ON DIFFERENT PARTS OF THE BUSHVELD COMPLEX

The Rustenburg Layered Suite (RLS) of the northwestern Bushveld is marked by a NE outcrop trend. The extreme NE end around Amandelbult and the Northam section dips and thickens toward the southeast in a step-like manner as revealed by the 3D models and fence diagrams. The step-like geometry in the northwestern Bushveld section (further confirmed by recent mining activities) is probably a series of south-trending half grabens initiated by extensional-fault reactivation due to the increasing magma influx and extension of the crust due to tectonic pull-apart. This might have led to differential offset of different stratigraphic levels by different amount with the bounding faults growing down-dip and forming horst and grabens structures, which indicate prevalent extensional system at such times. Either the dip parallel synformal geometry of this section is a primary feature, or as a result of incremental subsidence which might be due to magma cooling or isostatic adjustment to the increasing weight of additional magma influx (Einsele, 2000).

The Amandelbult and Northam section outcrop with step-like layering pattern probably shows evidence for multiple magma injection. The structural trend in this area is NNW as

defined by the centrally located downthrown section bounded by opposite dipping faults to form the Roodedem/Middellaagte graben. The NE-SW outcrop trend cuts across the NNW structural trend, and probably defines the magma influx direction. This area is also marked by the presence of folding to form a basin shape that is related to pothole structures. In the profile the length of the fold is mostly less than 1km and the height is not more than 500 m. L-shaped isopach contours around the central part of the Northwestern Bushveld Complex signify strike-slip movement. The Northern and Southern Gap area coincides with inferred fault planes. The Northern gap area slopes down towards the Amandelbult section while the Southern gap area slopes toward the Union section as indicated in Figure 4.6. The Upper Zone is also better developed around the gap areas, while the Upper Zone thickness exhibits a central NNW trend with sharp slopes along the gap area. There is an inverse relationship between structure and thickness of both regional and residual structures in the area, implying that the structures were already in place before the magma emplacement, although some of these structures were probably reactivated or modified during the emplacement. The widespread difference in structural pattern between the top of the Upper Zone and the base of the Main Zone unit in most parts of the western Bushveld might be due to slight changes in tectonic movement.

Several faults dominate the area around the Pilanesberg Complex as indicated on the geological map. Lower and Marginal Zone rocks are prominent in this area and appear folded and faulted around the Complex. The Lower Critical Zone is well-developed at the western part of the Complex. The southeastern part of the Pilanesberg Complex trends NNW-SSE and dips towards the centre. The structural trend and the outcrop trend are parallel to the trend of Rustenburg fault indicating that the NNW-SSE trend might have a strong influence on the magma migration path in the area.

The Southwestern Bushveld Complex indicates NNW trending structures while the outcrop trends E-W. The interval structural and isopach maps show more graben-shaped structures at the subsurface than indicated on the geological map of the area, has illustrated in chapter four –Figure 8A and 8B. This indicates the presence of blind faults and extensional regime at depth. Upper Zone rocks are more prominent in the eastern part of this section than on

the western side. The central part of this section exhibits very rugged morphology with presence of faults and grabens.

The Far western Bushveld or Nietverdiend sector dips slightly towards the main Western Bushveld, and the only identified structures in this area trends ENE. The central part of this section is slightly depressed (on the structure contour map) however; the depression is filled with thick deposits of Lower Critical Zone rocks (as indicated on the isopach map), surrounded by Marginal Zone rocks. The isopach map shows continuation to the west. There is an inverse relationship between structure and thickness in the area evident by the central depression filled with thick deposits of Lower Critical Zone rocks.

Regionally the Eastern Bushveld Complex compartment shows a prominent dip to the north, while the southern part is uplifted at depth. However, at the surface, the outcrop dips to the centre at the edges. The outcrop trends N-S (especially in the eastern parts) while the structure is rather irregular and includes N-S, NNW, E-W, and NE trends. A southward thickening trend is prominent in the Upper and Main Zone units. The widespread domain of all the RLS stratigraphic units and underlying units was observed on the 3D models. Similarities between the Main Zone interval structure contour patterns and the Archaean floor structure contours pattern indicate that structures here are probably floor rock controlled. However, not all parts of this compartment show the same inverse structure and thickness relation. Variations in the thickening trend in different parts of this limbis probably due to faulting and floor rock topography in the area. The outcrop trend of the Northeastern Bushveld Complex section indicates more of N-S and NNW. The Southeastern Bushveld Complex reveals inverse correlation in structure and thickness only in the Upper and the Main Zone units, while the other units exhibit similar structure and thickness. These heterogeneities in structure, thickness relationship and thickness trends are widespread in the Eastern Bushveld Complex. Structures in the northeastern Bushveld trend N-S and NNW while in the central section of the limb, the structural trend varies from E-W to ENE.

General gentle dipping and thickening toward the centre, especially in the Western Bushveld and Eastern Bushveld was related to subsidence after deposition according to

Gough and Van Niekerk (1959) and Hattingh (1995). However, thickening toward the centre as observed on the 3D models and from inverse correlation of structure and thickness in most parts of the Bushveld Complex probably suggest a pre-Bushveld emplacement feature. Otherwise, the edges of the Complex should be thicker than the subsided central section.

The Northern Bushveld compartment model exhibits northward dipping in the northern part, while the central part of the limb is dominated by prominent horst and graben structures together with several strike slip movement. The models also reveal that the RLS in this limb rests progressively on older rocks from south to north where it directly lies on the Archaean floor confirming the earlier observation by Ashwal et al. (2005) and Kinnaird et al. (2005). This progressive transgression of the RLS rocks reveals increasing northward dipping of underlying Archean floor rocks and corresponding northward thickening of the overlying Upper Zone rocks. This geometry probably resulted from the southward sliding of overlying Upper Zone rocks over the floor rocks. Further, southwards, the Upper Zone transgressed underlying RLS rocks to form a horst and graben structure tn the central sector. Presence of folds and step-like features in the floor of the central sector probably indicate imbricate staking due to thrusting which Friese (2004) had reported earlier in the area. However, the Lower Zone unit in the southern sector of the Northern Bushveld transgressed the overlying RLS rocks and rest directly on the Transvaal rocks. The regional outcrop trend is N-S to NNW while most of the structures trend E-W, ENE-WSW, NE and N-S. A number of folds, mostly NW dipping with ENE trend are also present, especially in the central and southern parts. A strong inverse correlation exists between the structures and thickness of RLS rocks and the Archaean floor, thus implying that most of the structures are probably pre-Bushveld and basement controlled. However, it was observed that faulting and folding within this compartment affected both the Archaean floor rocks and the RLS rock and might indicate that intense tectonic movement occurred after the emplacement of the Bushveld Complex. The horst and graben structure at the centre of the northern Bushveld, however, indicates an inversion, implying a formally uplifted area (as observed on the structure contour map) now shows pronounced thickening and graben shape on the thickness map. This shows that earlier structural high area that ought to have

received less magma influx probably experienced subsidence and faulting to form a graben and received more magma influx. The NE-ENE trending faults dominate the central section of the northern limb. Few N-S trending faults (with down-throw to the west); NNW-SSE, NE trending faults (parallel to Ysterberg-Planknek Fault) with a down-throw to the south; E-W trending faults (parallel to the Zebediela Fault) were identified in the southern part.
The Far Northern Bushveld sector is dominated by the Main Zone lithologies dipping to the southeast and a structural high that trends NNW in the southeast. Thickening in the SW (indicates low land area before magma influx) while there is thinning over the structural high or high land area at the southeast. This structure is not revealed on the surface of the Upper Zone unit but it is prominent in other stratigraphic units.
Most of the structures identified can be grouped as the product of reactivation spanning over 2 Ga. The regional stress conditions at the time of emplacement of the RLS supported the emplacement along existing NNW and ENE regional trends. The two trends can be correlated with tectonic events in the Kaapvaal Craton and also coincide with trend of weakness during the formation of the Kaapvaal Craton (de Wit et al., 1992).The ENE trend coincides with the depositional axis of the Transvaal basin and it is also oriented parallel to Thabazimbi-Murchison Lineament (Hunter, 1975). The NE-SW trend was described as a major compressional trend (which resulted from the collision of the Kaapvaal Craton with the Zimbabwe Craton) during Bushveld emplacement (Holzer et al., 1999). The surface geometry of the RLS is almost flat except for the inward dipping of the rims coupled with some doming which clearly shows up conspicuously on the models. This flat morphology might be parallel to the layering of the original sub-horizontal nature of the roof area while pre- and syn-Bushveld folding of the floor rock modified the basal portion of the layered suite (Sharpe, 1981).

The geometry of the RLS can be described as layers of multiple sills with roof and floor morphology modified by pre-, syn- and post-depositional structures (Cawthorn, 2012). Pre-Bushveld structures modified the emplacement of the intrusions; examples are: structures such as upfolds, domes, uplifts and downwarp of underlying floor rock; pre-Bushveld faulting (Du Plessis and Walraven, 1990), the Rustenburg fault (Coertze, 1962; Bumby et al., 1998), host and graben structures (Teigler et al., 1992). Syn-Bushveld structures

include cyclic lateral layering of RLS rocks. While post-Bushveld structures include faulting (thrusting and normal faulting) due to extensional and compressional movement and tilting of strata due to isostatic readjustment. Sharpe and Snyman (1980) proposed a NNE trend deposition for RLS at the basal section of the Transvaal Supergroup rocks.
Magma preferential migration pathway and geometry is influenced by crustal compression and extension as well as presence of pre-existing structures (Sibson, 2003; Hodge et al., 2012 and references therein). While extension in the crust will allow lateral migration of magma and create an obstruction to its upward migration, compression permits upward migration and acts as a barrier to lateral migration. Pre-existing structures act as weak zones and pathways through which magma can flow.

The geometric pattern interpretation of the stratigraphic intervals of the RLS in this study suggests continuous east-west horizontal to sub-horizontal emplacement of the Bushveld Complex, which was first distinguished as a northern and southern mass by Truter (1955) who, based on observation of transgressive contact. He made a distinction between an east-west oriented southern mass and an elongate north-south oriented northern mass. The geometry of the Bushveld Igneous Complex BIC was first described as a lopolith by Hall (1932). Further probe into the geometry revealed funnel-shaped intrusions (Willemse, 1964; Wager and Brown, 1967) while separate inward dipping sheet model was proposed by De Beer et al. (1987); Du Plessis and Kleywegt(1987). Gravity modelling by Webb et al. (2004), interpreted the Eastern and Western mafic units as connected sheets that were subsequently deformed. Campbell (2006, 2009) using seismic surveys identified widespread graben structures, floor domes, syn-Bushveld diapirs, and graben collapse structures within the RLS. Kgaswane et al. (2012) and Cole et al. (2012: 2014) reconfirmed continuous sheet model earlier proposed by Cawthorn et al. (1998), Cawthorn and Webb (2001), and Webb et al. (2004, 2011). The east-west orientation of the southern mass was attributed to tension in the east-west direction, contrary to the elongate northern mass, which was due to compression in the east-west direction. Evidence for the east-west elongation is supported by the location of the far western Bushveld Complex compartment to the west of the Western and Eastern Bushveld Complex compartments (;Eales and

Cawthorn, 1996: Mapeo et al., 2004) as well as variation in magma composition from north to south.

Formation of layered igneous suites such as the RLS might likely conform to rotation of maximum principal compressive stress σ_1 from vertical to horizontal according to Roberts et al. (2007), the principal stress at this point is vertical while the other two stress tensors will be horizontal and the magnitude of differential stress is minimal. Sills or sheet intrusion was thus formed when the magma pressure exceeds the vertical stress during upward migration of magma towards the surface. Horizontal to subhorizontal layering occurs along lithologic boundaries and surface of unconformity. Example of this is the Bushveld Complex, which was emplaced at the boundary between the Pretoria Group of the Transvaal Supergroup and overlying monzonitic residual roof rock (and the Rooiberg Group) as described by Cawthorn et al. (2006) and Cawthorn (2012). Another example is the Karoo Basin (Chevallier and Woodford, 1999; Burchardt, 2009) with references therein). Sill emplacement can also occur when the upper layer or the roof layer is more rigid according to Kavanagh et al. (2006).

Magma from magma chambers are transported upwards through conduits such as dykes and plugs. Attempts have been made through geophysical investigation by Van der Merwe (1976), Sharpe et al. (1980), Kinloch (1982), and du Plessis and Kleywegt, (1987) to identify magma feeders within the Bushveld Complex by relating anomalously high and positive gravity signature of thick mafic rock zones as feeder sites. In this study, a few of such anomalously thick zones were identified in some areas. These areas include the extreme NE part of the Western Bushveld (along Amandelbult and Northam section) where the down-dip or step-like deposit of over 2500 m (based on available borehole records), but described as more than 10 km by Maier et al. (2013) (based on recent mining activity in the area) was identified. The southeastern part of the Rustenburg fault on Schaapkraal farm; southeast part of the Steelpoort Fault on a Pietersburg farm in Eastern Bushveld limb; the eastern part of the central sector of the northern Bushveld and around Grasvally synformal structure in the southern sector are some of the areas that can be interpreted as feeder sites due to the anomalous thickness of the RLS units.

9.3 ECONOMIC IMPORTANCE OF STUDY

This study provides a synoptic view of the Rustenburg Layered Suite of the Bushveld Complex, allowing continuous trace of widely distributed terrain features and defines the geometry of the whole of the RLS. It also gives details of the geometry of contact zones revealing the subsurface structural features and emplacement models which are essential for future mineral exploration. Identification of thickening trends of each unit of the RLS proves to be significant for future exploration. Most of the synformal structures identified in our models coincide with the site of thick mineralization especially at Tweefontein where the synformal structure dips strongly to the SW,this was also reported by Nex (2005), the Grasvally structure that dips to the NW, also reported by Armitage (2011). Nex (2005) reported structural control on the distribution of sulphide in pre-Bushveld fold structures.The geometry and position of economic deposits are mostly controlled by ENE and NNW inherent structural trends in the Kaapvaal Craton during its development (von Gruenewaldt1979; Hunter1975, 1976). The ENE trend coincides with the Transvaal Basin depositional trend while the NNW trend is associated with the Vryburg arch depression. Intrusion exploited weak zones and fractures in the earth as pathways, while economic minerals are mostly deposited along fractures, such as veins and joints, fold axes and fault planes. The three-dimensional models produced in this study provide detail regional mapping and kinematic analysis of structures.

Major advantages of this study include the quality of data used (based on directly observation of borehole core log) and the perfect conformity of the results with previous field studies and geophysical investigation. Unsubstantiated inferences or assumption about the RLS subsurface features and geometry were conclusively evidenced, while very important additional information was added to the existing detail.

Visualisation of 3D models, grid models, fence diagrams and isopachs maps coupled with regional scale of study afforded good insight into the RLS geometry providing better understanding and enhanced thorough interpretation of geological relationships and associated structural features.

REFERENCES

AARNES, I., SVENSEN, H., POLTEAU, S. & PLANKE, S. 2011. Contact metamorphic devolatilization of shales in the Karoo Basin, South Africa, and the effects of multiple sill intrusions. *Chemical Geology,* 281**,** 181-194.

AGTERBERG, F. P. 1984. Trend surface analysis. *Spatial statistics and models.* Springer.

AMEGLIO, L. & VIGNERESSE, J. 1999. Geophysical imaging of the shape of granitic intrusions at depth: a review. *Geological Society, London, Special Publications,* 168**,** 39-54.

ARMITAGE, P. MCDONALD I., & TREDOUX M. (2007). A geological investigation of the Waterberg hydrothermal platinum deposit, Mookgophong, Limpopo Province, South Africa. *Appl. Earth Sci. (Trans. Inst. Min. Metall. B)*, **116**, B113-129.

ARMITAGE, P. E. B. 2011. *Development of the Platreef in the northern limb of the Bushveld Complex at Sandsloot, Mokopane District, South Africa.* University of Greenwich.

ASHWAL, L. D., WEBB, S. J. & KNOPER, M. W. 2005. Magmatic stratigraphy in the Bushveld Northern Lobe: continuous geophysical and mineralogical data from the 2950 m Bellevue drillcore. *South African Journal of Geology,* 108**,** 199-232.

AUGER, E., GASPARINI, P., VIRIEUX, J. & ZOLLO, A. 2001. Seismic evidence of an extended magmatic sill under Mt. Vesuvius. *Science,* 294**,** 1510-1512.

BAIRD, A., BAIRD, K. & MORTON, D. 1971. On deciding whether trend surfaces of progressively higher order are meaningful: discussion. *Geological Society of America Bulletin,* 82**,** 1219-1234.

BALLHAUS, C. G. 1988. Potholes of the Merensky Reef at Brakspruit Shaft, Rustenburg platinum mines; primary disturbances in the magmatic stratigraphy. *Economic Geology,* 83**,** 1140-1158.

BALLHAUS, C. G. & STUMPFL, E. F. 1985. Occurrence and petrological significance of graphite in the Upper Critical Zone, western Bushveld Complex, South Africa. *Earth and planetary science letters,* 74**,** 58-68.

BARCLAY, J., KRAUSE, F., CAMPBELL, R. & UTTING, J. 1990. Dynamic casting and growth faulting: Dawson Creek graben complex, Carboniferous-Permian Peace River embayment, western Canada. *Bulletin of Canadian Petroleum Geology,* 38**,** 115-145.

BARNES, S.-J., MAIER, W. & ASHWAL, L. 2004. Platinum-group element distribution in the main zone and upper zone of the Bushveld Complex, South Africa. *Chemical Geology,* 208**,** 293-317.

BARNES, S.J. & MAIER, W. D. 2002. Platinum-group element distributions in the Rustenberg Layered Suite of the Bushveld Complex, South Africa. . *The Geology, Geochemistry, Mineralogy and Mineral Beneficiation of Platinum-Group Elements.* Canadian Institute of Mining, Metallurgy and Petroleum.

BARNES, S. J., & MAIER, W. D. (1999). The fractionation of Ni, Cu and the noble metals in silicate and sulphide liquids. Dynamic processes in magmatic ore deposits and their application to mineral exploration. Geological Association of Canada, Short Course Notes, 13, 69-106.

BARTON, E. S., ALTERMANN, W., WILLIAMS, I. S. & SMITH, C. B. 1994. U-Pb zircon age for a tuff in the Campbell Group, Griqualand West Sequence, South Africa: Implications for Early Proterozoic rock accumulation rates. *Geology,* 22**,** 343-346.

BAYER, E. & DOOLEY, K.1990 New techniques for the generation of subsurface models. Offshore Technology Conference. Offshore Technology Conference.

BOHLING, G. 2005. Introduction to geostatistics and variogram analysis. *Kansas geological survey, 20p*.

BRISTOW, D. G., CAWTHORN, R. G., HARMER, J., LEE, C. A., TEGNER, C., VILJOEN, M. J., WALRAVEN, F. & J.R, W. 1993. Excursion guide—symposium on layering in igneous complexes. *Wager and Brown 25th Anniversary Commemorative Meeting.* Johannesburg.

BUMBY, A., ERIKSSON, P. & VAN DER MERWE, R. 1998. Compressive deformation in the floor rocks to the Bushveld Complex (South Africa): evidence from the Rustenburg Fault Zone. *Journal of African Earth Sciences,* 27**,** 307-330.

BURCHARDT, S. 2009. *Mechanisms of magma emplacement in the upper crust.* PhD Thesis-Geowissenschaftliches Zentrum der Georg-August Universität Göttingen.

BURROUGH, P. A.& MCDONNELL, R.A.1998. *Principles of geographical information systems*, Oxford university press Oxford.

CAHEN, L., SNELLING, N. J ., & DELHAL, J. 1984. *The geochronology and evolution of Africa* (Vol. 512). Oxford: Clarendon Press.

CAMERON, E. N. 1963. Structure and rock sequences of the Critical Zone of the eastern Bushveld Complex. *Min Soc Am Spec Pap,* 1**,** 93-107.

CAMERON, E. N. 1978. The lower zone of the eastern Bushveld Complex in the Olifants River trough. *Journal of Petrology,* 19**,** 437-462.

CAMERON, E. N. 1980. Evolution of the lower critical zone, central sector, eastern Bushveld Complex, and its chromite deposits. *Economic Geology,* 75**,** 845-871.

CAMERON, E. N. 1982. The upper critical zone of the eastern Bushveld Complex; precursor of the Merensky Reef. *Economic Geology,* 77**,** 1307-1327.

CAMPBELL, G. 1990. The seismic revolution in gold and platinum prospecting. *S Afr Geophys Assoc Yb BPI Geophys Univ Witwatersrand Johannesburg, S Afr***,** 37-45.

CAMPBELL, G. (1994). Geophysical contributions to mine-development planning: A risk reduction approach. In *Proceedings XV CMMI Congress: SAIMM Symposium Series* (pp. 283-325).

CAMPBELL, G. 2006. High resolution aeromagnetic mapping of "loss-of-ground" features at platinum and coal mines in South Africa. *South African Journal of Geology,* 109**,** 439-458.

CAMPBELL, G. 2009. Seismic Reflection Surveys and structural mapping: Faults, dips and domes. *11th SAGA Biennial Technical Meeting and Exhibition.* Swaziland.

CAMPBELL, G. 2011. Exploration geophysics of the Bushveld Complex in South Africa. *The Leading Edge,* 30**,** 622-638.

CAMPBELL, I. 1978. Some problems with the cumulus theory. *Lithos,* 11**,** 311-323.

CARR, H., KRUGER, F., GROVES, D. & CAWTHORN, R. 1999. The petrogenesis of Merensky Reef potholes at the Western Platinum Mine, Bushveld Complex: Sr-isotopic evidence for synmagmatic deformation. *Mineralium Deposita,* 34**,** 335-347.

CARR, H. W. & GROVES, D. I. 1994. The importance of synmagmatic deformation in the formation of Merensky Reef potholes in the Bushveld Complex. *Economic Geology,* 89**,** 1398-1410.

CAWTHORN, R. 1999. The platinum and palladium resources of the Bushveld Complex. *South African Journal of Science,* 95**,** 481-489.

CAWTHORN, R. 2012. MULTIPLE SILLS OR A LAYERED INTRUSION? TIME TO DECIDE. *South African Journal of Geology,* 115**,** 283-290.

CAWTHORN, R., EALES, H., WALRAVEN, F., UKEN, R. & WATKEYS, M. 2006. The Bushveld Complex. *The Geology of South Africa,* 691**,** 261-281.

CAWTHORN, R.G.,& MOLYNEUX, T. 1986. Vanadiferous magnetite deposits of the Bushveld Complex. *Mineral deposits of southern Africa,* 2**,** 1251-1266.

CAWTHORN, R. G., LEE, C. A., SCHOUWSTRA, R. P. & MELLOWSHIP, P. 2002. Relationship between PGE and PGM in the Bushveld Complex. *Canadian Mineralogist,* 40**,** 311-328.

CAWTHORN, R. G., MEYER, P. S. & KRUGER, F. J. 1991. Major addition of magma at the Pyroxenite Marker in the western Bushveld Complex, South Africa. *Journal of Petrology,* 32**,** 739-763.

CAWTHORN, R. G. & WALRAVEN, F. 1998. Emplacement and crystallization time for the Bushveld Complex. *J. Petrol.,* 39**,** 1669-1687.

CAWTHORN, R. G. & WEBB, S. J. 2001. Connectivity between the western and eastern limbs of the Bushveld Complex. *Tectonophysics,* 330**,** 195–209.

CHAMBERS, J. Q., HIGUCHI, N., SCHIMEL, J. P., FERREIRA, L. V. & MELACK, J. M. 2000. Decomposition and carbon cycling of dead trees in tropical forests of the central Amazon. *Oecologia,* 122**,** 380-388.

CHENEY, E. S. & TWIST, D. 1991. The conformable emplacement of the Bushveld mafic rocks along a regional unconformity in the Transvaal succession of South Africa. *Precambrian Research,* 52**,** 115-132.

CHEVALLIER, L. & WOODFORD, A. 1999. Morpho-tectonics and mechanism of emplacement of the dolerite rings and sills of the western Karoo, South Africa. *South African Journal of Geology,* 102**,** 43-54.

CHUNNETT, G. K. & ROMPEL, A. K. K. 2004. Data integration for structural interpretation in the Bushveld Complex. *International Platinum Conference: 'PlatinumAdding Value'*. The South African Institute of Mining and Metallurgy.

CLARKE, B. M., UKEN, R., WATKEYS, M. K. & REINHARDT, J. 2005. Folding of the Rustenburg layered suite adjacent to the Steelpoort pericline: implications for syn-Bushveld tectonism in the eastern Bushveld Complex. *South African Journal of Geology,* 108**,** 397-412.

CLARK, I. and HARPER, W.V., 2001. Practical Geostatistics 2000. Geostokos (Ecosse) Limited, 342 pp.

COERTZE, F. 1962. The Rustenburg Fault as a controlling factor of ore-deposition South-West of Pilanesberg. *Transactions Geological Society South Africa,* 65**,** 253-262.

COERTZE, F. 1970. The geology of the western part of the Bushveld Igneous Complex. *Geol. Soc. S. Afr. Spec. Publ,* 1**,** 5-22.

COERTZE, F. J. 1974. *The geology of the basic portion of the Western Bushveld Igneous Complex*, Geol. Surv. South Africa, Mem. 66, 148pp.

COLE, J., FINN, C. A. & WEBB, S. J. 2013. Overview of the magnetic signatures of the Palaeoproterozoic Rustenburg Layered Suite, Bushveld Complex, South Africa. *Precambrian Research,* 236**,** 193-213.

COLE, J., WEBB, S. J., & FINN, C. 2012,. Reassessing Geophysical Models of the Bushveld Complex in 3D. In *AGU Fall Meeting Abstracts* (Vol. 1, p. 08).

COLE, J., WEBB, S. J., & FINN, C. A. (2014). Gravity models of the Bushveld Complex–Have we come full circle?. *Journal of African Earth Sciences*, *92*, 97-118.

COLLINS JR, F. C. & BOLSTAD, P. V.1996 A comparison of spatial interpolation techniques in temperature estimation..

COOK, A. 1969. Trend-surface analysis of structure and thickness of Bulli Seam, Sydney Basin, New South Wales. *Journal of the International Association for Mathematical Geology,* 1**,** 53-78.

COUNCIL FOR GEOSCIENCE, 1997. Geological map of the Republic of South Africa and the Kingdoms of Lesotho and Swaziland 1:1 000 000. In: Geological Map Series.

COUSINS, C. 1959. The structure of the mafic portion of the Bushveld Igneous Complex. *Trans Geol Soc S Afr,* 62**,** 179-189.

COUSINS, C. A. & FERINGA, G. 1964. The chromite deposits of the western belt of the Bushveld Complex. In: The geology of some ore deposits in Southern Africa. *In:* HAUGHTON, S. (ed.). Johannesburg: Geol Soc S Afr, .

CROWSON, P. 2001. Mineral handbook 2000–2001. *Mining Journal Books, Edenbridge,* 486.

DAVIS, J. C. 1986. *Statistical and data analysis in geology*, J. Wiley.

DAVIS, J. C. 2002. *Statistics and data analysis in geology*, Wiley New York.

DAVIS, R. W. 1973. Quality of Near-Surface Waters in Southern Illinois. *Groundwater,* 11**,** 11-18.

DE BEER, J., MEYER, R. & HATTINGH, P. 1987. Geoelectrical and palaeomagnetic studies on the Bushveld complex. *Proterozic Lithospheric Evolution***,** 191-205.

DE KEMP, E. A. 2000. 3-D visualization of structural field data: examples from the Archean Caopatina Formation, Abitibi greenstone belt, Québec, Canada. *Computers & Geosciences,* 26**,** 509-530.

DE KLERK, W. J. 1992. *Petrogenesis of the upper critical zone in the western Bushveld complex with emphasis on the UG1 footwall and bastard units.* Rhodes University.

DE WIT, M. J., DE RONDE, C. E., TREDOUX, M., ROERING, C., HART, R. J., ARMSTRONG, R. A., GREEN, R. W., PEBERDY, E. & HART, R. A. 1992. Formation of an Archaean continent. *Nature,* 357**,** 553-562.

DU PLESSIS, A. & KLEYWEGT, R. 1987. A dipping sheet model for the mafic limbs of the Bushveld Complex. *South African journal of geology,* 90**,** 1-6.

DU PLESSIS, A. & LEVITT, J. G. 1987. On the structure of the Rustenburg layered suite—insight from seismic reflection data: . *Indaba on the tectonic setting of layered intrusives.* University of Pretoria, Institute for Geological Research: Geological Society of South Africa, Geological Survey of South Africa, .

DU PLESSIS, C. & WALRAVEN, F. 1990. The tectonic setting of the Bushveld Complex in Southern Africa, Part 1. Structural deformation and distribution. *Tectonophysics,* 179**,** 305-319.

EALES, H. 2002. Caveats in defining the magmas parental to the mafic rocks of the Bushveld Complex, and the manner of their emplacement: review and commentary. *Mineralogical Magazine,* 66**,** 815-832.

EALES, H., BOTHA, W., HATTINGH, P., DE KLERK, W., MAIER, W. & ODGERS, A. 1993. The mafic rocks of the Bushveld Complex: a review of emplacement and crystallization history, and mineralization, in the light of recent data. *Journal of African Earth Sciences (and the Middle East),* 16**,** 121-142.

EALES, H. & CAWTHORN, R. 1996. The Bushveld Complex. *Developments in Petrology,* 15**,** 181-229.

EALES, H., MARSH, J., MITCHELL, A., DE KLERK, W., KRUGER, F. & FIELD, M. 1986. Some geochemical constraints upon models for the crystallization of the Upper Critical Zone–Main Zone interval, Northwestern Bushveld Complex. *Mineralogical Magazine,* 50**,** 567-582.

EINSELE, G.2000. *Sedimentary basins: evolution, facies, and sediment budget*. Springer.

ELLIOTT, D. 1976. The energy balance and deformation mechanisms of thrust sheets. *Philosophical Transactions of the Royal Society of London. Series A, Mathematical and Physical Sciences,* 283**,** 289-312.

EMELEUS, C., CHEADLE, M., HUNTER, R., UPTON, B. & WADSWORTH, W. 1996. The Rum layered suite. *Developments in Petrology,* 15**,** 403-439.

ERIKSSON, P., HATTINGH, P. & ALTERMANN, W. 1995. An overview of the geology of the Transvaal Sequence and Bushveld Complex, South Africa. *Mineralium Deposita,* 30**,** 98-111.

ERIKSSON, P. & RECZKO, B. 1995. The sedimentary and tectonic setting of the Transvaal Supergroup floor rocks to the Bushveld Complex. *Journal of African Earth Sciences,* 21**,** 487-504.

ERIKSSON, P., SCHWEITZER, J., BOSCH, P., SCHEREIBER, U., VAN DEVENTER, J. & HATTON, C. 1993. The Transvaal sequence: an overview. *Journal of African Earth Sciences (and the Middle East),* 16**,** 25-51.

EVENICK, J. 2008. *Introduction to well logs and subsurface maps*, PennWell Books.

EVENICK, J.C., HATCHER, D.R., & BAKER, S.G. 2008. Trend surface residual anomaly mapping and well data may be underutilized combo. Oil and Gas journal.106.4.

FERGUSON, J., & BOTHA, E. (1963). Some aspects of igneous layering in the basic zones of the Bushveld Complex. *Trans Geol Soc South Afr*, *66*, 259-282.

FRIESE, A.E.W. (2004). Geology and tectono-magmatic evolution of the PPL concession area, Villa Nora-Potgietersrus Limb, Bushveld Complex. Geological Visitor Guide, Potgietersrus Platinums Limited, 57 pp.

GALINDO, I. & GUDMUNDSSON, A. 2012. Basaltic feeder dykes in rift zones: geometry, emplacement, and effusion rates. *Natural Hazards and Earth System Sciences,* 12**,** 3683-3700.

GIBSON, J., WALSH, J. & WATTERSON, J. 1989. Modelling of bed contours and cross-sections adjacent to planar normal faults. *Journal of Structural Geology,* 11**,** 317-328.

GODEL, B., BARNES, S.-J. & MAIER, W. D. 2011. Parental magma composition inferred from trace element in cumulus and intercumulus silicate minerals: An example from the Lower and Lower Critical Zones of the Bushveld Complex, South-Africa. *Lithos,* 125**,** 537-552.

GOUGH, D. I., & VAN NIEKERK, C. B. 1959. A study of the palaeomagnetism of the bushveld gabbrot. *Philosophical Magazine*, *4*(37), 126-136.

GOOVAERTS, P. 1997. *Geostatistics for natural resources evaluation*, Oxford university press.

GROSHONG JR, R. H. 2006. 3D Structural Geology–A Practical Guide to Quantitative Surface and Map Interpretation. Springer.

GROVES, D. I., GOLDFARB, R. J., KNOX-ROBINSON, C. M., OJALA, J., GARDOLL, S., YUN, G. Y. & HOLYLAND, P. 2000. Late-kinematic timing of orogenic gold deposits and significance for computer-based exploration techniques with emphasis on the Yilgarn Block, Western Australia. *Ore Geology Reviews,* 17**,** 1-38.

GROVES, D. I., HO, S. E., ROCK, N. M., BARLEY, M. E. & MUGGERIDGE, M. T. 1987. Archaean cratons, diamond and platinum: Evidence for coupled long-lived crust-mantle systems. *Geology,* 15**,** 801-805.

GUDMUNDSSON, A., FRIESE, N., ANDREW, R., PHILIPP, S. L., ERTL, G., LETOURNEUR, L., THORDARSON, T., SELF, S. & LARSEN, G. 2009. Effects of dyke emplacement and plate pull on mechanical interaction between volcanic systems and central volcanoes in Iceland. *Studies in volcanology: The legacy of George Walker: International Association of Volcanology and Chemistry of the Earth's Interior Special Publication,* 2**,** 331-347.

HALL, A. L. 1932. *The Bushveld igneous complex of the central Transvaal*, The Government printer.

HAMILTON, J. 1977. Sr isotope and trace element studies of the Great Dyke and Bushveld mafic phase and their relation to early Proterozoic magma genesis in southern Africa. *Journal of Petrology,* 18**,** 24-52.

HARMER, R. E. & ARMSTRONG, R. A. 2000. Duration of Bushveld Complex (sensu lato) magmatism: constraints from new SHRIMP zircon chronology. Workshop on the Bushveld Complex, Gethane Lodge, Burgersfort, University of the Witwatersrand, Johannesburg

HARMER, R. E. & VON GRUENEWALDT, G. 1991. A review of magmatism associated with the Transvaal Basin - implications for its tectonic setting. *South Afr. J. Geol.,* 94**,** 104-122.

HARNEY, D. M. W., MERKLE, R. K. W. & VON GRUENEWALDT, G. 1990. Plagioclase composition in the Upper zone, eastern Bushveld Complex - support for magma mixing at the Main Magnetite Layer. *Inst. Geol. Res. Bushveld Complex.* Univ. Pretoria

HARRIS, C. & CHAUMBA, J. 2000. Crustal contamination and fluid-rock interaction in the Platreef of the northern lobe of the Bushveld intrusion. *Journal of African Earth Sciences,* 31**,** 28-28.

HARTZER, F. 1989. Stratigraphy, structure, and tectonic evolution of the Crocodile River Fragment. *South African journal of geology,* 92**,** 110-124.

HARTZER, F. 1995. Transvaal Supergroup inliers: geology, tectonic development and relationship with the Bushveld Complex, South Africa. *Journal of African Earth Sciences,* 21**,** 521-547.

HATTINGH, P. J. (1995). Palaeomagnetic constraints on the emplacement of the Bushveld Complex. *Journal of African Earth Sciences*, *21*(4), 549-551.

HATTON, C. & SHARPE, M. 1988. *Significance and origin of boninite-like rocks associated with the Bushveld Complex*, University of Pretoria Institute for Geological Research on the Bushveld Complex.

HATTON, C. & VON GRUENEWALDT, G. 1987. The geological setting and petrogenesis of the Bushveld chromitite layers. *Evolution of chromium ore fields***,** 109-143.

HATTON, C. J., & Von GRUENEWALDT, G. (1985). Chromite from the Swartkop chrome mine; an estimate of the effects of subsolidus reequilibration. *Economic Geology*, *80*(4), 911-924.

HINTZE, W. H. 1971. Depiction of Faults on Stratigraphic Isopach Maps: Geological Note. *AAPG Bulletin,* 55**,** 871-879.

HODGE, K. F., CARAZZO, G. & JELLINEK, A. M. 2012. Experimental constraints on the deformation and breakup of injected magma. *Earth and Planetary Science Letters,* 325**,** 52-62.

HOGAN, J. P., PRICE, J. D. & GILBERT, M. C. 1998. Magma traps and driving pressure: consequences for pluton shape and emplacement in an extensional regime. *Journal of Structural Geology,* 20**,** 1155-1168.

HOLWELL, D. & MCDONALD, I. 2007. Distribution of platinum-group elements in the Platreef at Overysel, northern Bushveld Complex: a combined PGM and LA-ICP-MS study. *Contributions to Mineralogy and Petrology,* 154**,** 171-190.

HOLWELL, D. A. & MCDONALD, I. 2006. Petrology, geochemistry and the mechanisms determining the distribution of platinum-group element and base metal sulphide mineralisation in the Platreef at Overysel, northern Bushveld Complex, South Africa. *Mineralium Deposita,* 41**,** 575-598.

HOLZER, L., BARTON, J., PAYA, B. & KRAMERS, J. 1999. Tectonothermal history of the western part of the Limpopo Belt: tectonic models and new perspectives. *Journal of African Earth Sciences,* 28**,** 383-402.

HOYLE, P. 1993.Chemical and modal variations at the top of the Upper Zone in the Northwestern Bushveld Complex. Symposium on Layering in Igneous Complexes, Univ. Witwatersrand, Johannesburg. .

HUERTA, A. D. & RODGERS, D. W. 1996. Kinematic and dynamic analysis of a low-angle strike-slip fault: The Lake Creek fault of south-central Idaho. *Journal of Structural Geology,* 18**,** 585-593.

HULBERT, L. & VON GRUENEWALDT, G. 1985. Textural and compositional features of chromite in the lower and critical zones of the Bushveld Complex south of Potgietersrus. *Economic Geology,* 80**,** 872-895.

HUNTER, D.R.1975. The regional geological setting of the Bushveld Complex. (An adjunct to the provisional tectonic map of the Bushveld Complex). Econ.Geol. Res. Unit.Univ.Witwatersrand, Johannesburg, 18pp.

HUNTER, D. R. 1976. Some enigmas of the Bushveld Complex. *Economic Geology,* 71**,** 229-248.

ILJINA, M. J. & LEE, C. A. 2005. PGE deposits in the marginal series of layered intrusions. *Exploration for platinum group element deposits. Mineralog Assoc Can Short Course Series,* 35**,** 75-96.

IRVINE, T. N. (1987). Layering and related structures in the Duke Island and Skaergaard intrusions: similarities, differences, and origins. In *Origins of igneous layering* (pp. 185-245). Springer Netherlands.

JUDEEL, G. T. & HARTMANN, A. 2008. Ground support at Crocodile river mine located in the brits graben of the Western limb of the Bushveld Complex. 6th International Symposium on Ground Support in mining and civil engineering construction, 30th March -3rd April Cape Town, South Africa., 525-544.

KAVANAGH, J. L., MENAND, T. & SPARKS, R. S. J. 2006. An experimental investigation of sill formation and propagation in layered elastic media. *Earth and Planetary Science Letters,* 245**,** 799-813.

KGASWANE, E. M., NYBLADE, A. A., DURRHEIM, R. J., JULIÀ, J., DIRKS, P. H. & WEBB, S. J. 2012. Shear wave velocity structure of the Bushveld Complex, South Africa. *Tectonophysics,* 554**,** 83-104.

KEYSER, N., FOURIE, C. J. S. & COLE, P. 1997. *Geological Map of the Republic of South Africa and the Kingdoms of Lesotho and Swaziland 1997*, Council for Geoscience.

KINLOCH, E. 1982. Regional trends in the platinum-group mineralogy of the critical zone of the Bushveld Complex, South Africa. *Economic Geology,* 77**,** 1328-1347.

KINNAIRD, J. A. 2005. The Bushveld large igneous province. *Review Paper, The University of the Witwatersrand, Johannesburg, South Africa, 39pp*.

KINNAIRD, J. A., HUTCHINSON, D., SCHURMANN, L., NEX, P. & DE LANGE, R. 2005. Petrology and mineralisation of the southern Platreef: northern limb of the Bushveld Complex, South Africa. *Mineralium Deposita,* 40**,** 576-597.

KINNAIRD, J. A. & MCDONALD, I. 2005. An introduction to mineralisation in the northern limb of the Bushveld Complex. *Applied Earth Science: Transactions of the Institutions of Mining and Metallurgy: Section B,* 114**,** 194-198.

KLEMM, D., HENCKEL, J., DEHM, R. & VON GRUENEWALDT, G. 1985. The geochemistry of titanomagnetite in magnetite layers and their host rocks of the eastern Bushveld Complex. *Economic Geology,* 80**,** 1075-1088.

KOCA, D., SMITH, B. & SYKES, M. T. 2006. Modelling regional climate change effects on potential natural ecosystems in Sweden. *Climatic Change,* 78**,** 381-406.

KRESIC, N. 2006. *Hydrogeology and groundwater modelling*, CRC press.

KRESIC, N. & MIKSZEWSKI, A. 2012. *Hydrogeological Conceptual Site Models: Data Analysis and Visualization*, CRC Press.

KRIGE, D. 1951. *A Statistical Approach to Some Mine Valuation and Allied Problems on the Witwatersrand: By DG Krige.* University of the Witwatersrand.

KRIGE, D. G. & KRIGE, D. 1981. *Lognormal-de Wijsian geostatistics for ore evaluation*, South African Institute of mining and metallurgy Johannesburg.

KRUGER, F. 1994. The Sr-isotopic stratigraphy of the western Bushveld Complex. *S Afr J Geol,* 97**,** 393-398.

KRUGER, F. J. 2005a. The main zone of the Bushveld Complex: source of the Merensky Reef and the Platreef. In *10th Intl Pt Symp, Oulu*.

KRUGER, F. J. 2005b. Filling the Bushveld Complex magma chamber: lateral expansion, roof and floor interaction, magmatic unconformities, and the formation of giant chromitite, PGE and Ti-V-magnetitite deposits. *Mineralium Deposita,* 40**,** 451-472.

KRUGER, F., CAWTHORN, R. & WALSH, K. 1987. Strontium isotopic evidence against magma addition in the Upper Zone of the Bushveld Complex. *Earth and Planetary Science Letters,* 84**,** 51-58.

KRUGER, F. J. 1990. The stratigraphy of the Bushveld Complex: a reappraisal and the relocation of the Main Zone boundaries. *South African journal of geology,* 93**,** 376-381.

KRUMBEIN, W. 1959. Trend surface analysis of contour-type maps with irregular control-point spacing. *Journal of Geophysical Research,* 64**,** 823-834.

LEE, C. 1981. Post-deposition structures in the Bushveld Complex mafic sequence. *Journal of the Geological Society,* 138**,** 327-341.

LEE, C. & SHARPE, M. R. 1983. *The Structural Setting of the Bushveld Complex: An Assessment Aided by LANDSAT Imagery*, University of Pretoria Institute for Geological Research on the Bushveld Complex.

LEE, C. A. 1996. *A review of mineralization in the Bushveld Complex and some other layered intrusion. Developments in Petrology.15. 103-145.*

LEE, W. & MERRIAM, D. F. 1954. *Preliminary Study of the Structure of Western Kansas*, State Geological Survey of Kansas, University of Kansas.

LEMON, A. M. & JONES, N. L. 2003. Building solid models from boreholes and user-defined cross-sections. *Computers & Geosciences,* 29**,** 547-555.

LETTS, S., TORSVIK, T. H., WEBB, S. J. & ASHWAL, L. D. 2009. Palaeomagnetism of the 2054 Ma Bushveld Complex (South Africa): implications for emplacement and cooling. *Geophys. J. Int.,* 179**,** 850-872.

LI, J. &HEAP, A.D. 2008. *A review of spatial interpolation methods for environmental scientists*, Geoscience Australia Canberra.

LI, J. & HEAP, A. D. 2011. A review of comparative studies of spatial interpolation methods in environmental sciences: performance and impact factors. *Ecological Informatics,* 6**,** 228-241.

LU, G. Y. & WONG, D. W. 2008. An adaptive inverse-distance weighting spatial interpolation technique. *Computers & Geosciences,* 34**,** 1044-1055.

LUNARDI, A. 2009. *Interpolation theory*, Edizioni della Normale.

MAIER, W., BARNES, S.-J. & GROVES, D. 2013. The Bushveld Complex, South Africa: formation of platinum–palladium, chrome-and vanadium-rich layers via hydrodynamic sorting of a mobilized cumulate slurry in a large, relatively slowly cooling, subsiding magma chamber. *Mineralium Deposita,* 48**,** 1-56.

MAIER, W. & EALES, H. V. 1997. *Correlation within the UG2-Merensky Reef interval of the Western Bushveld Complex, based on geochemical, mineralogical and petrological data*, Geological Survey of South Africa, Council for Geoscience.

MAIER, W., RASMUSSEN, B., FLETCHER, I. & YANG, S. 2012. Direct precipitation of Pt alloys from basaltic magma in the 2.77 Ga Monts de Cristal Complex, Gabon. In *Abstr, 12th Int Ni–Cu–PGE symposium, Guiyang*.

MAIER, W. D., ARNDT, N. T. & CURL, E. A. 2000. Progressive crustal contamination of the Bushveld Complex: evidence from Nd isotopic analyses of the cumulate rocks. *Contributions to Mineralogy and Petrology,* 140**,** 316-327.

MAIER, W. D. & GROVES, D. I. 2011. Temporal and spatial controls on the formation of magmatic PGE and Ni–Cu deposits. *Mineralium Deposita,* 46**,** 841-857.

MANYERUKE, T. D. 2003. *The petrography and geochemistry of the Platreef on the farm Townlands, near Potgietersrus, northern Bushveld Complex.* University of Pretoria.

MAPEO, R. B. M., KAMPUNZU, A. B., RAMOKATE, L. V., CORFU, F., & KEY, R. M. 2004. Bushveld-age magmatism in Southeastern Botswana: evidence from U-Pb zircon and titanite geochronology of the Moshaneng Complex. *South African Journal of Geology*, *107*(1-2), 219-232.

MATHEZ, E., VANTONGEREN, J. & SCHWEITZER, J. 2013. On the relationships between the Bushveld Complex and its felsic roof rocks, part 1: petrogenesis of Rooiberg and related felsites. *Contributions to Mineralogy and Petrology,* 166**,** 435-449.

McCOURT, S. 1995. The crustal architecture of the Kaapvaal crustal block South Africa, between 3.5 and 2.0 Ga. *Mineralium Deposita,* 30**,** 89-97.

MCDONALD, I., HOLWELL, D. A. & ARMITAGE, P. E. 2005. Geochemistry and mineralogy of the Platreef and "Critical Zone" of the northern lobe of the Bushveld Complex, South Africa: implications for Bushveld stratigraphy and the development of PGE mineralisation. *Mineralium Deposita,* 40**,** 526-549.

MEI, S. 2009. Go sueologist-controlled trends versus computer-controlled trends: introducing a high-resolution approach tbsurface structural mapping using well-log data, trend surface analysis, and geospatial analysis. *Canadian Journal of Earth Sciences,* 46**,** 309-329.

Meyer, R., De Beer, H., 1987. Structure of the Bushveld Complex from resistivity measurements. Nature 325, 610–612.

MITCHELL, A. 1990. The stratigraphy, petrography and mineralogy of the Main Zone of the Northwestern Bushveld Complex.

MITCHELL, A. & SCOON, R. 1991. Discussion on The stratigraphy of the Bushveld Complex; a reappraisal and the relocation of the Main Zone boundaries. *South African journal of geology,* 94**,** 183-187.

MITCHELL, A. A., EALES, H. V. & KRUEGER, F. J. 1998. Magma replenishment, and the significance of poikilitic textures, in the Lower Main Zone of the western Bushveld Complex, South Africa. *Mineralogical Magazine,* 62**,** 435-450.

MOLYNEUX, T. 1974. A geological investigation of the Bushveld Complex in Sekhukhuneland and part of the Steelpoort valley. *Transactions of the Geological Society of South Africa,* 77**,** 329-338.

MOLYNEUX, T. G. 1970. *A geological investigation of the Bushveld Complex in Sekhukhuneland and part of the Steelpoort Valley, Eastern Transvaal with particular reference to the oxide minerals.* Universiteit van Pretoria.

MOSSOP, G. D. & SHETSEN, I. 1994. *Geological atlas of the Western Canada sedimentary basin*, Alberta Research, Council Canadian Society of Petroleum Geologists, Published jointly by the Canadian Society of Petroleum Geologists and the Alberta Research Council.

NALDRETT, A., WILSON, A., KINNAIRD, J., YUDOVSKAYA, M. & CHUNNETT, G. 2012. The origin of chromitites and related PGE mineralization in the Bushveld Complex: new mineralogical and petrological constraints. *Mineralium Deposita,* 47**,** 209-232.

NALDRETT, A. J. 2009. Fundamentals of magmatic sulfide deposits. In: Li C, Ripley EM (eds) New developments in magmatic Ni–Cu and PGE deposits. *Geol Publ House*.

NALDRETT, T., KINNAIRD, J., WILSON, A. & CHUNNETT, G. 2008. Concentration of PGE in the Earth's Crust with Special Reference to the Bushveld Complex. *Earth Science Frontiers,* 15**,** 264-297.

NASLUND, H. & McBIRNEY, A. 1996. Mechanisms of formation of igneous layering. *Developments in petrology,* 15**,** 1-43.

NEX, P. 2004. Formation of bifurcating chromitite layers of the UG1 in the Bushveld Igneous Complex, an analogy with sand volcanoes. *Journal of the Geological Society,* 161**,** 903-909.

NEX, P., KINNAIRD, J., INGLE, L., VAN DER VYVER, B. & CAWTHORN, R. 1998. A new stratigraphy for the Main Zone of the Bushveld Complex, in the Rustenburg area. *South African Journal of Geology,* 101**,** 215-223.

NEX, P. A. 2005. The structural setting of mineralisation on Tweefontein Hill, northern limb of the Bushveld Complex, South Africa. *Applied Earth Science: Transactions of the Institutions of Mining and Metallurgy: Section B,* 114**,** 243-251.

ODGERS, A. T. R., HINDS, R. C., & VON GRUENEWALDT, G. (1993). Interpretation of a seismic reflection survey across the southern Bushveld Complex. *South African journal of geology*, *96*(4), 205-212.

ODGERS, A. T. R. & DU PLESSIS, A. 1993. Interpretation of a regional reflection seismic survey in the north-eastern Bushveld Complex. In *3rd SAGA Biennial Conference and Exhibition*.

OLSSON, J., SÖDERLUND, U., KLAUSEN, M. & ERNST, R. 2010. U–Pb baddeleyite ages linking major Archean dyke swarms to volcanic-rift forming events in the Kaapvaal craton (South Africa), and a precise age for the Bushveld Complex. *Precambrian Research,* 183**,** 490-500.

PAULSON, O. L., & PEASCATORE F.T. 1979. *The Effects of the Phillips Fault Zone on Subsurface Jurassic Sediments and Petroleum Production of Jasper County, Mississippi*. Mississippi Mineral Resources Institute, University of Mississippi.

REID, D. & BASSON, I. 2002. Iron-rich ultramafic pegmatite replacement bodies within the Upper Critical Zone, Rustenburg Layered Suite, Northam Platinum Mine, South Africa. *Mineralogical Magazine,* 66**,** 895-914.

REISBERG, L., TREDOUX, M., HARRIS, C., COFTIER, A. & CHAUMBA, J. 2011. Re and Os distribution and Os isotope composition of the Platreef at the Sandsloot–Mogolakwena mine, Bushveld complex, South Africa. *Chemical Geology,* 281**,** 352-363.

REYNOLDS, I. M. 1985. The nature and origin of titaniferous magnetite-rich layers in the upper zone of the Bushveld Complex; a review and synthesis. *Economic Geology,* 80**,** 1089-1108.

REYNOLDS, I. M. (ed.) 1986. *The mineralogy and ore petrology of the Bushveld titaniferous magnetite-rich layers: In: Mineral deposits of southern Africa,* Johannesburg: Geol Soc S Afr.

ROBERTS, M., REID, D., MILLER, J., BASSON, I. 2007. The Merensky Cyclic Unit and its impact on footwall cumulates below Normal and Regional Pothole reef types in the Western Bushveld Complex. *Mineralium Deposita,* 42**,** 271-292.

ROSENBERG, C. & HANDY, M. 2005. Experimental deformation of partially melted granite revisited: implications for the continental crust. *Journal of Metamorphic Geology,* 23**,** 19-28.

SACS (SOUTH AFRICA COMMITTEE FOR STRATIGRAPHY) 1980. Stratigraphy of South Africa Part 1: Lithostratigraphy of the Republic of South Africa, South West

Africa/Namibia and the Republics of Bophuthatswana, Transkei and Venda. *Handbook Geological Survey South Africa.* Pretoria, South Africa.

SALVADOR, E. D. & RICCOMINI, C. 1995. Neotectoˆ nica de regia˜o do alto estrutural de Queluz. In: GrohmannC.H. Trend-surface analysis of morphometric parameters: A case study in Southeastern Brazil. *Revista Brasileira de Geociencias* 25, **,** 151–164.

SCHOUWSTRA, R., KINLOCH, E. & LEE, C. 2000. A short geological review of the Bushveld Complex. *Platinum Metals Review,* 44**,** 33-39.

SCOATES, J., WALL, C., FRIEDMAN, R., VANTONGEREN, J. & MATHEZ, E. 2011. Progress in resolving the duration of magmatism in the Paleoproterozoic Bushveld Complex. AGU Fall Meeting Abstracts, 2501.

SCOATES, J. S. & FRIEDMAN, R. M. 2008. Precise age of the platiniferous Merensky Reef, Bushveld Complex, South Africa, by the U-Pb zircon chemical abrasion ID-TIMS technique. *Econ. Geol.,* 103**,** 465-471.

SCOATES, J. S., WALL, C. J., FRIEDMAN, R. M., VANTONGEREN, J. A. & MATHEZ, E. A 2012. The age of the Bushveld Complex. Abstr, Goldschmidt Conference, Montreal, Canada.

SCOON, R. N. 2002. A new occurrence of Merensky reef on the flanks of the Zaaikloof dome, Southeastern Bushveld Complex: Relationship between diapirism and magma replenishment. *Economic Geology,* 97**,** 1037-1049.

SCOON, R. N. & MITCHELL, A. A. 1994. Discordant iron-rich ultramafic pegmatites in the Bushveld Complex and their relationship to iron-rich intercumulus and residual liquids. *Journal of Petrology,* 35**,** 881-917.

Sharpe, M.R & Snyman, lA (1980). A model for the emplacement of the eastern compartment of the Bushveld Complex. *Tectonophys ics,* 65, 85-11O.

SHARPE, M. 1981. The chronology of magma influxes to the eastern compartment of the Bushveld Complex as exemplified by its marginal border groups. *Journal of the Geological Society,* 138**,** 307-326.

SHARPE, M. R., BAHAT, D. & VON GRUENEWALDT, G. 1980. *The concentric elliptical structure of feeder sites to the Bushveld Complex and possible economic implications*, Institute for Geological Research on the Bushveld Complex, University of Pretoria.

SHEPPARD, S. R. 2005. Landscape visualisation and climate change: the potential for influencing perceptions and behaviour. *Environmental Science & Policy,* 8**,** 637-654.

SIBSON, R. H. 2003. Brittle-failure controls on maximum sustainable overpressure in different tectonic regimes. *AAPG bulletin,* 87**,** 901-908.

SILVER, P. G., FOUCH, M. J., GAO, S. S. & SCHMITZ, M. 2004. Seismic anisotropy, mantle fabric, and the magmatic evolution of Precambrian southern Africa. *South African Journal of Geology,* 107**,** 45-58.

SKYTTA, P., BAUER, T., HERMANSSON, T., DEHGHANNEJAD, M., JUHLIN, C., JUANATEY, M. D. L. A. G., HÜBERT, J. & WEIHED, P. 2013. Crustal 3-D geometry of the Kristineberg area (Sweden) with implications on VMS deposits. *Solid Earth,* 4**,** 387-404.

SMITH, D. S. & BASSON, I. J. 2006. Shape and distribution analysis of Merensky Reef potholing, Northam Platinum Mine, western Bushveld Complex: implications for pothole formation and growth. *Mineralium Deposita,* 41**,** 281-295.

SVENSEN, H., PLANKE, S., CHEVALLIER, L., MALTHE-SØRENSSEN, A., CORFU, F. & JAMTVEIT, B. 2007. Hydrothermal venting of greenhouse gases triggering Early Jurassic global warming. *Earth and Planetary Science Letters,* 256**,** 554-566.

TEARPOCK, D. J. & BISCHKE, R. E. 2002. *Applied subsurface geological mapping with structural methods*, Pearson Education.

TEGNER, C., CAWTHORN, R. G. & KRUGER, F. J. 2006. Cyclicity in the Main and Upper Zones of the Bushveld Complex, South Africa: crystallization from a zoned magma sheet. *Journal of Petrology,* 47**,** 2257-2279.

TEIGLER, B., EALES, H. & SCOON, R. 1992. The cumulate succession in the critical zone of the Rustenburg layered suite at Brits, western Bushveld Complex. *South African journal of geology,* 95**,** 17-28.

TEIGLER, B. & EALES, H. V. 1996. The lower and critical zones of the western limb of the Bushveld Complex, as indicated by the Nooitgedacht boreholes. *Geol Surv S Afr Bull***,** 126.

THOMAS, R., VON VEH, M. & MCCOURT, S. 1993. The tectonic evolution of southern Africa: an overview. *Journal of African Earth Sciences (and the Middle East),* 16**,** 5-24.

TOBLER, W. R. 1970. A computer movie simulating urban growth in the Detroit region. *Economic geography*, 234-240.

TRUTER, F. 1955. Modern concepts of the Bushveld igneous complex. *CCTA South Reg. Comm. Geol,* 1, 77-87.

UKEN, R. 1998. *The geology and structure of the Bushveld Complex metamorphic aureole in the Olifants River area.* University of Natal, Durban.

UKEN, R. & WATKEYS, M. K. 1997a. Diapirism initiated by the Bushveld complex, South Africa. *Geology,* 25, 723-726.

UKEN, R. & WATKEYS, M. K. 1997b. An interpretation of mafic dyke swarms and their relationship with major mafic magmatic events on the Kaapvaal Craton and Limpopo Belt. *South Afr. J. Geol.,* 100, 341-348.

UNWIN, D. 2009. Trend Surface Models. *Kitchin R, Thrift N. International Encyclopedia of Human Geography. Oxford: Elsevier,* 11, 484-488.

VAN DER MERWE, M. 1976. The layered sequence of the Potgietersrus limb of the Bushveld Complex. *Economic Geology,* 71, 1337-1351.

VAN DER MERWE, M. 1978. *The geology of the basic and ultramafic rocks of the Potgietersrus limb of the Bushveld Complex.* Universityof The Witwatersrand. Typescript (Photocopy). Contains 4 Maps In Back Pocket.

VANTONGEREN, J. & MATHEZ, E. 2013. Incoming Magma Composition and Style of Recharge below the Pyroxenite Marker, Eastern Bushveld Complex, South Africa. *Journal of Petrology,* 54, 1585-1605.

VANTONGEREN, J. A., MATHEZ, E. A. & KELEMEN, P. B. 2010. A felsic end to Bushveld differentiation. *Journal of Petrology,* 51, 1891-1912.

VERMAAK, C. F. 1995. *The Platinum-Group Metals: A Global Perspective,* Randburg, South Africa : Mintek, 1995.

VILJOEN, M.1994. A review of regional variations in facies and grade distribution of the Merensky Reef, Western Bushveld Complex with some mining implications. Proceedings XVth CMMI Congress, 1994. 183-194.

VILJOEN, M. 1999. The nature and origin of the Merensky Reef of the western Bushveld Complex based on geological facies and geological data. *South African Journal of Geology,* 102, 221-239.

VILJOEN, M. & HIEBER, R. 1986. The Rustenburg section of Rustenburg Platinum Mines Limited, with reference to the Merensky reef. *Mineral deposits of southern Africa,* 2**,** 1107-1134.

VILJOEN, M. J. & SCHURMANN, L. W. 1998. Platinum-group metals. *In:* WILSON, M. C. G. & ANHAEUSSER, C. R. (eds.) *The Mineral Resources of South Africa.* Council for Geoscience, Pretoria, South Africa.

VILJOEN, M. J. & SCOON, R. N. 1985. The distribution and main geologic features of discordant bodies of iron-rich ultramafic pegmatite in the Bushveld Complex. *Economic Geology,* 80**,** 1109-1128.

VIRING, R. & COWELL, M. 1999. The Merensky Reef on Northam Platinum Limited. *South African Journal of Geology,* 102**,** 192-208.

VON GRUENEWALDT, G. 1968. The Rooiberg felsite north of Middelburg and its relation to the layered sequence of the Bushveld Complex. *Trans. Geol. Soc. S. Afr,* 71**,** 151-154.

VON GRUENEWALDT, G. 1973. The main and upper zones of the Bushveld Complex in the Roossenekal area, eastern Transvaal. *Transactions of the Geological Society of South Africa,* 76**,** 207-227.

VON GRUENEWALDT, G. 1979. A review of some recent concepts of the Bushveld Complex with particular reference to sulfide mineralization.17, 233-256.

VON GRUENEWALDT, G. & HARMER, R. 1992. Tectonic setting of Proterozoic layered intrusions with special reference to the Bushveld Complex. *Developments in Precambrian Geology,* 10**,** 181-213.

VON GRUENEWALDT, G. 1977. Mineral-Resources Of Bushveld Complex. *Minerals Science and Engineering,* 9**,** 83-95.

WACKERNAGEL, H. 1995. Multivariable geostatistics: an introduction with applications. Berlin: Springer-Verlag.

WAGER, L. 1963. The mechanism of adcumulus growth in the layered series of the Skaergaard intrusion. *Mineralogical Society of America Special Paper,* 1**,** 1-9.

WAGER, L. R. & BROWN, G. M. 1967. Layered igneous rocks.

WALRAVEN, F. 1982. *Textural, geochemical and genetical aspects of the granophyric rocks of the Bushveld Complex.* University of the Witwatersrand.

WALRAVEN, F., ARMSTRONG, R. A. & KRUGER, F. J. 1990. A chronostratigraphic framework for the north central Kaapvaal craton the Bushveld Complex and the Vredefort Structure. *Tectonophysics,* 171**,** 23–48.

WALRAVEN, F. & HATTINGH, E. 1993. Geochronology of the Nebo Granite, Bushveld Complex. *South African Journal of Geology,* 96**,** 31-41.WEBB, S. J., ASHWAL, L. D., & CAWTHORN, R. G. (2011). Continuity between eastern and western Bushveld Complex, South Africa, confirmed by xenoliths from kimberlite. *Contributions to Mineralogy and Petrology*, *162*(1), 101-107.

WEBB, S. J., CAWTHORN, R. G., NGUURI, T. & JAMES, D. 2004. Gravity modelling of Bushveld Complex connectivity supported by Southern African seismic experiment results. *South African Journal of Geology,* 107**,** 207-218.

WHARTON, S.R. 1993. Trend Surface Mapping. Geo. Soc. of Trinidad and Tobago Newsletter 19.http://www.gstt.org/publications/news/Newsletter19/trend%20surface.htm

WILLEMSE, J. 1964. A brief outline of the geology of the Bushveld Igneous Complex. *The geology of some ore deposits in Southern Africa,* 11**,** 91-128.

WILSON, H. B. 1956. Structure of lopoliths. *Geological Society of America Bulletin,* 67**,** 289-300.

WILSON, J., CAWTHORN, R., KRUGER, F. & GRUNDVIG, S. 1994. Intrusive origin for the unconformable Upper Zone in the Northern Gap, western Bushveld Complex. *S Afr J Geol,* 97**,** 462-472.

WILSON, M. & ANHAEUSSER, C. 1998. The mineral resources of South Africa(Handbook 16).

WREN, A E. 1973. Trend Surface Analysis. Canadian J of Exploration Geophysics..09,01.

XU, S.-S., VELASQUILLO-MARTINEZ, L. G., GRAJALES-NISHIMURA, J. M., MURILLO-MUÑETÓN, G., GARCÍA-HERNÁNDEZ, J. & NIETO-SAMANIEGO, A. F. 2004. Determination of fault slip components using subsurface structural contours: methods and examples. *J. Petrol. Geol,* 27**,** 277-298.

YANG, S.-H., MAIER, W. D., LAHAYE, Y. & O'BRIEN, H. 2013. Strontium isotope disequilibrium of plagioclase in the Upper Critical Zone of the Bushveld Complex: evidence for mixing of crystal slurries. *Contributions to Mineralogy and Petrology,* 166**,** 959-974.

YOUSSOF, M., THYBO, H., ARTEMIEVA, I. M. & LEVANDER, A. 2013. Moho depth and crustal composition in Southern Africa. *Tectonophysics,* 609**,** 267–287.

YUDOVSKAYA, M. A., KINNAIRD, J. A., SOBOLEV, A. V., KUZMIN, D. V., MCDONALD, I. & WILSON, A. H. 2013. Petrogenesis of the Lower Zone olivine-rich cumulates beneath the Platreef and their correlation with recognized occurrences in the Bushveld Complex. *Economic Geology,* 108**,** 1923-1952.

ZHOU, W., CHEN, G., LI, H., LUO, H. & HUANG, S. L. 2007. GIS application in mineral resource analysis—a case study of offshore marine placer gold at Nome, Alaska. *Computers & geosciences,* 33**,** 773-788.

ZIEGLAR, D. L. 2005. Structure Contour Map Born in India. AAPG, EXPLORER archives.

APPENDIX 1

1.1 Introduction

One major problem in geological mapping is the sparse distribution of outcrops and the need to draw accurate and reliable geological boundary across outcrop locations. Mapping becomes more difficult, especially in areas where most of the rocks are concealed below the surface. The key challenge here is how to unravel the subsurface structure and geometry of geological terrain where field based mapping might not adequately describe the geometry of geological boundaries. When available, borehole data and reports becomes an alternative. A large volume of these borehole data and reports are readily available. To produce a complete and consistent three-dimensional representation of the subsurface from sparsely distributed borehole data a lot of inferences (interpolations) between borehole logs has to be made. However, due to the large volume and distribution of the borehole data the selection of best interpolation method that will give a geological reasonable solution that is closest to already known geology becomes imperative. Borehole data are primary data obtained by direct observation and are highly accurate (Wu et al., 2004).]. Borehole log data are particularly useful in interpreting geologic structures from structure contour maps (three dimensional representation of the subsurface), isopach maps profiles, fence diagrams and cross-sections (Mei, 2009). Computer models usually have a variety of parameters that can be utilized so that the model will better reflect reality. This write-up attempt to find a particular set of parameter which result in a maximal value of a likelihood function, usually by using an optimization method.

Geostatistics involves continuity modeling of spatial data. The main reason for modeling spatial continuity is to assess spatial uncertainty and interpret the spatial distribution (Journel, 1989). Spatial analysis is the use of statistical assumption and techniques to improve the interpretation of spatially referenced data using interpolation methods. Spatial interpolation corresponds to measuring the same parameter at different locations and using these to estimate for the data at unsampled points. Eight different interpolation techniques were compared to estimate variations in depth of the Rustenburg Layered Suite (RLS) stratigraphic units around the Northeastern parts of the Eastern Bushveld Complex. This has helped to determine spatial pattern, trends, distribution, and the relationship between the depth of occurrence and thickness of each stratigraphic unit.

It enhances the visualization of pattern, continuity, and a variability of spatial data. This is due to the ability of interpolation methods to create continuous surfaces from scattered observations by estimating the depth of occurrence of lithology and structures at unsampled (in-between borehole) points based on the premises that close observations are likely to have similar values than those that are far apart (Tobler, 1970). The surface here represents a continuous representation of data with x,y and z values. Flow chart of spatial analysis process.

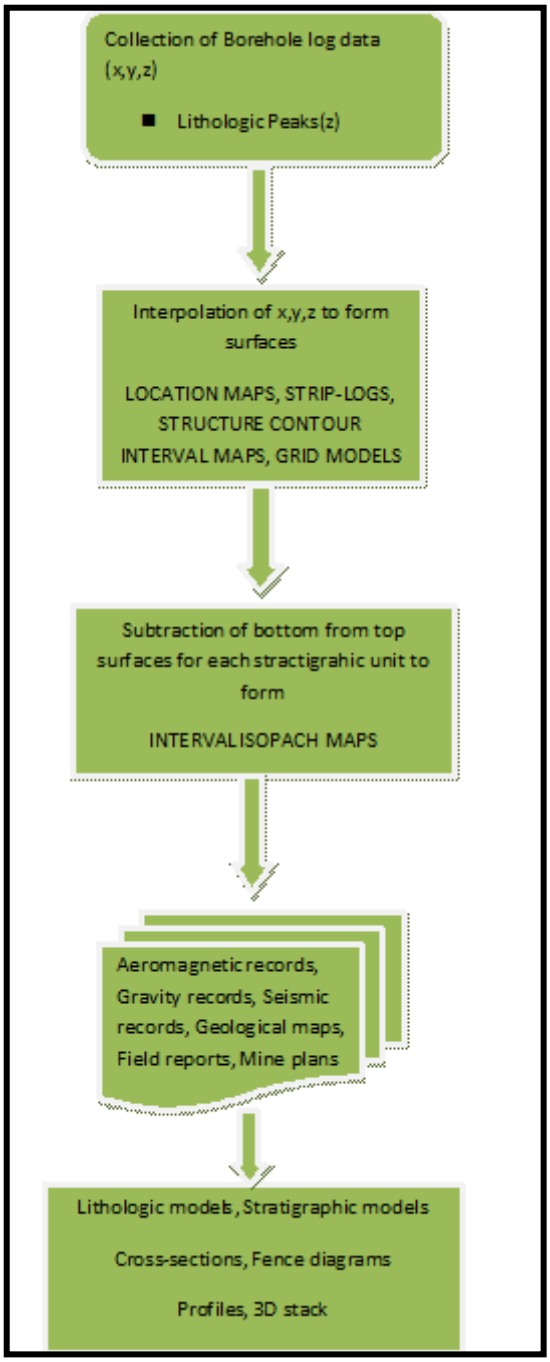

Figure 1A: Geospatial process flowchart

1.2 SELECTION OF APPROPRIATE INTERPOLATION METHOD

Selection of an appropriate spatial interpolation method it is a difficult task. The performance of the spatial interpolators according to (2008) depends on many factors including:

- the variable under study,
- the spatial configuration of the data,
- and the underlying assumptions of the spatial interpolation methods.

For this study, the best interpolation methods were selected based on closeness to know geology. It seems there is no simple answer regarding the choice of an appropriate spatial interpolator. The selection of best interpolation method for this study started with a collection of data over a subregion area (Northeastern parts of BIC) with known geology. Several search strategies were run over the sub region while trying to determine the best interpolation method. The best parameters that gives a result closest to known geology with the assumption that the difference in depth between two points on a surface is a function of distance and orientation.

A major factor in determining continuity among available data is the use of variogram. Variogram is used to display the variability between data points as a function of distance or direction. It can simply be defined as the direction along continuity (Journel, 1989). Variability increases and becomes stabilized at a given variability level called the sill. The range (zone of influence) is the distance at which the variogram reaches the sill value (Bourges et al., 2012).It is also useful in constructing three dimensional models that gives full interpretation of geologic continuity. This is based on the premises that close dataset are more related than distance dataset. Consequently, closely spaced data points show a low degree of variability while distant points show a higher degree of variability. This allows data, which were sampled at discreet units, to be modeled as a continuous function, and the value for any unknown point at any distance can be interpolated. This is also useful in determining the goodness of fit. This goodness of fit is determined by the correlation coefficient which could be positive or negative. Variogram determined from the measured or observed data were carefully fitted into available variogram models in rockworks. The result obtained using each of the eight variogram is presented below. The result shows that the model with Gaussian without nugget gave the highest correlation. This means that the nugget

effect is not allowed in a variogram, the resulting data grid may ultimately generate contours which honor the control points. It also shows the variability of the Z values for point pairs as a function of the distance between the points. RockWorks creates observed variograms of input data, and then finds the variogram model that offers the best fit - thus defining the distance and directional relationships in the input data.

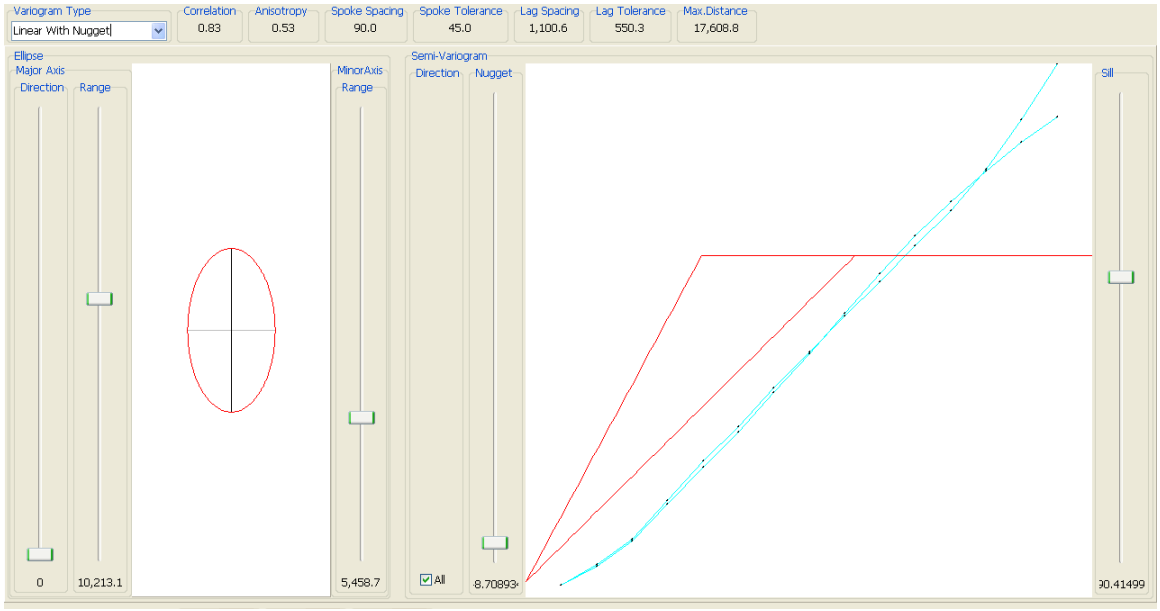

Figure 102: Variogram editor showing Linear with Nugget variogram with the directionality eclipse to the left, the observed variogram in blue and the calculated variogram in red (to the right).

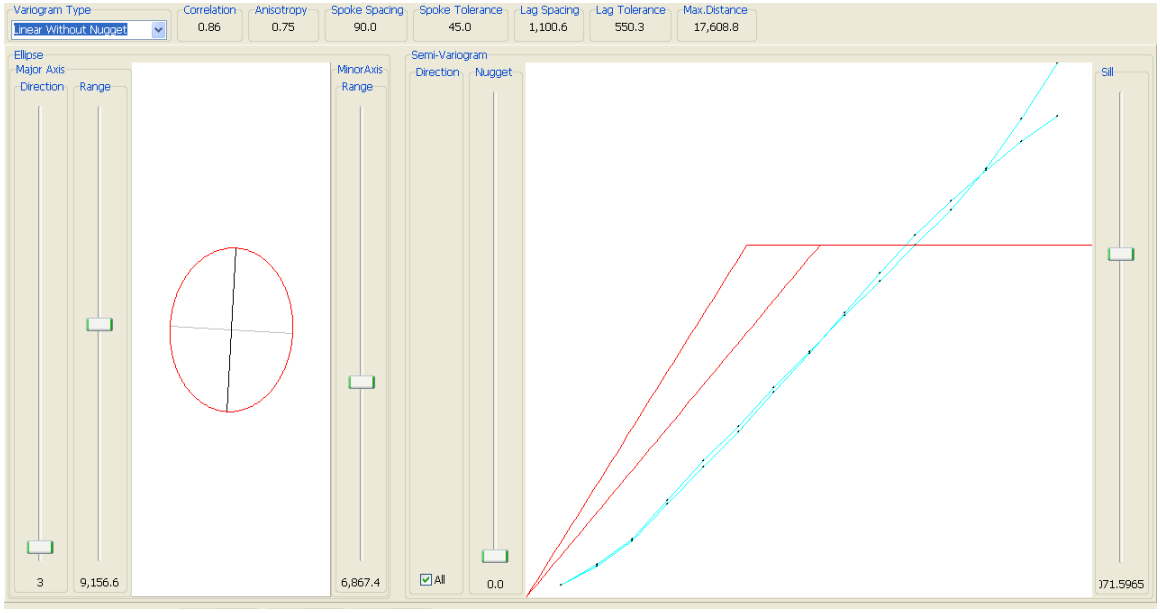

Figure 103: Variogram editor showing linear without Nugget option with directional eclipse to the left, the observed variogram in blue and the calculated variogram in red (to the right).

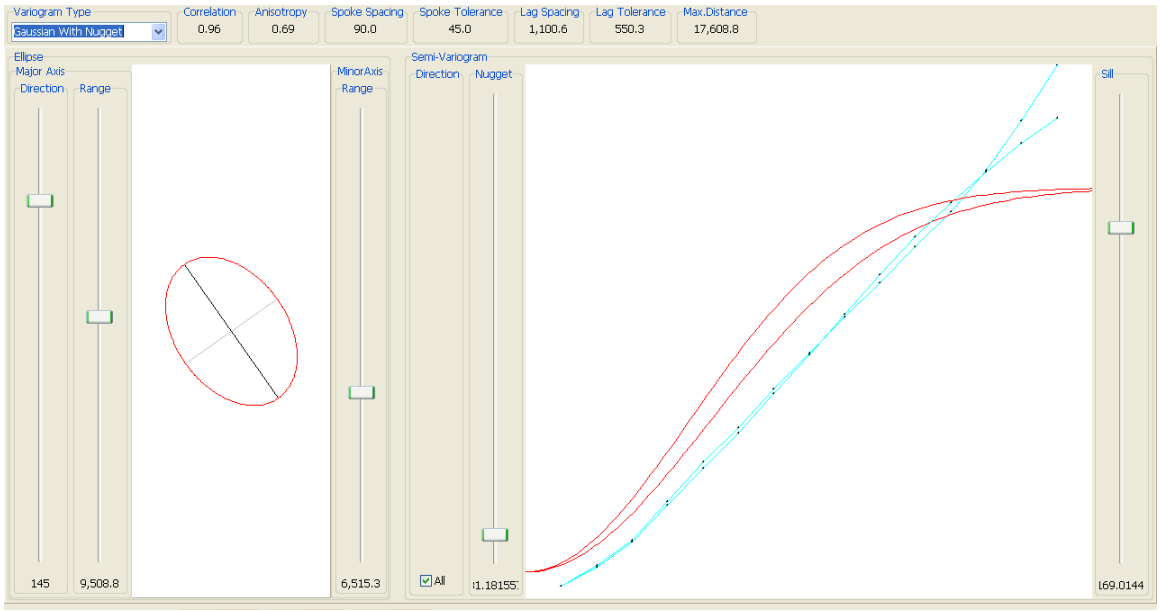

Figure 104: Variogram editor showing Gaussian with Nugget option with directional eclipse to the left, the observed variogram in blue and the calculated variogram in red (to the right).

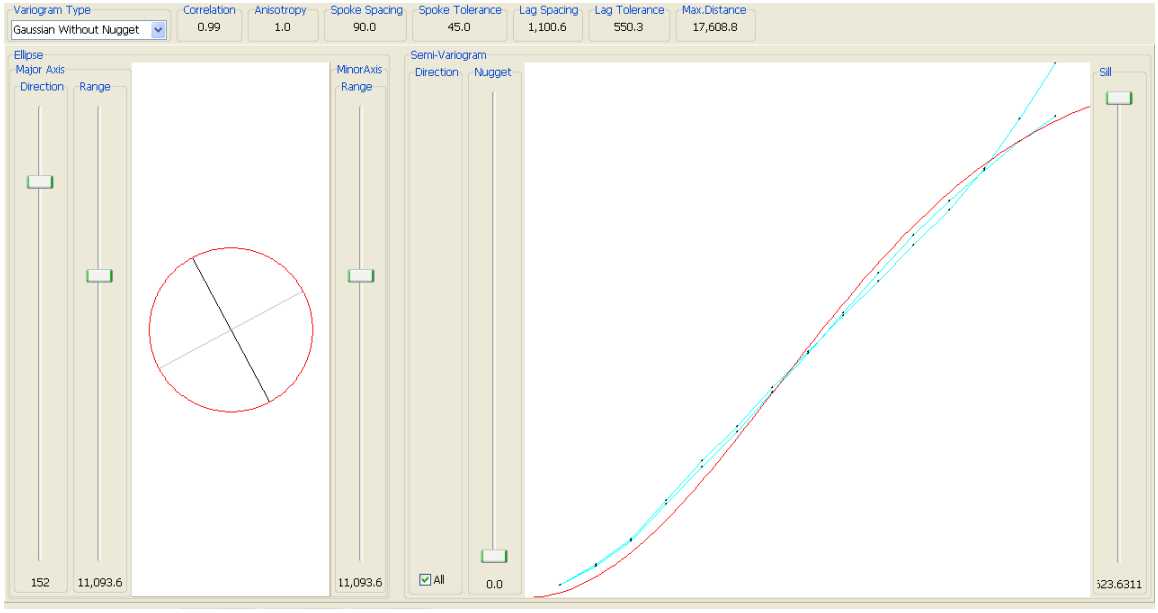

Figure 105: Variogram editor showing Gaussian without Nugget option with directional eclipse to the left, the observed variogram in blue and the calculated variogram in red (to the right).

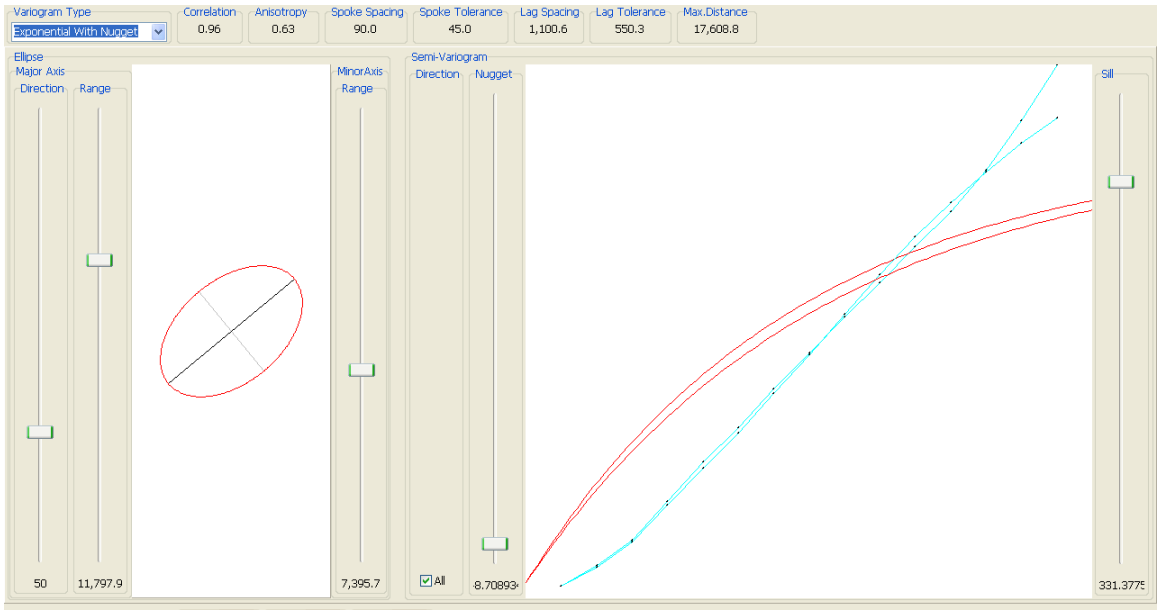

Figure 106: Variogram editor showing Spherical with Nugget option with directional eclipse to the left, the observed variogram in blue and the calculated variogram in red (to the right).

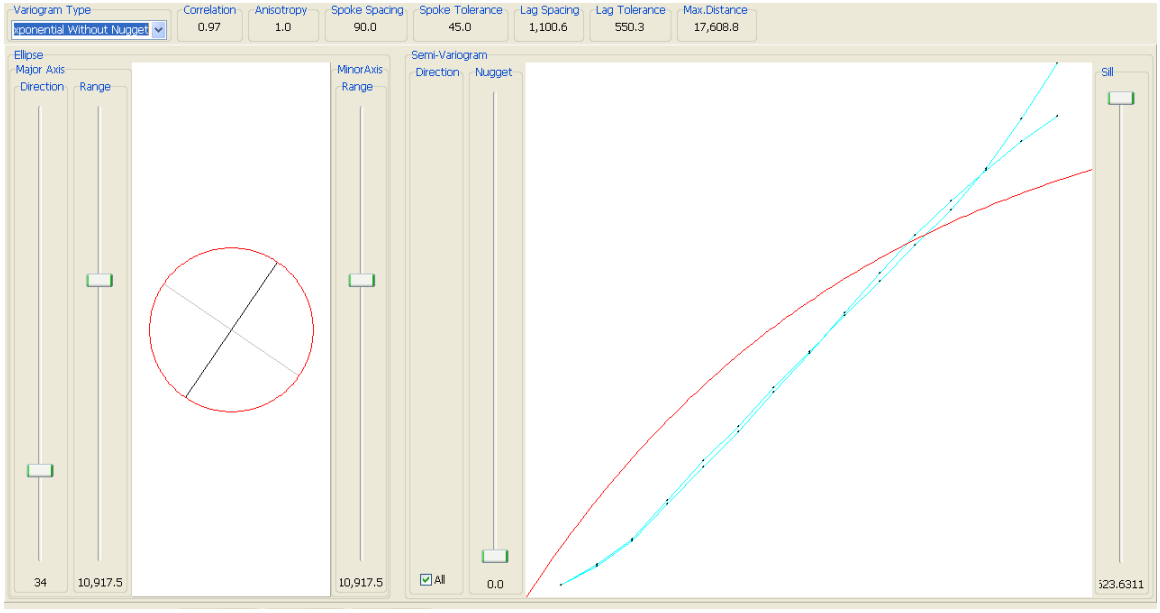

Figure 107: Variogram editor showing Spherical without Nugget option with directional eclipse to the left, the observed variogram in blue and the calculated variogram in red (to the right).

The most obvious factor on which to make this decision is the correlation shown between a particular variogram and observed data. The higher the correlation, the better the fit, the more accurate the model, and the more accurate the grid. The correlation coefficient is a representation of the correlation between the variogram and the lags, improperly selected lag dimensions (Manual kriging) won't necessarily be reflected by the correlation coefficient. In fact, very bad lag dimensions can produce high correlation coefficients.

Nugget means that the variogram does not go through the origin, i.e it did not go through the Y-axis. This signifies that the data varies at very close distance.

One other factor one might consider is the effect of the nugget is the resulting grids and contour maps. When the nugget effect is allowed in a variogram, the resulting data grid might generate contours, which do not honor the control points, thus showing you the error in data. However, with the advances in software engineering it is now possible to ensure that the contours honor the control points for better output. If the resultant contour map is objectionable, then re-kriging the data grid using a variogram with a suppressed nugget becomes a reasonable option.

1.3 INTERPOLATION METHODS

1.3.1 Inverse Distant Weighing (IDW)

$$\hat{v} = \frac{\sum_{i=1}^{n} \frac{1}{d_i} v_i}{\sum_{i=1}^{n} \frac{1}{d_i}}$$

v ˆ = value to be estimated
v i = known value
d_1..., d_n= distances from the *n* data points to the point estimated *n*

1.3.2 **Trangulation equation**

V = P(:,1).^2 + P(:,2).^2;

P= point

1.3.3 **Kriging interpolation method**

- Kriging types

Simple kriging requires that the mean of the variable over the field being estimated be constant and known (Wackernagel, 2003). Ordinary kriging does not require knowledge of the mean, as long as it remains constant over a specified field (Clark and Harper, 2001; Goovaerts, 1997). (Colin Childs, ArcUser,Jul-September,2004, ESRI educational services). The main advantage of Kriging

is that it is excellent at defining directional trends. The bull's-eye pattern of Inverse-Distance and the angularity of Triangulation are prevented with Kriging option.

Kriging with a trend model considers a variable mean, function of the coordinates values. That function is everywhere unknown but is of known functional form and could represent a local feature, while Universal Kriging assumes a trend component in the data Matheron (1969).
Block kriging estimates mean of variables over a block (Wackernagel, 2003). Cokriging entails the use of secondary variable in estimating the for the unsampled points (Goovaerts, 1997).

- Kriging equation

Where n represent the number of data Z is the parameter being measured at different locations. Z_α relate to the same attribute Z but at different locations

$x_\alpha \neq x_0$.

In this case, the depth of occurrence of a stratigraphic unit in the study area, is taken as $Z(x_0)$ at unsampled location x_0, *which is* estimated from *n* data $Z(x_\alpha)$ taken at *n* surrounding locations x_α:

$$Z^*(x_0)-m = \sum_{\alpha=1}^{n} \lambda_\alpha [Z(x_\alpha)-m] \qquad (1)$$

with m being the common expected value of the $(n + 1)$
RV's (random variables) $Z(x_0)$, $Z(x_\alpha)$, a = 1 , • • •, n. In practice, m would
be the mean of all Z data available within the same layer or stractigraphic unit
Defining the covariance function $C(h)$ as the covariance
between any two layer RV's $Z\{x)$, $Z(x + h)$, distant
of vector *h* but still within the same unit:

$C(h)$ = Cov $\{Z(x), Z(x + h)\}$

The simple kriging system (12) is:

$$\sum_{\beta=1}^{n} \lambda_\beta C(x_\alpha - X_0) = C(X_\alpha - X_0),\ \alpha = 1, \ldots n \qquad (2)$$

1.3.4 TREND SURFACE ANALYSIS (TSA)

Trend surface analysis involves fitting a simplified surface to the structure contour data using a regression matrix. The resultant (fitted) surfaces ultimately imitate the observed data as much as possible.

The principle of a TSA is a regression function that estimates the value Z_α at any location based on the X_α, Y_α coordinate of the location.

$Z_\alpha = f(X_\alpha, Y_\alpha)$

Z_α is property value at location α

X_α, Y_α are coordinate values at point α

F is regression function.

First order trend surface is described by

$$Z(X,Y) = a + bY + cX$$

Second order surface is a parabola described by equation

$$Z(X.Y) = a + bY + cX2 + dX + eX2 + fxy$$

Third order surface is defined by S shaped curve with equation

$$Z(X,Y) = a + bY + cY2 + dY3 + eX + fXY + gXY2 + hX2 + jX2Y + kX3$$

Not all the plot of the predicted or estimated versus the measured data will pass through the regression line. The vertical amount by which the line let-pass a datum is called the residual. It may be described as the measured data minus the predicted data. Random pattern of residual may not support a linear pattern. Non-linear data relationships are better observed in a residual plot than in a scatter plot (Stark, Philip B, 1997). Residuals with nonlinear association will plot around the X-axis, some will plot below the

X-axis as negative while some will plot above the X-axis as positives. This accounts for the negative values in some structure maps. Figure seven shows the plot of residual

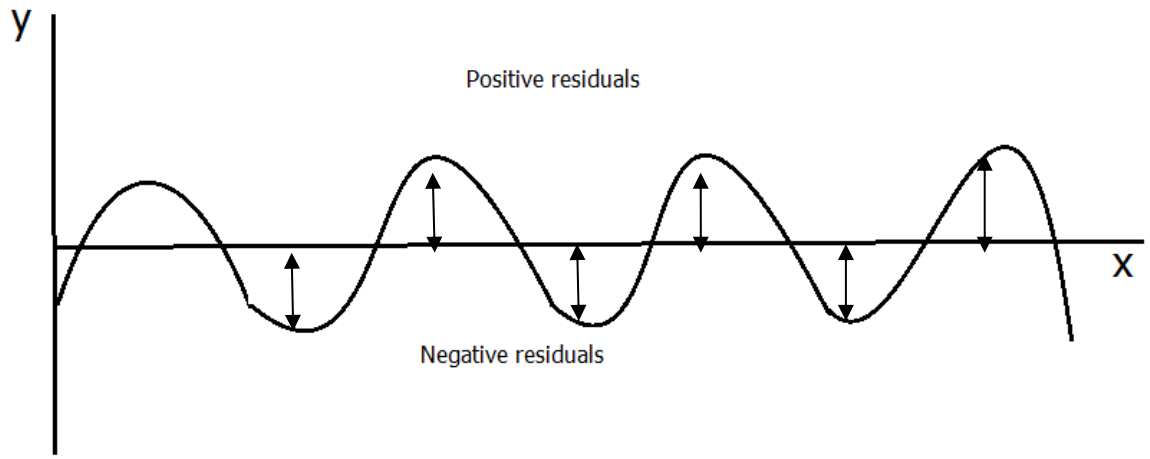

Figure 108: Example of a plot of predicted against original data and the calculated residuals

Beyond looking at the relationship between the measured and predicted data, goodness of fit and the use of global polynomial method to predict trend, Trend analysis can be used to geostatistically seperate the observed data into regional (trend or large scale component) and local (residual or small scale component) Mei, (). This method is employed in detecting subsurface structures. The method allows data manipulation and interpretation that reflect the geological input and expertise instead of the formal method that is primarily computer controlled (Mei, 2009). The regional component (trend surface) is defined by a global function that fits appropriately the entire map. In which case distant measured data are incorporated and given equal weight as close data in the analysis. The local component (residual map) only considers near data and attributes less weight to distant data. Further characterization of the original data was carried out by plotting Scattergram of observed/measured Z values of the Merensky reef versus computed node Z values for corresponding locations in an existing grid model. Different interpolation methods were plotted with the original data to determine the correlation between the original measured data and the calculated/ estimated data.The regression line/best fit line estimates the relationship between X and Y variables, it is used in characterizing the spread of the variables on a scattergram. High fidelity option was utilized to control the interpolation methods to honour the observed points as much as possible.

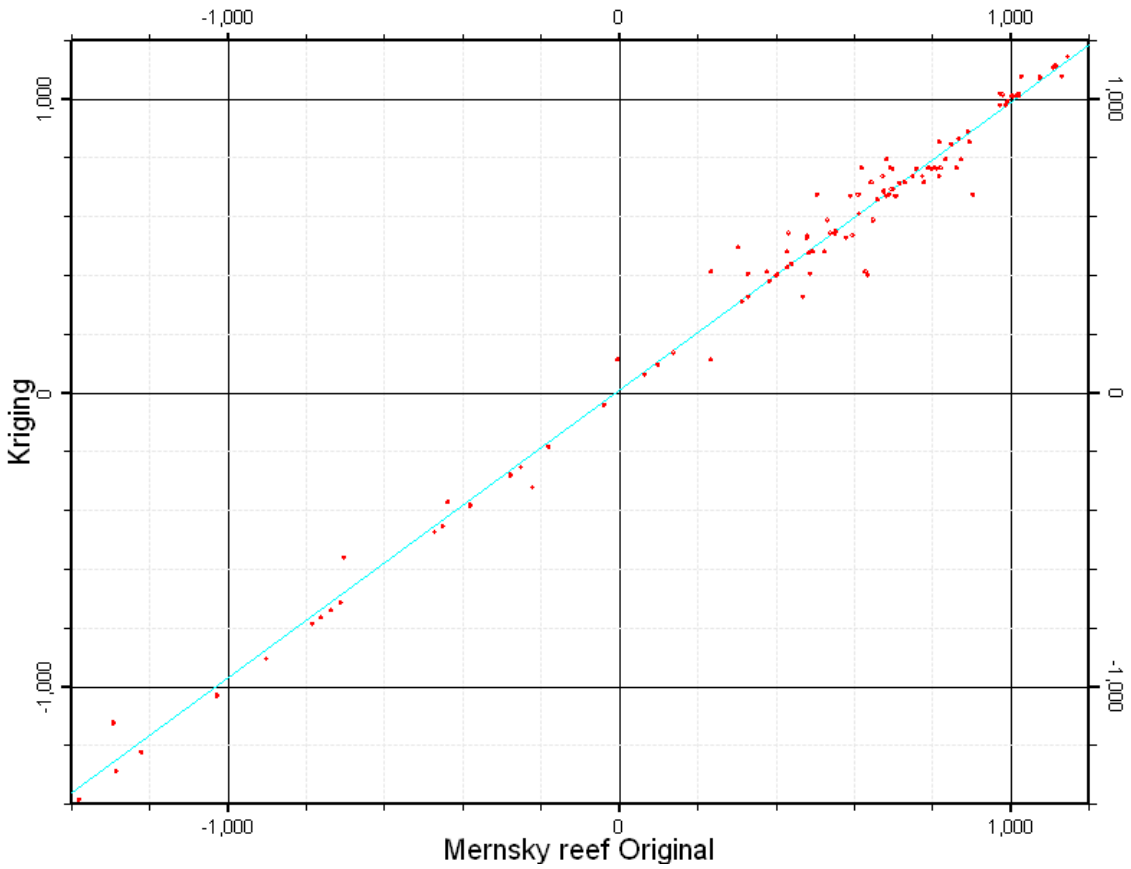

Figure 109: Scattergram of observed/measured Z values of the Merensky reef versus the estimated Z using krig interpolation.

The X,Y values define the location while the z values represent the elevation (in this study z represent the downhole depth at which each stratigraphic unit is encountered). Grids were constructed from these irregularly distributed data to provide values at regular rectangular nodes based on the degree of relationship or autocorrelation that exists between the data points. Contour lines were used to connect points of same elevation at the boundary of each stratigraphic unit. The isopach values were calculated by subtracting the stratigraphic top elevation from the elvation at the base.

TSA was applied to a small area within the RLS in order to demonstrate its usefulness in identifying subsurface structures; the result was compared with other interpolation methods and known geology. Before plotting, the stratigraphic intervals, all data were corrected to start form the mean sea level (MSL) thus eliminating topographical influence. First to sixth order trend and residuals were first determined from the available data. The first order is a linear regression function. Higher orders

(polynormial funcction) are used when the spatial distribution is more complex. The first and second order highlighted the residual structures more, while third and higher orders showed the trend. Lower orders were found to give good result even where the available data is sparse. The forth order in few cases showed very good trend that correlate well with the available records but most often the forth and higher order give erroneous result though they have higher correlation coefficient value. This further proves that statistical tests are not reliable guides in selecting appropriate TSA order. Rockworks 15 was used for most of the calculations.

Interpretation and choice of the order is therefore dependent on correlation with available surface mapping reports and geophysical records in the area. The TRA is fast, simple, and very useful in delineating small structures. The isopach maps were used in identifying pre, syn and post Bushveld structures.

Disadvantages of TSA method:

- when data points are few, anomalous values can seriously distort the surface;
- the surfaces are susceptible to edge effects.
- trend surfaces are inexact interpolators. extreme values of distant data points can exert an unduly large influence, resulting in poor local estimates of variable.

1.4 DATA ASSESSMENT AND CONTROL MEASURES

➢ HISTOGRAMS

Frequency diagrams were generated in-order to assess the distribution of observed data before contouring the data. This helps to determine the frequency or percentage of the total number of measurements for a particular variable e.g distribution of elevation at the contact of a stratigraphic unit. It also helps to determine the homogeneity of the statistical distribution and shows the dispersion of the values around the mean. Below is a plot of elevation (x) against frequency of occurrence for the Upper Zone, Main Zone and Merensky reef.

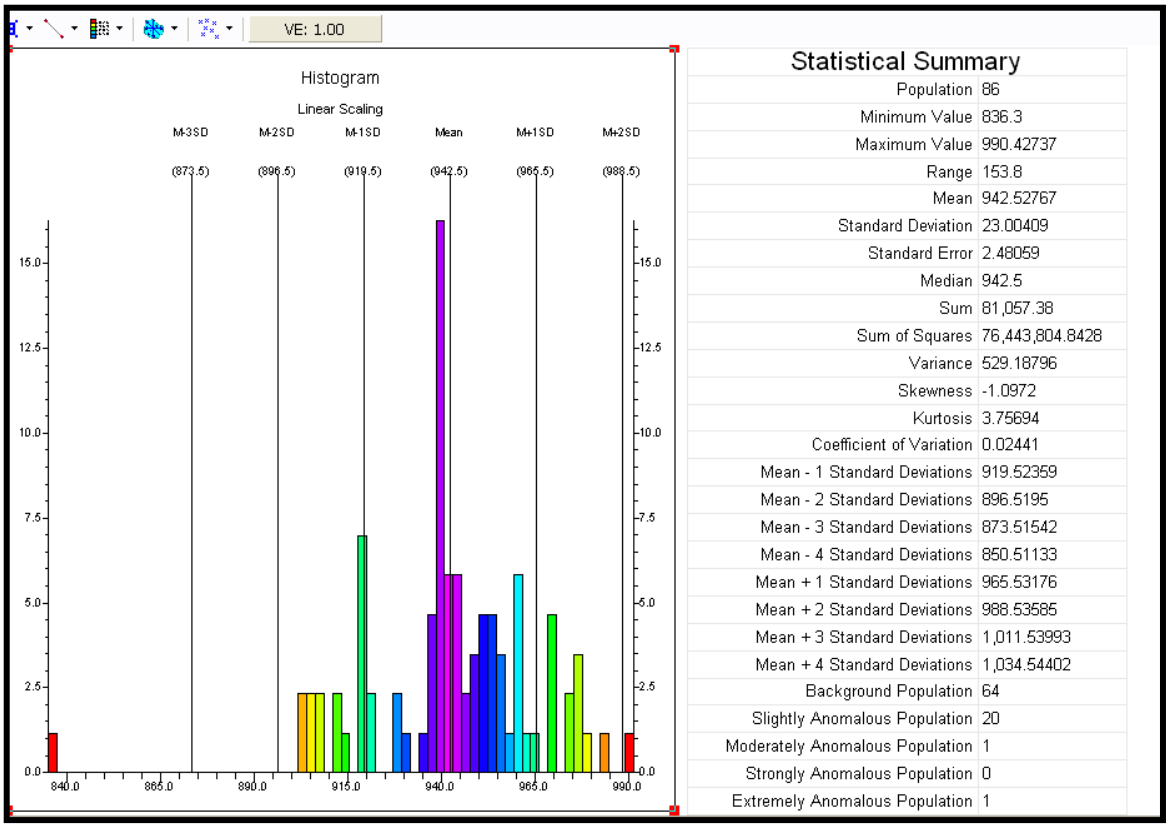

Figure 110: Histogram for 86 elevation data on Upper Zone stratigraphic contact at Amandelbult section of the Western Bushveld. This shows a single anomalous data, which was carefully crosschecked.

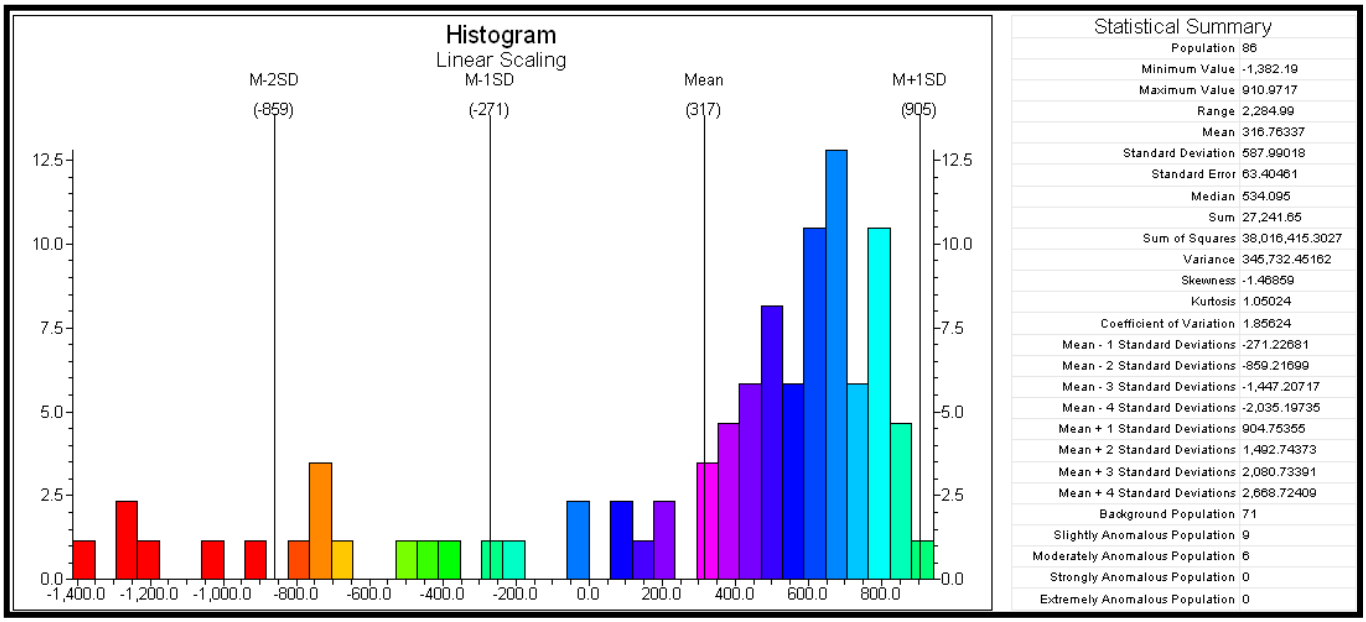

Statistical Summary

Population	86
Minimum Value	-1,382.19
Maximum Value	910.9717
Range	2,284.99
Mean	316.76337
Standard Deviation	587.99018
Standard Error	63.40461
Median	534.095
Sum	27,241.65
Sum of Squares	38,016,415.3027
Variance	345,732.45162
Skewness	-1.46859
Kurtosis	1.05024
Coefficient of Variation	1.85624
Mean - 1 Standard Deviations	-271.22681
Mean - 2 Standard Deviations	-859.21699
Mean - 3 Standard Deviations	-1,447.20717
Mean - 4 Standard Deviations	-2,035.19735
Mean + 1 Standard Deviations	904.75355
Mean + 2 Standard Deviations	1,492.74373
Mean + 3 Standard Deviations	2,080.73391
Mean + 4 Standard Deviations	2,668.72409
Background Population	71
Slightly Anomalous Population	9
Moderately Anomalous Population	6
Strongly Anomalous Population	0
Extremely Anomalous Population	0

Figure 111: Histogram for 86 elevation data on Main Zone stratigraphic contact at Amandelbult section of the Western Bushveld. The plot shows that the Main Zone unit occur more between 600 m and 800 m.

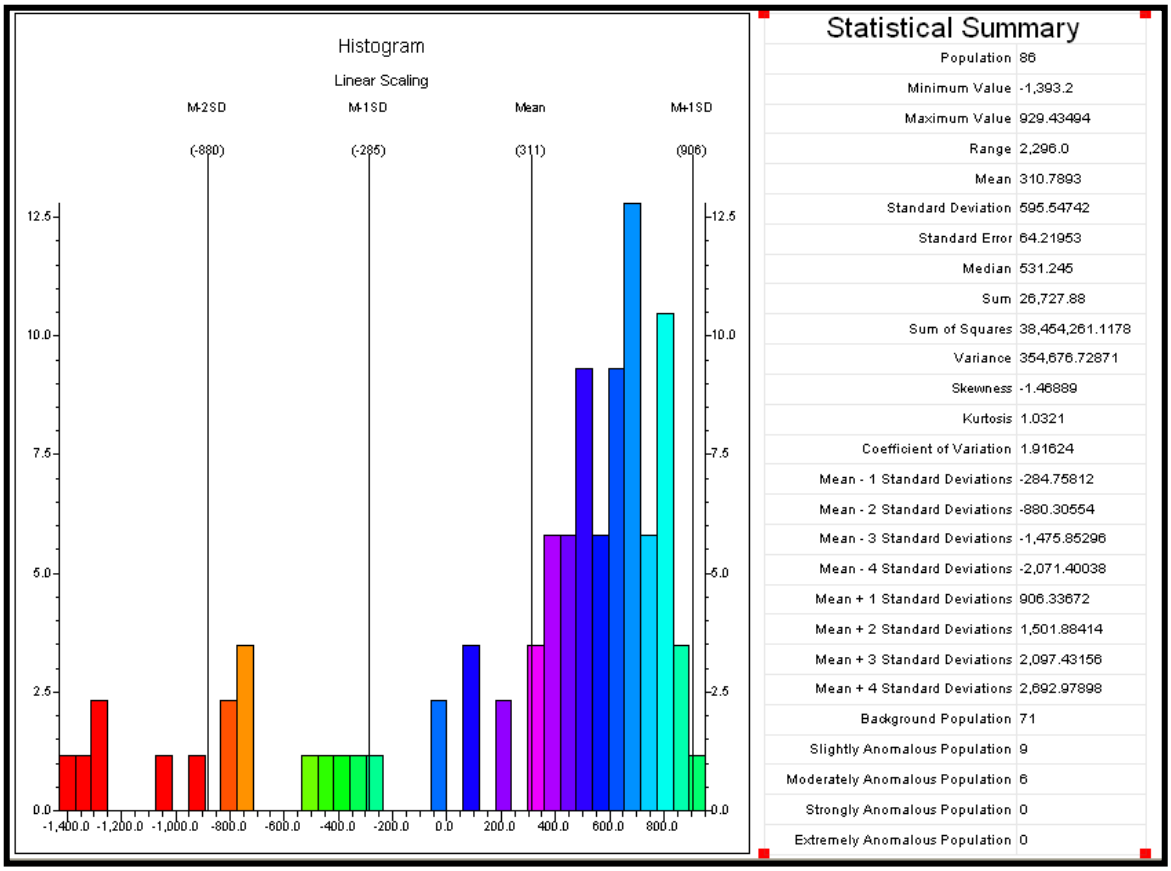

Figure 112: Histogram for 86 elevation data on Merensky reef contact at Amandelbult section of the Western Bushveld. The diagram illustrates the range and variability of elevations at the Main Zone contact. The average elevation is around -400.

Since no estimator (interpolation) is devoid of potential error, it becomes imperative to approximation (model) of the uncertainty underlying each estimate.

Deterministic interpolation techniques, including triangulation and inverse distance-weighting, which do not consider the possibility of a distribution of potential values for the unknown, they do not provide any measure of the reliability of the estimates.

1.5 COMPARISON OF RESULTS

Grid models of the northerneastern part of Eastern Bushveld Complex was compared with the result obtained and published by Lesego Platinum Mining, estimated the Merensky reef top to be approximately 2700 m. The grid models below show profiles drown from Phosiri Dome across the Phosiri ground (each showing the lowest level of the Phosiri ground on the Merensky reef top). All the interpolation method (Figures 12 to 20) applied gave estimates close to 2200 m except the Cummulative and Distance to point methods. Figure 21shows the depth to the top of the Upper Zonea around the BIC.

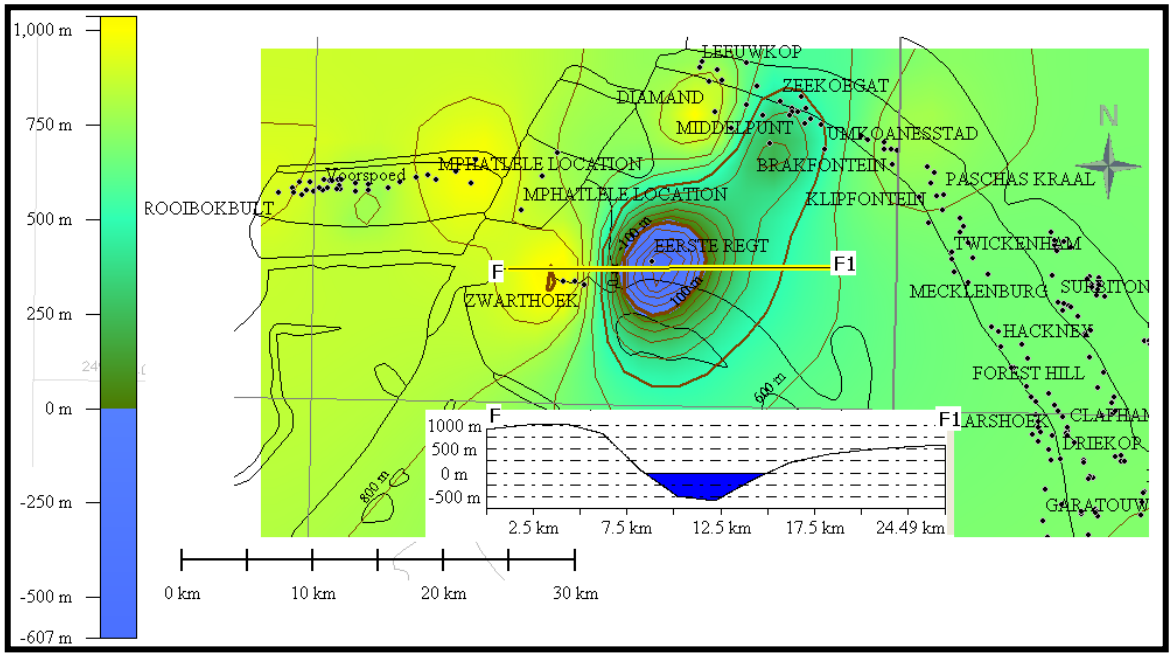

Figure12: Merensky reef isopach map of Northeastern Bushveld using Directional Weighing interpolation method in Rockworks

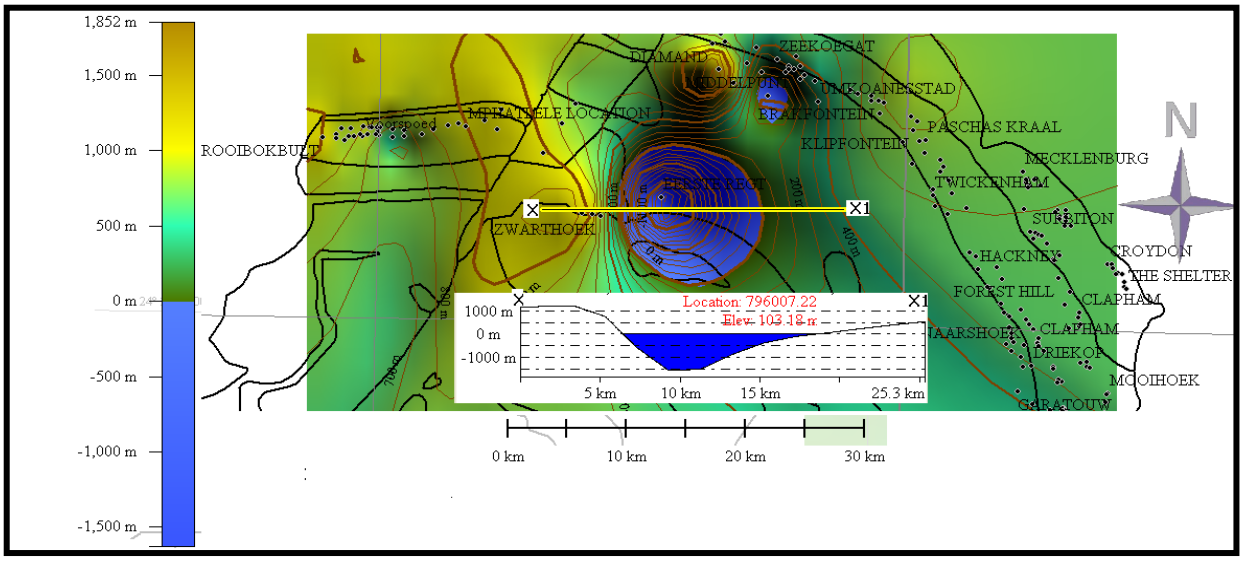

Figure13: Merensky reef isopach map of Northeastern Bushveld using trend surface interpolation method in Rockworks

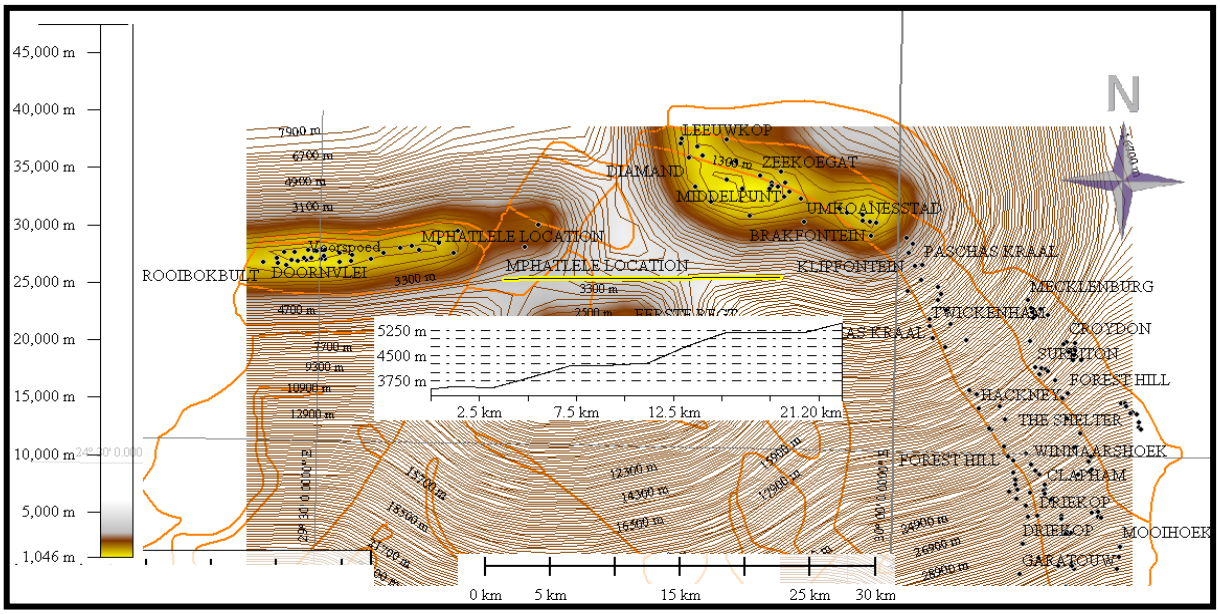

Figure14: Merensky reef isopach map of Northeastern Bushveld using Distance to point interpolation method in Rockworks

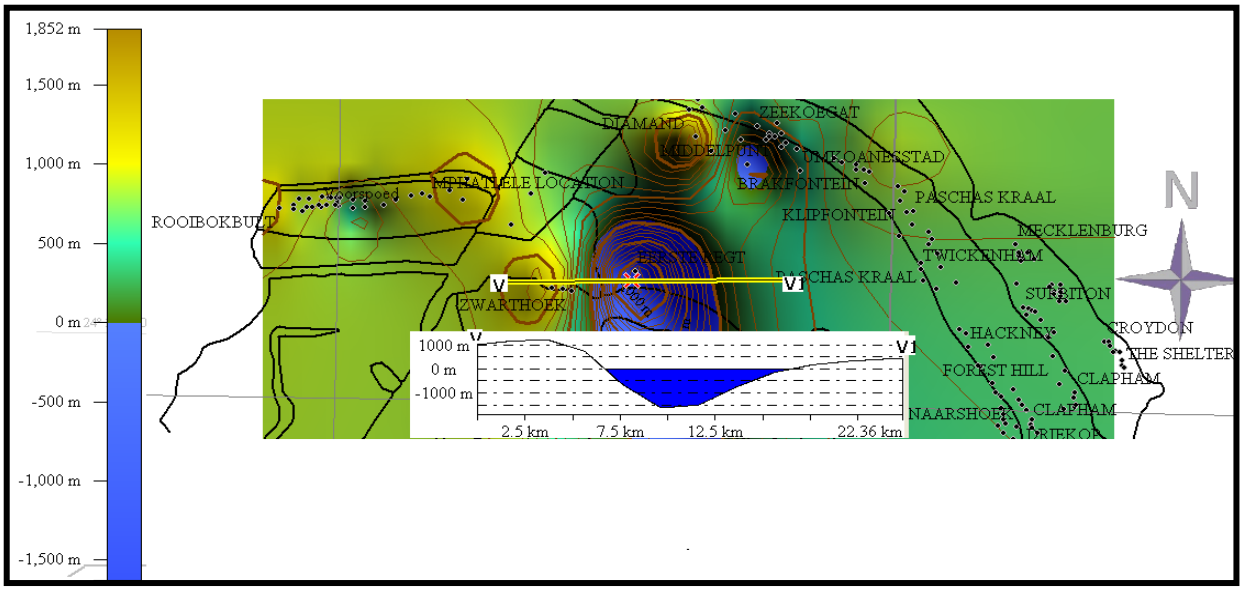

Figure 15: Merensky reef isopach map of Northeastern Bushveld using Kriging interpolation method in Rockworks

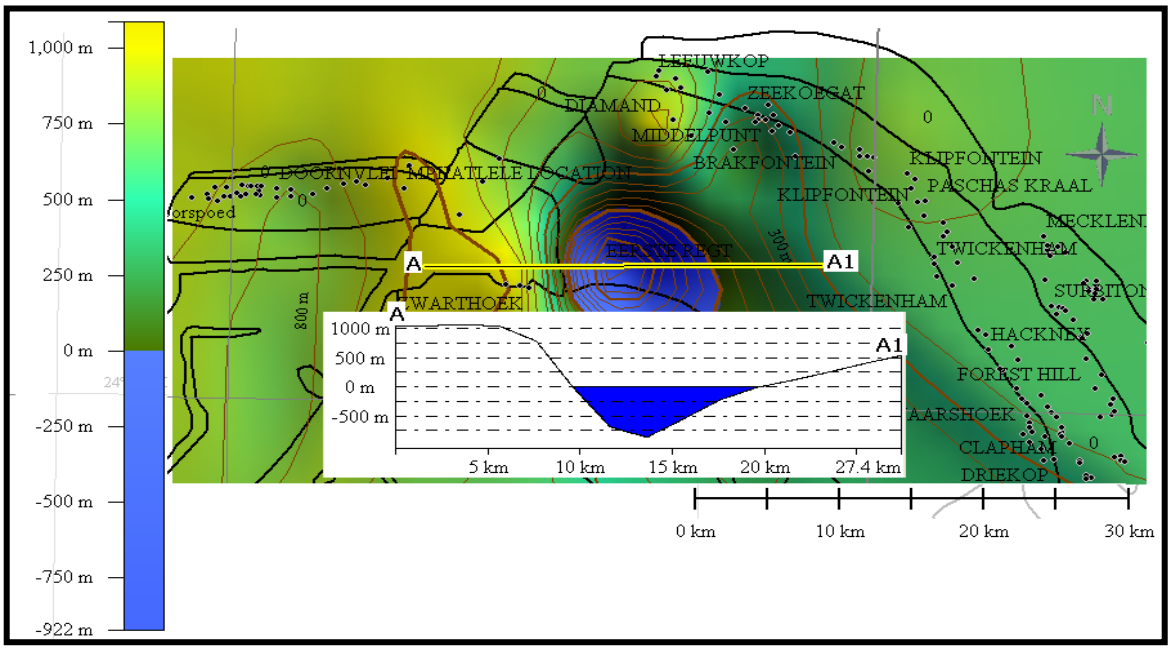

Figure 16: Merensky reef isopach map of Northeastern Bushveld using Inverse-distance weighing interpolation method in Rockworks

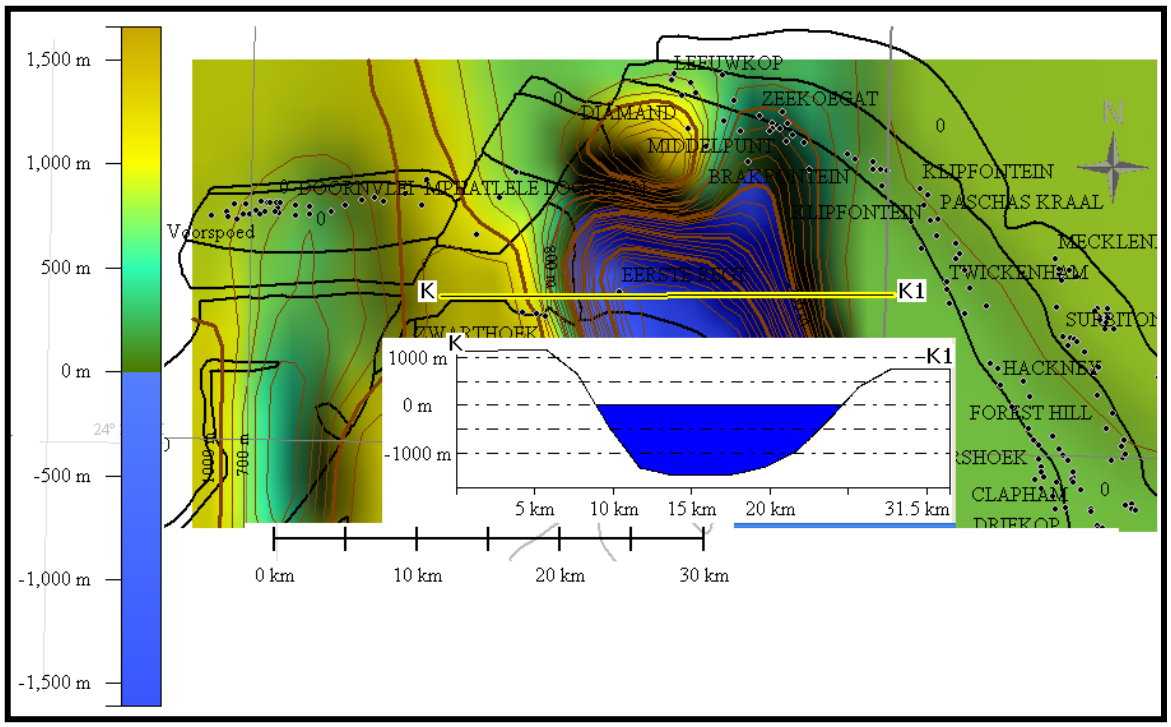

Figure 17: Merensky reef isopach map of Northeastern Bushveld using closest point distance interpolation method in Rockworks

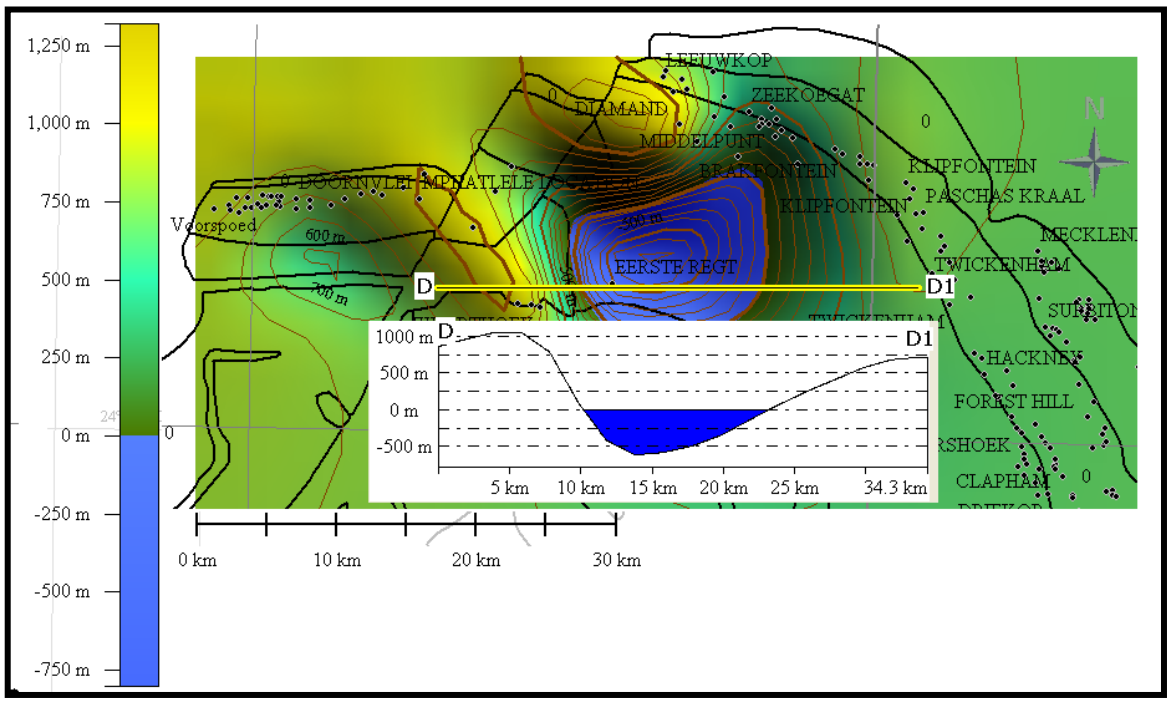

Figure 18: Merensky reef isopach map of Northeastern Bushveld using Trianglation interpolation method in Rockworks

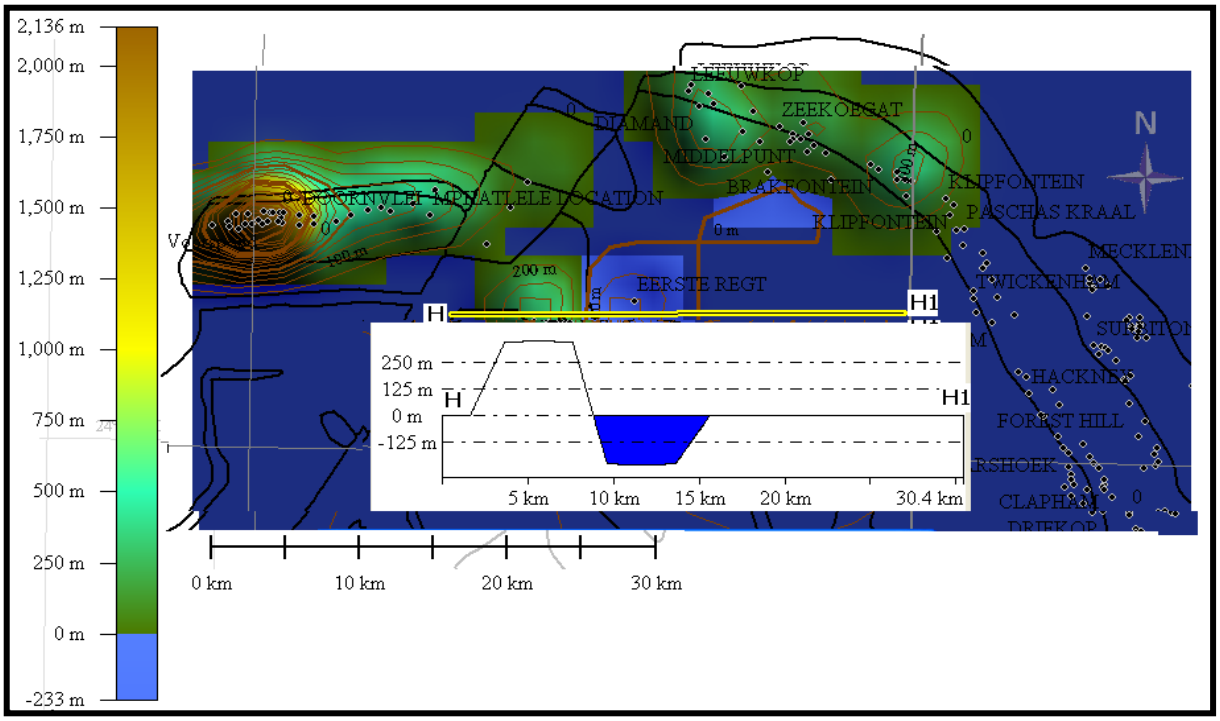

Figure 19:Merensky reef isopach map of Northeastern Bushveld using Cummulative interpolation method in Rockworks.

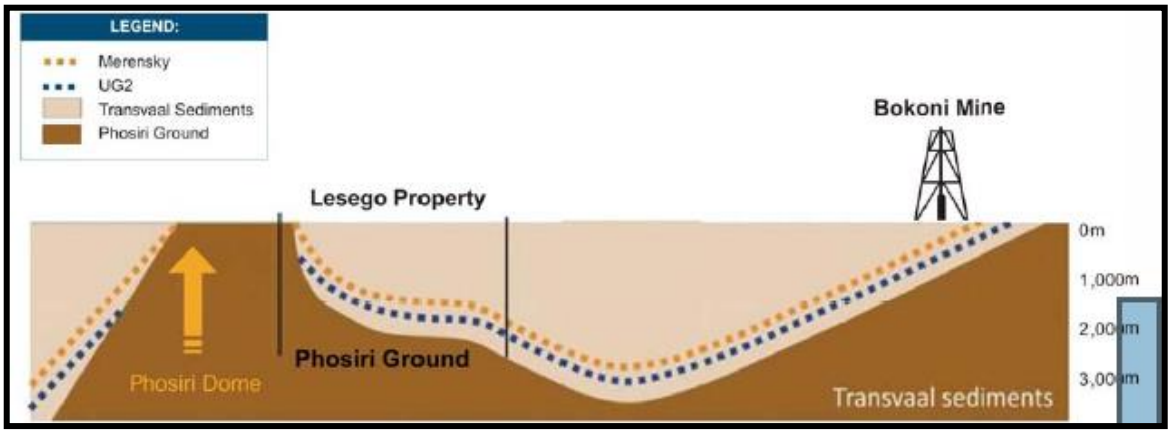

Figure 20: Diagram showing approximate depth of the Merensky reef and UG2 units from the investigation carried out by Lesego property in 2011.

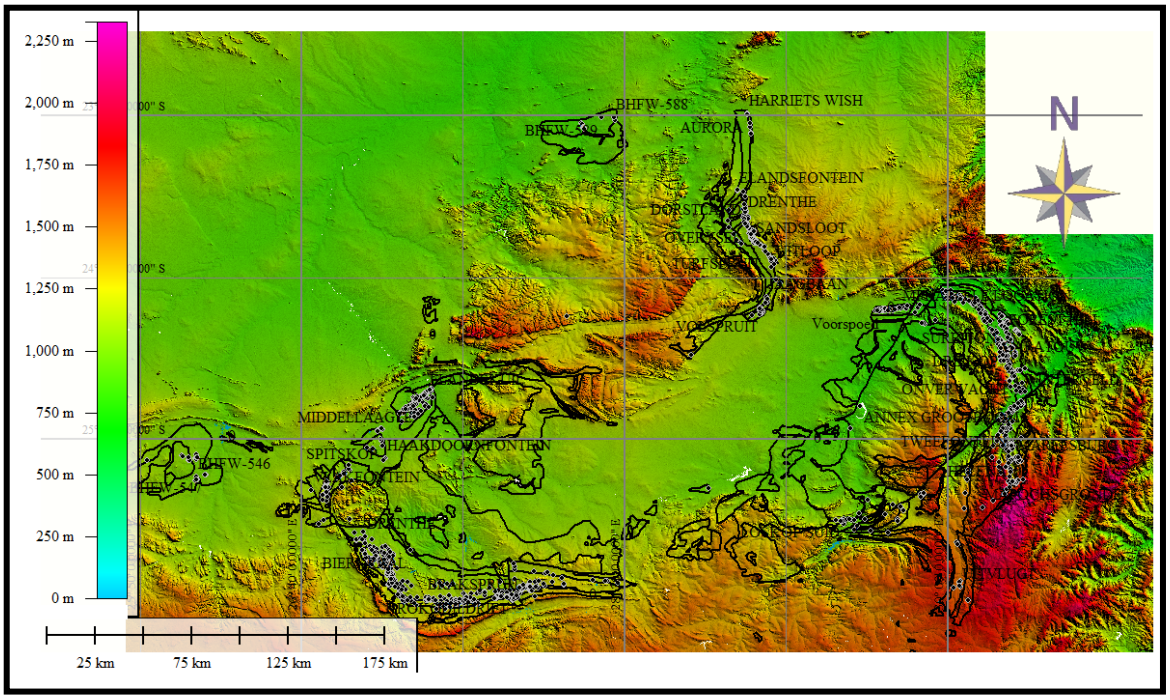

Figure 21: Depth to Bedrock around the BIC, obtained by subtracting the thickness of the overburden from the Digital Elevation Model (DEM)

REFERENCES

Bourges M., Mari Jean-Luc 2 and Jeann´ee1, N, 2012. A practical review of geostatistical processing applied to geophysical data: methods and applications. *Geophysical Prospecting,* 60, 400–412

Journel, A. G. 1989. Fundamentals of geostatistics in five lessons. Bibliography: p. 1. Geology-Statistical methods. American Geophysical Union, 2000 Florida Avenue, NW, Washington, DC 20009, U.S.A. SBN 0-87590-708-3.

Li, J. and Heap, A.D. 2008. *A review of spatial interpolation methods for environmental scientists*, Geoscience Australia Canberra.

Mei, S. 2009. Go sueologist-controlled trends versus computer-controlled trends: introducing a high-resolution approach tbsurface structural mapping using well-log data, trend surface analysis, and geospatial analysis. *Canadian Journal of Earth Sciences,* 46**,** 309-329.

Tobler, W. R. 1970. A computer movie simulating urban growth in the Detroit region. *Economic geography***,** 234-240.

Qiang Wua, HuaXu b, Xukai Zouc. 2004. An effective method for 3D geological modeling with multi-source data integration Computers & Geosciences 31 (2005) 35–43

APPENDIX 2

List of publications relevant to thesis

(a) Articles that have already appeared in learned Journals

(i) Bamisaiye, O.A., Eriksson, P.G., Van Rooy, J.L., Brynard, H.M., Foya, S., Nxumalo, V., Adeola, M., & Billay, A. (2014). Three dimensional geometry of the Rustenburg Layered Suite, South Africa. Canadian journal of tropical geography/Revue Canadienne de géographie tropicale. Laurientian University, Canada. Vol. (2) 1. 1-15.

(ii) Bamisaiye, O.A., (2015) Geo-Spatial Mapping of the Western Bushveld Rustenburg Layered Suite (Rls) in South Africa. Journal of Geography and Geology, Canada. Vol. 7, No. 4. 88-107.

(iii) Bamisaiye, O.A., Eriksson, P.G., Van Rooy, J.L., Brynard, H.M., Foya, S., Nxumalo, V., Adeola, M., & Billay, A. (2016). "Subsurface geometry of the Northwestern Bushveld complex, South Africa" Canadian journal of tropical geography/Revue canadienne de géographie tropicale. Laurientian University, Canada. Vol. (3) 1. 28-36.

(iv) Bamisaiye, O.A., .Eriksson, P.G., Van Rooy, J.L., Brynard, H.M., Foya, S (2016). Geo-Spatial Mapping of the Eastern Bushveld Rustenburg Layered Suite (RLS) in South Africa. Open Journal of Geology, 6, 285-301

(v) Bamisaiye, O.A., .Eriksson, P.G., Van Rooy, J.L., Brynard, H.M., Foya, S (2016). Geo-Spatial Mapping of the Northern Bushveld Rustenburg Layered Suite (RLS) in South Africa.Open Journal of Geology, 6, 302-313.

(vi). Bamisaiye, O.A., Eriksson, P.G., Van Rooy, J.L., Brynard, H.M., Foya, S., & Nxumalo, V. (2017). Subsurface Mapping of Rustenburg Layered Suite (RLS), Bushveld Complex, South Africa: Inferred Structural Features Using Borehole Data and Spatial Analysis. Journal of African Earth Sciences Vol.132. 139-167.

(b) Manuscripts submitted for publication:

vii. Bamisaiye, O.A., Van Rooy, J.L. (). The Bushveld Complex subsurface architecture: Results from geospatial analyses, 3D modelling and visualisation of the Rustenburg Layered Suite. Manuscript submitted to Computer and Geosciences Journal, currently under review. Manuscript ID:CAGEO-D-16-00425

(c) Published Conference Proceedings:

viii. Bamisaiye, O.A., Eriksson, P.G., Van Rooy, J.L., Brynard, H.M., & Foya, S. (2015) Subsurface Structural Mapping of the Rustenburg Layered Suite (RLS) of the Bushveld Igneous Complex in South Africa. Abstracts 1st Conference on Earth and Mineral Sciences, School of earth and Mineral Sciences (SEMS), Federal University of Technology, Akure, Ondo state, Nigeria, 29 June-2 July 2015.